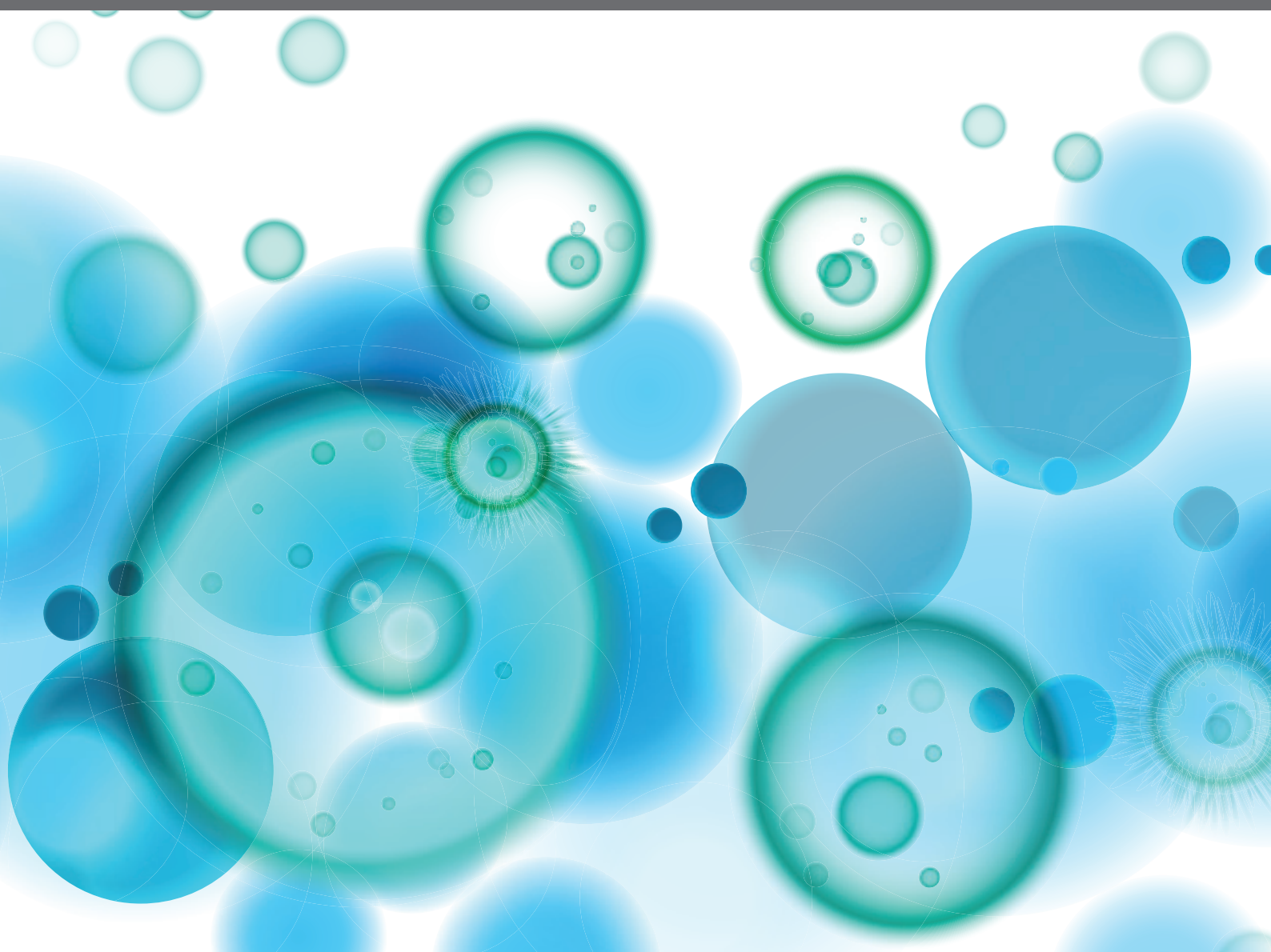


EXPLOITING NOVEL COMBINED HOST- AND PATHOGEN-DIRECTED THERAPIES FOR COMBATING BACTERIAL MULTIDRUG RESISTANCE

EDITED BY: Maurizio Fraziano, Roberto Nisini, Gian Maria Rossolini and
Marco Rinaldo Oggioni

PUBLISHED IN: *Frontiers in Immunology* and *Frontiers in Microbiology*





frontiers

Frontiers eBook Copyright Statement

The copyright in the text of individual articles in this eBook is the property of their respective authors or their respective institutions or funders. The copyright in graphics and images within each article may be subject to copyright of other parties. In both cases this is subject to a license granted to Frontiers.

The compilation of articles constituting this eBook is the property of Frontiers.

Each article within this eBook, and the eBook itself, are published under the most recent version of the Creative Commons CC-BY licence.

The version current at the date of publication of this eBook is CC-BY 4.0. If the CC-BY licence is updated, the licence granted by Frontiers is automatically updated to the new version.

When exercising any right under the CC-BY licence, Frontiers must be attributed as the original publisher of the article or eBook, as applicable.

Authors have the responsibility of ensuring that any graphics or other materials which are the property of others may be included in the CC-BY licence, but this should be checked before relying on the CC-BY licence to reproduce those materials. Any copyright notices relating to those materials must be complied with.

Copyright and source acknowledgement notices may not be removed and must be displayed in any copy, derivative work or partial copy which includes the elements in question.

All copyright, and all rights therein, are protected by national and international copyright laws. The above represents a summary only. For further information please read Frontiers' Conditions for Website Use and Copyright Statement, and the applicable CC-BY licence.

ISSN 1664-8714

ISBN 978-2-88966-307-1

DOI 10.3389/978-2-88966-307-1

About Frontiers

Frontiers is more than just an open-access publisher of scholarly articles: it is a pioneering approach to the world of academia, radically improving the way scholarly research is managed. The grand vision of Frontiers is a world where all people have an equal opportunity to seek, share and generate knowledge. Frontiers provides immediate and permanent online open access to all its publications, but this alone is not enough to realize our grand goals.

Frontiers Journal Series

The Frontiers Journal Series is a multi-tier and interdisciplinary set of open-access, online journals, promising a paradigm shift from the current review, selection and dissemination processes in academic publishing. All Frontiers journals are driven by researchers for researchers; therefore, they constitute a service to the scholarly community. At the same time, the Frontiers Journal Series operates on a revolutionary invention, the tiered publishing system, initially addressing specific communities of scholars, and gradually climbing up to broader public understanding, thus serving the interests of the lay society, too.

Dedication to Quality

Each Frontiers article is a landmark of the highest quality, thanks to genuinely collaborative interactions between authors and review editors, who include some of the world's best academicians. Research must be certified by peers before entering a stream of knowledge that may eventually reach the public - and shape society; therefore, Frontiers only applies the most rigorous and unbiased reviews.

Frontiers revolutionizes research publishing by freely delivering the most outstanding research, evaluated with no bias from both the academic and social point of view. By applying the most advanced information technologies, Frontiers is catapulting scholarly publishing into a new generation.

What are Frontiers Research Topics?

Frontiers Research Topics are very popular trademarks of the Frontiers Journals Series: they are collections of at least ten articles, all centered on a particular subject. With their unique mix of varied contributions from Original Research to Review Articles, Frontiers Research Topics unify the most influential researchers, the latest key findings and historical advances in a hot research area! Find out more on how to host your own Frontiers Research Topic or contribute to one as an author by contacting the Frontiers Editorial Office: researchtopics@frontiersin.org

EXPLOITING NOVEL COMBINED HOST- AND PATHOGEN-DIRECTED THERAPIES FOR COMBATING BACTERIAL MULTIDRUG RESISTANCE

Topic Editors:

Maurizio Fraziano, University of Rome Tor Vergata, Italy

Roberto Nisini, National Institute of Health (ISS), Italy

Gian Maria Rossolini, University of Florence, Italy

Marco Rinaldo Oggioni, University of Leicester, United Kingdom

Citation: Fraziano, M., Nisini, R., Rossolini, G. M., Oggioni, M. R., eds. (2020). Exploiting Novel Combined Host- and Pathogen-Directed Therapies for Combating Bacterial Multidrug Resistance. Lausanne: Frontiers Media SA. doi: 10.3389/978-2-88966-307-1

Table of Contents

- 05 Editorial: Exploiting Novel Combined Host- and Pathogen-Directed Therapies for Combating Bacterial Multidrug Resistance**
Roberto Nisini, Marco R. Oggioni, Gian Maria Rossolini and Maurizio Fraziano
- 08 From Petri Dish to Patient: Bioavailability Estimation and Mechanism of Action for Antimicrobial and Immunomodulatory Natural Products**
Nicholas John Sadgrove and Graham Lloyd Jones
- 34 Colistin Combined With Tigecycline: A Promising Alternative Strategy to Combat *Escherichia coli* Harboring bla_{NDM-5} and mcr-1**
Yu-Feng Zhou, Ping Liu, Chuan-Jian Zhang, Xiao-Ping Liao, Jian Sun and Ya-Hong Liu
- 45 Inhibition of Transglutaminase 2 as a Potential Host-Directed Therapy Against *Mycobacterium tuberculosis***
Ivana Palucci, Giuseppe Maulucci, Flavio De Maio, Michela Sali, Alessandra Romagnoli, Linda Petrone, Gian Maria Fimia, Maurizio Sanguinetti, Delia Goletti, Marco De Spirito, Mauro Piacentini and Giovanni Delogu
- 58 NSC 18725, a Pyrazole Derivative Inhibits Growth of Intracellular *Mycobacterium tuberculosis* by Induction of Autophagy**
Garima Arora, Gagandeep, Assirbad Behura, Tannu Priya Gosain, Ravi P. Shaliwal, Saqib Kidwai, Padam Singh, Shamseer Kulangara Kandi, Rohan Dhiman, Diwan S. Rawat and Ramandeep Singh
- 71 *Clostridium butyricum* Ameliorates Salmonella Enteritis Induced Inflammation by Enhancing and Improving Immunity of the Intestinal Epithelial Barrier at the Intestinal Mucosal Level**
Xiaonan Zhao, Jie Yang, Zijing Ju, Jianmin Wu, Lili Wang, Hai Lin and Shuhong Sun
- 82 Developing Novel Host-Based Therapies Targeting Microbicidal Responses in Macrophages and Neutrophils to Combat Bacterial Antimicrobial Resistance**
Katie Watson, Clark D. Russell, J. Kenneth Baillie, Kev Dhaliwal, J. Ross Fitzgerald, Timothy J. Mitchell, A. John Simpson, Stephen A. Renshaw and David H. Dockrell on behalf of the SHIELD consortium
- 94 Human Single-chain Variable Fragments Neutralize *Pseudomonas aeruginosa* Quorum Sensing Molecule, 3O-C12-HSL, and Prevent Cells From the HSL-mediated Apoptosis**
Sirijan Santajit, Watee Seesuy, Kodchakorn Mahasongkram, Nitat Sookrung, Pornpan Pumirat, Sumate Ampawong, Onrapak Reamtong, Manas Chongsa-Nguan, Wanpen Chaicumpa and Nitaya Indrawattana
- 111 Synergistic Effect of Berberine Hydrochloride and Fluconazole Against *Candida albicans* Resistant Isolates**
Jiangyan Yong, Ruiling Zu, Xiaoxue Huang, Yiman Ge and Yan Li

123 *Toxoplasma gondii* Dense Granule Proteins 7, 14, and 15 Are Involved in Modification and Control of the Immune Response Mediated via NF- κ B Pathway

Fumiaki Ihara, Ragab M. Fereig, Yuu Himori, Kyohko Kameyama, Kosuke Umeda, Sachi Tanaka, Rina Ikeda, Masahiro Yamamoto and Yoshifumi Nishikawa

141 *Liposomes Loaded With Phosphatidylinositol 5-Phosphate Improve the Antimicrobial Response to Pseudomonas aeruginosa in Impaired Macrophages From Cystic Fibrosis Patients and Limit Airway Inflammatory Response*

Noemi Poerio, Federica De Santis, Alice Rossi, Serena Ranucci, Ida De Fino, Ana Henriquez, Marco M. D'Andrea, Fabiana Ciciriello, Vincenzina Lucidi, Roberto Nisini, Alessandra Bragonzi and Maurizio Fraziano

154 *Etiopathogenesis, Challenges and Remedies Associated With Female Genital Tuberculosis: Potential Role of Nuclear Receptors*

Shalini Gupta and Pawan Gupta



Editorial: Exploiting Novel Combined Host- and Pathogen-Directed Therapies for Combating Bacterial Multidrug Resistance

Roberto Nisini¹, Marco R. Oggioni^{2,3}, Gian Maria Rossolini⁴ and Maurizio Fraziano^{5*}

¹ Department of Infectious Diseases, Istituto Superiore di Sanità, Roma, Italy, ² Department of Genetics and Genome Biology, University of Leicester, Leicester, United Kingdom, ³ Dipartimento di Farmacia e Biotecnologie, Università di Bologna, Bologna, Italy, ⁴ Clinical Microbiology and Virology Unit, Careggi University Hospital, Florence, Italy, ⁵ Department of Biology, University of Rome Tor Vergata, Rome, Italy

Keywords: multidrug resistance, bacteria, host-directed therapy, pathogen-directed therapy, innate immunity

OPEN ACCESS

Edited and reviewed by:

Ian Marriott,
University of North Carolina at
Charlotte, United States

*Correspondence:

Maurizio Fraziano
fraziano@bio.uniroma2.it

Specialty section:

This article was submitted to
Microbial Immunology,
a section of the journal
Frontiers in Immunology

Received: 12 October 2020

Accepted: 15 October 2020

Published: 04 November 2020

Citation:

Nisini R, Oggioni MR, Rossolini GM
and Fraziano M (2020) Editorial:
Exploiting Novel Combined
Host- and Pathogen-Directed
Therapies for Combating
Bacterial Multidrug Resistance.
Front. Immunol. 11:616486.
doi: 10.3389/fimmu.2020.616486

Editorial on the Research Topic

Exploiting Novel Combined Host- and Pathogen-Directed Therapies for Combating Bacterial Multidrug Resistance

The golden age of antibiotic therapy started in 1928 with the discovery of penicillin and reached a peak at the mid-1950s. Thereafter, antibiotic discovery and development of new molecules gradually declined with the parallel emergence of drug resistance of many human bacterial pathogens. These circumstances led to the current therapeutical crisis due to antimicrobial resistance (1). Today, the frequency and spectrum of antibiotic resistance in specific bacterial pathogens continues to increase worryingly, with particular concerns on *Mycobacterium tuberculosis* and on several Gram-positive (e.g., *Streptococcus pneumoniae*, *Staphylococcus aureus*, and enterococci) as well as Gram-negative bacteria (e.g., *Klebsiella pneumoniae*, *Escherichia coli*, *Enterobacter* spp, *Acinetobacter baumannii*, and *Pseudomonas aeruginosa*). The slow-pace of discovery of novel antimicrobial agents, the dearth of new antibiotics already in the drug development pipeline, and the emergence and rapid diffusion of strains resistant to last resort antibiotics, make novel therapeutic approaches an urgent need to reduce the burden of infectious diseases. It is estimated that deaths due to antibiotic resistant bacterial pathogens may pass from the actual 700,000 cases to about 10 million per year by 2050, if adequate countermeasures are not undertaken.

Novel antimicrobials or antimicrobial combinations may help to overcome this global emergence. Zhou et al. report data showing that the combined use of the antibiotics colistin and tigecycline may represent a valuable therapeutic option against multi-drug resistant *E. coli* harbouring bla_{NDM-5} and mcr-1 expression. Yong et al. show that berberine hydrochloride, a commonly used traditional Chinese medicine with known antimicrobial effects, in combination

with fluconazole, may be an effective therapeutic option for infections related to FLC-resistant *C. albicans*. Sadgrove and Jones highlight the importance of pharmacokinetic and pharmacodynamic analysis in the field of ethnopharmacology, before extrapolating enteral and topical therapeutic value of natural compounds.

However, the evolution of bacteria towards resistance to antimicrobial agents, including multidrug resistance, is an unavoidable phenomenon because it reflects an aspect of the general evolution of bacteria which is unstoppable (2) and, for many bacterial infections, drug resistant mutants are likely present by the time antibiotic treatment starts. Nevertheless, such infections can be successfully cleared and it is commonly assumed that this is due to the combined action of the drug and of the immune response, the latter facilitating clearance of the resistant bacterial population (3). Novel anti-infectious therapeutic approaches based on the modulation of host response (Host-directed therapy, HDT) have been proposed to counteract the emergence of antimicrobial resistance. HDT is defined as a therapeutic approach based on strategies aimed at improving innate or adaptive protective response needed for pathogen control and/or at limiting immunopathology. In this context, the vaccination may be considered as a prototypical host-directed approach that counteracts antibiotic resistance and prevents bacterial diseases (4). HDT may also comprise any drug that can activate effector mechanisms of the antimicrobial response (ROS generation, autophagy, phagolysosome maturation, antimicrobial peptide production) and/or down-modulate tissue-damaging immune responses (5).

In this special topic, Arora et al. identify a nitroso containing pyrazolo derivative compound, which was directly effective against *M. tuberculosis*, and show a synergistic effect with isoniazid and an additive effect with other molecules. Interestingly, this molecule is also capable of inducing autophagy in host cells and this mechanism is demonstrated as the major mechanism for killing of intracellular slow- and fast-growing mycobacteria. Palucci et al. identify host trasglutaminase 2 as a possible gene target for novel host directed therapy and its inhibition by cystamine or cysteamine promotes intracellular killing of *M. tuberculosis*, and acts synergistically with a second-line anti-TB drug amikacin. Improvement in HDT strategies may also require studies focusing on the identification of microbial gene products, which could be targeted by immune responses. Thus, Santajit et al. generate a fully human single-chain variable fragment (HuscFvs) binding to N-(3-oxododecanoyl)-L-homoserine lactone (3O-C12-HSL) of *P. aeruginosa*, a quorum sensing signalling molecule that contributes to the pathogenesis of infection by regulating expression of bacterial virulence factors causing intense inflammation and toxicity in the infected host. In this study, HuscFvs is capable of neutralizing 3O-C12 -HSL activity and preventing host cell apoptosis. Finally, Ihara et al. demonstrate that dense granule proteins 7, 14 and 15 from type II *Toxoplasma gondii* strains induced host immunity via NF- κ B activation and can limit parasite expansion.

The emergence of antimicrobial resistant strains is often caused by an inefficient immune response, which promotes the persistence

of naturally occurring MDR strains within a bacterial population. Thus, patients with defective immune responses and that are unresponsive to standard antibiotic treatments are often characterized by a chronic tissue damaging inflammatory response. In the present collection, Watson et al. suggest a focused host-directed therapeutic approach capable of enhancing pauci-inflammatory microbial killing in myeloid phagocytes, which maximizes pathogen clearance while minimizing the harmful consequences of the inflammatory responses. The combined down-modulation of the pathogenic inflammatory response and activation of the antimicrobial response has been described by Poerio et al. The authors show that the treatment with apoptotic body-like liposomes loaded with phosphatidylinositol 5-phosphate promotes phagosome maturation, which is naturally subverted in cells from CF patients, and intracellular bacterial killing of MDR *P. aeruginosa*, while simultaneously limiting inflammatory response both *in vitro* and *in vivo*. Immunosuppression is also an important risk factor for extrapulmonary tuberculosis. Gupta and Gupta discuss novel therapeutic approaches against female genital tuberculosis, representing one of the most perilous forms of extrapulmonary tuberculosis, and suggest that nuclear receptors could be major new therapeutic targets and/or diagnostic biomarkers.

An additional interesting approach, targeting local microbiota, has been described by Zhao et al. who report the use of *Clostridium butyricum*, a common human and animal gut commensal bacterium often used as a probiotic, as a possible treatment for *Salmonella enteritidis* infection. Here, *C. butyricum* attenuates inflammation and epithelial barrier damage, alters intestinal microbial composition, and increases the diversity of bacterial communities in the intestine of *Salmonella* infected chickens.

In conclusion, novel and heterogeneous therapeutic approaches to reduce the global burden of antimicrobial resistance have been proposed and discussed in this special issue. Based upon these studies, we suggest that a combination of both host- and pathogen- directed therapeutic approaches may represent a valuable and exploitable strategy, over single therapies, to i) control multidrug resistant infections, ii) minimize the risk of emergence of drug resistance and iii) reduce the time of therapy. This would, in turn, help reduce patient management costs in low- and middle-income countries where the social and economic impact of MDR burden has dramatic consequences.

AUTHOR CONTRIBUTIONS

All authors listed have made a substantial, direct, and intellectual contribution to the work and approved it for publication.

FUNDING

This work was supported by the Italian Cystic Fibrosis Research Foundation (FFC#19/2019).

REFERENCES

1. Hutchings MI, Truman AW, Wilkinson B. Antibiotics: past, present and future. *Curr Opin Microbiol* (2019) 51:72–80. doi: 10.1016/j.mib.2019.10.008
2. Courvalin P. Why is antibiotic resistance a deadly emerging disease? *Clin Microbiol Infect* (2016) 22:405–7. doi: 10.1016/j.cmi.2016.01.012
3. Happel KI, Bagby GJ, Nelson S. Host defense and bacterial pneumonia. *Semin Respir Crit Care Med* (2004) 25:43–52. doi: 10.1055/s-2004-822304
4. Tagliabue A, Rappuoli R. Changing Priorities in Vaccinology: Antibiotic Resistance Moving to the Top. *Front Immunol* (2018) 9:1068. doi: 10.3389/fimmu.2018.01068
5. Kaufmann SHE, Dorhoi A, Hotchkiss RS, Bartenschlager R. Host-directed therapies for bacterial and viral infections. *Nat Rev Drug Discov* (2018) 17:35–56. doi: 10.1038/nrd.2017.162

Conflict of Interest: The authors declare that the research was conducted in the absence of any commercial or financial relationships that could be construed as a potential conflict of interest.

Copyright © 2020 Nisini, Oggioni, Rossolini and Fraziano. This is an open-access article distributed under the terms of the Creative Commons Attribution License (CC BY). The use, distribution or reproduction in other forums is permitted, provided the original author(s) and the copyright owner(s) are credited and that the original publication in this journal is cited, in accordance with accepted academic practice. No use, distribution or reproduction is permitted which does not comply with these terms.



From Petri Dish to Patient: Bioavailability Estimation and Mechanism of Action for Antimicrobial and Immunomodulatory Natural Products

Nicholas John Sadgrove^{1,2*} and Graham Lloyd Jones¹

¹ Pharmaceuticals and Nutraceuticals (PAN) Group, School of Science and Technology, University of New England, Armidale, NSW, Australia, ² Jodrell Science Laboratory, Royal Botanic Gardens, Kew, Richmond, United Kingdom

OPEN ACCESS

Edited by:

Natalia V. Kirienko,
Rice University, United States

Reviewed by:

Carlos Henrique Gomes Martins,
Federal University of Uberlândia, Brazil
Maurizio Fraziano,
University of Rome Tor Vergata, Italy
Masood Sepehrimanesh,
Gilan University of Medical Sciences,
Iran

*Correspondence:

Nicholas John Sadgrove
n.sadgrove@kew.org

Specialty section:

This article was submitted to
Antimicrobials, Resistance
and Chemotherapy,
a section of the journal
Frontiers in Microbiology

Received: 15 August 2019

Accepted: 15 October 2019

Published: 31 October 2019

Citation:

Sadgrove NJ and Jones GL
(2019) From Petri Dish to Patient:
Bioavailability Estimation
and Mechanism of Action
for Antimicrobial
and Immunomodulatory Natural
Products. *Front. Microbiol.* 10:2470.
doi: 10.3389/fmicb.2019.02470

The new era of multidrug resistance of pathogens against frontline antibiotics has compromised the immense therapeutic gains of the ‘golden age,’ stimulating a resurgence in antimicrobial research focused on antimicrobial and immunomodulatory components of botanical, fungal or microbial origin. While much valuable information has been amassed on the potency of crude extracts and, indeed, purified compounds there are too many reports that uncritically extrapolate observed *in vitro* activity to presumed ingestive and/or topical therapeutic value, particularly in the discipline of ethnopharmacology. Thus, natural product researchers would benefit from a basic pharmacokinetic and pharmacodynamic understanding. Furthermore, therapeutic success of complex mixtures or single components derived therefrom is not always proportionate to their MIC values, since immunomodulation can be the dominant mechanism of action. Researchers often fail to acknowledge this, particularly when ‘null’ activity is observed. In this review we introduce the most up to date theories of oral and topical bioavailability including the metabolic processes affecting xenobiotic biotransformation before and after drugs reach the site of their action in the body. We briefly examine the common methodologies employed in antimicrobial, immunomodulatory and pharmacokinetic research. Importantly, we emphasize the contribution of synergies and/or antagonisms in complex mixtures as they affect absorptive processes in the body and sometimes potentiate activity. Strictly in the context of natural product research, it is important to acknowledge the potential for chemotypic variation within important medicinal plants. Furthermore, polar head space and rotatable bonds give *a priori* indications of the likelihood of bioavailability of active metabolites. Considering this and other relatively simple chemical insights, we hope to provide the basis for a more rigorous scientific assessment, enabling researchers to predict the likelihood that observed *in vitro* anti-infective activity will translate to *in vivo* outcomes in a therapeutic context. We give worked examples of tentative pharmacokinetic assessment of some well-known medicinal plants.

Keywords: polar head space, rotatable bonds, pharmacokinetics, pharmacodynamics, transdermal penetration

INTRODUCTION

The pharmacotherapeutic value of antimicrobial and immunomodulatory (anti-infective) drugs critically depends on the orchestration of properties influencing pharmacokinetics and pharmacodynamics. In the former, the discipline of pharmacokinetics was born out of the need to monitor and maintain optimal physiological concentration of a drug to achieve a positive therapeutic outcome. Optimal concentration is above an 'active' threshold but below contraindicated (and possibly toxic) levels. In clinical practice, to achieve optimal concentration, factors under consideration include efficiency of absorption, drug half-life and hence, dose and intervals of drug administration. In a broader sense, characteristics influencing pharmacokinetic fate of a specific drug critically depend on its chemical functional groups, which are the basis for *a priori* insight into the possibility of absorption or transdermal penetration.

However, pharmacodynamics is a more preliminary step in that the mechanism of the drug is fully or tentatively explained and the therapeutic and/or toxicity thresholds are established. One of the bigger challenges in pharmacodynamics is the translation to the pharmacokinetic context, from *in vitro* models to *in vivo* environments where several physiological processes may compromise the presumed positive therapeutic outcomes. The most important of these challenges include absorption and biotransformation of ingested therapies occurring in the liver and by the gut microbiota. Such challenges are commonly neglected in ethnopharmacological or natural product research, particularly those involving crude extracts as commonly administered in herbal medicine.

After the turn of the century most of the research concerning anti-infectives has focused on natural plant, marine or endophyte extracts. Since this research usually starts with a bioactivity guided fractionation of a crude extract, structural elucidation studies commence at a relatively late stage. Ideally, the preliminary steps taken before measuring biological activity should involve tentative interpretation in the context of pharmacokinetics by closer examination of polar functional groups known to influence absorption and the number of rotatable bonds. This is critical when therapies are ingested and expected to act non-locally (not in the digestive tract) and therefore require sufficiently high systemic concentration. Understandably, since most investigations measure activity first and compound structure second, with pharmacokinetic interpretation as a final step, there are a plethora of published studies reporting successful *in vitro* outcomes which are naively and often uncritically extrapolated to presumed *in vivo* therapeutic value.

Fortunately, by remembering only a few generic guidelines a greater understanding of pharmacokinetics can be acquired, empowering the researcher to more critically assess *in vitro* outcomes for potential *in vivo* reproducibility. Thus, the current review highlights the most common problems with the presentation of *in vitro* outcomes and provides insight into how data could be interpreted to provide more relevant conclusions on therapeutic potential.

THE 'DARK AGE' OF ANTIBIOTICS

The 'dark age' of antibiotics is a time of resistance development against the antibiotics discovered in the 'golden era' (Lyddiard et al., 2016). Ironically, even before the 'Waksman platform,' which led to the discovery of most of the antibiotics in use today, we were warned that this time would come. On receipt of his 1945 Nobel prize for the discovery of penicillin, Alexander Fleming made the prescient observation that the '*thoughtless person playing with penicillin treatment is morally responsible for the death of the man who succumbs to infection with the penicillin-resistant organism*' (Cheesman et al., 2017).

It could be argued that the modern techniques of molecular docking and rational drug design have demonstrated little success by comparison with the much less sophisticated screening methods employed during the 'golden era' of antibiotic discovery and this gives impetus to calls for a new iteration of natural product screening in the search for new efficacious drugs and novel drug scaffolds (Lyddiard et al., 2016). Yet another lesson we could learn from the 'dark age,' and Fleming's grim yet accurate prediction, is to direct research efforts toward development of combination therapy drugs, by contrast with the monotherapy drug approach that ushered in the resistance paradigm (Cock, 2018).

Most of the antimicrobial compounds identified as secondary metabolites from natural products have a low degree of specificity in their mechanisms of action (MOA) and yet the most successful antibiotics have a high degree of specificity. This prompts the question of whether there is a correlation between degree of specificity and potency of drugs that are safe in human use. If this is indeed true, then the trade-off may be that with higher specificity and potency comes greater probability of resistance development. Adjuvants can, in some cases, disrupt resistance mechanisms (Cock, 2018), but combination therapies that target two or more sites provide arguably the best strategy for preventing further resistance development. Thus, this new paradigm of dual-therapy drugs opens a potential niche for the common non-specific antimicrobials found in natural product research that could be used to complement the conventional antibiotics that are losing potency in the unrelenting march of microbial resistance.

PHARMACODYNAMICS OF DRUGS

Mechanism of Action (MOA) and Structure-Activity Relationships (SAR)

Van Vuuren and Holl (2017) suggested that the criteria for describing the levels of antimicrobial activity in natural products be specific for types of extract, using the terms 'moderate,' 'strong,' 'very strong,' and 'noteworthy'. In the case of crude extracts from medicinal plants, noteworthy activity is ascribed for activity ≤ 160 $\mu\text{g/ml}$, for essential oils it is ≤ 1000 $\mu\text{g/ml}$ and for pure compounds it is ≤ 16 $\mu\text{g/ml}$.

In antimicrobial research a pronounced distinction can be made between susceptibility of Gram-negative and Gram-positive bacteria, where Gram-negative organisms tend to be

less susceptible on average. This is due to the presence of an outer membrane and hydrophilic periplasmic space in Gram-negative bacteria, which influences penetration and the fate of antibiotics. Thus, there are many antibiotics that have specificity for the Gram-positive organisms. For example, vancomycin is too large to cross the outer cell membrane of Gram-negative bacteria and thus has little to no activity against them. Furthermore, in the context of penicillins, Gram-negative bacteria have a privileged site for the accumulation of β -lactamases, with increased expression in the presence of β -lactam antibiotics (Zeng and Lin, 2013); a resistance mechanism that substantially reduces penicillin efficacy. However, antibiotics with broad spectrum activity have activity across both Gram-types. All such antibiotics have α -hydrophilic groups which aid passage across the lipophobic periplasmic space of Gram-negative bacteria (Patrick, 2013).

For the most successful antibiotics currently in use, five main categories of mode of action are known, which are: (1) Inhibition of enzyme activity (antimetabolites), (2) Disruption of cell wall synthesis, (3) Plasma membrane interference, (4) Prevention of protein synthesis at ribosomes, and (5) Inhibition of DNA transcription and replication. The main types of drugs used in the pharmaceutical industry and their mechanisms are listed in Tables 1, 2.

In most antimicrobial research protocols, such conventional antibiotics are included in assays as a positive control, not merely to convey a contrast of efficacy to the study but also as an internal validation of correct execution of the protocol. More importantly, since research on alternatives now embraces the possibility of adjuvancy to counteract resistance mechanisms against these frontline antibiotics, it is important to have a clear understanding of their mechanisms to guide selection of antibiotics for synergism-antagonism testing.

An appreciation of structure-activity relationships draws attention to the prevalence of amine functional groups and amine-alkaloids (Figure 1) that emerged from the ‘golden era’ as antibiotics with a high degree of specificity. This is not a coincidence. Not only do amine groups enhance solubility whilst retaining lipophilic character (by easy equilibration of ionized and non-ionized forms) but they are often involved in the drug’s binding interactions with its target through specific hydrogen bonding and/or formation of salt bridges.

The high degree of specificity of penicillin comes from its ability to mimic the dimer of D-alanine (D-Ala-D-Ala), a dipeptide amine used in bacterial cell wall synthesis (Figure 1). Other classes of antibiotics include compounds that can disrupt protein synthesis by binding to the 30S or 50S ribosomal subunit, preventing either the reading of mRNA, or translocation or binding of aminoacyl-tRNA (streptomycin, tetracycline, macrolides). At pH 7.4 (homeostatic pH), the cationic amine groups of many classes of antibiotic give them binding affinity to negatively charged pockets in RNA, rRNA or auto catalytic ribozymes (Jia et al., 2013). Antimetabolite drugs such as the sulfonamides, which mimic *p*-aminobenzoic acid, bind irreversibly to dihydropteroate synthetase and prevent biosynthesis of tetrahydrofolate. Ionic interactions of amine groups with various negatively charged pockets in the bacterial

TABLE 1 | The penicillins; their chemical groups and subtle differences in modes of action (MOA) against bacterial cell wall biosynthesis (Patrick, 2013).

Sub-group	Benzyl/penicillin	Aminopenicillins	Carboxypenicillins	Ureidopenicillins	Acid-resistant	Penicillinase-resistant	Penicillin prodrug
Sub-structure	6-benzyl substituted	6-amino substituted	α -carboxy substituted	α -urea substituted	6-electron withdrawal substituted	6-steric shield substituted	Ampicillin esters of carboxyl moiety
MOA	Cell wall, inhibition of transpeptidase enzyme						
Sub-MOA	Lipophilic, but unstable in stomach acid	Broad spectrum, higher hydrophilicity, crosses Gram-negative cell wall			Stable in stomach acid	Blocks β -lactamase	Ampicillin has poor absorption, esters aid absorption and are hydrolyzed in phase-1 metabolism
Inhibition	Bactericidal						
Examples	Penicillin G	Ampicillin, Amoxicillin, Penicillin N, Penicillin T	Carbenicillin, carfecillin (prodrug), ticarcillin	Azlocillin, mezlocillin, piperacillin	Penicillin V, ampicillin, amoxicillin	Methicillin, nafcillin, temocillin, oxacillin, cloxacillin, flucloxacillin, dicloxacillin	Pivampicillin, talampicillin, bacampicillin

TABLE 2 | Other frontline antibiotics (Patrick, 2013).

Group	Glycopeptides	Aminoglycosides	Tetracyclines	Macrolides	Chloramphenicol	Lincosamides	Streptogramins
Sub-structure	Polyphenolic glycopeptides	Carbohydrate, basic amine groups	Tetracyclic, two enols, one amide	O-glycosylated lactone rings	Dichloroacetamide, nitrophenyl	Thiosugar amine	Lactone macrocycles
MOA	Bind to cell wall building blocks			Inhibit protein synthesis by binding to ribosomes			
Inhibition	Bactericidal	Bactericidal	Bacteriostatic	Bacteriostatic	Bacteriostatic	Bacteriostatic	Bacteriostatic
Examples	Vancomycin, teicoplanin, eremomycin	Streptomycin, gentamicin C1a	Chlortetracycline, tetracycline, doxycycline, demeclocycline	Erythromycin, clarithromycin, azithromycin, telithromycin	Chloramphenicol	Lincomycin, clindamycin	Pritinamycin, quinupristin, dalbapristin
Group	Oxazolidinones	Quinolones	Fluoroquinolones	Aminoacridines	Rifamycins	Nitroimidazoles	Cephalosporins
Sub-structure	N-heterocycle, lactone, fluoride	N-heterocyclic quinone	Piperazine fluoride quinone		Naphthalenic lactone in macrocycle	Pentene, N-heterocycles	β -lactam with adjoining thiohexacycline
MOA	Bind to 50S subunit	Inhibit topoisomerase enzymes		Intercalate with DNA, toxic to humans	Inhibit RNA polymerase	Inhibit protozoa and anaerobes	Cell wall, transpeptidase inhibition Bactericidal
Inhibition	Bacteriostatic	Bactericidal	Bactericidal	Bactericidal	Bacteriostatic	Bactericidal	
Examples	Linezolid	Nalidixic acid	Ciprofloxacin, enoxacin, ofloxacin, levofloxacin, moxifloxacin	Proflavine	Rifamycin B, rifampicin	Metronidazole, nitrofurantoin	Cephalothin, cefalexin, cefazolin, cefoxitin, cefuroxime, cefotaxime, ceftazidime, ceftriaxone, cefpirome
Group	Ionophores	Cyclic lipopeptides	Sulfonamide	Sulfones			
Sub-structure	Macrocycle with hydrophobic semi-circle		SO ₂ NH ₁	SO ₂			
MOA	Act on plasma membrane, disrupt ion channels		Inhibition of dihydropteroate synthetase				
Inhibition	Bactericidal	Bactericidal	Bacteriostatic	Bacteriostatic			
Examples	Valinomycin, gramicidin, polymyxin B	Valinomycin, daptomycin	Sulfamethoxazole	-			

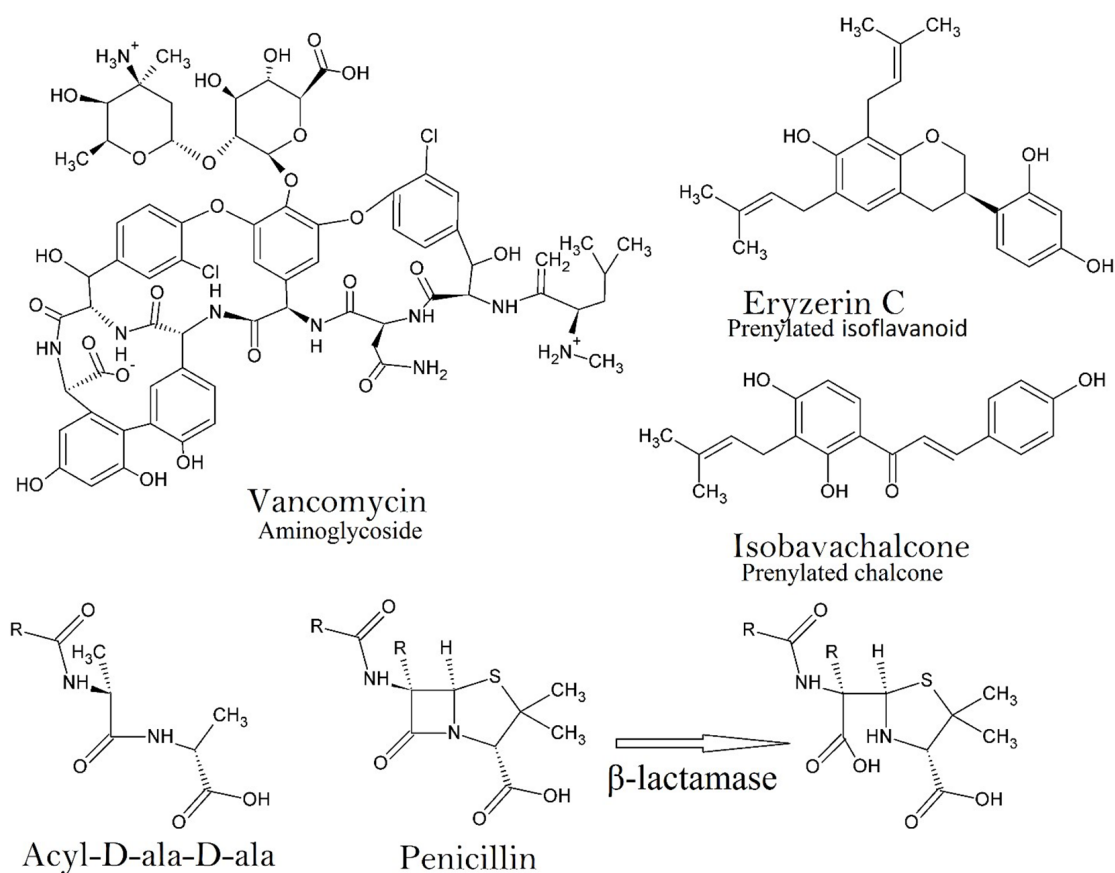


FIGURE 1 | An example of the chemical structure of an aminoglycoside (Vancomycin) showing the complexity of just one of some of the frontline antibiotics. Two structures are depicted that are representative of category 1 antimicrobials (Eryzerin C – prenylated flavonoid; Isobavachalcone – prenylated chalcone), which are among the most potent plant derived nitrogen deficient antimicrobial compounds in nature. The prenyl group enhances lipophilicity and bacterial membrane penetration, the adjacent phenolic OH group (on the same ring as the prenyl group) is essential for efficacy. The structural similarity of acyl-D-ala-D-ala to penicillin is important for the specificity of penicillin since human proteins have no D-amino acids. The activity of β -lactamase against penicillin is on the β -lactam moiety, which hydrolyzes the amide bond (Patrick, 2013).

membrane also occur, creating pores that enable hydrophilic aminoglycosides to enter the bacterial cytoplasm. Thus, the importance of the amine groups in specificity is evident.

Natural product screening for antimicrobial compounds may conveniently be broken into two major categories; (1) Nitrogen-deficient compounds constructed of C, H, and O atoms (oxygenated hydrocarbons) or C and H only (hydrocarbons), where generalized activity is expected. Specific modes of action are less common but have been reported for aromatics, such as chalcones or flavonoids (**Figure 1**); and (2) Nitrogenous compounds constructed of C, H and N (and O) atoms (alkaloids, amines, amides, anilines and imines) or C, H, S, O and N atoms (sulfonamides), where the possibility for absolute specificity exists. It is common for compounds in the second category to be synthesized from natural product scaffolds in the first category.

Nitrogen Deficient Compounds

In this first category, constituting the predominant class of compounds isolated from plant species, in most (but not all) cases generalized activity against bacterial cell walls or

membranes is the expected outcome. It is obvious that simple terpenes or phenylpropanoids, such as those in essential oils, typically demonstrate only low to modest antimicrobial activity attributable to perturbations of the lipid fraction of the cell membrane, enhancing permeability and spilling cellular contents or enabling entry into the cytoplasm (Trombetta et al., 2005). While such activity is, at first blush, unimpressive, such therapies are finding place as topical adjuvants or alternatives to antibiotics. As alternatives, they may mitigate the selective pressure on antibiotics and buy time before resistance development. As adjuvants, sometimes additive or synergistic effects occur, but also on occasion these small lipophilic compounds may antagonize resistance mechanisms and therefore restore efficacy of antibiotics. This is certainly the case with essential oils and volatiles that inhibit efflux pumps, a mechanism that bacteria have evolved to remove antibiotics from bacterial cytoplasm (Aelenei et al., 2016).

Perhaps the two best performing nitrogen deficient classes of antimicrobial compound with ‘noteworthy’ activity are flavonoids and chalcones (**Figure 1**). The most

potent activity in the literature gives values ranging from 0.06 to 2.4 $\mu\text{g/ml}$ against Gram-positive organisms for prenylated flavonoids and chalcones such as panduratin A and isobavachalcone respectively (Cushnie and Lamb, 2011). In terms of structure activity relationships, prenylated isoflavones and chalcones with aromatic hydroxyl groups adjacent to the prenyl moiety give the most pronounced activity (Cushnie and Lamb, 2011; Mukne et al., 2011). The prenyl group is important since it acts as a lipophilic arm and enhances penetration into the phospholipid membrane while the hydroxyl group accommodates the process by interaction with the polar head group of these lipids (He et al., 2014).

Flavonoids and chalcones are special in that multiple modes of antimicrobial specificity have been claimed, mainly against topoisomerases such as DNA gyrase (topo-II) in *Escherichia coli* (Wu et al., 2013) and topo-IV (Mukne et al., 2011). This activity is similar to the mechanism of action of the quinolones and fluoroquinolones of conventional antimicrobial therapy (Patrick, 2013).

The literature dealing with MOA of flavonoids and chalcones is ambiguous but an examination of structural differences, such as glycosylated and aglycone forms, indicates that a single general MOA is unlikely, due to variations in ability to cross cell membrane interfaces. However, the multitude of proposed mechanisms reported in the literature may be an exaggeration, where factors such as 'cause and effect' and issues of aggregation of purified enzymes *in vitro* may complicate the interpretation of data (Cushnie and Lamb, 2011). Whilst the possibility of multiple MOAs across flavonoids or chalcones in general is realistic, more comprehensive testing is necessary to confirm this. This should include screening a group of flavonoids or chalcones across a diverse range of MOA assays.

In this context it should be noted that evolutionary pressures would likely select for biosynthesis of secondary metabolites that confer antimicrobial activity via mechanisms unfavorable to resistance development. Drugs with multiple MOAs yield a similar outcome to combination therapies, in that single mutations in microbes are unlikely to create comprehensive resistance mechanisms against multiple targets.

Many follow-up studies have confirmed some of the MOAs reported for flavonoids and chalcones, such as topoisomerase inhibition (Cushnie and Lamb, 2011). Given the previous discussion on the importance of amine functional groups, it follows that the activity of flavonoids might be enhanced by production of amine derivatives. The validity of this approach was demonstrated in the synthesis of a tricyclic sulfur-amino flavonoid, which demonstrated most impressive inhibition of the Gram-positive species *Staphylococcus aureus* down to concentrations of 0.24 $\mu\text{g/ml}$ (Babii et al., 2016), with the mechanism related to the impairment of cell membrane integrity and cell agglutination.

Nitrogenous Compounds

As previously stated, compounds from the second category, containing nitrogen and/or sulfur atoms, have hitherto demonstrated the most pronounced antimicrobial activity,

with absolute specificity. These have almost exclusively been isolated from bacteria and fungi, but some studies have reported the isolation of such compounds from plants. Natural quinolone alkaloids were isolated from the fruit of a species in *Rutaceae* and screened for antimicrobial activity and in some cases demonstrated noteworthy activity against Gram-positive species. The structures differed by a homologous series of alkyl side-chain moieties, which significantly impacted on MIC values, with chains within the range of 9–13 carbons as yielding the most pronounced activity, as low as 4 $\mu\text{g/ml}$ (Wang et al., 2013). Such a structure-activity profile suggests that cell membrane penetration is enhanced by the alkyl sidechain.

On Why Some Antimicrobial Agents Fail Supply Challenges

Most antibiotics in common clinical use are of bacterial or fungal origin. This may give the impression of the intrinsic inferiority of plant-extracted compounds. However, this pattern of prioritization of bacterial and fungal metabolites is more related to logistics than efficacy *per se*. Microorganisms can be cultured and are characterized by rapid growth, which makes the supply aspect of a commercial product non-limiting. By contrast, plant derived metabolites require long waiting periods for maturation of plantations, followed by a complex extraction protocol and generally low yield. This makes supply a limiting factor. Sometimes a valuable alternative to the cultivation of plants is realized, but only if it can be demonstrated that microbial endophytes are responsible for the *de novo* biosynthesis of the relevant plant metabolite. In this case, the endophyte can be isolated and cultured as in classical antibiotic production. Alternatively, genetically modified yeasts may also be used to produce specialized metabolites provided the yeasts themselves are not susceptible to the product or its intermediates.

Although the supply of natural antibiotics is a major logistical concern, *de novo* and semi-synthetic approaches can also be employed to make them commercially viable should the need arise. More fundamental challenges to the efficacy of noteworthy antimicrobial drugs are related to the pharmacotherapeutic obstacles encountered *in vivo*. Thus, pharmacotherapeutic challenges could be related to negative side effects, such as toxicity, or failure to translate *in vitro* activity into useful therapeutic activity because of poor absorption, bacterial resistance or biotransformation in the gut or liver.

Pharmacodynamic Challenges

Strictly in the context of pharmacodynamics, resistance mechanisms and toxicity are the biggest problems. While many researchers are now seeking to identify compounds effective against resistant strains, far fewer studies employ synergism-antagonism assays, which may lead to the discovery of antimicrobial compounds that work in combinations. The best example of the success of this approach comes from the synergistic effects of clavulanic acid, a weak antibiotic that is related to penicillin by the presence of a β -lactam ring. Since resistance mechanisms in bacteria now include

the induction of the enzyme β -lactamase, which cleaves the β -lactam ring (**Figure 1**) and inactivates penicillin derived antibiotics, inhibiting this enzyme restores the activity of β -lactam antibiotics. Clavulanic acid is classified as a 'suicide substrate' in that the β -lactam site is cleaved by β -lactamase in the usual way, but the presence of an enol ether over the fused heterocyclic ring (O in the place of S) causes the drug to bind to the enzyme irreversibly. Thus, combinations of clavulanic acid and β -lactam antibiotics restores the potency of these drugs. This is currently in clinical practice with a product called Augmentin®, which combines amoxycillin and clavulanic acid (Cock, 2018).

Another resistance mechanism is the aminoglycoside riboswitch (Jia et al., 2013), which regulates expression of the anti-aminoglycoside enzymes, aminoglycoside acetyl transferase and glycoside adenyl transferase, in response to binding to the aminoglycosides. The expressed enzymes modify the structures of aminoglycosides and inactivate them (Aghdam et al., 2014). Methods to counteract this resistance mechanism are still under development, but some headway has been made with the realization of unique binding activity of paromomycin, which makes a transient hydrogen bond at 6'-OH with A17, diminishing interactions with more important coding regions of the riboswitch, leading to deactivation (Kulik et al., 2018). Researchers are now looking at paromomycin derivatives as new aminoglycoside drugs (Zárate et al., 2018).

No research has yet been published demonstrating combinations that attenuate the riboswitch resistance mechanism. Research has focused more on efflux inhibition, anti-quorum sensing, anti-virulence and anti-infective mechanisms at sub-MIC concentrations that attenuate both pathogenicity and resistance (Cushnie and Lamb, 2011).

Pharmacokinetic Challenges

It is apparent that even the lowest MIC values achieved by natural products is still many folds higher than the possible systemic concentrations achieved *in vivo* for oral therapies (not topical). This implies that the antimicrobial outcomes, no matter how impressive, will not be actualized *in vivo* unless other factors are taken into consideration. One neglected area of research is to examine compound accumulation in specific tissues. Another area of research is to redirect efforts toward immunomodulation either in the context of stimulation or conversely, anti-inflammatory (suppression). This aspect is further explored in the section titled 'routine absorption and immunomodulatory assays.'

'Potentiators' to Counteract Resistance

Researchers will refer to drugs that antagonize resistance mechanisms as the 'potentiator' (Cock, 2018). Thus, compounds that have poor antimicrobial activity may nevertheless affect the virulence or pathogenicity of microorganisms. For example, antimicrobial assays assess activity against bacteria in planktonic growth (as colonies) rather than as biofilms, which are formed because of quorum sensing activities. Since the biofilm itself, and surface adhesion, confers resistance to the immune response and slows antibiotic activity, antagonism of quorum sensing

can reduce virulence. Flavonoids, and polyphenols such as catechins, have demonstrated anti-quorum sensing activities. Furthermore, other virulence and pathogenicity factors are antagonized by many polyphenols and flavonoids, such as sortase inhibition (another enzyme implicated in biofilm formation), urease inhibition (for *Helicobacter* to survive stomach acid), listeriolysin inhibition (for surviving phagosomes and entering the cytosol of host cells) or neutralization of bacterial toxins (reducing pathogenicity) (Cushnie and Lamb, 2011).

Drugs that block efflux pumps are potentiators of antibiotics. The intracellular efflux pumps in bacteria have become increasingly capable of excreting a wide array of antibiotics, with the tetracyclines receiving the most attention. Many examples of efflux inhibitors have been discovered, which often include flavonoids and polyphenols at sub-MIC values (Cheesman et al., 2017).

Compounds that antagonize bacterial resistance, virulence and pathogenicity are evidently good potentiators of both the immune system and antibiotics. Thus, they should be seriously considered as adjuvants to conventional therapies (Cock, 2018). However, compounds that are antagonistic of bacterial resistance development *per se* have received the least attention in antimicrobial research. For example, drugs with multiple modes of action, or combination therapies, antagonize resistance development by maintaining efficacy against mutant strains that develop single resistance mechanisms.

Combination therapies can also combine bactericidal drugs with bacteriostatic drugs to counteract resistance development. Such combinations are also beneficial because immunocompromised patients are fully dependent upon the drug and it is difficult to maintain optimal plasma concentrations of bacteriostatic drugs over the course of the infection. Antimetabolite drugs, such as the sulfonamides, are bacteriostatic (Patrick, 2013), but many flavonoids and chalcones have demonstrated bactericidal activities (Cushnie and Lamb, 2011), so this combination may achieve positive outcomes.

Sometimes combinations achieve synergistically enhanced antimicrobial activity, which means that the MIC value is enhanced by more than the sum of the two activities of each drug combined (greater than the sum of its parts). Alternatively, sometimes there are interactions that antagonize activity. Researchers generally test for these effects in a synergism-antagonism assay (Van Vuuren and Viljoen, 2011). The methodology involves testing the combinations at different ratios across different dilutions to produce a 'fractional inhibitory concentration index' (Σ FIC). It is obvious that synergistically enhanced activity in combinations is beneficial, but less obvious that it has the potential for providing a wider gap between MIC values and median lethal dose (LD50), if relevant.

Toxicity

Several methods for measuring LD50 and LC50 values are in practice for describing a compound's toxicity. Brine shrimp lethality is for some researchers a first step, giving broad implications for human contact (Sarah et al., 2017) but greater specificity is acquired using mammalian cell lines (Ekwall et al., 1990). It is important that drugs with potent antimicrobial

activity have much higher toxicity concentrations as compared to MIC values, since concentrations required to kill bacteria should not be damaging to the host. However, when interpreting toxicity studies, one must be aware of research that specifically tests for toxicity against cancer cell lines without appropriate comparison to non-cancerous cells. Obviously, high toxicity to cancer cells but low toxicity to healthy mammalian cells is a positive outcome in this context.

Unfortunately, without knowledge of, or access to, the biotransformed conjugate of the drug as it would appear in the host after metabolism, it is difficult to comment specifically on the toxicity of a drug, if it is an ingested therapy. In antimicrobial outcomes, some of the activity is maintained in the pre-conjugated form, and sometimes as well after conjugation, but toxicity after conjugation is difficult to control for. The fates of xenobiotics after absorption and transformation provide the most common challenges for understanding the pharmacotherapeutics of the drug and this is the jurisdiction of pharmacokinetics.

THE CORE OF PHARMACOKINETICS: LIPOPHILICITY, HYDROPHOBICITY AND 'BIOAVAILABILITY'

It is no surprise that the vast majority of prospective drug candidates are poorly soluble in aqueous solvents. One pharmaceutical company estimates that 30% of drug candidates have aqueous solubility at $<5 \mu\text{g/ml}$ (Lipinski, 2001). While lipophilicity of a drug is an important factor influencing absorption and distribution into the lipid membranes characterizing many human tissues, at least some aqueous solubility is necessary to enable distribution in and from the human GIT. This issue is illustrated in the intestinal permeability prediction assays, such as the caco-2 cell culture, but this problem is replicated in the human gastrointestinal tract.

While exceptions can be made for compounds of low aqueous solubility that are liquids at body temperature, such as with essential oils, [indeed, melting point was considered a contributor in earlier transdermal models (Magnusson et al., 2004)], solid insoluble compounds are not generally bioavailable. While aqueous solubility and lipophilicity are generally treated as opposites, they are not exactly inversely proportional, especially in fluorinated molecules. There are many examples of compounds that are amphiphilic (high solubility in both), such as saponins, but the lipophilic moiety itself is considered important in bringing about bioavailability.

Drugs that are small and strongly lipophilic are often regarded as having good bioavailability. In contrast, high molecular mass drugs only have good bioavailability if they convey fewer rotatable bonds and an optimal balance of lipophilic and hydrophilic moieties, where lipophilic moieties enable passive *trans*-membrane or *trans*-dermal diffusion and polar groups enact biological interactions. In addition, polar groups enhance aqueous solubility and prevent flocculation in the gastrointestinal tract, which aids absorption.

Despite their considerably higher lipophilicity, their typically small molecular size means that essential oils have good

bioavailability, but their high lipophilicity means that they may also cross the blood-brain barrier. This outcome could be favorable if essential oils confer immunomodulatory effects, particularly where anti-inflammatory activities are potentially useful. However, one of the most controversial side-effects of some lipophilic drugs is psychoactivity. Almost all psychoactive drugs have high lipophilicity, some of which occur in essential oils, such as elemicin, a psychoactive phenylpropanoid that also confers anti-inflammatory effects (Sa et al., 2014). Pre-conjugated forms (pre-metabolized forms) of essential oils also rapidly dissolve in the fat tissues, giving a shorter half-life in the first instance and creating a reserve or 'storage' of potentially bioactive compounds in the second instance.

Ingestion of aromatic foods over time will lead to an accumulation of essential oils in adipose tissue. For example, grazing on the aromatic fodder plant *Penzia incana* leads to an accumulation of *Artemisia*-type terpenes in the fat tissue of South Africa's 'Karoo Lamb', which confers a distinctive flavor to the meat when roasted (Hulley et al., 2018) and prolongs the immunomodulatory effects of components such as linalyl acetate (Sa et al., 2013). Another example involves the bioaccumulation of cannabinoids in fat tissues of cannabis smokers. Lipolysis induced by exercise or starvation can provide the user with a recycled 'high' (Gunasekaran et al., 2009), a side-effect that occurs together with a range of immunomodulatory effects mediated by agonism of cannabinoid receptors (type 2) (Olah et al., 2017). Strains used for medicinal cannabis have higher yields of cannabidiol and less tetrahydrocannabinol (Rom and Persidsky, 2013) to achieve more positive and less psychoactive effects. Due to their high lipophilicity the cannabinoids have very long half-lives, conferring immunomodulatory effects for sustained periods after smoking.

Thus, the activity of anti-infective drugs with good tissue or fat solubility may be prolonged as they are slowly released back into the host's circulation from such tissues (Patrick, 2013). The drug is usually released from fat stores at a lower concentration as compared to the active systemic concentration, but repeated drug administration enhances this effect. For example, the anesthetic thiopental is highly lipophilic, so its peak concentration is rapidly decreased due to redistribution to more slowly perfused fatty tissues, at which time it is slowly released from fat storage at subanaesthetic concentrations. However, after repeated doses the fat sink is fuller, and thiopental is then released at an active concentration, which keeps the patient anesthetized. This also occurs with drugs that accumulate within cells, such as the anti-malarial drug chloroquine, which accumulates in white blood and liver cells, reaching concentrations thousands of times higher than in plasma.

As drugs become slightly more hydrophilic their aqueous solubility increases and accumulation in adipose and other body tissues becomes less relevant, but as aqueous solubility continues further issues of absorption become prominent. It is therefore important to be able to judge *a priori* the approximate solubility character of a molecule from the number of polar moieties, before it becomes clear if it has potential as a drug candidate. Other important factors include numbers of rotatable bonds and hydrogen donors/acceptors (closely

related to polar surface area). Some rudimentary guidelines will now be given.

INDICATIONS THAT A DRUG HAS 'GOOD BIOAVAILABILITY'

The classical approach used to judge the bioavailability of a drug was 'the rule of 5', which is a set of 4 guidelines that prescribe numerical parameters as a factor of 5. Hence, 1) molecular weight needs to be <500 Da, 2) there must be less than 5 hydrogen bond donor groups, 3) and no more than 10 hydrogen bond acceptor groups, 4) and a calculated log *P* value of less than + 5 (drug hydrophobicity measurement) (Patrick, 2013).

Today it is clear that a substantial number of bioavailable drugs break this rule of 5; drugs commonly referred to as 'in the space beyond the rule of 5' (bRo5 space) (Doak et al., 2014). New parameters for prediction of oral bioavailability now acknowledge that molecular size is insignificant, provided that the polar surface area is $\leq 140 \text{ \AA}^2$ and that the number of rotatable bonds is fewer than 10 (Veber et al., 2002). Percutaneous penetration is a different matter, where molecular size continues to be regarded as significant, but macromolecules that are rapidly absorbed have also been identified (Pino et al., 2012). Thus, there are ample examples where molecules that are easily absorbed break the modern rules.

Unlike polar surface area, the number of rotatable bonds leading to molecular flexibility, is a parameter that is not so intuitive. However, since molecular flexibility tends to become a limiting factor in larger molecules ($\geq 500 \text{ Da}$), a first assessment for smaller molecules should only be for a compound's polarity, which is easily judged by the number of polar groups and how polar they are.

It is relatively easy to get an approximate estimate of the hydrophobicity of a molecule according to the number of amides, amines, alcohols (hydroxyl), aldehydes, ketones, ethers and acid (ester) groups attached. The order of polarity goes amide > acid > phenol > alcohol > ketone > aldehyde > amine > ester > ether > hydrocarbon (alkane) (**Figure 2**). For example, sugar groups (glycosides) are pharmacokinetically negative. Generally, when small molecules ($\leq 400 \text{ Da}$) have six or more hydroxyl groups the bioavailability is substantially low. However, monoglycosides (one sugar) are more easily orally absorbed than diglycosides (two sugars), which are better than triglycosides (three sugars) and so on.

By contrast, amines generally have a weaker dipole moment (lower polarity) as compared to hydroxyl groups and have higher bioavailability. They are cationic at pH 7.4 and can interact with the anionic components of the stratum corneum or intestinal epithelium, enabling passage of anionic drugs (Pandey et al., 2014). Surprisingly, small molecules with carboxylic acids and amides are also bioavailable. Accordingly, amino acids are used as penetration enhancers (Sarpotdar et al., 1988), and this effect may be enhanced by esterification of the carboxylic acid moiety (Hrabálek et al., 1994).

As the numbers of polar groups increase relative to the alkane bonds the bioavailability decreases (**Figure 3**), decreasing further

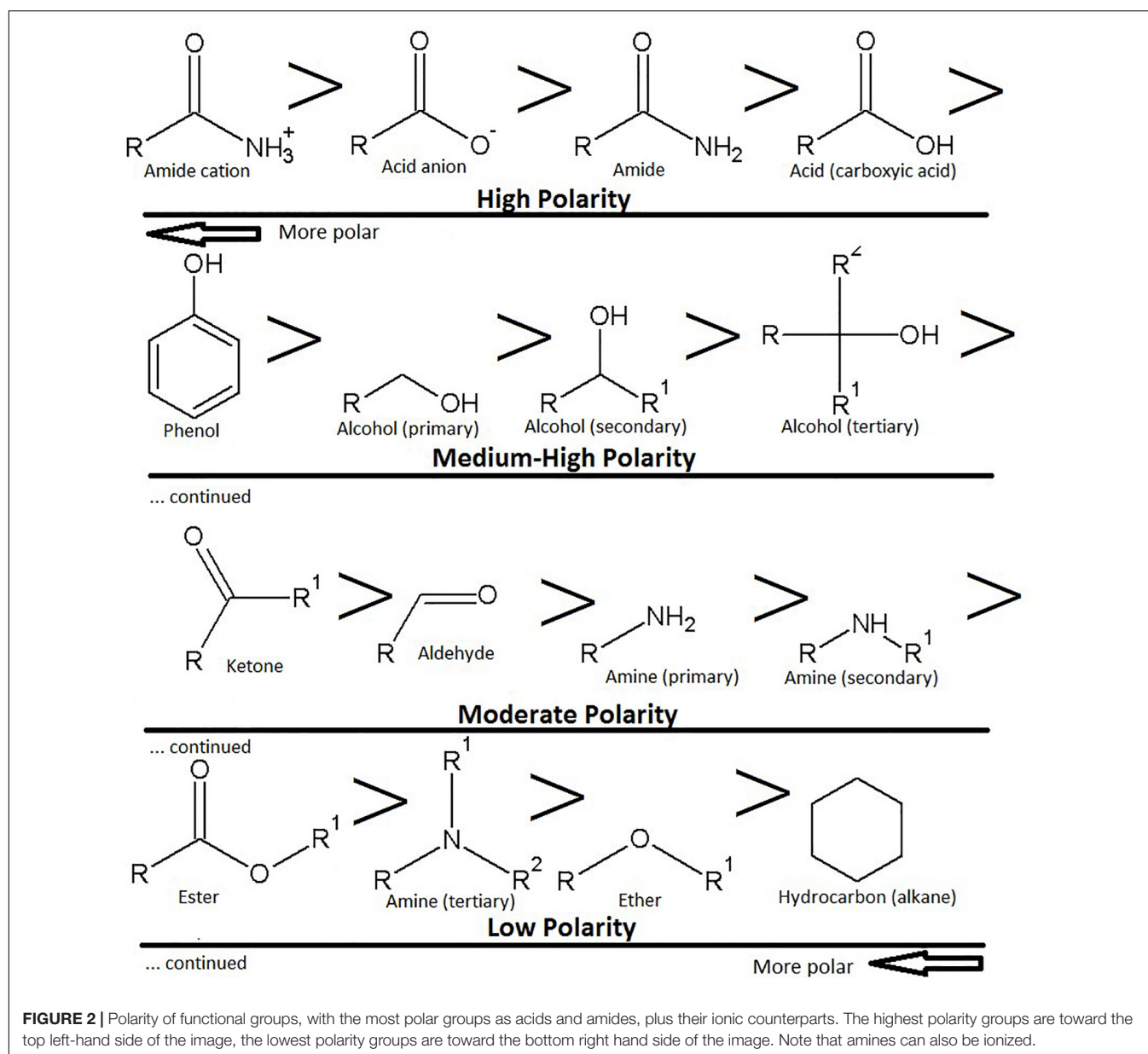
as the number of rotatable groups increases. The segmentation of molecules into hydrophilic and hydrophobic moieties can enhance penetration across skin, but an even distribution of polar groups on a molecule has the opposite effect. It is not clear if this is the case for intestinal absorption but it is clear that a sugar such as glucose illustrates this implicitly. In sugars there is a 1:1 ratio of carbon to oxygen atoms with each carbon adjacent to an oxygen, five of which are hydroxyl groups. To counteract poor bioavailability, sugars are actively transported in the human digestive tract and are not absorbed across the stratum corneum.

When sugar groups are sterically oriented around a lipophilic triterpene core, this attenuates the interaction of the molecule with the lipid fraction of the epidermis and antagonizes bioavailability. Tannins and saponins are model examples of this effect (Seo et al., 2002; Seeram et al., 2004). Indeed, these two classes of secondary metabolites arguably demonstrate the lowest oral bioavailability in the natural product world and following ingestion are mostly absorbed as much smaller deglycosylated species. Whilst some saponins are absorbed orally it is generally at a very slow rate and rather than crossing into the cell through its plasma membrane, which is comprised by hydrophobic phospholipids, they are either actively transported or enter portal circulation passively by paracellular transport across the tight junction, passing through pores between epithelial cells.

MORE ON BIOAVAILABILITY ESTIMATION

While it is convenient to glance at a molecular structure and make tentative predictions about its bioavailability, more comprehensive predictions can be made by following some clear guidelines. As previously mentioned, the number of rotatable bonds (≤ 10) and polar surface area ($\leq 140 \text{ \AA}^2$) gives the best prediction for oral bioavailability (Veber et al., 2002) and rotatable bonds and molecular weight ($\leq 500 \text{ Da}$) for transdermal or percutaneous ability (skin penetration) (Grice et al., 2010). Although there is much overlap between oral bioavailability and percutaneous penetration, the influence of polar surface area is apparently less significant in the latter. Other differences occur due to active transport mechanisms, which are dependent upon the site of absorption (intestinal space or topical). In the case of compounds that completely break the rules, such as the macromolecules named avicins (Pino et al., 2012), pronounced differences between oral and transdermal bioavailability are likely (see next section).

Nevertheless, it is good to be able to accurately predict polar surface area and the number of rotatable bonds. Polar surface area represents the sum of all polar surface areas, including the electronegative atoms nitrogen and oxygen, and their attached hydrogen atoms. These estimations replace the previous convention of the octanol/water partition coefficient (log *P*). Generally, calculation of polar surface area can take 10 or more minutes per molecule, using specialized software that generates 3D structures *in silico*. Since polar surface area estimations require some time and organization, a cruder strategy which involves counting hydrogen donor and acceptor groups



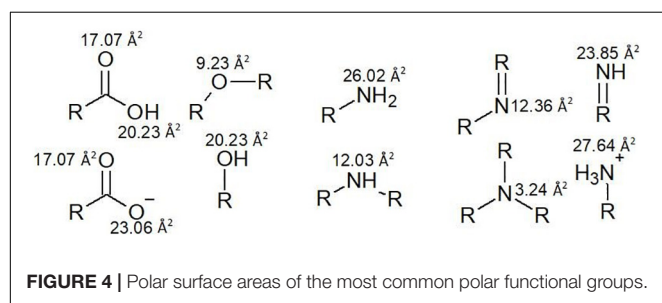
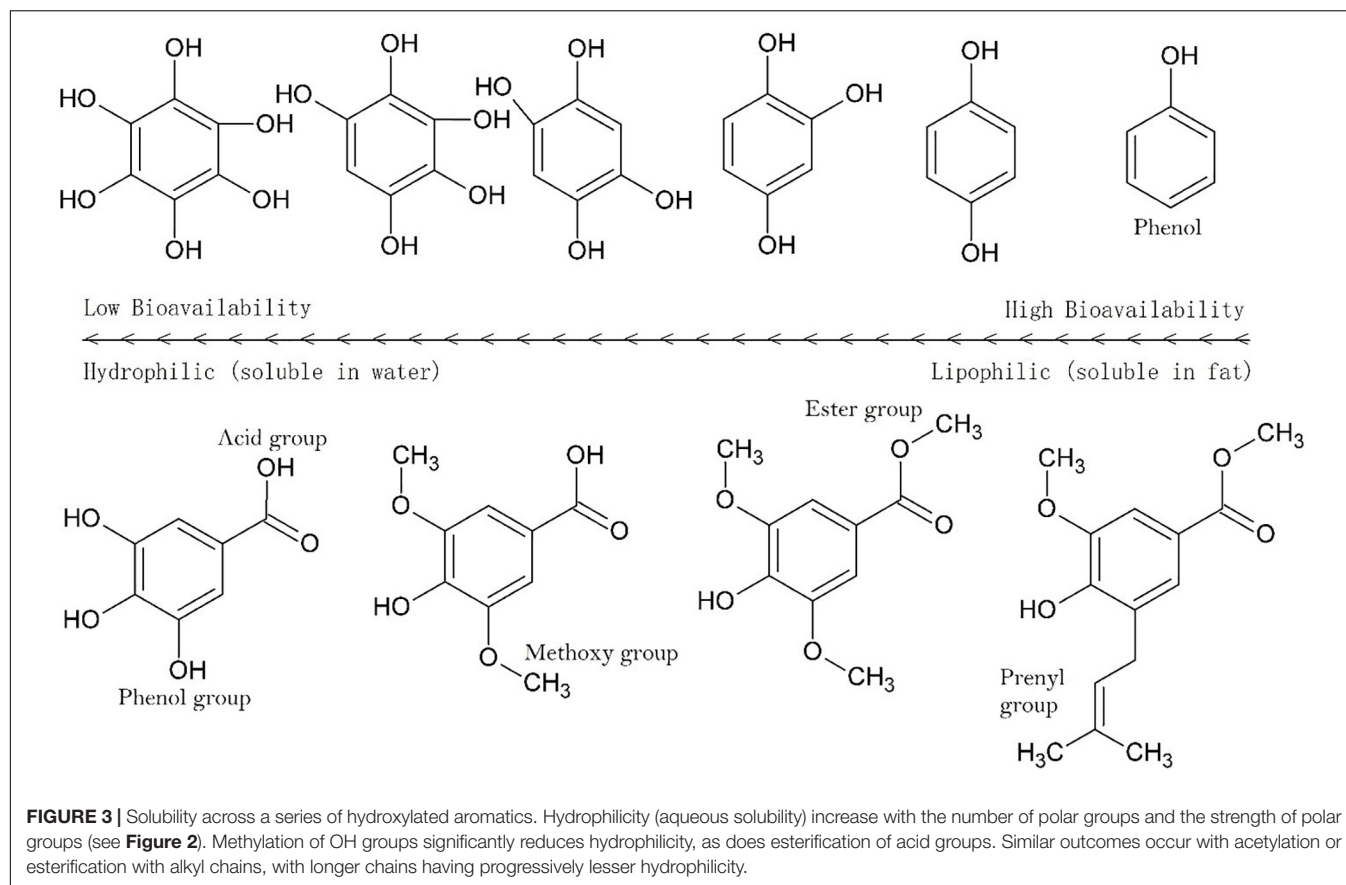
(≤ 12) is used to create *a priori* estimates (Veber et al., 2002). However, use of polar surface area is more accurate, so a faster and more approachable method for this calculation has been proposed by Ertl et al. (2000), which involves assigning standard surface areas to polar groups and summing the values. Some examples from a list of 43 by Ertl et al. (2000) are illustrated in Figure 4 and some examples of the calculation are given in Figure 5.

For the calculation of rotatable bonds Veber et al. (2002) was a little vague on exclusion criteria, stating only that they are 'defined as any single bond, not in a ring, bound to a non-terminal heavy (i.e., non-hydrogen) atom. Excluded from the count are amide C-N bonds because of their high rotational energy barrier'. Other types of bonds also have a high rotational energy barrier, which means that most chemists also exclude thioamides, sulfonamide bonds,

the C-O in ester bonds and single bonds between aromatic groups with three or more ortho substituents. These are illustrated in Figure 6.

THE PHARMACOKINETIC JOURNEY: FROM PETRI DISH TO THE SITE OF INFECTION

Generally, the pharmacokinetic journey follows the drug up to the site of infection, but then beyond, to the point of elimination. The entire fate of a drug is therefore framed by the acronym ADME, which is an abbreviation of absorption, distribution, metabolism and elimination, as previously mentioned.



The most prominent pharmacokinetic obstacles faced by drugs include transdermal penetration (topical therapies), acid pH of the stomach, digestive enzymes in the human GIT or of bacterial origin, intestinal absorption (oral therapies), first pass metabolism, absorption into the various tissues and organs of the body and blood brain barrier penetration (if relevant).

Thus, oral bioavailability is reflective of the amount of drug in the system after deductions are made for all of these factors, which includes the fraction escaping gut-wall and hepatic elimination (El-Kattan and Varma, 2012). Giving all of these factors some consideration, the school of bioavailability ranks transdermal or gut-wall penetration as the leading obstacle controlling the success of drugs proven *in vitro*, which alone controls the necessary route of administration. Administration routes can be broadly divided into enteral (sublingual, oral,

rectal) and parenteral (topical, inhaled, injection). These will now be elaborated upon.

Parenteral: Topical Therapies

By comparison with ingestive therapies, the efficacy of topically applied remedies for local afflictions is more often reflective of observed *in vitro* outcomes, since compounds are not digested, nor are they subjected to the first pass effect in liver metabolism. Thus, dermal penetration is the only outstanding pharmacokinetic parameter in play, becoming less of an obstacle in damaged or infected tissues.

The pharmacokinetics of topically applied therapeutics is also less complex as compared to ingested drugs. While topical routes are often utilized for administration of systemic drugs expected to act non-locally (e.g., nicotine patch), the following discussion is directed at therapies that target local afflictions, such as pathogenic microbes, infections or inflammation.

Most pathogenic organisms are superficial and easily reached by inhibitory molecules. For example, fungal infections, such as *Trichophyton rubrum*, *T. mentagrophytes* or *T. interdigitalis* (Tinea pathologies), are superficial, since they are external to the dermal layers and can therefore be inhibited *in vivo* as efficiently as observed *in vitro* outcomes. By contrast, the penetration of compounds into an abscess is difficult, even with compounds having high bioavailability. The degree of penetration is influenced by duration of infection and stage of encapsulation

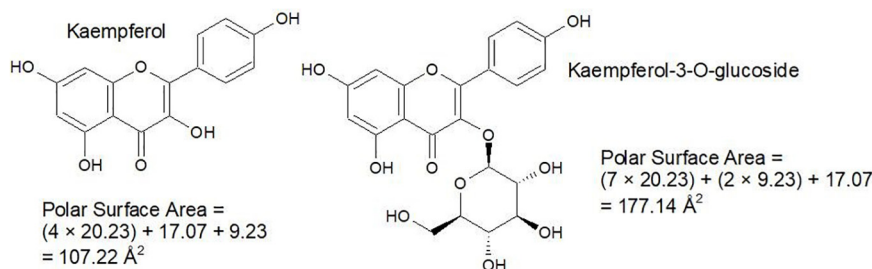
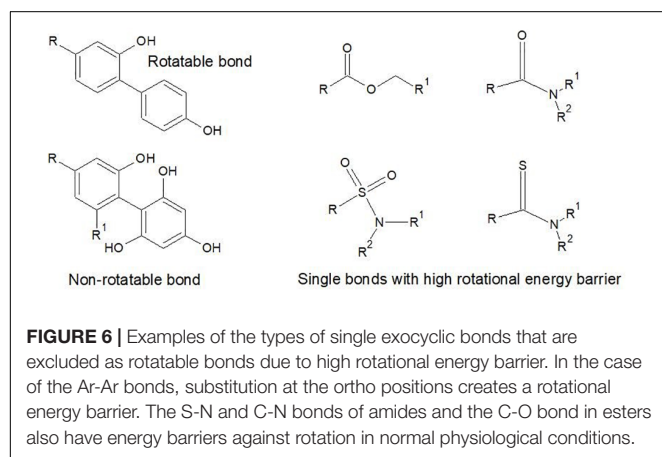


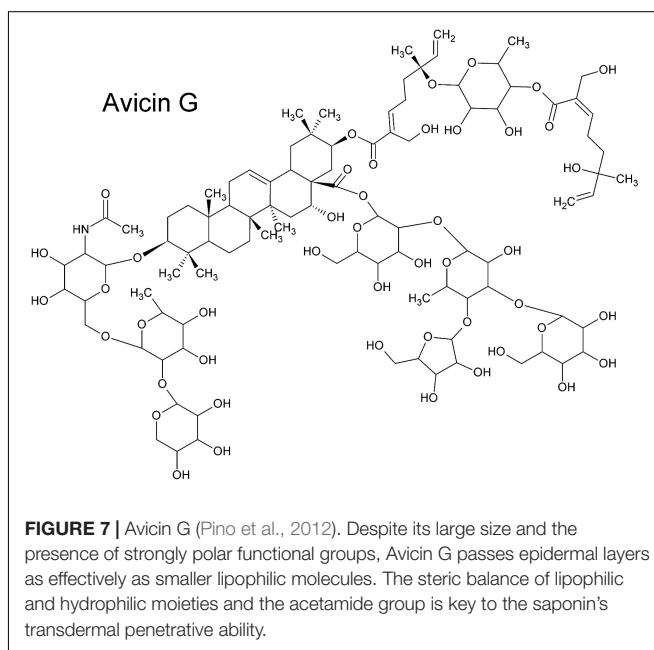
FIGURE 5 | Simple examples for the calculation of polar surface area.



(Wagner et al., 2006). Inflammation has also been implicated in changes of drug transport efficiency, with penetration being antagonized in many instances (Schmith and Foss, 2008).

Nevertheless, a general rule is that small molecules (≤ 500 Da) that are lipophilic can passively cross dermal layers. As compounds increase in polarity and size the skin permeability substantially reduces. Some larger hydrophilic compounds can also passively cross dermal layers, provided that a low number of rotatable bonds are present. In some cases, polar and apolar moieties are sterically optimized for penetration, but this is not often reported. For example, Pino et al. (2012) discovered that avicins, glycosylated triterpenes (acetamide saponins) with a molecular mass > 2000 Da, pass the dermal layers as rapidly as smaller lipophilic molecules. The key to the structure's success in this regard is the combination of a geranyl ester moiety (monoterpene), an acetamide group and a tetrasaccharide (**Figure 7**), conferring both hydrophilic and hydrophobic properties in an optimal spatial (steric) arrangement (Pino et al., 2012).

Poorly bioavailable compounds, such as saponins, may still find a place in topical therapies. Ruptured skin tissue, occurring in conditions such as eczema, provides a privileged passage to important sites. Another privileged passage follows hair follicles, to the dermal papilla, a site of increased permeability with high capillary networking and density of immune cells (Herman and Herman, 2016). Sebum secretions line the inside of the



follicle infundibulum, which may be considered a hydrophobic barrier that can be easily breached by lipophilic or amphiphilic compounds, such as saponins. The infundibulum may therefore be a site for the penetration of higher molecular mass compounds with strong detergent-like character.

The fates of compounds in topical therapies as components of complex mixtures applied as extracts are not entirely limited by their individual bioavailability. Other compounds, such as the sterically balanced avicins (Pino et al., 2014) or small lipophilic molecules, can temporarily modify the stratum corneum and allow passive transport of molecules with intrinsically poor bioavailability. Thus, in commenting on the pharmacokinetics of topically applied therapies one must take note of the presence of potential penetration enhancers in extracts. These include high quantities of volatile terpenes (Paduch et al., 2007), phenylpropanoids or others as described by Karande et al. (2005).

Parenteral: Injection

Due to poor oral bioavailability, or challenges related to modifications by gut microbes, many antibiotics are injected

rather than ingested. In the 1950's it became common knowledge that some antibiotics could be absorbed in the alimentary canal, and some required intramuscular or intravenous injection (Finland, 1958). Those that could be absorbed orally were penicillin, erythromycin, tetracyclines, chloramphenicol and novobiocin. Those that had poor absorption and required injection were streptomycin, neomycin, viomycin, nystatin, vancomycin, ristocetin and various polypeptide antibiotics.

Antibiotics that are absorbed in the intestines can also be given by injection but common practice is to convert to sodium or potassium salts to enhance aqueous solubility. By contrast, those with high aqueous solubility can be injected without conversion. Thus, except for ionized penicillin, the degree of absorption is reflective of aqueous solubility. High aqueous solubility then influences the drug's ability to reach the target site within the body. This is generally not a problem in antimicrobial research, since most infections are extracellular.

Enteral: Oral, Stomach Acid as the First Obstacle

At the mastication stage there is the possibility of absorption of lipophilic compounds through the area around and under the tongue, which is known as the sublingual route. In this case absorbed drugs are not subjected to liver metabolism or acid hydrolysis in the stomach. However, the sublingual route is limited, and most patients prefer not to taste their medicines.

Orally administered drugs or therapies generally survive mastication, but it is common practice to preserve drug contents for release further along in the alimentary canal, by encapsulation into a soluble capsule or fashioning into a pill with or without a sugar coating. In most cases pills or capsules release contents into the stomach. Sometimes stomach acids can break down or transform drugs, particularly if electron dense hydrogen acceptors are on the molecule. For example, the first penicillin used clinically was unstable in stomach acid and had to be administered intravenously. Ampicillin is an example of a penicillin derivative that is modified to give resistance to acid hydrolysis in the stomach, by placement of an electron-withdrawing substituent on the α -carbon of the side chain to draw electrons away from the carbonyl group.

Thus, depending upon acid stability, drug capsules can be fashioned for solubility either in the stomach or upon entry into the small intestine. Less commonly employed today, a previously widely used enterosoluble coating came from a gum called 'sandarac,' which could be made from the Australian Black Cypress tree (*Callitris endlicheri*) (Sadgrove and Jones, 2014b, 2015), or the actual sandarac tree (*Tetraclinis articulata*).

Enteral: Oral, GIT Metabolism as the Second Obstacle

In the intestines microbial transformations can also be a significant challenge (the domain of pharmacomicrobiomics). For example, although warfarin survived stomach acid, mixed therapeutic results observed in patients were hypothesized to be related to individual differences in the gut microbiome (Das et al., 2016). Digoxin is another drug that is susceptible to the

microbiota, but unlike warfarin, it is consistently transformed into a less active form (Jourova et al., 2016). To curb such effects drugs can be administered together with a general antibiotic to kill off the microbiome and prevent transformations. This is the procedure for the anti-inflammatory drug sulfasalazine (Jourova et al., 2016). Obviously, this latter procedure is undesirable.

By contrast, microbial transformations of non-active 'prodrugs' can in some cases create potent antimicrobial drugs. In 1935 it was discovered that the red dye called prontosil had antimicrobial activity *in vivo*, but this was not evident *in vitro*. It was discovered that prontosil was metabolized by bacteria in the small intestine into sulphanilamide by reductive removal of the benzamine moiety. Today, many such prodrugs are known. The most important derivatives come from ampicillin. Lipophilic prodrugs are made by esterification with substitution groups, such as acyloxymethyl or pthalide, to remove the potential ionization of the carboxylate and aid absorption. The ester is subsequently hydrolyzed in phase-1 metabolism to produce active ampicillin.

Nearly all biotransformation reactions occur on the more electronegative atoms, such as oxygen and nitrogen, or with atoms that have non-bonding electron pairs, such as the former two atoms and sulfur, or atoms conjugated to oxygen, such as alpha-beta unsaturated ketones. Thus, in addition to alkenes and α -alkene carbons where hydroxylation commonly occurs, these three heteroatoms are where most of the transformations take place (Patrick, 2013).

Intestinal passage usually reduces the size of compounds via reductive and/or hydrolytic processes. Whilst reduction tends to increase polarity, the overall outcome may generate higher lipophilicity, such as by dehydroxylation or removal of a sugar moiety (Figure 8; Jourova et al., 2016). For example, in many instances the reductive process of hydrolysis creates aglycone moieties of glycosides (Day et al., 2000), which sees a substantial increase in lipophilic character of the aglycone moiety, making systemic absorption passive (Németh et al., 2003). This process has a most significant potential impact in research on natural products because it is obvious yet neglected. Other significant transformations include hydrolysis of esters and amides, particularly peptides (Patrick, 2013).

Generally, by the time glycosides enter systemic circulation they are present as aglycones or mono-glycosylated glycosides (less commonly di-glycosides). Glycosides are mostly absorbed by active mechanisms in the small intestine (Németh et al., 2003) but larger molecules enter between cells through pores. Lipids are digested to release free fatty acids. Alkyl esters or alkyl amides are often cleaved but can also be absorbed intact, with combinations of both appearing in blood plasma, such as those homologous alkylamides from *Echinacea* (Matthias et al., 2007), which are modulators of the immune system (Raduner et al., 2006).

Enteral: Absorption as the Third Obstacle

As previously mentioned, polar surface area and the number of rotatable bonds will influence the absorption rate or efficiency of a drug. While most absorption occurs passively, on occasion, metabolites enter circulation via active mechanisms. The major implication is that even strongly polar groups can be

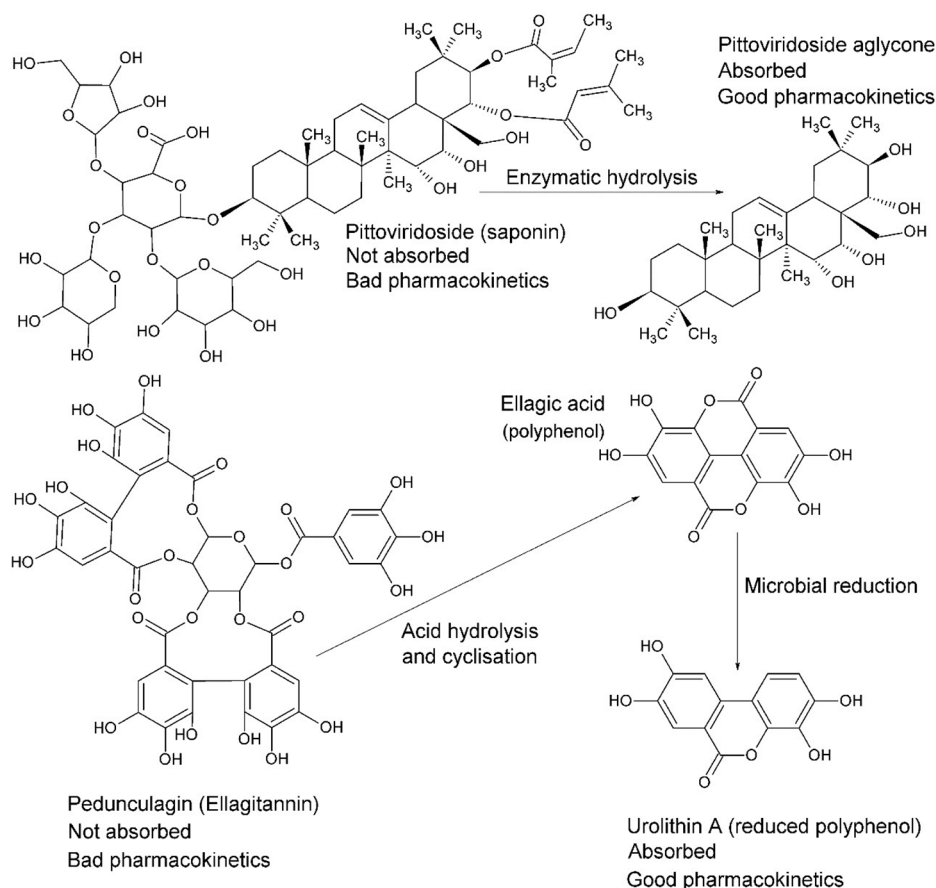


FIGURE 8 | The fate of complex glycosides in human digestion involves cleavage of sugar moieties, either by β -glucosidases of the small intestine (or bacteria) in the case of saponins, such as pittoviridoside (Seo et al., 2002), or by acid hydrolysis in the stomach, such as pedunculagin (Seeram et al., 2004). Ellagic acid is metabolized into urolithin A by gut bacteria before absorption; however, both are systemic. The pentacyclic triterpene of pittoviridoside is absorbed after hydrolysis of the sugar and butenoic ester moieties.

absorbed, provided that there is compatibility with one of the transport routes.

Surprisingly, even a small hydrophilic molecule, such as the simple sugar glucose, requires active transport for absorption. It was once thought to be passively absorbed but it has long since been demonstrated that the Na^+ /glucose cotransporter is responsible for absorption in the small intestine (Chen et al., 2016). This has implications for mechanisms of absorption of glycosides in general. Although they are predominantly absorbed passively after deglycosylation (**Figure 8**), they can be actively transported as monoglycosides on the hexose transport pathway by interaction with the sugar moiety (Gee et al., 2000). Nevertheless, the fate of glycosides that enter the portal circulation is deglycosylation by liver metabolism, but xenobiotics that make the first pass in metabolism may enact biological interactions before phase-1 transformation in the second pass.

A pharmacokinetic study of flavonoid or chalcone aglycones and saponins in rats gives insight into the differences of absorption from the GIT between these two types of compound. Relatively apolar compounds, with fewer hydrogen donor and

acceptor groups, reach peak plasma concentration in 5–30 min (Ying-Yuan et al., 2019). A similar outcome was observed with monoglycosides. But the diglycosides demonstrated completely different kinetics, with peak concentrations being seen after 8 h on average. The ginsenosides specifically had long half-lives (12–25 h) but other diglycosides were more similar to the less polar compounds (2–11 h). This study shows that it is definitely possible for diglycosides to enter systemic circulation, albeit much slower by comparison with less polar compounds.

Following absorption, post-metabolized drugs can be returned to the GIT where they are metabolized to their pre-conjugated or phase-1 metabolized state. For example, glucuronidated drugs enter the GIT for excretion but are cleaved by intestinal microbes that express β -glucuronidase enzymes and reabsorbed (Pellock and Redinbo, 2017).

Enteral: 'First Pass' Metabolism

The discipline of pharmacokinetics encourages us to consider the potential biological effects of more polar conjugated drug forms, or 'xenobiotics,' as they are metabolized during the body's elimination response by phase-1 and phase-2 enzymes, such as

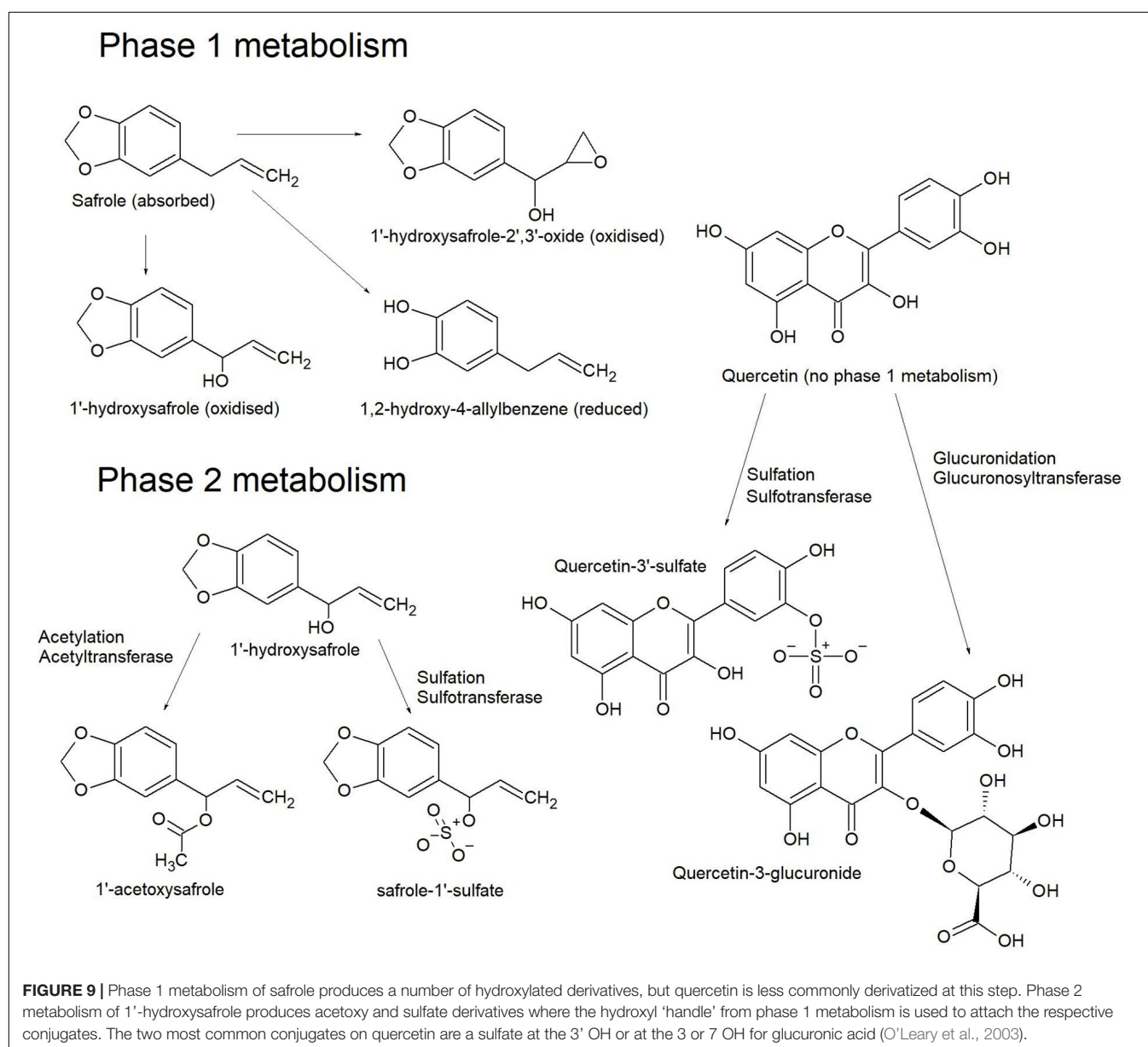
cytochrome P450 isozymes (phase-1) and/or transferase enzymes (phase-2) such as glucuronosyltransferase. This complex series of enzymatic transformations occurring mainly in the liver may, depending on the chemistry of the original compounds, either enhance or attenuate activity and/or toxicity.

Antimicrobial compounds that are absorbed (now called xenobiotics) and become 'first pass' have the capacity to enact biological effects provided they are distributed to the site of infection. In some cases, however, a significant amount of drug will be metabolized before becoming systemic. Phase-1 reactions may continue the reductive and hydrolytic process started in digestion, particularly on actively absorbed glycosides that were absorbed from the intestine before microbial modifications. Thus, much like the microbial processes, nitro, azo and carbonyl groups are the most common sites for reduction, and amides,

esters and glycosides are the sites for hydrolysis (Patrick, 2013). The predominant group of enzymes responsible for these phase-1 reactions are the cytochrome P450 isozymes.

In the liver, phase-1 reductions are less common than oxidative processes. Oxidations typically occur on N-methyl and aromatic groups, thiols, the terminal position of alkyl chains and sterically favorable positions on an alicyclic moiety. These reactions commonly put OH groups on carbon atoms (hydroxylation) (**Figure 9**) and aliphatic primary amines; oxygen anions on N-methyl groups or N-heteroaromatic rings; keto groups on thiols, with conversion of thiol amines to sulfonamides and so on. Such reactions are said to create a 'handle' for subsequent phase-2 oxidative processes (Patrick, 2013).

Phase-2 oxidative processes use the 'handle' created in phase-1 reactions (**Figure 9**) to attach a strongly polar group.



These are mostly conjugation reactions catalyzed by transferase enzymes, installing a polar group such as sulfate, O-glucuronide, C-glucuronide, glutathione and less commonly apolar groups, such as methyl groups or cholesterol. Conjugated xenobiotics are usually inactive but sometimes toxic compounds are created (Patrick, 2013).

By far the most common transferase reactions are glucuronidation and sulfation (**Figure 9**), particularly with aromatics such as flavonoids (O'Leary et al., 2003). In this reaction glucuronic acid is conjugated to phenols, alcohols, hydroxylamines, carboxylic acids, amides, amines and thiols. Sulfate conjugation also occurs on phenols, alcohols and amines. Furthermore, carboxylic acids (and cleaved esters) can be conjugated to cholesterol or amino acids. Glutathione conjugates form with the nucleophilic thiol group of the tripeptide moiety by reactions with electrophilic functional groups, such as epoxides, alkyl halides, sulfonamides, disulfides and radical species. Glutathione conjugates can also be transformed to mercapturic acids.

Some conjugation processes decrease the polarity of xenobiotics, such as methylation or cholesterol esterification. While methylation often happens in conjunction with glucuronidation (Williamson et al., 2005), it is also possible that some of the transformations are not specifically designed to remove metabolites. For example, at pH 7.4 some flavonoids are stabilized by glucuronidation, which then can be actively transported across cell interfaces by de-glucuronidation and re-glucuronidation at convenient locations. Less frequently, some conjugated xenobiotics such as flavonoids and chalcones (Williamson et al., 2005), maintain bioactivity consistent with pre-conjugated forms. For a drug to be approved for use in therapies it is a requirement that all the potential conjugated forms, including enantiomers, epimers and other isomers, be screened for biological activity, testing for efficacy or toxicity. However, all possible conjugates will be an overestimate. In due course the actual conjugate forms will be revealed by *in vivo* studies that screen blood plasma and urine for the xenobiotics on their exit from the host. Such studies are the only real way to know of the relevant conjugate forms for any particular drug.

Nutraceuticals, functional foods and complementary therapies (including Traditional Chinese Medicine, TCM) do not require this level of approval and *in vivo* studies can be conducted as a preliminary step to identify the conjugated forms, which can be synthesized or isolated in follow-up to screen for bioactivities and toxicity. In such pharmacokinetic studies the pre-conjugated form of the absorbed compound is detected, together with biotransformed derivatives representative of both phase-1 and phase-2 metabolism.

Circulation to the Site of Infection

Once a drug enters systemic circulation it will easily go into the fluid surrounding the various tissues, cells and organs, since extracellular space is relatively porous, allowing passage of most molecules that are smaller than proteins. In some cases, drugs bind to plasma proteins and are slow to leave the systemic circulation. In a similar way to the adipose 'sink,' protein bound drugs are slowly released as plasma concentrations reduce.

In general, a drug's lipophilicity influences its ability to penetrate a mammalian or bacterial cell wall. For example, streptomycin is evidently strongly polar, a consequence of the trisaccharide moiety. To overcome the issue of absorption, and deglycosylation in the intestines, streptomycin is therefore given by parenteral routes, but since its mode of action is against the bacterial ribosome, absorption across bacterial cell wall and membrane interfaces must occur. Indeed, this is the case, with a cationic charge in alkaline environments the aminoglycoside interacts with the outer membrane of Gram-negative bacteria and displaces magnesium and calcium ions, disrupting ionic bridges and creating pores through which the drug enters the cytoplasm.

LESSONS FOR ETHNOPHARMACOLOGY

The presumed route of therapeutic application influences how closely the outcomes of *in vitro* anti-infective studies will be reflected *in vivo*. For example, inhaled therapies for bronchial afflictions are expected to closely reflect *in vitro* outcomes, provided only the volatiles are screened, including hydrodistilled essential oils and/or other volatiles with moderate aqueous solubility that dissolve into the hydrosol. In the case of 'smoked' therapies a wider selection of volatiles than those present in essential oils or hydrosols are expected to be relevant. For example, often diterpenes, amines, pyranocoumarins, cannabinoids or drimane sesquiterpenes (Khumalo et al., 2018) are present in acrid steamy smoke. These larger compounds are not present in essential oils because they require higher temperatures than those employed in hydrodistillation to become volatile (Sadgrove et al., 2016). Furthermore, heat derived artifacts that dramatically increase the antimicrobial activity, such as genifuranal (Sadgrove et al., 2014a), are a rare occurrence, but if observed should nevertheless be included in antimicrobial assays.

In ethnopharmacology there is a pronounced difference between topical and ingestive therapies, particularly in the context of anti-infectives. Since it is so common for antimicrobial therapies to demonstrate *in vitro* activity that is only moderate, it is only practical to interpret contact inhibition in the context of topical applications. Where ingestive therapies are being studied, a failure to identify highly potent antimicrobial active compounds encourages us to examine immunomodulatory activities in interpreting their presumed therapeutic value.

However, ingestive therapies are inherently more complex to interpret. Often the fate of natural products is to be judged as toxic, due to inhibition of cytochrome P450 isozymes. Unfortunately many natural products, nutraceuticals and herbs are considered as either toxic or as having the potential for negative interaction with pharmaceuticals (Sasaki et al., 2017). Nevertheless, these studies often neglect the poor absorption of 'toxic' components and fail to screen metabolized forms. Alternatively, natural therapies that contain compounds that confer cytochrome P450 inhibition may also be considered as adjuvants in the context of enhancement of drug half-life. Such adjuvancy is seen to be important in the administration of antiretroviral therapies (Dresser et al., 2000). Thus, such

interactions must be considered more broadly both for their potential adverse and/or beneficial effects.

Routine Antimicrobial Assays

Two methods are commonly employed to generate *in vitro* antimicrobial outcomes, the first being the disc (or disk) diffusion assay and the second more precise method, the two-fold serial broth dilution assay, which generates a minimum inhibitory concentration (MIC) value in a 96-well microtiter plate.

The classical 'disk diffusion' is a well-established method for screening of antibacterial activity, using an absorbent paper disk that is loaded with an extract or purified compound and placed on the surface of a petri dish containing a medium (usually agar based) inoculated with a test organism. After incubation for 24–48 h, the diameter of the clearing zone around the disk reflects the inhibitory power of the sample. The simple disk diffusion protocol is no longer regarded as the preferred method but continues to be used today as a pre-screening tool to aid prioritizing samples for the more conventional method of testing.

Thus, today the standard *in vitro* method for measuring antimicrobial activity is the two-fold serial broth dilution, minimum inhibitory concentration (MIC) assay (Eloff, 1998; Andrews, 2000) that is now controlled by the Clinical Laboratory and Standards Institute (CLSI, 2017). While this approach measures bacterial inhibition of an extract or compound, the protocol can be made more comprehensive by determining bactericidal concentration (MBC) in subsequent steps. MBC receives the least attention in antimicrobial research, since most antimicrobial natural products are bactericidal, due to generalized MOA. It is less common to find drugs that are bacteriostatic only (like tetracycline), thus, MIC and MBC concentrations are usually within proximal range.

The MIC assay is a serial dilution method, where the concentration of pure compound or complex mixture screened against microbes is successively half the previous concentration. For example, starting at 32 µg/ml, tetracycline dilutions will be 32, 16, 8, 4, 2, 1, 0.5, 0.25 µg/ml et cetera. Problematically, it is common for reviewers to demand standard deviations. The data is ordinal not continuous and so standard error or deviation is not meaningful, but it is acceptable to represent the data as an average of individual assays. Furthermore, MIC values represent an upper maximum, with the actual value in between the MIC value and the next dilution.

Since data is reported as µg/ml, the MIC value is not representative of the actual efficiency of the compound, as it would be if represented as molarity or molecules per CFU. For example, since bacterial cell density is diluted to approximately 5×10^5 CFU/ml, a compound with MIC value of 1 µg/ml and mass of 444.5 g/mol inhibits with 2.7×10^9 molecules per CFU, but for a compound with double the mass, with the same MIC value, it is 1.4×10^9 molecules per CFU, apparently showing double the efficiency.

It is a common fallacy that the inclusion of frontline antibiotics as a positive control is to show the efficacy of a drug in the context of the expected outcomes from the pharmaceutical industry, with positive control and treatment drug as competitors for the lowest MIC value. Whilst such a comparison is important, expected

MIC values from leading antibiotics are widely known (Andrews, 2000). The inclusion of a positive control is more about validation of the experimental protocol as executed by the researcher by comparing results against expected outcomes. This is to provide a higher level of standardization and quality control to create more realistic and confident comparisons between research outcomes from different laboratory environments. Whilst low MIC values are of value, it is more important to consider the toxicity of a new drug, its pharmacokinetics and the logistics of administration. This is because the true efficacy of an antimicrobial therapy lies in the quantities that can be safely administered to achieve optimal MIC plasma concentration and its ability to be circulated to the site of infection. If it is a safe and cost-effective drug, that is easily absorbed, such as a flavonoid, then it is theoretically better than a drug with an exponentially lower MIC value that has a narrower toxicity threshold.

For example, purely in the ethnopharmacological context, it is a common mistake to judge only the activity of the molecule *in vitro* and not consider its relative abundance in the extract or raw plant material. However, from a traditional practitioner's perspective, high concentration of a compound with medium activity is better than very low concentration of a compound with noteworthy activity. An example that illustrates this concerns the volatiles from *Eremophila longifolia* (Sadgrove et al., 2011), a species that is comprised of many individual chemotypes. Some chemotypes have extremely high yields of essential oils (isomenthone and menthone) that have only low antimicrobial activity, but other chemotypes have low yields of essential oils (containing borneol and α -terpineol) that have more moderate activity. Topical use of either chemotype will likely produce a similar antimicrobial outcome. Systemic circulation is not important in this context since the extracts are applied directly to the site of infection and transdermal penetration is all that is required. In ethnopharmacological studies, provided that active antimicrobial ingredients (or active combinations) are extracted by the traditional method at a higher concentration than the value given by MIC, then bacterial or fungal inhibition is possible.

However, where systemic concentrations are relevant, such as where oral therapies are used, it is often the case that *in vitro* values are not possible, yet anecdotal accounts continue to argue in favor of the efficacy of the botanical therapy. In such cases, it is conceivable that other mechanisms can explain infectious control. In this regard, there has not yet been enough interest invested in immunomodulatory compounds.

Routine Absorption and Immunomodulatory Assays

A vast number of assays are used to create *in vitro* estimates of bioavailability and immunomodulation, but researchers often use animal skins (pig or rat) for transdermal measurements and human epithelial colorectal adenocarcinoma cells (Caco-2) or jejunum *ex vivo* for intestinal absorptivity measurements (Angelis and Turco, 2011).

Outcomes from animal skin models are reported as either maximum flux (J_{\max} in mol/cm² per hour) or a permeability coefficient (K_p in cm.s⁻¹). The permeability coefficient merely

gives rate but of more importance is the maximum flux (J_{\max}) because it denotes the quantity of drug absorbed (Grice et al., 2010). The maximum absorbable dose (MAD) for Caco-2 and jejunum permeability is also given as a J_{\max} value.

Challenges to absorptivity occur in cases of poor aqueous solubility, which can pose a significant problem to the intravenous and ingestive approach to drug delivery; but this does not negate the possibility of transdermal absorption, since solubilizing agents and penetration enhancers can be used in topical applications. Many transdermal penetration enhancers are known and include a long list of essential oil ingredients (Aqil et al., 2007; Chen et al., 2015), triterpene glycosides (saponins) (Shastri et al., 2008), other surfactants (Pandey et al., 2014), amino acids (Sarpotdar et al., 1988) and esters of omega amino acids (Hrabálek et al., 1994), just to name a few.

As previously mentioned, inflammation can antagonize bioavailability of topical antimicrobial drugs, with the encapsulated boil (abscess) being the clearest example. Thus, anti-inflammatory activities not only favor symptomatic relief but expedite the activity of anti-infective drugs by enhancing tissue penetration.

Animal (*in vivo*) and *in vitro* methods are commonly used to predict anti-inflammatory activity, either by direct observation of inflammation or measurement of inflammatory markers, regulatory proteins or pro-inflammatory cytokines. This follows the deduction that inflammation can be prevented either by inhibition of regulatory proteins or binding to pro-inflammatory cytokines.

The most common inflammatory pathways considered *in vitro* include mitogen activated protein kinase (MAPK) and nuclear factor kappa B inhibitor alpha (IkB- α), which are activated when phosphorylated (Harbeoui et al., 2019), leading to release of MAPKs or nuclear factor kappa B (NF- κ B) respectively, signaling expression of pro-inflammatory cytokines such as tumor necrosis factor- α (TNF- α) and interleukins (IL- β , IL-6). Another inflammatory pathway is controlled by cyclooxygenase (COX) isoenzymes, which mediate expression of the lipid-based prostaglandins, such as prostaglandin E₂ (PGE₂) (Ricciotti and FitzGerald, 2011; Nile and Park, 2013). This latter pathway is better known in the context of arthritic pain.

Markers of inflammation also include nitric oxide (NO), inducible isoform of nitric oxide synthase (iNOS), 15-lipoxygenase (15-LOX) and hypoxanthine oxidase or xanthine oxidase (HX/XO) (Nowakowska, 2007; Harbeoui et al., 2019; Lawal et al., 2019) leading to secretion of the superoxide anion in the latter. These are more often measured to predict the level of inflammation, rather than explain cause and effect.

The most common *in vitro* anti-inflammatory biomarkers reported in the literature describe downregulation of the proinflammatory cytokines (TNF- α , IL- β , IL-6), markers of inflammation (NO, iNOS, 15-LOX, HX, XO), hormones (PGE₂) or regulatory proteins (MAPKs, NF- κ B, COX-2).

A common *in vitro* method to make such prediction uses lipopolysaccharide (LPS) induced macrophages, such as the RAW 264.7 cell line (Harbeoui et al., 2019) and measuring attenuation of any of the above inflammatory markers. In the natural product world, studies often show that species

with proanthocyanidins (Lawal et al., 2019) and chalcones (Nowakowska, 2007) often demonstrate attenuation and may therefore have anti-inflammatory effects, provided that the chemical species are bioavailable in the first instance and in the second, demonstrate the same activity *in vivo*. Thus, it is important for researchers to not only be aware of *in vitro* outcomes from studies of poorly bioavailable compounds, but to take into consideration the possibility of multiple activities of the compound. For example, often phenols (flavonoids, chalcones) non-selectively bind to all or most free enzymes. Without selectivity (or absolute specificity) the perception of anti-inflammatory activity is unlikely to be vindicated *in vivo* because of problems of acute toxicity, which compromise potential therapeutic effects.

Even at the very low concentrations demonstrated *in vitro* for antimicrobial or anti-inflammatory therapies, it is often the case that the same concentrations are not reached *in vivo* when administered orally. In such cases presumed efficacy may possibly be explained by such phenomena as bioaccumulation and concentration in source tissue (lipophilic actively transported) or another mechanism altogether involving immunomodulation as previously mentioned.

One exciting area of research that has not yet received enough attention is cannabinoid receptor-2 agonism (CB₂) (Rom and Persidsky, 2013). While CB₁ is associated with the psychoactive effects of cannabis smoking, the CB₂ receptor mediates anti-inflammatory and immunomodulatory activity. However, activation of CB₂ is considered immunosuppressive rather than the converse (Olah et al., 2017). Almost counterintuitively, immune-stimulating compounds are generally proinflammatory (Kang and Min, 2012; Tsai et al., 2018) but can do so at substantially lower systemic concentrations than required for direct antimicrobial effects. Other neglected areas of research include insulin mediated T cell stimulation (Tsai et al., 2018) and toll-like receptor agonism (Chen and Yu, 2016). The latter, toll-like receptors, have 13 known types to date and are present on various immune cells as innate pathogen recognition defense mechanisms. Fortunately some information on toll-like receptor agonism by natural products can be garnished from the literature (Chen and Yu, 2016), but it is clear that a paradigm shift in the natural products world is called for, where natural products are screened for toll-like receptor agonists particularly type 4, in conjunction with the continuing effort to find antimicrobial candidates.

Ingestive Therapies

Some of the important pharmacokinetic factors introduced in this review that are most neglected in ethnopharmacological studies include the effects of biotransformation of ingested therapies, synergisms and antagonisms of mixtures and the possibility of chemical variability (chemotypes) of the botanical species studied.

The occurrence of chemotypes in medicinal species, if not recognized, can compromise the reproducibility of bioassays. Plants often demonstrate high degrees of intraspecific variability of secondary metabolites. For example, the Australian species *Eremophila longifolia*, highly regarded as an anti-infective

medicinal plant by indigenous populations, is known to have at least 10 different chemotypes (Sadgrove and Jones, 2014a). Furthermore, species may have taxonomic issues, with heterogeneous species aggregates complicating taxonomic determination, which will inevitably introduce chemical variability (Sadgrove et al., 2014b). Thus, the results of studies that screen crude extracts without further chemical characterization of the components can fail the test of reproducibility in subsequent research. Alternatively, if an active ingredient is identified the effects of chemovariability can be elucidated and issues with reproducibility can be explained.

Where chemical studies are undertaken, as previously mentioned researchers often measure antimicrobial activities against compounds that are evidently not absorbed or are entirely broken down in digestion. For example, many South African medicinal barks, or tubers, that are high in hydrolyzable and condensed tannins are used to target gastrointestinal pathologies (Van Wyk et al., 2009). Tannins are non-specific protein poisons and, at the concentrations extracted by these medicinal plants, will not only erase the gut microbiome but will also knock out an epidermal layer. However, only condensed tannins will get as far as the small intestine since hydrolyzable tannins are destroyed in the acid pH of the stomach and broken into their component phenolic acids and sugars (Figure 8). Condensed tannins and some phenolic acids are poorly absorbed but since the site of infection is in the gut, gastrointestinal pathologies are easily antagonized by these therapies.

In a similar way to tannins, ingestion of saponins above a certain threshold can also kill off the gut microbiome before passing out in the stool, mostly undigested. But ingestion to achieve saponin concentration below inhibitory concentration accommodates digestion into aglycones (Figure 8), which are absorbed more efficiently than the saponin itself. Thus, studies that elucidate biological roles for saponins must be considered in the context of topical versus internal application as well as dosage.

For example, dried and pulverized leaves of the Australian medicinal plant *Pittosporum angustifolium* are widely traded on the 'underground complementary therapies market' with claims of anticancer activity following ingestion (Sadgrove and Jones, 2014c) together with effective reversal of gastrointestinal pathologies. Inspired by such claims, studies examined cytotoxicity of the main saponins against cancer cells, demonstrating a positive outcome (Bäcker et al., 2014a,b). These saponins are very large, with four or more sugar units, meaning they are barely absorbed. It is likely that the O-linked sugars are hydrolyzed and only the aglycone is absorbed or its monosaccharide form. Thus, it makes more sense to screen the triterpene aglycone moieties for bioactivity, since triterpenes generally demonstrate positive outcomes across a range of pathologies (Yamai et al., 2009). However, at one stage herbalists were prescribing impractically high quantities, which would kill the microbiome, thereby preventing digestion of the saponins. Nevertheless, if they were targeting a gastrointestinal pathology it is useful in the short-term to ingest such high quantities. However, chronic consumption at such high concentrations may be contraindicated, since the microbiome has importance in digestion and indeed in modulating the immune response.

Anti-infective compounds that are not absorbed could be given via parenteral routes to target non-local infections. But high systemic concentrations of saponins is likely to be dangerous, due to the hemolytic (detergent-like) effects. Such hemolytic effects may explain the moderate antimicrobial activity of aqueous leaf extracts of *P. angustifolium* against Gram-positive organisms, which has little relevance for pathologies requiring absorption (Sadgrove and Jones, 2013). By contrast, the traditional use of *P. angustifolium* is most commonly topical, for amelioration of eczema where infective microorganisms could be a comorbidity (Sadgrove and Jones, 2013). Thus, *in vitro* bioassays of the saponins could be informative for topical applications, whereas extrapolation to use as an ingested therapy is problematic. It is therefore better to look at possible immunomodulatory effects occurring at lower concentrations, mediated either by the saponin itself or the aglycone moiety.

A pharmacokinetic study of ingestion of Chinese herbs demonstrated that the monoterpene and flavonoid glycosides were completely absent in the serum of human candidates and the respective free aglycones were only present in trace amounts, with dominant conjugated forms as sulfates and glucuronides (Figure 9; Lee Chao et al., 2006). It is common for some flavonoids to be absorbed as glucosides, the most prominent being quercetin-3-glucoside (Németh et al., 2003). The mechanism of absorption is active, via the glucose carrier SGLT-1 across the brush border membrane of the small intestine (Wolfram et al., 2002).

A similar study of the stevia glycosides demonstrated that only the aglycone diterpene 'steviol' was absorbed in both rats and humans and was dependent upon the cleavage process in digestion (Koyama et al., 2003), which was then metabolized to steviol glucuronide. The steviosides are evidently hydrolyzed by the gut microbiome, a process that requires β -glucosidase enzymes. Although the steviosides are more popularly known as natural alternatives to sugar for sweetening of beverages, these diterpene glycosides have been recognized as conferring anti-inflammatory and other immunomodulatory effects (Boonkaewwan and Burodom, 2013), wherein the activity of the metabolite steviol was more pronounced than the glycoside.

Most natural glycosides contain β -glycosidic linkages, which are easily cleaved by enzymes secreted by gastrointestinal bacteria. However, it is also common for the host plant to have β -glucosidase isozymes (Boonclarm et al., 2006). There is good evidence that moderate heating of a mixture of herbs within the range of 40–70°C can influence flavonoid β -glycosides and β -glucosidase, driving enzyme activity, which produces aglycones, but the enzyme denatures at higher temperatures (Zhang et al., 2014). In ethnopharmacological research, therefore, care must be taken to observe subtleties in methods of preparing traditional medicines that could produce similar effects.

Aside from the gut microbiome, the human small intestine is one of the most significant sites for the secretion of β -glucosidases, making it the most important site for the absorption of flavonoid aglycones (Németh et al., 2003). As previously stated, differences in bioactivity of compounds in their

glycosidic Vs aglycone forms challenges the reproducibility of antimicrobial or immunomodulatory outcomes.

The role for essential oils as anti-infective agents is another of the problematic ethnopharmacological research areas. Antimicrobial outcomes are naively extrapolated to pathologies that require dangerously high systemic concentrations to achieve contact inhibition. Generally, antimicrobial outcomes with essential oils are expected to have implications mainly for topical therapies, because MIC concentrations are not realistically achieved systemically. However, essential oils confer immunomodulatory effects at substantially lower concentrations.

Positive therapeutic outcomes may be a possibility, but a more detailed examination of mechanism of action is necessary. In the 1960s a sweetener called saffrole was added to beverages. It was subsequently demonstrated to lead to hepatotoxicity and cancers in mice, so its use was discontinued. Although no significant antimicrobial activity has been attributed to the pre-conjugated form of saffrole, a role in immunomodulation has been identified (Sa et al., 2014). Many essential oils, not just phenylpropanoids, have demonstrated immunomodulatory effects (Anastasiou and Buchbauer, 2017) emphasizing again that antimicrobial assays *per se* may not wholly explain the presumed therapeutic efficacy of an aromatic medicinal plant.

Essential oil metabolites may have lower MIC values or may even be toxic. As previously mentioned, it is difficult to predict how the conjugated xenobiotic will look, but insight can be garnished from *in vivo* pharmacokinetic studies. For example, studies on saffrole demonstrated that the carcinogenic compound was not actually saffrole, but the phase-1 metabolites 1'-hydroxysaffrole and 1'-hydroxy-2',3'-oxide. In addition, phase-2 metabolites 1'-acetoxysaffrole and saffrole-1'-sulfate, were shown to be mutagenic (Wislocki et al., 1997). These metabolites (Figure 9) were identified by detailed study of the urine of mice.

Knowledge of the metabolite form of sulfate esters of coumarins is another research area that could contribute to our understanding of the immunomodulatory activity of many species. Most notably, not much is known of the sulfate esters of coumarins in *Pelargonium sidoides* (Hauer et al., 2010), a South African medicinal root that is now marketed out of Germany under the name 'Umckaloabo'. Its main therapeutic claim is for coughs and colds, but extracts show low activity upon screening for antimicrobial compounds against respiratory pathogens. In this case, the putative active compounds are possibly created during metabolism. Alternatively, anti-infective activity may be partly or wholly explained by immunomodulatory effects, but this requires further investigation.

The commercial success of *Pelargonium sidoides* as a treatment for respiratory afflictions under the name of Umckaloabo (EPs® 7630) is due to the efforts of Charles Henry Stevens (Brendler and Van Wyk, 2008), who in 1897 traveled from England to South Africa upon recommendation from his doctor to experience relief from tuberculosis. It was believed at the time that the clean air was the point of difference that accommodated recovery from his affliction. After consultation with a Lesotho sangoma he was prescribed a remedy that greatly accelerated his recovery, or so the legend goes. As previously mentioned, today the mechanism of this remedy has eluded researchers,

but some indication of immunomodulation is evident *in vitro* (Brendler, 2009).

VITAMIN D

While it is conceivable that 'clean air' may have played a role in Steven's recovery from tuberculosis, recent studies indicate that the 'African sun' is more likely to have been an important complement to the efficacy of Umckaloabo. Vitamin D deficiency has been correlated with incidences of infection, particularly tuberculosis, and it is believed that supplementation or sunlight exposure (leading to Vitamin D UV-synthesis) can promote recovery (Gombart, 2009). However, using oral doses, clinical trials have not demonstrated consistent outcomes (Gombart, 2009) which may be related to insufficient dose or variable oral bioavailability (Alsaqr et al., 2015). The transdermal route is one proposed solution, but higher oral dose can also be useful, using rich natural sources, such as the Australian food species *Tasmannia lanceolata* (Poir.) A.C. Smith (Winteraceae) or *Solanum centrale* J.M. Black (desert resin: Solanaceae) (Black et al., 2017).

The immunomodulatory effects of Vitamin D₃ (from sunlight) and Vitamin D₂ (from dietary sources) starts with the phase-1 liver metabolite 25(OH)D (Figure 10), which is converted to its active form 1,25(OH)₂D by the mitochondrial 1 α -hydroxylase enzyme, the majority of which occurs in the primary renal tubules of the kidney (Gombart, 2009). It is postulated that 1,25(OH)₂D regulates specific genes encoding for antimicrobial peptides. To date no studies have demonstrated a bioactivity difference between D₂ and D₃ forms of 1,25(OH)₂D or the effects of using transdermal routes of precursors to by-pass 'first-pass' metabolism, which is inevitable in oral routes, and hence increase the half-life of its pre-conjugated form. Furthermore, no studies have explained or nullified the potential superiority of UV-synthesized routes of Vitamin D.

BIOAVAILABILITY ESTIMATION IN PRACTICE: WORKED EXAMPLES

Another 'nitrogen deficient' class of compound that confers noteworthy antimicrobial activity, comparable to the chalcones and prenylated isoflavones, is the acylphloroglucinol, such as the synthetic PPAP 23 (MIC 1 μ g/mL) (Wang et al., 2019), or the naturally occurring hyperforin (Figure 11) from St John's Wort (*Hypericum perforatum* L. Hypericaceae) (Lyles et al., 2017), also with an MIC value at 1 μ g/mL against *Staphylococcus aureus* (Reichling et al., 2001). Although today St John's Wort is commonly prescribed for psychological ailments, it was once prized for topical anti-infective effects. Its efficacy was reinforced by a doctrine of signatures comparison to human skin;

"The little holes where of the leaves of Saint John's wort are full, doe resemble all the pores of the skin and therefore it is profitable for all hurts and wounds that can happen thereunto." Coles, William (1657). Adam in Eden, or, Natures paradise. OCLC 217197164

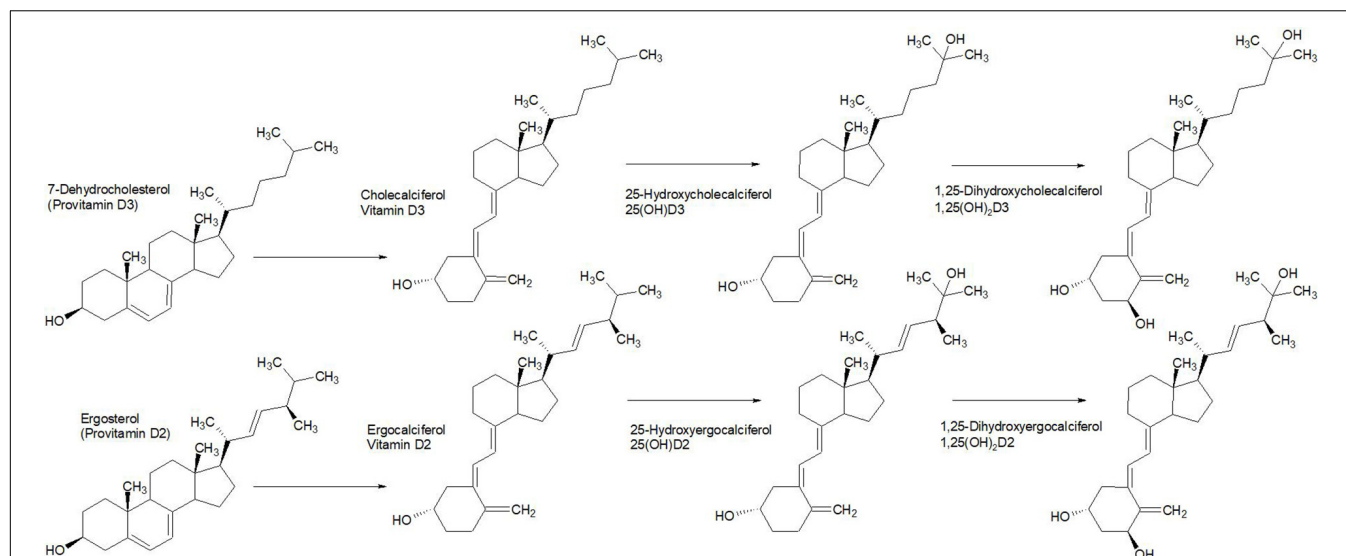


FIGURE 10 | Biosynthetic precursors to Vitamin D3 (top) and D2 (bottom). Vitamin D3 and D2 differ by their alkyl substituent branching from the 5 membered ring. This difference is also evident in the 1,25-dihydroxy derivatives, which are the active immunomodulatory forms. No research has yet elucidated salient differences in biological functions.

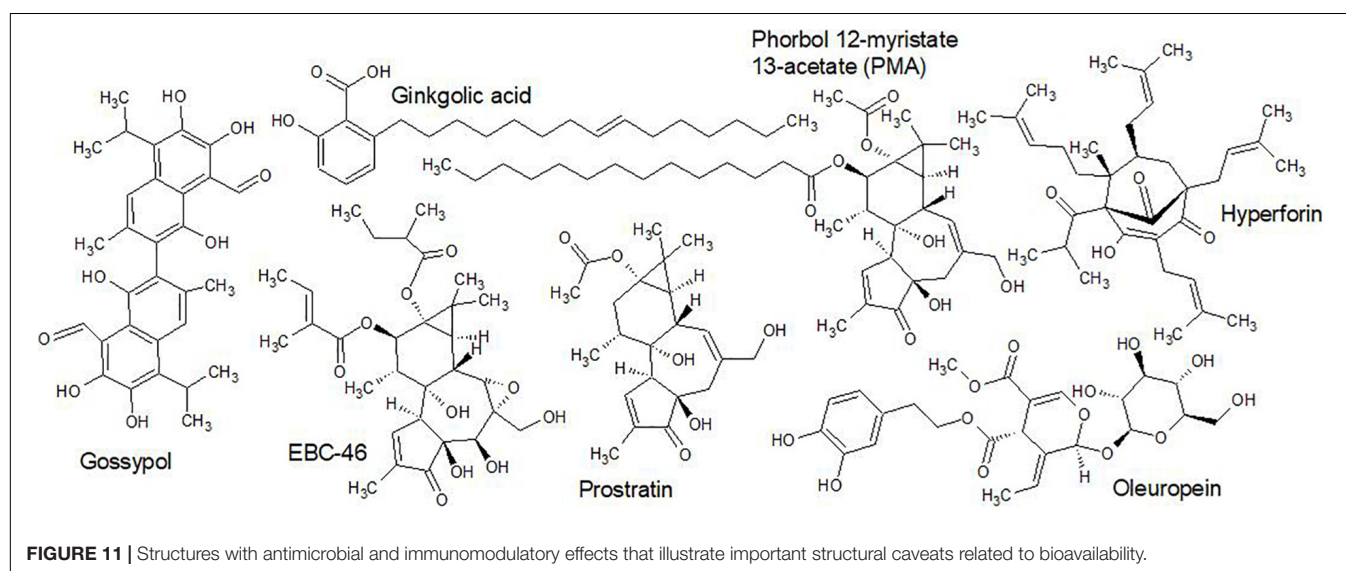


FIGURE 11 | Structures with antimicrobial and immunomodulatory effects that illustrate important structural caveats related to bioavailability.

An examination of the structure of hyperforin (**Figure 11**) using Veber's descriptors (Veber et al., 2002) demonstrates that the polar headspace of 71.44 \AA^2 is nearly half of the prescribed cut off for bioavailability (140 \AA^2). Thus, its presence in the oil extract used in Kosovar traditional medicine (Lyles et al., 2017) is consistent with this observation, since low polar headspace values correlate to increased lipophilicity. The estimation of rotatable bonds, using the current definition, gives 11, which is above the cut off at 10 prescribed by Veber et al. (2002). However, some ambiguity may be experienced with single bonds to sp^2 hybridized orbitals (single bond to a double bonded carbon). This is exemplified by examination of the 5,6-*trans* bond (*E*) in vitamin D and derivatives (**Figure 10**) where free rotation about the

single bond replaces *trans* with *cis* bonds, which evidently doesn't happen without energy input. Thus, rotation about a single bond between two sp^2 hybridized carbons does not happen. This is slightly different to hyperforin however, since the single bond is between a methylene and a singular sp^2 orbital (not between two sp^2 hybridized carbons). Nevertheless, exclusion of these bonds from the count of 'free' rotatable bonds lowers the total to 6, which may have significant implications for the interpretation of the bioavailability of this structure. In oral bioavailability studies maximum plasma levels were reached in 3 h (Biber et al., 1998), indicating good absorption, an apparent contradiction of the bioavailability estimation, if the definition of rotatable bonds is not tightened.

Another area of ambiguity is on structures with alkyl or fatty acid ester side chains. Chains longer than 10 carbons have 10 or more rotatable bonds, theoretically but not actually reducing bioavailability. In reality, alkyl chains are considered to enhance bioavailability by conferring lipophilicity to one side of the molecule. Lengths in the range of 10–15 carbons often optimize for antimicrobial efficacy against Gram-positive organisms. Ginkgolic acid from leaves and seeds of *Ginkgo biloba* L. (Ginkgoaceae) is a good example of this (Hua et al., 2017), with 14 rotatable bonds and polar head space of 57.53 Å² (Figure 11). But due to poor aqueous solubility, it is unclear how suitably applied ginkgolic acid would be without adequate formulation. After ingestion by mice, plasma concentrations were measured, confirming oral bioavailability. With rapid metabolism and return to the bowel, ginkgolic acid is eliminated almost exclusively in feces (Xia et al., 2013). Nevertheless, it is advisable to exercise caution when interpreting numbers of rotatable bonds where homologous series of methylene carbons are present (repeating CH₂ units; i.e., -CH₂-CH₂-CH₂- and so on), such as with alkyl or fatty acid ester groups.

Fatty acid esters in phorbols can increase toxicity by enhancing penetration into phospholipid membranes, the site where the drug's mechanisms are enacted (Goel et al., 2007). Phorbol esters belong to a class that is reputedly either toxic or in a dramatic twist, significantly therapeutic. They are best known for tumor promotion by activation of protein kinase c (PKC). The standard tumor promoter that is used as a positive control in toxicity studies is phorbol 12-myristate-13-acetate (PMA), which as the name suggests, has a fatty acid ester, substantially increasing hydrophobicity (Boyle et al., 2014). The number of rotatable bonds is 17, or 4 if the myristate moiety is merely counted as one and polar headspace is 130.36 Å² (Figure 11). Evidently this highly toxic bioavailable phorbol ester breaks the rules set out by Veber et al. (2002) if it is not recognized that the number of rotatable bonds in the fatty chain complicates the process of bioavailability estimation.

It is ironic that in the same class of compound as PMA, one of the most potent anticancer drugs are found, which is now in phase-2 human clinical trials. Tigilano tiglate (EBC-46; Figure 11) was isolated from the Australian rainforest species *Fontainea picrosperma* C.T.White (Euphorbiaceae). This drug also regulates PKC expression, but it activates a more specific subset of isoforms compared to the previously mentioned PMA (Boyle et al., 2014). With 8 rotatable bonds and polar headspace of 159.82 Å² this drug is slightly more hydrophilic than is acceptable by the guidelines proposed by Veber et al. (2002). However, this drug is normally administered by injection directly into the tumor mass (intratumoral).

When the immunomodulatory Polynesian drug prostratin (Figure 11), a phorbol ester, was first isolated from a medicinal species in Samoa (*Homalanthus nutans* (G.Forst.) Guill, Euphorbiaceae), it was immediately assumed it would be dangerous in human use, but *in vitro* studies demonstrated its safety and further identified HIV activation of latently infected CD4⁺ T cells and exposing them to immune response, which

reduces the pathogenicity of the HIV virus (Beans et al., 2013). Although prostratin is normally given by infusion, with a polar headspace of 139.59 Å² and only 3 rotatable bonds, it is a good candidate for the transdermal or oral route, such as in the traditional Samoan practice. Indeed, a concept for a slow release oral tablet has been proposed (Brown and Hezarah, 2012).

Another HIV inhibitory compound, also with antimalarial and antibacterial properties, is the polyphenol gossypol, which is isolated from the cotton plant (*Gossypium hirsutum* Malvaceae) (Polsky et al., 1989). This drug is a dimer of heptyl-substituted naphthalene, with aldehyde and OH substituents (Figure 11). It is worthy of mention because of the unconventional chiral center as the bridge of the dimer, which is a single C-C bond. Due to the OH substitution of the aromatic carbons adjacent to the single bond free rotation is prevented, causing two enantiomeric forms to exist (Keshmiri-Neghab and Goliaei, 2014). Generally, the negative enantiomer is most cited in association with bioactivities. Since the bridging bond is not freely rotatable, the structure has only 4 rotatable bonds and a slightly high polar headspace of 155.52 Å², which may slow the rate of absorption of this compound.

The final example is of oleuropein (Figure 11), an immunomodulatory seco-iridoid with a sugar moiety that is most famously derived from aerial parts of the olive tree (*Olea europaea* L.) (Vezza et al., 2017). Not only is this drug able to confer anti-inflammatory effects in the tissues of the intestines, but it also modifies the immune response in a positive way by increasing IFN-γ production, which is associated with higher absolute numbers of CD8⁺ and NK (natural killer) cells (Magrone et al., 2018). Oleuropein has 10 freely rotatable bonds and a polar headspace of 201.67 Å² it is unlikely to be absorbed passively in the human intestine. However, active transport of monoglycosides occurs on the Na⁺/glucose cotransporter.

Thus, while there are many valuable natural products that break rules related to passive bioavailability, exceptions can often be made where factors related to active transport mechanisms, alkyl side chains, rotational energy barriers or optimal steric placement of functional groups can influence bioavailability. Such factors need to be given careful consideration when bioavailability estimation is attempted.

CONCLUSION

The widespread emergence of common pathogens resistant to frontline antibiotics has prompted an increasingly desperate search not just for new 'magic bullets' but also for new strategies to deploy and administer existing drugs. Plant secondary metabolites provide a potential treasure trove in this regard. In this review we have surveyed a range of pertinent investigations from our own and other laboratories. By introducing a number of important caveats, we warn against naive extrapolation from *in vitro* laboratory results to therapies that may be available to clinicians at some future date. Our aim is not to discourage the very valuable work currently being undertaken, particularly in the

ethnopharmacological domain, but rather to provide indications based on relatively simple metabolic and chemical principles that may sharpen and concentrate the focus of researchers in the field.

REFERENCES

- Aelenei, P., Miron, A., Trifan, A., Bujor, A., Gille, E., and Aprotosoaie, A. C. (2016). Essential oils and their components as modulators of antibiotic activity against Gram-negative bacteria. *Medicines* 3:19. doi: 10.3390/medicines3030019
- Aghdam, E. M., Hejazi, M. E., Hejazi, M. S., and Barzegar, A. (2014). Riboswitches as potential targets for aminoglycosides compared with rRNA molecules: *in silico* studies. *J. Microb. Biochem. Technol.* 2014:S9.
- Alsaqr, A., Rasoully, M., and Musteata, F. M. (2015). Investigating transdermal delivery of Vitamin D3. *AAPS PharmSciTech* 16, 963–972. doi: 10.1208/s12249-015-0291-3
- Anastasiou, C., and Buchbauer, G. (2017). Essential oils as immunomodulators: some examples. *Open Chem.* 15, 352–370.
- Andrews, J. M. (2000). Determination of minimum inhibitory concentrations. *J. Antimicrob. Chemother.* 48, 5–16. doi: 10.1093/jac/48.suppl_1.5
- Angelis, I. D., and Turco, L. (2011). Caco-2 cells as a model for intestinal absorption. *Curr. Protoc. Toxicol.* 47, 20.6.1–20.6.15.
- Aqil, M., Ahad, A., Sultana, Y., and Ali, A. (2007). Status of terpenes as skin penetration enhancers. *Drug Discov. Today* 12, 1061–1067. doi: 10.1016/j.drudis.2007.09.001
- Babii, C., Bahrin, L. G., Neagu, A. N., Gostin, I., Mihasan, M., Birsă, L. M., et al. (2016). Antibacterial activity and proposed action mechanism of a new class of synthetic tricyclic flavonoids. *J. Appl. Microbiol.* 120, 630–637. doi: 10.1111/jam.13048
- Bäcker, C., Jenett-Siems, K., Boddke, A., and Lindequist, U. (2014a). Polyphenolic compounds from the leaves of *Pittosporum angustifolium*. *Biochem. Systemat. Ecol.* 55, 101–103. doi: 10.1016/j.bse.2014.02.015
- Bäcker, C., Jenett-Siems, K., Siems, K., Wurster, M., Boddke, A., and Lindequist, U. (2014b). Cytotoxic saponins from the seeds of *Pittosporum angustifolium*. *Z. Naturforsch. C* 69, 191–198. doi: 10.5560/znc.2014-0011
- Beans, E. J., Fournogerakis, D., Gauntlett, C., Heumann, L. V., Kramer, R., Marsden, M. D., et al. (2013). Highly potent, synthetically accessible prostratin analogs induce latent HIV expression *in vitro* and *ex vivo*. *Proc. Natl. Acad. Sci.* 110, 11698–11703. doi: 10.1073/pnas.1302634110
- Biber, A., Fischer, H., Romer, A., and Chatterjee, S. S. (1998). Oral bioavailability of hyperforin from hypericum extracts in rats and human volunteers. *Pharmacopsychiatry* 31, 36–43. doi: 10.1055/s-2007-979344
- Black, L. J., Lucas, R. M., Sherriff, J. L., Bjorn, L. O., and Bornman, J. F. (2017). In pursuit of vitamin D in plants. *Nutrients* 9:E136. doi: 10.3390/nu9020136
- Boonclarm, D., Sornwatana, T., Arthan, D., Kongsaree, P., and Svasti, J. (2006). β -Glucosidase catalyzing specific hydrolysis of an iridoid β -Glucoside from *Plumeria obtusa*. *Acta Biochim. Biophys. Sin.* 38, 563–570. doi: 10.1111/j.1745-7270.2006.00196.x
- Boonkaewwan, C., and Burodom, A. (2013). Anti-inflammatory and immunomodulatory activities of stevioside and steviol on colonic epithelial cells. *J. Sci. Food Agric.* 93, 3820–3825. doi: 10.1002/jsfa.6287
- Boyle, G. M., D'Souza, M. M. A., Pierce, C. J., Adams, R. A., Cantor, A. S., Johns, J. P., et al. (2014). Intra-lesional injection of the novel PKC activator EBC-46 rapidly ablates tumors in mouse models. *PLoS One* 9:e108887. doi: 10.1371/journal.pone.0108887
- Brendler, T. (2009). “Umckaloabo: from a patent remedy to a modern herbal pharmaceutical based on *Pelargonium sidoides* with clinically proven efficacy,” in *Proceedings of the African Natural Plant Products: New Discoveries and Challenges in Chemistry and Quality*, ACS Symposium Series, eds H. R. Juliani, J. E. Simon, and H. Chi-Tang (Oxford: Oxford University Press), 295–319. doi: 10.1021/bk-2009-1021.ch017
- Brendler, T., and Van Wyk, B.-E. (2008). A historical, scientific and commercial perspective on the medicinal use of *Pelargonium sidoides* (Geraniaceae). *J. Ethnopharmacol.* 119, 420–433. doi: 10.1016/j.jep.2008.07.037
- Brown, S. J., and Hezarah, M. (2012). *Methods of Administering Prostratin and Structural Analogs Thereof*, Application EP-2276478-A4. Los Angeles, CA: AIDS Research Alliance.
- Cheesman, M. J., Ilanko, A., Blonk, B., and Cock, I. E. (2017). Developing new antimicrobial therapies: are synergistic combinations of plant extracts/compounds with conventional antibiotics the solution? *Pharmacog. Rev.* 11, 57–72. doi: 10.4103/phrev.phrev_21_17
- Chen, J., Jiang, Q.-D., Wu, Y.-M., Liu, P., Yao, J.-H., Lu, Q., et al. (2015). Potential of essential oils as penetration enhancers for transdermal administration of ibuprofen to treat dysmenorrhoea. *Molecules* 20, 18219–18236. doi: 10.3390/molecules201018219
- Chen, L., Tuo, B., and Dong, H. (2016). Regulation of intestinal glucose absorption by ion channels and transporters. *Nutrients* 8:43. doi: 10.3390/nu8010043
- Chen, L., and Yu, J. (2016). Modulation of toll-like receptor signaling in innate immunity by natural products. *Int. J. Immunopharmacol.* 37, 65–70. doi: 10.1016/j.intimp.2016.02.005
- CLSI (2017). *Performance Standards for Antimicrobial Susceptibility Testing; 23rd Informational Supplement*, CLSI document M100-S27. Wayne, PA: Clinical and Laboratory Standards Institute.
- Cock, I. E. (2018). Is the pharmaceutical industry's preoccupation with the monotherapy drug model stifling the development of effective new drug therapies? *Inflammopharmacology* 26, 861–879. doi: 10.1007/s10787-018-0488-7
- Cushnie, T. T., and Lamb, A. J. (2011). Recent advances in understanding the antibacterial properties of flavonoids. *Int. J. Antimicrob. Agents* 38, 99–107. doi: 10.1016/j.ijantimicag.2011.02.014
- Das, A., Srinivasan, M., Ghosh, T. S., and Mande, S. S. (2016). Xenobiotic metabolism and gut microbiomes. *PLoS One* 11:e0163099. doi: 10.1371/journal.pone.0163099
- Day, A. J., Cañada, F. J., Diaz, J. C., Kroon, P. A., Mclauchlan, R., Faulds, C. B., et al. (2000). Dietary flavonoid and isoflavone glycosides are hydrolysed by the lactase site of lactase phlorizin hydrolase. *FEBS Lett.* 438, 166–170. doi: 10.1016/S0014-5793(00)01211-4
- Doak, B. C., Over, B., Giordanetto, F., and Kihlberg, J. (2014). Oral druggable space beyond the rule of 5: insights from drugs and clinical candidates. *Chem. Biol. Rev.* 21, 1115–1142. doi: 10.1016/j.chembiol.2014.08.013
- Dresser, G. K., Spence, J. D., and Bailey, D. G. (2000). Pharmacokinetic-pharmacodynamic consequences and clinical relevance of cytochrome P450 3A4 inhibition. *Clin. Pharmacokinet.* 38, 41–57. doi: 10.2165/00003088-200038010-00003
- Ekwall, B., Silano, V., Stamatopaganuzzi, A., and Zucco, F. (1990). “Chapter 7 – Toxicity tests with mammalian cell cultures,” in *Short-Term Toxicity Tests for Non-Genotoxic Effects*, eds P. Bourdeau, E. Sommers, G. Mark Richardson, and J. R. Hickman (Hoboken, NJ: John Wiley and Sons).
- El-Kattan, A., and Varma, M. (2012). “Oral absorption, intestinal metabolism and human oral bioavailability,” in *Topics on Drug Metabolism*, ed. J. Paxton (London: InTechOpen), 1–34.
- Eloff, J. N. (1998). A sensitive and quick microplate method to determine the minimal inhibitory concentration of plant extracts for bacteria. *Planta Med.* 64, 711–713. doi: 10.1055/s-2006-957563
- Ertl, P., Rohde, B., and Selzer, P. (2000). Fast calculation of molecular polar surface area as a sum of fragment-based contributions and its application to the prediction of drug transport properties. *J. Med. Chem.* 43, 3714–3717. doi: 10.1021/jm000942e
- Finland, M. (1958). Current concepts in therapy: antibiotics. III. Absorption and excretion and toxicity. *N. Engl. J. Med.* 258, 544–546.
- Gee, J. M., DuPont, M. S., Day, A. J., Plumb, G. W., Williamson, G., and Johnson, I. T. (2000). Intestinal transport of quercetin glycosides in rats involves both deglycosylation and interaction with the hexose transport pathway. *J. Nutr.* 130, 2765–2771. doi: 10.1093/jn/130.11.2765
- Goel, G., Makkar, H. P. S., Francis, G., and Becker, K. (2007). Phorbol esters: structure, biological activity, and toxicity in animals. *Int. J. Toxicol.* 26, 279–288. doi: 10.1080/10915810701464641

AUTHOR CONTRIBUTIONS

NS wrote the manuscript. GJ assisted with edits.

- Gombart, A. F. (2009). The vitamin D-antimicrobial peptide pathway and its role in protection against infection. *Future Microbiol.* 4, 1151–1165. doi: 10.2217/fmb.09.87
- Grice, J. E., Cross, S. E., Brownlie, C., and Roberts, M. S. (2010). The application of molecular structural predictors of intestinal absorption to screening of compounds for transdermal penetration. *J. Pharm. Pharmacol.* 62, 750–755. doi: 10.1211/jpp.62.06.0011
- Gunasekaran, N., Long, L. E., Dawson, B. L., Hansen, G. H., Richardson, D. P., Li, K. M., et al. (2009). Reintoxication: the release of fat-stored Δ^9 -tetrahydrocannabinol (THC) into blood is enhanced by food deprivation or ACTH exposure. *Br. J. Pharmacol.* 158, 1330–1337. doi: 10.1111/j.1476-5381.2009.00399.x
- Harbeoui, H., Hichami, A., Wannes, W. A., Lemput, J., Tounsi, M. S., and Khan, N. A. (2019). Anti-inflammatory effect of grape (*Vitis vinifera* L.) seed extract through the downregulation of NF-KB and MAPK pathways in LPS-induced RAW264.7 macrophages. *S. Afr. J. Bot.* 125, 1–8. doi: 10.1016/j.sajb.2019.06.026
- Hauer, H., Germer, S., Elsässer, J., and Ritter, T. (2010). Benzopyranones and their sulfate esters from *Pelargonium sidoides*. *Planta Med.* 76, 350–352. doi: 10.1055/s-0029-1186167
- He, M., Wu, T., Pan, S., and Xu, X. (2014). Antimicrobial mechanism of flavonoids against *Escherichia coli* ATCC25922 by model membrane study. *Appl. Surf. Sci.* 305, 515–521. doi: 10.1016/j.apsusc.2014.03.125
- Herman, A., and Herman, A. P. (2016). Mechanism of action of herbs and their active constituents used in hair loss treatment. *Fitoterapia* 114, 18–25. doi: 10.1016/j.fitote.2016.08.008
- Hrabálek, A., Dolezal, P., Roman, M., Machacek, M., and Sklbalova, Z. (1994). Esters of omega-amino acids as flexible penetration enhancers. *Die Pharmazie* 49, 325–328.
- Hua, Z., Wu, C., Fan, G., Tang, Z., and Cao, F. (2017). The antibacterial activity and mechanism of ginkgolic acid C15:1. *BMC Biotechnol.* 17:5. doi: 10.1186/s12896-12016-10324-12893
- Hulley, I. M., Sadgrove, N. J., Tilney, P. M., Özek, G., Yur, S., Özek, T., et al. (2018). Essential oil composition of *Pentzia incana* (Asteraceae), an important natural pasture plant in the Karoo region of South Africa. *Afr. J. Range Forage Sci.* 35, 137–145. doi: 10.2989/10220119.2018.1495265
- Jia, X., Zhang, J., Sun, W., He, W., Jiang, H., Chen, D., et al. (2013). Riboswitch control of aminoglycoside antibiotic resistance. *Cell* 152, 68–81. doi: 10.1016/j.cell.2012.12.019
- Jourova, L., Anzenbacher, P., and Anzenbacherova, E. (2016). Human gut microbiota plays a role in the metabolism of drugs. *Biomed. Pap. Med. Fac. Univ. Palacky Olomouc Czech Repub.* 160, 317–326. doi: 10.5507/bp.2016.039
- Kang, S., and Min, H. (2012). Ginseng, the 'Immunity Boost': the effects of *Panax ginseng* on immune system. *J. Ginseng Res.* 36, 354–368. doi: 10.5142/jgr.2012.36.4.354
- Karande, P., Jain, A., Ergun, K., Kispersky, V., and Mitragotri, S. (2005). Design principles of chemical penetration enhancers for transdermal drug delivery. *Proc. Natl. Acad. Sci. U.S.A.* 102, 4688–4693.
- Keshmiri-Neghab, H., and Goliaei, B. (2014). Therapeutic potential of gossypol: an overview. *Pharmaceutical Biology* 52, 124–128. doi: 10.3109/13880209.2013.832776
- Khumalo, G. P., Sadgrove, N. J., Van Vuuren, S. F., and Van Wyk, B.-E. (2018). Antimicrobial activity of volatile et al. (Canellaceae) against skin and respiratory pathogens. *S. Afr. J. Bot.* 115:290.
- Koyama, E., Sakai, N., Ohori, Y., Kitazawa, K., Izawa, O., Kakegawa, K., et al. (2003). Absorption and metabolism of glycosidic sweeteners of stevia mixture and their aglycone, steviol, in rats and humans. *Food Chem. Toxicol.* 41, 875–883. doi: 10.1016/s0278-6915(03)00039-5
- Kulik, M., Mori, T., Sugita, Y., and Trylska, J. (2018). Molecular mechanisms for dynamic regulation of N1 riboswitch by aminoglycosides. *Nucleic Acids Res.* 46, 9960–9970. doi: 10.1093/nar/gky833
- Lawal, F., Bapela, M. J., Adebayo, S. A., Nkadameng, S. M., Yusuf, A. A., Malterud, K. E., et al. (2019). Anti-inflammatory potential of South African medicinal plants used for the treatment of sexually transmitted infections. *S. Afr. J. Bot.* 125, 62–71. doi: 10.1016/j.sajb.2019.06.023
- Lee Chao, P. D., Hsiu, S. L., and Hou, Y. C. (2006). Bioavailability, metabolism, and pharmacokinetics of glycosides in Chinese herbs. *ACS Sym. Ser.* 925, 212–223. doi: 10.1021/bk-2006-0925.ch016
- Lipinski, C. A. (2001). Avoiding investment in doomed drugs: is poor solubility an industry wide problem? *Curr. Drug Discov.* 1, 17–19.
- Lyddiard, D., Jones, G. L., and Greatrex, B. W. (2016). Keeping it simple: lessons from the golden era of antibiotic discovery. *FEMS Microbiol. Ecol.* 363:fnw084. doi: 10.1093/femsle/fnw084
- Lyles, J. T., Kim, A., Nelson, K., Bullard-Roberts, A. L., Hajdari, A., Mustafa, B., et al. (2017). The chemical and antibacterial evaluation of St John's Wort Oil macerates used in Kosovar traditional medicine. *Front. Microbiol.* 8:1639. doi: 10.3389/fmicb.2017.01639
- Magnusson, B. M., Anissimov, Y. G., Cross, S. E., and Roberts, M. S. (2004). Molecular size as the main determinant of solute maximum flux across the skin. *J. Invest. Dermatol.* 122, 993–999. doi: 10.1111/j.0022-202x.2004.22413.x
- Magrone, T., Spagnoletta, A., Salvatore, R., Magrone, M., Dentamaro, F., Russo, M. A., et al. (2018). Olive leaf extracts act as modulators of the human immune response. *Endocr. Metab. Immune Disord. Drug Targets* 18, 85–93. doi: 10.2174/1871530317666171116110537
- Matthias, A., Addison, R. S., Agnew, L. L., Bone, K. M., Watson, K., and Lehmann, R. P. (2007). Comparison of Echinacea alkylamide pharmacokinetics between liquid and tablet preparations. *Phytomedicine* 14, 587–590. doi: 10.1016/j.phymed.2006.12.021
- Mukne, A. P., Viswanathan, V., and Phadatar, A. G. (2011). Structure prerequisites for isoflavones as effective antibacterial agents. *Pharmacog. Rev.* 5:13. doi: 10.4103/0973-7847.79095
- Németh, K., Plumb, G. W., Berrin, J.-G., Juge, N., Jacob, R., Naim, H. Y., et al. (2003). Deglycosylation by small intestinal epithelial cell β -glucosidases is a critical step in the absorption and metabolism of dietary flavonoid glycosides in humans. *Eur. J. Nutr.* 42, 29–42. doi: 10.1007/s00394-003-0397-3
- Nile, S. H., and Park, S. W. (2013). Optimized methods for *in vitro* and *in vivo* anti-inflammatory assays and its applications in herbal and synthetic drug analysis. *Mini Rev. Med. Chem.* 13, 95–100. doi: 10.2174/1389557511307010095
- Nowakowska, Z. (2007). A review of anti-infective and anti-inflammatory chalcones. *Eur. J. Med. Chem.* 42, 125–137. doi: 10.1016/j.ejmech.2006.09.019
- Olah, A., Szekanecz, Z., and Biro, T. (2017). Targeting cannabinoid signaling in the immune system: "High"-ly exciting questions, possibilities, and challenges. *Front. Immunol.* 8:1487. doi: 10.3389/fimmu.2017.01487
- O'Leary, K. A., Day, A. J., Needs, P. W., Mellon, F. A., O'Brien, N. M., and Williamson, G. (2003). Metabolism of quercetin-7- and quercetin-3-glucuronides by an *in vitro* hepatic model: the role of human β -glucuronidase, sulfotransferase, catechol-O-methyltransferase and multi-resistant protein 2 (MRP2) in flavonoid metabolism. *Biochem. Pharmacol.* 65, 479–491. doi: 10.1016/s0006-2952(02)01510-1
- Paduch, R., Kandefer-Szerszeń, M., Trytek, M., and Fiedurek, J. (2007). Terpenes: substances useful in human healthcare. *Arch. Immunol. Ther. Exp.* 55:315. doi: 10.1007/s00005-007-0039-1
- Pandey, A., Mittal, A., Chauhan, N., and Alam, S. (2014). Role of surfactants as penetration enhancer in transdermal drug delivery system. *J. Mol. Pharmac. Org. Process Res.* 2, 2–7.
- Patrick, G. L. (2013). *An Introduction to Medicinal Chemistry*. Oxford: Oxford University Press.
- Pellock, S. J., and Redinbo, M. R. (2017). Glucuronides in the gut: sugar-driven symbioses between microbe and host. *J. Biol. Chem.* 292, 8569–8576. doi: 10.1074/jbc.R116.767434
- Pino, C. J., Gutterman, J. U., Vonwil, D., Mitragotri, S., and Shastri, V. P. (2012). Glycosylation facilitates transdermal transport of macromolecules. *Proc. Natl. Acad. Sci. U.S.A.* 109, 21283–21288. doi: 10.1073/pnas.1200942109
- Pino, C. J., Scherer, M. A., and Shastri, V. P. (2014). Investigation of the transdermal transport of charged local anesthetics in the presence of triterpene saponin glycosides. *Drug Deliv. Transl. Res.* 4, 131–138. doi: 10.1007/s13346-013-0186-3
- Polsky, B., Segal, S. J., Baron, P. A., Gold, J. W. M., Ueno, H., and Armstrong, D. (1989). Inactivation of human immunodeficiency virus *in vitro* by gossypol. *Contraception* 39, 579–587. doi: 10.1016/0010-7824(89)90034-6
- Raduner, S., Majewska, A., Chen, J.-Z., Xie, X.-Q., Hamon, J., Faller, B., et al. (2006). Alkylamides from Echinacea are a new class of cannabinomimetics. *J. Biol. Chem.* 281, 14192–14206. doi: 10.1074/jbc.m601074200

- Reichling, J., Weseler, A. R., and Saller, R. (2001). A current review of the antimicrobial activity of *Hypericum perforatum* L. *Pharmacopsychiatry* 34, S116–S118.
- Ricciotti, E., and FitzGerald, G. A. (2011). Prostaglandins and inflammation. *Arterioscler. Thromb. Vasc. Biol.* 31, 986–1000. doi: 10.1161/ATVBAHA.110.207449
- Rom, S., and Persidsky, Y. (2013). Cannabinoid receptor 2: potential role in immunomodulation and neuroinflammation review. *J. Neuroimmune Pharmacol.* 8, 608–620. doi: 10.1007/s11481-013-9445-9
- Sa, R. C. S., Andrade, L. N., de Oliveira, R. R. B., and de Sousa, D. P. (2014). A review on anti-inflammatory activity of phenylpropanoids found in essential oils. *Molecules* 19, 1459–1480. doi: 10.3390/molecules19021459
- Sa, R. C. S., Andrade, L. N., and de Sousa, D. P. (2013). A review on anti-inflammatory activity of monoterpenes. *Molecules* 18, 1227–1254. doi: 10.3390/molecules18011227
- Sadgrove, N., and Jones, G. L. (2013). Chemical and biological characterisation of solvent extracts and essential oils from leaves and fruit of two Australian species of *Pittosporum* (Pittosporaceae) used in aboriginal medicinal practice. *J. Ethnopharmacol.* 145, 813–821. doi: 10.1016/j.jep.2012.12.019
- Sadgrove, N., and Jones, G. L. (2014a). Cytochrome P450 of essential oil chemotypes of *Eremophila longifolia* F. Muell (Scrophulariaceae). *Phytochemistry* 105, 43–51. doi: 10.1016/j.phytochem.2014.05.005
- Sadgrove, N., and Jones, G. L. (2014b). Medicinal compounds, chemically and biologically characterised from extracts of Australian *Callitris endlicheri* and *C. glaucophylla* (Cupressaceae): used traditionally in Aboriginal and colonial pharmacopoeia. *J. Ethnopharmacol.* 153, 872–883. doi: 10.1016/j.jep.2014.03.054
- Sadgrove, N., Jones, G. L., and Greatrex, B. W. (2014a). Isolation and characterisation of (-)-genifuranal: the principal antimicrobial component in traditional smoking applications of *Eremophila longifolia* (Scrophulariaceae) by Australian Aboriginal peoples. *J. Ethnopharmacol.* 154, 758–766. doi: 10.1016/j.jep.2014.05.003
- Sadgrove, N. J., Telford, I. R. H., Greatrex, B. W., and Jones, G. L. (2014b). Composition and antimicrobial activity of essential oils from the *Phebalium squamulosum* species complex (Rutaceae) in New South Wales, Australia. *Phytochemistry* 97, 38–45. doi: 10.1016/j.phytochem.2013.10.015
- Sadgrove, N., Mijajlovic, S., Tucker, D. J., Watson, K., and Jones, G. L. (2011). Characterization and bioactivity of essential oils from novel chemotypes of *Eremophila longifolia* (F. Muell) (Myoporaceae): a highly valued traditional Australian medicine. *Flav. Fragr. J.* 26, 341–350.
- Sadgrove, N. J., and Jones, G. L. (2014c). "Phytochemical variability of *Pittosporum angustifolium* Lodd. (Pittosporaceae): a traditional and contemporary Aboriginal Australian medicine," in *Proceedings of the XXIX International Horticultural Congress on Horticulture: Sustaining Lives, Livelihoods and Landscapes (IHC2014): V World Congress on Medicinal and Aromatic Plants and International Symposium on Plants, as Factories of Natural Substances, Edible and Essential Oils*, Vol. 1125, (Brisbane, QLD), 303–308. doi: 10.17660/actahortic.2016.1125.39
- Sadgrove, N. J., and Jones, G. L. (2015). A contemporary introduction to essential oils: chemistry, bioactivity and prospects for Australian agriculture. *Agriculture* 5, 48–102. doi: 10.3390/agriculture5010048
- Sadgrove, N. J., Lyddiard, D., Collins, T. L., Greatrex, B. W., and Jones, G. L. (2016). "Genifuranal and other derivatives: smoking desert plants," in *Proceedings of the XXIX International Horticultural Congress on Horticulture: Sustaining Lives, Livelihoods and Landscapes (IHC2014): V World Congress on Medicinal and Aromatic Plants and International Symposium on Plants, as Factories of Natural Substances, Edible and Essential Oils*, Vol. 1125, (Brisbane, QLD), 181–188. doi: 10.17660/actahortic.2016.1125.22
- Sarah, Q. S., Anny, F. C., and Misbahuddin, M. (2017). Brine shrimp lethality assay. *Bangladesh J. Pharmacol.* 12:2017.
- Sarpotdar, P. P., Gaskill, J. L., Giannini, R. P., and Daniels, C. R. (1988). *L-α-Amino Acids as Transdermal Penetration Enhancers*, US06/754,805. Washington, DC: Wyeth LLC.
- Sasaki, T., Sato, Y., Kumagai, T., Yoshinari, K., and Nagata, K. (2017). Effect of health foods on cytochrome P450-mediated drug metabolism. *J. Pharm. Health Care Sci.* 3:14. doi: 10.1186/s40780-017-0083-x
- Schmith, V. D., and Foss, J. F. (2008). Effects of inflammation on pharmacokinetics/pharmacodynamics: increasing recognition of its contribution to variability in response. *Clin. Pharmacol. Ther.* 83, 809–811. doi: 10.1038/clpt.2008.62
- Seeram, N. P., Lee, R., and Heber, D. (2004). Bioavailability of ellagic acid in human plasma after consumption of ellagitannins from pomegranate (*Punica granatum* L.) juice. *Clin. Chim. Acta* 348, 63–68. doi: 10.1016/j.cccn.2004.04.029
- Seo, Y., Berger, J. M., Hoch, J., Neddermann, K. M., Bursuker, I., Mamber, S. W., et al. (2002). A new triterpene saponin from *Pittosporum viridiflorum* from the Madagascar rainforest. *J. Nat. Prod.* 65, 65–68.
- Shastri, V. P., Pino, C. J., Scherer, M. A., and Guan, C. M. (2008). "Triterpene saponin glycosides impact the percutaneous delivery of water soluble drugs," in *Proceedings of the 2008 MRS Fall Meeting conference*, (Boston, MA).
- Trombetta, D., Castelli, F., Sarpietro, M. G., Venuti, V., Cristani, M., Daniele, C., et al. (2005). Mechanisms of antibacterial action of three monoterpenes. *Antimicrob. Agents Chemother.* 49, 2474–2478. doi: 10.1128/aac.49.6.2474-2478.2005
- Tsai, S., Clemente-Casares, X., Zhou, A. C., Lei, H., Ahn, J. J., Chan, Y. T., et al. (2018). Insulin receptor-mediated stimulation boosts T cell immunity during inflammation and infection. *Cell Metab.* 28, 933–934. doi: 10.1016/j.cmet.2018.08.003
- Van Vuuren, S. F., and Holl, D. (2017). Antimicrobial natural product research: a review from a South African perspective for the years 2009–2016. *J. Ethnopharmacol.* 208, 236–252. doi: 10.1016/j.jep.2017.07.011
- Van Vuuren, S. F., and Viljoen, A. M. (2011). Plant-based antimicrobial studies - methods and approaches to study the interaction between natural products. *Planta Med.* 77, 1168–1182. doi: 10.1055/s-0030-1250736
- Van Wyk, B.-E., Oudtshoorn, B., and Gericke, N. (2009). *Medicinal Plants of South Africa*, 2nd Edn. Pretoria: Briza Publications.
- Veber, D. F., Johnson, S. R., Cheng, H.-Y., Smith, B. R., Ward, K. W., and Kopple, K. D. (2002). Molecular properties that influence oral bioavailability of drug candidates. *J. Med. Chem.* 42, 2615–2623. doi: 10.1021/jm020017n
- Veza, T., Algieri, F., Rodriguez-Nogales, A., Garrido-Msa, J., Utrilla, M. P., Talhao, N., et al. (2017). Immunomodulatory properties of *Olea europaea* leaf extract in intestinal inflammation. *Mol. Nutr. Food Res.* 61:1601066. doi: 10.1002/mnfr.201601066
- Wagner, C., Saueremann, R., and Joukhadar, C. (2006). Principles of antibiotic penetration into abscess fluid. *Pharmacology* 78, 1–10. doi: 10.1159/000094668
- Wang, H., Kraus, F., Popella, P., Baykal, A., Guttroff, C., Francois, P., et al. (2019). The polycyclic polyphenylated acylphloroglucinol antibiotic PPAP 23 targets the membrane and iron metabolism in *Staphylococcus aureus*. *Front. Microbiol.* 10:14. doi: 10.3389/fmicb.2019.00014
- Wang, X.-X., Zan, K., Shi, S.-P., Zeng, K.-W., Jiang, Y., Guan, Y., et al. (2013). Quinolone alkaloids with antibacterial and cytotoxic activities from the fruits of *Evoidia rutaecarpa*. *Fitoterapia* 89, 1–7. doi: 10.1016/j.fitote.2013.04.007
- Williamson, G., Barron, D., Shimoi, K., and Terao, J. (2005). In vitro biological properties of flavonoid conjugates found in vivo. *Free Radic. Res.* 39, 457–469. doi: 10.1080/10715760500053610
- Wislocki, P. G., Miller, E. C., Miller, J. A., McCoy, E. C., and Rosenkranz, H. S. (1997). Carcinogenic and mutagenic activities of saffrole, 1'-hydroxysaffrole, and some known or possible metabolites. *Cancer Res.* 37, 1883–1891.
- Wolfram, S., Block, M., and Ader, P. (2002). Quercetin-3-glucoside is transported by the glucose carrier SGLT-1 across the brush border membrane of rat small intestine. *J. Nutr.* 132, 630–635. doi: 10.1093/jn/132.4.630
- Wu, T., Zang, X., He, M., Pan, S., and Xu, X. (2013). Structure–activity relationship of flavonoids on their anti-*Escherichia coli* activity and inhibition of DNA gyrase. *J. Agric. Food Chem.* 61, 8185–8190. doi: 10.1021/jf402222v
- Xia, H., Liu, Z., Hu, H., Zhou, H., and Zeng, S. (2013). Identification of ginseng acid (15:1) metabolites in rat following oral administration by high-performance liquid chromatography coupled to tandem mass spectrometry. *Xenobiotica* 43, 454–460. doi: 10.3109/00498254.2012.725141
- Yamai, H., Sawada, N., Yoshida, T., Seike, J., Takizawa, H., Kenzaki, K., et al. (2009). Triterpenes augment the inhibitory effects of anticancer drugs on growth of human esophageal carcinoma cells in vitro and suppress experimental metastasis in vivo. *Int. J. Cancer* 125, 952–960. doi: 10.1002/ijc.24433
- Ying-Yuan, L., Jin-Feng, C., Jin-Yang, S., Zhi-Yong, D., Jin-Long, W., Yi, Q., et al. (2019). Pharmacokinetics study of 16 representative components from Baoyuan decoction in rat plasma by LC-MS/MS with a large-volume direct injection method. *Phytomedicine* 57, 148–157. doi: 10.1016/j.phymed.2018.09.002

- Zárate, S. G., De la Cruz Claire, M. L., Benito-Arenas, R., Revuelta, J., Santana, A. G., and Bastida, A. (2018). Overcoming aminoglycoside enzymatic resistance: design of novel antibiotics and inhibitors. *Molecules* 23:E284. doi: 10.3390/molecules23020284
- Zeng, X., and Lin, J. (2013). Beta-lactamase induction and cell wall metabolism in Gram-negative bacteria. *Front. Microbiol.* 4:128. doi: 10.3389/fmicb.2013.00128
- Zhang, W. L., Chen, J. P., Lam, K. Y. C., Zhan, J. Y. X., Yao, P., Dong, T. T. X., et al. (2014). Hydrolysis of glycosidic flavonoids during the preparation of Danggui Buxue Tang: an outcome of moderate boiling of chinese herbal mixture. *Evid. Based Complement. Alter. Med.* 2014:608721. doi: 10.1155/2014/608721

Conflict of Interest: The authors declare that the research was conducted in the absence of any commercial or financial relationships that could be construed as a potential conflict of interest.

Copyright © 2019 Sadgrove and Jones. This is an open-access article distributed under the terms of the Creative Commons Attribution License (CC BY). The use, distribution or reproduction in other forums is permitted, provided the original author(s) and the copyright owner(s) are credited and that the original publication in this journal is cited, in accordance with accepted academic practice. No use, distribution or reproduction is permitted which does not comply with these terms.



Colistin Combined With Tigecycline: A Promising Alternative Strategy to Combat *Escherichia coli* Harboring *bla*_{NDM-5} and *mcr-1*

Yu-Feng Zhou^{1,2}, Ping Liu^{1,2}, Chuan-Jian Zhang^{1,2}, Xiao-Ping Liao^{1,2}, Jian Sun^{1,2} and Ya-Hong Liu^{1,2,3*}

¹ National Risk Assessment Laboratory for Antimicrobial Resistance of Animal Origin Bacteria, College of Veterinary Medicine, South China Agricultural University, Guangzhou, China, ² Guangdong Provincial Key Laboratory of Veterinary Pharmaceutics Development and Safety Evaluation, South China Agricultural University, Guangzhou, China, ³ Jiangsu Co-innovation Center for the Prevention and Control of Important Animal Infectious Disease and Zoonosis, Yangzhou University, Yangzhou, China

OPEN ACCESS

Edited by:

Gian Maria Rossolini,
University of Florence, Italy

Reviewed by:

Jianfeng Wang,
Jilin University, China
Song Lin Chua,
Hong Kong Polytechnic University,
Hong Kong

*Correspondence:

Ya-Hong Liu
lyh@scau.edu.cn

Specialty section:

This article was submitted to
Antimicrobials, Resistance,
and Chemotherapy,
a section of the journal
Frontiers in Microbiology

Received: 12 September 2019

Accepted: 09 December 2019

Published: 08 January 2020

Citation:

Zhou Y-F, Liu P, Zhang C-J,
Liao X-P, Sun J and Liu Y-H (2020)
Colistin Combined With Tigecycline:
A Promising Alternative Strategy
to Combat *Escherichia coli* Harboring
*bla*_{NDM-5} and *mcr-1*.
Front. Microbiol. 10:2957.
doi: 10.3389/fmicb.2019.02957

Infections due to carbapenem-resistant NDM-producing *Escherichia coli* represent a major therapeutic challenge, especially in situations of pre-existing colistin resistance. The aim of this study was to investigate combinatorial pharmacodynamics of colistin and tigecycline against *E. coli* harboring *bla*_{NDM-5} and *mcr-1*, with possible mechanisms explored as well. Colistin disrupted the bacterial outer-membrane and facilitated tigecycline uptake largely independent of *mcr-1* expression, which allowed a potentiation of the tigecycline-colistin combination. A concentration-dependent decrease in colistin MIC and EC₅₀ was observed with increasing tigecycline levels. Clinically relevant concentrations of colistin and tigecycline combination significantly decreased bacterial density of colistin-resistant *E. coli* by 3.9 to 6.1-log₁₀ cfu/mL over 48 h at both inoculums of 10⁶ and 10⁸ cfu/mL, and were more active than each drug alone (*P* < 0.01). Importantly, colistin and tigecycline combination therapy was efficacious in the murine thigh infection model at clinically relevant doses, resulting in >2.0-log₁₀cfu/thigh reduction in bacterial density compared to each monotherapy. These data suggest that the use of colistin and tigecycline combination can provide a therapeutic alternative for infection caused by multidrug-resistant *E. coli* that harbored both *bla*_{NDM-5} and *mcr-1*.

Keywords: carbapenem-resistant Enterobacteriaceae, carbapenem-resistance, colistin-resistance, combination therapy, MCR-1, New Delhi metallo-β-lactamases-5

INTRODUCTION

Infections caused by carbapenem-resistant Enterobacteriaceae (CRE), especially the New Delhi metallo-β-lactamases (NDM)-producing *Escherichia coli*, have become a global therapeutic challenge in clinical and public health settings (Perez and Bonomo, 2018). In general, isolates carrying *bla*_{NDM} tend to carry other resistance genes thus limiting treatment options (Falagas et al., 2014; Liu et al., 2019). Currently, the polymyxin antibiotics (polymyxin B and colistin) have reemerged as the last-line therapy against CRE. However, the clinical efficacy of polymyxin

antibiotics has been significantly compromised by the widespread emergence of mobile colistin resistance gene *mcr-1* (Liu et al., 2016). Worryingly, the MCR-1-producing *E. coli* that coexist with NDM-1, NDM-5, and NDM-9 have been recently reported worldwide, and these isolates possess resistance to fluoroquinolones, sulfonamides, β -lactams, tetracycline, and aminoglycosides (Du et al., 2016; Yao et al., 2016). Fortunately, the level of *mcr-1*-mediated colistin resistance is moderate (Sun et al., 2018), thus the use of colistin-based combinations would be of considerable clinical significance.

Tigecycline is the first of glycylcycline class that exhibited mainly bacteriostatic activity (Meagher et al., 2005). Of note, the decreased clinical efficacy and increased mortality have been previously reported regarding tigecycline monotherapy in the treatment of severe infections (Yahav et al., 2011). Therefore, clinicians should avoid tigecycline monotherapy to reserve it as another last-resort drug.

In this study, we systemically investigated the activity of colistin and tigecycline combination at the clinically achievable concentrations *in vitro* and in a murine thigh infection model against carbapenem-resistant *E. coli* harboring *bla*_{NDM-5}, especially in situations of pre-existing the *mcr-1* gene and high bacterial burdens. Additionally, we explored the underlying mechanisms of this combination (Figure 1) by determination of bacterial out-membrane integrity and tigecycline accumulation.

MATERIALS AND METHODS

Organisms, Media, and Antibiotics

Five well-described *E. coli* strains used in this study were 2630 (ST3902, *bla*_{NDM-5}), 3112 (ST1011, *mcr-1*), 1320 (ST648; *bla*_{NDM-5}, *mcr-1*), 2610 (ST101; *bla*_{NDM-5}, *mcr-1*), and 2121 (ST156; *bla*_{NDM-5}, *mcr-1*) (Sun et al., 2016a,b; Zhou et al., 2017). The *E. coli* strain ATCC 25922 (ST73) served as the negative control. The organisms were grown, subcultured, and quantified in cation-adjusted Mueller-Hinton broth (CAMHB) and agar (MHA; Difco Laboratories, Detroit, MI, United States). Colistin (CST), tigecycline (TGC), and other used antibiotics were purchased from Sigma-Aldrich (Shanghai, China) and prepared as fresh stock solutions in sterile water or medium prior to experiments.

Combinatorial Susceptibility Testing

The MICs of colistin for each *E. coli* strain were determined in the absence and presence of twofold increasing tigecycline concentrations (0.13–0.5 mg/L) using a modified broth microdilution method (Wiegand et al., 2008). The interaction of this combination was evaluated in duplicate for each isolate with a checkerboard assay (CST range 0.25–32 mg/L; TGC range 0.015–32 mg/L). Inhibition was read visually to calculate the fractional inhibitory concentration index (FICI), with an FICI \leq 0.5 deemed synergistic. In addition, cell density was assessed using a spectrometer to estimate cell densities for MacSynergy II analysis (Prichard and Shipman, 1990). The MacSynergy II program uses the Bliss independence algorithm to generate a 3-dimensional response profile of the

synergy-antagonism landscape by representing the theoretical indifferent surface. Peaks and troughs represent synergy and antagonism, respectively, and the extents of these were defined using interaction volumes (μM^2): <25 , additive; 25 to 50, minor but significant; 50 to 100, moderate; and >100 , strong synergy or antagonism (Deshpande et al., 2016; Lai et al., 2016). The results were expressed as the mean interaction volumes calculated at the 95% confidence level from three independent experiments.

Assessment of Colistin-Induced Outer-Membrane Disruption

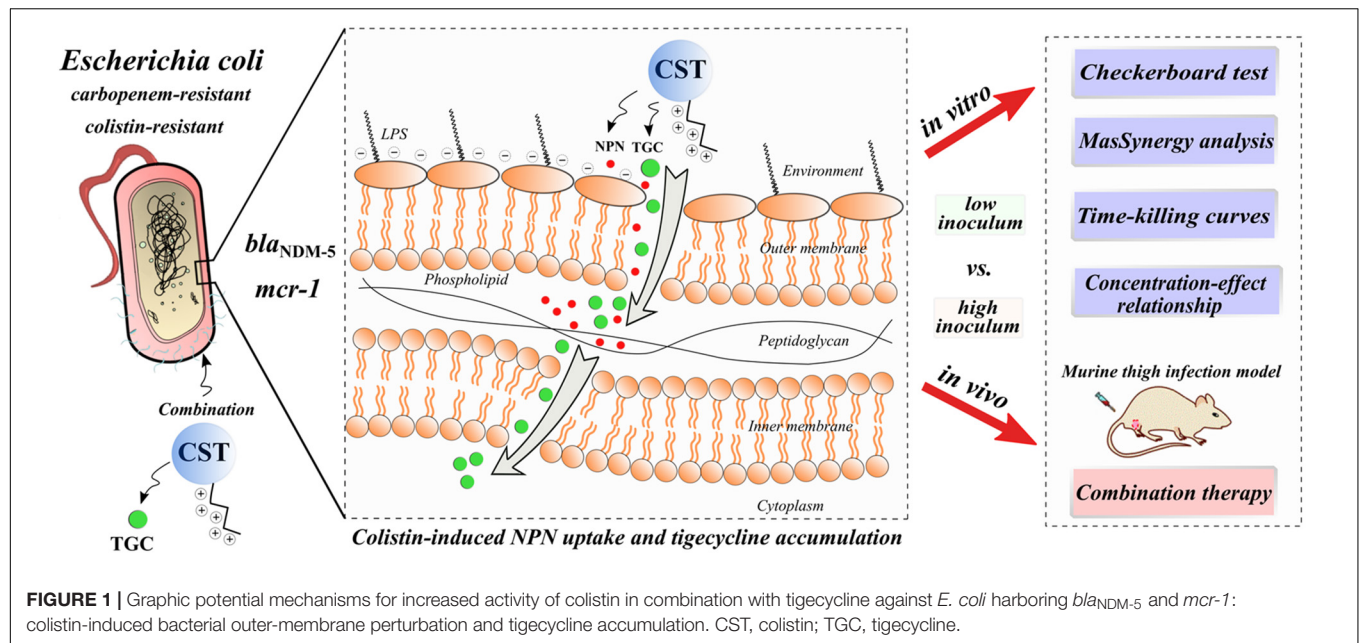
The 1-*N*-phenyl-*naphthylamine* (NPN) assay was performed to assess bacterial outer-membrane permeability to colistin as previously described (Buyck et al., 2012). Uptake of NPN by *E. coli* cells was a measure of the degree of permeability, and the subsequent fluorescence indicated a permeability breakdown (Macnair et al., 2018). Thus, NPN uptake was used to quantitatively indicate the colistin-induced outer membrane disruption. Mid-logarithmic cultures of *E. coli* strains were washed and suspended in PBS to a density of 10^9 cfu/mL (i.e., OD_{600nm} = 1.0). Bacterial cells were added to PBS containing NPN (10 μM) and varying concentrations of colistin in black 96-well microplates. After 1 h of incubation at 37°C, fluorescence was read using an EnSight multimode plate reader (PerkinElmer, Waltham, MA, United States) at 355 nm excitation and 405 nm emission wavelengths. NPN uptake (%) was calculated for each *E. coli* strain as described elsewhere (Macnair et al., 2018). Full NPN uptake (100%) was achieved by adding 100 mg/L of colistin.

Intracellular Accumulation of Tigecycline

The levels of tigecycline accumulation by *mcr-1*-positive and -negative *E. coli* strains in the absence and presence of colistin were determined as our previously described (Chen et al., 2017). Overnight cultures of *E. coli* strains were diluted to 10^9 cfu/mL into CAMHB and grown in the same medium for 20 min with 10 mg/L of tigecycline alone and in combination with 2 mg/L of colistin. Bacterial cells were collected by centrifugation at $3000 \times g$ for 10 min, washed with sterile normal saline and dried to obtain the dry weight. Bacteria cells were lysed by sonication for 15 min and then centrifuged at $3000 \times g$ for 10 min to remove the cell debris. Tigecycline concentrations in the resulting cell extracts were determined by a LC-MS/MS method (Sun et al., 2019; details are given in the **Supplementary Material**). All experiments were performed at least five independent biological replicates. Results were expressed as amount of tigecycline incorporated per dry weight of bacteria.

In vitro Time-Kill Experiments

In vitro time-kill experiments were conducted to characterize the activity of the colistin and tigecycline combination using previously described methods (Rao et al., 2016). In brief, overnight *E. coli* cultures ($\sim 10^6$ or 10^8 cfu/mL) were exposed to colistin (2 and 8 mg/L) alone and in combination with tigecycline (0.25 mg/L) over a period of 48 h. The choice of colistin concentrations was based on the clinically achievable serum steady-state concentration (C_{ss}) and peak concentration (C_{max})



in humans, while the tigecycline concentration was chosen to simulate the average C_{ss} at the clinical dose of 50 mg every 12 h (Van Wart et al., 2006; Tran et al., 2016; Nation et al., 2017). Serial samples were obtained at 0, 1, 3, 6, 9, 12, 24, 27, 30, 33, and 48 h after incubation at 37°C. Bacterial counts were determined based on the quantitative cultures on MHA plates. Historical time-kill data of colistin alone for portion of study strains were obtained from our previous report (Zhou et al., 2017).

In vitro Pharmacodynamic (PD) Analysis

The concentration-effect curves were used to quantitatively evaluate the potency of colistin and tigecycline combination against *E. coli* strains harboring *bla*_{NDM-5} and *mcr-1*, at initial inoculums of 10^6 and 10^8 cfu/mL, respectively. The testing procedure consisted of four groups, and each group included tubes with twofold increasing concentrations of colistin from 0.5 to 16 mg/L, in the absence and presence of tigecycline at 0.13, 0.25, and 0.5 mg/L. After 48 h of incubation, the microbiological response was measured by the \log_{10} change in bacterial density vs. pre-exposure at 0 h. The relationships between colistin concentrations and antibacterial response to single and combination therapies were fit to the Hill sigmoid E_{max} model: $E = E_0 + E_{max} \times C^N / (EC_{50}^N + C^N)$, where E_0 is the \log_{10} change in bacterial count without colistin, E_{max} is the maximal effect, EC_{50} is the colistin concentration required to achieve 50% of E_{max} and N is the slope of concentration-effect curve. The PD analysis was carried out by the non-linear least-squares regression in WinNonlin software Version 6.1 (Pharsight, Sunnyvale, CA, United States) (Zhou et al., 2017). The coefficient of determination (R^2) was used to estimate the variance of PD regression analysis. Mann-Whitney test was used to compare the parameters of E_{max} and EC_{50} between *mcr-1*-positive and -negative strains. Differences of PD parameter at 10^6 vs. 10^8 cfu/mL inoculum were determined using Wilcoxon signed-rank

test in GraphPad Prism 8 software (San Diego, CA, United States) and a P value of <0.05 was considered significant.

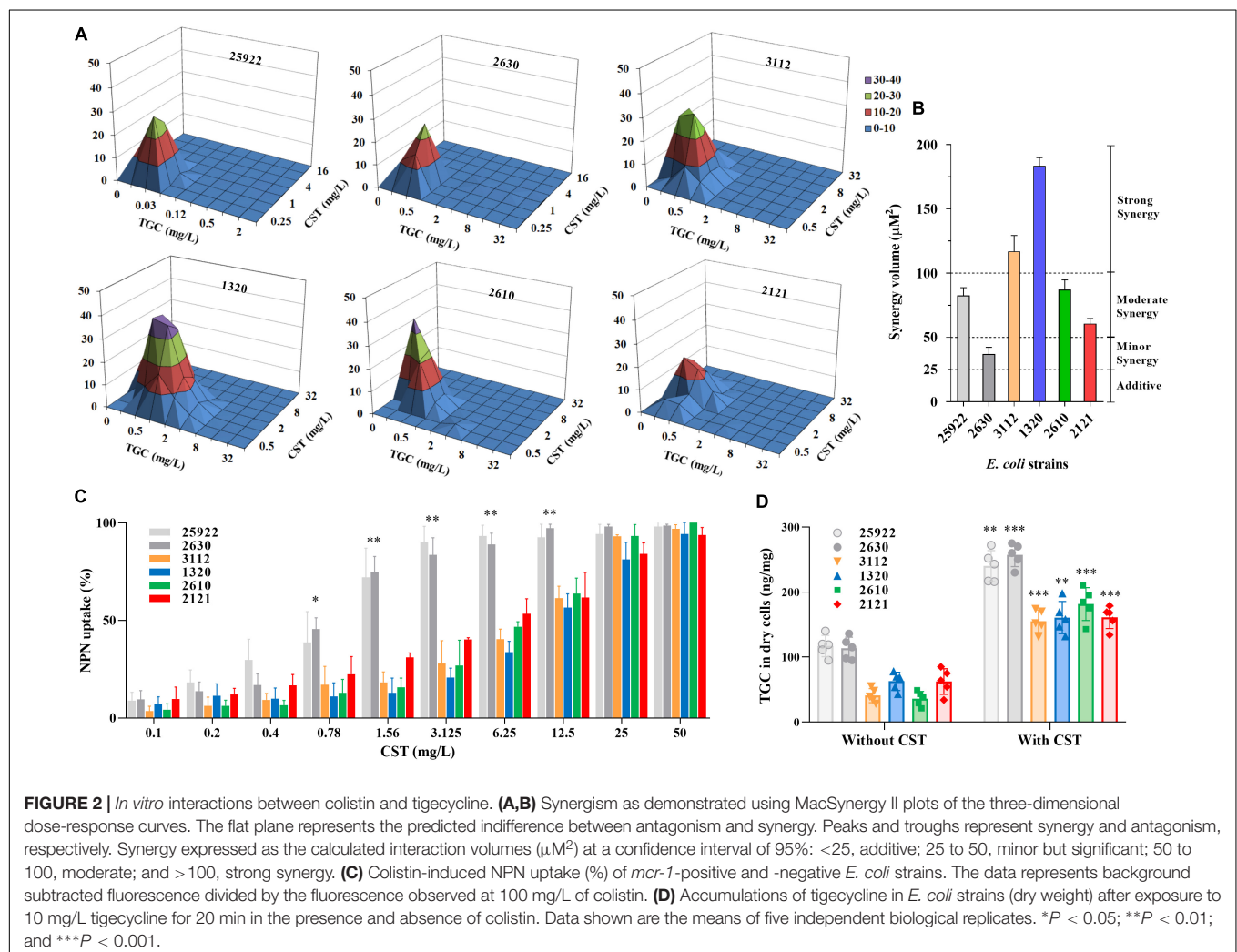
Murine Thigh Infection Model and Treatment Regimens

All animal experimental protocols were approved by South China Agricultural University (SCAU) Institutional Animal Ethics Committee (Guangzhou, China) and performed in accordance with the SCAU Institutional Laboratory Animal Care and Use guidelines. Six-week-old, 25–27 g, specific-pathogen-free, female ICR mice (Hunan SJA Laboratory Animal, Changsha, China) were rendered neutropenic by administration of cyclophosphamide intraperitoneally as previously described (Zhou et al., 2018). Thigh infections with each *E. coli* were produced by injecting 0.1 mL of bacterial suspension in normal saline ($10^{6.5}$ and $10^{8.5}$ cfu/mL). At 2 h after infection, mice were randomized to receive (i) no therapy (control), (ii) colistin at 7.5 mg/kg intraperitoneally (i.p.) twice a day (bid), (iii) tigecycline at 5 mg/kg subcutaneously (s.c.) bid, or (iv) combination of colistin and tigecycline. The current usual doses of colistin (3 MIU, equivalent to 240 mg, every 8 h) and tigecycline (100 mg initially, then 50 mg bid) were acceptable for the treatment of severe infections in humans (Meagher et al., 2005; Docobo-Perez et al., 2012). In this study, the drug doses in mice were selected to mimic the pharmacokinetic profiles of human clinical doses of 300 and 200 mg, respectively (Meagher et al., 2005; Karnik et al., 2013; Zhou et al., 2017; Zhao et al., 2018). Control and antibiotic-treated mice were sacrificed at 24 h after start of therapy. Thigh muscles were aseptically removed, homogenized and bacteria were cultured quantitatively using the plate counting method, and results were expressed as the \log_{10} cfu/thigh. Three mice (i.e., six thighs) were included in each group. The Mann-Whitney U -test was used to compare bacterial densities in target tissue between mono- and combination therapies.

TABLE 1 | Genotype summary, *in vitro* antimicrobial susceptibility profiles, and MICs of colistin in the absence and presence of tigecycline at 0.13, 0.25, and 0.5 mg/L against study *E. coli* strains^a.

<i>E. coli</i> strain	Relevant genotype	MIC (mg/L)								CST MIC (mg/L)				FIC index
		AMP	CTX	MEM	GEN	CIP	RIF	TET	TGC	CST alone	TGC 0.13	TGC 0.25	TGC 0.5	
25922	ST73; ATCC strain	4	0.06	0.03	0.5	0.008	4	1	0.13	1	NA	NA	NA	0.5
2630	ST3902; <i>bla</i> _{NDM-5}	256	256	64	16	256	32	128	1	0.5	0.5	0.25	0.13	0.75
3112	ST1011; <i>mcr-1</i>	256	128	0.13	256	128	256	64	1	8	2	2	1	0.37
1320	ST648; <i>bla</i> _{NDM-5} / <i>mcr-1</i>	128	64	16	32	128	8	128	2	4	2	0.5	0.5	0.37
2610	ST101; <i>bla</i> _{NDM-5} / <i>mcr-1</i>	256	256	16	64	256	256	64	1	4	2	1	1	0.5
2121	ST156; <i>bla</i> _{NDM-5} / <i>mcr-1</i>	256	256	16	128	128	4	128	1	8	4	2	0.5	0.5

^aAMP, ampicillin; CTX, cefotaxime; MEM, meropenem; GEN, gentamicin; CIP, ciprofloxacin; RIF, rifampicin; TET, tetracycline; TGC, tigecycline; CST, colistin; NA, not applicable.



RESULTS

In vitro Susceptibility and Interaction Assessment

The carbapenem-resistant *E. coli* strains were highly resistant to almost all tested antibiotics (Table 1). As expected, *E. coli* strain 2630 lacking *mcr-1* was susceptible to colistin, with an

MIC of 0.5 mg/L in the absence of tigecycline (Table 1). However, the strains that harbored *bla*_{NDM-5} and *mcr-1* were resistant both to meropenem (MIC ≥ 16 mg/L) and colistin (MIC ≥ 4 mg/L). Interestingly, colistin MICs for *mcr-1*-positive CRE strains decreased to 1/4 to 1/16 of the original levels as tigecycline concentration was raised from 0 to 0.5 mg/L (Table 1). This was confirmed using the checkerboard assay that showed

synergistic effects of the colistin and tigecycline combination. The FICI values varied from 0.38 to 0.5 for all except the colistin susceptible strain 2630 (Table 1). In particular, *E. coli* 1320 that carried both *bla*_{NDM-5} and *mcr-1* displayed a highly significant synergistic response to this combination across the range of drug concentrations tested, with a clear peak at 0.5 mg/L tigecycline and 1 or 2 mg/L colistin (Figure 2A). Different degrees of synergy were observed for all study *E. coli* strains with synergy volumes that ranged from 36.9 to 183 μM^2 (Figure 2B).

Colistin-Induced Outer-Membrane Perturbation and Tigecycline Accumulation

Carriage of *mcr-1* in carbapenem-resistant *E. coli* strains increased their resistance to colistin-induced outer-membrane

disruption as expected. NPN uptake in *mcr-1*-harboring *E. coli* was significantly less than *E. coli* 2630 after exposure to colistin at 0.78 to 12.5 mg/L (Figure 2C; $P < 0.05$), with corresponding colistin MIC increases from 8- to 16-fold (Table 1). The colistin concentrations required to achieve the comparable levels of NPN uptake increased eightfold in *mcr-1*-positive compared to -negative *E. coli* strains. For example, 45% of NPN uptake was observed at 0.78 mg/L colistin for colistin-susceptible *E. coli* 2630, while similar NPN uptake (38% to 53%) occurred at 6.25 mg/L colistin for *mcr-1*-harboring strains (Figure 2C). It seems that the additional levels of outer-membrane perturbation in a colistin-susceptible strain can be achieved by increasing the concentration of colistin eightfold in *mcr-1*-harboring *E. coli* strains. Importantly, when combined with the clinically relevant concentration of colistin at 2 mg/L, intracellular accumulations of tigecycline markedly increased in all study *E.*

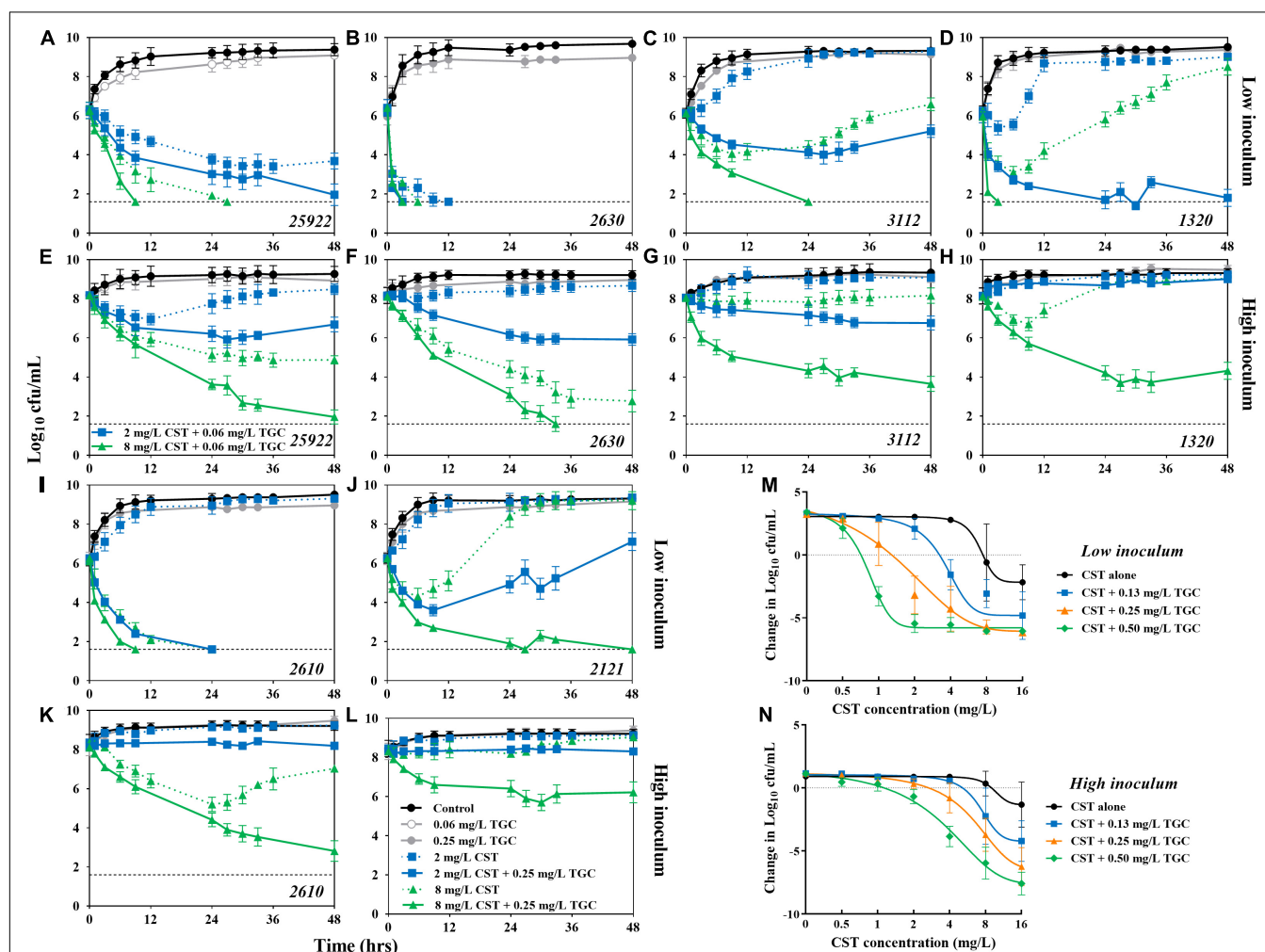


FIGURE 3 | Combinatorial bactericidal activity of colistin and tigecycline against *mcr-1*-positive and -negative *E. coli* strains harboring *bla*_{NDM-5}. (A–L) *In vitro* time-kill experiments of colistin (2 and 8 mg/L) alone and in combination with tigecycline (0.25 mg/L) against all study *E. coli* strains at low and high inoculums over 48 h. The horizontal dotted line represents the limit of detection for bacterial count (40 cfu/mL). Historical time-kill data of colistin alone for portion of strains was obtained from our previous study (Zhou et al., 2017). (M,N) The concentration-effect profiles of colistin against *E. coli* strains harboring both *bla*_{NDM-5} and *mcr-1* (i.e., 1320, 2610, and 2121) at low (M) and high (N) inoculums following treatment with colistin (0–16 mg/L) at fixed concentrations of tigecycline (0–0.5 mg/L). Each symbol represents the log_{10} change in bacterial burdens over a 48 h study period. Data points below the line represent killing and points above the line represent growth.

coli strains ($P < 0.01$; **Figure 2D**). Although the concentration of 2 mg/L colistin alone was insufficient to inhibit growth of *E. coli* harboring both *bla*_{NDM-5} and *mcr-1* (**Figures 3H–J**), it provided sufficient outer-membrane perturbation to facilitate tigecycline uptake and subsequent tigecycline-induced growth inhibition (**Figure 2D**).

In vitro Time-Kill Experiments

At a low inoculum (10^6 cfu/mL), colistin alone at 2 mg/L achieved complete the bactericidal activity ($>6.3\text{-log}_{10}$ reduction) over 24 h against colistin-susceptible strain 2630. The activity was not further improved at higher colistin levels or in combination with tigecycline (**Figure 3B**). Against the colistin-resistant *E. coli* 1320, the clinically achievable concentrations of colistin resulted in early bactericidal activity only, with a 1.3- to 3.2- \log_{10} reduction in bacterial density, followed by rapid regrowth beyond 6 h. However, complete bacterial eradication was attained with the combination of 8 mg/L colistin and 0.25 mg/L tigecycline (**Figure 3D**). Similarly, in the presence of 0.25 mg/L tigecycline, substantial killing of *E. coli* 2610 was achieved with >2 mg/L colistin (**Figure 3I**). Interestingly, despite the lack of activity that was observed for all colistin monotherapies against *E. coli* 2121, tigecycline displayed the ability to increase killing activity over 48 h of exposure to colistin (**Figure 3J**).

Monotherapy with a high colistin concentration (8 mg/L) or the combination of 0.25 mg/L tigecycline and 2 mg/L colistin exhibited sustained bactericidal activity at the high inoculum (10^8 cfu/mL) of *E. coli* 2630 (**Figure 3F**). However, even the high colistin levels of 8 mg/L were inactive for the colistin-resistant strains, whereas in combination with 0.25 mg/L tigecycline resulted in a 2.1- to 3.9- \log_{10} reduction in bacterial density (**Figures 3H,K–L**). Tigecycline monotherapy at 0.06 or 0.25 mg/L performed no different from the growth control against all study *E. coli* at both low and high inoculums (**Figure 3**).

Concentration-Effect Relationships

The concentration-effect relationship was fitted to a Hill-type equation ($R^2 > 0.95$), and the PD parameter of EC_{50} representing colistin potency was significantly greater in *mcr-1*-harboring strains compared with *E. coli* 2630 ($P < 0.01$; **Table 2**). In addition, the EC_{50} values at 10^8 cfu/mL inoculum were 1.5- to 18.4-times higher than those at 10^6 cfu/mL inoculum (mean = 5.3, $P < 0.001$). In the three strains that harbored *bla*_{NDM-5} and *mcr-1*, a clear tendency toward higher E_{\max} values were seen with a 10^8 cfu/mL inoculum, whereas no significant difference was noted at 10^6 cfu/mL (**Table 2**).

Overall, we found similar dose-dependent shifts with increasing tigecycline levels to a lower colistin concentration required to suppress the growth of *E. coli* at both inoculums (**Figures 3M,N**). For example, at 10^6 cfu/mL, inhibition of *E. coli* 2630 occurred at the colistin concentration of 0.75 mg/L and decreased threefold to 0.25 mg/L in the presence of tigecycline (**Supplementary Figure S1C**). Carriage of *mcr-1* increased the colistin concentration required for growth inhibition to 8 mg/L, which was 11-fold greater than for *E. coli* 2630 (**Figure 3M**). However, in combination with tigecycline from 0.13 to 0.5 mg/L, the colistin levels for growth inhibition were only 0.75 mg/L or

TABLE 2 | Hill PD parameters describing the concentration-response profiles of colistin (0–16 mg/L) in the presence of fixed tigecycline concentrations (0–0.5 mg/L) at low and high inoculums^a.

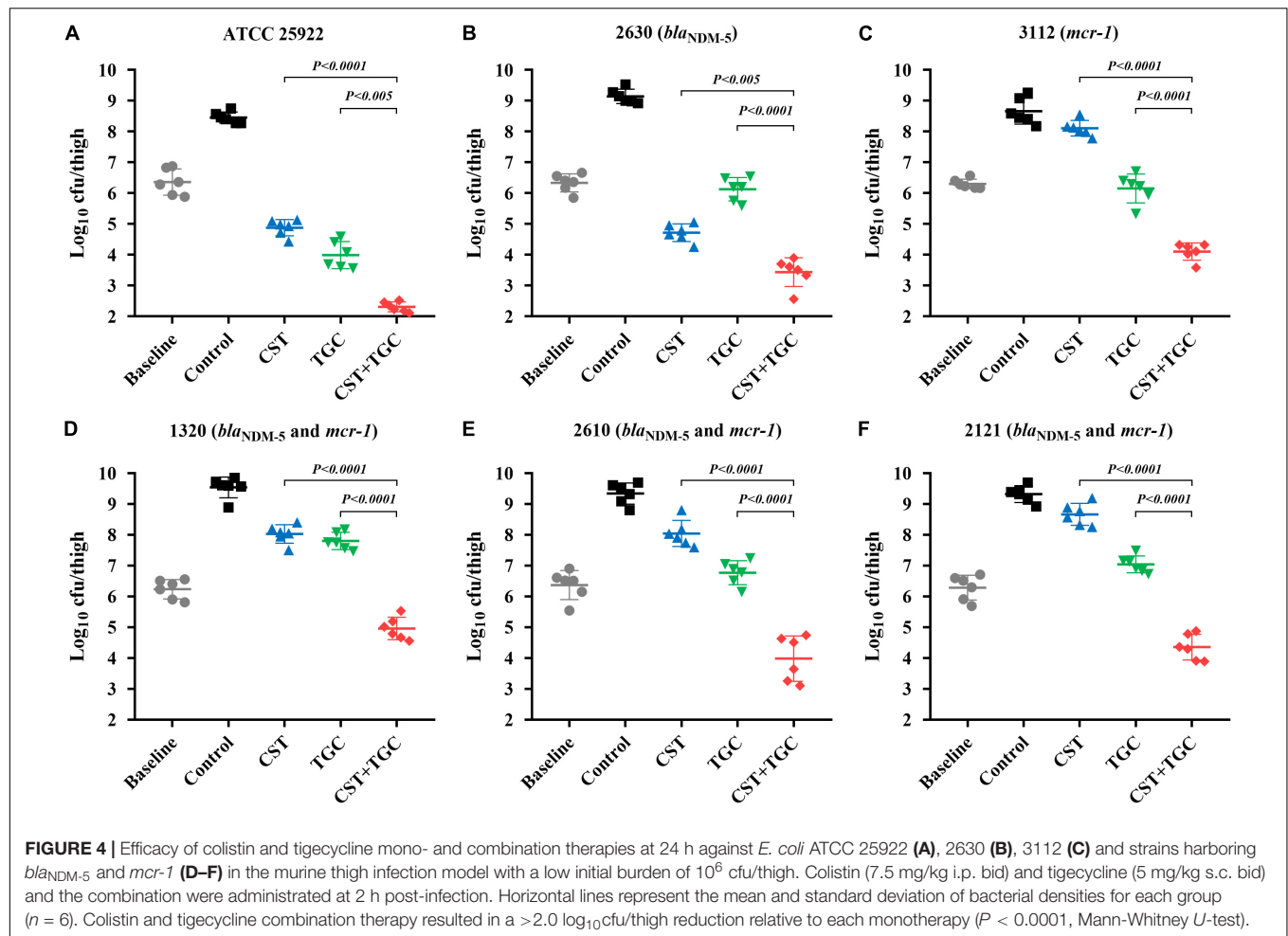
TGC (mg/L) in combination	10 ⁶ cfu/mL			10 ⁸ cfu/mL		
	E _{max}	EC ₅₀	N	E _{max}	EC ₅₀	N
PD parameters for <i>E. coli</i> ATCC 25922						
0	−9.61	1.58	2.24	−6.46	6.19	1.94
0.03	−9.85	1.01	1.53	−8.95	4.95	1.12
0.06	−8.74	0.83	1.30	−9.09	3.47	1.40
0.13	−7.22	0.55	1.73	−9.13	2.01	1.43
PD parameters for <i>E. coli</i> carrying <i>bla</i>_{NDM-5} (i.e., isolate 2630)						
0	−9.43	0.82	8.13	−9.11	6.75	4.68
0.13	−9.68	0.49	10.7	−9.14	5.45	3.71
0.25	−9.56	0.27	10.1	−9.17	4.98	1.18
0.50	−9.57	0.26	12.9	−9.41	2.36	1.22
PD parameters for <i>E. coli</i> carrying <i>mcr-1</i> only (i.e., isolate 3112)						
0	−5.60	5.98	2.07	−2.28	8.68	1.04
0.13	−9.48	3.96	2.55	−4.33	6.01	1.71
0.25	−9.42	2.34	2.37	−7.05	3.55	1.49
0.50	−9.30	1.05	1.84	−7.52	3.48	1.59
Mean PD parameters for <i>E. coli</i> carrying <i>bla</i>_{NDM-5} and <i>mcr-1</i> (i.e., 1320, 2610, and 2121)						
0	−6.53	7.37	5.66	−2.31	10.6	4.34
0.13	−8.23	5.50	3.97	−5.25	9.91	3.69
0.25	−9.42	2.09	2.56	−7.49	7.02	2.83
0.50	−9.36	0.80	4.17	−8.60	3.98	2.13

^a E_{\max} , maximum effect compared to the no drug control for a \log_{10} change of bacterial density after the 48 h study period; EC_{50} , colistin concentration required to achieve 50% E_{\max} ; N, slope of the concentration-effect curve.

twofold and fourfold greater than the concentration needed to synergize with tigecycline against *E. coli* 2630 (**Figure 3M** and **Supplementary Figure S1C**). It seems that the *mcr-1* gene only provided protection against colistin monotherapy, but not an ability to resist the colistin and tigecycline combination therapy.

In vivo Efficacy of Mono- and Combination Therapies

During thigh infection with a low initial burden, colistin monotherapy led to decreased bacterial density by 1.62- \log_{10} cfu/thigh for colistin-susceptible *E. coli* 2630, compared to the untreated control at 0 h (**Figure 4B**). However, for colistin-resistant strains, neither colistin nor tigecycline monotherapy showed a significant reduction in bacterial density after 24 h of therapy. Interestingly, colistin and tigecycline combination proved efficacious, resulting in >2.0 \log_{10} cfu/thigh reduction compared to each monotherapy ($P < 0.0001$, Mann-Whitney *U*-test; **Figures 4C–F**). The high initial burden in the murine thigh infection model was used to stimulate the severe infections that result in high mortality, and the effectiveness of combination therapy is a general proof of principle. Monotherapy with colistin or tigecycline did not achieve notable antibacterial effects against *E. coli* harboring *bla*_{NDM-5} and *mcr-1* at the high initial inoculum (**Figure 5**). Importantly, the combination of colistin and tigecycline significantly increased killing activity



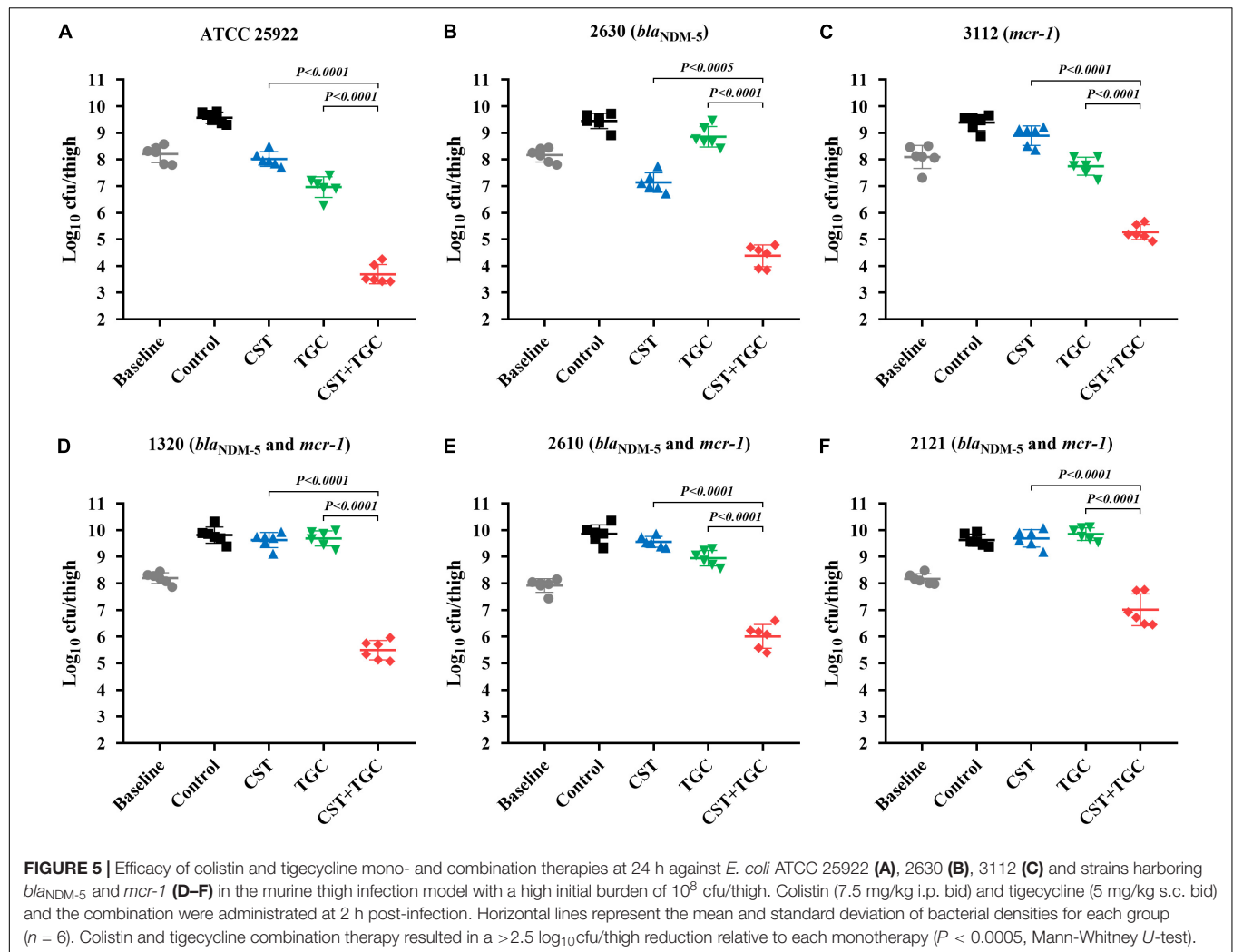
at 24 h by 1.1- to 2.7- log₁₀cfu/thigh reduction in bacterial density compared to control at 0 h or >2.5-log₁₀cfu/thigh compared to each monotherapy (*P* < 0.0005, Mann-Whitney U-test; Figures 5D–F).

DISCUSSION

Treatment options for carbapenem-resistant *E. coli* infections are very limited especially if the *mcr-1* gene is also present in the infecting strains. Tigecycline and colistin are currently the last-resort antibiotics for the treatment of severe infections (Sun et al., 2019). However, tigecycline demonstrates mainly bacteriostatic activity with low serum levels (Van Wart et al., 2006). Concerns have been raised regarding the efficacy of tigecycline monotherapy in the light of decreased clinical success rates (Yahav et al., 2011). Indeed, in the current study, tigecycline monotherapy did not achieve positive outcomes in a murine thigh infection model when the study *E. coli* strains harbored both *bla*_{NDM-5} and *mcr-1*, despite the fact that most of strains (5/6) remained susceptible to tigecycline except the strain 1320. Fortunately, the presence of *mcr-1* only slightly increased the MIC of colistin (Zhou et al., 2017).

Consequently, there was a compelling reason to use colistin and tigecycline in combination.

Colistin and tigecycline combination therapy against CRE infection had varying outcomes from synergy to indifference (Bercot et al., 2011; Karaoglan et al., 2013; Rao et al., 2016; Cai et al., 2017; Ku et al., 2017). In this study, combination of clinically achievable concentration of colistin and tigecycline produced a synergistic activity *in vitro* against *E. coli* harboring *bla*_{NDM-5} and *mcr-1*, resulting in a >4.0-log₁₀cfu/mL reduction by 48 h. An additional *in vivo* synergistic effect was indeed observed in the murine thigh model, at both low and high inoculums. Supporting our findings, colistin displayed a similar synergistic interaction with tigecycline for carbapenem-resistant *A. baumannii* and *K. pneumoniae* (Pournaras et al., 2011; Karaoglan et al., 2013; Ku et al., 2017). Data from previous case reports also showed beneficial activity of tigecycline and colistin combination therapy against *K. pneumoniae* bacteremia (Cobo et al., 2008). Interestingly, the higher dose of tigecycline has been shown to be associated with better synergistic outcomes against multidrug-resistant CRE, compared with the conventional dosing regimen (De Pascale et al., 2014; Cai et al., 2017). In contrast, a potential trend toward antagonism was observed at lower tigecycline concentrations (Albur et al., 2012).



Of note, previous studies that used this combination employed different methods, and the isolates were not well-described genotypically, making the results difficult to generalize. Here, we demonstrated increased activity of colistin in combination with tigecycline against *E. coli* strains that harbored *bla*_{NDM-5} and *mcr-1*, including the pandemic clonal complex ST648 (Hornsey et al., 2011). The clinical impact of infections due to colistin-resistant NDM-5-producing *E. coli* is currently unknown, but our findings provide an alternative approach to combat such resistant strains. In support of this view, a recent report indicated that colistin and tigecycline combination was able to prevent the emergence of high-level resistance to these antibiotics (Cai et al., 2017).

The potentiation effect of this combination is most likely related to their different mechanisms of action at separate bacterial targets. Tigecycline acts in the cytoplasm by binding to the ribosomal complex that requires drug to enter the bacterial cells first (Bauer et al., 2004). In general, uptake of tigecycline across the bacterial cell wall and cytoplasmic membrane includes two ways: passive diffusion and an energy-dependent active transport system (Schnappinger and Hillen, 1996; Chopra and Roberts, 2001). In Gram-negative bacteria, the cell wall is

surrounded by the outer-membrane and tigecycline moves through membranes via porin channels in the absence of colistin (Roberts, 2003). Colistin resulted in bacterial outer-membrane disruption and instable regions in cytoplasmic membrane that may facilitate tigecycline passive accumulation (Macnair et al., 2018). Supporting this speculation, our NPN uptake and intracellular tigecycline accumulation assays demonstrated that exposure to colistin did promote tigecycline uptake and subsequent tigecycline-induced growth inhibition independent of *mcr-1* expression. This scenario has been reported for colistin in combination with minocycline, the prodrug of tigecycline (Liang et al., 2011). However, the precise details of how colistin affects the energy-dependent transport of tigecycline still remain unclear.

Owing to the paucity of novel antibiotics, colistin-based combination therapy was therefore regarded as an alternative approach to combat colistin-resistant CRE infections. A synergistic effect of colistin with amikacin, rifampicin, and osthole has been reported (Lagerback et al., 2016; Liu X. et al., 2016; Zhou et al., 2017, 2019). However, systemic administration of colistin is associated with nephrotoxicity despite the fact that

toxicity is dose-dependent and reversible on discontinuation of treatment (Biswas et al., 2012). Therefore, the clinical utility of colistin should be prudent when used in combination with other nephrotoxic antibiotics such as gentamicin and amikacin. Previous nephrotoxicity studies in mice indicated that only mild kidney damage was observed until an accumulated dose of 72 mg/kg colistin, and suggested an acceptable colistin single dose ranges within 40 mg/kg in mice (Cheah et al., 2015; Roberts et al., 2015). Therefore, the much lower colistin dose (7.5 mg/kg) that used in this study should be safe for mice by comparison. In fact, many previous studies have employed 7.5 mg/kg colistin to carry out *in vivo* efficacy studies in mice (Liu et al., 2016; Zhou et al., 2017; Macnair et al., 2018). In the present study, tigecycline demonstrated bactericidal activity against *E. coli* harboring *bla*_{NDM-5} and *mcr-1* when combined with the clinically relevant concentration of colistin at 2 mg/L, which is considered as the appropriate partnered concentration to avoid renal impairment (Tran et al., 2016). Importantly, the combination of tigecycline with colistin we studied here may allow lower colistin dose sparing regimens that reduce nephrotoxicity for treating colistin-resistant CRE infections. Previous comparative observational studies also showed a lower-than-expected toxicity for tigecycline and colistin combination therapy (Zhang et al., 2013). Even patients with kidney disease could benefit from colistin-based combination therapy, when provided with a lower daily dose of colistin achieving comparable efficacy (Falagas et al., 2006; Biswas et al., 2012). In addition, a retrospective cohort study indicated that colistin is a valuable antibiotic with acceptable nephrotoxicity (<7%) and considerable efficacy that depends on daily dose (Falagas et al., 2010).

Our investigation has several limitations. For example, the combination was evaluated in a small number of strains despite the different clonal types. In addition, the murine thigh model is a local infection model, and additional study is needed to evaluate the usefulness of this combination in the clinical setting. Moreover, based on our current results, we do not know whether the colistin-induced increased accumulation of tigecycline in bacterial cells is “drug specific” or more broad range for other antibiotics. Although this is beyond the scope of this study, future studies should examine this potential mechanism.

In summary, this study demonstrated increased activity of colistin and tigecycline combination against *E. coli* harboring *bla*_{NDM-5} and *mcr-1*. Importantly, a potentiation effect occurred at the clinically relevant concentrations of colistin and tigecycline, and was efficacious in the murine thigh infection model. In addition, we demonstrated for the first time that colistin permeabilization of the bacterial outer-membrane facilitates

the uptake of tigecycline, contributing to increased activity of the combination.

DATA AVAILABILITY STATEMENT

The raw data supporting the conclusions of this article will be made available by the authors, without undue reservation, to any qualified researcher.

ETHICS STATEMENT

This study was carried out in accordance with the recommendations of ethical guidelines of South China Agricultural University. All animal experimental protocols and isolation procedures for *E. coli* strains were reviewed and approved by the South China Agricultural University Institutional Animal Ethics Committee (2019B161 and 2018B095). Individual written informed consent for the use of isolates was obtained.

AUTHOR CONTRIBUTIONS

Y-HL and Y-FZ designed the study and wrote the manuscript. Y-FZ, PL, and C-JZ carried out the experiments. JS and X-PL analyzed the data. All authors read and approved the final manuscript.

FUNDING

This study was supported by the National Key Research and Development Program of China (2016YFD0501300), the National Natural Science Foundation of China (31730097 and 31772793), the Program of Changjiang Scholars and Innovative Research Team in University of Ministry of Education of China (IRT_17R39), and the Foundation for Innovation and Strengthening School Project of Guangdong, China (2016KCXTD010).

SUPPLEMENTARY MATERIAL

The Supplementary Material for this article can be found online at: <https://www.frontiersin.org/articles/10.3389/fmicb.2019.02957/full#supplementary-material>

REFERENCES

- Albur, M., Noel, A., Bowker, K., and Macgowan, A. (2012). Bactericidal activity of multiple combinations of tigecycline and colistin against NDM-1-producing *Enterobacteriaceae*. *Antimicrob. Agents Chemother.* 56, 3441–3443. doi: 10.1128/AAC.05682-11
- Bauer, G., Berens, C., Projan, S. J., and Hillen, W. (2004). Comparison of tetracycline and tigecycline binding to ribosomes mapped by dimethylsulphate and drug-directed Fe²⁺ cleavage of 16S rRNA. *J. Antimicrob. Chemother.* 53, 592–599. doi: 10.1093/jac/dkh125
- Bercot, B., Poirer, L., Dortet, L., and Nordmann, P. (2011). In vitro evaluation of antibiotic synergy for NDM-1-producing *Enterobacteriaceae*. *J. Antimicrob. Chemother.* 66, 2295–2297. doi: 10.1093/jac/dkr296
- Biswas, S., Brunel, J. M., Dubus, J. C., Reynaud-Gaubert, M., and Rolain, J. M. (2012). Colistin: an update on the antibiotic of the 21st century. *Expert Rev. Anti Infect. Ther.* 10, 917–934. doi: 10.1586/eri.12.78

- Buyck, J. M., Plesiat, P., Traore, H., Vanderbist, F., Tulkens, P. M., and Van Bambeke, F. (2012). Increased susceptibility of *Pseudomonas aeruginosa* to macrolides and ketolides in eukaryotic cell culture media and biological fluids due to decreased expression of *oprM* and increased outer-membrane permeability. *Clin. Infect. Dis.* 55, 534–542. doi: 10.1093/cid/cis473
- Cai, X., Yang, Z., Dai, J., Chen, K., Zhang, L., Ni, W., et al. (2017). Pharmacodynamics of tigecycline alone and in combination with colistin against clinical isolates of multidrug-resistant *Acinetobacter baumannii* in an *in vitro* pharmacodynamic model. *Int. J. Antimicrob. Agents* 49, 609–616. doi: 10.1016/j.ijantimicag.2017.01.007
- Cheah, S. E., Wang, J., Nguyen, V. T., Turnidge, J. D., Li, J., and Nation, R. L. (2015). New pharmacokinetic/pharmacodynamic studies of systemically administered colistin against *Pseudomonas aeruginosa* and *Acinetobacter baumannii* in mouse thigh and lung infection models: smaller response in lung infection. *J. Antimicrob. Chemother.* 70, 3291–3297. doi: 10.1093/jac/dkv267
- Chen, Y., Hu, D., Zhang, Q., Liao, X. P., Liu, Y. H., and Sun, J. (2017). Efflux Pump overexpression contributes to tigecycline heteroresistance in *Salmonella enterica* serovar Typhimurium. *Front. Cell Infect. Microbiol.* 7:37. doi: 10.3389/fcimb.2017.00037
- Chopra, I., and Roberts, M. (2001). Tetracycline antibiotics: mode of action, applications, molecular biology, and epidemiology of bacterial resistance. *Microbiol. Mol. Biol. Rev.* 65, 232–260. doi: 10.1128/mmr.65.2.232-260.2001
- Cobo, J., Morosini, M. I., Pintado, V., Tato, M., Samaranch, N., Baquero, F., et al. (2008). Use of tigecycline for the treatment of prolonged bacteremia due to a multiresistant VIM-1 and SHV-12 beta-lactamase-producing *Klebsiella pneumoniae* epidemic clone. *Diagn. Microbiol. Infect. Dis.* 60, 319–322. doi: 10.1016/j.diagmicrobio.2007.09.017
- De Pascale, G., Montini, L., Pennisi, M., Bernini, V., Maviglia, R., Bello, G., et al. (2014). High dose tigecycline in critically ill patients with severe infections due to multidrug-resistant bacteria. *Crit. Care* 18:R90. doi: 10.1186/cc13858
- Deshpande, D., Srivastava, S., Nuernberger, E., Pasipanodya, J. G., Swaminathan, S., and Gumbo, T. (2016). Concentration-dependent synergy and antagonism of linezolid and moxifloxacin in the treatment of childhood tuberculosis: the dynamic duo. *Clin. Infect. Dis.* 63, s88–s94. doi: 10.1093/cid/ciw473
- Docobo-Perez, F., Nordmann, P., Dominguez-Herrera, J., Lopez-Rojas, R., Smani, Y., Poirer, L., et al. (2012). Efficacies of colistin and tigecycline in mice with experimental pneumonia due to NDM-1-producing strains of *Klebsiella pneumoniae* and *Escherichia coli*. *Int. J. Antimicrob. Agents* 39, 251–254. doi: 10.1016/j.ijantimicag.2011.10.012
- Du, H., Chen, L., Tang, Y. W., and Kreiswirth, B. N. (2016). Emergence of the *mcr-1* colistin resistance gene in carbapenem-resistant *Enterobacteriaceae*. *Lancet Infect. Dis.* 16, 287–288. doi: 10.1016/s1473-3099(16)00056-6
- Falagas, M. E., Lourida, P., Poulidakos, P., Rafailidis, P. I., and Tansarli, G. S. (2014). Antibiotic treatment of infections due to carbapenem-resistant *Enterobacteriaceae*: systematic evaluation of the available evidence. *Antimicrob. Agents Chemother.* 58, 654–663. doi: 10.1128/AAC.01222-13
- Falagas, M. E., Rafailidis, P. I., Ioannidou, E., Alexiou, V. G., Matthaiou, D. K., Karageorgopoulos, D. E., et al. (2010). Colistin therapy for microbiologically documented multidrug-resistant Gram-negative bacterial infections: a retrospective cohort study of 258 patients. *Int. J. Antimicrob. Agents* 35, 194–199. doi: 10.1016/j.ijantimicag.2009.10.005
- Falagas, M. E., Rafailidis, P. I., Kasiakou, S. K., Hatzopoulou, P., and Michalopoulos, A. (2006). Effectiveness and nephrotoxicity of colistin monotherapy vs. colistin-meropenem combination therapy for multidrug-resistant Gram-negative bacterial infections. *Clin. Microbiol. Infect.* 12, 1227–1230. doi: 10.1111/j.1469-0691.2006.01559.x
- Hornsey, M., Phee, L., and Wareham, D. W. (2011). A novel variant, NDM-5, of the New Delhi metallo-beta-lactamase in a multidrug-resistant *Escherichia coli* ST648 isolate recovered from a patient in the United Kingdom. *Antimicrob. Agents Chemother.* 55, 5952–5954. doi: 10.1128/AAC.05108-11
- Karaoglan, I., Zer, Y., Bosnak, V. K., Mete, A. O., and Namiduru, M. (2013). *In vitro* synergistic activity of colistin with tigecycline or beta-lactam antibiotic/beta-lactamase inhibitor combinations against carbapenem-resistant *Acinetobacter baumannii*. *J. Int. Med. Res.* 41, 1830–1837. doi: 10.1177/0300060513496172
- Karnik, N. D., Sridharan, K., Jadhav, S. P., Kadam, P. P., Naidu, R. K., Namjoshi, R. D., et al. (2013). Pharmacokinetics of colistin in critically ill patients with multidrug-resistant Gram-negative bacilli infection. *Eur. J. Clin. Pharmacol.* 69, 1429–1436. doi: 10.1007/s00228-013-1493-9
- Ku, Y. H., Chen, C. C., Lee, M. F., Chuang, Y. C., Tang, H. J., and Yu, W. L. (2017). Comparison of synergism between colistin, fosfomycin and tigecycline against extended-spectrum beta-lactamase-producing *Klebsiella pneumoniae* isolates or with carbapenem resistance. *J. Microbiol. Immunol. Infect.* 50, 931–939. doi: 10.1016/j.jmii.2016.12.008
- Lagerback, P., Khine, W. W., Giske, C. G., and Tangden, T. (2016). Evaluation of antibacterial activities of colistin, rifampicin and meropenem combinations against NDM-1-producing *Klebsiella pneumoniae* in 24 h *in vitro* time-kill experiments. *J. Antimicrob. Chemother.* 71, 2321–2325. doi: 10.1093/jac/dkw213
- Lai, Y. W., Campbell, L. T., Wilkins, M. R., Pang, C. N., Chen, S., and Carter, D. A. (2016). Synergy and antagonism between iron chelators and antifungal drugs in *Cryptococcus*. *Int. J. Antimicrob. Agents* 48, 388–394. doi: 10.1016/j.ijantimicag.2016.06.012
- Liang, W., Liu, X. F., Huang, J., Zhu, D. M., Li, J., and Zhang, J. (2011). Activities of colistin- and minocycline-based combinations against extensive drug resistant *Acinetobacter baumannii* isolates from intensive care unit patients. *BMC Infect. Dis.* 11:109. doi: 10.1186/1471-2334-11-109
- Liu, S., Zhang, J., Zhou, Y., Hu, N., Li, J., Wang, Y., et al. (2019). Pterostilbene restores carbapenem susceptibility in NDM-producing isolates via inhibiting the activity of NDM enzymes. *Br. J. Pharmacol.* [Epub ahead of print].
- Liu, X., Zhao, M., Chen, Y., Bian, X., Li, Y., Shi, J., et al. (2016). Synergistic killing by meropenem and colistin combination of carbapenem-resistant *Acinetobacter baumannii* isolates from Chinese patients in an *in vitro* pharmacokinetic/pharmacodynamic model. *Int. J. Antimicrob. Agents* 48, 559–563. doi: 10.1016/j.ijantimicag.2016.07.018
- Liu, Y. Y., Wang, Y., Walsh, T. R., Yi, L. X., Zhang, R., Spencer, J., et al. (2016). Emergence of plasmid-mediated colistin resistance mechanism MCR-1 in animals and human beings in China: a microbiological and molecular biological study. *Lancet Infect. Dis.* 16, 161–168. doi: 10.1016/S1473-3099(15)00424-7
- Macnair, C. R., Stokes, J. M., Carfrae, L. A., Fiebig-Comyn, A. A., Coombes, B. K., Mulvey, M. R., et al. (2018). Overcoming *mcr-1* mediated colistin resistance with colistin in combination with other antibiotics. *Nat. Commun.* 9:458. doi: 10.1038/s41467-018-02875-z
- Meagher, A. K., Ambrose, P. G., Grasela, T. H., and Ellis-Grosse, E. J. (2005). The pharmacokinetic and pharmacodynamic profile of tigecycline. *Clin. Infect. Dis.* 41(Suppl. 5), S333–S340.
- Nation, R. L., Garonzik, S. M., Thamlikitkul, V., Giamarellos-Bourboulis, E. J., Forrest, A., Paterson, D. L., et al. (2017). Dosing guidance for intravenous colistin in critically-ill patients. *Clin. Infect. Dis.* 64, 565–571. doi: 10.1093/cid/ciw839
- Perez, F., and Bonomo, R. A. (2018). Evidence to improve the treatment of infections caused by carbapenem-resistant Gram-negative bacteria. *Lancet Infect. Dis.* 18, 358–360. doi: 10.1016/s1473-3099(18)30112-9
- Pournaras, S., Vriani, G., Neou, E., Dendrinos, J., Dimitroulia, E., Poulou, A., et al. (2011). Activity of tigecycline alone and in combination with colistin and meropenem against *Klebsiella pneumoniae* carbapenemase (KPC)-producing *Enterobacteriaceae* strains by time-kill assay. *Int. J. Antimicrob. Agents* 37, 244–247. doi: 10.1016/j.ijantimicag.2010.10.031
- Prichard, M. N., and Shipman, C. Jr. (1990). A three-dimensional model to analyze drug-drug interactions. *Antiviral Res.* 14, 181–205. doi: 10.1016/0166-3542(90)90001-n
- Rao, G. G., Ly, N. S., Diep, J., Forrest, A., Bulitta, J. B., Holden, P. N., et al. (2016). Combinatorial pharmacodynamics of polymyxin B and tigecycline against heteroresistant *Acinetobacter baumannii*. *Int. J. Antimicrob. Agents* 48, 331–336. doi: 10.1016/j.ijantimicag.2016.06.006
- Roberts, K. D., Azad, M. A., Wang, J., Horne, A. S., Thompson, P. E., Nation, R. L., et al. (2015). Antimicrobial activity and toxicity of the major lipopeptide components of polymyxin B and colistin: last-line antibiotics against multidrug-resistant gram-negative bacteria. *ACS Infect. Dis.* 1, 568–575. doi: 10.1021/acsinfecdis.5b00085
- Roberts, M. C. (2003). Tetracycline therapy: update. *Clin. Infect. Dis.* 36, 462–467. doi: 10.1086/367622
- Schnappinger, D., and Hillen, W. (1996). Tetracyclines: antibiotic action, uptake, and resistance mechanisms. *Arch. Microbiol.* 165, 359–369. doi: 10.1007/s002030050339
- Sun, J., Chen, C., Cui, C. Y., Zhang, Y., Liu, X., Cui, Z. H., et al. (2019). Plasmid-encoded *tet(X)* genes that confer high-level tigecycline resistance

- in *Escherichia coli*. *Nat. Microbiol.* 4, 1457–1464. doi: 10.1038/s41564-019-0496-4
- Sun, J., Li, X. P., Yang, R. S., Fang, L. X., Huo, W., Li, S. M., et al. (2016a). Complete nucleotide sequence of an IncI2 plasmid coharboring blaCTX-M-55 and mcr-1. *Antimicrob. Agents Chemother.* 60, 5014–5017. doi: 10.1128/AAC.00774-16
- Sun, J., Yang, R. S., Zhang, Q., Feng, Y., Fang, L. X., Xia, J., et al. (2016b). Co-transfer of blaNDM-5 and mcr-1 by an IncX3-X4 hybrid plasmid in *Escherichia coli*. *Nat. Microbiol.* 1:16176. doi: 10.1038/nmicrobiol.2016.176
- Sun, J., Zhang, H., Liu, Y. H., and Feng, Y. (2018). Towards understanding MCR-like colistin resistance. *Trends Microbiol.* 26, 794–808. doi: 10.1016/j.tim.2018.02.006
- Tran, T. B., Velkov, T., Nation, R. L., Forrest, A., Tsuji, B. T., Bergen, P. J., et al. (2016). Pharmacokinetics/pharmacodynamics of colistin and polymyxin B: are we there yet? *Int. J. Antimicrob. Agents* 48, 592–597. doi: 10.1016/j.ijantimicag.2016.09.010
- Van Wart, S. A., Owen, J. S., Ludwig, E. A., Meagher, A. K., Korth-Bradley, J. M., and Cirincione, B. B. (2006). Population pharmacokinetics of tigecycline in patients with complicated intra-abdominal or skin and skin structure infections. *Antimicrob. Agents Chemother.* 50, 3701–3707. doi: 10.1128/aac.01636-05
- Wiegand, I., Hilpert, K., and Hancock, R. E. (2008). Agar and broth dilution methods to determine the minimal inhibitory concentration (MIC) of antimicrobial substances. *Nat. Protoc.* 3, 163–175. doi: 10.1038/nprot.2007.521
- Yahav, D., Lador, A., Paul, M., and Leibovici, L. (2011). Efficacy and safety of tigecycline: a systematic review and meta-analysis. *J. Antimicrob. Chemother.* 66, 1963–1971. doi: 10.1093/jac/dkr242
- Yao, X., Doi, Y., Zeng, L., Lv, L., and Liu, J. H. (2016). Carbapenem-resistant and colistin-resistant *Escherichia coli* co-producing NDM-9 and MCR-1. *Lancet Infect. Dis.* 16, 288–289. doi: 10.1016/s1473-3099(16)00057-8
- Zhang, H. Z., Zhang, J. S., and Qiao, L. (2013). The *Acinetobacter baumannii* group: a systemic review. *World J. Emerg. Med.* 4, 169–174. doi: 10.5847/wjem.j.1920-8642.2013.03.002
- Zhao, M., Wu, X. J., Fan, Y. X., Zhang, Y. Y., Guo, B. N., Yu, J. C., et al. (2018). Pharmacokinetics of colistin methanesulfonate (CMS) in healthy Chinese subjects after single and multiple intravenous doses. *Int. J. Antimicrob. Agents* 51, 714–720. doi: 10.1016/j.ijantimicag.2017.12.025
- Zhou, Y., Wang, J., Guo, Y., Liu, X., Liu, S., Niu, X., et al. (2019). Discovery of a potential MCR-1 inhibitor that reverses polymyxin activity against clinical mcr-1-positive *Enterobacteriaceae*. *J. Infect.* 78, 364–372. doi: 10.1016/j.jinf.2019.03.004
- Zhou, Y. F., Tao, M. T., Feng, Y., Yang, R. S., Liao, X. P., Liu, Y. H., et al. (2017). Increased activity of colistin in combination with amikacin against *Escherichia coli* co-producing NDM-5 and MCR-1. *J. Antimicrob. Chemother.* 72, 1723–1730. doi: 10.1093/jac/dkx038
- Zhou, Y. F., Tao, M. T., He, Y. Z., Sun, J., Liu, Y. H., and Liao, X. P. (2018). In Vivo bioluminescent monitoring of therapeutic efficacy and pharmacodynamic target assessment of tofloxacin against *Escherichia coli* in a neutropenic murine thigh infection model. *Antimicrob. Agents Chemother.* 62:e01281-17. doi: 10.1128/AAC.01281-17

Conflict of Interest: The authors declare that the research was conducted in the absence of any commercial or financial relationships that could be construed as a potential conflict of interest.

Copyright © 2020 Zhou, Liu, Zhang, Liao, Sun and Liu. This is an open-access article distributed under the terms of the Creative Commons Attribution License (CC BY). The use, distribution or reproduction in other forums is permitted, provided the original author(s) and the copyright owner(s) are credited and that the original publication in this journal is cited, in accordance with accepted academic practice. No use, distribution or reproduction is permitted which does not comply with these terms.



Inhibition of Transglutaminase 2 as a Potential Host-Directed Therapy Against *Mycobacterium tuberculosis*

Ivana Palucci^{1,2†}, Giuseppe Maulucci^{1,3†}, Flavio De Maio^{1,2}, Michela Sali^{1,2}, Alessandra Romagnoli⁴, Linda Petrone⁵, Gian Maria Fimia^{4,6}, Maurizio Sanguinetti^{1,2}, Delia Goletti⁵, Marco De Spirito^{1,3}, Mauro Piacentini^{4,7*} and Giovanni Delogu^{1,2,8*}

¹ Fondazione Policlinico Universitario A. Gemelli IRCCS, Rome, Italy, ² Institute of Microbiology, Università Cattolica del Sacro Cuore, Rome, Italy, ³ Institute of Physics, Università Cattolica del Sacro Cuore, Rome, Italy, ⁴ Electron Microscopy and Cell Biology Unit, Department of Epidemiology and Preclinical Research, "L. Spallanzani" National Institute for Infectious Diseases (INMI), IRCCS, Rome, Italy, ⁵ Translational Research Unit, Department of Epidemiology and Preclinical Research, "L. Spallanzani" National Institute for Infectious Diseases (INMI), IRCCS, Rome, Italy, ⁶ Department of Molecular Medicine, Sapienza University of Rome, Rome, Italy, ⁷ Department of Biology, University of Rome "Tor Vergata", Rome, Italy, ⁸ Mater Olbia Hospital, Olbia, Italy

OPEN ACCESS

Edited by:

Maurizio Fraziano,
University of Rome Tor Vergata, Italy

Reviewed by:

Andreas Kupz,
James Cook University, Australia
Ricardo Silvestre,
University of Minho, Portugal

*Correspondence:

Mauro Piacentini
mauro.piacentini@uniroma2.it
Giovanni Delogu
giovanni.delogu@unicatt.it

[†]These authors have contributed
equally to this work

Specialty section:

This article was submitted to
Microbial Immunology,
a section of the journal
Frontiers in Immunology

Received: 24 September 2019

Accepted: 11 December 2019

Published: 24 January 2020

Citation:

Palucci I, Maulucci G, De Maio F,
Sali M, Romagnoli A, Petrone L,
Fimia GM, Sanguinetti M, Goletti D, De
Spirito M, Piacentini M and Delogu G
(2020) Inhibition of Transglutaminase 2
as a Potential Host-Directed Therapy
Against *Mycobacterium tuberculosis*.
Front. Immunol. 10:3042.
doi: 10.3389/fimmu.2019.03042

Host-directed therapies (HDTs) are emerging as a potential valid support in the treatment of drug-resistant tuberculosis (TB). Following our recent report indicating that genetic and pharmacological inhibition of transglutaminase 2 (TG2) restricts *Mycobacterium tuberculosis* (*Mtb*) replication in macrophages, we aimed to investigate the potentials of the TG2 inhibitors cystamine and cysteamine as HDTs against TB. We showed that both cysteamine and cystamine restricted *Mtb* replication in infected macrophages when provided at equimolar concentrations and did not exert any antibacterial activity when administered directly on *Mtb* cultures. Interestingly, infection of differentiated THP-1 mRFP-GFP-LC3B cells followed by the determination of the autophagic intermediates pH distribution (AIPD) showed that cystamine inhibited the autophagic flux while restricting *Mtb* replication. Moreover, both cystamine and cysteamine had a similar antimicrobial activity in primary macrophages infected with a panel of *Mtb* clinical strains belonging to different phylogeographic lineages. Evaluation of cysteamine and cystamine activity in the human ex vivo model of granuloma-like structures (GLS) further confirmed the ability of these drugs to restrict *Mtb* replication and to reduce the size of GLS. The antimicrobial activity of the TG2 inhibitors synergized with a second-line anti-TB drug as amikacin in human monocyte-derived macrophages and in the GLS model. Overall, the results of this study support the potential usefulness of the TG2-inhibitors cysteamine and cystamine as HDTs against TB.

Keywords: tuberculosis, transglutaminase 2, host-directed therapy, *Mycobacterium tuberculosis*, macrophage, MDR-TB

INTRODUCTION

Tuberculosis (TB) is a leading cause of death worldwide with 10 million new TB cases and 1.6 million deaths in 2017 alone (1). The emergence and spread of *Mycobacterium tuberculosis* (*Mtb*) strains resistant to the two most common drugs isoniazid and rifampicin (multidrug-resistant *Mtb*, MDR-TB) are a cause of major concern. Among the half million cases of MDR-TB estimated in 2017, 8.5% are expected to have a pattern of extensively drug resistant-TB (XDR-TB), defined as the additional non-susceptibility to fluoroquinolones and an injectable drug (1). Drug

regimens for MDR-TB patients are much more complex and toxic compared to those commonly administered to patients with drug-susceptible TB and consist in the combined administration of at least four drugs for up to 20 months (2, 3). Despite the introduction of new drugs, therapeutic regimens of MDR-TB and XDR-TB patients show poor success rates that rarely exceed 50% in high-burden countries (4). Moreover, these regimens are very expensive; combining direct and indirect costs, in EU states and the US, the average cost for an MDR-TB patient is five to six times higher than a drug-susceptible patient and increases up to 20 times for XDR-TB (2, 5). These high costs associated with the treatment of drug-resistant TB pose a major burden to many countries, with relevant health, social, and economic consequences (2).

There is an urgent need of improved treatment options for TB, and the introduction of the new drugs delamanid and bedaquiline, while widening the therapeutic options, has already led to the emergence of *Mtb* strains resistant to these drugs (6), frustrating the hopes of scientists, public health authorities, and patients. In the last few years, also thanks to new insights in TB pathogenesis, several host-directed therapies (HDTs) have been proposed as adjunct therapy against TB and primarily against the drug-resistant forms that do not respond to the available treatments (7–9). Some of these HDTs are based on the repurposing of old drugs which have already shown a good safety record in previous clinical trials (7, 8), as is the case for metformin (10), statins (11), and other drugs (12). These treatments may enhance the host antimicrobial defenses or provide beneficial effects by interfering with the mechanisms exploited by the pathogen to persist in host tissues or by lessening inflammation and reducing tissue damage. These beneficial effects of HDTs can synergize with the anti-TB regimens, resulting in improved clinical outcomes and reduced risk for emergence of drug resistance, and may lead to shorter anti-TB regimens.

Transglutaminase 2 (TG2) is a pleiotropic enzyme belonging to the transglutaminase family involved in several important cellular processes including cell death/survival and autophagy (13–15). We have recently shown that genetic or pharmacological inactivation of TG2 enhances the anti-mycobacterial properties of *Mtb*-infected macrophages, which intriguingly correlate with reduced cell death and impairment of the LC3/autophagy homeostasis (16). Interestingly, two TG2 inhibitors, cystamine and cysteamine, have already been tested in clinical trials and showed a good safety record (17, 18). Briefly, cystamine inhibits most of the extracellular transglutaminases, while its reduced form cysteamine can more efficiently reach the cytoplasm and inhibit transglutaminase intracellular activities (19). In this study, we aimed to investigate in relevant *in vitro* and *ex vivo* models of human *Mtb* infection whether these two TG2 inhibitors act as HDTs against TB.

RESULTS

Cystamine and Cysteamine Act as a Host-Directed Therapy Against *Mtb*

We have recently shown that treatment of murine and human primary macrophages with cystamine, a TG2 inhibitor, enhances

the anti-tuberculosis activity of macrophages (16). The reduced form of cystamine, cysteamine, is an orphan drug also well-known as TG2 inhibitor already tested in clinical studies to treat non-infectious diseases (18). To investigate whether cysteamine had an anti-microbial activity against *Mtb* in macrophages, THP-1 monocyte-derived macrophages were infected with *Mtb* H37Rv and then treated with cystamine and cysteamine at concentrations compatible to those achieved *in vivo* (16). As shown in **Figure 1A**, treatment with cysteamine resulted in a dose-dependent reduction of intracellular bacteria that reached a similar activity with cystamine when administered at equimolar concentrations (400 μ M cystamine, 800 μ M cysteamine). At these concentrations, treatment with cystamine or cysteamine did not reduce macrophage cell viability (as assessed by measuring lactate dehydrogenase, data not shown) nor inhibit *Mtb* H37Rv viability in axenic culture (**Figure 1B**), similar to what was previously shown for cystine or cysteine (20). Moreover, the combined use of isoniazid with these two drugs, at concentrations previously used in macrophages, provided only a slight delay in the emergence of drug-resistant bacteria. Besides, these treatments did not result in the sterilization or strong inhibition of the persistent population (**Figure 1B**), as previously observed with other molecules with a free-thiol group [though when administered at higher concentration as is the case of N-acetylcysteine (NAC) at 4 mM; **Figure 1B**] (20). Taken together these results indicate that cystamine and cysteamine, at the concentrations shown to inhibit *Mtb* replication in macrophages, do not exert any direct antimicrobial effect on *Mtb*.

Cystamine Restricts *Mtb* Replication in Macrophages While Inhibiting Autophagy

We previously showed that genetic inactivation of TG2 in murine macrophages results in the impairment of the LC3/autophagy homeostasis, which nevertheless correlates with the restriction of *Mtb* intracellular replication (16). To further investigate the impact of the two TG2 inhibitors cystamine and cysteamine on autophagy, we quantitatively evaluated the autophagic flux by confocal pH-imaging of the autophagic intermediates on THP-1 cells transfected with mRFP-GFP-LC3B (21). The number and pH of autophagic intermediates are expressed by autophagic intermediates pH distribution (AIPD), the pH distribution of the number of autophagic intermediates per cell. AIPD shape and amplitude are sensitive to alterations in the autophagy pathway induced by drugs or environmental states and allow a quantitative estimation of autophagic flux by retrieving the concentrations of autophagic intermediates. Briefly, the total area of the AIPD corresponds to the total number of autophagic intermediates. An increase of high F_G/F_R organelles indicates an increase of autophagosomes. Formation of autolysosomes (autophagosome-lysosome fusion) is indicated by a shift of AIPD toward low F_G/F_R values, caused by a decrease of the pH of autophagic intermediates. Thus, this assay is not only a marker of autophagy activation but also allows for an accurate estimation of the autophagic flux (21).

We first assessed the suitability of the assay following infection with the virulent *Mtb* H37Rv and the attenuated strain *Mycobacterium bovis* BCG, which is unable to inhibit

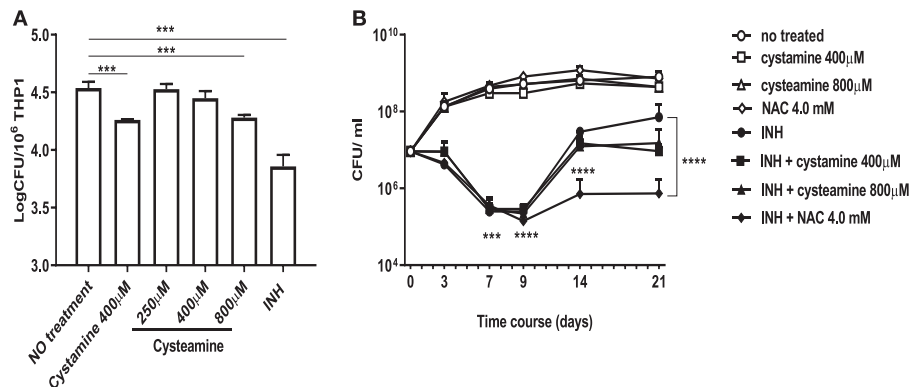


FIGURE 1 | Cystamine and cysteamine exert anti-mycobacterial activity only in infected macrophages. **(A)** THP-1 cells were infected with *Mtb* at MOI 1:10 and treated with the drugs starting at 4 h p.i. until harvesting of intracellular CFU at 2 days p.i. Cystamine (400 μM) or cysteamine at different concentrations (from 250 to 800 μM) and isoniazid at MIC concentration were administered to infected macrophages 4 h p.i. The graph shows intracellular CFU at 2 days p.i. for the untreated and treated THP-1. Data were analyzed by one-way ANOVA followed by Dunnett's multiple-comparisons test (***p* < 0.005, compared with *Mtb* H37Rv no treatment). **(B)** Viability of *Mtb* treated with INH (7.3 μM, 20 times the MIC), cystamine (400 μM) or cysteamine (800 μM), NAC (4.0 mM), and combination of these with INH. The experiments, in which the combinations are shown, were performed using the same concentrations of drugs as the individual treatments. Aliquots were taken at indicated times and plated to determine CFU. Average with SD is plotted (*n* = 1). Values are expressed as a mean of three independent experiments. Data were analyzed by one-way ANOVA with Dunnett's multiple-comparisons test against *Mtb* H37Rv untreated (***p* < 0.005, *****p* < 0.001).

autophagy and is readily degraded by macrophages (22). Infection with *Mtb* and BCG expressing the Ds-Red Cherry fluorescent protein, followed by the confocal analysis of autophagic intermediates (21), allows distinguishing autophagic activation and flux in infected and non-infected cells (Figure 2). A visual inspection of the AIPDs reveals that, in BCG-infected cells (Figure 2A), not only autophagosomes are formed at 2 h post-infection (p.i.) (increase of high F_G/F_R shoulder) but also autolysosomes are forming (simultaneous shift of AIPD toward low F_G/F_R values). The observed decrease of the total number of intermediates during the time course indicates an increased autophagic flux accompanied by a gradual autophagy inactivation (intermediates almost disappear at 24 h). Therefore, this indicates that the overall duration of the autophagy process in THP-1 cells infected with BCG is ≈24 h (Figures 2A–C).

Infection with virulent *Mtb* (Figures 2B–D) activates autophagy, though the AIPD shift toward acidic pH is less pronounced compared to BCG-infected cells and is accompanied by an increase of the neutral organelles. In contrast with the correspondent non-infected cells, the peak of autophagosomes (high F_G/F_R values) is higher than the peak of autolysosomes (low F_G/F_R values; Figure 2B). This change in the shape of the distribution indicates *Mtb* inhibition of the autophagic flux following infection by preventing intermediate acidification, in line with previous findings (22–24). Another important difference between BCG- and *Mtb*-infected macrophages is that AIPD in the latter does not undergo important changes in shape over the same 24-h time course, indicating that cells keep autophagy activated even at 24 h p.i. These results underscore the usefulness of the quantitative analysis of AIPD to monitor autophagy in macrophages infected with *Mtb*. Of note, we also observed autophagic flux induction in non-infected macrophages (in BCG- and *Mtb*-infected cells), probably resulting from the

cytokines released by infected cells (24, 25) that can act in paracrine mode.

To investigate the impact of the TG2 inhibitors on autophagy, THP-1 mRFP-GFP-LC3B cells were infected with *Mtb* H37Rv Ds-Red Cherry and then treated with rapamycin, cystamine, and cysteamine immediately after infection, and AIPD was measured at 24 h later (Figure 3). As expected, treatment with rapamycin readily induced an increase in autophagic flux; AIPD displays an acidification of intermediates (Figure 3A) with respect to untreated *Mtb*-infected macrophages (Figure 3B). Conversely, treatment with cysteamine resulted in a decrease of autophagosome acidification (Figures 3A,B), thus indicating a partial inhibition of the autophagic flux at the level of autophagosome maturation. To quantify the extent of the activation or inhibition of the autophagic flux, we reported in Figure 3C the ratio *A/B* between the AIPD area at the left (*A*) and at the right (*B*) of a fixed threshold value ($F_G/F_R = 0.55$). An increase in *A/B* value corresponds to an increase in the autophagic flux. These findings are in full agreement with the impairment of late autophagic stages reported in TG2 knockout mice (26). Taken together, these results indicate that treatment with cystamine, and to a lesser extent cysteamine, of THP-1 mRFP-GFP-LC3B cells infected with *Mtb* results in the inhibition of the autophagic flux.

Pharmacological Inhibition of TG2 Restricts *Mtb* Replication of Modern and Ancient *Mtb* Clinical Isolates

Mtb strains belonging to different phylogeographic lineages show different pathogenetic properties, with implications in terms of virulence, extent of disease, transmission, and epidemic potentials (25, 27–29). *Mtb* strains belonging to modern lineages showed enhanced virulence compared with strains of the

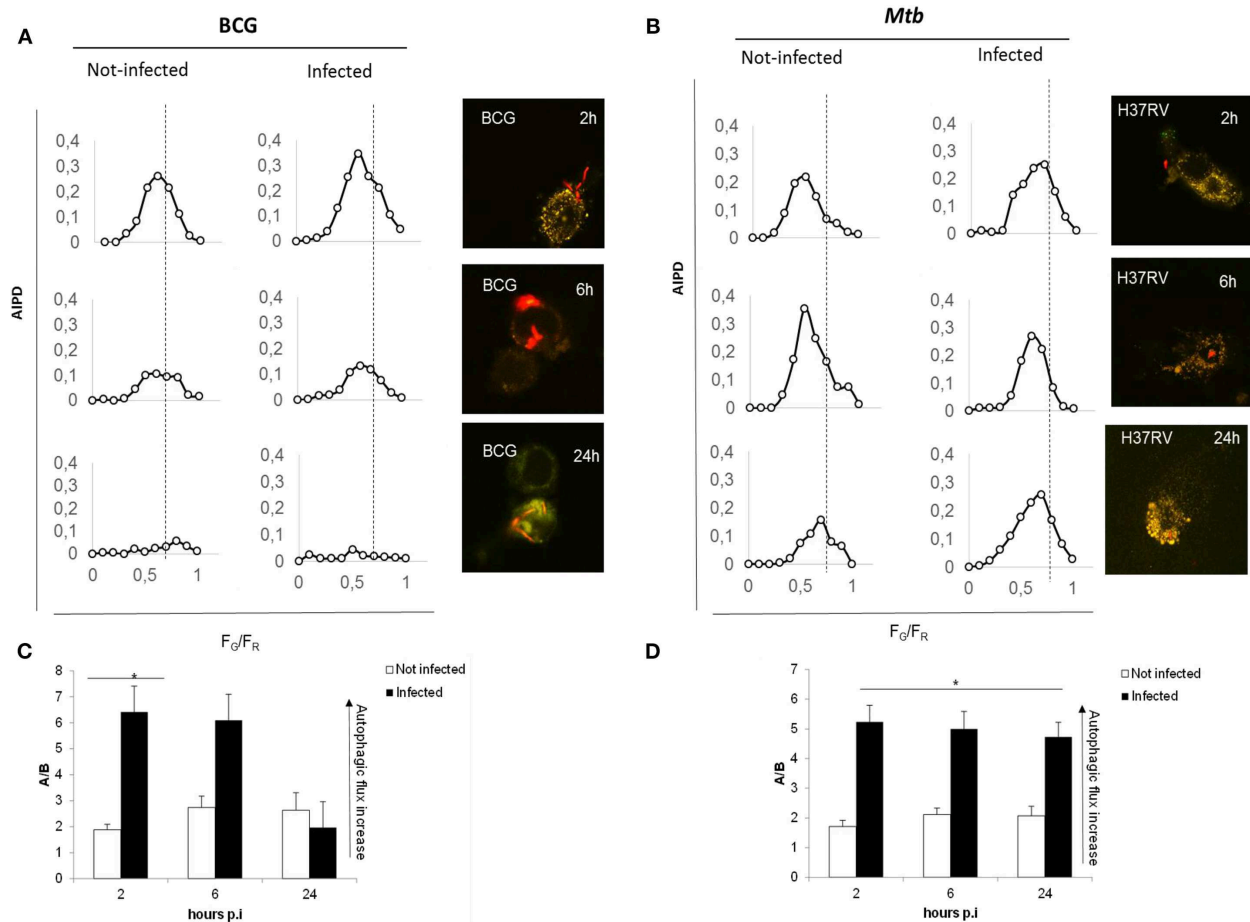
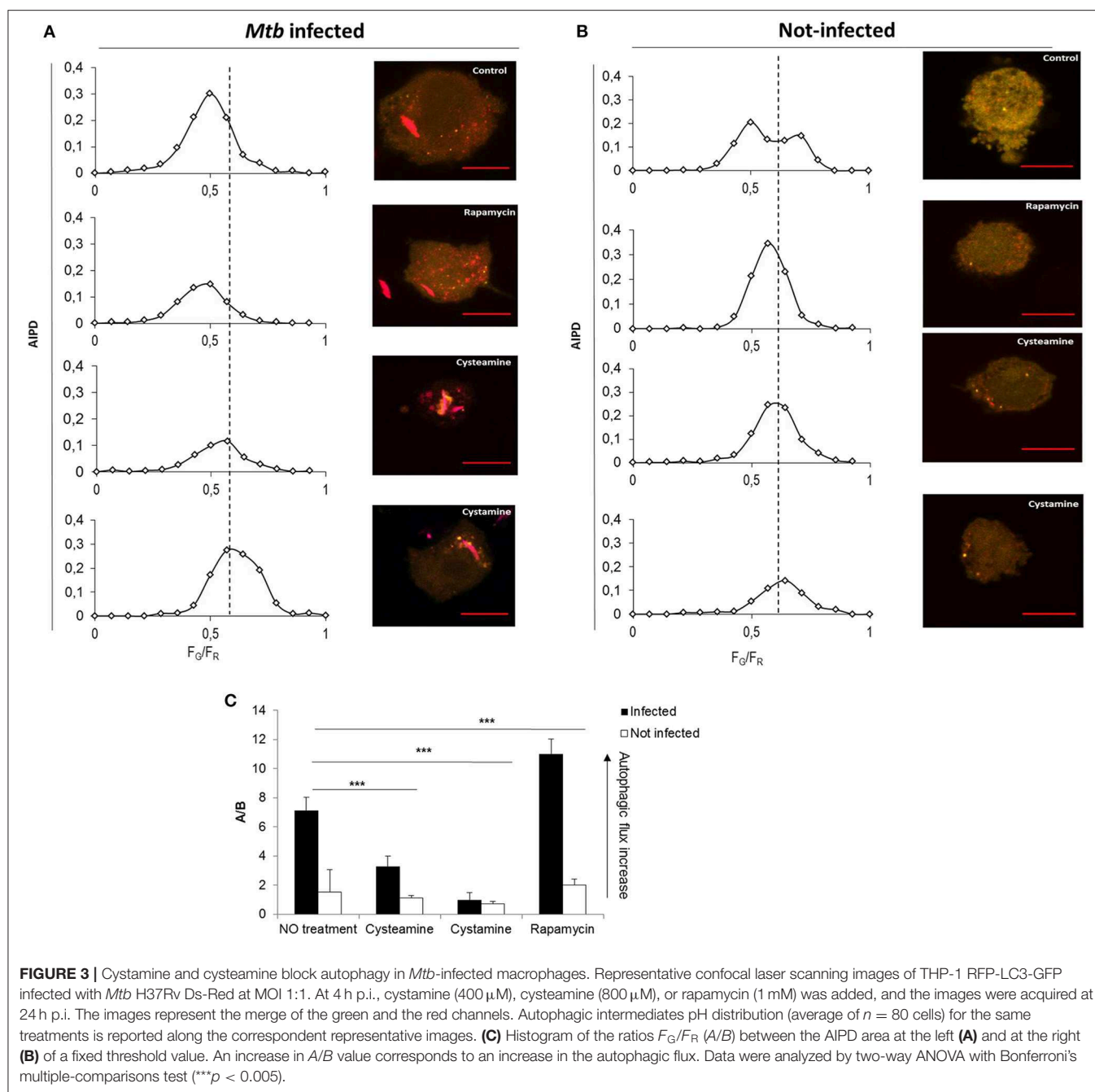


FIGURE 2 | Autophagic flux is altered in virulent *Mtb* H37Rv strain compared to *M. bovis* BCG. THP-1 RFP-LC3-GFP cells infected with *M. bovis* BCG Ds-Red Cherry at MOI 5:1 (A) and with virulent *Mtb* H37Rv Ds-Red Cherry at MOI 1:1 (B). Quantitative assessment of autophagic flux during the time interval lasting 24 h post-infection. Reported in the graphs are the number and pH of autophagic intermediates expressed by AIPD, the pH distribution of the number of autophagic intermediates per cell. AIPD shape and amplitude are sensitive to alterations in the autophagy pathway induced by drugs or environmental states and allow a quantitative estimation of autophagic flux by retrieving the concentrations of autophagic intermediates. An increase of high F_0/F_R organelles indicates an increase of autophagosomes. A shift of AIPD toward low F_0/F_R values indicates that the pH of autophagic intermediates is shifting to acidic values and autolysosomes formation. (C,D) Bar graphs on the trend of autophagy during infection of *M. bovis* BCG and *Mtb*, respectively, expressed as ratios F_0/F_R (A/B) between the AIPD area of a fixed threshold value. Data were analyzed by two-way ANOVA with Bonferroni's multiple-comparisons test (* $p < 0.05$).

ancient lineages, and recent data from our group indicate a different ability to induce and evade autophagy by modern vs. ancient strains (25). To investigate whether treatment with TG2 inhibitors could restrict the intracellular replication of *Mtb* belonging to different lineages, THP-1 cells were infected with *Mtb* clinical isolates of the modern Euro-American (H3 clade) and East Asian (Beijing) lineages and of the ancient lineage EAI (EAI_MAN). As shown in **Figure 4**, treatment with cysteamine and cystamine were equally effective in restricting *Mtb* replication of strains of different clades, with a decrease over the untreated control that ranged between 35 and 50% (**Figure 4B**). Interestingly, we show a 50% decrease in THP-1 cells infected with the Beijing *Mtb* strain. These results indicate that cysteamine and cystamine promote an antimicrobial activity in macrophages effective against clinical isolates representative of the *Mtb* genetic diversity at global level.

Cystamine Synergizes With Capreomycin in Restricting *Mtb* Replication in Primary Human Monocyte-Derived Macrophages

HDTs against TB have the potential to synergize with antimicrobial drugs to enhance the efficacy of therapy. This is of utmost importance during treatment of drug-resistant TB, which relies on antibiotics that are less powerful than the first-line drugs (9). As a proof of concept, to investigate the potential usefulness of the TG2-inhibitors under study, human monocyte-derived macrophages (hMDM) were infected with *Mtb* and then treated with cystamine, cysteamine alone, or in combination with the second-line anti-TB drug capreomycin. As shown in **Figure 5**, cystamine reduced *Mtb* replication in macrophages at a higher level compared to rapamycin (16) and similarly to capreomycin when these drugs were administered



at 4 h p.i. and intracellular *Mtb* evaluated after 2 days of infection. Interestingly, the combined use of cystamine and capreomycin further reduced *Mtb* replication in macrophages, indicating a synergistic effect of these drugs. A similar experiment was repeated with amikacin, an aminoglycoside included in group C of drugs endorsed for use in longer MDR-TB regimens (30). As shown in **Figure 5B**, in hMDM, amikacin significantly reduced *Mtb* intracellular growth even more than the reduction generated by capreomycin (capreomycin = -0.32 log colony-forming units (CFU)/ 10^6 cells; amikacin = -0.89 log CFU/ 10^6 cells). Remarkably, the combined use of amikacin and cystamine or cysteamine further reduced *Mtb* replication

in hMDM, providing a decrease of -1.22 log CFU/ 10^6 cells for combination with cystamine and -1.24 log CFU/ 10^6 cells for cysteamine over untreated infected hMDM (**Figure 5B**). Interestingly, the respective anti-*Mtb* activity of amikacin and capreomycin was lower at day 7 p.i. compared to what was observed at day 2 p.i. (**Figure 5C**); differently, the combination of aminoglycosides, particularly amikacin, with cystamine and cysteamine resulted in a persistent and highly significant reduction of intracellular CFU (**Figure 5C**). Taken together, these results indicate that cystamine and cysteamine can synergize with amikacin to enhance anti-TB activity in infected hMDM.

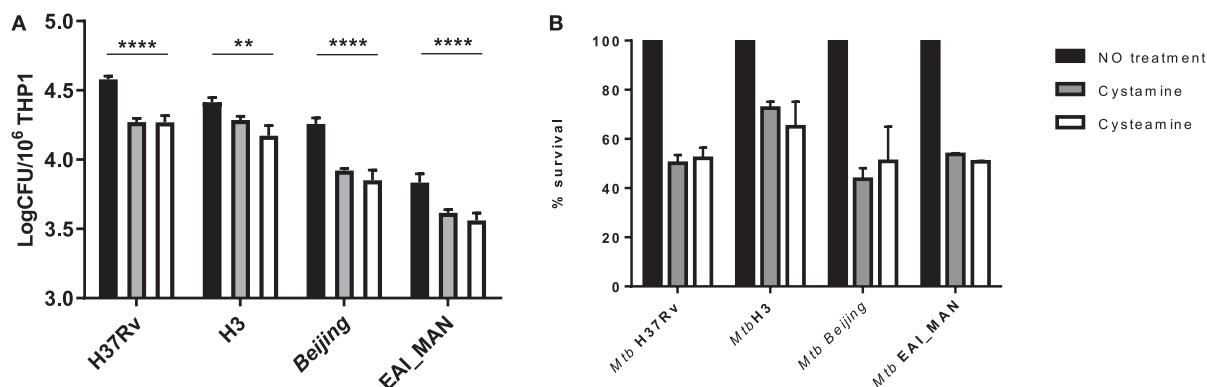


FIGURE 4 | Evaluation of cystamine and cysteamine effects in macrophages infected with different *Mtb* strains belonging to different lineages. Differentiated THP-1 cells were infected with MTBC clinical strains belonging to different clades (H3, Beijing, EAI_MAN) (25) at MOI 1:1. At 4 h p.i., the cells were treated with cystamine (400 μ M) and cysteamine (800 μ M), and at 2 days p.i., cells were lysed to measure intracellular CFU **(A)**. Values are expressed as a mean of three independent experiments. **(B)** To compare the activity of the two drugs, results are expressed as percentage of mean value of CFU in triplicate of treated vs. untreated strains in panels. Data were analyzed by two-way ANOVA with Dunnett's multiple-comparisons test against each strain with untreated condition (** $p < 0.01$, **** $p < 0.001$).

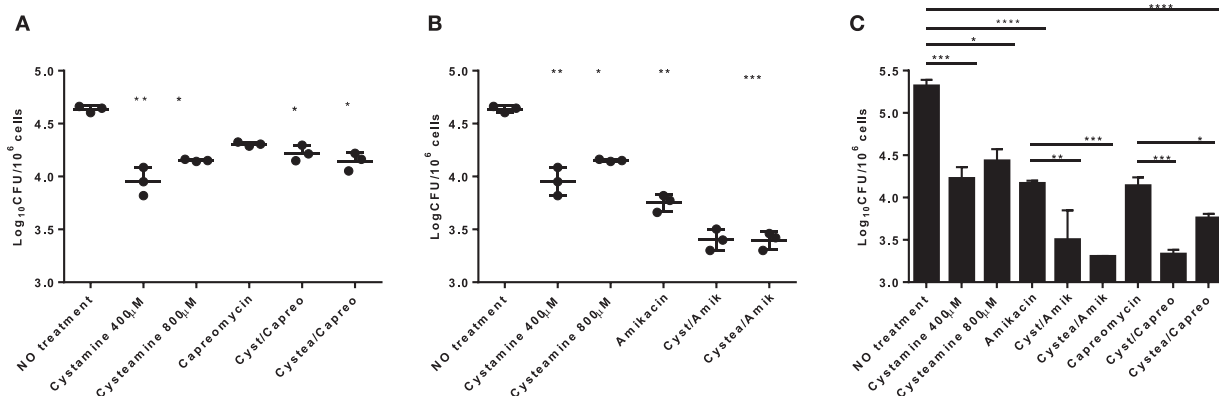


FIGURE 5 | Evaluation of the synergistic effect of cystamine and cysteamine with aminoglycosides in human primary monocyte-derived macrophages (hMDM). hMDM were infected with *Mtb* H37Rv at MOI 1:1, and at 4 h p.i., we added different drugs: cystamine (400 μ M), cysteamine (800 μ M); the antibacterial drugs belonging to the aminoglycosides class capreomycin (4 μ g/ml, **A**) and amikacin (1 μ g/ml, **B**) and the combination of the aminoglycosides with cystamine and cysteamine. Two days after infection, cells were lysed to assess intracellular CFU, and results are shown as log CFU/10⁶ cells. **(C)** To measure the long-term effect in this *in vitro* model of *Mtb* infection, hMDM were maintained up to 7 days p.i., and CFU were determined. Values are expressed as a mean of three independent experiments. Data were analyzed by one-way ANOVA followed by Dunnett's multiple-comparisons test (* $p < 0.05$, ** $p < 0.01$, *** $p < 0.005$, **** $p < 0.001$ compared with *Mtb* H37Rv no treatment). To measure the synergistic effect of cystamine and cysteamine in combination with capreomycin or amikacin in prolonged treatment, we compared groups treated with antibiotic alone with those receiving the same antibiotic in combination with cysteamine or cystamine (** $p < 0.01$, *** $p < 0.005$ for amikacin treatments; * $p < 0.05$, *** $p < 0.001$ for capreomycin treatment). Data obtained from single independent infections are reported in **Supplementary Figure 1**.

Cysteamine and Cystamine Are Active Against *Mtb* in the Human *ex vivo* Model of Granuloma-Like Structures

Infection of human peripheral blood monocyte cells (PBMCs) with *Mtb* results in the formation of granuloma-like structures (GLS) that are emerging as a valuable *ex vivo* model of TB (31, 32). To investigate the activity of these HDTs against TB, PBMCs were infected with *Mtb* H37Rv and with the clinical strain *Mtb* H3, which in hMDM showed enhanced virulence compared with other *Mtb* reference and clinical strains (25). Following infection with *Mtb*, cysteamine, or cystamine was added in infected GLS at day 6 p.i. at the concentrations previously used

in macrophages. At day 12 p.i., the total CFU counts were evaluated, and some GLS parameters were analyzed. As shown in **Figures 6A–D**, treatment with cysteamine and cystamine resulted in a reduction in the number of GLS per field compared with untreated GLS, while no differences were observed in the average surface area of these GLS. Interestingly, *Mtb* H37Rv load was significantly reduced in these GLS, confirming the antimycobacterial activity of these two TG2 inhibitors. Infection of PBMCs with *Mtb* H3 resulted in fewer GLS with smaller areas compared with the results obtained with *Mtb* H37Rv (**Figures 6E–G**). Again, cystamine significantly reduced the total CFU of *Mtb* H3-infected GLS, while the activity of cysteamine

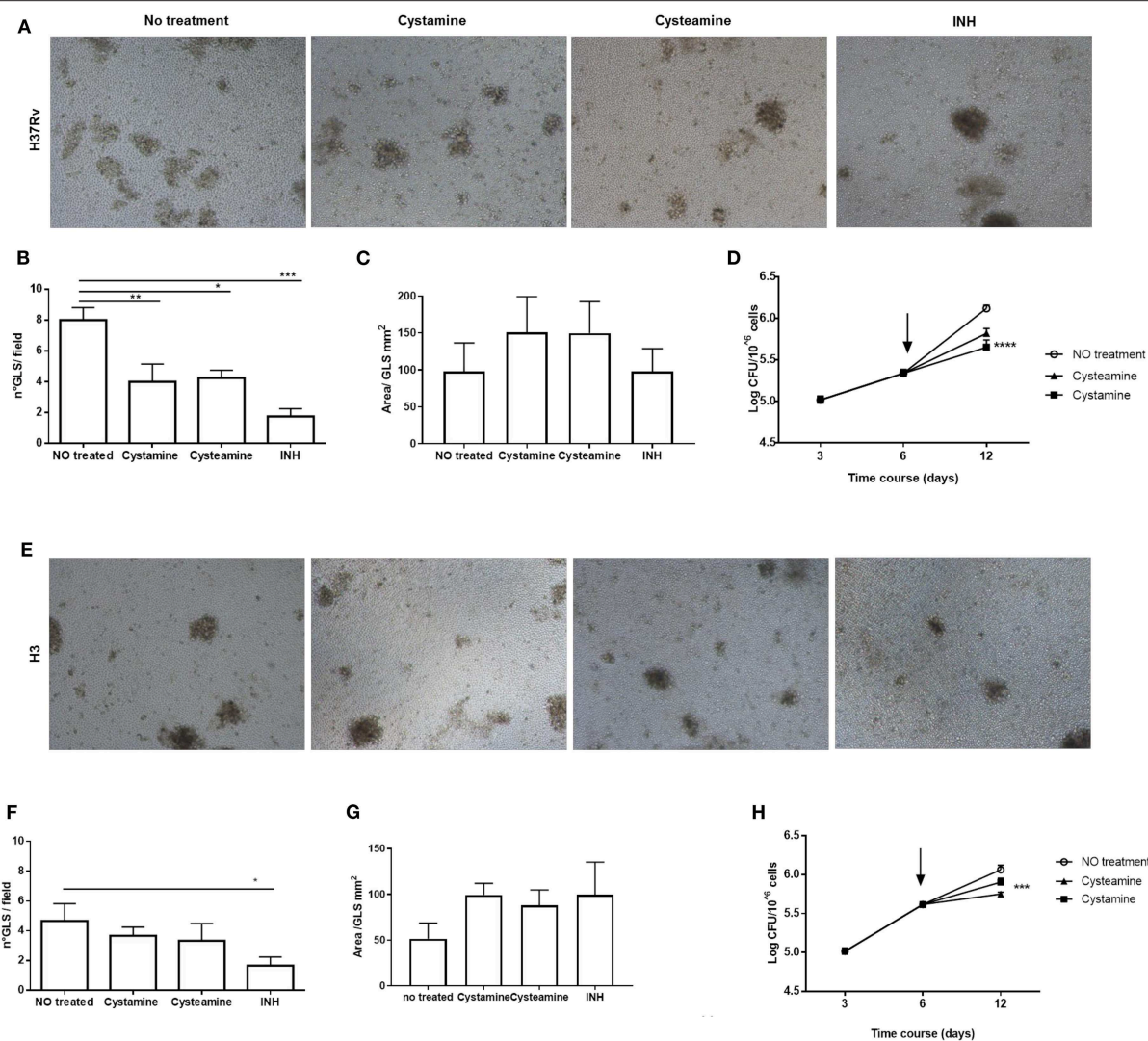


FIGURE 6 | Cystamine and cysteamine reduce the fitness of *Mtb* in an *in vitro* granuloma model containing human innate and adaptive immune cells. PBMCs obtained from healthy donors were infected with *Mtb* H37Rv and *Mtb* H3 (MOI 1:1) for up to 12 days. Representative images of granuloma-like structure formed *in vitro* 10 days after infection with *Mtb* reference strain H37Rv (A) and H3 clinical strain (E). Magnification, $\times 40$. Granuloma formation was scored for each condition; the means \pm standard deviations of scores representative of three experiments each are given in the images. GLS were treated with different drugs at 3 days post-infection; the medium was replaced: cystamine (400 μ M), cysteamine (800 μ M), and INH at MIC concentration. The measurement of the number of GLS and area was applied on day 10 p.i., 12 fields per sample were evaluated (B,C for *Mtb* H37Rv; F,G for *Mtb* H3), and CFU were determined at 3, 6, and 12 days post-infection (D) and for clinical strain *Mtb* H3 (H), arrows represent the beginning of treatments ($^*p < 0.05$, $^{**}p < 0.01$, $^{***}p < 0.005$, $^{****}p < 0.001$).

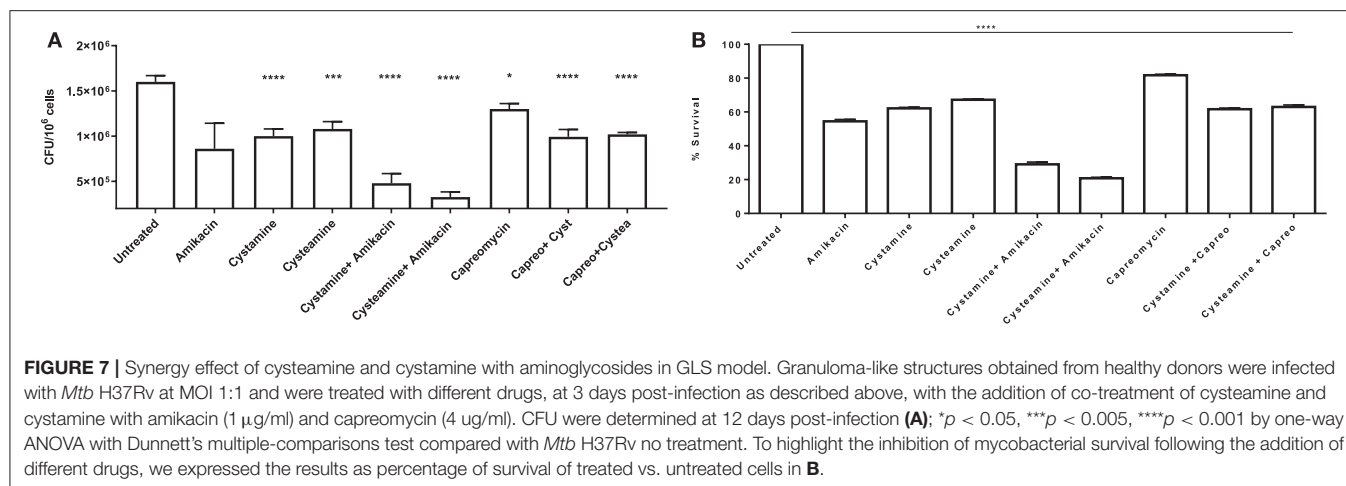
was lower compared with the results observed in *Mtb* H37Rv-infected GLS (Figure 6H). Taken together, these results indicate that cystamine and cysteamine reduce *Mtb* growth in the human *ex vivo* model of GLS.

To further assess the potentials of these two TG2 inhibitors as HDTs for TB, the respective activity of cystamine and cysteamine was assessed in combination with capreomycin and amikacin in the GLS model. As shown in Figure 6G, treatment with cysteamine or cystamine significantly reduced *Mtb* replication even more efficiently than the treatment with capreomycin in GLS, and the combined administration of capreomycin with the TG2 inhibitors did not provide any additive effect. Conversely,

the combined administration of amikacin with cystamine or cysteamine warranted an enhanced restriction of intracellular *Mtb* compared with the treatment with any of these drugs alone. Taken together, these results indicate that cystamine and cysteamine can synergize with a second-line anti-TB drug as amikacin, supporting their potential usefulness as HDTs for TB (Figures 7A,B).

DISCUSSION

Our recent report indicating that genetic and pharmacological inhibition of TG2 restricts *Mtb* replication in macrophages (16)



prompted us to investigate the potential usefulness of the TG2 inhibitors cystamine and cysteamine as HDTs against TB. In this study, using a panel of *in vitro* experimental assays, we show that cysteamine and cystamine, two known inhibitors of TG2, can restrict *Mtb* replication in macrophages infected with the *Mtb* H37Rv reference strain and a panel of clinical isolates representative of different phylogeographic lineages. Interestingly, we analyzed the AIPD in THP-1 mRFP-GFP-LC3B cells infected with *Mtb* and observed, for the first time, that cystamine inhibited autophagy while restricting *Mtb* replication, confirming our previous observation (16). Overall, the results of this study support the potential usefulness of the TG2 inhibitors cysteamine and cystamine as HDTs against TB.

TG2 is known to contribute to a few important pathologies (15). Among the drugs that inhibit TG2, there are two small molecules, cystamine and cysteamine. These two drugs are safe when administered in humans; cysteamine is used to treat cystinosis (33, 34), and both cysteamine and cystamine have been used in human clinical trials in the treatment of diseases which directly or indirectly implicate TG2 and autophagy deregulation such as Huntington disease (35), cystic fibrosis (36, 37), and celiac disease (38). It is noteworthy that cystamine has been used as a support treatment in cancer therapy (39). In keeping with the data reported in this study, TG2 and autophagy are both up-regulated in cancer, playing a crucial role in oncogenesis (39, 40). Thus, the inhibitory action exerted by cysteamine and cystamine both on autophagy and TG2 could represent an efficient approach to favor the sensitization of cancer cells to chemo/radio/immune therapy. Our results showing that cysteamine and cystamine have an anti-TB activity when administered in a monocyte-derived macrophage cell line, in primary macrophages, or PBMCs infected with *Mtb* suggest that these drugs can be safely used as HDTs for TB (9).

Cystamine and cysteamine are reducing agents that can affect cell metabolism by increasing glutathione and L-cysteine level (35, 41). Recently, it has been demonstrated that L-cysteine or NAC can promote respiration in axenic *Mtb* culture, preventing the emergence of drug tolerance against the two

most powerful anti-TB drugs, isoniazid and rifampicin (20). In these experiments, L-cysteine or NAC were administered at a concentration of 4 mM, which is five times higher than the concentration we used in our experiments involving *Mtb*-infected macrophages. Indeed NAC administered at a concentration of 10 mM was shown to directly decrease *Mtb* replication (42). However, in this study, we show a reproduction of the experimental conditions indicated in Vilcheze et al. (20), wherein cystamine or cysteamine, when administered at the concentrations used in *Mtb*-infected macrophages (400 and 800 μ M, respectively), did not exert any direct activity against *Mtb* cultured in axenic media and did not prevent the emergence of drug tolerance against isoniazid. It follows that the anti-tuberculosis activity of cysteamine and cystamine that we observed in THP-1 monocyte-derived macrophages, primary macrophages, and PBMCs is not the result of a direct effect on *Mtb*. Moreover, Vilcheze et al. (20) showed that only the molecules with a free thiol group (as L-cysteine and NAC) may enhance *Mtb* metabolism, while the oxidized form, as cystine, does not exert any activity. Conversely, in our experiments, both cysteamine and cystamine similarly inhibit *Mtb* intracellularly in infected macrophages. This suggests that the mechanism of the anti-TB activity of the two anti-TG2 drugs described in the present study is different from that observed when L-cysteine or NAC is administered at a much higher concentration in *Mtb* axenic cultures.

It remains to be elucidated how the impairment of autophagy homeostasis by cysteamine and cystamine may contribute to restrict *Mtb* replication. It is well-established that induction of autophagy by various stimuli, such as rapamycin, IFN- γ , and Vitamin D3, promotes the lysosomal degradation of *Mtb* (43). However, the role of basal autophagy in infected macrophages appears to be more complex. We have recently demonstrated that *Mtb* strains from ancient and modern lineages have a different impact on the basal autophagy flux (25). While the ancient lineages impair the autophagic flux, infection with the modern strains leads to a stimulation of this process, which is dependent on the increased production of

IL1- β triggered by these mycobacteria (25). This induction of autophagy is however ineffective in restricting *Mtb* growth but rather correlates with more exuberant *Mtb* replication, perhaps by sustaining its metabolic requirements in the infected cells (25, 44). These observations lend support to the hypothesis that a blanket inhibition of the autophagic flux in *Mtb*-infected macrophages may be detrimental for *Mtb*, perhaps because it would activate apoptosis, and that *Mtb* may manipulate this process in a more complex and dynamic way (45, 46). Autophagy is a complex and conserved process that involves multiple autophagy-associated enzymes; yet, apart from Atg5, autophagy-deficient mice do not show increased susceptibility to *Mtb* infection (47). Interestingly, the dramatic difference in the inflammatory response was the predominant driver for the enhanced susceptibility to *Mtb* infection in ATG5-deficient mice (47), highlighting the remarkable consequences that disruption of autophagic homeostasis can have during *Mtb* infection. These experimental observations suggest that *Mtb* has developed multiple strategies to escape autophagy engulfment and regulate the autophagy flux to fine-tune its pathogenetic strategies. Based also on the evidences generated in this study, we propose that impairment of the autophagic flux by the TG2 inhibitors is detrimental for *Mtb* intracellular growth. Further experiments are required to elucidate the functional link between impairment of autophagy homeostasis and *Mtb* growth and its consequences on inflammation when cells are treated with cysteamine and cystamine.

Mycobacterium tuberculosis complex (MTBC) is a genetically monomorphic species which evolved by clonal expansion since more than 100,000 years ago, leading to seven phylogeographic lineages which show different pathogenetic and virulence properties (27, 28). Most of the human TB cases at global level are caused by *Mtb* strains belonging to the modern lineages L2, L3, and L4, which seem to show enhanced pathogenic properties (29, 48, 49). More recent evidences indicate that even within these modern lineages, some clades or clusters may be more successful or virulent than others, indicating that the relative little genetic variability within *Mtb* can nevertheless have significant impact on infection outcome (28, 49). We and others have recently shown that *Mtb* strains of diverse lineages and clades can differently manipulate the autophagic process in infected macrophages, with consequences in terms of intracellular survival and cytokine/chemokine secretion (25, 50, 51). In this study, we show that the inhibition of TG2 by cysteamine or cystamine can effectively inhibit intracellular *Mtb* regardless of MTBC lineage. Indeed *Mtb* strains of the H3 and Beijing clade, which are characterized by an enhanced *in vitro* virulence compared to the other lineages (25), were inhibited by the anti-TG2 drugs, although at a lower level compared with the results observed with the other *Mtb* strains. Since *Mtb* H3 was shown to modulate the autophagy flux differently compared to the other *Mtb* strains, exploiting the autophagic process for its own survival (25), it is possible that the anti-TG2 drugs cysteamine and cystamine are less effective in inhibiting the intracellular *Mtb* H3. Nonetheless, these results demonstrate that cysteamine and cystamine have an antibacterial activity against several *Mtb* clinical strains representative of the global diversity of MTBC and

support the finding that these anti-TG2 molecules are acting as HDTs by boosting macrophage antimicrobial responses.

Inhibition of TG2 and the ensuing effect on autophagy, in addition with the capability of these drugs to increase the generation of glutathione-S-transferase (52), may have consequences on the pattern of chemokines and cytokines secreted by infected macrophages. To evaluate the activity of cystamine and cysteamine in a more complex system, involving multiple cell types, we implemented the *ex vivo* model of GLS (31, 53). Treatment with cystamine or cysteamine of PBMCs infected with the *Mtb* H37Rv reference strain and the *Mtb* clinical strain H3 indicates a significant reduction in the total bacterial burden in GLS, although no major differences in GLS size were observed. These results indicate that the two anti-TG2 molecules can exert their anti-TB activity even in this *ex vivo* model of infection, further supporting their role as HDTs for TB.

HDTs against TB shall ideally serve to improve and eventually shorten current anti-TB regimens during treatment of drug-susceptible TB and, most importantly, drug-resistant TB. In fact, regimens against MDR-TB are longer and more toxic primarily because second-line drugs show reduced antimicrobial activity compared to isoniazid and rifampicin. Since the success rate for drug-susceptible TB is around 95% (54), we anticipate that any HDTs against TB will be tested and the activity will be measured in MDR-TB patients receiving second-line drugs. It is remarkable that cysteamine, and more robustly cystamine, can reduce intracellular *Mtb* growth similarly to the two aminoglycosides tested, underscoring on one side the potential antimicrobial activity of these two molecules and on the other the poor activity of the second-line drugs. Given the important potential clinical implications, we investigated the synergistic activity of the two anti-TG2 molecules with second-line drugs as those of the aminoglycoside class. The finding that cysteamine and cystamine synergized when administered in combination with capreomycin and most importantly with amikacin in primary human macrophages infected with *Mtb* and in the GLS *ex vivo* model of infection further highlights the potential usefulness of these two anti-TG2 inhibitors as HDTs against TB.

In conclusion, this study shows for the first time that cystamine and cysteamine display anti-*Mtb* activity while inhibiting host cell autophagy. These safe FDA-approved drugs have high potential applications against *Mtb* infection in combination with canonical anti-TB regimen to improve and shorten regimens against drug-susceptible TB and most importantly during treatment of MDR-TB patients or of patients which are at higher risk of non-compliance as migrants or homeless. In the future, specifically designed clinical trials should validate the efficacy for their utilization in the clinical practice, opening a new avenue in the treatment of TB.

MATERIALS AND METHODS

Reagents and Bacterial Strains

The *M. tuberculosis* strain H37Rv, *Mtb* complex clinical strains (MTBC), and *M. bovis* BCG were isolated at the Fondazione Policlinico Gemelli IRCCS, Università Cattolica del Sacro Cuore (25, 55). The strains were grown in Middlebrook 7H9 (Difco,

Sparks, MD) supplemented with 10% (vol/vol) oleic acid-albumin-dextrose-catalase (OADC; Difco), with 0.2% glycerol (Microbiol, Cagliari, Italy) and 0.05% Tween 80 (Sigma-Aldrich, St. Louis, MO) at 37°C. Mycobacterial cultures were harvested at late log phase, glycerol was added at 20% final concentration, and 1-ml aliquots stored at -80°C. All experiments with *Mtb* strains were carried out in biosafety laboratory level 3 (BSL-3), following standard safety procedures.

Growth of *Mtb* in vitro Cultures

Mtb H37Rv cultures were diluted until a final concentration of $\approx 10^7$ CFU/ml, treated with the appropriate chemicals (cystamine 400 μ M, cysteamine 800 μ M, NAC 4 mM, INH 7.3 μ M, or the combination INH/Cystamine, INH/cysteamine, INH/NAC using the same concentrations as the individual treatment), AND incubated at 37°C with shaking for the duration of the experiment, and CFU were obtained by plating serial dilutions. Plates were incubated at 37°C for up to 6 weeks. All experiments were carried out in BSL-3.

Study Participants

The PBMCs were derived from healthy donors. Participants were recruited among people who had recently tested negative for QFT negative, not vaccinated with BCG, male, Caucasian, and aged between 30 and 35 years. Written informed consent was obtained from each donor.

Cell Cultures

Human THP-1 cells *wt* were stably transduced with a retroviral vector encoding GFP-RFP-LC3 (56). *Wt* and transgenic THP-1 were grown in RPMI 1640 supplemented with glutamine (2 mM) and 10% FBS. Cells were treated with 20 nM PMA (Sigma-Aldrich, St. Louis, MO) for 24 h to induce their differentiation into macrophages, then washed three times with PBS, and maintained in 5% FCS.

Peripheral blood mononuclear cells (PBMCs) were obtained from healthy donors. PBMCs were isolated by density gradient centrifugation. Monocytes were purified from PBMCs by positive sorting, using anti-CD14-conjugated magnetic microbeads (Miltenyi Biotec, Auburn, CA). Human monocyte-derived macrophages (hMDM) were obtained by cultivating adherent monocytes for 5–6 days in X-Vivo 15 medium (Lonza, Walkersville, MD), 2% human serum (Euroclone, Paignton, United Kingdom) at 37°C in a 5% humidified atmosphere until macrophage differentiation (25).

Human cells were infected with different strains of MTBC [multiplicity of infection (MOI) 1: 1], and at various time-points (4 h, 2 and 7 days for hMDM), cells were washed twice with sterile phosphate-buffered saline (PBS) to remove extracellular bacteria, lysed in 0.01% Triton-X100 (Sigma-Aldrich, St. Louis, MO) and intracellular bacterial loads (in CFU) determined as previously described (57).

To assess the synergistic effect of cystamine and cysteamine with standard antibacterial drugs, we added 4 h and 3 days post-infection, respectively for hMDM instead of hMMO and GLS, capreomycin (4 μ g/ml) (Sigma-Aldrich, St. Louis,

MO), amikacin (1 μ g/ml) (Sigma-Aldrich, St. Louis, MO) and combination of these drugs with cystamine and cysteamine.

Granuloma-Like Structure Formation and Quantification

PBMCs were obtained from healthy donors and isolated as described above. PBMCs (containing $\sim 1 \times 10^5$ monocytes) were immediately infected with *Mtb* at a MOI of 1:1 and incubated for up to 10–12 days, during which time granuloma was developed and analyzed (31, 58). The analysis of stage of GLS has been done daily by using an inverted light microscope. At least 12 separate fields per sample were used to establish the area and total number of GLS (31). Intracellular bacterial growth was assessed by counting the CFU; infected GLS were lysed at different time-points (3, 6, and 12 days post-infection) as described previously (57).

Confocal Microscopy

Images were obtained by using an inverted confocal microscope; the slides were then placed on the inverted confocal microscope (Nikon A1 MP) equipped with an on-stage incubator ($T = 37^\circ\text{C}$, 5% CO_2 , OKOLAB), and 32 channel spectral images were obtained using a $\times 60$ objective (NA 1.4) under 488-nm excitation for Nile Red. Internal photon multiplier tubes collected images in 16-bit, unsigned images at 0.25 ms dwell time. mRFP-GFP-LC3 was excited by an argon-ion laser line (excitation wavelength, 488 nm; emission ranges, 500–550, 570–620 nm). DsRED fluorescence was monitored in the channel 500–550 nm. Photomultiplier tube gain values were kept fixed during the experiment. Pinhole was set to 1 A.U.Z-. Analysis of images acquired was performed with ImageJ 1.41 (NIH). AIPD determination was obtained following Maulucci et al. (21). Briefly, the *R* index was obtained by calculating the ratio between fluorescence emissions in the 500–550 nm (F_G) and 570–620 nm (F_R) ranges, upon sample excitation at 488 nm. By mapping *R* over the entire microscope scanning field, *R* images can be created with the homemade downloadable software Redox Maps Generator Green (59), and red images were overlaid; maxima of red and green channels, representing autophagy intermediates (“puncta”), were retrieved by the FIND MAXIMA plugin (ImageJ). Regions of interests, including whole organelles, were manually drawn in correspondence of the maxima, and fluorescence intensity values were measured directly on the *R* image through the SYNC WINDOWS plug-in (ImageJ). Puncta without detectable EGFP fluorescence were minimized to <5% of the total number by setting adequate values for photomultipliers. At least 50 cells per sample were analyzed to build the histogram. Fluorescence intensities and intensity ratio data were presented as mean \pm SD, and differences were assessed by using χ^2 -test. Values of $p < 0.05$ were considered as significant.

Statistics

Data were analyzed using the GraphPad Prism software, version 7.02 for Windows (GraphPad Software, San Diego, CA). All experiments were performed at least three times in triplicate. Growth of *Mtb* H37Rv in *in vitro* cultures was evaluated using one-way ANOVA with Dunnett’s multiple-comparisons

test against *Mtb* H37Rv untreated; the statistical significance of the differences between MTBC strains was evaluated using two-way ANOVA with Dunnett's multiple-comparisons test against each strain with untreated condition. The healthy donors used for GLS formation were adult (18–45 years of age), uninfected, and non-vaccinated. Differences were considered significant if *p*-values were ≤ 0.05 .

DATA AVAILABILITY STATEMENT

All datasets generated for this study are included in the article/**Supplementary Material**.

ETHICS STATEMENT

The studies involving human participants were reviewed and approved by L. Spallanzani National Institute for Infectious Diseases-IRCCS (INMI) Ethical Committee (approval number: parere 4/2009, amendment of February 2018; approval number: parere 68/2018). The patients/participants provided their written informed consent to participate in this study. Healthy donors were prospectively enrolled from January 2017 until March 2019.

AUTHOR CONTRIBUTIONS

IP, GD, and MP conceived the study. IP designed and performed the experiments, analyzed data, interpreted results, prepared figures, and wrote manuscript. GD analyzed data, interpreted results, and took the lead in writing the manuscript. DG, MP, and MSan contributed to analyze the data. GM performed and analyzed all data

with confocal microscopy. GM and MD interpreted results and prepared figures that associate the *Mtb* infection and autophagy omeostasis. FD and MSal maintained, cultivated and prepared different TB strains. FD and MSal collected samples and contributed to perform the experiments. LP, AR, and GF contributed reagents and analyzed the data. AR and GF produced the transfected cells RFP-LC3-GFP. MSan interpreted results. All authors critically reviewed the manuscript.

FUNDING

This work has been supported by the Università Cattolica del Sacro Cuore (Linea D3.2 and Linea D1 awarded to GD), in part by grants from the AIRC (IG2015-17404 to GF and IG2018-21880 to MP), the Italian Ministry of University and Research (PRIN 2015 20152CB22L to GF), the Italian Ministry of Health (Ricerca Corrente and Ricerca Finalizzata RF2010 2305199), Fondazione Fibrosi Cistica (FFC#8/2015 to MP), and Regione Lazio (Gruppi di Ricerca to MP). The authors also acknowledge the support of the grant from the Russian Government Programme for the Recruitment of the Leading Scientists into the Russian Institutions of Higher Education (14.W03.31.0029 to MP). The confocal analysis has been performed at Labcemi, UCSC, Rome.

SUPPLEMENTARY MATERIAL

The Supplementary Material for this article can be found online at: <https://www.frontiersin.org/articles/10.3389/fimmu.2019.03042/full#supplementary-material>

REFERENCES

- World Health Organization. *Global Tuberculosis Report* (2018).
- Dheda K, Gumbo T, Maartens G, Dooley KE, McNerney R, Murray M, et al. The epidemiology, pathogenesis, transmission, diagnosis, and management of multidrug-resistant, extensively drug-resistant, and incurable tuberculosis. *Lancet Respir Med.* (2017). doi: 10.1016/S2213-2600(17)30079-6
- World Health Organization. *WHO Consolidated Guidelines on Drug-Resistant Tuberculosis* (2019).
- Hughes J, Snyman L. Palliative care for drug-resistant tuberculosis: when new drugs are not enough. *Lancet Respir Med.* (2018) 6:251–2. doi: 10.1016/S2213-2600(18)30066-3
- Diel R, Vandeputte J, de VG, Stillo J, Wanlin M, Nienhaus A. Costs of tuberculosis disease in the European Union: a systematic analysis and cost calculation. *Eur Respir J.* (2014) 43:554–65. doi: 10.1183/09031936.00079413
- Bloemberg GV, Keller PM, Stucki D, Trauner A, Borrell S, Latshang T, et al. Acquired resistance to bedaquiline and delamanid in therapy for tuberculosis. *N Engl J Med.* (2015) 373:1986–8. doi: 10.1056/NEJMc1505196
- Kaufmann SHE, Dorhoi A, Hotchkiss RS, Bartenschlager R. Host-directed therapies for bacterial and viral infections. *Nat Rev Drug Discov.* (2018) 17:35–56. doi: 10.1038/nrd.2017.162
- Maeurer M, Rao M, Zumla A. Host-directed therapies for antimicrobial resistant respiratory tract infections. *Curr Opin Pulm Med.* (2016) 22:203–11. doi: 10.1097/MCP.0000000000000271
- Palucci I, Delogu G. Host directed therapies for tuberculosis: futures strategies for an ancient disease. *Chemotherapy.* (2018) 63:172–80. doi: 10.1159/000490478
- Singhal A, Jie L, Kumar P, Hong GS, Leow MK, Paleja B, et al. Metformin as adjunct antituberculosis therapy. *Sci Transl Med.* (2014) 6:263ra159. doi: 10.1126/scitranslmed.3009885
- Parihar SP, Guler R, Khutlang R, Lang DM, Hurdal R, Mhlanga MM, et al. Statin therapy reduces the *Mycobacterium tuberculosis* burden in human macrophages and in mice by enhancing autophagy and phagosome maturation. *J Infect Dis.* (2014) 209:754–63. doi: 10.1093/infdis/jit550
- Kolloli A, Subbian S. Host-directed therapeutic strategies for tuberculosis. *Front Med.* (2017) 4:171. doi: 10.3389/fmed.2017.00171
- Fesus L, Piacentini M. Transglutaminase 2: an enigmatic enzyme with diverse functions. *Trends Biochem Sci.* (2002) 27:534–9. doi: 10.1016/S0968-0004(02)02182-5
- D'Eletto M, Farrace MG, Rossin F, Strappazzon F, Giacomo GD, Cecconi F, et al. Type 2 transglutaminase is involved in the autophagy-dependent clearance of ubiquitinated proteins. *Cell Death Differ.* (2012) 19:1228–38. doi: 10.1038/cdd.2012.2
- Piacentini M, D'Eletto M, Farrace MG, Rodolfo C, Del NF, Ippolito G, et al. Characterization of distinct sub-cellular location of transglutaminase type II: changes in intracellular distribution in physiological and pathological states. *Cell Tissue Res.* (2014) 358:793–805. doi: 10.1007/s00441-014-1990-x
- Palucci I, Matic I, Falasca L, Minerva M, Maulucci G, De SM, et al. Transglutaminase type 2 plays a key role in the pathogenesis of *Mycobacterium tuberculosis* infection. *J Intern Med.* (2018) 283:303–13. doi: 10.1111/joim.12714
- De SD, Villella VR, Esposito S, Tosco A, Sepe A, De GF, et al. Restoration of CFTR function in patients with cystic fibrosis carrying the F508del-CFTR mutation. *Autophagy.* (2014) 10:2053–74. doi: 10.4161/15548627.2014.973737

18. Tosco A, De GF, Esposito S, De SD, Sana I, Ferrari E, et al. A novel treatment of cystic fibrosis acting on-target: cysteamine plus epigallocatechin gallate for the autophagy-dependent rescue of class II-mutated CFTR. *Cell Death Differ.* (2016) 23:1380–93. doi: 10.1038/cdd.2016.22
19. Jeitner TM, Pinto JT, Cooper AJL. Cystamine and cysteamine as inhibitors of transglutaminase activity *in vivo*. *Biosci Rep.* (2018) 38:BSR20180691. doi: 10.1042/BSR20180691
20. Vilcheze C, Hartman T, Weinrick B, Jain P, Weisbrod TR, Leung LW, et al. Enhanced respiration prevents drug tolerance and drug resistance in *Mycobacterium tuberculosis*. *Proc Natl Acad Sci USA.* (2017) 114:4495–500. doi: 10.1073/pnas.1704376114
21. Maulucci G, Chiarpotto M, Papi M, Samengo D, Pani G, De SM. Quantitative analysis of autophagic flux by confocal pH-imaging of autophagic intermediates. *Autophagy.* (2015) 11:1905–16. doi: 10.1080/15548627.2015.1084455
22. Romagnoli A, Etna MP, Giacomini E, Pardini M, Remoli ME, Corazzari M, et al. ESX-1 dependent impairment of autophagic flux by *Mycobacterium tuberculosis* in human dendritic cells. *Autophagy.* (2012) 8:1357–70. doi: 10.4161/auto.20881
23. Gutierrez MG, Master SS, Singh SB, Taylor GA, Colombo MI, Deretic V. Autophagy is a defense mechanism inhibiting BCG and *Mycobacterium tuberculosis* survival in infected macrophages. *Cell.* (2004) 119:753–66. doi: 10.1016/j.cell.2004.11.038
24. Petruccioli E, Romagnoli A, Corazzari M, Coccia EM, Butera O, Delogu G, et al. Specific T cells restore the autophagic flux inhibited by *Mycobacterium tuberculosis* in human primary macrophages. *J Infect Dis.* (2012) 205:1425–35. doi: 10.1093/infdis/jis226
25. Romagnoli A, Petruccioli E, Palucci I, Camassa S, Carata E, Petrone L, et al. Clinical isolates of the modern *Mycobacterium tuberculosis* lineage 4 evade host defense in human macrophages through eluding IL-1 β -induced autophagy. *Cell Death Dis.* (2018) 9:624. doi: 10.1038/s41419-018-0640-8
26. D'Eletto M, Farrace MG, Falasca L, Reali V, Oliverio S, Melino G, et al. Transglutaminase 2 is involved in autophagosome maturation. *Autophagy.* (2009) 5:1145–54. doi: 10.4161/auto.5.8.10040
27. Portevin D, Gagneux S, Comas I, Young D. Human macrophage responses to clinical isolates from the *Mycobacterium tuberculosis* complex discriminate between ancient and modern lineages. *PLoS Pathog.* (2011) 7:e1001307. doi: 10.1371/journal.ppat.1001307
28. Stucki D, Brites D, Jeljeli L, Coscolla M, Liu Q, Trauner A, et al. *Mycobacterium tuberculosis* lineage 4 comprises globally distributed and geographically restricted sublineages. *Nat Genet.* (2016) 48:1535–43. doi: 10.1038/ng.3704
29. Reiling N, Homolka S, Walter K, Brandenburg J, Niwinski L, Ernst M, et al. Clade-specific virulence patterns of *Mycobacterium tuberculosis* complex strains in human primary macrophages and aerogenically infected mice. *MBio.* (2013) 4:e00250–13. doi: 10.1128/mBio.00250-13
30. World Health Organization. Key Changes to Treatment of Multidrug- and Rifampicin-Resistant Tuberculosis (MDR/RR-TB). (2018). Ref Type: Report
31. Guirado E, Mbawuike U, Keiser TL, Arcos J, Azad AK, Wang SH, et al. Characterization of host and microbial determinants in individuals with latent tuberculosis infection using a human granuloma model. *MBio.* (2015) 6:e02537–e02514. doi: 10.1128/mBio.02537-14
32. Refai A, Gritli S, Barbouche MR, Essafi M. *Mycobacterium tuberculosis* virulent factor ESAT-6 drives macrophage differentiation toward the pro-inflammatory M1 phenotype and subsequently switches it to the anti-inflammatory M2 phenotype. *Front Cell Infect Microbiol.* (2018) 8:327. doi: 10.3389/fcimb.2018.00327
33. Iwata F, Kuehl EM, Reed GF, McCain LM, Gahl WA, Kaiser-Kupfer MI. A randomized clinical trial of topical cysteamine disulfide (cystamine) versus free thiol (cysteamine) in the treatment of corneal cystine crystals in cystinosis. *Mol Genet Metab.* (1998) 64:237–42. doi: 10.1006/mgme.1998.2725
34. Kleta R, Gahl WA. Pharmacological treatment of nephropathic cystinosis with cysteamine. *Expert Opin Pharmacother.* (2004) 5:2255–62. doi: 10.1517/14656566.5.11.2255
35. Borrell-Pages M, Canals JM, Cordelieres FP, Parker JA, Pineda JR, Grange G, et al. Cystamine and cysteamine increase brain levels of BDNF in Huntington disease via HSJ1b and transglutaminase. *J Clin Invest.* (2006) 116:1410–24. doi: 10.1172/JCI27607
36. Ferrari E, Monzani R, Vilella VR, Esposito S, Saluzzo F, Rossin F, et al. Cysteamine re-establishes the clearance of *Pseudomonas aeruginosa* by macrophages bearing the cystic fibrosis-relevant F508del-CFTR mutation. *Cell Death Dis.* (2017) 8:e2544. doi: 10.1038/cddis.2016.476
37. Rossin F, Vilella VR, D'Eletto M, Farrace MG, Esposito S, Ferrari E, et al. TG2 regulates the heat-shock response by the post-translational modification of HSF1. *EMBO Rep.* (2018) 19:e45067. doi: 10.15252/embr.201745067
38. Song M, Hwang H, Im CY, Kim SY. Recent progress in the development of transglutaminase 2 (TGase2) inhibitors. *J Med Chem.* (2017) 60:554–67. doi: 10.1021/acs.jmedchem.6b01036
39. Agnihotri N, Mehta K. Transglutaminase-2: evolution from pedestrian protein to a promising therapeutic target. *Amino Acids.* (2017) 49:425–39. doi: 10.1007/s00726-016-2320-2
40. Maiuri MC, Kroemer G. Therapeutic modulation of autophagy: which disease comes first? *Cell Death Differ.* (2019) 26:680–9. doi: 10.1038/s41418-019-0290-0
41. Lesort M, Lee M, Tucholski J, Johnson GV. Cystamine inhibits caspase activity. Implications for the treatment of polyglutamine disorders. *J Biol Chem.* (2003) 278:3825–30. doi: 10.1074/jbc.M205812200
42. Amaral EP, Conceicao EL, Costa DL, Rocha MS, Marinho JM, Cordeiro-Santos M, et al. N-Acetyl-cysteine exhibits potent anti-mycobacterial activity in addition to its known anti-oxidative functions. *BMC Microbiol.* (2016) 16:251. doi: 10.1186/s12866-016-0872-7
43. Goletti D, Petruccioli E, Romagnoli A, Piacentini M, Fimia GM. Autophagy in *Mycobacterium tuberculosis* infection: a passepartout to flush the intruder out? *Cytokine Growth Factor Rev.* (2013) 24:335–43. doi: 10.1016/j.cytogfr.2013.01.002
44. O'Neill LA, Pearce EJ. Immunometabolism governs dendritic cell and macrophage function. *J Exp Med.* (2016) 213:15–23. doi: 10.1084/jem.20151570
45. Chandra P, Ghanwat S, Matta SK, Yadav SS, Mehta M, Siddiqui Z, et al. *Mycobacterium tuberculosis* inhibits RAB7 recruitment to selectively modulate autophagy flux in macrophages. *Sci Rep.* (2015) 5:16320. doi: 10.1038/srep16320
46. Chandra P, Kumar D. Selective autophagy gets more selective: uncoupling of autophagy flux and xenophagy flux in *Mycobacterium tuberculosis*-infected macrophages. *Autophagy.* (2016) 12:608–9. doi: 10.1080/15548627.2016.1139263
47. Kimmey JM, Huynh JP, Weiss LA, Park S, Kambal A, Debnath J, et al. Unique role for ATG5 in neutrophil-mediated immunopathology during *M. tuberculosis* infection. *Nature.* (2015) 528:565–9. doi: 10.1038/nature16451
48. Brites D, Gagneux S. Co-evolution of *Mycobacterium tuberculosis* and *Homo sapiens*. *Immunol Rev.* (2015) 264:6–24. doi: 10.1111/imr.12264
49. Gagneux S. Ecology and evolution of *Mycobacterium tuberculosis*. *Nat Rev Microbiol.* (2018) 16:202–13. doi: 10.1038/nrmicro.2018.8
50. Ribeiro SC, Gomes LL, Amaral EP, Andrade MR, Almeida FM, Rezende AL, et al. *Mycobacterium tuberculosis* strains of the modern sublineage of the Beijing family are more likely to display increased virulence than strains of the ancient sublineage. *J Clin Microbiol.* (2014) 52:2615–24. doi: 10.1128/JCM.00498-14
51. Etna MP, Giacomini E, Severa M, Coccia EM. Pro- and anti-inflammatory cytokines in tuberculosis: a two-edged sword in TB pathogenesis. *Semin Immunol.* (2014) 26:543–51. doi: 10.1016/j.smim.2014.09.011
52. Jeitner TM, Delikatny EJ, Ahlqvist J, Capper H, Cooper AJ. Mechanism for the inhibition of transglutaminase 2 by cystamine. *Biochem Pharmacol.* (2005) 69:961–70. doi: 10.1016/j.bcp.2004.12.011
53. Agrawal N, Streat I, Pei G, Weiner J, Kotze L, Bandermann S, et al. Human monocytic suppressive cells promote replication of *Mycobacterium tuberculosis* and alter stability of *in vitro* generated granulomas. *Front Immunol.* (2018) 9:2417. doi: 10.3389/fimmu.2018.02417
54. Nuernberger EL, Spigelman MK, Yew WW. Current development and future prospects in chemotherapy of tuberculosis. *Respirology.* (2010) 15:764–78. doi: 10.1111/j.1440-1843.2010.01775.x

55. Camassa S, Palucci I, Iantomasi R, Cubeddu T, Minerva M, De ME, et al. Impact of pe_pgrs33 gene polymorphisms on *Mycobacterium tuberculosis* infection and pathogenesis. *Front Cell Infect Microbiol.* (2017) 7:137. doi: 10.3389/fcimb.2017.00137
56. Antonioli M, Albiero F, Nazio F, Vescovo T, Perdomo AB, Corazzari M, et al. AMBRA1 interplay with cullin E3 ubiquitin ligases regulates autophagy dynamics. *Dev Cell.* (2014) 31:734–46. doi: 10.1016/j.devcel.2014.11.013
57. Palucci I, Camassa S, Cascioferro A, Sali M, Anoosheh S, Zumbo A, et al. PE_PGRS33 contributes to *Mycobacterium tuberculosis* entry in macrophages through interaction with TLR2. *PLoS ONE.* (2016) 11:e0150800. doi: 10.1371/journal.pone.0150800
58. Puissegur MP, Botanch C, Duteyrat JL, Delsol G, Caratero C, Altare F. An *in vitro* dual model of mycobacterial granulomas to investigate the molecular interactions between mycobacteria and human host cells. *Cell Microbiol.* (2004) 6:423–33. doi: 10.1111/j.1462-5822.2004.00371.x
59. Maulucci G, Labate V, Mele M, Panieri E, Arcovito G, Galeotti T, et al. High-resolution imaging of redox signaling in live cells through

an oxidation-sensitive yellow fluorescent protein. *Sci Signal.* (2008) 1:pl3. doi: 10.1126/scisignal.143pl3

Conflict of Interest: The authors declare that the research was conducted in the absence of any commercial or financial relationships that could be construed as a potential conflict of interest.

The handling editor declared a shared affiliation, though no other collaboration, with one of the authors, MP.

Copyright © 2020 Palucci, Maulucci, De Maio, Sali, Romagnoli, Petrone, Fimia, Sanguinetti, Goletti, De Spirito, Piacentini and Delogu. This is an open-access article distributed under the terms of the Creative Commons Attribution License (CC BY). The use, distribution or reproduction in other forums is permitted, provided the original author(s) and the copyright owner(s) are credited and that the original publication in this journal is cited, in accordance with accepted academic practice. No use, distribution or reproduction is permitted which does not comply with these terms.



NSC 18725, a Pyrazole Derivative Inhibits Growth of Intracellular *Mycobacterium tuberculosis* by Induction of Autophagy

Garima Arora^{1†}, Gagandeep^{2†}, Assirbad Behura³, Tannu Priya Gosain¹, Ravi P. Shaliwal¹, Saqib Kidwai¹, Padam Singh¹, Shamseer Kulangara Kandi², Rohan Dhiman³, Diwan S. Rawat² and Ramandeep Singh^{1*}

¹ Tuberculosis Research Laboratory, Translational Health Science and Technology Institute, Faridabad, India, ² Department of Chemistry, Faculty of Science, University of Delhi, New Delhi, India, ³ Laboratory of Mycobacterial Immunology, Department of Life Science, National Institute of Technology, Rourkela, India

OPEN ACCESS

Edited by:

Roberto Nisini,
Istituto Superiore di Sanità (ISS), Italy

Reviewed by:

Mary O'Sullivan,
Trinity College Dublin, Ireland
Babak Javid,
Tsinghua University, China
Alok Kumar Singh,
Johns Hopkins Medicine,
United States

*Correspondence:

Ramandeep Singh
ramandeep@thsti.res.in

[†] These authors have contributed
equally to this work

Specialty section:

This article was submitted to
Antimicrobials, Resistance
and Chemotherapy,
a section of the journal
Frontiers in Microbiology

Received: 09 September 2019

Accepted: 18 December 2019

Published: 28 January 2020

Citation:

Arora G, Gagandeep, Behura A, Gosain TP, Shaliwal RP, Kidwai S, Singh P, Kandi SK, Dhiman R, Rawat DS and Singh R (2020) NSC 18725, a Pyrazole Derivative Inhibits Growth of Intracellular *Mycobacterium tuberculosis* by Induction of Autophagy. *Front. Microbiol.* 10:3051. doi: 10.3389/fmicb.2019.03051

The increasing incident rates of drug-resistant tuberculosis (DR-TB) is a global health concern and has been further complicated by the emergence of extensive and total drug-resistant strains. Identification of new chemical entities which are compatible with first-line TB drugs, possess activity against DR-, and metabolically less active bacteria is required to tackle this epidemic. Here, we have performed phenotypic screening of a small molecule library against *Mycobacterium bovis* BCG and identified 24 scaffolds that exhibited MIC₉₉ values of at least 2.5 μ M. The most potent small molecule identified in our study was a nitroso containing pyrazole derivative, NSC 18725. We observed a significant reduction in viable bacilli load of starved *Mycobacterium tuberculosis* upon exposure to NSC 18725. The action of NSC 18725 was “synergistic” with isoniazid (INH) and “additive” with other drugs in our checkerboard assays. Structure-activity relationship (SAR) studies of the parent compound revealed that pyrazole derivatives without a functional group at fourth position lacked anti-mycobacterial activity *in vitro*. The derivative with *para*-chlorophenyl substitution at the first position of the pyrazole ring was the most active scaffold. We also demonstrate that NSC 18725 is able to induce autophagy in differentiated THP-1 macrophages. The induction of autophagy by NSC 18725 is the major mechanism for the killing of intracellular slow and fast-growing mycobacteria. Taken together, these observations support the identification of NSC 18725 as an antimycobacterial compound, which synergizes with INH, is active against non-replicative mycobacteria and induces autophagy in macrophages.

Keywords: *Mycobacterium tuberculosis*, phenotypic screening, pyrazole scaffold, NSC-18725, autophagy

INTRODUCTION

Tuberculosis (TB), is responsible for the highest number of annual deaths among the infectious diseases (Glaziou et al., 2018). Furthermore, approximately 1.7 billion individuals are estimated to be latently infected with *Mycobacterium tuberculosis*. These individuals are asymptomatic, non-infectious but at a risk of developing disease during their lifetime (Glaziou et al., 2018). The

current regimen for TB treatment comprises of an intensive phase of 2 months of administration of isoniazid (INH), rifampicin (RIF), ethambutol (EMB), and pyrazinamide (PZA) followed by a 4-month continuation phase for INH and RIF administration (Snider and Roper, 1992; Bass et al., 1994). Several factors, such as poor patient compliance, low tolerability, and sub-optimal drug concentration contribute to the emergence of drug resistant (DR-) strains. Approximately, 3.5% of newly diagnosed and 18% of previously treated TB cases are estimated to be multi-drug resistant TB (MDR-TB), which are defined as having resistance to both INH and RIF. Among cases of MDR-TB, 8.5% are extensively drug resistant TB (XDR-TB), defined as individuals having resistance to at least one fluoroquinolone and a second-line injectable drug in addition to INH and RIF (Horsburgh et al., 2015). The cure rates in individuals with drug-susceptible TB (DS-TB), MDR-TB and XDR-TB, are 82, 55, and 34%, respectively (Glaziou et al., 2018). Therefore, it is imperative to design better tolerated and shorter drug regimens to eliminate both DS- and DR-TB. The new candidate drug should (i) target a novel metabolic pathway, (ii) possess activity against DR-strains and metabolically dormant bacteria, and (iii) be compatible with current first-line TB and anti-retroviral therapy.

High-throughput phenotypic screening is the most successful approach for identification of new chemical entities against *M. tuberculosis*. Phenotypic screening addresses challenges associated with cell wall penetration, pro-drug activation and results in the identification of accessible and essential bacterial targets (Swinney, 2013; Dhiman and Singh, 2018; Yuan and Sampson, 2018). Several groups have performed modified phenotypic screening by incorporating conditions such as acidic, low oxygen, nutrient starvation, reactive nitrogen intermediates, and fatty acids as carbon source in their screening assays (Cho et al., 2007; Mak et al., 2012; Grant et al., 2013; VanderVen et al., 2015; Early et al., 2019). In addition, high-content screening has also resulted in identification of compounds that inhibit growth of intracellular *M. tuberculosis* (Christophe et al., 2009, 2010; Brodin et al., 2010; Pethe et al., 2013; Stanley et al., 2014). Target-based phenotypic screening combines the advantage of both phenotypic and target-based screening for validation of various metabolic pathways as drug-targets and identification of small molecules targeting these essential enzymes (Bogatcheva et al., 2010; Wilson et al., 2013; Moreira et al., 2015). The combination of phenotypic screening and whole-genome sequencing of the DR-strains has led to identification of various scaffolds that are currently being evaluated in different stages of clinical trials (Dhiman and Singh, 2018; Yuan and Sampson, 2018). Among these, Bedaquiline (BDQ, targeting ATP synthase), Pretomanid (PA-824), and Delamanid (OPC-68683, targeting bacterial respiration) have been recently FDA-approved for administration in individuals with MDR-TB (Diacon et al., 2014; Li H. et al., 2019; Li Y. et al., 2019).

In the present study, we have performed conventional phenotypic screening to identify small molecules that possess anti-tubercular activity. Among the identified anti-mycobacterial compounds, NSC 18725 was the most potent scaffold that displayed an MIC₉₉ value of 0.3125 μ M against both fast and slow growing mycobacteria in liquid cultures. The lead

compound possessed activity against starved *M. tuberculosis* and was synergistic with first-line TB drug, INH *in vitro*. Using medicinal chemistry approach, we demonstrate that the nitroso functional group is important for NSC 18725 activity. Further, we show that NSC 18725 induces autophagy and inhibits survival of intracellular *M. tuberculosis* in human macrophages. Taken together, we have identified an anti-tubercular lead compound for future mechanistic and structure-based drug design studies.

MATERIALS AND METHODS

Cell Culture and Reagents

The maintenance and differentiation of THP-1, a human monocytic cell line, into macrophages (THP-1) was performed as previously described (Mawatwal et al., 2017). The details of cell culture reagents used in the present study are provided in **Supplementary Text 1**.

Bacterial Strains and Growth Conditions

The culturing of various mycobacterial strains was carried out in Middlebrook (MB) 7H9 medium supplemented with 0.2% glycerol, 1 \times Albumin-Dextrose-Saline (ADS), 0.05% Tween-80, or 7H11 agar supplemented with 1 \times Oleic acid-Albumin-Dextrose-Saline (OADS) as previously described (Singh et al., 2013). For MIC₉₉ determination assays, *Staphylococcus aureus* (ATCC-BAA-976), *Klebsiella pneumoniae* (ATCC-33495), and *Pseudomonas aeruginosa* (ATCC-2785) were cultured in Mueller-Hinton broth. *Enterococcus faecium* (ATCC-19434), *Acinetobacter baumannii* (ATCC-BAA-2800), and *Escherichia coli* MSG1655 were cultured in brain heart infusion broth, tryptic soy broth, and Luria-Bertani broth, respectively.

Phenotypic Screening and MIC₉₉ Determination Assays

In vitro MIC₉₉ determination assays against various bacterial strains were determined as reported previously (Kidwai et al., 2017). Preliminary screening of small molecular library at 10 μ M concentration was performed using *Mycobacterium bovis* BCG as a host strain. For actual MIC₉₉ determination, the plates were incubated at 37°C for 1 day in the case of ESKAPE pathogens, 2 days in the case of *Mycobacterium smegmatis* and 10–14 days in the case of *M. bovis* BCG and *M. tuberculosis*. The lowest concentration of drug at which no visible growth was observed is reported as the MIC₉₉ values. All assay plates included no drug, medium only controls, and positive controls such as INH for *M. tuberculosis* and *M. bovis* BCG and ampicillin or tetracycline for ESKAPE pathogens. We also determined the synergy of the lead compound NSC 18725 with various first-line TB drugs, INH, RIF, or EMB and drugs in clinical trials, BTZ043 or BDQ or PA-824 using checkerboard assay. The fractional inhibitory concentration index (Σ FIC) in various drug-combinations was calculated as previously described (Odds, 2003). For *in vitro* killing experiments, early logarithmic cultures (OD_{600 nm} ~0.2) and nutritionally starved cultures were exposed to various drugs at 10 \times MIC₉₉ concentration as described previously

(Betts et al., 2002; Kidwai et al., 2017). For nutritionally starved bacteria, mid-log phase cultures were washed with $1 \times$ PBS, resuspended in $1 \times$ PBS and exposed to $10 \times$ MIC₉₉ of drugs. After 7 days of exposure, 10-fold serial dilutions were prepared and plated on MB7H11 plates at 37°C for 3–4 weeks.

Cell Viability and Intracellular Killing Experiments

Cell viability of THP-1 cells after exposure to drugs was determined using Cell Proliferation Reagent, WST-1 as per manufacturer's recommendation (Sigma-Aldrich, St. Louis, MO, United States). For macrophage killing experiments, THP-1 cells were infected with single-cell bacterial suspensions as previously described (Mawatwal et al., 2017). After 4 h post-infection, the extracellular bacteria were removed by overlaying macrophages with RPMI medium containing 200 µg/ml of amikacin. After 2 h of incubation, cells were washed and infected macrophages were overlaid with RPMI medium containing drugs for indicated time points. In another experiment, infected macrophages were pre-treated for 1 h with 3-methyl adenine (3-MA, 10 mM), a selective PI3K inhibitor that inhibits autophagy before treating with NSC 18725 for varied time points. Co-localization experiments were performed by infecting THP-1 cells with GFP labeled *M. bovis* BCG at a MOI of 1:10 as described above followed by treatment with NSC 18725 treatment for 12 h. For bacterial enumeration, 10-fold serial dilutions were prepared and plated on MB7H11 plates at 37°C for 3–4 weeks.

Confocal Microscopy Experiments

The formation and counting of LC3 puncta were estimated using a previously published protocol (Mawatwal et al., 2017). Briefly, drug-treated macrophages were fixed, permeabilized, and stained with specific antibodies. The formation of LC3 puncta was manually counted in approximately 50 cells for each experiment. In a separate experiment, vacuolar ATPase inhibitor, Bafilomycin A1 (Baf-A1, 50 nM) was added 3 h prior to completion of NSC 18725 treatment followed by estimation of LC3 puncta. Further, monodansylcadaverine (MDC) staining was also performed in drug treated THP-1 macrophages as previously described (Mawatwal et al., 2018). The images were acquired using confocal scanning laser microscope (CSLM, Leica Microsystems, Wetzlar, Germany) and were finally processed for presentation using Adobe Photoshop software. In co-localization experiments, macrophages were fixed, stained for LC3 and visualized under confocal microscope using same methodology as discussed above. The % co-localization between GFP labeled *M. bovis* BCG and LC3 was calculated by counting more than 50 bacteria in at least five or six random fields.

Western Blot Analysis

The expression analysis of various autophagy markers such as Beclin-1 and Atg 3 in THP-1 macrophages was quantified by Western blot analysis as per manufacturer's recommendations. Briefly, the protein samples were prepared in radioimmunoprecipitation assay (RIPA) buffer containing protease inhibitors. The samples were fractionated through

SDS-PAGE, transferred to nitrocellulose membrane, probed with appropriate antibodies, and detected using ECL kit. The relative fold intensities in drug treated samples in comparison to control samples were quantified using ImageJ software (NIH, United States).

Chemical Synthesis of Various Pyrazole Derivatives

The reagents for chemical synthesis of pyrazole derivatives were purchased from Spectrochem, India. The formation of the final products was monitored by thin-layer chromatography (TLC). The purification of the final products was performed by column chromatography using silica gel. The melting points of various compounds were recorded on EZ-Melt automated melting point apparatus, Stanford Research Systems and are uncorrected. IR-spectra were recorded on Perkin-Elmer FT-IR spectrophotometer using KBr pellets, and the values are expressed in cm^{-1} . ^1H NMR (400 MHz) and ^{13}C NMR (100 MHz) spectra were recorded on Jeol ECX spectropin instrument using CDCl_3 as a solvent with TMS as an internal reference. The chemical shift values were expressed on δ scale and the coupling constant (J) in Hz. The mass data were recorded in Jeol-Accu TOF JMS-T100LC and micromass LCT mass spectrometer/Data system. The synthesis and characterization details of various small molecules are described in **Supplementary Text 1**.

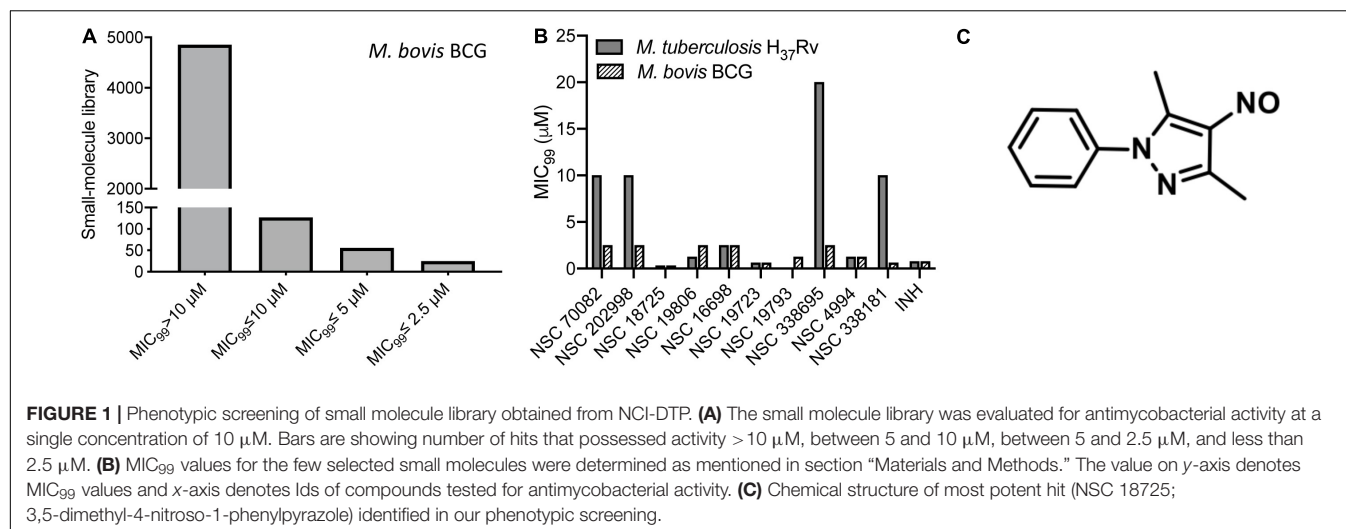
Statistical Analysis

Differences between groups were determined by paired (two-tailed) t test. Differences were considered significant at a P value of <0.05 . GraphPad Prism version 8 (GraphPad Software Inc., San Jose, CA, United States) was used for statistical analysis and the generation of graphs.

RESULTS

Identification of NSC 18725 as a Highly Potent and Specific Hit for *Mycobacterium tuberculosis*

In order to identify novel scaffolds with anti-tubercular activity, we screened approximately 5,000 small molecules using *M. bovis* BCG as a host strain. The small molecule library was procured from the National Institutes of Health and compounds belonged to either Open Set II or Oncology Set V. Initially, the preliminary screening was performed at a single concentration of 10 µM, and we observed a hit rate of 4.14% with 207 compounds inhibiting bacterial growth by more than 99% (**Figure 1A**). These active scaffolds were re-evaluated for MIC₉₉ determination in a dose dependent manner. Among the active scaffolds, 127, 56, and 24 compounds displayed MIC₉₉ value in the range of 5–10 µM, 2.5– 5 µM, and less than 2.5 µM, respectively (**Figure 1A**). Among the scaffolds that displayed MIC₉₉ below 2.5 µM, we selected 10 preliminary hits, and these were evaluated for their anti-tubercular activity (**Table 1** and **Supplementary Figure S1**). As shown in **Figure 1B**, we observed that MIC₉₉ values of NSC



18725, NSC 19806, NSC 16698, NSC 19723, NSC 19793, and NSC 4994 were comparable against both *M. bovis* BCG and *M. tuberculosis*. However, NSC 70082, NSC 202998, NSC 338695, and NSC 338181 showed less potency against *in vitro* grown cultures of *M. tuberculosis* in comparison to their activity against *M. bovis* BCG (Figure 1B). The most potent hits identified in our phenotypic screening were NSC 18725 and NSC 19723, and their activity was comparable to the activity observed for INH, a front-line TB drug (Table 1).

In the subsequent sections, we would discuss results of structure-activity relationship (SAR) and activity of NSC 18725 against mycobacteria *in vitro* and in macrophages (Figure 1C). We next determined the antimicrobial spectrum of NSC 18725 by evaluating its activity against well-characterized ESKAPE pathogens. As shown in Table 2, we noticed that NSC 18725 was inactive against *E. coli* and ESKAPE pathogens *in vitro* even at 25 μ M. As shown in Table 2, the control drugs inhibited the growth of ESKAPE pathogens *in vitro* in the expected range. We also evaluated NSC 18725 for activity against fast-growing mycobacterial species *M. smegmatis* and observed that the MIC₉₉ value was similar to that obtained against slow growing mycobacteria (Table 2). Taken together, these results demonstrate that NSC 18725 inhibits a metabolic pathway that is vital for *in vitro* growth of mycobacteria. We next determined the mode of mycobacterial killing by NSC 18725 *in vitro*. As shown in Figure 2A, we observed that exposure of *M. bovis* BCG early logarithmic cultures to NSC 18725 resulted in reduction of bacterial counts by ~ 9.0 folds in comparison to untreated samples ($*P < 0.05$). As expected, exposure of early logarithmic cultures to INH for 7 days resulted in ~ 450 -fold reduction in bacterial counts (Figure 2A, $**P < 0.01$). Several studies have shown that *M. tuberculosis* enters into dormancy in host tissues by slowing down its metabolism, and this metabolically less active dormant bacteria is tolerant to front-line TB drugs (Wayne and Sohaskey, 2001; Peddireddy et al., 2017). Next, the activity of NSC 18725 was evaluated against non-replicating persistent *M. tuberculosis* using nutrient-starvation model (Betts et al., 2002). Interestingly, we observed

that exposure to NSC 18725 results in the killing of starved bacteria in a bactericidal manner. As shown in Figure 2B, the bacterial counts declined by ~ 24.0 -fold upon exposure to NSC 18725 ($*P < 0.05$). As expected, nutrient deprived-cultures of *M. tuberculosis* were resistant to killing by INH after 7 days of exposure (Figure 2B). These observations indicate that NSC 18725 targets a metabolic pathway that is essential for *M. tuberculosis* to survive in nutrient limiting growth conditions.

NSC 18725 Potentiates the Anti-tubercular Efficacy of Front-Line Anti-tubercular Drugs and Drugs in Clinical Trials

In order to tackle the threat imposed by anti-microbial resistance, there is an urgent need to identify small molecules that are compatible with first-line TB drugs and possess activity against DR-TB. Hence, we investigated the interactions between NSC 18725 and other front-line TB drugs or drugs in clinical trials. We measured the activity of NSC 18725 either alone or in combination with either INH or RIF or EMB or BDQ or BTZ043 or PA-824 using checkerboard assay. As shown in Figure 2C, NSC 18725 synergizes with INH against *M. tuberculosis* with a Σ FIC value of 0.375 in our checkerboard experiments. This combination improved the individual MIC₉₉ values of NSC 18725 and INH by 8.0 fold and 4.0 fold, respectively. The Σ FIC of NSC 18725 with RIF, EMB, BDQ, BTZ043, and PA-824 was approximately 0.75, 2, 1, 0.75, and 1, respectively suggesting the additive effect in these drug-combinations (Figure 2C). Taken together, these data augur well for future evaluation of NSC18725 in combination with first-line TB drugs in particular INH against *M. tuberculosis*.

Structure-Activity Relationship Studies of NSC 18725

The parent compound, NSC 18725 (compound 5b, 3,5-dimethyl-4-nitroso-1-phenyl-1H-pyrazole), was chemically synthesized and evaluated for its activity against slow growing mycobacteria

TABLE 1 | List of compounds displaying MIC₉₉ values less than 2.5 μM identified from phenotypic screening performed in the present study.

S. No	NSC number	Compound name	Molecular weight (Daltons)	MIC ₉₉ (<i>M. bovis</i> BCG)
1	NSC 19893	5-Fluorouracil	130.08	0.156
2	NSC 15558	(4-Fluorophenyl)(oxo)arsane	186.01	1.25
3	NSC 70082	Diethylcarbamodithioic acid; tellurium	276.9	2.5
4	NSC 203105	Mercury, bis(1-butanethiolato)-	290.78	2.5
5	NSC 202998	Phenazine 5-oxide	196.2	2.5
6	NSC 18725	3,5-Dimethyl-4-nitroso-1-phenylpyrazole	201.22	0.3125
7	NSC 19806	Cinnamaldehyde, alpha-bromo-	211.05	2.5
8	NSC 16698	2-Methoxy-4-[(Z)-2-methyl-3-nitroprop-1-enyl]phenol	223.22	2.5
9	NSC 12470	Ethyl 2-acetamido-2-cyano-5-oxopentanoate	226.23	0.156
10	NSC 338695	Benzo[g]isoquinoline-5,10-dione	209.2	2.5
11	NSC 4830	Pyridylmercuric acetate	337.73	1.25
12	NSC 4773	Phenylmercuric hydroxide	295.71	0.156
13	NSC 4994	1-Chloro-5-nitroanthraquinone	287.65	1.25
14	NSC 338181	5-[(4-Chlorophenyl)hydrazinylidene]-2-(dimethylamino)-6-methylpyrimidin-4-one	291.73	0.625
15	NSC 269612	7-Chloro-[1,4]dithiino[2,3-b]quinoxaline-2,3-dicarbonitrile	302.8	1.25
16	NSC 19723	[(E)-(4-Prop-2-enoxyphenyl)methylideneamino]thiourea	235.31	0.625
17	NSC 19793	(1Z)-1-(4-Chlorophenyl)-2-diazonio-3-methoxy-3-oxoprop-1-en-1-olate	238.63	1.25
18	NSC 338107	1-(2H-Tetrazol-5-ylhydrazinylidene)naphthalen-2-one	240.22	1.25
19	NSC 4603	Chloro(2,2-dimethylpropyl)mercury	307.18	0.156
20	NSC 63142	N-[(E)-1-(3-Bromophenyl)ethylideneamino]pyridine-4-carboxamide	318.17	1.25
21	NSC 4772	Nitrooxy(phenyl)mercury or Phermernite	339.7	0.156
22	NSC 60777	3-Methoxyestra-1,3,5(10)-triene-16,17-dione 16-oxime	313.4	2.5
23	NSC 36758	Tolonium chloride, (7-amino-8-methylphenothiazin-3-ylidene)-dimethylazanium;chloride	305.8	1.56
24	NSC 171303	3-Nitro-N-(5-nitro-1,3-thiazol-2-yl) benzamide	294.25	2.5

TABLE 2 | Activity of NSC 18725 against *Mycobacterium smegmatis* and ESKAPE Pathogens.

Strain name	NSC 18725 (μM)	Tetracycline (μg/ml)	Ampicillin (μg/ml)	Rifampicin (μM)
<i>E. coli</i> MG1655	50	0.38	Not done	Not done
<i>S. aureus</i> (ATCC-BAA-976)	50	<0.09	Not done	Not done
<i>K. pneumoniae</i> (ATCC – 33495)	25	25	Not done	Not done
<i>P. aeruginosa</i> (ATCC-2785)	50	12.5	Not done	Not done
<i>E. faecium</i> (ATCC-19434)	> 100	0.39	3.125	10
<i>A. baumannii</i> (ATCC-BAA-2800)	25	> 50	> 200	10
<i>M. smegmatis</i> mc ² 155	0.39–0.78	Not done	Not done	Not done

in liquid cultures. The synthesized parent compound (5b) displayed a MIC₉₉ value of 0.3125 μM, and this was similar to the activity obtained from our phenotypic screening (Table 3). In order to design a more potent analog, we synthesized series of NSC 18725 structural analogs using medicinal chemistry approach and evaluated their *in vitro* anti-mycobacterial activity. We synthesized two series of compounds. In Series I the substituted phenyl ring was attached to the N-1 position of the pyrazole ring and lacked any substitution at the fourth position of the pyrazole ring (3a–3f, Figure 3A). In Series II, the nitroso group was introduced at the fourth position of the pyrazole ring and the substituted phenyl ring was varied at the N-1 position of the pyrazole ring (5b–5k, Figure 3B). Subsequently, the nitroso group of the parent compound (5b) was reduced by catalytic hydrogenation using H₂ gas in the presence of a catalyst, Pd/C (6a, Figure 4A). Finally, the halogen groups were introduced at

the fourth position of the pyrazole ring by reacting 3,5-dimethyl-1-phenyl-1H-pyrazole (3b) with either *N*-bromosuccinimide or *N*-chlorosuccinimide (7a, 7b, Figure 4B). The details of the synthesis and characterization of various scaffolds are provided in Supplementary Text 1.

In our MIC₉₉ determination assays, we observed that pyrazole derivatives (3a–3f) lacking a functional group at the fourth position were inactive against *M. tuberculosis* and displayed an MIC₉₉ value greater than 50 μM (Table 3). We also noticed that derivatives (5b–5k) having the nitroso functional group at the fourth position were active and displayed MIC₉₉ value in the range of 0.039–6.25 μM. Among these molecules, pyrazole derivative with *para*-chlorophenyl at the first position displayed the highest activity in the range of 0.039–0.078 μM against *M. tuberculosis* (5f, Table 3). The pyrazole derivative with *p*-tolyl substitution also displayed 4.0-fold higher activity in comparison

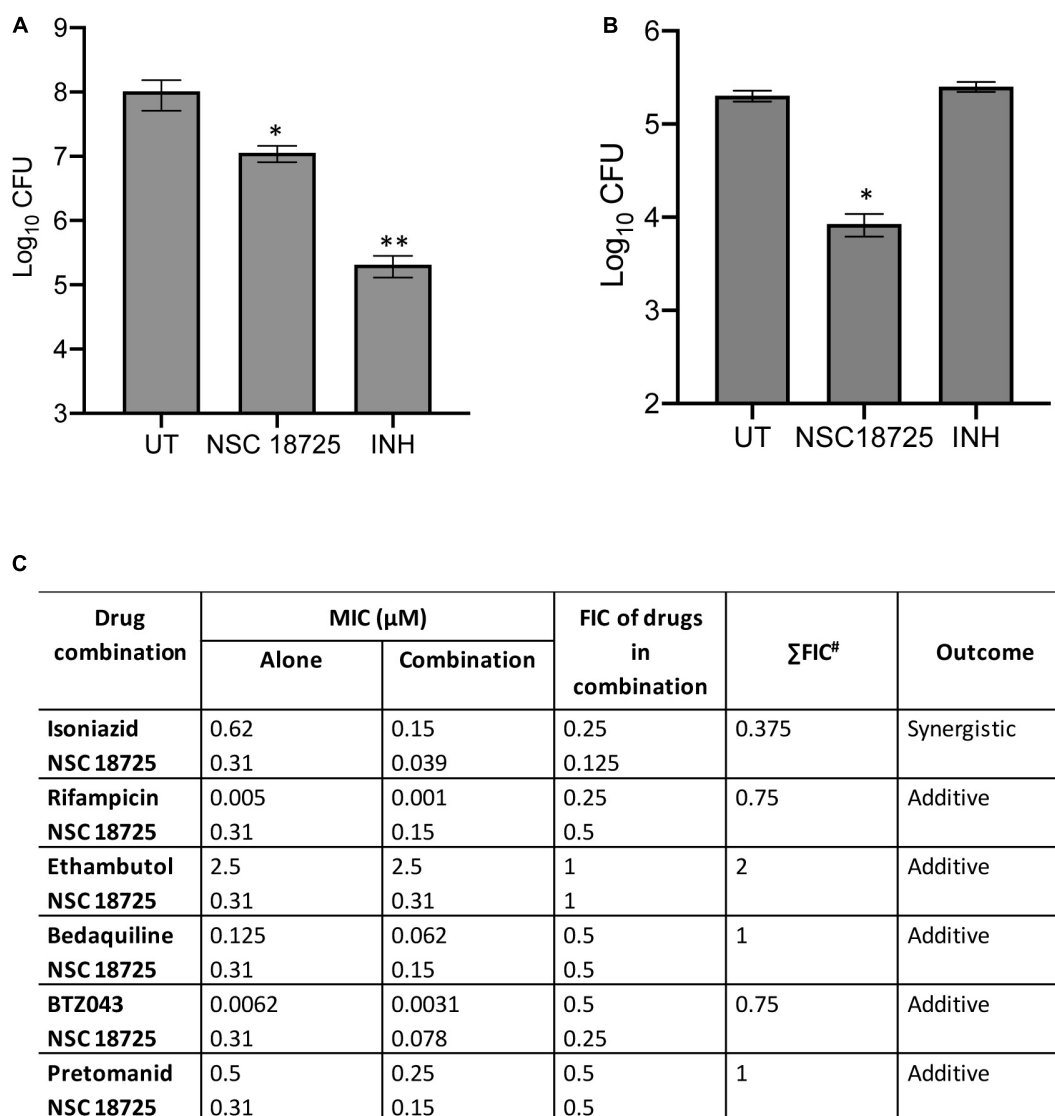
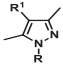


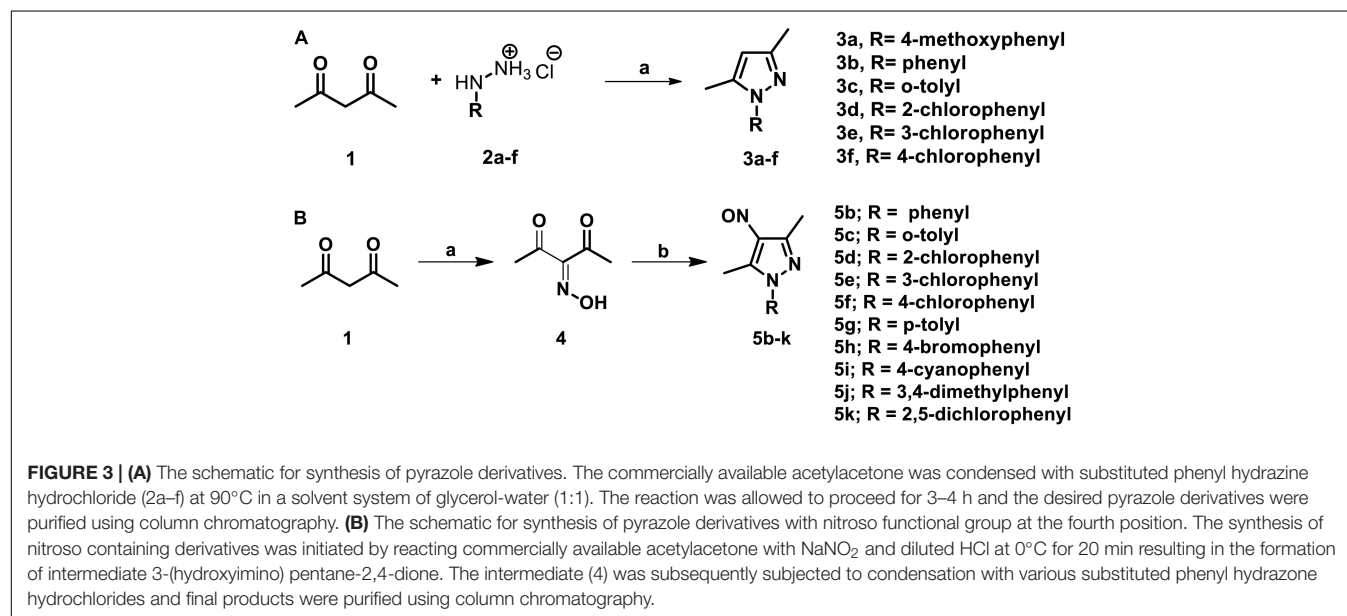
FIGURE 2 | (A,B) Time kill kinetics of NSC 18725 against *Mycobacterium bovis* BCG and *Mycobacterium tuberculosis*. **(A)** *M. bovis* BCG was grown till early logarithmic phase ($OD_{600\text{ nm}} \sim 0.2$) and subsequently exposed to either NSC 18725 or INH for 7 days. **(B)** The starved *M. tuberculosis* cultures were exposed to either NSC 18725 or INH for 7 days. For bacterial enumeration, 10.0-fold serial dilutions were prepared and 100 µl was plated on MB7H11 plates at 37°C for 3–4 weeks. The data shown in panels **(A,B)** are mean \pm SE of CFU obtained from three independent experiments. $P < 0.05$ and $P < 0.01$ are represented as * and **, respectively. **(C)** Synergy experiments of NSC 18725 with first-line TB drugs and drugs in clinical trials against *M. tuberculosis* using checkerboard assay. Two-fold serial dilutions of NSC 18725 prepared horizontally were cross-diluted vertically with two-fold serial dilutions of other drugs and Σ FIC values were calculated for each combination. Combinations with best Σ FIC values are shown.

to the parent compound (5g, **Table 3**). We also observed that pyrazole derivative with nitrile substitution at *para*-position of the phenyl ring (5i) enhanced the activity of the parent compound by 2.0-fold (**Table 3**). However, a derivative with a bromo-group (5h) substitution at *para*-position of the phenyl group displayed MIC₉₉ values that were comparable to those observed for the parent compound. Next, we determined the effect of *ortho*- and *meta*-position substitution of the phenyl ring on NSC 18725 activity. We noticed that changing the position of substitution from *para*- to *ortho*- and *meta*-position resulted in a decrease of activity by 2.0-fold (5c, with methyl substitution at

ortho-position), 4.0-fold (5d, with chloro substitution at *ortho*-position) and 4.0-fold (5e, with chloro substitution at *para*-position). Further, multiple substitutions on the phenyl ring resulted in reduced activity (5j; MIC₉₉ = 0.3125–0.6250 µM and 5 k; MIC₉₉ = 0.3125 µM) in comparison to mono-substituted compounds (**Table 3**). We observed that the derivatives with multiple substitutions (5j, 5k) on the phenyl ring displayed MIC₉₉ values similar to those obtained for the parent compound (**Table 3**). These observations suggest that nitroso substitution at the fourth position of the pyrazole ring is essential for NSC 18725 activity *in vitro*. Also, substitution at the *para*-position of the

TABLE 3 | *In vitro* MIC₉₉ determination of NSC 18725 and its derivatives against both *Mycobacterium tuberculosis* H37Rv and *Mycobacterium bovis* BCG.


S. No.	Compound code	R	R ¹	MIC ₉₉ (μM) (<i>M. tuberculosis</i> H ₃₇ Rv)	MIC ₉₉ (<i>M. bovis</i> BCG)
1	3a	4-methoxyphenyl	H	>50	>50
2	3b	Phenyl	H	>50	>50
3	3c	o-tolyl	H	>50	>50
4	3d	2-chlorophenyl	H	>50	>50
5	3e	3-chlorophenyl	H	>50	>50
6	3f	4-chlorophenyl	H	>50	>50
7	5b	Phenyl	NO	0.3125	0.3125
8	5c	o-tolyl	NO	0.156	0.078–0.156
9	5d	2-chlorophenyl	NO	0.3125–0.625	0.3125
10	5e	3-chlorophenyl	NO	0.3125	0.3125–0.625
11	5f	4-chlorophenyl	NO	0.039–0.078	0.039
12	5g	p-tolyl	NO	0.078	0.078–0.156
13	5h	4-bromophenyl	NO	0.3125	0.3125
14	5i	4-cyanophenyl	NO	0.156	0.156
15	5j	3,4dimethylphenyl	NO	0.3125	0.3125
16	5k	2,5-dichlorophenyl	NO	0.3125–0.625	0.3125
17	6	Phenyl	NH ₂	>50	>50
18	7a	Phenyl	Br	>50	>50
19	7b	Phenyl	Cl	>50	>50

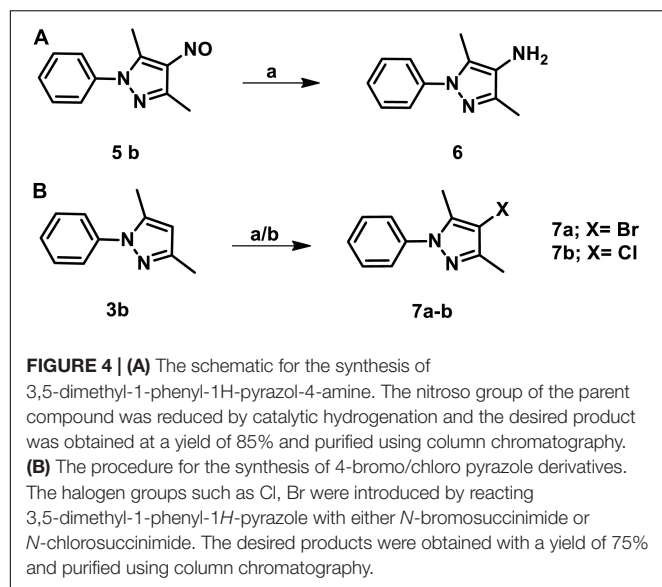


phenyl ring with chloro and methyl functional groups improves NSC 18725 anti-tubercular activity.

NSC 18725 Induces Autophagy in Differentiated THP-1 Macrophages and Inhibits Growth of Intracellular *Mycobacterium tuberculosis*

Being a facultative intracellular pathogen, *M. tuberculosis* is able to adapt to various stress conditions encountered

in the host and to replicate inside the host macrophage. Macrophages employ numerous antimicrobial mechanisms such as production of reactive oxygen intermediates, reactive nitrogen intermediates, and phagosome lysosome fusion to combat infections. Autophagy is a lysosomal degradative process and can be used by the macrophages to inhibit growth of intracellular *M. tuberculosis* (Lowrie and Andrew, 1988; Bah and Vergne, 2017). Several studies have shown that small molecules inducing autophagy are able to clear intracellular DR- and DS-TB (Kidwai et al., 2017; Mawatwal et al., 2017; Dhiman and Singh, 2018).



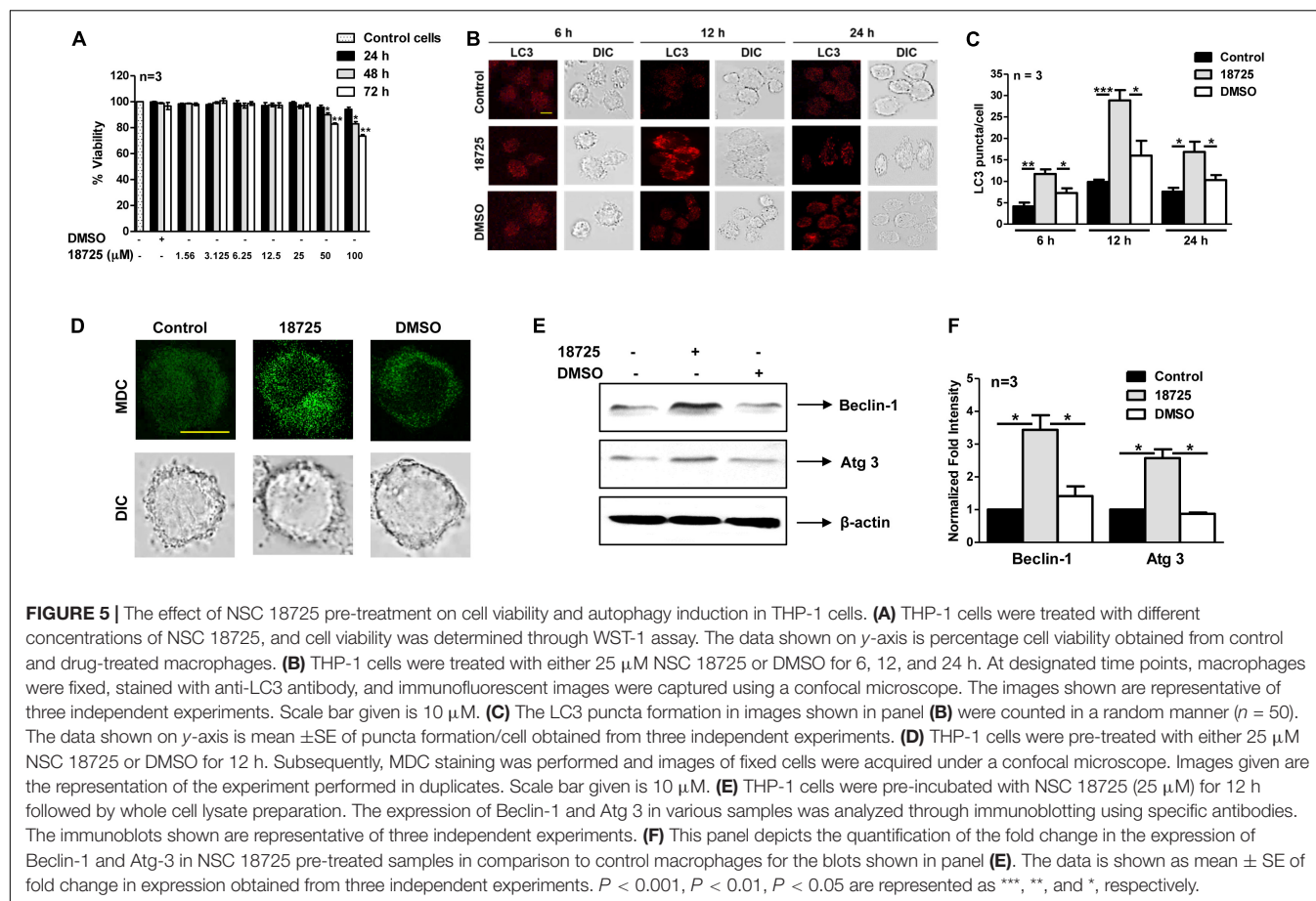
In order to investigate whether NSC 18725 is able to induce autophagy, we first determined cell viability of THP-1 cells in the presence of different concentrations of drug. We observed that NSC 18725 at 25 μ M concentration was non-cytotoxic to THP-1 cells till 72 h of incubation and subsequent experiments were performed at this concentration (**Figure 5A**). We observed that exposure of THP-1 cells to NSC 18725 at 25 μ M concentration resulted in significant LC3 puncta formation after 12 h of incubation, hence this time point was selected for future experiments (**Figures 5B,C**, $*P < 0.05$, $**P < 0.01$ and $***P < 0.001$). In concordance, MDC staining revealed significant autophagic vacuole formation in NSC 18725 treated THP-1 macrophages, and this observation was further corroborated with specific upregulation of autophagic markers such as Beclin-1 and Atg 3 at protein level in drug-treated samples (**Figures 5D,E**). As shown in **Figure 5F**, we observed that Beclin-1 and Atg 3 expression was increased by ~ 3.0 -fold and 2.5-fold, respectively, in NSC 18725 treated macrophages (**Figure 5F**, $*P < 0.05$).

Previous studies have shown that there is an accumulation of LC3 puncta or autophagic vacuole formation during autophagy inhibition, therefore, we next performed autophagy experiments in NSC 18725 treated THP-1 cells in the presence of Baf-A1 (Yoshii and Mizushima, 2017). In concordance with our earlier results, we observed that Baf-A1 addition significantly enhanced LC3 puncta and autophagic vacuole formation in NSC 18725 pre-treated THP-1 cells in comparison to untreated macrophages (**Figures 6A–D**, $*P < 0.05$, $**P < 0.01$, and $***P < 0.001$). These observations were further validated by quantifying co-localization between GFP labeled *M. bovis* BCG and LC3 in NSC 18725 treated THP-1 cells in the absence or presence of Baf-A1. As shown in **Figures 6E,F**, significant co-localization was observed in treated THP-1 cells in the presence of Baf-A1 in comparison to only NSC 18725 treated cells ($37.9 \pm 1.9\%$ vs. $26.4 \pm 2.8\%$, $*P < 0.05$). These observations indicate that NSC 18725 induces autophagy in human macrophages. Several reports

have shown that modulation of autophagy by small molecules results in faster clearance of intracellular *M. tuberculosis*, therefore, we further evaluated the antimicrobial efficacy of NSC 18725 against the pathogen replicating inside macrophages (Kidwai et al., 2017; Mawatwal et al., 2017; Dhiman and Singh, 2018). In concordance with previous studies, we observed that autophagy induction upon NSC 18725 treatment inhibited the growth of mycobacteria in human macrophages. We observed that exposure to NSC 18725 resulted in approximately 64 and 78% significant reduction in bacterial counts of *M. smegmatis* and *M. bovis* BCG, respectively in comparison to untreated and DMSO treated macrophages (**Figures 6G,H**, $*P < 0.05$, $**P < 0.01$, $***P < 0.001$). We next studied whether 3-MA inhibited the killing activity of NSC 18725. In concordance with our earlier observations, we demonstrated that preincubation of macrophages with 3-MA reduced the intracellular killing of NSC 18725 (**Figure 6I**, $*P < 0.05$, $**P < 0.01$). As expected, pre-incubation with 3-MA only has no effect on the intracellular growth of both *M. bovis* BCG and *M. smegmatis*. These findings elucidate that induction of autophagy is the mechanism by which NSC 18725 inhibits the survival of intracellular mycobacteria. Taken together, the observations presented in this study demonstrate that modulation of autophagy by NSC 18725 in human macrophages can be exploited further to design novel therapeutics against TB.

DISCUSSION

The current scenario of TB epidemiology stresses for the development of new diagnostic tools, vaccines, and drugs to tackle the challenge of DR- and DS-TB. Despite the availability of various scaffolds in clinical pipeline, there is an urgent need to develop new lead molecules that possess activity against DR- and metabolically dormant bacilli. Till date, phenotypic and target-based screening have been extensively utilized for identification and validation of novel anti-tubercular agents. Although, the target-based approach has been the backbone for drug discovery in pharmaceutical industry in past decades, it has failed to show ample success in the area of antitubercular drug discovery. This lack of whole-cell activity for small molecules identified from target-based screening is attributed to their poor penetration. Phenotypic screening has led to identification of various antitubercular scaffolds with a novel mechanism of action (Dhiman and Singh, 2018). The highly infectious and pathogenic nature of *M. tuberculosis* along with the prerequisite for complex infrastructure for handling *M. tuberculosis* led us to use *M. bovis* BCG as a surrogate host for initial screening. In the present study, we have performed whole cell based screening and identified 24 scaffolds that possessed anti-mycobacterial activity below 2.5 μ M. In concordance, with previous studies, majority of these compounds showed comparable activity against both *M. bovis* BCG and *M. tuberculosis* *in vitro* (Taneja and Tyagi, 2007; Altaf et al., 2010; Stanley et al., 2012; Kidwai et al., 2017). However, NSC 70082, NSC 202998, NSC 338695, and NSC 338181 displayed better activity against *M. bovis* BCG in comparison to *M. tuberculosis*. This differential activity could be

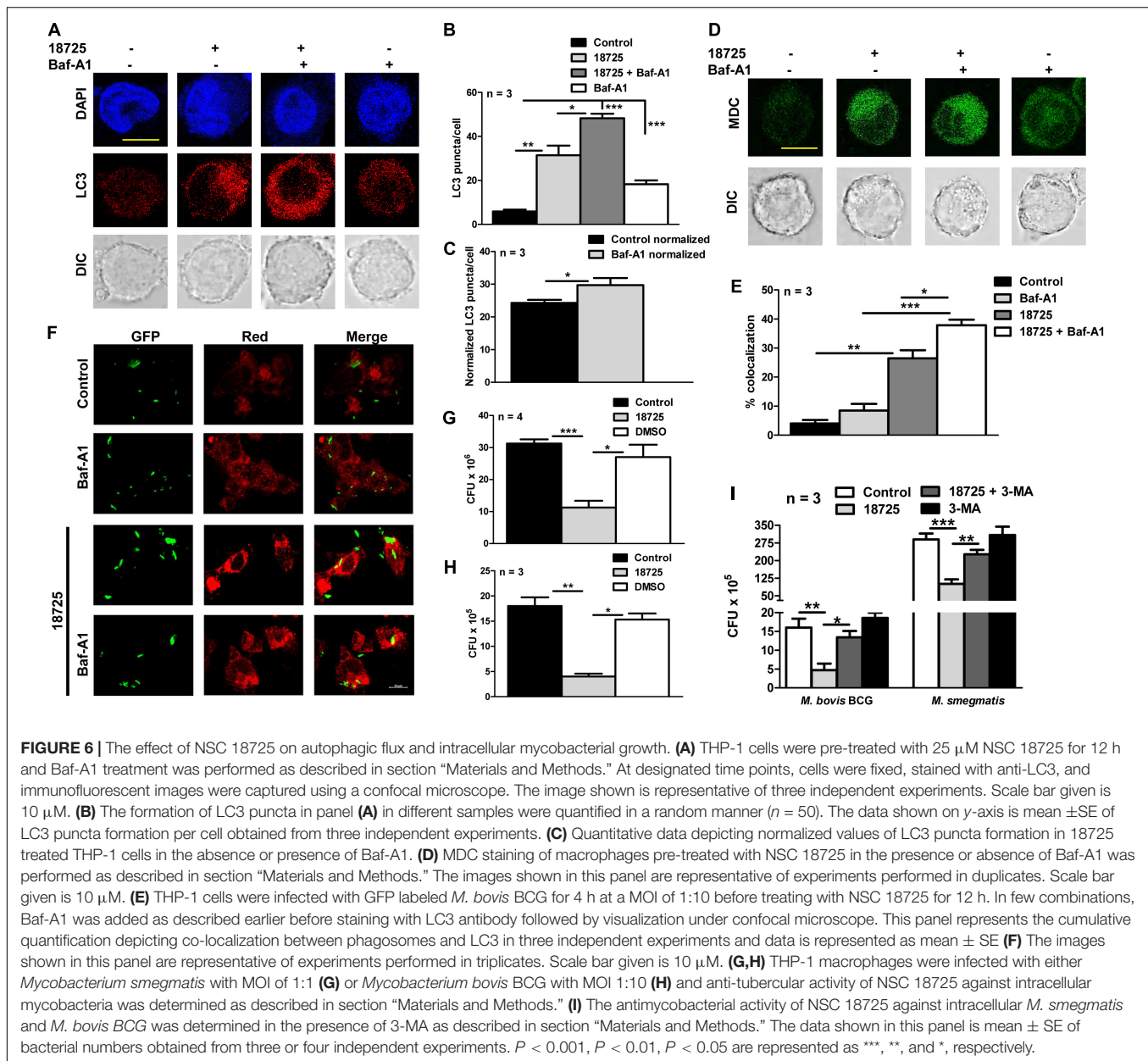


attributed to (i) altered expression levels of their respective drug-targets in *M. bovis* BCG and *M. tuberculosis* (ii) modification of the drug-target in *M. tuberculosis* or (iii) differential ability of the small molecules to penetrate in *M. bovis* BCG and *M. tuberculosis*.

In the present study, we have performed detailed characterization of NSC 18725 (3,5-dimethyl-4-nitroso-1-phenylpyrazole), the most active compound identified in our phenotypic screening. Pyrazoles containing pharmaco-active agents are potent medicinal scaffolds and exhibit a broad spectrum of biological activities such as antimicrobial, anti-inflammatory, anti-cancer, analgesic, and neuroprotection (Wilfred et al., 1956, 1958; Slack, 1957; Daidone et al., 1992; Bekhit et al., 2005; Chandra et al., 2010; Ahsan et al., 2011; Keche et al., 2012; Maurya et al., 2013; Alegaon et al., 2014; Pathak et al., 2014; Naim et al., 2016). We also observed that NSC 18725 displayed MIC₉₉ value of ~ 0.3125 μ M against slow growing mycobacteria and was non-cytotoxic to THP-1 macrophages even at 25 μ M concentration. SAR studies revealed that the nitroso group is important for anti-tubercular activity associated with this series. In concordance previous studies have also shown that nitro or nitroso functional groups are essential for the anti-tubercular activity of small molecules (Singh et al., 2008; Kidwai et al., 2017, 2019). We also show that substitution at the *para*-position of the phenyl ring with either electron withdrawing group such as (chloro and cyano)

or electron donating groups (such as methyl) improved NSC 18725 activity *in vitro*. A major limitation in the field of drug development is target identification of small molecules identified from phenotypic screens. In the present work, we have also tried to generate resistant mutant strains against NSC 18725 but all these attempts have been unsuccessful.

Indiscriminate use of antimicrobial drugs globally has resulted in increased incident rates of various DR-TB strains. Several studies have shown that pyrazole derivatives possess activities against various microbial species such as *S. aureus*, *P. aeruginosa*, *Bacillus subtilis*, *E. Coli*, and *Salmonella typhi* as well as fungal strains such as *Aspergillus niger* and *Candida albicans* (Keche et al., 2012; Naim et al., 2016; Karrouchi et al., 2018). Therefore, we also evaluated the ability of NSC 18725 against a panel of resistant strains that constitute ESKAPE pathogens. However, we observed that NSC 18725 failed to inhibit the *in vitro* growth of the tested ESKAPE pathogens thereby indicating that these pyrazole derivatives lack cross resistance with existing drugs and target a mycobacteria specific metabolic pathway. Another challenge in the field of TB chemotherapy is that among various clinical candidates very few scaffolds are able to inhibit the growth of dormant bacteria. Here, we show that NSC 18725 is able to kill the dormant population of *M. tuberculosis* thereby indicating that NSC 18725 might target a metabolic pathway which is essential for *M. tuberculosis* to



survive in nutrient limiting growth conditions. Most of the compounds that are currently in different stages of clinical trials possess activity against both DS- and DR- strains *in vitro* and show synergistic effect with the current TB drugs. We also observed that NSC 18725 shows synergistic effect with INH and additive effect with other tested TB drugs. Our results demonstrate that if used in combination, NSC 18725 can potentially reduce the dosage associated toxicity associated with TB drugs. These observations suggest that evaluation of NSC 18725 in combination with other first- and second-line drugs could help design better regimens against both DS- and DR-TB infection.

In the present study, we also validated the activity of NSC 18725 against intracellular mycobacteria in macrophage model

of infection. We observed that pre-incubation with NSC 18725 resulted in LC3 puncta formation and increased expression of autophagy markers such as Atg 3 and Beclin-1. This NSC18725 mediated modulation of autophagy resulted in inhibition of growth of mycobacteria in infected macrophages. We also observed that pre-incubation of THP-1 macrophages with 3-MA completely abrogated the intracellular activity associated with NSC 18725. Therefore, we hypothesize, that induction of autophagy is the main mechanism by which NSC 18725 inhibits intracellular bacterial growth in macrophages. These observations are in concordance with previous reports showing that induction of autophagy can be harnessed as a host-directed therapy (HDT) either alone or in combination with first-line TB drugs (Dara et al., 2019). Despite identification of autophagy

inducers, enough information is not available about the co-operative action of various known or unknown mechanisms regulated by autophagy (Paik et al., 2019). Therefore, evaluation of promising autophagy inducers as host-directed therapy either alone or in combination with first-line TB drugs will refine therapeutic interventions against TB.

Taken together, we have identified a pyrazole derivative that possesses anti-mycobacterial activity. We showed that this compound is active against both actively growing, dormant bacteria, and the nitroso group is essential for the observed anti-tubercular activity. Finally, we also show that NSC 18725 induces autophagy and inhibits the growth of intracellular mycobacteria in macrophages. Further experiments include (i) designing of structural analogs with better therapeutic index, (ii) understanding the mechanism of action of NSC 18725 *in vitro*, (iii) pharmacokinetics and pharmacodynamic studies to determine stability of these series of compounds in serum or plasma of animals, and (iv) evaluating the *in vivo* efficacy of this series in mice model of infection.

CONCLUSION

In conclusion, we have identified NSC 18725 as an anti-tubercular compound with the activity comparable to INH, first-line TB drug. In addition, NSC 18725 also possesses activity against dormant *M. tuberculosis* *in vitro*. We also demonstrate that NSC 18725 augments the host defense mechanisms by inducing autophagy and inhibits *M. tuberculosis* survival in macrophages. Furthermore, NSC 18725 showed synergy with INH and additive effect with other tested drugs in checkerboard assays. We also demonstrated that the nitroso group is essential for the anti-mycobacterial activity of the parent compound. Further, substitution at the *para*-position of the phenyl ring enhanced NSC 18725 activity *in vitro*. Future studies would involve more detailed SAR studies to improve NSC 18725 activity *in vitro* and evaluate the efficacy of this series in aerosol infected mice.

DATA AVAILABILITY STATEMENT

All datasets generated for this study are included in the article/**Supplementary Material**.

REFERENCES

- Ahsan, M. J., Samy, J. G., Khalilullah, H., Bakht, M. A., and Hassan, M. Z. (2011). Synthesis and antimycobacterial evaluation of 3a,4-dihydro-3H-indeno [1,2-c] pyrazole-2-carboxamide analogues. *Eur. J. Med. Chem.* 46, 5694–5697. doi: 10.1016/j.ejmech.2011.09.035
- Alegao, S. G., Alagawadi, K. R., Garg, M. K., Dushyant, K., and Vinod, D. (2014). 1,3,4-Trisubstituted pyrazole analogues as promising anti-inflammatory agents. *Bioorg. Chem.* 54, 51–59. doi: 10.1016/j.bioorg.2014.04.001
- Altaf, M., Miller, C. H., Bellows, D. S., and O'Toole, R. (2010). Evaluation of the *Mycobacterium smegmatis* and BCG models for the discovery of *Mycobacterium*

AUTHOR CONTRIBUTIONS

RS conceived the idea and supervised the experiments. The microbiology related experiments were performed by GA, TG, RPS, SK, and PS. Gagandeep and SKK performed chemical synthesis of NSC 18725 analogs. AB performed the autophagy experiments. RD supervised the autophagy experiments. DR supervised the experiments related to chemical synthesis. RS, GA, Gagandeep, and PS wrote the manuscript with inputs from other authors.

FUNDING

RS acknowledges the financial support received from THSTI and Department of Biotechnology (BT/COE/34/15219/2015). RS is a recipient of Ramalingaswami fellowship (BT/HRD/35/02/18/2009) and National Bioscience Award (BT/HRD/NBA/37/01/2014). The financial assistance provided by the Department of Science and Technology, Government of India (EMR/2016/000048, EEQ/2016/000205, and DST/INSPIRE/Faculty award/2014/DST/INSPIRE/04/2014/01662) and Ministry of Human Resource Development (MHRD), Government of India to RD is duly acknowledged. The funders had no role in study design, results, analysis, and preparation of manuscript.

ACKNOWLEDGMENTS

We acknowledge the University of Delhi South Campus for providing access to the BSL-3 facility. Department of Biotechnology (GA, TG), Department of Science and Technology (PS, AB), and Council of Scientific and Industrial Research (Gagandeep, SKK) are acknowledged for providing research fellowships. We acknowledge Dr. Deepak Kumar Saini for critical reading of the manuscript. We also acknowledge the technical help provided by Mr. Sher Singh and Mr. Rajesh.

SUPPLEMENTARY MATERIAL

The Supplementary Material for this article can be found online at: <https://www.frontiersin.org/articles/10.3389/fmicb.2019.03051/full#supplementary-material>

tuberculosis inhibitors. *Tuberculosis* 90, 333–337. doi: 10.1016/j.tube.2010.09.002

- Bah, A., and Vergne, I. (2017). Macrophage autophagy and bacterial infections. *Front. Immunol.* 8:1483. doi: 10.3389/fimmu.2017.01483
- Bass, J. B. Jr., Farer, L. S., Hopewell, P. C., O'Brien, R., Jacobs, R. F., Ruben, F., et al. (1994). Treatment of tuberculosis and tuberculosis infection in adults and children. American Thoracic Society and the centers for disease control and prevention. *Am J. Respir. Crit. Care Med.* 149, 1359–1374. doi: 10.1164/ajrccm.149.5.8173779
- Bekhit, A. A., Ashour, H. M., and Guemei, A. A. (2005). Novel pyrazole derivatives as potential promising anti-inflammatory antimicrobial agents. *Arch. Pharm.* 338, 167–174. doi: 10.1002/ardp.200400940

- Betts, J. C., Lukey, P. T., Robb, L. C., McAdam, R. A., and Duncan, K. (2002). Evaluation of a nutrient starvation model of *Mycobacterium tuberculosis* persistence by gene and protein expression profiling. *Mol. Microbiol.* 43, 717–731. doi: 10.1046/j.1365-2958.2002.02779.x
- Bogatcheva, E., Hanrahan, C., Chen, P., Gearhart, J., Sacksteder, K., Einck, L., et al. (2010). Discovery of dipiperidines as new antitubercular agents. *Bioorg. Med. Chem. Lett.* 20, 201–205. doi: 10.1016/j.bmcl.2009.10.135
- Brodin, P., Poquet, Y., Levillain, F., Peguillet, I., Larrouy-Maumus, G., Gilleron, M., et al. (2010). High content phenotypic cell-based visual screen identifies *Mycobacterium tuberculosis* acyltrehalose-containing glycolipids involved in phagosome remodeling. *PLoS Pathog.* 6:e1001100. doi: 10.1371/journal.ppat.1001100
- Chandra, T., Garg, N., Lata, S., Saxena, K. K., and Kumar, A. (2010). Synthesis of substituted acridinyl pyrazole derivatives and their evaluation for anti-inflammatory activity. *Eur. J. Med. Chem.* 45, 1772–1776. doi: 10.1016/j.ejmech.2010.01.009
- Cho, S. H., Warit, S., Wan, B., Hwang, C. H., Pauli, G. F., and Franzblau, S. G. (2007). Low-oxygen-recovery assay for high-throughput screening of compounds against nonreplicating *Mycobacterium tuberculosis*. *Antimicrob. Agents Chemother.* 51, 1380–1385. doi: 10.1128/aac.00055-06
- Christophe, T., Ewann, F., Jeon, H. K., Cechetto, J., and Brodin, P. (2010). High-content imaging of *Mycobacterium tuberculosis*-infected macrophages: an in vitro model for tuberculosis drug discovery. *Future Med. Chem.* 2, 1283–1293. doi: 10.4155/fmc.10.223
- Christophe, T., Jackson, M., Jeon, H. K., Fenistein, D., Contreras-Dominguez, M., Kim, J., et al. (2009). High content screening identifies decaprenyl-phosphoribose 2' epimerase as a target for intracellular antimycobacterial inhibitors. *PLoS Pathog.* 5:e1000645. doi: 10.1371/journal.ppat.1000645
- Daidone, G., Plescia, S., Raffa, D., Maggio, B., and Schillaci, D. (1992). Synthesis and evaluation of antimicrobial activity of new 4-nitroso and 4-diazopyrazole derivatives. *Farmaco* 47, 203–217.
- Dara, Y., Volcani, D., Shah, K., Shin, K., and Venketaraman, V. (2019). Potentials of host-directed therapies in tuberculosis management. *J. Clin. Med.* 8:E1166. doi: 10.3390/jcm8081166
- Dhiman, R., and Singh, R. (2018). Recent advances for identification of new scaffolds and drug targets for *Mycobacterium tuberculosis*. *IUBMB Life* 70, 905–916. doi: 10.1002/iub.1863
- Diacon, A. H., Pym, A., Grobusch, M. P., de los Rios, J. M., Gotuzzo, E., Vasilyeva, I., et al. (2014). Multidrug-resistant tuberculosis and culture conversion with bedaquiline. *N. Engl. J. Med.* 71, 723–732.
- Early, J., Ollinger, J., Darby, C., Alling, T., Mullen, S., Casey, A., et al. (2019). Identification of compounds with pH-Dependent bactericidal activity against *Mycobacterium tuberculosis*. *ACS Infect. Dis.* 5, 272–280. doi: 10.1021/acscinfdis.8b00256
- Glaziou, P., Floyd, K., and Raviglione, M. C. (2018). Global epidemiology of tuberculosis. *Semin. Respir. Crit. Care Med.* 39, 271–285. doi: 10.1055/s-0038-1651492
- Grant, S. S., Kawate, T., Nag, P. P., Silvis, M. R., Gordon, K., Stanley, S. A., et al. (2013). Identification of novel inhibitors of nonreplicating *Mycobacterium tuberculosis* using a carbon starvation model. *ACS Chem. Biol.* 8, 2224–2234. doi: 10.1021/cb4004817
- Horsburgh, C. R. Jr., Barry, C. E. III, and Lange, C. (2015). Treatment of Tuberculosis. *N. Engl. J. Med.* 373, 2149–2160.
- Karrouchi, K., Radi, S., Ramli, Y., Taoufik, J., Mabkhot, Y. N., Al-Aizari, F. A., et al. (2018). Synthesis and pharmacological activities of pyrazole derivatives: a review. *Molecules* 23:E134. doi: 10.3390/molecules23010134
- Keche, A. P., Hatnapure, G. D., Tale, R. H., Rodge, A. H., and Kamble, V. M. (2012). Synthesis, anti-inflammatory and antimicrobial evaluation of novel 1-acetyl-3,5-diaryl-4,5-dihydro (1H) pyrazole derivatives bearing urea, thiourea and sulfonamide moieties. *Bioorg. Med. Chem. Lett.* 22, 6611–6615. doi: 10.1016/j.bmcl.2012.10.118
- Kidwai, S., Bouzeyen, R., Chakraborti, S., Khare, N., Das, S., Gosain, T. P., et al. (2019). NU-6027 inhibits growth of *Mycobacterium tuberculosis* by targeting Protein Kinase D and Protein Kinase G. *Antimicrob. Agents Chemother.* 63:e00996-19. doi: 10.1128/AAC.00996-19
- Kidwai, S., Park, C. Y., Mawatwal, S., Tiwari, P., Jung, M. G., Gosain, T. P., et al. (2017). Dual Mechanism of Action of 5-Nitro-1,10-Phenanthroline against *Mycobacterium tuberculosis*. *Antimicrob. Agents Chemother.* 61:e00969-17. doi: 10.1128/AAC.00969-17
- Li, Y., Sun, F., and Zhang, W. (2019). Bedaquiline and delamanid in the treatment of multidrug-resistant tuberculosis: Promising but challenging. *Drug Dev. Res.* 80, 98–105.
- Li, H., Salinger, D. H., Everitt, D., Li, M., Del Parigi, A., Mendel, C., et al. (2019). Long-term effects on QT prolongation of pretomanid, alone and in combinations, in patients with tuberculosis. *Antimicrob. Agents Chemother.* 63:e00445-19. doi: 10.1128/AAC.00445-19
- Lowrie, D. B., and Andrew, P. W. (1988). Macrophage antimycobacterial mechanisms. *Br. Med. Bull.* 44, 624–634. doi: 10.1093/oxfordjournals.bmb.a072272
- Mak, P. A., Rao, S. P., Ping Tan, M., Lin, X., Chyba, J., Tay, J., et al. (2012). A high-throughput screen to identify inhibitors of ATP homeostasis in non-replicating *Mycobacterium tuberculosis*. *ACS Chem. Biol.* 7, 1190–1197. doi: 10.1021/cb2004884
- Maurya, H. K., Verma, R., Alam, S., Pandey, S., Pathak, V., Sharma, S., et al. (2013). Studies on substituted benzo[h]quinazolines, benzo[g]indazoles, pyrazoles, 2,6-diarylpyridines as anti-tubercular agents. *Bioorg. Med. Chem. Lett.* 23, 5844–5849. doi: 10.1016/j.bmcl.2013.08.101
- Mawatwal, S., Behura, A., Ghosh, A., Kidwai, S., Mishra, A., Deep, A., et al. (2017). Calcimycin mediates mycobacterial killing by inducing intracellular calcium-regulated autophagy in a P2RX7 dependent manner. *Biochim. Biophys. Acta Gen. Subj.* 1861, 3190–3200. doi: 10.1016/j.bbagen.2017.09.010
- Mawatwal, S., Behura, A., Mishra, A., Singh, R., and Dhiman, R. (2018). Calcimycin induced IL-12 production inhibits intracellular mycobacterial growth by enhancing autophagy. *Cytokine* 111, 1–12. doi: 10.1016/j.cyto.2018.07.033
- Moreira, W., Ngan, G. J., Low, J. L., Poulsen, A., Chia, B. C., Ang, M. J., et al. (2015). Target mechanism-based whole-cell screening identifies bortezomib as an inhibitor of caseinolytic protease in mycobacteria. *MBio* 6:e00253-15. doi: 10.1128/mBio.00253-15
- Naim, M. J., Alam, O., Nawaz, F., Alam, M. J., and Alam, P. (2016). Current status of pyrazole and its biological activities. *J. Pharm. Bioallied Sci.* 8, 2–17. doi: 10.4103/0975-7406.171694
- Odds, F. C. (2003). Synergy, antagonism, and what the checkerboard puts between them. *J. Antimicrob. Chemother.* 52:1. doi: 10.1093/jac/dkg301
- Paik, S., Kim, J. K., Chung, C., and Jo, E. K. (2019). Autophagy: a new strategy for host-directed therapy of tuberculosis. *Virulence* 10, 448–459. doi: 10.1080/21505594.2018.1536598
- Pathak, V., Maurya, H. K., Sharma, S., Srivastava, K. K., and Gupta, A. (2014). Synthesis and biological evaluation of substituted 4,6-diarylpyrimidines and 3,5-diphenyl-4,5-dihydro-1H-pyrazoles as anti-tubercular agents. *Bioorg. Med. Chem. Lett.* 24, 2892–2896. doi: 10.1016/j.bmcl.2014.04.094
- Peddireddy, V., Doddam, S. N., and Ahmed, N. (2017). Mycobacterial dormancy systems and host responses in tuberculosis. *Front. Immunol.* 8:84. doi: 10.3389/fimmu.2017.00084
- Pethe, K., Bifani, P., Jang, J., Kang, S., Park, S., Ahn, S., et al. (2013). Discovery of Q203, a potent clinical candidate for the treatment of tuberculosis. *Nat. Med.* 19, 1157–1160. doi: 10.1038/nm.3262
- Singh, R., Manjunatha, U., Boshoff, H. I., Ha, Y. H., Niyomrattanakit, P., Ledwidge, R., et al. (2008). PA-824 kills nonreplicating *Mycobacterium tuberculosis* by intracellular NO release. *Science* 322, 1392–1395. doi: 10.1126/science.1164571
- Singh, R., Singh, M., Arora, G., Kumar, S., Tiwari, P., and Kidwai, S. (2013). Polyphosphate deficiency in *Mycobacterium tuberculosis* is associated with enhanced drug susceptibility and impaired growth in guinea pigs. *J. Bacteriol.* 195, 2839–2851. doi: 10.1128/JB.00038-13
- Slack, W. A. F. A. R. (1957). *Improvements in or Relating to Pyrazole Compounds and Compositions Containing Them*. United Kingdom Patent No GB786753A. Munich: European Patent Office.
- Snider, D. E. Jr., and Roper, W. L. (1992). The new tuberculosis. *N. Engl. J. Med.* 326, 703–705.
- Stanley, S. A., Barczak, A. K., Silvis, M. R., Luo, S. S., Sogi, K., Vokes, M., et al. (2014). Identification of host-targeted small molecules that restrict intracellular *Mycobacterium tuberculosis* growth. *PLoS Pathog.* 10:e1003946. doi: 10.1371/journal.ppat.1003946
- Stanley, S. A., Grant, S. S., Kawate, T., Iwase, N., Shimizu, M., Wivagg, C., et al. (2012). Identification of novel inhibitors of *M. tuberculosis* growth using whole

- cell based high-throughput screening. *ACS Chem. Biol.* 7, 1377–1384. doi: 10.1021/cb300151m
- Swinney, D. C. (2013). Phenotypic vs. target-based drug discovery for first-in-class medicines. *Clin. Pharmacol. Ther.* 93, 299–301. doi: 10.1038/clpt.2012.236
- Taneja, N. K., and Tyagi, J. S. (2007). Resazurin reduction assays for screening of anti-tubercular compounds against dormant and actively growing *Mycobacterium tuberculosis*, *Mycobacterium bovis* BCG and *Mycobacterium smegmatis*. *J. Antimicrob. Chemother.* 60, 288–293. doi: 10.1093/jac/dkm207
- VanderVen, B. C., Fahey, R. J., Lee, W., Liu, Y., Abramovitch, R. B., Memmott, C., et al. (2015). Novel inhibitors of cholesterol degradation in *Mycobacterium tuberculosis* reveal how the bacterium's metabolism is constrained by the intracellular environment. *PLoS Pathog.* 11:e1004679. doi: 10.1371/journal.ppat.1004679
- Wayne, L. G., and Sohaskey, C. D. (2001). Nonreplicating persistence of *Mycobacterium tuberculosis*. *Annu. Rev. Microbiol.* 55, 139–163.
- Wilfred, A. F., East, B., Pain, D. L., Rainham, and Slack, R. (1958). *Heterocyclic compounds*. US Patent No 2831866.
- Wilfred, A. F., East, B., and Slack, R. (1956). *Isomeric Nitroso-1-phenyl pyrazoles*. US patent No 2751395.
- Wilson, R., Kumar, P., Parashar, V., Vilcheze, C., Veyron-Churlet, R., Freundlich, J. S., et al. (2013). Antituberculosis thiophenes define a requirement for Pks13 in mycolic acid biosynthesis. *Nat. Chem. Biol.* 9, 499–506. doi: 10.1038/nchembio.1277
- Yoshii, S. R., and Mizushima, N. (2017). Monitoring and measuring autophagy. *Int. J. Mol. Sci.* 18:1865. doi: 10.3390/ijms18091865
- Yuan, T., and Sampson, N. S. (2018). Hit generation in TB drug discovery: from genome to granuloma. *Chem. Rev.* 118, 1887–1916. doi: 10.1021/acs.chemrev.7b00602
- Conflict of Interest:** The authors declare that the research was conducted in the absence of any commercial or financial relationships that could be construed as a potential conflict of interest.

Copyright © 2020 Arora, Gagandeep, Behura, Gosain, Shaliwal, Kidwai, Singh, Kandi, Dhiman, Rawat and Singh. This is an open-access article distributed under the terms of the Creative Commons Attribution License (CC BY). The use, distribution or reproduction in other forums is permitted, provided the original author(s) and the copyright owner(s) are credited and that the original publication in this journal is cited, in accordance with accepted academic practice. No use, distribution or reproduction is permitted which does not comply with these terms.



Clostridium butyricum Ameliorates *Salmonella* Enteritis Induced Inflammation by Enhancing and Improving Immunity of the Intestinal Epithelial Barrier at the Intestinal Mucosal Level

Xiaonan Zhao^{1,2}, Jie Yang¹, Zijing Ju¹, Jianmin Wu¹, Lili Wang¹, Hai Lin^{1*} and Shuhong Sun^{1*}

OPEN ACCESS

Edited by:

Marco Rinaldo Oggioni,
University of Leicester,
United Kingdom

Reviewed by:

Jie Wen,
Institute of Animal Sciences (CAAS),
China
Annalisa Ciabattini,
University of Siena, Italy
Janet Yakubu Nale,
University of Leicester,
United Kingdom

*Correspondence:

Hai Lin
Hailin@sdaa.edu.cn
Shuhong Sun
jqybfkyjs@163.com

Specialty section:

This article was submitted to
Microbial Immunology,
a section of the journal
Frontiers in Microbiology

Received: 14 October 2019

Accepted: 10 February 2020

Published: 26 February 2020

Citation:

Zhao X, Yang J, Ju Z, Wu J,
Wang L, Lin H and Sun S (2020)
Clostridium butyricum Ameliorates
Salmonella Enteritis Induced
Inflammation by Enhancing and
Improving Immunity of the Intestinal
Epithelial Barrier at the Intestinal
Mucosal Level.
Front. Microbiol. 11:299.
doi: 10.3389/fmicb.2020.00299

¹ College of Animal Science and Technology, Shandong Agricultural University, Tai'an, China, ² Institute of Animal Science and Veterinary Medicine, Shandong Academy of Agricultural Sciences, Jinan, China

This study was aimed to investigate the effects of *Clostridium butyricum* (*C. butyricum*) immunity and intestinal epithelial barrier function at the intestinal mucosal level, by using *Salmonella* enteritidis (*S. enteritidis*) to infect specific-pathogen-free (SPF) chickens and intestinal epithelial cells (IEC). We found that *C. butyricum* could decrease cytokine levels (IFN- γ , IL-1 β , IL-8, and TNF- α) via the TLR4-, MyD88-, and NF- κ B-dependent pathways in intestinal tissues and intestinal epithelial cells. Additionally, *C. butyricum* could attenuate bacteria-induced intestinal damage and increase the expression level of muc-2 and ZO-1 in the intestine and intestinal epithelial cells. Furthermore, *C. butyricum* altered the intestinal microbial composition, increased the diversity of the bacterial communities in the cecum of *Salmonella*-infected chickens. In conclusion, *C. butyricum* effectively attenuated inflammation and epithelial barrier damage, altered the intestinal microbial composition, increased the diversity of the bacterial communities in the intestine of *Salmonella*-infected chickens. The result suggests that *C. butyricum* might be an effective and safe therapy for the treatment of *Salmonella* infection.

Keywords: *C. butyricum*, *Salmonella* enteritidis, immunity, intestine, intestinal microflora

INTRODUCTION

Salmonella is a common bacterial entero-pathogen and one of the leading causes of serious illness in humans and animals, such as enteritis and diarrhea (Mathur et al., 2012). Over 20 million individuals suffer from typhoid fever, and more than 220,000 deaths each year have been reported around the world (Majowicz et al., 2010; Feasey et al., 2012).

Chickens have been recognized as an important reservoir for *Salmonella* (Chen and Jiang, 2014). The most frequently isolated serovar from chickens is *S. enteritidis* (Zhao et al., 2017). After oral ingestion in chickens, *Salmonella* initially breaches the epithelial lining, which is the first line of defense against the invasion of microbes and their associated lipopolysaccharide (LPS) and toxins. Impaired epithelial barrier function may predispose to various intestinal disorders, such as inflammation (Juan et al., 2018; Xiao et al., 2018). In addition, Mucins are the

primary components of intestinal mucus layer that are part of the innate immune system and act as a barrier against luminal pathologies (Forstner et al., 1995; Huang et al., 2015).

In recent years, antibiotics have been effectively used to treat *Salmonella* infection. Unfortunately, the widespread use of antibiotics has increased bacterial resistance and led to intestinal flora imbalance, which considerably diminish the efficacy of chemical antibiotics (Parry and Threlfall, 2008). Alternatively, the use of probiotic bacteria can modulate systemic and mucosal immune function, improve intestinal barrier function, alter gut micro-ecology, induce secretion of cytokines and Ig in serum, and perturb the MyD88 signaling pathway (Kusumawati et al., 2006; Shanahan, 2010; Madsen, 2012; Kemgang et al., 2014; Lim et al., 2017).

Clostridium butyricum is a gram-positive, obligate anaerobe and endospore-forming probiotic, which has been widely used for repairing intestinal epithelium, thereby improving gastrointestinal function (Cao et al., 2012). A preliminary study demonstrated that *C. butyricum* could reduce the colonization of pathogenic bacteria, weakening the inflammatory response (Zhang et al., 2016). However, the mechanism of protection remains to be elucidated.

In this study, we aimed to explore the mechanism by which *C. butyricum* could suppress the pathogenic strain *S. enterica* using the specific-pathogen-free (SPF) chicken model with an emphasis on the response at the intestinal mucosal level.

MATERIALS AND METHODS

Ethics Statement

All procedures were approved by the Animal Care and Use Committee of Shandong Agricultural University (SDAUA-2016-016), and all husbandry practices and euthanasia were performed with full consideration of animal welfare.

Bacterial Strains

Clostridium butyricum (AQQF01000149) was obtained from Dalian Sanyi Animal Medicine Company (China). The strain was cultured anaerobically with Reinforced Clostridial Medium (RCM) broth at 37°C for 48 h. According to the plate count method as described by Wei et al. (2013), the concentration of the bacteria was adjusted to 10⁶ colony forming units (CFU)/mL.

A virulent *Salmonella enteritidis* strain was obtained from the Avian Disease Centre of Shandong Agricultural University, and it was selected for the challenge study due to the invasive characteristic previously described (Zhao et al., 2017). The *S. enteritidis* strain was cultured with nutrient broth at 37°C for 12 h. To eliminate the possible LPS contamination, *S. enteritidis* cells were collected by centrifugation at 7,000 × *g* for 10 min and washed twice with PBS (pH 7.2), followed by dilution with PBS to a final cell count of 10⁶ colony forming units (CFU)/mL according to the LD50.

Animals

Specific-pathogen-free chickens were obtained from Jinan SPFAFAS Poultry Company (Jinan, China). SPF chickens refer to

animals that do not have specific microorganisms or parasites, but may carry non-specific microorganisms and parasites, also known as third-class animals (The European Pharmacopoeia 7.0, 2010). Chickens were reared in the animal room of Shandong Agricultural University. Chickens were reared in metal cages, and the temperature was maintained at 30°C for the first 3 days and gradually reduced to 28°C during the last days of the experiment. Chickens were fed with a commercial diet and had free access to feed and water during the whole experimental period. The nutrient levels of the basal diet met the nutritional requirement of the chickens (NRC, 1994) (Table 1). At 1 and 7 days of age, birds were tested for the absence of *Salmonella* by taking cloacal swabs. Thereafter, a total of 60 health chickens were randomly assigned to three groups (*n* = 20/group): (Mathur et al., 2012) orally administered 0.2 mL sterile saline solution per chicken once every day from day 1 through day 14 [negative control group (NC)]; (Feasey et al., 2012) orally administered 0.2 mL sterile saline solution per chicken once every day from day 1 through day 14 and challenged with 0.2 mL *S. enteritidis* (10⁶ CFU/mL) on day 8 [*S. enteritidis* infected group, positive control (PC)]; and (Majowicz et al., 2010) orally administered 0.2 mL *C. butyricum* (10⁶ CFU/mL) once every day from day 1 through day 14 and challenged with 0.2 mL *S. enteritidis* (10⁶ CFU/mL) on day 8 [*C. butyricum* + *S. enteritidis* treatment (EXP)]. At the age of 14 days (6 dpi), all birds were euthanized via cervical dislocation. The tissues of duodenum, jejunum, ileum, and cecum were collected and stored in liquid nitrogen for mRNA and histological analysis. The cecal contents were collected and stored at −80°C for microbial composition analysis.

Histological Study of the Cecum

One inch of the cecum of chickens was removed, fixed in 4% paraformaldehyde and prepared for histological studies as described by Sainte-Marie (1962). Paraffin sections of 5 μm were deparaffinized in xylene and stained with hematoxylin and eosin

TABLE 1 | The composition and nutrients of basal diet.

Ingredient	Content (%)	Chemical composition	Content
Corn	55.23	CP,%	20.90
Soybean meal	30.67	ME, Mcal/kg	3.00
Wheat shorts	4.00	Calcium,%	1.00
Fish meal	3.00	Total P,%	0.65
Soybean oil	2.90	Available P,%	0.45
DL-Methionine	0.27	Methionine + cysteine,%	0.90
NaCl	0.27	Lysine,%	1.05
Limestone	1.33		
Calcium phosphate	1.33		
Vitamin-mineral premix	1.00		

^aCrude protein content is 62.5% and metabolizable energy is 2.79 Mcal/kg.

^bMetabolizable energy is 8.8 Mcal/kg. ^cSupplied per kilogram of diet: vitamin A (retinyl acetate), 1,500 IU; cholecalciferol, 200 IU; vitamin E (DL-α-tocopheryl acetate), 10 IU; riboflavin, 3.5 mg; pantothenic acid, 10 mg; niacin, 30 mg; cobalamin, 10 μg; choline chloride, 1,000 mg; biotin, 0.15 mg; folic acid, 0.5 mg; thiamine 1.5 mg; pyridoxine 3.0 mg; Fe, 80 mg; Zn, 40 mg; Mn, 60 mg; I, 0.18 mg; Cu, 8 mg; Se, 0.15 mg.

(H&E) for microscopic examination, and the overall quality of villi was observed.

Microbial Composition Analysis

100 mg cecum contents samples were collected and microbial genomic DNA was extracted from cecum contents using TIANamp Stool DNA Kit (Tiangen, Beijing, China) according to the manufacturer's instructions. The V4 hypervariable region of the 16S rRNA gene was amplified by PCR using 515F and 806R primers. Eighteen samples ($n = 6/\text{group}$) were sequenced on an Illumina MiSeq platform provided by Personalbio (Shanghai, China). Paired-end reads from the original DNA fragments were merged using FLASH. Clustering was performed using the UPARSE pipeline, and sequences were assigned to operational taxonomic units at 97% similarity (Schloss et al., 2009). The diversity and composition of the bacterial community was determined by α diversities according to Personalbio's recommendations. The Chao1 and ACE indexes simply refer to the number of species in the community, regardless of the abundance of each species in the community, the Shannon's diversity index considers both richness and evenness, the higher Chao1, ACE and Shannon index are, the higher the species diversity are.

Real-Time PCR

Total RNA was extracted from duodenal, jejunal, ileal, and cecal tissues using Trizol reagent (Invitrogen, United States) according to the manufacturer's instructions. Briefly, 50–100 mg tissue samples were ground to powder with liquid nitrogen and transferred to a tube with 1 ml of Trizol; after centrifuged at 4°C, 0.2 ml chloroform was added to the supernatant; after centrifuged at 4°C, the supernatant containing the intact RNA was transferred to a new tube, RNA was then precipitated with equal volume of isopropyl alcohol, and washed with 80% ethanol. The RNA was solubilized in RNase free water. RNA quantity and quality were evaluated using a NanoDrop™ 2000 spectrophotometer (Thermo Fisher Scientific, Waltham, MA, United States), followed by cDNA synthesis via the Transcriptor First-Strand cDNA Synthesis Kit (Roche, China) using 2 µg RNA template. Real-time PCR was performed using SYBR Green I Master mix (Roche). Two microliters of cDNA, 5 µl SYBR Green buffer 2 × (Roche) and 2.5 pmol of each primer were combined for a total reaction volume of 10 µl. The thermocycler protocol consisted of a 5 min pre-incubation at 95°C for 20 s, 60°C for 30 s and 72°C for 20 s, and melt curves were added. The β -actin reference gene was chosen for the relative expression of targeted genes. mRNA relative expression was calculated using the $2^{-\Delta\Delta C_t}$ method. The primers used in this study are listed in Table 2.

Primary Chicken Intestinal Epithelial Cell Culture

Specific-pathogen-free eggs were purchased from Jinan SPAFAS Poultry Company (China). Chicken intestinal epithelial cells (IECs) were prepared from 19-day-old SPF chicken embryos as described previously (Pierzchalska et al., 2012) with some modifications. Briefly, the duodenum was excised, cut into small

TABLE 2 | Primer sequences of targeted and reference genes.

Gene	Sequence (5'–3')	References
TLR4	Forward: AGTCTGAAATTGCTGAGCTCAAAT Reverse: GCGACGTTAAGCCATGGAAG	Zhao et al., 2017
MyD88	Forward: TGATGCCTTCATCTGCTACTG Reverse: TCCCTCCGACACCTTCTTTCTA	Zhao et al., 2017
NF-κB	Forward: CAGCCCATCTATGACAACCG	Zhao et al., 2017
IFN-γ	Reverse: TCCCTGCGTCTCCTCTGTGA Forward: CTGACGGTGGACCTATTATTGTAG Reverse: GTTTGATGTGCGGCTTTGA	Zhao et al., 2017
IL-1β	Forward: GTGAGGCTCAACATTGCGCTGTA Reverse: TGTCCAGGCGGTAGAGATGAAG	Zhao et al., 2017
IL-8	Forward: ATGAACGGCAAGCTTGGAGCTG Reverse: TCCAAGCACACCTCTCTTCCATCC	Zhao et al., 2017
TNF-α	Forward: TGCTGTTCTATGACCGCC Reverse: CTTTCAGAGCATCAACGCA	Zhao et al., 2017
Muc-2	Forward: AGGCCAGTTCTATGGAGCACAGTT Reverse: TTGAGTGCCGAGGGACATTTC	Huang et al., 2015
ZO-1	Forward: GCGCCTCCCTATGAGGAGCA Reverse: CAAATCGGGTTGTGCCGGA	Zuo et al., 2014
Occludin	Forward: TCGTGCTGTGCATCGCCATC Reverse: CGCTGGTTACCCCTCCGTA	Zuo et al., 2014
β-Actin	Forward: GAGAAATTGTGCTGACATCA Reverse: CCTGAACCTCTCATTGCCA	Zhao et al., 2017

pieces with a sterile scalpel blade, and dissected perpendicularly to expose the lumen. Small duodenal pieces were transferred to a tube filled with DMEM/Ham's/F12 (Gibco, Grand Island, NY, United States) medium with 1% fetal bovine serum (Gibco), 50 µg/ml gentamycin (Invitrogen, Carlsbad, CA, United States), 100 µl/ml penicillin/streptomycin (10,000 U/ml/10,000 µg/ml) (Invitrogen, Carlsbad, CA, United States), 1 U/ml dispase II (Roche, Basel, Switzerland) and 75 U/ml collagenase (Gibco). Digestion was performed at 37°C under steady agitation for 2 h. The material was filtered, and larger pieces were discarded, while medium containing single cells and small pieces was centrifuged at 100 × g for 3 min. To separate mucus and IECs, a centrifugation step of 10 min was performed at 400 × g. Mucus covering the cell pellet was discarded. The remaining cell pellet was subsequently washed several times until the suspension was clear, and finally, 1×10^7 cells were cultured in six-well plates and incubated at 37°C with 5% CO₂. After incubation for 48 h, IECs were treated under three different conditions as follows: (NC) DMEM alone; (PC) *S. enteritidis* (10⁶ CFU) infection only; and (EXP) pre-incubation with *C. butyricum* (10⁶ CFU) for 2 h prior to exposure to *S. enteritidis*. At 2 and 6 h after *S. enteritidis* challenge, a portion of the cells were then collected and treated with lysis buffer to extract total RNA for real-time PCR.

Statistical Analysis

Statistical evaluations were performed using a one-way ANOVA followed by a Duncan multiple range test or a Fisher least significant difference test using SPSS 16.0 (SPSS, Chicago, IL, United States). Data were visualized using GraphPad Prism 5 software (GraphPad Software, Inc., San Diego, CA, United States). $P < 0.05$ was considered significant.

RESULTS

C. butyricum Improved Morphology and Integrity in the Cecum

Microscopic examination revealed that chicken infected with *S. enteritidis* in the PC group showed surface damage and disruption to villi. Cecal tissue of chickens pre-treated with *C. butyricum* in the EXP group showed less severe surface damage to villi than did cecal tissue of chickens in the PC group. These observations demonstrate that pretreatment of *C. butyricum* resulted in a reduction of bacteria-induced intestinal damage (Figure 1).

Determination of Cytokine Levels in Intestines

Cytokine levels were measured to test the hypothesis that early pretreatment of chicken with *C. butyricum* may alter cytokine production in intestinal tissue following *S. enteritidis* challenge.

The gene expression levels of cytokines IFN- γ , IL-1 β , IL-8, and TNF- α in intestinal tissue (i.e. duodenum, jejunum, ileum, and cecum) were also evaluated. The results showed that at 6 days post-infection, no significant differences were found in IFN- γ and TNF- α among NC, PC, and EXP groups in intestinal tissue (i.e. duodenum, jejunum, ileum, and cecum) ($P > 0.05$) (Figures 2A,D). The gene expression level of IL-1 β in the duodenum was significantly elevated in the PC group compared to the NC and EXP group ($P < 0.05$), but there was no significant difference between the NC and EXP groups ($P > 0.05$); in the jejunum, the gene expression level of IL-1 β was significantly elevated in the PC group compared to the EXP group ($P < 0.05$), but there was no significant difference between the NC and EXP groups and the same change between NC and PC groups ($P > 0.05$); in the ileum, no significant difference of IL-1 β was found among NC, PC, and EXP groups ($P > 0.05$); in the cecum, the gene expression level of IL-1 β was significantly elevated in the PC group compared to the NC group ($P < 0.05$), but no significant difference was found between the NC and EXP groups and the same change between PC and EXP groups ($P > 0.05$) (Figure 2B). The gene expression level of IL-8 in the jejunum was significantly elevated in the PC group compared to the NC and EXP groups ($P < 0.05$), but no significant difference was found between the NC and EXP groups ($P > 0.05$); of note, no significant difference of

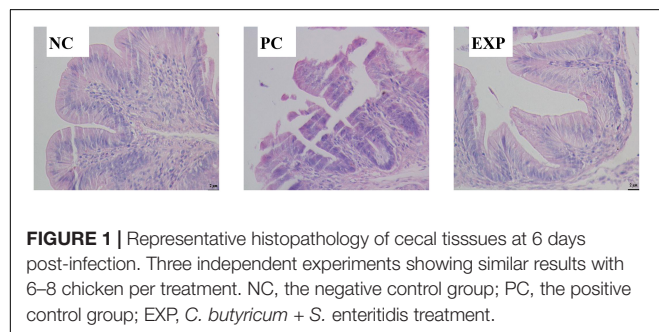
IL-8 in duodenum, ileum, and cecum was found among NC, PC and EXP groups ($P > 0.05$) (Figure 2C). Furthermore, we investigated the effects of *C. butyricum* on cytokine expression in IECs *in vitro*. The results showed that after 2 h of infection, the expression level of IFN- γ was significantly elevated in the PC group compared to the NC and EXP groups ($P < 0.05$), but there was no significant difference between the NC and EXP groups ($P > 0.05$) (Figure 3A). The expression level of IL-8 was significantly elevated in the PC and EXP groups compared to the NC group ($P < 0.05$), but there was no significant difference between the PC and EXP groups ($P > 0.05$). Regarding the expression levels of IL-1 β and TNF- α , no significant difference was found among the NC, PC, and EXP groups ($P > 0.05$) (Figures 3B–D). After 6 h of infection, the expression levels of IFN- γ and TNF- α were significantly elevated in the PC group compared to the NC and EXP groups ($P < 0.05$), but there was no significant difference between the NC and EXP groups ($P > 0.05$) (Figures 3A,D). The gene expression levels of IL-1 β and IL-8 were significantly elevated in the PC group compared to the NC group ($P < 0.05$), but there was no significant difference between the NC and EXP groups, and the same change between PC and EXP groups ($P > 0.05$) (Figures 3B,C).

C. butyricum Modulated muc2 Expression in Intestines of *S. Enteritidis*-Infected Chickens

The expression of muc2 in chicken intestines was detected via real-time PCR. The results showed that the expression level of muc2 in the jejunum was decreased in the PC group compared to the EXP groups ($P < 0.05$), but there was no significant difference between the NC and EXP groups, and the same change between PC and NC groups ($P > 0.05$). Of note, *C. butyricum* effectively attenuated the *S. enteritidis*-induced changes to muc2 expression in the jejunum. There were no significant differences in muc2 expression in the duodenum, ileum, or cecum among any of the groups ($P > 0.05$) (Figure 2E). Furthermore, we investigated the effects of *C. butyricum* on the muc2 expression in IECs *in vitro*, and our data showed that after 2 and 6 h post-infection, the gene expression level of muc2 was not significantly different among the different groups ($P > 0.05$) (Figure 3E).

C. butyricum Increased Intestinal Barrier Function in *S. Enteritidis*-Infected Chickens

In this study, we evaluated the effects of *C. butyricum* on epithelial barrier function in the chicken intestines by detecting the expression level of Zonula occludens-1 (ZO-1) and Occludin via real-time PCR. The results showed that at 6 days post-infection, the expression level of ZO-1 in duodenum and jejunum was significantly decreased in the PC group compared with the EXP group ($P < 0.05$), but there was no significant difference between the NC and EXP groups, and the same change between PC and NC groups ($P > 0.05$). There were no significant differences in ZO-1 expression in either the ileum or cecum among any of the groups ($P > 0.05$) (Figure 2F). Similarly, no significant difference in Occludin levels was found in intestines among the



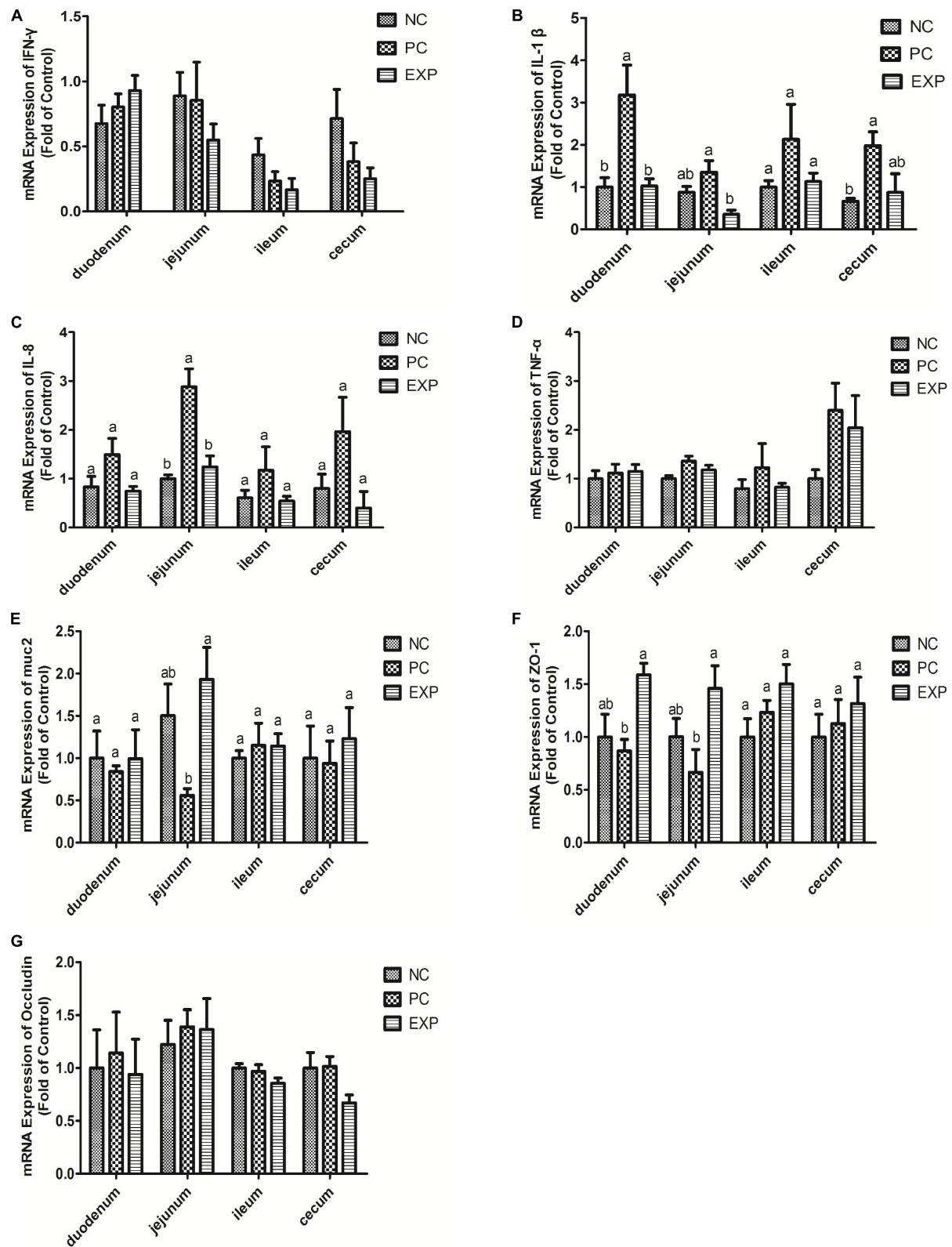


FIGURE 2 | Expression level of cytokines (IFN- γ , IL-1 β , IL-8, and TNF- α), muc2 mucin and the tight junction proteins (ZO-1 and Occludin) (A–G) in intestine tissues (duodenum, jejunum, ileum, and cecum) were estimated by real-time PCR. The bars represent the mean \pm SD ($n = 6/\text{group}$). Different letters over the bars indicate statistically differences between the groups ($P < 0.05$), same letters over the bars indicate no statistically differences between the groups ($P > 0.05$). NC, the negative control group; PC, the positive control group; EXP, *C. butyricum* + *S. enteritidis* treatment.

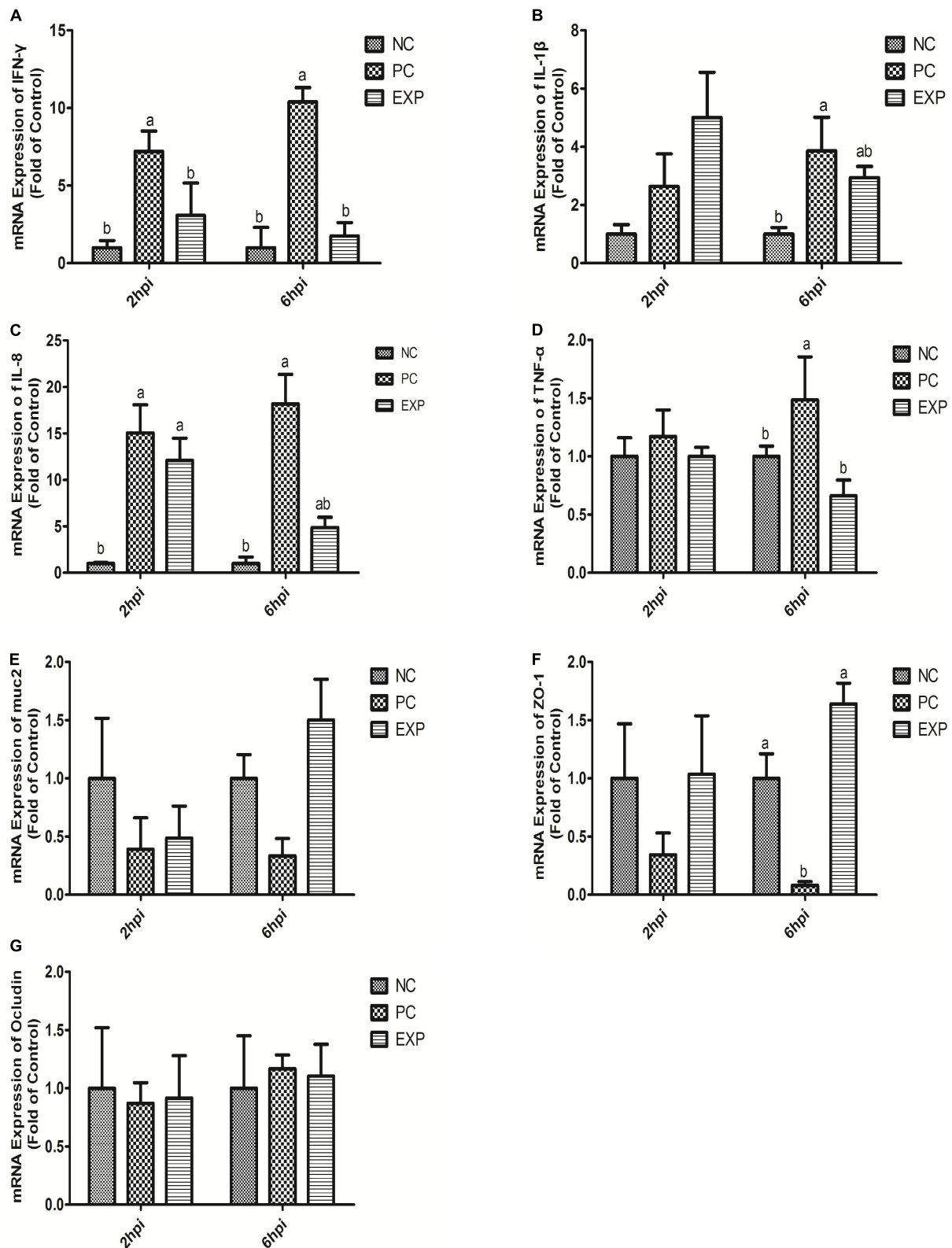


FIGURE 3 | Expression level of cytokines (IFN- γ , IL-1 β , IL-8, and TNF- α), muc2 mucin and the tight junction proteins (ZO-1 and Occludin) (A–G) in intestinal epithelial cells were estimated by real-time PCR. The bars represent the mean \pm SD ($n = 6$ /group). Different letters over the bars indicate statistically differences between the groups ($P < 0.05$), same letters over the bars indicate no statistically differences between the groups ($P > 0.05$). NC, the negative control group; PC, the positive control group; EXP, *C. butyricum* + *S. enteritidis* treatment.

NC, PC, and EXP groups ($P > 0.05$) (Figure 2G). We also investigated the effects of *C. butyricum* on tight junction (TJ) expression in IECs *in vitro*. The data show that after 2 h post-infection, the expression levels of ZO-1 and Occludin were not significantly different among NC, PC and EXP groups ($P > 0.05$) (Figures 3F,G); but after 6 h post-infection, the expression of ZO-1 was significantly decreased in the PC group compared to the EXP group ($P < 0.05$), and there was no significant difference between the NC and EXP groups ($P > 0.05$) (Figure 3F). The expression of Occludin 6 h post-infection was not significantly different among any of the groups ($P > 0.05$) (Figure 3G).

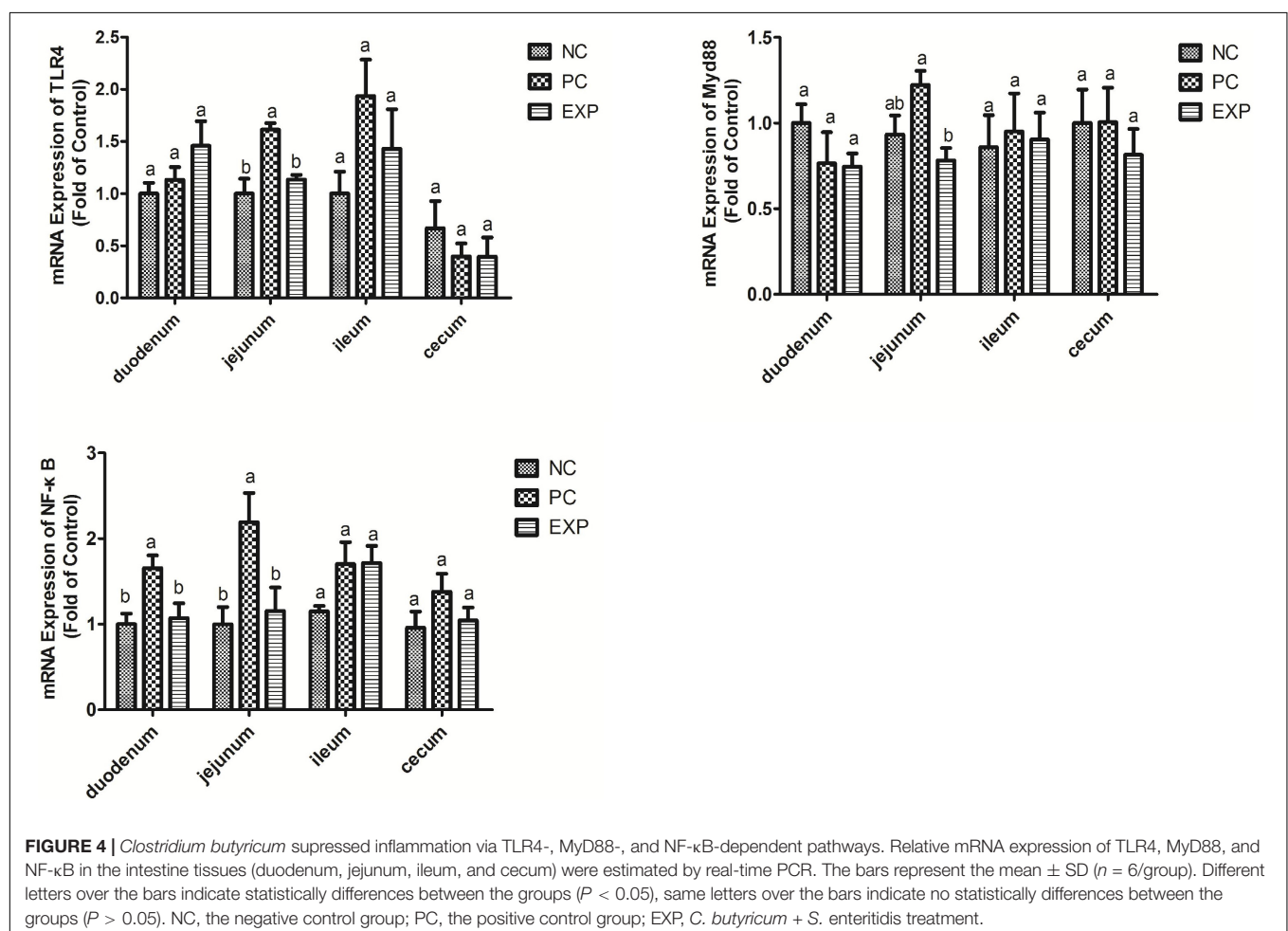
C. butyricum Suppressed TLR4-, MyD88-, and NF- κ B-Dependent Inflammation Pathways

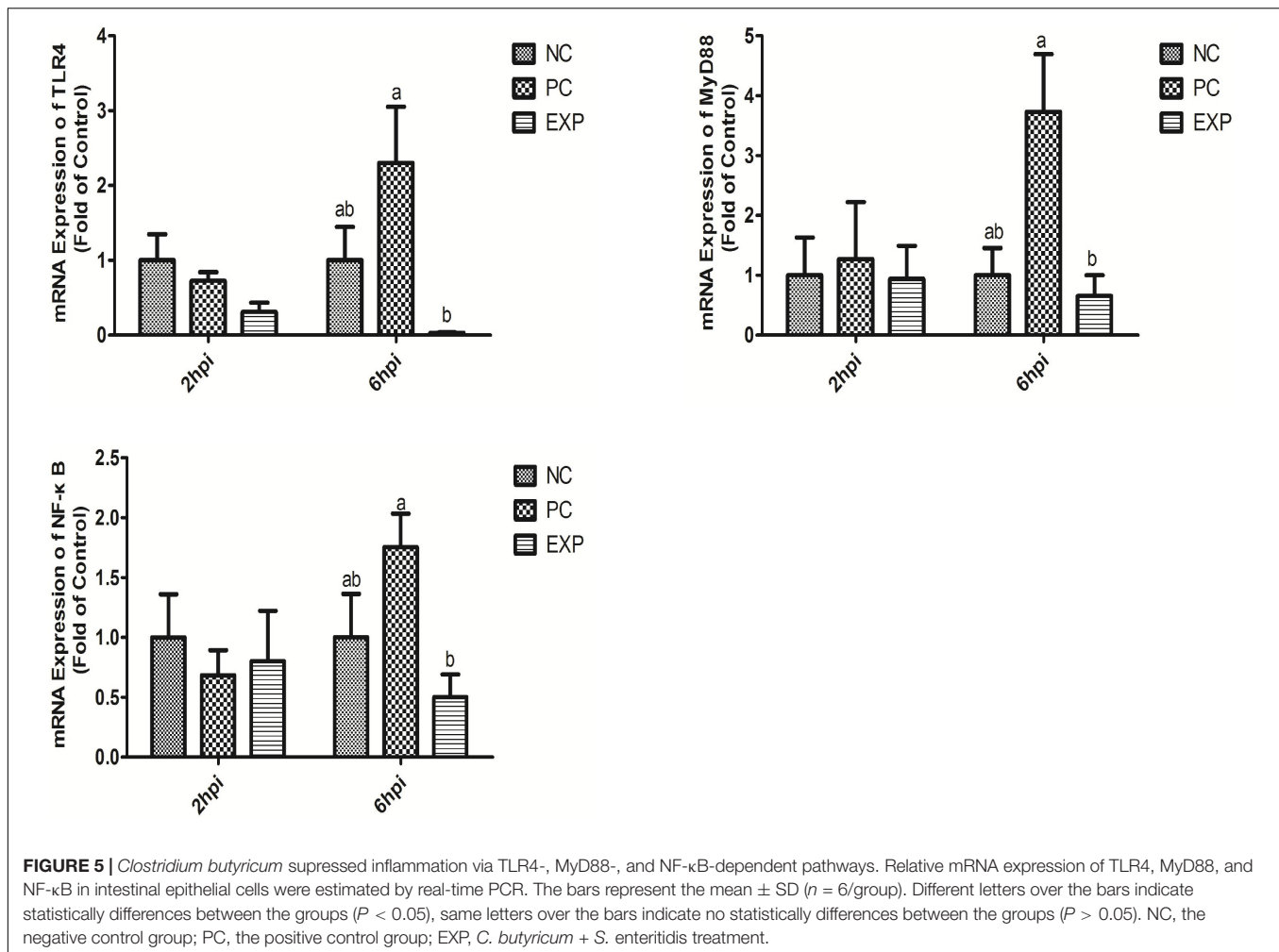
Chickens in the EXP group had decreased gene expressions of TLR4, MyD88, and NF- κ B in the jejunum compared to those in the PC group ($P < 0.05$), but there was no significant difference between the NC and EXP groups and the same change between PC and NC groups regarding the gene expressions of MyD88 ($P > 0.05$), which indicates a direct effect of *C. butyricum*. There were no significant differences in TLR4 and MyD88 expression

in the duodenum, ileum, or cecum among any of the groups ($P > 0.05$). The expression level of NF- κ B in duodenum was significantly elevated in the PC group compared with the EXP and NC groups ($P < 0.05$), but there was no significant difference between the NC and EXP groups ($P > 0.05$) (Figure 4). We further investigated the effects of *C. butyricum* on the TLR4, MyD88, and NF- κ B expression levels in IECs *in vitro* and our results show that, after 2 h post-infection, the gene expression levels of TLR4, MyD88, and NF- κ B were not significantly different among any of the groups ($P > 0.05$) (Figure 5); but after 6 h post-infection, *C. butyricum* decreased the gene expression levels of TLR4, MyD88, and NF- κ B in the EXP group compared with the PC group ($P < 0.05$), but there was no significant difference between the NC and EXP groups and the same change between PC and NC groups ($P > 0.05$) (Figure 5).

The Effects of *C. butyricum* on the Bacterial Community Within Chicken Cecum

We evaluated the effects of *C. butyricum* on the microbiota in chicken cecum using Illumina sequencing of the 16S rRNA V4 region. Firmicutes, Tenericutes, and proteobacteria were





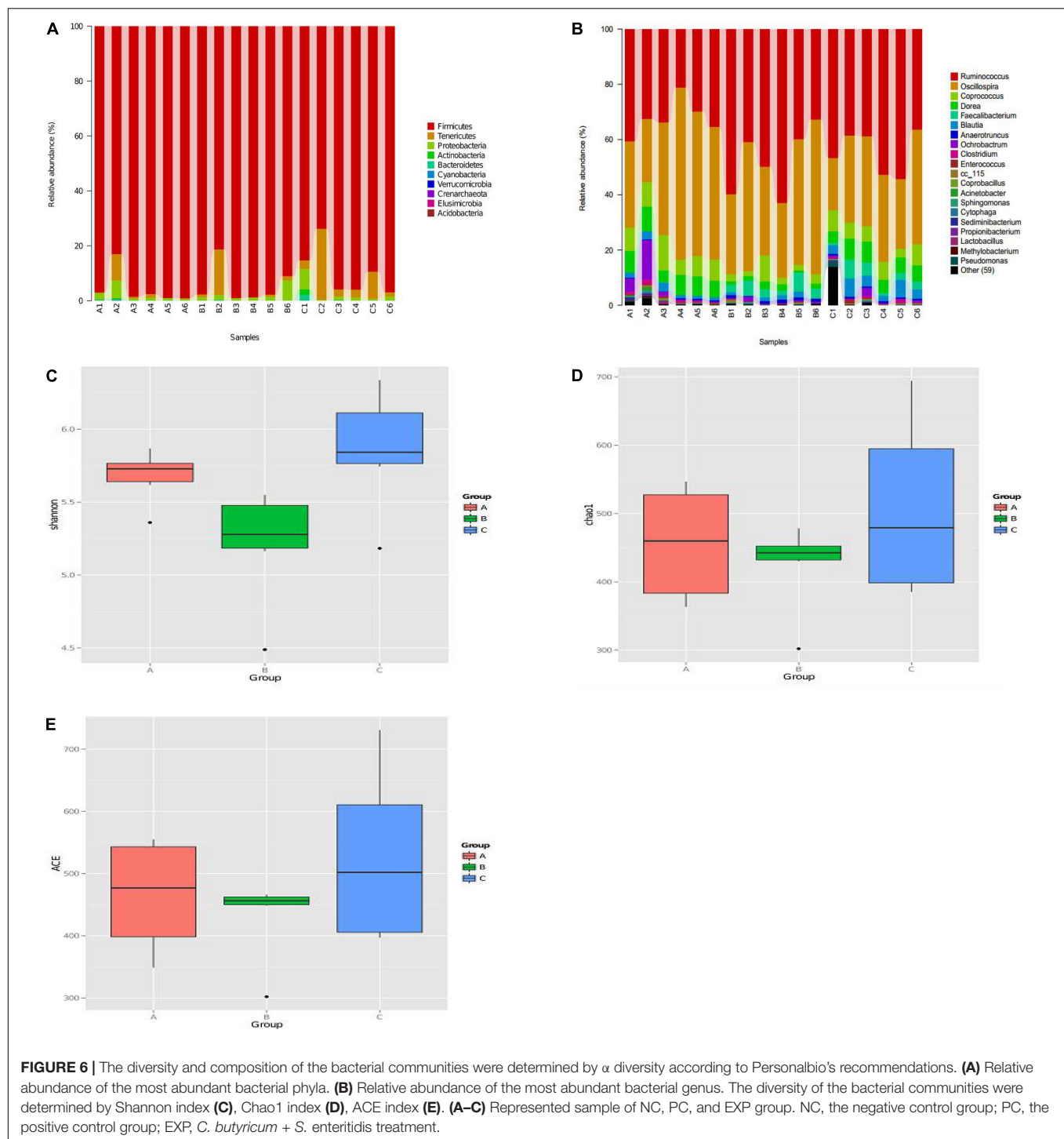
the three most abundant bacterial phyla in all samples, and *C. butyricum* increased the proportion of Tenericutes in the EXP chickens compared to the NC and PC groups (Figure 6A). The genera Ruminococcus, Oscillospira, Coprococcus, and Dorea were the most prevalent in all of the groups, and the proportion of Coprococcus and Dorea in NC and EXP groups was increased compared to the PC group (Figure 6B). The diversity of the intestinal bacterial community was determined by Shannon, Chao1, and AEC indices. The results show that *C. butyricum* increased the diversity of the bacterial community in the EXP group compared to the NC and PC groups (Figures 6C–E). Collectively, these data suggest that *C. butyricum* affects bacterial composition in the cecum of chickens.

DISCUSSION

Gram-negative *S. enterica* was identified as the most common cause of food poisoning in China (Ran et al., 2011) and is known to disrupt the intestinal epithelial layer during its infection (Coburn et al., 2007). In this study, *C. butyricum* protected the integrity of the villi in the cecum, limited the invasion of *Salmonella*;

attenuated *Salmonella*-induced microbiota disruption in the intestine of chickens; improved intestinal epithelial barrier function through the modulation of Muc-2 and ZO-1 expression. Our results suggest that *C. butyricum* is a potential therapy for *Salmonella* infection or other intestinal diseases.

It has been reported that *Salmonella* could easily colonize the gut and induce a strong intestinal inflammatory response due to the defective microbial barriers and innate immune systems in the newly-hatched chicks (Brown et al., 2006). In the present study, *C. butyricum* significantly decreased the expression level of the pro-inflammatory cytokine (IL-1β and IL-8) production in intestines and the expression level of the pro-inflammatory cytokine (IFN-γ, IL-1β, IL-8, and TNF-α) in intestinal epithelial cells of chickens after *Salmonella* infection. The protective action of *C. butyricum* was similar to that of other probiotics (Castillo et al., 2013) and it maybe depended on its antibacterial activity. Furthermore, we found that *C. butyricum* suppressed intestinal inflammation by downregulating the TLR4-, MyD88-, and NF-κB-dependent pathways in chickens with *Salmonella* infection, consistent with previous studies that *C. butyricum* can decrease pro-inflammatory cytokine levels by inhibiting the NF-κB signaling pathway in broiler chickens with *Salmonella*



infection (Zhao et al., 2017). The result suggests the linkage of TLR4/NF- κ B pathway may involved in the suppression of *C. butyricum* on *Salmonella* infection.

Muc2 is the major gel-forming mucin of the intestine and is the main structural component of the mucus gel. It is generally assumed that muc2 is essential for epithelial protection (Gill et al., 2011). In this study, muc2 production was decreased in

the jejunum of chickens with *Salmonella* infection. However, *C. butyricum* attenuated the *Salmonella*-induced disruption of muc2 production, which is consistent with another study that showed supplementation of LGG before and after DON/ZEA exposure appeared to increase muc2 (Murphy et al., 2016), but our results are different than those reported in mice (Gaudier et al., 2005), that mucin gene expression was not altered by

probiotic administration, this may be due to the differences in probiotic strains.

Tight junctions play a very important role in the intestinal mucosal barrier against macromolecular transmission (Ballard et al., 1995). ZO-1 and Occludin are important proteins responsible for the structural and functional organization of tight junctions (Fanning et al., 1998). In this study, we demonstrated that *C. butyricum* enhanced epithelial barrier function by increasing the expression of ZO-1 in intestinal tissue and IECs infected with *Salmonella*, which is consistent with a previous report showing that mRNA levels of ZO-1 in broiler chickens fed a 300 or 450 g/ton β -mannanase diet were significantly higher (Zuo et al., 2014).

Dietary supplementation of *C. butyricum* strains as a probiotic has become an effective alternative to the use of antibiotics to increase health and growth performance of chickens, as it has been shown that probiotics can positively affect the gut microbiota, which plays an important role in health and nutrient digestion in chickens (Yang et al., 2012). In this study, we found that *C. butyricum* treatment could alter the intestinal microbial composition and increase the diversity of the bacterial community, which could directly or indirectly impact chicken health and reduce or inhibit the presence of opportunistic pathogens and it may be due to its ability to produce metabolites, which can regulate the pH (acid change) of intestinal, inhibit pathogenic bacteria, and thus adjust the bacterial community structure. Our study aligns with another study that showed a diet supplemented with *Enterococcus faecalis* could shift microbial diversity in the porcine gut and inhibit pathogens (Li et al., 2016).

CONCLUSION

Clostridium butyricum effectively attenuated inflammation and epithelial barrier damage, altered the intestinal microbial composition by increasing the diversity of the bacterial

community, and promoted immune function in the intestines of *Salmonella*-infected chicken. *C. butyricum* might be an effective and safe therapy for *Salmonella* infection.

Future Work

In future work, we will supplement the detection of *Salmonella* and *Clostridium butyricum* counts during the course of the experiments to further verify that the organism of the bacteria colonized the gut.

DATA AVAILABILITY STATEMENT

The datasets generated for this study are available on request to the corresponding author.

ETHICS STATEMENT

The animal study was reviewed and approved by The Animal Care and Use Committee of Shandong Agricultural University.

AUTHOR CONTRIBUTIONS

HL, SS, and XZ conceived and designed the study. XZ, JY, ZJ, JW, and LW performed the experiments and analyzed the data. HL, SS, and XZ wrote and revised the manuscript.

FUNDING

This work was supported by the National Key R&D Project (2016YFD0501608 and 2016 YFD0500510), Taishan Scholar Program (201511023), Funds of Shandong “Double Tops” Program, and Shandong Agricultural Major Applied Technology Innovation Project (SD2019XM009).

REFERENCES

- Ballard, S. T., Hunter, J. H., and Taylor, A. E. (1995). Regulation of tight-junction permeability during nutrient absorption across the intestinal epithelium. *Annu. Rev. Nutr.* 15, 35–55. doi: 10.1146/annurev.nu.15.070195.000343
- Brown, S. P., Cornell, S. J., Sheppard, M., Grant, A. J., Maskell, D. J., and Mastroeni, P. (2006). Intracellular demography and the dynamics of *Salmonella enterica* infections. *PLoS Biol.* 4:349. doi: 10.1371/journal.pbio.0040349
- Cao, G. T., Xiao, Y. P., Yang, C. M., Chen, A. G., Liu, T. T., Zhou, L., et al. (2012). Effects of *Clostridium butyricum* on growth performance, nitrogen metabolism, intestinal morphology cecal microflora in broiler chickens. *J. Anim. Vet. Adv.* 11, 2665–2671. doi: 10.3923/javaa.2012.2665.2671
- Castillo, N. A., de Moreno de LeBlanc, A., Galdeano, M. C., and Perdigon, G. (2013). Comparative study of the protective capacity against *Salmonella* infection between probiotic and nonprobiotic *lactobacilli*. *J. Appl. Microbiol.* 114, 861–876. doi: 10.1111/jam.12074
- Chen, Z., and Jiang, X. (2014). Microbiological safety of chicken litter or chicken litter-based organic fertilizers: a review. *Agriculture* 4, 1–29. doi: 10.3390/agriculture4010001
- Coburn, B., Grassl, G. A., and Finlay, B. B. (2007). *Salmonella*, the host and disease: a brief review. *Immunol. Cell Biol.* 85, 112–118. doi: 10.1038/sj.icb.7100007
- Fanning, A. S., Jameson, B. J., Jesaitis, L. A., and Anderson, J. M. (1998). The tight junction protein ZO-1 establishes a link between the transmembrane protein occludin and the actin cytoskeleton. *J. Biol. Chem.* 273, 29745–29753. doi: 10.1074/jbc.273.45.29745
- Feasey, N. A., Dougan, G., Kingsley, R. A., Heyderman, R. S., and Gordon, M. A. (2012). Invasive nontyphoidal *Salmonella* disease: an emerging and neglected tropical disease in Africa. *Lancet* 379, 2489–2499. doi: 10.1016/S0140-6736(11)61752-2
- Forstner, J., Oliver, M., and Sylvester, F. (1995). *Production, Structure and Biologic Relevance of Gastrointestinal Mucins*. New York, NY: Raven Press.
- Gaudier, E., Michel, C., Segain, J. P., Cherbut, C., and Hoebler, C. (2005). The VSL# 3 probiotic mixture modifies microflora but does not heal chronic dextran-sodium sulfate-induced colitis or reinforce the mucus barrier in mice. *J. Nutr.* 135, 2753–2761.
- Gill, N., Wlodarska, M., and Finlay, B. B. (2011). Roadblocks in the gut: Barriers to enteric infection. *Cell Microbiol.* 13, 660–669. doi: 10.1111/j.1462-5822.2011.01578.x
- Huang, Q. Q., Wei, Y. N., Lv, Y. J., Wang, Y. X., and Hu, T. M. (2015). Effect of dietary inulin supplements on growth performance and intestinal immunological parameters of broiler chickens. *Livest. Sci.* 180, 172–176. doi: 10.1016/j.livsci.2015.07.015

- Juan, D. L., Adhikari, B., Park, S. H., Teague, K. D., Graham, L. E., Mahaffey, B. D., et al. (2018). Evaluation of the epithelial barrier function and ileal microbiome in an established necrotic enteritis challenge model in broiler chickens. *Front. Vet. Sci.* 5:199. doi: 10.3389/fvets.2018.00199
- Kemgang, S. T., Kapila, S., Shanmugam, V. P., and Kapila, R. (2014). Cross-talk between probiotic *Lactobacilli* and host immune system. *J. Appl. Microbiol.* 117, 303–319. doi: 10.1111/jam.12521
- Kusumawati, D. I., Harmayani, E., and Asmara, W. (2006). Effect of probiotic *Lactobacillus* sp. *Dad13* on humoral immune response of balb/C mice infected with *Salmonella typhimurium*, Indonesian. *J. Biotechnol.* 11, 870–877.
- Li, P. H., Niu, Q., Wei, Q. T., Zhang, Y. Q., Ma, X., Kim, S. W., et al. (2016). Microbial shifts in the porcine distal gut in response to diets supplemented with *Enterococcus Faecalis* as alternatives to antibiotics. *Sci. Rep.* 7:41395. doi: 10.1038/srep41395
- Lim, S. M., Jang, H. M., Jeong, J. J., Han, M. J., and Kim, D. H. (2017). *Lactobacillus johnsonii* CJLJ103 attenuates colitis and memory impairment in mice by inhibiting gut microbiota lipopolysaccharide production and NF- κ B activation. *J. Funct. Foods* 34, 359–368. doi: 10.1016/j.jff.2017.05.016
- Madsen, K. L. (2012). Enhancement of epithelial barrier function by probiotics. *J. Epithelial Biol. Pharmacol.* 5, 55–59. doi: 10.2174/1875044301205010055
- Majowicz, S. E., Musto, J., Scallan, E., Angulo, F. J., Kirk, M., O'Brien, S. J., et al. (2010). The global burden of nontyphoidal *Salmonella* gastroenteritis. *Clin. Infect. Dis.* 50, 882–889. doi: 10.1086/650733
- Mathur, R., Oh, H., Zhang, D., Park, S. G., Seo, J., Koblansky, A., et al. (2012). A mouse model of *Salmonella typhi* infection. *Cell* 151, 590–602. doi: 10.1016/j.cell.2012.08.042
- Murphy, L. Y. W., Paul, C. T., Kevin, J. A., and Hani, E. N. (2016). *Lactobacillus rhamnosus* GG modulates intestinal mucosal barrier and inflammation in mice following combined dietary exposure to deoxy nivalenol and zearalenone. *J. Funct. Foods* 22, 34–43. doi: 10.1016/j.jff.2016.01.014
- Parry, C. M., and Threlfall, E. J. (2008). Antimicrobial resistance in typhoidal and nontyphoidal *Salmonellae*. *Curr. Opin. Infect. Dis.* 21, 531–538. doi: 10.1097/QCO.0b013e32830f453a
- Pierzchalska, M., Grabacka, M., Michalik, M., Zyla, K., and Pierzchaski, P. (2012). Prostaglandin E2 supports growth of chicken embryo intestinal organoids in Matrigel matrix. *Biotechniques* 52, 307–315. doi: 10.2144/0000113851
- Ran, L., Wu, S., Gao, Y., Zhang, X., Feng, Z., Wang, Z., et al. (2011). Laboratory-Based Surveillance of Nontyphoidal *Salmonella* infections in China. *Foodborne Pathog. Dis.* 8, 921–927. doi: 10.1089/fpd.2010.0827
- Sainte-Marie, G. A. (1962). Paraffin embedding technique for studies employing immunofluorescence. *J. Histochem. Cytochem.* 10, 150–156.
- Schloss, P. D., Westcott, S. L., Ryabin, T., Hall, J. R., Hartmann, M., Hollister, E. B., et al. (2009). Introducing mothur: open-source, platform-independent, community-supported software for describing and comparing microbial communities. *App. Environ. Microb.* 75, 7537–7541. doi: 10.1128/AEM.01541-09
- Shanahan, F. (2010). Probiotics in perspective. *Gastroenterology* 139, 1808–1812. doi: 10.1053/j.gastro.2010.10.025
- The European Pharmacopoeia 7. 0, (2010). *General Text 5.2.2. Chicken Flocks Free From Specified Pathogens for the Production and Quality Control of Vaccines*. Strasbourg: The European Pharmacopoeia commission, 527–530.
- Wei, C. L., Chao, S. H., Tsai, W. B., Lee, P. S., Tsau, N. H., Chen, J. S., et al. (2013). Analysis of bacterial diversity during the fermentation of inyu, a high-temperature fermented soy sauce, using nested PCR-denaturing gradient gel electrophoresis and the plate count method. *Food Microbiol.* 33, 252–261. doi: 10.1016/j.fm.2012.10.001
- Xiao, M., Mi, Y., Liu, L., Lv, C., Zeng, W., Zhang, C., et al. (2018). Taurine regulates mucosal barrier function to alleviate lipopolysaccharide-induced duodenal inflammation in chicken. *Amino Acids* 50, 1637–1646. doi: 10.1007/s00726-018-2631-6
- Yang, C. M., Cao, G. T., Ferket, P. R., Liu, T. T., Zhou, L., Zhang, L., et al. (2012). Effects of probiotic, *Clostridium butyricum*, on growth performance, immune function, and cecal microflora in broiler chickens. *Poult. Sci.* 91, 2121–2129. doi: 10.3382/ps.2011-02131
- Zhang, L., Zhang, L., Zhan, X., Zeng, X., Zhou, L., Cao, G., et al. (2016). Effects of dietary supplementation of probiotic, *Clostridium butyricum*, on growth performance, immune response, intestinal barrier function, and digestive enzyme activity in broiler chickens challenged with *Escherichia coli* K88. *J. Anim. Sci. Biotechnol.* 7, 107–115. doi: 10.1186/s40104-016-0061-4
- Zhao, X. N., Yang, J., Wang, L. L., Lin, H., and Sun, S. H. (2017). Protection mechanism of *Clostridium butyricum* against *Salmonella* enteritidis infection in broilers. *Front. Microbiol.* 8:1523. doi: 10.3389/fmicb.2017.01523
- Zuo, J. J., Guo, A. H., Yan, X. Y., Xu, M., Xia, W. G., and Feng, D. Y. (2014). Supplementation of β -Mannanase in diet with energy adjustment on affect performance, intestinal morphology and tight junction proteins mRNA expression in broiler chickens. *J. Anim. Vet. Adv.* 13, 144–151.

Conflict of Interest: The authors declare that the research was conducted in the absence of any commercial or financial relationships that could be construed as a potential conflict of interest.

Copyright © 2020 Zhao, Yang, Ju, Wu, Wang, Lin and Sun. This is an open-access article distributed under the terms of the Creative Commons Attribution License (CC BY). The use, distribution or reproduction in other forums is permitted, provided the original author(s) and the copyright owner(s) are credited and that the original publication in this journal is cited, in accordance with accepted academic practice. No use, distribution or reproduction is permitted which does not comply with these terms.



Developing Novel Host-Based Therapies Targeting Microbicidal Responses in Macrophages and Neutrophils to Combat Bacterial Antimicrobial Resistance

Katie Watson^{1,2}, Clark D. Russell^{1,2,3}, J. Kenneth Baillie³, Kev Dhaliwal², J. Ross Fitzgerald³, Timothy J. Mitchell⁴, A. John Simpson⁵, Stephen A. Renshaw⁶ and David H. Dockrell^{1,2*} on behalf of the SHIELD consortium

¹ Department of Infection Medicine, University of Edinburgh, Edinburgh, United Kingdom, ² Centre for Inflammation Research, University of Edinburgh, Edinburgh, United Kingdom, ³ Roslin Institute, University of Edinburgh, Edinburgh, United Kingdom, ⁴ Institute of Microbiology and Infection, University of Birmingham, Birmingham, United Kingdom, ⁵ Institute of Cellular Medicine, Newcastle University and Newcastle Hospitals NHS Foundation Trust, Newcastle upon Tyne, United Kingdom, ⁶ Department of Infection, Immunity and Cardiovascular Disease, University of Sheffield Medical School, Sheffield, United Kingdom

OPEN ACCESS

Edited by:

Marco Rinaldo Oggioni,
University of Leicester,
United Kingdom

Reviewed by:

Arshad Khan,
University of Texas Health Science
Center at Houston, United States
Catherine Ropert,
Federal University of Minas
Gerais, Brazil
Joseph Wanford,
University of Leicester,
United Kingdom

*Correspondence:

David H. Dockrell
david.dockrell@ed.ac.uk

Specialty section:

This article was submitted to
Microbial Immunology,
a section of the journal
Frontiers in Immunology

Received: 14 February 2020

Accepted: 07 April 2020

Published: 05 June 2020

Citation:

Watson K, Russell CD, Baillie JK, Dhaliwal K, Fitzgerald JR, Mitchell TJ, Simpson AJ, Renshaw SA and Dockrell DH (2020) Developing Novel Host-Based Therapies Targeting Microbicidal Responses in Macrophages and Neutrophils to Combat Bacterial Antimicrobial Resistance. *Front. Immunol.* 11:786. doi: 10.3389/fimmu.2020.00786

Antimicrobial therapy has provided the main component of chemotherapy against bacterial pathogens. The effectiveness of this strategy has, however, been increasingly challenged by the emergence of antimicrobial resistance which now threatens the sustained utility of this approach. Humans and animals are constantly exposed to bacteria and have developed effective strategies to control pathogens involving innate and adaptive immune responses. Impaired pathogen handling by the innate immune system is a key determinant of susceptibility to bacterial infection. However, the essential components of this response, specifically those which are amenable to re-calibration to improve host defense, remain elusive despite extensive research. We provide a mini-review focusing on therapeutic targeting of microbicidal responses in macrophages and neutrophils to de-stress reliance on antimicrobial therapy. We highlight pre-clinical and clinical data pointing toward potential targets and therapies. We suggest that developing focused host-directed therapeutic strategies to enhance “pauci-inflammatory” microbial killing in myeloid phagocytes that maximizes pathogen clearance while minimizing the harmful consequences of the inflammatory response merits particular attention. We also suggest the importance of One Health approaches in developing host-based approaches through model development and comparative medicine in informing our understanding of how to deliver this strategy.

Keywords: antimicrobial resistance, macrophage, neutrophil, host-based therapies, innate immunity

INTRODUCTION

Antimicrobial chemotherapy has formed the cornerstone of our therapeutic strategy against bacterial disease since penicillin was first developed. Prior to this, developing host-based therapy was a major focus, including Fleming’s original work on lysozyme, a humoral microbicide he isolated while seeking antimicrobial factors in pus (1). The first therapeutic use of penicillin in 1930

(treating eye infections in babies in Sheffield by Cecil Paine), and the pioneering work of Florey, Chain and colleagues in Oxford who developed innovations in penicillin synthesis to allow the first clinical trials in 1941, established antimicrobial chemotherapy as the pre-eminent therapeutic approach to bacterial disease (2). This has had a major impact on human health but arguably diverted focus away from host-based approaches other than vaccination.

Recent public health estimates suggest antimicrobial resistant bacteria cause 131 infections/100,000 population in Europe and that two-thirds are nosocomial (3). The disability adjusted life years of these infections approximates tuberculosis, influenza and HIV combined (3). In addition, development of new antimicrobials has been declining (4). There is thus a pressing need to develop new antimicrobials, improved antimicrobial stewardship, better diagnostics to identify the patients who truly need antimicrobials, and alternative approaches, for example those involving bacteriophage therapy, nanoparticle-based therapy, photodynamic light therapy and antimicrobial peptides (AMP) to manage infection with antimicrobial resistant ESKAPE (*Enterococcus faecium*, *Staphylococcus aureus*, *Klebsiella pneumoniae*, *Acinetobacter baumannii*, *Pseudomonas aeruginosa*, and *Enterobacter* spp.) pathogens (5). While vaccination remains a major focus, the concept of developing host-based therapy is gaining traction.

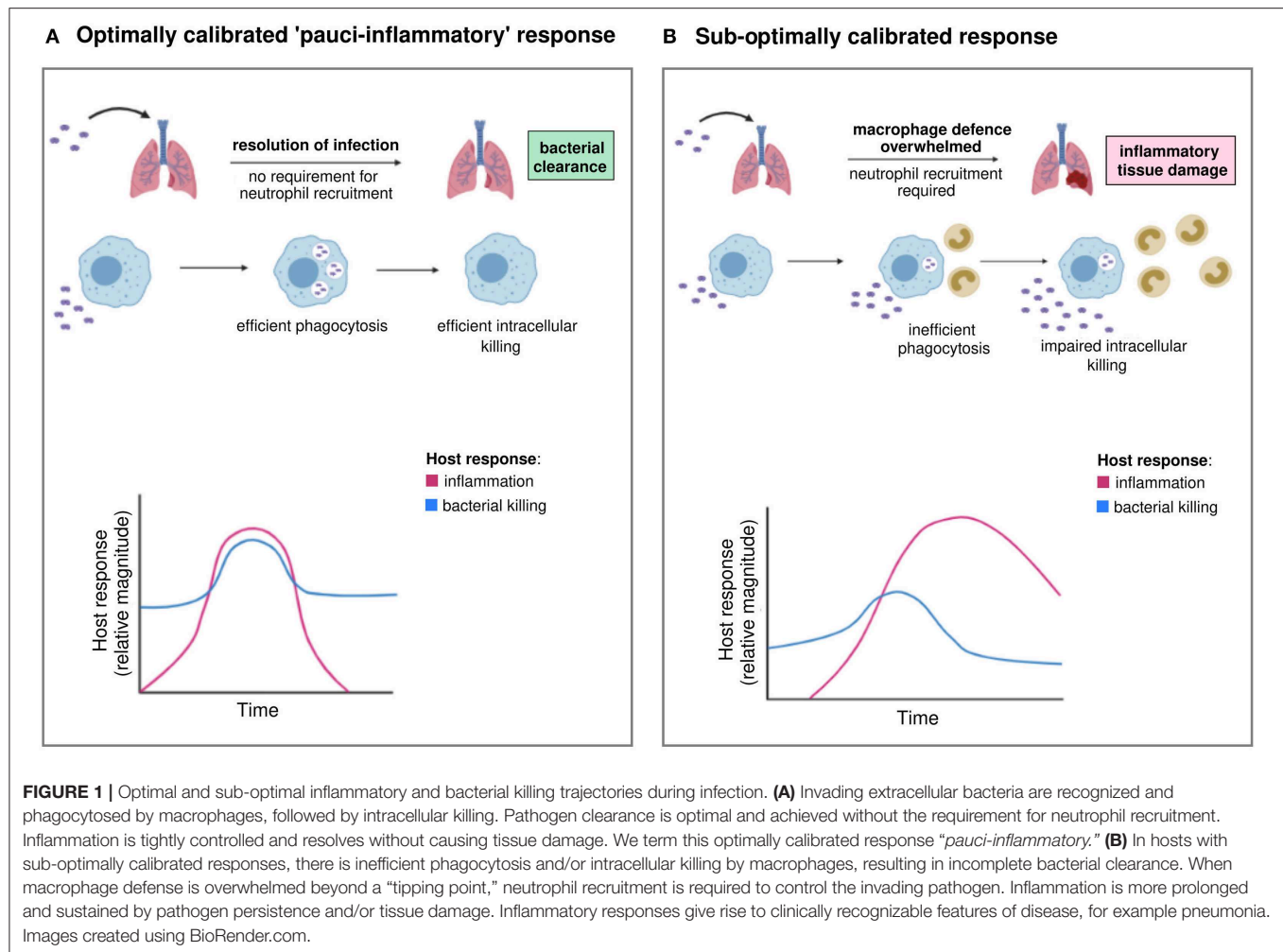
CHARACTERISTICS OF OPTIMAL INNATE IMMUNE RESPONSES TO PATHOGENIC BACTERIA

Pathogenic bacteria commonly colonize healthy individuals without causing disease. *S. aureus* is carried by >40% of infants after birth and ~50% of adults are permanent or intermittent carriers (6, 7). Uropathogenic *Escherichia coli* is typically part of an individual's fecal microbiota and healthy individuals carry a large number of potentially pathogenic strains (8). In other cases, pathogens are harmless microbiome constituents but cause opportunistic infections in patients whose immune system is impaired by medical co-morbidity, such as nosocomial enterococcal infections (9). This apparent paradox, between common carriage but uncommon disease, suggests most infections are readily controlled by the host yet the specific microbicidal responses that control infection when small numbers of colonizing bacteria translocate to new sites is incompletely defined. Broadly, the innate immune system ensures a rapid response, working in concert with any adaptive immune responses to the pathogen. There are many components to the innate immune system including mucosal barrier function, humoral factors released in mucosal secretions and a range of innate cellular responses that are not restricted to myeloid phagocytes but also include innate lymphoid cells. These responses are modified through adaptive immune responses, but the focus of this review is exclusively on myeloid phagocyte responses.

Professional phagocytes (macrophages and neutrophils) clear bacteria from mucosa associated with a low-density microbiome,

for example the distal airway or bladder (10). Macrophages play a critical role in the initial response as the resident phagocytes in tissues, using pattern recognition receptors (PRRs) to detect pathogens and orchestrate the inflammatory response. They are efficient at phagocytosing bacteria and utilize a range of microbicidal strategies to kill ingested bacteria. Tissue macrophage function is tightly controlled by activation state which is regulated by a cell network including epithelial, endothelial, T- and B- lymphocytes, as well as tissue resident innate lymphoid cells. The resulting cytokine networks reflect the importance of environmental cues (11). Innate immune memory ensures previous pathogen exposure modulates macrophage function via epigenetic imprinting of monocytes to induce "training" (enhanced microbicidal responses to repeat challenge) and "tolerance" (reduced deleterious responses to repeat challenge) to pathogen-associated molecular patterns (12, 13). Lipopolysaccharide (LPS) engagement of Toll-like receptor (TLR) 4 is just one example amongst several of a microbial stimulus that can on repeat stimulation be associated with tolerance manifest as reduced generation of pro-inflammatory cytokines and reactive species (14). This has implications for monocyte-derived macrophage populations but the extent to which it also influences resident macrophage populations with distinct ontogeny remains to be established. Though capable of avid phagocytosis, tissue macrophages have a finite capacity to kill ingested bacteria (15). This capacity can be diminished by interactions with other microorganisms e.g., viruses, environmental factors or co-morbidity, resulting in increased susceptibility to bacterial disease. For example, both HIV-1 infection and chronic obstructive pulmonary disease (COPD) impair alveolar macrophage (AM) killing of pneumococci (16, 17). Furthermore, pathogenic bacteria have evolved mechanisms to withstand microbicides, such as antioxidant systems (18). Successful pathogens such as *S. aureus* inhibit phagosomal maturation contributing to intracellular survival (19), while others that are more readily killed may escape killing in subsets of macrophages, as exemplified by survival of pneumococci in permissive CD169+ splenic macrophages in murine and porcine models (20). Several potentially AMR pathogens such as *K. pneumoniae* and *P. aeruginosa* can subvert phagosomal maturation in macrophages (21, 22). Traditional paradigms of intracellular and extracellular bacteria are blurring and the intracellular fate of the so-called extracellular bacteria (including medically important ESKAPE pathogens, *Haemophilus influenzae* and *Streptococcus pneumoniae*) is likely a major determinant of infection outcome.

When the intracellular killing capacity of resident tissue macrophages is overwhelmed, they orchestrate recruitment of neutrophils and other inflammatory cells. Murine models of clodronate-mediated AM depletion illustrate how escalating bacterial challenge shifts the role of AM from primary effectors of bacterial clearance to regulators of the inflammatory response, with neutrophils required for pathogen clearance (15, 23). The exhaustion of macrophage clearance capacity is likely also a feature of systemic infections, as evidenced for Kupffer cells in the liver and is augmented by commensal bacteria (24). This represents the transition from sub-clinical infection to



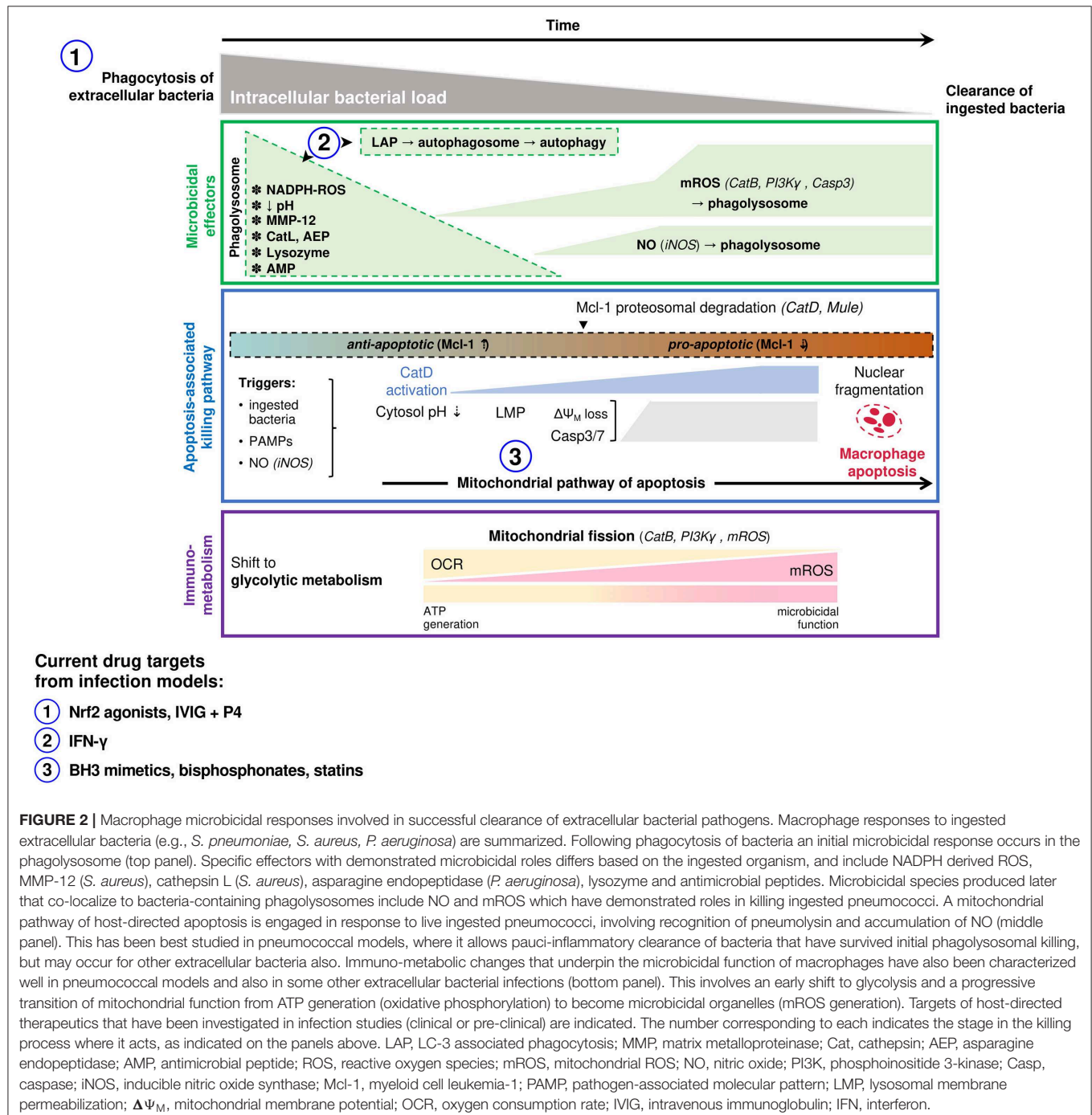
clinical disease, and signs of neutrophilic inflammation are used to establish a clinical diagnosis. The inflammatory response, however, contributes to tissue injury since potent microbicides, such as reactive oxygen species (ROS), can cause tissue injury and organ dysfunction (25). Nevertheless, this inflammatory response is essential and neutrophil deficiency results in severe bacterial infection (26). Neutrophil microbicidal responses have been extensively characterized and include ROS, AMP, divalent metal iron-sequestering proteins (e.g., lactoferrin), proteases such as the serine proteases contained in azurophilic granules (e.g., cathepsin G and neutrophil elastase) and acid hydrolases in lysosomes (26). The pre-eminence of ROS as a direct microbicidal mechanism has been challenged by observations that it is the associated ionic changes in the phagosome, activating granule-associated serine proteases, that actually mediate microbicidal killing (27). Neutrophils can also release granule contents and DNA extracellular traps to kill bacteria (28).

The challenge is therefore to generate an effective response that maximizes pathogen clearance and minimizes the inflammatory response, either by enhancing the macrophage response to raise the threshold for induction of neutrophilic

inflammation or by ensuring the neutrophilic component achieves pathogen clearance yet limits bystander tissue injury. We term this desirable microbicidal profile a “pauci-inflammatory microbicidal response” recognizing that its characteristics include rapid induction, effective pathogen killing, and controlled recruitment of inflammatory cells when needed, but also early resolution and tightly regulated production of potentially damaging microbicidal species (Figure 1). It builds on concepts articulated by Sears and colleagues in chronic parasitic infections where the cost of the host response (immunopathology) is weighed against resistance to the pathogen (29). In the case of common “extracellular” bacterial disease, the primary cost becomes tissue injury/organ dysfunction due to the microbicidal response and chronic infection is a rare outcome. If initial microbicidal responses by phagocytes are sub-optimal, the inflammatory response is escalated with increased recruitment of neutrophils, macrophages and lymphocytes that have the potential to promote self-propagating waves of inflammation driven by release of damage-associated molecular patterns in response to tissue injury. Excessive production

of cytokines, reactive species, proteases, phospholipids and eicosanoids mediate inflammatory tissue injury, induction of various cell death paradigms and ultimately loss of tissue homeostasis. These principles are well-exemplified by the development of acute respiratory distress syndrome (ARDS) (30). Organ specific injury is also associated with a systemic inflammatory response which can cause multiorgan failure (31). In addition, the generalized inflammatory response can lead to immunosuppression with impaired immune responses on

subsequent pathogen challenge (32). It is therefore essential to limit these dysregulated inflammatory responses and induce a more limited inflammatory response with optimal pathogen clearance, by targeting microbicidal responses. To target potential bottlenecks in the host microbicidal response, we must identify optimal responses that promote resilience in the healthy population and patient groups in whom these fail. We need to develop assays to assess the host response and effect of therapy.



IDENTIFYING HOST RESPONSES AS TARGETS FOR IMMUNOMODULATION

A critical bottleneck in host defense involves macrophage bacterial clearance (19, 33). However, therapeutic modulation of this is impeded by limitations in our understanding of microbicidal responses in tissue macrophages, which are often inferred from neutrophils, monocytes or monocytic cell lines. Well-established microbicidal mechanisms in other phagocytes may not operate in tissue macrophages, which (excluding those in atherosclerotic plaques) lack the ability to produce the more potent halogenated ROS like hypochlorous acid (34, 35). Some microbicidal responses are more convincingly demonstrated in mice than man, for example those involving nitric oxide (NO), which may be produced at lower levels in human macrophages, although several groups have detected it following bacterial challenge (36). Effective responses likely require combinations of microbicides. Defining these has been limited by how well *in vitro* macrophage cultures mirror tissue macrophages *in vivo*. Many tissue macrophages with low-level homeostatic turnover arise from embryonic yolk sac or fetal liver hematopoietic stem cell progenitors and are maintained by division of resident cells, e.g., AM derived from fetal liver precursors (37). Monocyte-derived macrophages (MDM) give rise to macrophages in the gut and peritoneum, populations associated with a higher turnover, but we cannot assume their microbicidal responses are identical to macrophages derived from embryonic progenitors. In addition, tissue macrophage maturation is heavily influenced by environmental cues and their transcriptional profiles are as distinct as they are from monocytes (38).

Irrespective of these limitations there are many similarities between microbicidal mechanisms of different macrophage populations. A range of primary human macrophages (including MDM and AM) and murine models demonstrate an initial phase of extensive intracellular killing, activated in the phagosome. For pathogens such as pneumococci, this is followed by a delayed phase of bacterial killing, involving apoptosis-associated killing that clears residual viable bacteria (16, 19, 33). These responses often involve combinations of microbicides (**Figure 2**), for example ROS and NO, which helps subvert pathogen resistance (33). Tissue macrophages modify the phagosomal environment to inhibit bacterial survival; phagolysosomal acidification and restriction of divalent metal cations inhibits bacterial enzymes, including manganese-containing superoxide dismutase. Nevertheless, the role of these responses is more established in killing intracellular bacteria, compared to internalized extracellular bacteria (39). These defenses are complemented by AMP and proteases. Matrix metalloproteinase 12 contributes to early killing of bacteria in macrophages (40). The cathelicidin LL-37 enhances killing of bacteria including *S. aureus* in macrophages and is taken up from exogenous sources to complement ROS generation and lysosome fusion (41). AMR in *E. coli* can increase the sensitivity to AMP, suggesting host-based strategies can synergize with antimicrobials or with antimicrobial selective pressure (42). Similarly, a synthetic peptide derived from human lactoferrin synergizes with antimicrobials against

a carbapenemase-producing *K. pneumoniae* (43). However, there are also examples where mutations inducing AMR may also enable resistance to AMP; modification of *K. pneumoniae* lipid A not only enables resistance to polymyxins but also β -defensins and human neutrophil peptide-1 (44). Many other AMP and proteases contribute to microbicidal responses, but the mechanism may be indirect. For example cathepsin D enhances apoptosis-associated killing by increasing proteasomal degradation of the anti-apoptotic Bcl-2 family member Mcl-1 (45).

The ability to perform lentiviral delivery of genome-scale clustered regularly interspaced short palindromic repeats (CRISPR)-associated nuclease Cas9 knock-out (GeCKO) pooled libraries to human cells allows whole genome screening with the potential to shed new light on microbicidal mechanisms (46, 47). A further potential approach is to harness comparative biology and aims to use convergent evolution of pathogens as they shift species tropism (48) or divergent evolution within species as they rapidly evolve under a host-selective pressure (49), to probe microbicidal mechanisms. Nevertheless, identifying microbicidal mechanisms as targets for immunomodulation will also require evidence that these are sub-optimally calibrated in patient groups with increased susceptibility to bacterial disease. For example, AM from patients with COPD fail to enhance mitochondrial ROS (mROS) production following bacterial challenge (16). This is important since mROS has recently emerged as a key microbicide affecting bacterial killing in the macrophage phagolysosome (33, 50). Evaluation of potential microbicidal targets will also require application of super-resolution microscopy and other advanced imaging modalities, combined with advances in probes, optics and analytics to provide temporal and spatial resolution of microbicidal generation. In the past, generation at a population level using automated systems such as flow cytometry has been assumed to be a surrogate for this but may be insufficient to allow optimal characterization. *In vivo* imaging is also a valuable adjunct and comparative medicine using large animals such as pigs, whose immune system is similar to humans, and studies in humans will aid translation in models of infection (51, 52).

RECALIBRATING MICROBICIDAL RESPONSES IN CLINICAL SETTINGS

Only a few strategies to modulate the host response to bacteria have progressed to clinical trials, and specific assessment of target microbicidal responses is often lacking (**Table 1**). Interferon (IFN)- γ is established in the treatment of chronic granulomatous disease (CGD), a genetic disorder in which deficiency in one of the components of the nicotinamide adenine dinucleotide phosphate (NADPH) oxidase leads to increased susceptibility to a range of infections. While this is an extreme case of adjusting an immune response, it shows immunomodulation can be used to enhance microbicidal responses. Clinical trial data shows IFN- γ reduces the frequency of severe infections in CGD and it has also been investigated for multi-drug resistant tuberculosis, *Mycobacterium avium*

TABLE 1 | Examples of host-directed therapies in infectious diseases from clinical and pre-clinical studies.

Therapy	Level of evidence	Target			Pathogen or disease	Outcomes	References
		Cell type	Cellular pathway	Microbicidal response			
IFN- γ	Clinical trial (RCT)	Neutrophil	NADPH-mediated ROS production	Phagosomal intracellular killing	Patients with chronic granulomatous disease ($n = 128$)	↓ frequency of serious infections in patients receiving IFN- γ (22 vs. 46%, $p = 0.0006$). No serious toxicity.	(53)
GM-CSF	Clinical trial (RCT)	Neutrophil	RhoA GTPase pathway and actin polymerisation	Phagocytosis	Critically ill adults with ↓ <i>ex vivo</i> neutrophil phagocytosis ($n = 38$)	<i>Ex vivo</i> reversal of defective neutrophil phagocytosis. No serious toxicity.	(54)
IL-7	Clinical trial (RCT)	Lymphocyte	IL-7R signaling via Jak/STAT and PI3K/Akt pathways	T-cell apoptosis	Adults with septic shock and lymphopenia ($n = 27$; most commonly pneumonia or intra-abdominal infection)	↑ absolute lymphocyte count. ↑ CD8 ⁺ and CD4 ⁺ T-cell count. ↑ T-cell proliferation and activation. No serious toxicity	(55)
IFN- γ	Clinical trial	Monocyte	HLA-DR expression	Monocyte activation	Critically ill adults with sepsis and ↓ monocyte HLA-DR expression ($n = 9$)	↑ <i>ex vivo</i> monocyte LPS-induced TNF- α production. ↑ <i>ex vivo</i> monocyte HLA-DR expression. No serious toxicity.	(56)
Anti-PD1 mAb + IFN- γ^*	Case report	Lymphocyte	PD-1/PDL-1 interactions	T-cell apoptosis	1 patient with invasive mucormycosis	Clinical cure. ↑ absolute lymphocyte count. ↑ monocyte HLA-DR expression. ↑ CD8 ⁺ T-cell count. ↓ T-cell PD-1 expression.	(57)
IFN- γ^*	Case report	Monocytes	HLA-DR expression	Monocyte activation	1 patient with persistent <i>S. aureus</i> bacteraemia and metastatic infection	Clinical cure. ↑ MHC-II pathway transcription. ↑ HLA-DR expression. ↑ antigen-specific T-reg cells. Shift from Th2 to Th1/Th17.	(58)
IFN- γ	Pre-clinical	Macrophage	p62 tagging of intracellular bacteria and autophagosome formation.	Autophagic killing of intracellular bacteria	<i>B. cenocepacia</i> (cystic fibrosis)	MDM from patients with cystic fibrosis <i>in vitro</i> : ↑ intracellular killing ↓ IL-1 β production	(59)
P4 peptide + IVIG	Pre-clinical	Neutrophils and macrophages	Fc- γ R	Phagocytosis	<i>S. pneumoniae</i>	Murine pneumococcal disease model: ↑ survival ↑ bacterial clearance ↑ Fc- γ R expression (neutrophils) Murine macrophages: ↑ phagocytosis.	(60)
P4 peptide	Pre-clinical	Neutrophils and monocytes	Phagosome	Phagocytosis and killing	<i>S. pneumoniae</i>	Neutrophils from adults with severe sepsis: ↑ neutrophil bacterial killing ↑ neutrophil and monocyte ROS	(61)
Nrf2 agonists	Pre-clinical	Macrophage	Antioxidant response (phase II detoxifying enzymes)	Phagocytosis	<i>S. pneumoniae</i> , <i>H. influenzae</i>	Alveolar macrophages from patients with COPD: ↑ phagocytosis.	(62)

(Continued)

TABLE 1 | Continued

Therapy	Level of evidence	Target			Pathogen or disease	Outcomes	References
		Cell type	Cellular pathway	Microbicidal response			
BH3 mimetics Clodronate	Pre-clinical	Macrophage	Inhibition of anti-apoptotic BCL-2 family members or induction of apoptosis in case of clodronate	Apoptosis-associated killing	<i>S. pneumoniae</i> , <i>L. pneumophila</i>	Murine pneumonia models: ↑ survival ↑ bacterial clearance (lung) ↓ neutrophil recruitment ↑ alveolar macrophage apoptosis	(33, 63)
Statins	Pre-clinical	Macrophage	Cholesterol biosynthesis	Phagosomal maturation and autophagy	<i>M. tuberculosis</i>	MDM from statin-treated patients: ↓ intracellular bacterial growth Murine tuberculosis model: ↓ bacterial burden and lung micro-abscesses Statin-treated murine BMDM: ↓ intracellular bacterial growth	(64)
Statins	Pre-clinical	Macrophages	Cholesterol biosynthesis	Apoptosis-associated killing	<i>S. enterica</i> serovar Typhimurium	Statin-treated RAW 264.7 cells: ↓ intracellular bacterial growth ↑ apoptosis and CatD localisation to SCV Murine model (intra-peritoneal): ↓ bacterial burden (liver and spleen)	(65)
Statins	Pre-clinical	Neutrophils	Cholesterol biosynthesis	NETosis Phagocytosis ROS	<i>S. aureus</i>	Statin-treated neutrophils: ↑ extracellular killing & NETosis ↓ phagocytosis ↓ oxidative burst Murine pneumonia model: ↑ bacterial clearance (lung) ↓ lung inflammation ↑ NETosis	(66)
Statins	Pre-clinical	Macrophages	Cholesterol biosynthesis JNK pathway	Phagocytosis ROS Fc-γR signaling	<i>S. aureus</i>	Statin-treated MDM: ↓ phagocytosis, ROS & intracellular killing ↑ Fc-γR-mediated TNF-α production	(67)

GM-CSF: granulocyte-macrophage colony-stimulating factor; IL: interleukin; IFN: interferon; RCT: randomised-controlled trial; ROS: reactive oxygen species; mAb: monoclonal antibody; IVIG: intravenous immunoglobulin; BMDM: bone marrow-derived macrophages; MDM: monocyte-derived macrophages; CatD: cathepsin D; SCV: Salmonella-containing vacuole; NET: neutrophil extracellular trap.

*Administered in addition to appropriate antimicrobials.

complex and *Cryptococcus neoformans* infections (53, 68). IFN-γ enhances several microbicidal mechanisms and has been shown to correct defective *ex vivo* killing of the intracellular pathogen *Burkholderia cenocepacia* in cystic fibrosis (CF) MDM by enhancing autophagy, a regulated cellular process that enables removal and recycling of macromolecules and organelles to promote cellular homeostasis and a related cell process using autophagy machinery that leads to killing of ingested bacteria termed xenophagy (59). However, nebulized IFN-γ did not

reduce bacterial density or inflammation in a clinical trial in CF (69). In critically ill adults, clinical trial data demonstrates that IFN-γ is associated with clearance of persistent bacteremia and improved cytokine profiles in the setting of sepsis-induced immunosuppression. Further investigation in clinical trials in sepsis is ongoing (70). It has also been shown to correct HLA-DR expression on monocytes in patients with sepsis which provides a useful marker of response (56). In a case report, IFN-γ enabled clearance of persistent *S. aureus* bacteremia in

association with transcriptional profiles associated with a shift toward Th1/Th17 responses and antigen-specific T-regs, though the specific consequences for microbicidal responses were not examined (58). In patients with septic shock and lymphopenia, IL-7 has been shown to reverse sepsis-induced lymphopenia (55).

GM-CSF and G-CSF enhance macrophage and neutrophil phagocytosis and microbicidal responses *in vitro* and are used to restore functional phagocyte numbers in patients receiving bone marrow-suppressive chemotherapy. GM-/G-CSF have also been investigated in patients with sepsis, with a meta-analysis suggesting a trend toward benefit (71, 72). Timing may be important with GM-CSF and it may have most efficacy when targeted to patients with low monocyte HLA-DR (73). Whilst the impact on microbicidal responses is often not studied, a recent clinical trial showed GM-CSF targeted to critically ill patients with defects in *ex vivo* neutrophil phagocytosis could ameliorate this defect and increase monocyte HLA-DR (54). Both GM-CSF and IFN- γ will, with subtle differences, contribute to macrophage activation phenotypes that promote microbicidal responses, particularly against pathogens with significant intracellular survival. Other cytokines will have similar effects (74). As with many other approaches listed, each can impact more than one cellular process directly or indirectly, affecting microbicidal responses (Table 2). For example, IFN- γ can also enhance myeloid cell recruitment in clinical trials (68).

Other investigational approaches include the use of checkpoint inhibitors, such as anti-programmed cell death protein-1 (anti-PD-1) or anti-cytotoxic T-lymphocyte-associated protein-4 (CTLA-4) monoclonal antibodies (73). These inhibitors aim to reverse suppression of T-cell inflammatory responses. Nivolumab, an anti-PD-1 monoclonal antibody, is being tested in a clinical trial in sepsis, and while such therapies are anticipated to modulate the inflammatory response, they may also target microbicidal responses. For example, there is a case report of Nivolumab being used in combination with IFN- γ to successfully treat an intractable fungal infection (57). A PD-1 ligand inhibitor has also been shown to increase monocyte HLA-DR expression (76). Other immune modulating strategies that can be expected to modulate microbicidal responses include recombinant IL-7, which corrects lymphopenia and will enhance IFN- γ , and intravenous immunoglobulin (IVIG), which in addition to immunomodulation enhances pathogen clearance through phagocytosis (73). Immunomodulatory peptides have also been combined with IVIG, specifically the P4 peptide (derived from the immunomodulatory pneumococcal lipopeptide Pneumococcal surface adhesin A), resulting in increased pneumococcal clearance in mice and enhanced neutrophil and monocyte bacterial killing (60, 61).

REPURPOSED DRUGS TO TARGET MICROBICIDAL RESPONSES IN PRE-CLINICAL MODELS

Studies in relevant *in vitro* and animal models, and human patient groups, can identify host microbicidal targets. But there is then a need to develop therapeutic approaches to modulate these

targets. This will inevitably be constrained by cost, but this can potentially be reduced by re-purposing existing agents that are found to modify the host response of interest (75).

Critical illness can be associated with the compensatory anti-inflammatory response syndrome and temporary immunoparesis, after the initial stages of innate immune activation. This is characterized by reduced Th1 and monocyte responses, which increase the risk of nosocomial infection (77). Reducing PRR engagement and subsequent immune activation, such as through reduction in TLR activation in the early stages of illness, could potentially reverse this phenomenon and the turmeric constituent curcumin appears to down-regulate signaling through a range of TLRs (78, 79).

Phagocytosis of bacteria activates phagosomal microbicidal responses in myeloid cells (80). Although phagocytosis is not usually a rate limiting process, in conditions such as COPD macrophage phagocytosis may be reduced. This is associated with increased airway bacterial burden (62). This defect is related to cellular oxidative stress (62, 81). Nrf2 agonists are in development, which enhance the host cell's anti-oxidant host defenses, and in COPD AM can enhance phagocytosis as well as clearance of *P. aeruginosa* in mice exposed to cigarette smoke (62, 82).

Xenophagy is selective autophagy that aids clearance of intracellular pathogens such as *Mycobacterium tuberculosis* (83) and some extracellular bacteria. Of note, *Streptococcus pyogenes* subverts this process in endothelial cells (84). Activation of autophagy via inhibition of inhibitory pathways, such as class I phosphoinositide-3-kinase, mitogen-activated protein kinases or 5'-AMP-activated protein kinases, could be a tractable microbicidal strategy and drugs already under development for other indications could be re-purposed (75).

Another novel microbicidal response in macrophages and potentially other myeloid cells involves apoptosis-associated killing. BH3 mimetics enhance killing of *S. pneumoniae* and *Legionella pneumophila* in murine models through augmentation/restoration of this pathway (33, 63). Bisphosphonates also enhance macrophage apoptosis-associated killing of bacteria (33), while fluoroquinolones cause lysosomal permeabilization, sensitizing cells to this pathway (45, 85).

3-hydroxy-3-methyl-glutaryl-CoA (HMG-CoA) reductase inhibitors, termed statins, are used as cholesterol lowering medicines. Statins enhance bacterial clearance in a murine sickle cell model of pneumococcal disease. The impact was limited to the sickle cell mice with no response seen in wild type (86). One potential mechanism was downregulation of platelet-activating factor receptor required for bacterial translocation from the lung in the sickle cell mice. However, the microbicidal basis for the enhanced clearance was not established beyond the association of increased clearance with reduced sickle cell-associated inflammation. In the case of *M. tuberculosis*, statins enhance phagosomal maturation and xenophagy (64), while for *Salmonella enterica* serovar Typhimurium they enhance cathepsin D localization to phagosomes and apoptosis induction (65). Whether they also enhance these processes for extracellular pathogens is not established. They can enhance neutrophil and monocyte killing by extracellular traps (66). However, they

TABLE 2 | Summary of strategies of host-directed therapy.

Strategy	Therapy	References
↑ microbicidal activity through canonical killing mechanisms	IFN- γ	(53)
	GM-CSF	(54)
	Statins (undetermined mechanism, presumed canonical)	(64–66)
	Anti-PD1 (nivolumab)	(57)
	IL-7	(73)
↑ apoptosis-associated killing (macrophages)	P4 peptide	(61)
	BH3 mimetics	(33, 63)
	Clodronate	(33)
	Statins	(65)
↑ xenophagy	IFN- γ	(59)
	Statins	(64)
	PI3K, MAPK 5' AMP kinases	(75)
↑ monocyte activation	IFN- γ	(56, 58)
	GM-CSF	(54, 73)
	PDL1 inhibitor	(76)
Enhancing T cell numbers to indirectly increase microbicidal responses	IL-7	(73)
↑ Phagocytosis as basis of increased microbicidal response	GM-CSF	(54)
	IVIG	(60)
	P4 peptide	(61)
	Nrf2 agonists	(62)
	Statins	(66, 67)

inhibit phagocytosis and microbicidal responses in other models such as Fc γ -receptor mediated uptake of opsonized *S. aureus* (67) and reduce bacterial killing by neutrophils in a murine pneumonia model (87). Therefore, how they would be best used requires further elucidation, as reflected in contradictory findings from clinical studies. For example, a reduced risk of community-acquired *S. aureus* bacteremia (88) and reduced mortality in pneumonia were reported (89, 90) yet no reduction in mortality was observed in another pneumonia study (91) or in a study of ventilator-associated pneumonia (92).

CHALLENGES

Recalibrating responses will likely require a personalized medicine approach. Individual pathogens would need varying degrees of engagement of a given response. *S. aureus* inhibits apoptosis-associated killing in macrophages so might need a greater degree of enhancement, or might require an alternative approach, while for *S. pneumoniae* in which apoptosis-associated killing is already engaged, the adjustment might only need to be of a more modest extent in a

subset of individuals (33). Certain responses might need engagement in select patient groups such as those with medical comorbidities that adjust the response. Alternatively these responses might not be suitable for enhancement in certain groups. For example, patients with COPD might not be amenable to enhancement of mROS production or might require reduction in high baseline levels of antioxidants to enhance this microbicidal response (16). Such personalized approaches would require validated tests to help calibrate an individual response.

Another challenge is that where responses need to be recalibrated it will be important that responses do not over shoot and result in overproduction of factors that could lead to tissue injury if there is excessive production of microbicides or inflammatory cells (30). This is most likely to be prevented where the responses enhanced are intracellular, generated at high levels adjacent to bacteria and transient. Responses will require application of techniques to measure the individuals response through use of appropriate biomarkers or imaging modalities and would benefit from approaches that combine these measures with microdosing experiments and endomicroscopy (the application of *in vivo* microscopy applied through endoscopy to allow optical biopsy) to test the efficacy of recalibration (93).

CONCLUSIONS

The ineluctable progression of AMR necessitates investigation of novel strategies for treating bacterial disease. Based on the observation that exposure to potentially pathogenic bacteria infrequently leads to disease, we contend that identification and exploitation of specific determinants of host defense represents a tractable alternative to antimicrobials (host-based therapy). While there are many potential aspects of the host response that represent tractable targets, including humoral factors (e.g., AMP), epithelial barrier function, and lymphoid populations, we suggest approaches that promote pauci-inflammatory macrophage and neutrophil microbicidal responses can improve outcomes. We have highlighted a number of promising *in vitro*, animal model, human and pre-clinical observations that support this viewpoint and provide a roadmap for future research.

AUTHOR CONTRIBUTIONS

KW, CR, and DD wrote the initial drafts of the article. JB, KD, JE, TM, AS, and SR provided critical comment and revised the document.

FUNDING

The authors are supported by the MRC SHIELD consortium investigating novel host based antimicrobial responses to antimicrobial resistant bacteria (MRNO2995X/1).

REFERENCES

- Hare R. The scientific activities of Alexander Fleming, other than the discovery of penicillin. *Med Hist.* (1983) 27:347–72. doi: 10.1017/s0025727300043386
- Arseculeratne SN, Arseculeratne G. A re-appraisal of the conventional history of antibiotics and Penicillin. *Mycoses.* (2017) 60:343–7. doi: 10.1111/myc.12599
- Cassini A, Hogberg LD, Plachouras D, Quattrocchi A, Hoxha A, Simonsen GS, et al. Attributable deaths and disability-adjusted life-years caused by infections with antibiotic-resistant bacteria in the EU and the European Economic Area in 2015: a population-level modelling analysis. *Lancet Infect Dis.* (2019) 19:56–66. doi: 10.1016/S1473-3099(18)30605-4
- Czaplewski L, Bax R, Clokie M, Dawson M, Fairhead H, Fischetti V, et al. Alternatives to antibiotics—a pipeline portfolio review. *Lancet Infect Dis.* (2016) 16:239–51. doi: 10.1016/S1473-3099(15)00466-1
- Mulani MS, Kamble EE, Kumkar SN, Tawre MS, Pardesi KR. Emerging Strategies to combat ESKAPE pathogens in the era of antimicrobial resistance: a review. *Front Microbiol.* (2019) 10:539. doi: 10.3389/fmicb.2019.00539
- Peacock SJ, Justice A, Griffiths D, de Silva GDI, Kantzanou MN, Crook D, et al. Determinants of acquisition and carriage of *Staphylococcus aureus* in infancy. *J Clin Microbiol.* (2003) 41:5718–25. doi: 10.1128/jcm.41.12.5718-5725.2003
- Wertheim HF, Melles DC, Vos MC, van Leeuwen W, van Belkum A, Verbrugh HA, et al. The role of nasal carriage in *Staphylococcus aureus* infections. *Lancet Infect Dis.* (2005) 5:751–62. doi: 10.1016/S1473-3099(05)70295-4
- Nielsen KL, Dynesen P, Larsen PN, Frimodt-Moller. Faecal *Escherichia coli* from patients with *E. coli* urinary tract infection and healthy controls who have never had a urinary tract infection. *J Med Microbiol.* (2014) 63:582–9. doi: 10.1099/jmm.0.068783-0
- Gao W, Howden BP, Stinear TP. Evolution of virulence in *Enterococcus faecium*, a hospital-adapted opportunistic pathogen. *Curr Opin Microbiol.* (2018) 41:76–82. doi: 10.1016/j.mib.2017.11.030
- Turvey SE, Broide DH. Innate immunity. *J Allergy Clin Immunol.* (2010) 125(Suppl. 2):S24–32. doi: 10.1016/j.jaci.2009.07.016
- Mortha A, Burrows K. Cytokine networks between innate lymphoid cells and myeloid cells. *Front Immunol.* (2018) 9:191. doi: 10.3389/fimmu.2018.00191
- Ifrim DC, Quintin J, Joosten LAB, Jacobs C, Jansen T, Jacobs L, Gow NAR, et al. Trained immunity or tolerance: opposing functional programs induced in human monocytes after engagement of various pattern recognition receptors. *Clin Vaccine Immunol.* (2014) 21:534–45. doi: 10.1128/CI.00688-13
- Saeed S, Quintin J, Kerstens HH, Rao NA, Sharifi N, Janssen-Megens EM, et al. Epigenetic programming of monocyte-to-macrophage differentiation and trained innate immunity. *Science.* (2014) 345:1251086. doi: 10.1126/science.1251086
- Medvedev AE, Sabroe I, Hasday JD, Vogel SN. Tolerance to microbial TLR ligands: molecular mechanisms and relevance to disease. *J Endotoxin Res.* (2006) 12:133–50. doi: 10.1179/096805106X102255
- Dockrell DH, Marriott HM, Prince LR, Ridger VC, Ince PG, Hellewell PG, et al. Alveolar macrophage apoptosis contributes to pneumococcal clearance in a resolving model of pulmonary infection. *J Immunol.* (2003) 171:5380–8. doi: 10.4049/jimmunol.171.10.5380
- Bewley MA, Preston JA, Mohasin M, Marriott HM, Budd RC, Swales J, et al. Impaired mitochondrial microbicidal responses in chronic obstructive pulmonary disease macrophages. *Am J Respir Crit Care Med.* (2017) 196:845–55. doi: 10.1164/rccm.201608-1714OC
- Collini PJ, Bewley MA, Mohasin M, Marriott H, Miller RF, Geretti A-M, et al. HIV gp120 in the lungs of antiretroviral therapy-treated individuals impairs alveolar macrophage responses to pneumococci. *Am J Respir Crit Care Med.* (2018) 197:1604–15. doi: 10.1164/rccm.201708-1755OC
- Aberdein JD, Cole J, Bewley MA, Marriott H, Dockrell DH. Alveolar macrophages in pulmonary host defence the unrecognized role of apoptosis as a mechanism of intracellular bacterial killing. *Clin Exp Immunol.* (2013) 174:193–202. doi: 10.1111/cei.12170
- Jubrail J, Morris P, Bewley MA, Stoneham S, Johnston SA, Foster SJ, et al. Inability to sustain intraphagolysosomal killing of *Staphylococcus aureus* predisposes to bacterial persistence in macrophages. *Cell Microbiol.* (2016) 18:80–96. doi: 10.1111/cmi.12485
- Ercoli G, Fernandes VE, Chung WY, Wanford J, Thomson S, Bayliss CD, et al. Intracellular replication of *Streptococcus pneumoniae* inside splenic macrophages serves as a reservoir for septicemia. *Nat Microbiol.* (2018) 3:600–10. doi: 10.1038/s41564-018-0147-1
- Cano V, March C, Insua JL, Aguiló N, Llobet E, Llobet E, Moranta D, et al. *Klebsiella pneumoniae* survives within macrophages by avoiding delivery to lysosomes. *Cell Microbiol.* (2015) 17:1537–60. doi: 10.1111/cmi.12466
- Mukherjee K, Khatua B, Mandal C. Sialic acid-siglec-e interactions during *Pseudomonas aeruginosa* infection of macrophages interferes with phagosome maturation by altering intracellular calcium concentrations. *Front Immunol.* (2020) 11:332. doi: 10.3389/fimmu.2020.00332
- Knapp S, Leemans JC, Florquin S, Branger J, Maris NA, Pater J, et al. Alveolar macrophages have a protective antiinflammatory role during murine pneumococcal pneumonia. *Am J Respir Crit Care Med.* (2003) 167:171–9. doi: 10.1164/rccm.200207-698OC
- Boldock E, Surewaard BGJ, Shamarina D, Na M, Fei Y, Ali A, et al. Human skin commensals augment *Staphylococcus aureus* pathogenesis. *Nat Microbiol.* (2018) 3:881–90. doi: 10.1038/s41564-018-0198-3
- Mittal M, Siddiqui MR, Tran K, Reddy SP, Malik AB. Reactive oxygen species in inflammation and tissue injury. *Antioxid Redox Signal.* (2014) 20:1126–67. doi: 10.1089/ars.2012.5149
- Segal W. How neutrophils kill microbes. *Annu Rev Immunol.* (2005) 23:197–223. doi: 10.1146/annurev.immunol.23.021704.115653
- Reeves EP, Lu H, Jacobs HL, Messina CGM, Bolsover S, Gabella G, et al. Killing activity of neutrophils is mediated through activation of proteases by K⁺ flux. *Nature.* (2002) 416:291–7. doi: 10.1038/416291a
- Brinkmann V, Reichard U, Goosmann C, Fauler B, Uhlemann Y, Weiss D, et al. Neutrophil extracellular traps kill bacteria. *Science.* (2004) 303:1532–5. doi: 10.1126/science.1092385
- Sears BF, Rohr JR, Allen JE, Martin LB. The economy of inflammation: when is less more? *Trends Parasitol.* (2011) 27:382–7. doi: 10.1016/j.pt.2011.05.004
- Han S, Mallampalli RK. The acute respiratory distress syndrome: from mechanism to translation. *J Immunol.* (2015) 194:855–60. doi: 10.4049/jimmunol.1402513
- Meduri GU, Annane D, Chrousos GP, Marik PE, Sinclair SE, et al. Activation and regulation of systemic inflammation in ARDS: rationale for prolonged glucocorticoid therapy. *Chest.* (2009) 136:1631–43. doi: 10.1378/chest.08-2408
- Buttenschoen K, Kornmann M, Berger D, Leder G, Beger H, Vasilescu GC. Endotoxemia and endotoxin tolerance in patients with ARDS. *Langenbecks Arch Surg.* (2008) 393:473–8. doi: 10.1007/s00423-008-0317-3
- Preston JA, Bewley MA, Marriott HM, McGarry Houghton A, Mohasin M, Jubrail J, et al. Alveolar macrophage apoptosis-associated bacterial killing helps prevent murine pneumonia. *Am J Respir Crit Care Med.* (2019) 200:84–97. doi: 10.1164/rccm.201804-0646OC
- Koeffler HP, Ranyard J, Pertcheck M. Myeloperoxidase: its structure and expression during myeloid differentiation. *Blood.* (1985) 65:484–91
- Sugiyama S, Okada Y, Sukhova GK, Virmani R, Heinecke JW, Libby P, et al. Macrophage myeloperoxidase regulation by granulocyte macrophage colony-stimulating factor in human atherosclerosis and implications in acute coronary syndromes. *Am J Pathol.* (2001) 158:879–91. doi: 10.1016/S0002-9440(10)64036-9
- Thomas AC, Mattila JT. “Of mice and men”: arginine metabolism in macrophages. *Front Immunol.* (2014) 5:479. doi: 10.3389/fimmu.2014.00479
- Ginhoux F, Williams M. Tissue-resident macrophage ontogeny and homeostasis. *Immunity.* (2016) 44:439–49. doi: 10.1016/j.immuni.2016.02.024
- Gautier EL, Shay T, Miller J, Greter M, Jakubczik C, Ivanov S, et al. Gene-expression profiles and transcriptional regulatory pathways that underlie the identity and diversity of mouse tissue macrophages. *Nat Immunol.* (2012) 13:1118–28. doi: 10.1038/ni.2419
- Flannagan RS, Cosio G, Grinstein S. Antimicrobial mechanisms of phagocytes and bacterial evasion strategies. *Nat Rev Microbiol.* (2009) 7:355–66. doi: 10.1038/nrmicro2128
- Houghton AM, Hartzell WO, Robbins CS, Gomis-Rüth FX, Shapiro SD, et al. Macrophage elastase kills bacteria within murine macrophages. *Nature.* (2009) 460:637–41. doi: 10.1038/nature08181
- Tang X, Basavarajappa D, Haeggstrom JZ, Wan M. P2X7 receptor regulates internalization of antimicrobial peptide LL-37 by human macrophages that

- promotes intracellular pathogen clearance. *J Immunol.* (2015) 195:1191–201. doi: 10.4049/jimmunol.1402845
42. Lazar V, Martins A, Spohn R, Daruka L, Grezal G, Fekete G, et al. Antibiotic-resistant bacteria show widespread collateral sensitivity to antimicrobial peptides. *Nat Microbiol.* (2018) 3:718–31. doi: 10.1038/s41564-018-0164-0
 43. Morici P, Florio W, Rizzato C, Ghelardi E, Tavanti A, Rossolini G, et al. Synergistic activity of synthetic N-terminal peptide of human lactoferrin in combination with various antibiotics against carbapenem-resistant *Klebsiella pneumoniae* strains. *Eur J Clin Microbiol Infect Dis.* (2017) 36:1739–48. doi: 10.1007/s10096-017-2987-7
 44. Kidd TJ, Mills G, Sa-Pessoa J, Dumigan A, Frank CG, Insua JL, et al. A *Klebsiella pneumoniae* antibiotic resistance mechanism that subdues host defences and promotes virulence. *EMBO Mol Med.* (2017) 9:430–47. doi: 10.15252/emmm.201607336
 45. Bewley MA, Marriott HM, Tulone C, Francis SE, Mitchell TJ, et al. A cardinal role for cathepsin d in co-ordinating the host-mediated apoptosis of macrophages and killing of pneumococci. *PLoS Pathog.* (2011) 7:e1001262. doi: 10.1371/journal.ppat.1001262
 46. Shalem O, Sanjana NE, Hartenian E, Shi X, Scott DA, Mikkelsen T, et al. Genome-scale CRISPR-Cas9 knockout screening in human cells. *Science.* (2014) 343:84–7. doi: 10.1126/science.1247005
 47. Li B, Clohisey SM, Chia BS, Wang B, Cui A, Eisenhaure T, et al. Genome-wide CRISPR screen identifies host dependency factors for influenza A virus infection. *Nat Commun.* (2020) 11:164. doi: 10.1038/s41467-019-13965-x
 48. Viana D, Comos M, McAdam PR, Ward MJ, Selva L, Guinane CM, et al. A single natural nucleotide mutation alters bacterial pathogen host tropism. *Nat Genet.* (2015) 47:361–6. doi: 10.1038/ng.3219
 49. Witznath M, Pache F, Lorenz D, Koppe U, Gutbier B, Tabeling C, et al. The NLRP3 inflammasome is differentially activated by pneumolysin variants and contributes to host defense in pneumococcal pneumonia. *J Immunol.* (2011) 187:434–40. doi: 10.4049/jimmunol.1003143
 50. West AP, Brodsky IE, Rahner C, Woo DK, Erdjument-Bromage H, Tempst P, et al. TLR signalling augments macrophage bactericidal activity through mitochondrial ROS. *Nature.* (2011) 472:476–80. doi: 10.1038/nature09973
 51. Akram AR, Chankeshwara SV, Scholefield E, Aslam T, McDonald N, Megia-Fernandez A, et al. *In situ* identification of gram-negative bacteria in human lungs using a topical fluorescent peptide targeting lipid A. *Sci Transl Med.* (2018) 10:eaal0033. doi: 10.1126/scitranslmed.aal0033
 52. Meurens F, Summerfield A, Nauwynck H, Saif L, Gerdt V. The pig: a model for human infectious diseases. *Trends Microbiol.* (2012) 20:50–7. doi: 10.1016/j.tim.2011.11.002
 53. A controlled trial of interferon gamma to prevent infection in chronic granulomatous disease. The international chronic granulomatous disease cooperative study group. *N Engl J Med.* (1991) 324:509–16. doi: 10.1056/NEJM199102213240801
 54. Pinder EM, Rostron AJ, Hellyer TP, Ruchaud-Sparagano MH, Scott J, Macfarlane JG, et al. Randomised controlled trial of GM-CSF in critically ill patients with impaired neutrophil phagocytosis. *Thorax.* (2018) 73:918–25. doi: 10.1136/thoraxjnl-2017-211323
 55. Francois B, Jeannot R, Daix T, Walton AH, Shotwell MS, Unsinger J, et al. Interleukin-7 restores lymphocytes in septic shock: the IRIS-7 randomized clinical trial. *JCI Insight.* (2018) 3:98960. doi: 10.1172/jci.insight.98960
 56. Döcke WD, Randow F, Syrbe U, Krausch D, Asadullah K, Reinke P, et al. Monocyte deactivation in septic patients: restoration by IFN-gamma treatment. *Nat Med.* (1997) 3:678–81. doi: 10.1038/nm0697-678
 57. Grimaldi D, Pradier O, Hotchkiss RS, Vincent JL. Nivolumab plus interferon-gamma in the treatment of intractable mucormycosis. *Lancet Infect Dis.* (2017) 17:18. doi: 10.1016/S1473-3099(16)30541-2
 58. Nalos M, Santner-Nanan B, Parnell G, Tang B, McLean AS, Nanan R. Immune effects of interferon gamma in persistent staphylococcal sepsis. *Am J Respir Crit Care Med.* (2012) 185:110–2. doi: 10.1164/ajrcm.185.1.110
 59. Assani K, Tazi ME, Amer AO, Kopp BT. IFN-gamma stimulates autophagy-mediated clearance of Burkholderia cenocepacia in human cystic fibrosis macrophages. *PLoS ONE.* (2014) 9:e96681. doi: 10.1371/journal.pone.0096681
 60. Bangert M, Bricio-Moreno L, Gore S, Rajam G, Ades EW, Gordon SB, et al. P4-mediated antibody therapy in an acute model of invasive pneumococcal disease. *J Infect Dis.* (2012) 205:1399–407. doi: 10.1093/infdis/jis223
 61. Morton B, Mitsi E, Pennington SH, Reiné J, Wright AD, Parker R, et al. Augmented passive immunotherapy with P4 peptide improves phagocyte activity in severe sepsis. *Shock.* (2016) 46:635–41. doi: 10.1097/SHK.0000000000000715
 62. Bewley MA, Budd RC, Ryan E, Cole J, Collini P, Marshall J, et al. Opsonic phagocytosis in chronic obstructive pulmonary disease is enhanced by Nrf2 agonists. *Am J Respir Crit Care Med.* (2018) 198:739–50. doi: 10.1164/rccm.201705-0903OC
 63. Speir M, Lawlor KE, Glaser SP, Abraham G, Chow S, Vogrin A, et al. Eliminating Legionella by inhibiting BCL-XL to induce macrophage apoptosis. *Nat Microbiol.* (2016) 1:15034. doi: 10.1038/nmicrobiol.2015.34
 64. Parihar SP, Guler R, Khutlang R, Lang DM, Hurdal R, Mhlanga MM, et al. Statin therapy reduces the *Mycobacterium tuberculosis* burden in human macrophages and in mice by enhancing autophagy and phagosome maturation. *J Infect Dis.* (2014) 209:754–63. doi: 10.1093/infdis/jit550
 65. Catron DM, Lange Y, Borensztajn J, Sylvester MD, Jones BD, Haldar K. *Salmonella enterica* serovar Typhimurium requires nonsterol precursors of the cholesterol biosynthetic pathway for intracellular proliferation. *Infect Immun.* (2004) 72:1036–42. doi: 10.1128/iai.72.2.1036-1042.2004
 66. Chow OA, von Kockritz-Blickwede M, Bright AT, Hensler ME, Zinkernagel AS, Cogen AL, et al. Statins enhance formation of phagocyte extracellular traps. *Cell Host Microbe.* (2010) 8:445–54. doi: 10.1016/j.chom.2010.10.005
 67. Benati D, Ferro M, Savino MT, Ulivieri C, Schiavo E, Nuccitelli A, et al. Opposite effects of simvastatin on the bactericidal and inflammatory response of macrophages to opsonized *S. aureus*. *J Leukoc Biol.* (2010) 87:433–42. doi: 10.1189/jlb.0409273
 68. Miller CH, Maher SG, Young HA. Clinical use of interferon-gamma. *Ann N Y Acad Sci.* (2009) 1182:69–79. doi: 10.1111/j.1749-6632.2009.05069.x
 69. Moss RB, Mayer-Hamblett N, Wagener J, Daines C, Hale K, Ahrens R, et al. Randomized, double-blind, placebo-controlled, dose-escalating study of aerosolized interferon gamma-1b in patients with mild to moderate cystic fibrosis lung disease. *Pediatr Pulmonol.* (2005) 39:209–18. doi: 10.1002/ppul.20152
 70. Payen D, Faivre V, Miatello J, Leentjens J, Brumpt C, Tissieres P, et al. Multicentric experience with interferon gamma therapy in sepsis induced immunosuppression. A case series. *BMC Infect Dis.* (2019) 19:931. doi: 10.1186/s12879-019-4526-x
 71. Bo L, Wang F, Zhu J, Li J, Deng X. Granulocyte-colony stimulating factor (G-CSF) and granulocyte-macrophage colony stimulating factor (GM-CSF) for sepsis: a meta-analysis. *Crit Care.* (2011) 15:R58. doi: 10.1186/cc10031
 72. Mathias B, Szpila BE, Moore FA, Efron PA, Moldawer LL. A review of GM-CSF therapy in sepsis. *Medicine.* (2015) 94:e2044. doi: 10.1097/MD.0000000000002044
 73. Davies R, O'Dea K, Gordon A. Immune therapy in sepsis: Are we ready to try again? *J Intensive Care Soc.* (2018) 19:326–44. doi: 10.1177/1751143718765407
 74. Murray PJ, Allen JE, Biswas SK, Fisher EA, Gilroy DW, Goerdt S, et al. Macrophage activation and polarization: nomenclature and experimental guidelines. *Immunity.* (2014) 41:14–20. doi: 10.1016/j.immuni.2014.06.008
 75. Brown D. Antibiotic resistance breakers: can repurposed drugs fill the antibiotic discovery void? *Nat Rev Drug Discov.* (2015) 14:821–32. doi: 10.1038/nrd4675
 76. Hotchkiss RS, Colston E, Yende S, Angus DC, Moldawer LL, Crouser ED, et al. Immune checkpoint inhibition in sepsis: a phase 1b randomized, placebo-controlled, single ascending dose study of antiprogrammed cell death-ligand 1 antibody (BMS-936559). *Crit Care Med.* (2019) 47:632–42. doi: 10.1097/CCM.0000000000003685
 77. Ward NS, Casserly B, Ayala A. The compensatory anti-inflammatory response syndrome (CARS) in critically ill patients. *Clin Chest Med.* (2008) 29:617–25. doi: 10.1016/j.ccm.2008.06.010
 78. Gradišar H, Keber MM, Pristovsek P, Jerala R. MD-2 as the target of curcumin in the inhibition of response to LPS. *J Leukoc Biol.* (2007) 82:968–74. doi: 10.1189/jlb.1206727
 79. Shuto T, Ono T, Ohira Y, Shimasaki S, Mizunoe S, Watanabe K, et al. Curcumin decreases toll-like receptor-2 gene expression and function in human monocytes and neutrophils. *Biochem Biophys Res Commun.* (2010) 398:647–52. doi: 10.1016/j.bbrc.2010.06.126
 80. DeLeo FR, Allen LA, Apicella M, Nauseef WM. NADPH oxidase activation and assembly during phagocytosis. *J Immunol.* (1999) 163:6732–40

81. Belchamber KBR, Singh R, Batista CM, Whyte MK, Dockrell DH, Kilty I, et al. Defective bacterial phagocytosis is associated with dysfunctional mitochondria in COPD macrophages. *Eur Respir J*. (2019) 54:1802244. doi: 10.1183/13993003.02244-2018
82. Harvey CJ, Thimmulappa RK, Sethi S, Kong X, Yarmus L, Brown RH, et al. Targeting Nrf2 signaling improves bacterial clearance by alveolar macrophages in patients with COPD and in a mouse model. *Sci Transl Med*. (2011) 3:78ra32. doi: 10.1126/scitranslmed.3002042
83. Sharma V, Verma S, Seranova E, Sarkar S, Kumar D. Selective autophagy and xenophagy in infection and disease. *Front Cell Dev Biol*. (2018) 6:147. doi: 10.3389/fcell.2018.00147
84. Cheng YL, Kuo CF, Lu SL, Hiroko O, Wu YN, Hsieh CL, et al. Group A *Streptococcus* induces liposomes via SLO/beta1 integrin/NOX2/ROS pathway in endothelial cells that are ineffective in bacterial killing and suppress xenophagy. *mBio*. (2019) 10:e02148–19. doi: 10.1128/mBio.02148-19
85. Bewley MA, Naughton M, Preston J, Mitchell A, Holmes A, Marriott HM, et al. Pneumolysin activates macrophage lysosomal membrane permeabilization and executes apoptosis by distinct mechanisms without membrane pore formation. *mBio*. (2014) 5:e01710–14. doi: 10.1128/mBio.01710-14
86. Rosch JW, Boyd AR, Hinojosa E, Pestina T, Hu Y, Persons DA, et al. Statins protect against fulminant pneumococcal infection and cytotoxicity in a mouse model of sickle cell disease. *J Clin Invest*. (2010) 120:627–35. doi: 10.1172/JCI39843
87. Fessler MB, Young SK, Jeyaseelan S, Lieber JG, Arndt PG, Nick JA, et al. A role for hydroxy-methylglutaryl coenzyme A reductase in pulmonary inflammation and host defense. *Am J Respir Crit Care Med*. (2005) 171:606–15. doi: 10.1164/rccm.200406-729OC
88. Smit J, López-Cortés LE, Thomsen RW, Schönheyder HC, Nielsen H, Frølev T, et al. Statin use and risk of community-acquired *Staphylococcus aureus* bacteremia: a population-based case-control study. *Mayo Clin Proc*. (2017) 92:1469–1478. doi: 10.1016/j.mayocp.2017.07.008
89. Schlienger RG, Fedson DS, Jick SS, Jick H, Meier CR. Statins and the risk of pneumonia: a population-based, nested case-control study. *Pharmacotherapy*. (2007) 27:325–32. doi: 10.1592/phco.27.3.325
90. Thomsen RW, Riis A, Kornum JB, Christensen S, Johnsen SP, Sørensen HT. Preadmission use of statins and outcomes after hospitalization with pneumonia: population-based cohort study of 29,900 patients. *Arch Intern Med*. (2008) 168:2081–7. doi: 10.1001/archinte.168.19.2081
91. Majumdar SR, McAlister FA, Eurich DT, Padwal RS, Marrie TJ. Statins and outcomes in patients admitted to hospital with community acquired pneumonia: population based prospective cohort study. *BMJ*. (2006) 333:999. doi: 10.1136/bmj.38992.565972.7C
92. Papazian L, Roch A, Charles PE, Penot-Ragon C, Perrin G, Roulier P, et al. Effect of statin therapy on mortality in patients with ventilator-associated pneumonia: a randomized clinical trial. *JAMA*. (2013) 310:1692–700. doi: 10.1001/jama.2013.280031
93. Robles-Medrand C. Confocal endomicroscopy: Is it time to move on? *World J Gastrointest Endosc*. (2016) 8:1–3. doi: 10.4253/wjge.v8.i1.1

Conflict of Interest: The authors declare that the research was conducted in the absence of any commercial or financial relationships that could be construed as a potential conflict of interest.

Copyright © 2020 Watson, Russell, Baillie, Dhaliwal, Fitzgerald, Mitchell, Simpson, Renshaw and Dockrell. This is an open-access article distributed under the terms of the Creative Commons Attribution License (CC BY). The use, distribution or reproduction in other forums is permitted, provided the original author(s) and the copyright owner(s) are credited and that the original publication in this journal is cited, in accordance with accepted academic practice. No use, distribution or reproduction is permitted which does not comply with these terms.



Human Single-chain Variable Fragments Neutralize *Pseudomonas aeruginosa* Quorum Sensing Molecule, 3O-C12-HSL, and Prevent Cells From the HSL-mediated Apoptosis

Sirijan Santajit¹, Watee Seesuary², Kodchakorn Mahasongkram², Nitat Sookrung^{2,3}, Pornpan Pumirat¹, Sumate Ampawong⁴, Onrapak Reamtong⁵, Manas Chongsa-Nguan⁶, Wanpen Chaicumpa² and Nitaya Indrawattana^{1*}

OPEN ACCESS

Edited by:

Marco Rinaldo Oggioni,
University of Leicester,
United Kingdom

Reviewed by:

Song Lin Chua,
The Hong Kong Polytechnic
University, Hong Kong
Rodolfo Garcia-Contreras,
National Autonomous University
of Mexico, Mexico

*Correspondence:

Nitaya Indrawattana
nitaya.ind@mahidol.ac.th

Specialty section:

This article was submitted to
Antimicrobials, Resistance
and Chemotherapy,
a section of the journal
Frontiers in Microbiology

Received: 18 December 2019

Accepted: 07 May 2020

Published: 24 June 2020

Citation:

Santajit S, Seesuary W, Mahasongkram K, Sookrung N, Pumirat P, Ampawong S, Reamtong O, Chongsa-Nguan M, Chaicumpa W and Indrawattana N (2020) Human Single-chain Variable Fragments Neutralize *Pseudomonas aeruginosa* Quorum Sensing Molecule, 3O-C12-HSL, and Prevent Cells From the HSL-mediated Apoptosis. *Front. Microbiol.* 11:1172. doi: 10.3389/fmicb.2020.01172

¹ Department of Microbiology and Immunology, Faculty of Tropical Medicine, Mahidol University, Bangkok, Thailand, ² Center of Research Excellence on Therapeutic Proteins and Antibody Engineering, Department of Parasitology, Faculty of Medicine Siriraj Hospital, Mahidol University, Bangkok, Thailand, ³ Biomedical Research Unit, Department of Research, Faculty of Medicine Siriraj Hospital, Mahidol University, Bangkok, Thailand, ⁴ Department of Tropical Pathology, Faculty of Tropical Medicine, Mahidol University, Bangkok, Thailand, ⁵ Department of Tropical Molecular Biology and Genetics, Faculty of Tropical Medicine, Mahidol University, Bangkok, Thailand, ⁶ Faculty of Public Health and Environment, Pathumthani University, Pathum Thani, Thailand

The quorum sensing (QS) signaling molecule, *N*-(3-oxododecanoyl)-L-homoserine lactone (3O-C12-HSL), contributes to the pathogenesis of *Pseudomonas aeruginosa* by regulating expression of the bacterial virulence factors that cause intense inflammation and toxicity in the infected host. As such, the QS molecule is an attractive therapeutic target for direct-acting inhibitors. Several substances, both synthetic and naturally derived products, have shown effectiveness against detrimental 3O-C12-HSL activity. Unfortunately, these compounds are relatively toxic to mammalian cells, which limits their clinical application. In this study, fully human single-chain variable fragments (HuscFvs) that bind to *P. aeruginosa* haptenic 3O-C12-HSL were generated based on the principle of antibody polyspecificity and molecular mimicry of antigenic molecules. The HuscFvs neutralized 3O-C12-HSL activity and prevented mammalian cells from the HSL-mediated apoptosis, as observed by Annexin V/PI staining assay, sub-G1 arrest population investigation, transmission electron microscopy for ultrastructural morphology of mitochondria, and confocal microscopy for nuclear condensation and DNA fragmentation. Computerized homology modeling and intermolecular docking predicted that the effective HuscFvs interacted with several regions of the bacterially derived ligand that possibly conferred neutralizing activity. The effective HuscFvs should be tested further *in vitro* on *P. aeruginosa* phenotypes as well as *in vivo* as a sole or adjunctive therapeutic agent against *P. aeruginosa* infections, especially in antibiotic-resistant cases.

Keywords: *Pseudomonas aeruginosa*, quorum sensing, *N*-3-oxo-dodecanoyl-L-homoserine lactone (3O-C12-HSL), apoptosis, human scFv

INTRODUCTION

Pseudomonas aeruginosa, a versatile and ubiquitous Gram-negative bacterium, is an opportunistic microorganism that frequently causes severe nosocomial infections, particularly among immunocompromised patients and those suffering from cystic fibrosis, burns, HIV infection, and cancer (Tang et al., 1996; Sadikot et al., 2005; Silva Filho et al., 2013; Malhotra et al., 2019; Waters and Goldberg, 2019). The pathogenicity of *P. aeruginosa* is attributable mainly, if not solely, to the regulons of two complete *N*-acyl homoserine lactone (AHL)-dependent quorum sensing (QS) systems, called LasI/R and RhlI/R (Preston et al., 1997; Venturi, 2006). The two QS systems act in a hierarchical manner, i.e., the LasI/R system controls the activity of the rhlI/R circuit (Pearson et al., 1994, 1995). During bacterial infection, the LasI and RhlI synthases produce *N*-(3-oxododecanoyl)-*L*-homoserine lactone (3O-C12-HSL) and *N*-butanoyl-*L*-homoserine lactone (C4-HSL), respectively. The QS molecules then interact with their cognate LasR and RhlR, causing transcription of hundreds of target genes, including those coding for virulence factors such as lectins, elastases, proteases, exotoxin A, pyocyanin, and surface-active rhamnolipids important in the late stages of biofilm development, as well as genes involved in antibiotic resistance (Wagner et al., 2003; Venturi, 2006; Rutherford and Bassler, 2012; Moradali et al., 2017).

N-(3-Oxododecanoyl)-*L*-homoserine lactone (3O-C12-HSL) is the prominent autoinducer of the *P. aeruginosa* QS system (Duan and Surette, 2007; Rasamiravaka and El Jaziri, 2016). 3O-C12-HSL is a small, fatty acid-like, membrane-permeant signaling molecule that comprises a hydrophilic homoserine lactone ring linked to the hydrophobic 12-carbon-atom-long acyl side chain via an amide bond (Eberhard et al., 1981; Pearson et al., 1995; Ritchie et al., 2007; O'Connor et al., 2015). The roles of 3O-C12-HSL in pathogenesis and modulation of the host immune responses have been reviewed (Liu et al., 2015). Owing to its lipophilicity, the 3O-C12-HSL can traverse the mammalian cell membrane (Ritchie et al., 2007), causing mitochondrial damage and dysfunction, which subsequently activates the caspase pathway leading to apoptosis of several cell types, including macrophages, neutrophils, T lymphocytes, human vascular endothelial cells, murine fibroblasts, airway epithelial cells, goblet cells, and breast carcinoma cells (Tateda et al., 2003; Li et al., 2004; Shiner et al., 2006; Jacobi et al., 2009; Schwarzer et al., 2012; Tao et al., 2016, 2018). *P. aeruginosa* QS signaling molecules also modulate host immune responses by down-regulating the expression of co-stimulatory molecules on dendritic cells (DCs), leading to inhibition of DC maturation and their ability to activate effector T-cell responses (Boontham et al., 2008). Because the 3O-C12-HSL plays an important role in the virulence and pathogenesis of *P. aeruginosa* and host immunity suppression, it is an attractive target for novel therapeutics for *P. aeruginosa* infection. Substances that interfere with *P. aeruginosa* 3O-C12-HSL activity should mitigate bacterial-associated disease severity, although blocking the QS system alone does not necessarily abrogate all *P. aeruginosa* virulence factors, such as T3SS (Blevins et al., 2005; López-Jácome et al.,

2019; Soto-Aceves et al., 2019). A therapeutic approach based on QS interference and/or attenuation of QS signals should result in greater sensitivity of the *P. aeruginosa* to stresses, such as antimicrobial drugs (Rasmussen and Givskov, 2006; Defoirdt et al., 2010; Maeda et al., 2012; Kalia et al., 2014; Krzyżek, 2019).

Recently, a murine monoclonal antibody (mAb), RS2-1G9, against a lactam mimetic of 3O-C12-HSL has been shown to prevent apoptosis through p38 mitogen-activated protein kinase activation and protected murine bone marrow-derived macrophages from the cytotoxic effects of the QS molecule (Kaufmann et al., 2006, 2008). The RS2-1G9 paratope was shown to enclose the polar lactam moiety of the 3O-C12-HSL molecule in the co-crystal structure of the Fab fragment of the RS2-1G9 mAb and the target 3O-C12-HSL completely (Debler et al., 2007). Active immunization of mice with 3O-C12-HSL-protein conjugate protected immunized mice from lethal *P. aeruginosa* infection (Miyairi et al., 2006). Antibody-based therapy directed to the QS molecule should not only block bacterial virulence, but also rescue the host immunity that had been modulated/suppressed by the QS system (Kaufmann et al., 2008; Palliyil and Broadbent, 2009). The present study generated engineered, fully human, single-chain antibody variable fragments (HuscFvs) that neutralize 3O-C12-HSL bioactivity. The HuscFvs should be tested, step-by-step, toward clinical application as a sole or adjunct therapy for the currently failing antibiotic treatment of patients with *P. aeruginosa* infection.

MATERIALS AND METHODS

P. aeruginosa

N-(3-Oxododecanoyl)-*L*-Homoserine Lactone (3O-C12-HSL)

The QS molecule was synthesized commercially (Cayman Chemical, Ann Arbor, MI, United States) under the IUPAC name: 3-oxo-*N*-[(3*S*)-2-oxooxolan-3-yl]-dodecanamide. 3O-C12-HSL was stored in 100% dimethyl-sulfoxide (DMSO) and diluted with phosphate-buffered saline, pH 7.4 (PBS), to the desired concentration for use.

Preparation of HuscFv to *P. aeruginosa* 3O-C12-HSL

The human single-chain variable fragments (HuscFvs) to the 3O-C12-HSL were generated based on the principles of the polyspecific property of an antibody, i.e., one antibody can bind different antigens by paratope adaptation to accommodate distinct antigens, such as through differential engagements of the complementarity determining regions (CDRs), and the molecular mimicry of the antigens (different antigens can share surface topologies in terms of shape or chemical nature) (Tapryal et al., 2013). In this study, HB2151 *Escherichia coli* clones carrying phagemids with inserted HuscFv genes (*huscFvs*) were previously selected from a HuscFv phage display library (Kulkeaw et al., 2009) using *Pseudomonas* exotoxin A (ETA) as antigen in the phage-biopanning process (Santajit et al., 2019). Genes coding for

HuscFvs of individual *E. coli* clones were sequenced and deduced, and the canonical CDRs and framework regions (FRs) of both VH and VL domains were determined based on the numbering scheme of Chotia and Kobat (Abhinandan and Martin, 2008).

Three dimensional (3D) models of the selected HuscFvs were generated by subjecting their deduced amino acid sequences to the I-TASSER online server (Yang et al., 2015). The HuscFvs-3D models from the I-TASSER were further refined to improve local geometric and physical quality using ModRefiner (Xu and Zhang, 2011). The quality of the generated homology models of HuscFvs was then evaluated using the PROCHECK server to provide Ramachandran plots (Laskowski et al., 1993). Thereafter, the 3D structures of the individual HuscFvs were superimposed with the 3D structure of the mAb RS2-1G9 F(ab')₂ (PDB ID: 2NTF) (previously shown to neutralize 3O-C12-HSL pathogenic activity; hence, the mAb has been designated as a “quorum quenching antibody”) (Kaufmann et al., 2006, 2008) using the CLICK server, i.e., the topology-independent tool comparing 3D structures without a scoring function measuring structural similarity (Nguyen et al., 2011). The HuscFvs showing top-scored topological similarity with the RS2-1G9 antigen-binding site were selected. The 3D structure of 3O-C12-HSL was retrieved from the PubChem database, a resource of chemical molecules and their bioactivities (PubChem CID: 3246941) (Kim et al., 2015). The modeled-3O-C12-HSL F(ab')₂ was docked with the 3D model of each HuscFv receptor binding pocket using Autodock Vina software (Trott and Olson, 2010; Forli et al., 2016). The conformation of each HuscFv-ligand complex with the lowest binding free energy (ΔG) at the best docking position was selected for interaction analysis and visualization through the Discovery studio visualizer 3.5 program.

Large-Scale Production of HuscFvs

The *E. coli* clones carrying phagemids containing the DNA coding for the selected HuscFvs were subjected to sub-cloning for large scale HuscFv production. The *huscFvs* were PCR-amplified from the *huscFv*-pCANTAB5E phagemids of HB2151 *E. coli* clones using a Phusion High-Fidelity DNA polymerase (Thermo Fisher Scientific, Carlsbad, CA, United States). The PCR specific primers were forward-*huscFv*-LIC: 5'-GGTTGGGAATTGCAAGCGGC CCAGCCGGCC-3' and reverse-*E-tag*-LIC: 5'-GGAGATGGGA AGTCATTAACGCGGTTCCAGCGGATCC-3'. The *huscFv* inserts were designed to consist of a HuscFv-coding sequence linked to specific sequences for ligation independent cloning (LIC) protocol (Thermo Fisher Scientific). The amplified *huscFv-E-tag* DNAs were cloned separately into the pLATE52 vector (Thermo Fisher Scientific). Recombinant pLATE52-*huscFv* plasmids were transformed into JM109 *E. coli* by the heat-shock method. After PCR screening and DNA sequencing, the recombinant plasmids were introduced into an expression host, NiCo21(DE3) *E. coli* (New England Biolabs, St. Albans, Herts, United Kingdom), and the transformed bacteria were grown at 37°C for 16 h on LB agar containing 100 µg/ml of ampicillin. A single colony of each transformed clone was cultured in LB broth containing 100 µg/ml ampicillin with

shaking (250 rpm) at 37°C for 16 h. The overnight cultures (12.5 ml) were separately inoculated into the fresh LB medium (250 ml) containing ampicillin and grown at 37°C until an OD_{600 nm} reached ~0.6–0.8. Recombinant HuscFv expression was induced by adding isopropyl-β-D-1-thiogalactopyranoside (IPTG) to a final concentration of 1 mM and incubated at 30°C for 6 h. The bacterial pellets were collected by centrifugation at 5,000 × g at 4°C for 20 min.

The recombinant HuscFvs were purified from the bacterial inclusion bodies (IBs) as described previously (Jittavisutthikul et al., 2016). Two grams of *E. coli* wet cell pellets were resuspended in 10 ml of BugBuster™ protein extraction reagent (Novagen, Schwalbach, Germany) and 20 µl of Lysonase™ bioprocessing reagent (Novagen) were added to each preparation. The preparations were kept at 25°C on a rotator for 20 min and cell pellets were collected after centrifugation at 8,000 × g at 4°C for 30 min. The IBs were washed with Wash-100 reagent [50 mM sodium phosphate buffer, pH 8.0; 500 mM NaCl; 5 mM EDTA; 8% (w/v) glycerol; and 1% (v/v) Triton X-100] twice and once with Wash-114 buffer [50 mM Tris-HCl, pH 8.0; 300 mM NaCl; and 1% (v/v) Triton X-114] with shaking at high speed for 40 min, and the IB pellets were then collected. The IBs were then washed with Wash-Solvent solution [50 mM Tris-HCl, pH 8.0; and 60% (v/v) isopropanol] and sterile ultrapure distilled water on ice, also with vigorous shaking, and centrifuged. Thereafter, 2.5 mg of purified IB pellets were solubilized in 5 ml of solubilizing buffer [50 mM CAPS, pH 11.0; 0.3% (w/v) *N*-lauryl sarcosine; and 1 mM dithiothreitol (DTT)] and kept at 4°C for 16 h. After dissolving completely, the protein was loaded into Snakeskin dialysis tubing with a molecular weight cut-off of 10 kDa (Thermo Fisher Scientific), and dialyzed against 750 ml of refolding buffer (20 mM imidazole, pH 8.5, supplemented with 0.1 mM DTT) at 4°C with slow stirring. After 3 h, the buffer was changed to a fresh refolding buffer, and dialysis was continued for 16 h. The refolded protein was subsequently dialyzed against a dialysis buffer without DTT with slow stirring at 4°C for 16 h. Each preparation was filtered through a 0.2-µm low protein binding Acrodisc® Syringe Filter (Pall, Port Washington, NY, United States) and kept at 30°C in a water bath for 3 h before adding 60 mM trehalose. The protein concentration of the refolded HuscFvs was determined using Pierce® BCA Protein Assay, while the quality and purity of the recombinant proteins were analyzed by SDS-PAGE and stained with Coomassie Brilliant Blue G-250 (Bio-rad, Hercules, CA, United States). Refolded HuscFv preparations were concentrated using Amicon® Ultra 4 ml 3K centrifugal filter devices (Merck Millipore, Darmstadt, Germany) and stored at –20°C until use.

Circular Dichroism

The buffer of the HuscFv preparations was changed to 20 mM sodium phosphate buffer, pH 8.5, at a protein concentration of 0.1 mg/ml, and the antibodies were subjected to CD measurement. The data were recorded using a JASCO spectrometer (model J-815) equipped with a Peltier temperature controller system (Jasco, Tokyo, Japan) in a 1 mm path-length quartz cuvette. The proteins were scanned at 50 nm/min

at 25°C. The CD spectra were collected over a wavelength range of 190–260 nm.

Cell Line

Human cervical carcinoma, HeLa, cells were cultured in Dulbecco's Modified Eagle's Medium (DMEM; Gibco, Carlsbad, CA, United States) supplemented with 10% (v/v) fetal bovine serum (Hyclone, Novato, CA, United States) and 1% (v/v) penicillin-streptomycin (complete DMEM) at 37°C in a 5% CO₂ atmosphere.

Determination of the Biocompatibility of the HuscFvs to Mammalian Cells

The monolayer of HeLa cells established in individual wells of a 24-well tissue culture plate ($\sim 2 \times 10^5$ cells/well) were washed with sterile PBS, added with 2 μ M of individual HuscFv preparations in complete DMEM, and incubated at 37°C in 5% CO₂ atmosphere for 24 h. Cells in the medium alone served as a background control. After 24 h, the percent viability of cells of each treatment was analyzed using an FITC-Annexin V Apoptosis Detection Kit (BD Biosciences, San Jose, CA, United States) according to the manufacturer's protocols. The cells were washed with Dulbecco's phosphate-buffered saline (DPBS) and resuspended in binding buffer. Five microliters of Annexin V-FITC conjugate and 5 μ l of propidium iodide (PI) were added. After 15-min incubation at room temperature (25°C) in darkness, apoptotic cells were enumerated by flow cytometric analysis (BD LSRFortessa™, San Jose, CA, United States) using BD FACSDiva™ software (BD Biosciences). At least 20,000 events of single cells per sample were collected.

Cellular Apoptosis Mediated by 3O-C12-HSL

HeLa cells ($\sim 2 \times 10^5$ cells/well) were treated with various concentrations of 3O-C12-HSL, i.e., 10, 25, 50, 75, and 100 μ M. The background control comprised of cells incubated with medium alone. After incubation at 37°C in a CO₂ incubator for 18 h, the cells were harvested and subjected to Annexin V/PI binding assay, as described above.

Neutralization of 3O-C12-HSL-mediated-Cytotoxicity by HuscFvs

Fifty micromolars of 3O-C12-HSL in 0.25% DMSO were mixed with various concentrations of individual HuscFv preparations (0.25, 0.5, 1.0, and 1.2 μ M) for 1 h before adding to HeLa cells ($\sim 2 \times 10^5$ cells/well) and incubated at 37°C in a CO₂ incubator for 18 h. After incubation, the cells were collected, washed, double-stained with Annexin V-FITC and PI, and analyzed by flow cytometry, as described above. Three independent experiments were performed.

Neutralization of 3O-C12-HSL-mediated Cell Cycle Arrest by HuscFvs

HeLa cells ($\sim 2 \times 10^5$ cells/well) were treated with a mixture of 50 μ M 3O-C12-HSL and 1 μ M of individual HuscFvs for

18 h. HeLa cells exposed to medium alone served as a control. After incubation, cells were washed with ice-cold PBS, fixed in 70% ethanol, and kept at –20°C overnight. Cells were then washed 3 times with ice-cold PBS and incubated in 500 μ l of stain solution [10 μ g/ml PI, 100 μ g/ml RNase, and 0.1% (v/v) Triton X-100 in DPBS, pH 7.4] at room temperature in darkness for 30 min. The DNA contents of the cells were measured, and cell cycle histograms/distributions were generated. Then, the percentage of cells in the sub-G1 phase was determined by flow cytometry (BD LSRFortessa™) using BD FACSDiva™ software (BD Biosciences), with at least 10,000 recorded events per sample.

Analysis of Nuclear Damage by Fluorescence Staining

Nuclear damage was studied using 4',6-diamidino-2-phenylindole (DAPI) staining. Briefly, HeLa cells (1×10^6 cells) were seeded on a 22 \times 22 mm square coverslip (Menzel-Glaser, Braunschweig, Germany) in a 6-well plate (Costar, New York, NY, United States) and kept at 37°C in a 5% CO₂ incubator for 24 h. The culture medium was removed and the cells were replenished with complete DMEM containing a mixture of 3O-C12-HSL (50 μ M) and HuscFvs (2 μ M). After 18 h, the cells were washed and fixed with 4% (v/v) paraformaldehyde in PBS, permeabilized with 1% (v/v) Triton X-100 in PBS, blocked with 3% (w/v) bovine serum albumin (BSA) in PBS at room temperature for 30 min, then washed. The permeabilized cells were stained and mounted with DAPI (1:5,000) (Molecular Probes, Carlsbad, CA, United States) in the anti-fade mounting medium. DNA fragmentation and chromatin condensation were observed under a confocal microscope (Carl Zeiss Laser Scanning System LSM 700, Jena, Germany). Images were processed using the Zeiss LSM Image Browser (version 6.0.0.309).

Transmission Electron Microscopy

Transmission electron microscopy (TEM) was used to examine the ultrastructural changes of the HeLa cell mitochondria after various treatments. The cells from each treatment group were fixed with 2.5% (v/v) glutaraldehyde in 0.1 M sucrose phosphate buffer (SPB) at room temperature for 1 h, washed three times with 0.1 M SPB, post-fixed with 1.0% (w/v) osmium tetroxide in the same buffer for 1 h, and dehydrated with a graded series of ethanol. The dehydrated cells were infiltrated with pure LR white embedded medium (EMS®, Hatfield, PA, United States) in 70% (v/v) ethanol, embedded in a capsule beam, and incubated at 65°C for 48 h. The ultrathin (100 nm) sections of the cells were prepared; the sections were positioned on a 200 square-mesh copper grid and stained with ethanolic uranyl acetate and lead citrate. The morphological and structural characteristics of mitochondria were observed under a transmission electron microscope (model HT7700, Hitachi, Tokyo, Japan).

Statistical Analysis

Statistical analyses of all experiments were performed using GraphPad Prism 5 software (La Jolla, CA, United States). One-way ANOVA followed by Tukey's *post hoc* multiple comparison tests were used to analyze the differences between groups. All data

are shown as mean \pm SD. Statistically significant difference was set at $p < 0.05$.

RESULTS

HuscFvs to 3O-C12-HSL

The refined models of HuscFvs for the selected HB2151 *E. coli* clones derived from phage biopanning with *P. aeruginosa* exotoxin A revealed that HuscFvs of three *E. coli* clones, i.e., E44 (HuscFv-E44), F15 (HuscFv-F15), and F19 (HuscFv-F19), showed reliable Ramachandran plots. The percent residues in the most favored regions, the additional allowed regions, the generously allowed regions, and the disallowed regions of the Ramachandran diagrams of the HuscFv-E44, HuscFv-F15, and HuscFv-F19 were 90.1, 6.8, 1.0, and 2.1 %; 91.3, 7.7, 0.5, and 0.5%; and 88.2, 9.4, 1.0, and 1.5%, respectively (Supplementary Figure S1).

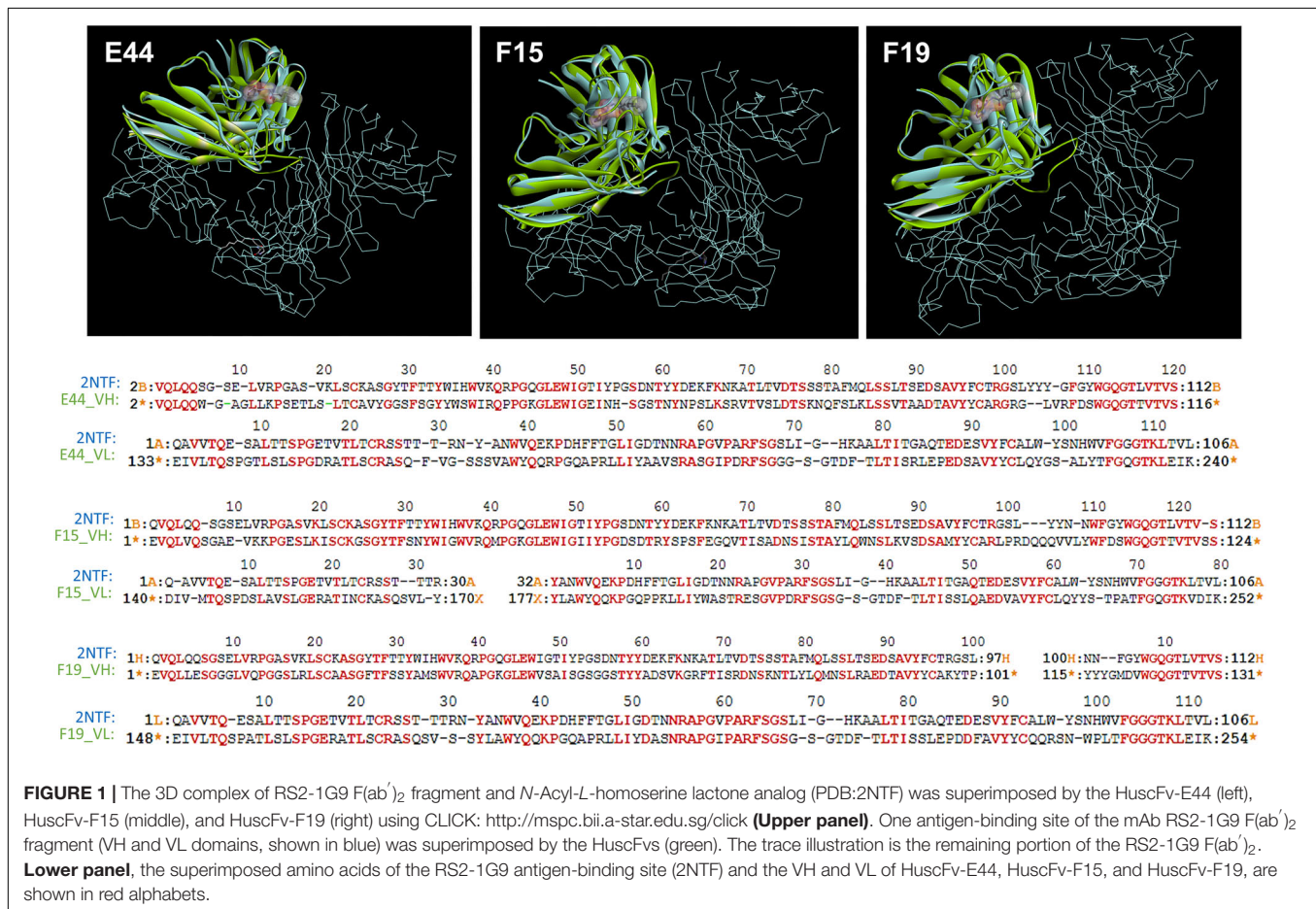
From structural comparisons of individual HuscFvs with the antigen-binding site of the well-characterized quorum quenching mAb, i.e., RS2-1G9 (shown previously to bind to and neutralize the activities of *P. aeruginosa* 3O-C12-HSL), it was found that the binding pockets of the three HuscFvs were superimposed with the antigen-binding site of RS2-1G9. The

coverage percentages of the overlapping structures between the modeled HuscFv-E44, HuscFv-F15, and HuscFv-F19 and the RS2-1G9 were 90.83, 89.29, and 88.58%, respectively (Figure 1 and Supplementary Table S1).

Homology Modeling and Intermolecular Docking Between HuscFvs and 3O-C12-HSL

In silico intermolecular docking was performed to investigate the interaction of the HuscFvs with the 3O-C12-HSL. The residues of HuscFv-E44, HuscFv-F15, and HuscFv-F19 that tentatively formed interactive bonds with the haptenic 3O-C12-HSL target are shown in Figure 2 and Table 1. The Gibbs free energy (ΔG) of the representative complexes of respective HuscFvs with the ligand were -5.6 , -5.8 , and -5.4 kcal/mol, respectively.

The HuscFv-E44 used residues from VH-CDR2 and VL-CDR3, as well as help from VH-FR2, VH-FR3, VL-FR1, and VL-FR4 to form contact interfaces with the functional groups of 3O-C12-HSL. The interactions were three hydrogen bonds between L45 of VH-FR2 with the NH group of the coordinated 3O-C12-HSL (2.18 Å) and N60 of VH-CDR2, and W47 of VH-FR2 with the 3O-C12-HSL carbonyl oxygen of 3-oxo-group of the acyl chain (2.97 and 2.44 Å, respectively). There was one



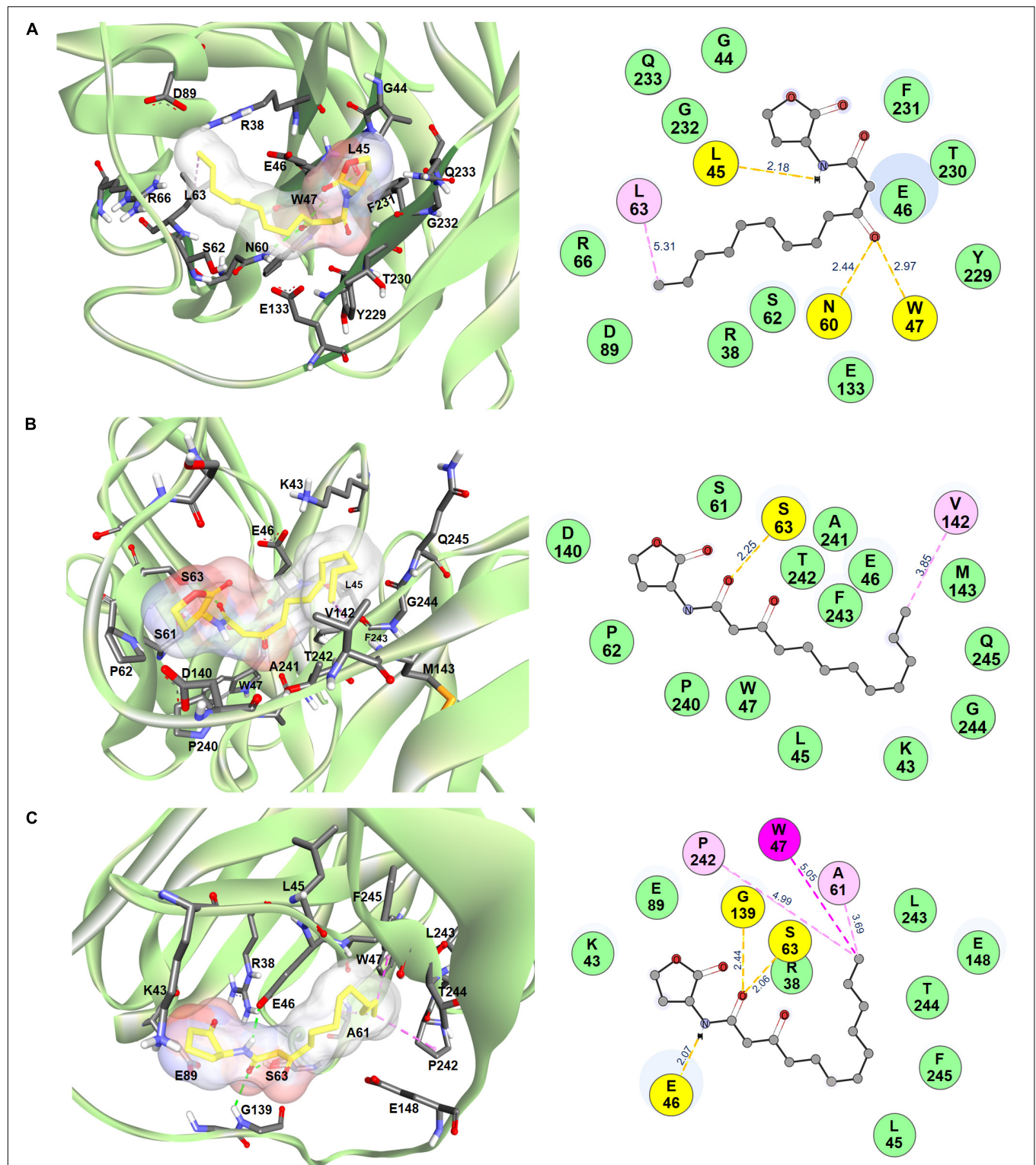


FIGURE 2 | Computerized contact interfaces between 3O-C12-HSL and HuscFvs. **(A–C)** on the left side of the panels show interaction between 3D structures of 3O-C12-HSL (yellow stick) and green ribbons of **(A)** HuscFv-E44, **(B)** HuscFv-F15, **(C)** HuscFv-F19. Right side of the panels **(A–C)** show residues of the respective HuscFvs and the HuscFv-3O-C12-HSL interactive bonds (yellow, hydrogen bond; light pink, alkyl; magenta, Pi-alkyl; green, van der Waals force).

TABLE 1 | Residues of *Pseudomonas aeruginosa* 3O-C12-HSL predicted to form contact interfaces with the effective HuscFv-E44, HuscFv-F15, and HuscFv-F19.

3O-C12-HSL position	HuscFv-E44		Interactive bond
	Residue (s)	Domain	
Ketone group of HSL ring	E46	VH-FR2	Van de Waals
C3 of HSL ring	G44	VH-FR2	Van de Waals
	G232	VL-FR4	Van de Waals
C4 of HSL ring	G44	VH-FR2	Van de Waals
NH-group	L45	VH-FR2	Hydrogen
	E46	VH-FR2	Van de Waals
	F231	VL-FR4	Van de Waals
1-oxo-group	T230	VL-CDR3	Van de Waals
	F231	VL-FR4	Van de Waals
C2 of acyl chain	E46	VH-FR2	Van de Waals
	T230	VL-CDR3	Van de Waals
3-oxo-group	W47	VH-FR2	Hydrogen
	N60	VH-CDR2	Hydrogen
	E46	VH-FR2	Van de Waals
	Y229	VL-CDR3	Van de Waals
C5 of acyl chain	E133	VL-FR1	Van de Waals
C9 of acyl chain	S62	VH-CDR2	Van de Waals
C10, C11 of acyl chain	R38	VH-FR2	Van de Waals
	R66	VH-FR3	Van de Waals
C12 of acyl side chain	L63	VH-CDR2	Hydrophobic (alkyl)
C12 of acyl side chain	R38	VH-FR2	Van de Waals
	R66	VH-FR3	Van de Waals
	N89	VH-FR3	Van de Waals

3O-C12-HSL position	HuscFv-F15		Interactive bond
	Residue(s)	Domain	
C3 of HSL ring	P62	VH-CDR2	Van de Waals
C3, C4 of HSL ring	D140	VL-FR1	Van de Waals
1-oxo-group	W47	VH-FR2	Van de Waals
	S61	VH-CDR2	Van de Waals
	S63	VH-CDR2	Hydrogen
C2 of acyl chain	W47/A241	VH-FR2	Van de Waals
3-oxo-group	P240/A241/T242	VL-CDR3	Van de Waals
	W47	VH-FR2	Van de Waals
	A241	VL-CDR3	Van de Waals
C4 of acyl chain	W4	VH-FR2	Van de Waals
	F243	VL-FR4	Van de Waals
	A241/T242	VL-CDR3	Van de Waals
C5 of acyl chain	E46, W47	VH-FR2	Van de Waals
	F243	VL-FR4	Van de Waals
C6 of acyl chain	F243	VL-FR4	Van de Waals
C7 of acyl chain	L45, E46	VH-FR2	Van de Waals
	F243	VL-FR4	Van de Waals
C8 of acyl chain	K43, E46	VH-FR2	Van de Waals
C9 of acyl chain	K43	VH-FR2	Van de Waals
C10 of acyl chain	F243/G244/Q245	VL-FR4	Van de Waals
	F243/G244/Q245	VL-FR4	Van de Waals
C12 of acyl chain	V142	VL-FR1	Hydrophobic (alkyl)
	M143	VL-FR1	Van de Waals
	T242	VL-CDR3	Van de Waals
	F243	VL-FR4	Van de Waals

(Continued)

TABLE 1 | Continued

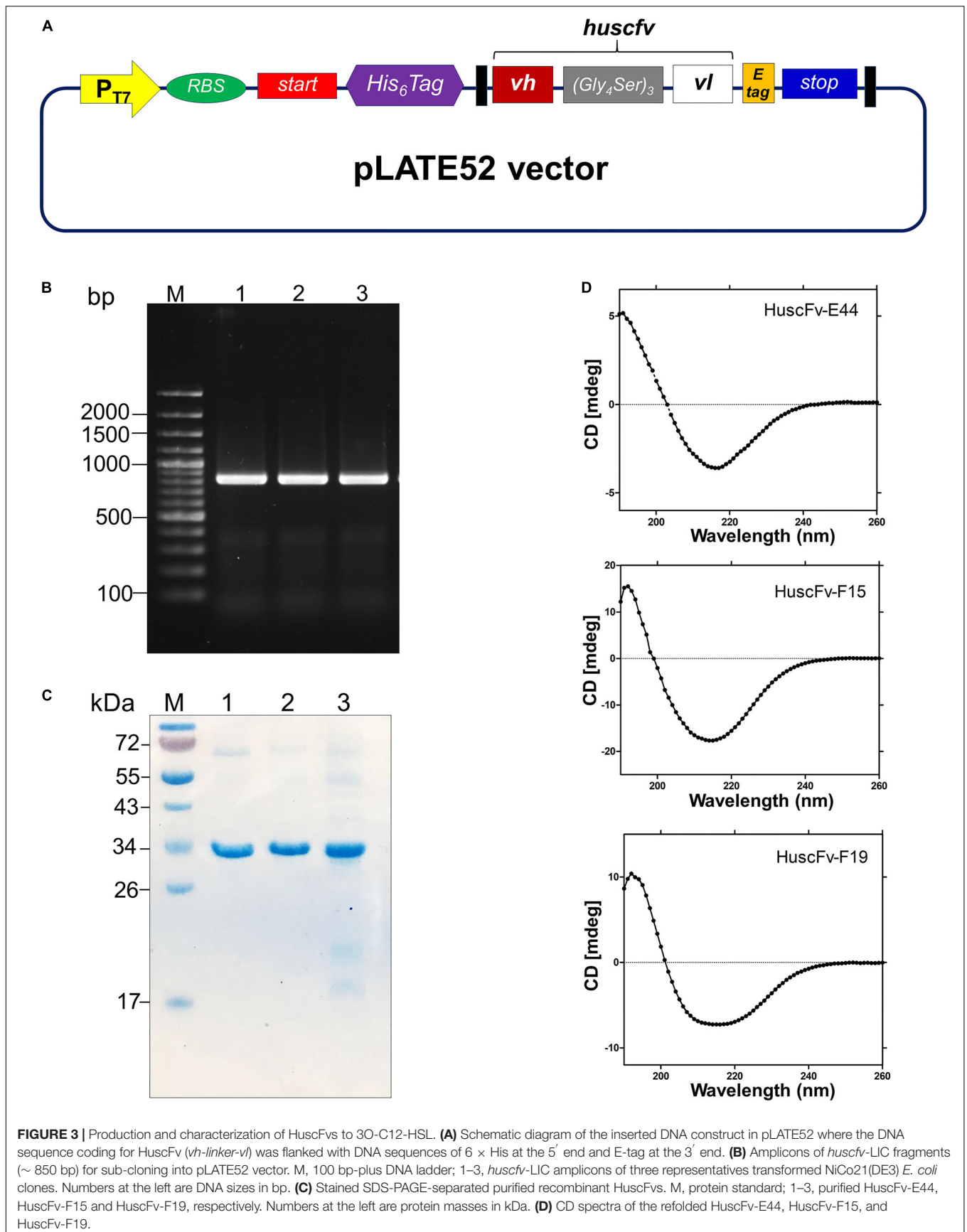
3O-C12-HSL position	HuscFv-F19		Interactive bond
	Residue(s)	Domain	
Ketone group of HSL ring	R38	VH-FR2	Van de Waals
	E89	VH-FR3	Van de Waals
C3, C4 of HSL ring	K43	VH-FR2	Van de Waals
Oxygen of HSL ring	E89	VH-FR3	Van de Waals
NH-group	R38, E46	VH-FR2	Hydrogen
	R38	VH-FR2	Van de Waals
	S63	VH-CDR2	Hydrogen
1-oxo-group	G139	Linker	Hydrogen
	R38	VH-FR2	Van de Waals
	L45	VH-FR2	Van de Waals
C2 of acyl side chain	F245	VL-FR4	Van de Waals
C7, C8 of acyl chain	T244	VL-CDR3	Van de Waals
	F245	VL-FR4	Van de Waals
C9 of acyl side chain	E148	VL-FR1	Van de Waals
C10 of acyl chain	L243	VL-CDR3	Van de Waals
C11 of acyl chain	W47	VH-FR2	Hydrophobic (π -alkyl)
	A61	VH-CDR2	Hydrophobic (alkyl)
	P242	VL-CDR3	Hydrophobic (alkyl)

hydrophobic interaction (alkyl) formed between L63 of VH-CDR2 and C12 of the acyl chain of AHL. HuscFv-E44 also used many residues in different domains to form contact interfaces via van der Waals forces with the 3O-C12-HSL, including S62 of VH-CDR2; Y229 and T230 of VL-CDR3; R38, G44, and E46 of VH-FR2; R66 and D89 of VH-FR3; E133 of VL-FR1; and F231, G232, and Q233 of VL-FR4 (Table 1).

HuscFv-F15 formed a hydrogen bond (2.25 Å) with the carbonyl oxygen of the 1-oxo-group of the fatty acid-like ligand through S63 of VH-CDR2. This antibody also used V142 of VL-FR1 to form hydrophobic contact (alkyl) with the C12 of the hapten acyl chain. Several other positions of the 3O-C12-HSL molecule have interacted via van der Waals forces with several residues of the HuscFv-F15 including S61 and P62 of VH-CDR2; P240, A241, and T242 of VL-CDR3; K43, L45, E46, and W47 of VH-FR2; D140 and M143 of VL-FR1; and F243, G244, and Q245 of VL-FR4.

Serine 63 of VH-CDR2 and G139 of the HuscFv-F19 linker formed contact with the carbonyl oxygen of the 1-oxo-group of the 3O-C12-HSL via hydrogen bonds (2.06 and 2.44 Å, respectively). Hydrogen bonding also occurred between E46 of VH-FR2 and the NH-group of the HSL backbone (2.07 Å). The last carbon atom of the long acyl side chain of the 3O-C12-HSL formed π -alkyl hydrophobic interaction with W47 of VH-FR2 as well as the alkyl hydrophobic interaction with A61 of VH-CDR2 and P242 of VL-CDR3. In addition, the HuscFv-F19 formed van der Waals contacts with the 3O-C12-HSL by using L243 and T244 of VL-CDR3; R38, K43, and L45 of VH-FR2; E89 of VH-FR3; E148 of VL-FR1; and F245 of VL-FR4.

The results of the structural comparison of the HuscFvs with the quorum quenching mAb, RS2-1G9, and the intermolecular docking between the HuscFvs and the 3O-C12-HSL enticed us



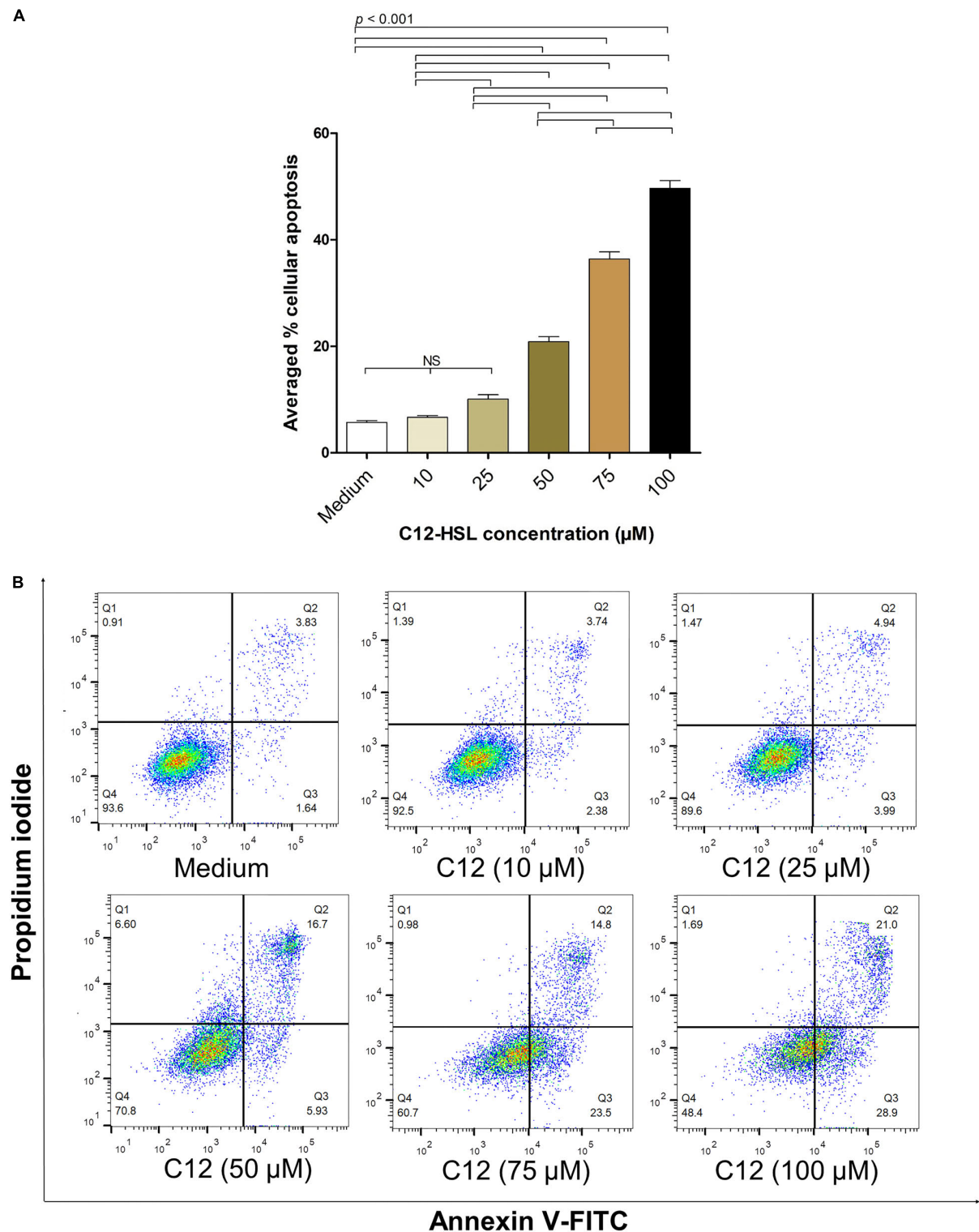


FIGURE 4 | The percentages of apoptotic HeLa cells exposed to different concentrations of 3O-C12-HSL. **(A)** Bar graph of average percentages (means \pm SD) of apoptotic cells from three independent experiments after exposure to 10, 25, 50, 75, and 100 μ M of C12-HSL, compared with the cells in medium alone. **(B)** The density plots of HeLa cells after treatment with 10, 25, 50, 75, and 100 μ M of C12-HSL, and control cells stained by Annexin V-FITC/PI and subjected to flow cytometric analysis (representative of three independent experiments). The cytotoxic activity of the 3O-C12-HSL was dose-dependent. Q1, necrotic cells (Annexin V negative/PI positive); Q2, late apoptotic cells (Annexin V positive/PI positive); Q3, early-apoptotic cells (Annexin V positive/PI negative), and Q4, viable cells (Annexin V negative/PI negative).

to test further the ability of HuscFvs to neutralize *P. aeruginosa* 3O-C12-HSL activities.

Large-Scale Production of HuscFvs

The *huscfv* inserts in the pCANTAB5E phagemids of the *E. coli* clones E44, F15, and F19 were sub-cloned into the pLATE52 vector. The DNA construct in the vector is shown in **Figure 3A**. The amplicon of DNA coding for 6 × His tagged-HuscFv formed a PCR amplicon band at ~ 850 bp, as revealed on agarose gel (**Figure 3B**). The refolded and purified HuscFv-E44, HuscFv-F15, and HuscFv-F19, with molecular sizes of about 34 kDa, are shown in **Figure 3C**.

Secondary structures of the refolded HuscFvs were determined by far-UV CD spectroscopy. The far-UV CD spectra (190–260 nm) for all HuscFvs revealed their β -sheet structures, which shared a similar CD spectra pattern (**Figure 3D**). The antibody preparations did not form aggregates.

Biocompatibility of HuscFvs to Mammalian Cells

HeLa cells exposed to 2 μ M of HuscFv-E44, HuscFv-F15, and HuscFv-F19 for 24 h showed more than 90% viability, which was not different from the cells in medium alone ($p > 0.05$) (**Supplementary Figure S2**) indicating biocompatibility of the HuscFvs to the representative mammalian cells.

HuscFvs-bound 3O-C12-HSL Had Impairment in Inducing Mammalian Cell Apoptosis

The average percentages of apoptotic HeLa cells treated with 10, 25, 50, 75, and 100 μ M of 3O-C12-HSL dissolved in 0.25% DMSO, from three independent experiments, were 6.67 ± 0.53 , 10.08 ± 1.41 , 20.85 ± 1.62 , 36.37 ± 2.32 , and $49.63 \pm 2.51\%$, respectively, while the background apoptotic cells of the control (cells in culture medium) was $5.71 \pm 0.59\%$ (**Figure 4A**). **Figure 4B** shows the results of the flow cytometric analysis of apoptotic cells (stained with Annexin V/PI) from one representative experiment. The background apoptotic cells (% cell viability) with and without 0.25% DMSO in the culture medium were not different (**Supplementary Figure S3**).

The percentages of apoptotic HeLa cells exposed to 50 μ M of HuscFv-bound 3O-C12-HSL (0.25, 0.5, 1.0, and 1.2 μ M of individual HuscFvs) were significantly decreased compared with those without HuscFvs (**Table 2** and **Figure 5**). The HuscFvs of all three *E. coli* clones could neutralize 3O-C12-HSL, leading to reduced HeLa-cell apoptosis.

HuscFv-bound-C12-HSL Had Reduced Ability to Induce sub-G1 Arrest of HeLa Cells

Exposure of HeLa cells with 50 μ M 3O-C12-HSL for 18 h resulted in $3.79 \pm 0.52\%$ of apoptotic cells in the hypodiploid DNA peak (sub-G1 population, which were apoptotic cells) as determined by flow cytometric analysis of the PI-stained cellular DNA. The numbers of cells with a hypodiploid DNA peak induced

TABLE 2 | Flow cytometric results evaluating the efficacy of HuscFvs using Annexin V-FITC/PI staining for 3O-C12-HSL-mediated cell apoptosis.

HeLa cells treated with	Percent cellular apoptosis	Percent cellular survival
Medium alone	6.77 ± 0.20	92.50 ± 0.28
3O-C12-HSL (50 μ M)	21.05 ± 2.23	72.15 ± 1.91
3O-C12-HSL + HuscFv-E44 (0.25 μ M)	15.03 ± 0.49	83.57 ± 0.50
3O-C12-HSL + HuscFv-E44 (0.5 μ M)	13.31 ± 0.12	85.33 ± 0.25
3O-C12-HSL + HuscFv-E44 (1.0 μ M)	12.99 ± 0.41	86.10 ± 0.35
3O-C12-HSL + HuscFv-E44 (1.2 μ M)	11.74 ± 0.66	87.30 ± 0.70
3O-C12-HSL + HuscFv-F15 (0.25 μ M)	16.04 ± 1.06	82.07 ± 1.20
3O-C12-HSL + HuscFv-F15 (0.5 μ M)	12.31 ± 0.49	85.97 ± 0.50
3O-C12-HSL + HuscFv-F15 (1.0 μ M)	12.88 ± 0.75	86.27 ± 0.75
3O-C12-HSL + HuscFv-F15 (1.2 μ M)	12.88 ± 0.48	85.53 ± 0.47
3O-C12-HSL + HuscFv-F19 (0.25 μ M)	13.53 ± 0.46	84.27 ± 0.49
3O-C12-HSL + HuscFv-F19 (0.5 μ M)	12.93 ± 0.18	85.80 ± 0.17
3O-C12-HSL + HuscFv-F19 (1.0 μ M)	10.71 ± 0.60	88.67 ± 0.64
3O-C12-HSL + HuscFv-F19 (1.2 μ M)	10.63 ± 0.91	88.60 ± 0.87

by the 3O-C12-HSL bound by the HuscFv-E44, HuscFv-F15, and HuscFv-F19, were decreased to 2.58 ± 0.10 , 2.71 ± 0.10 , and $1.79 \pm 0.11\%$, respectively. The cells in medium alone had $1.04 \pm 0.04\%$ apoptotic cells (**Figure 6**). The results of the sub-G0/G1 analysis were conformed to those of the Annexin V/PI binding assay data.

Degrees of Nuclear Damage Mediated by HuscFv-bound 3O-C12-HSL

DAPI staining and confocal microscopy were used to observe the intact HeLa nuclei and nuclear DNA damage induced by the 3O-C12-HSL and the HuscFv-bound 3O-C12-HSL (**Figure 7**). Intact nuclei of normal HeLa cells were stained weakly by the dye (**Figure 7A**), while the fragmented nuclei of the 3O-C12-HSL-exposed cells were stained brightly (**Figure 7B**). Damage to the nuclear DNA was reduced in cells exposed to HuscFv-F19-bound 3O-C12-HSL, as shown by the dimly stained nuclei (**Figure 7C**).

Mitigation of the 3O-C12-HSL Induced-mitochondrial Injuries by HuscFvs

Transmission electron microscopy was used to study mitochondrial changes of the HeLa cells after exposure to the 3O-C12-HSL and HuscFv-bound 3O-C12-HSL, using the cells in medium alone as a normal control. As shown in **Figures 8A,B**, the mitochondria of the normal cells revealed an intact mitochondrial subcellular structure. In contrast, mitochondria of the cells treated with 50 μ M of 3O-C12-HSL for 18 h exhibited a swollen appearance, with single or multiple distensions of the intercellular matrix in association with severe loss of cristae and double membranes (**Figures 8C,D**). The pathological changes of the mitochondria were ameliorated in the cells exposed to HuscFv-F19-bound 3O-C12-HSL (representative), i.e., mild mitochondrial swelling and more cristae (**Figures 8E,F**), compared with the 3O-C12-HSL-exposed cells.

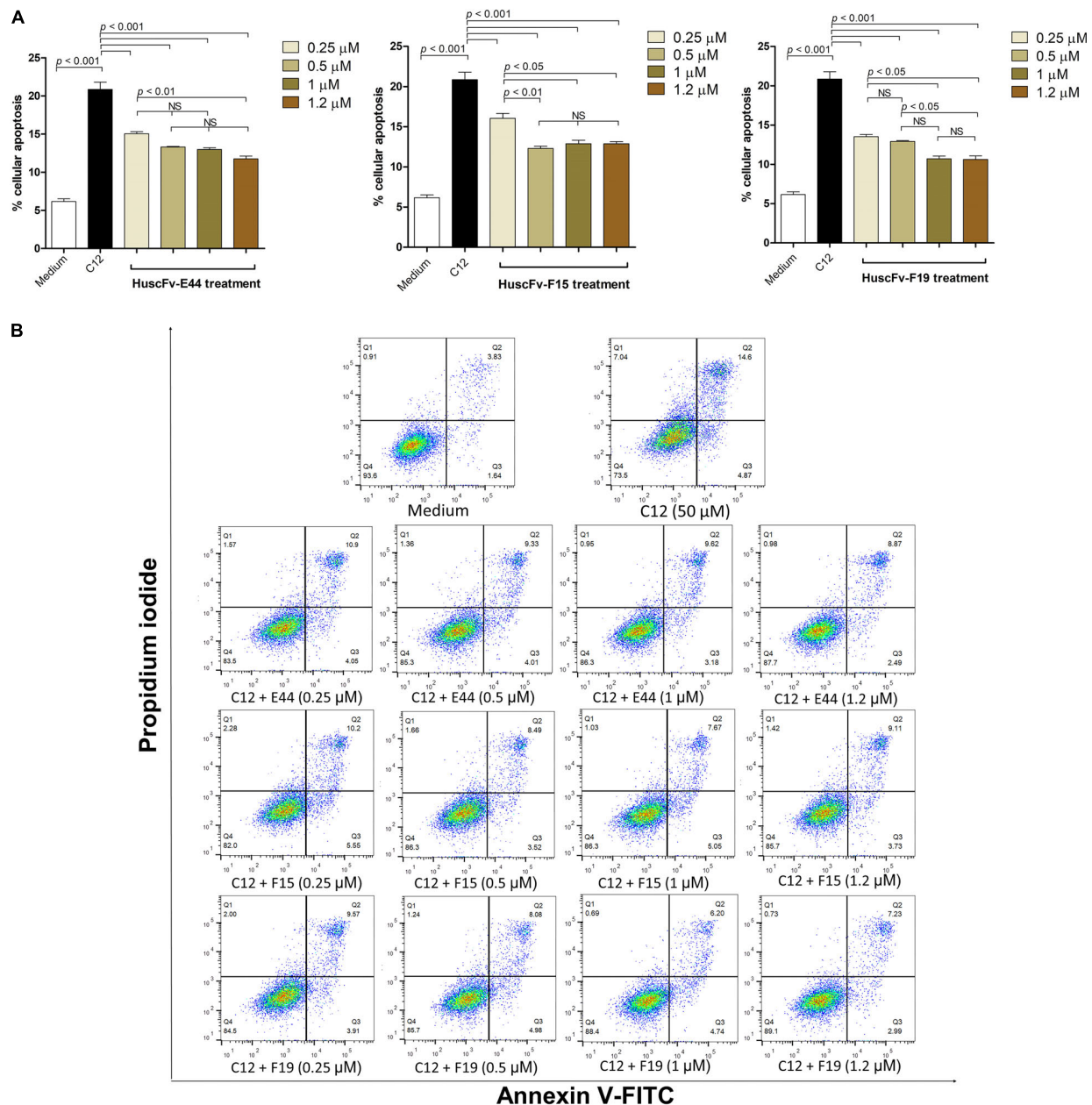


FIGURE 5 | HuscFvs rescue HeLa cells from 3O-C12-HSL-mediated apoptosis. **(A)** The percentages of apoptotic cells of different treatment conditions, i.e., HeLa cells in medium alone, cells exposed to 50 μ M 3O-C12-HSL (C12), cells added with 3O-C12-HSL mixed with various amounts of HuscFvs. **(B)** Density plots of flow cytometric analysis of doubly stained HeLa cells as in **(A)** (representative of one of the three reproducible experiments). The percent apoptotic cells caused by the 3O-C12-HSL was reduced significantly in the presence of HuscFvs.

DISCUSSION

Pseudomonas aeruginosa 3O-C12-HSL not only regulates virulence factors of the bacteria, but also causes inflammation in the infecting host by the induction of pro-inflammatory cytokine and chemokine synthesis (Smith et al., 2002). The 3O-C12-HSL killed mammalian cells through programmed cell death, i.e., an apoptotic mechanism at concentrations ranging from 10 to 100 μ M by rapidly triggering depolarization of

mitochondrial membrane potential and release of cytochrome *c* into cytosol, which activates the caspase cascades (Sultan and Sokolove, 2001; Tateda et al., 2003; Kravchenko et al., 2006; Schwarzer et al., 2012; Tao et al., 2016, 2018). The apoptotic cells manifest mitochondrial permeability transition (MPT), caspase activation, nuclear fragmentation, phosphatidylserine externalization, and cell shrinkage with apoptotic bodies (Wyllie et al., 1980; Cummings and Schnellmann, 2004). Mitochondrial swelling, depolarization, and membrane permeability are the

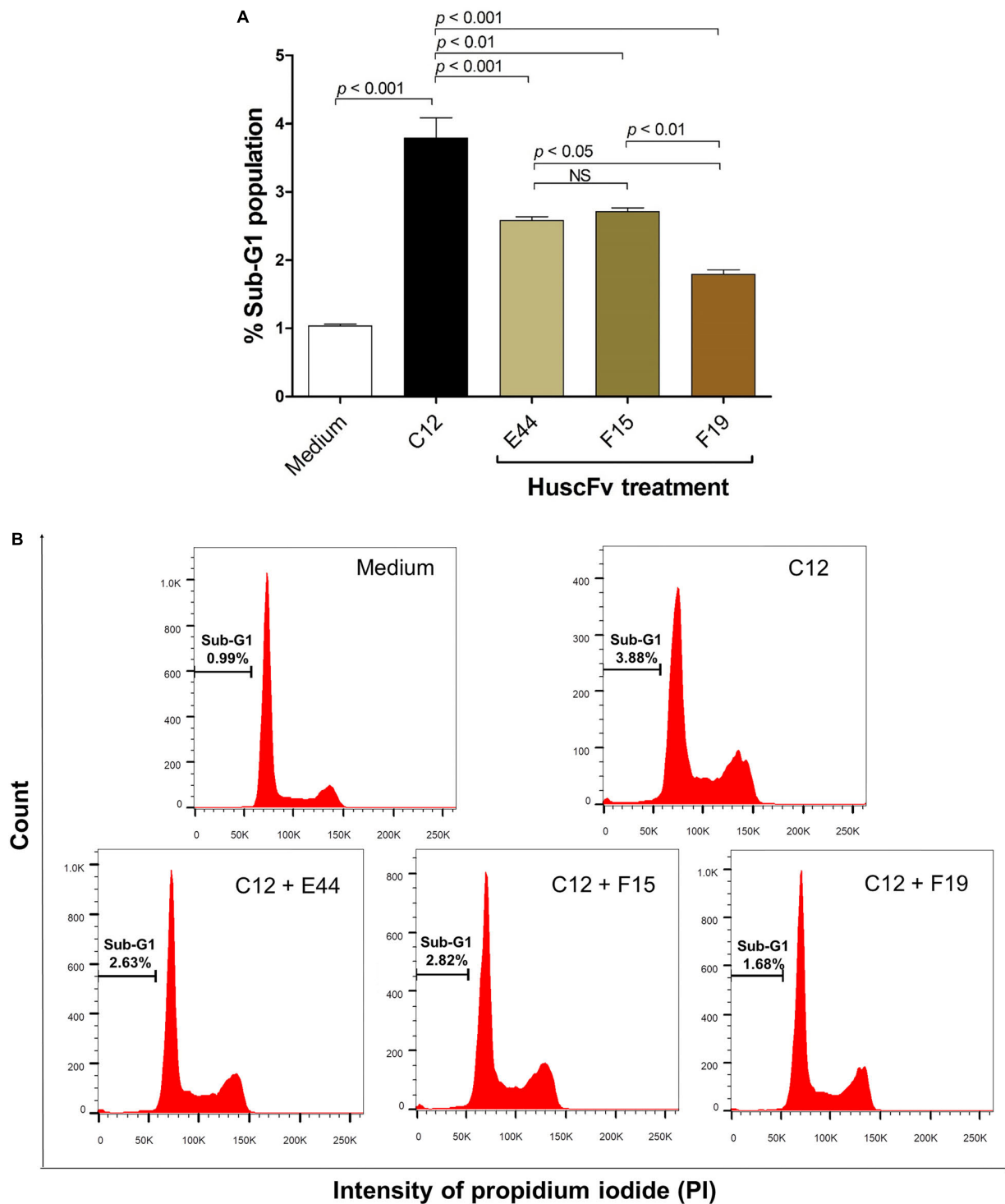


FIGURE 6 | Reduction of sub-G1 arrest population of 3O-C12-HSL-exposed cells by HuscFvs. **(A)** Percent sub-G1 population (mean \pm SD of triplicate individual experiments) after different treatments. **(B)** Histograms of cell cycle distribution. The percentage of apoptotic cells in the hypodiploid DNA peak (sub-G1 population) of each treatment is indicated in each plot.

key markers of the MPT that indicates mitochondria-stimulated programmed cell death in the pathogenesis of several diseases. Upon response to external stimuli or oxidative stress, the

cells undergo continuous opening of permeability transition pores (PTP) in the mitochondrial inner membrane, which augments colloidal osmotic pressure in the matrix together

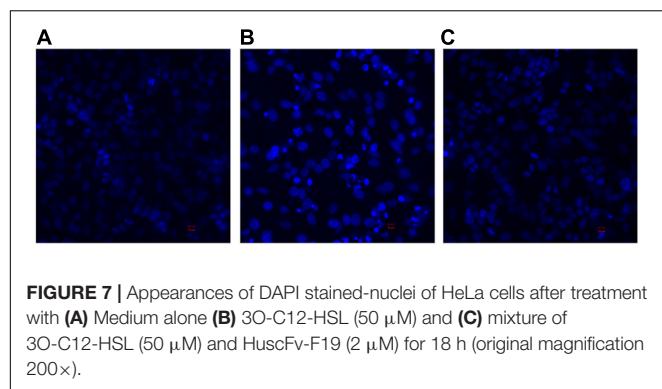


FIGURE 7 | Appearances of DAPI stained-nuclei of HeLa cells after treatment with (A) Medium alone (B) 3O-C12-HSL (50 μ M) and (C) mixture of 3O-C12-HSL (50 μ M) and HuscFv-F19 (2 μ M) for 18 h (original magnification 200 \times).

with mitochondrial membrane depolarization, resulting in mitochondrial swelling (Chapa-Dubocq et al., 2018) followed by rupture of the mitochondrial outer membrane and release of cytochrome *c* into the cytosol and activation of caspase cascades (Petronilli et al., 2001). The stimulated caspase-3 activates endogenous endonuclease, which cleaves nuclear DNA (Zhang and Ming, 2000). Cells with apoptotic fragmented DNA or sub-G1 population are used as a marker of apoptosis (Riccardi and Nicoletti, 2006). In this study, 3O-C12-HSL produced a significant dose-dependent increment in mammalian cell death by inducing apoptosis, which validates previous notions on the cytotoxicity of *P. aeruginosa* QS substance.

Deletion of *lasI* or *lasI* and *rhlI* diminished the lung-colonization ability of *P. aeruginosa* in a mouse model of acute pneumonitis (Smith et al., 2002). *P. aeruginosa* mutants with defective QS are known to have less virulence and be more susceptible to antibiotic treatments and host immunity than the respective wild-type (Hentzer et al., 2003). As such, *P. aeruginosa* QS systems are attractive targets for direct-acting therapeutic agents, of which the expected treatment consequences are mitigation of the severity of the bacteria-associated diseases (Penesyan et al., 2015). During the past decades, several groups of *P. aeruginosa* QS inhibitors/modulators have been identified: small chemical molecules, i.e., AHL analogs (phenylpropionyl homoserine lactones and phenyloxycetyl homoserine lactones of the *N*-aryl homoserine lactone library) (Geske et al., 2008), *N*-acyl cyclopentylamides (Ishida et al., 2007), halogenated furanone compound (Hentzer et al., 2002), other furanone derivatives (Kim et al., 2008), aspirin (El-Mowafy et al., 2014), and itaconimides and citraconimides (Fong et al., 2018); and natural inhibitors, such as secondary metabolites of the Australian marine macroalgae, *Delisea pulchra* (Givskov et al., 1996), patulin and penicillic acid from extracts of *Penicillium* species (Rasmussen et al., 2005), an organosulfur compound found in garlic extracts, named Ajoene (Jakobsen et al., 2012), and derivatives of ellagic acid (dilactone of hexahydroxydiphenic acid) from black or chebulic myrobalan, *Terminalia chebula* Retz (Sarabhai et al., 2013). Unfortunately, these compounds are relatively toxic to mammalian cells, which limits their therapeutic use (Ni et al., 2009). Recently, natural plant-derived compounds, *trans*-cinnamaldehyde (CA), and salicylic acid (SA) have been shown to effectively downregulate both *las* and *rhl*

QS systems, reduce the production of extracellular virulence factors, i.e., protease, elastase, and pyocyanin, and reduce biofilm formation, concomitantly with repressed rhamnolipid gene expression (Ahmed et al., 2019). However, the sole use of QS inhibitors at high concentrations to eradicate bacterial infection completely is of legitimate concern due to potential toxicity (Shreaz et al., 2016).

Passive immunization has been used as an intervention for post-exposure morbidity and/or treatment of diseases since the late 18th century (Keller and Stiehm, 2000). An antibody molecule uses multiple amino acid residues in several CDRs (sometimes with the help of FRs) to form multiple non-covalent bonds with the target molecule, thus, making it difficult for pathogens to create antibody escape mutants, compared with small molecular drugs/inhibitors, from which resistant variants emerge rather easily and frequently. Therapeutic antibodies may be in the form of intact molecules (two antigen-binding sites with Fc fragment- when the bioactivities of the Fc are required for effectiveness) or merely smaller antibody fragments, i.e., F(ab')₂, Fab, scFv, or single domain (VH, V_HH) with higher tissue penetrating ability than the intact four-chain counterpart when the Fc is dispensable. For *P. aeruginosa* infection, specific murine mAb, RS2-1G9, directed toward bacterial 3O-C12-HSL has been generated for use as an immunotherapeutic agent (Kaufmann et al., 2006, 2008). This murine antibody displayed the cytoprotective effect of 3O-C12-HSL-exposed host cells (Kaufmann et al., 2006, 2008; Debler et al., 2007). In addition, sheep-mouse chimeric mAb recognized native AHL protected mice from lethal *P. aeruginosa* infection (Palliyil et al., 2014). Nevertheless, while these 3O-C12-HSL-specific antibodies have therapeutic potential, their immunogenicity in human recipients, with possible adverse consequences, such as serum sickness, should be of concern.

Nowadays, any engineered fully human antibody format can be generated *in vitro* using phage display technology, invented by Nobel laureate, George Pearson Smith (Smith, 1985) as a biological tool (Santajit et al., 2019). The target antigens, such as proteins or peptides, attached to a carrier surface, e.g., fixed cell, plastic bead, or well of an ELISA plate, can be used as bait to fish out phage clones that display recombinant antibodies binding to the antigen from an antibody phage display library (Kulkeaw et al., 2009). Suppressor *E. coli*, such as strain HB2151 transfected with antigen-bound phages, when grown in appropriate conditioned medium, produces antigen-specific antibodies, and these antibodies can be isolated from the bacterial lysate/homogenate (Glab-Ampai et al., 2017; Santajit et al., 2019). Nevertheless, attachment of the small molecular haptens, like 3O-C12-HSL, to solid surfaces (as well as retaining the native configuration of the molecule) for conventional phage biopanning, is a relatively complicated process compared with proteins or peptides. Therefore, in this study, an alternative method was used to produce fully human scFvs (HuscFvs) to the synthetic *P. aeruginosa* 3O-C12-HSL based on the principle of antibody polyspecificity and antigenic molecular mimicry, i.e., completely unrelated molecules can share common receptors, possibly through similar structural and/or chemical features involved in recognition and binding (Wing, 1995;

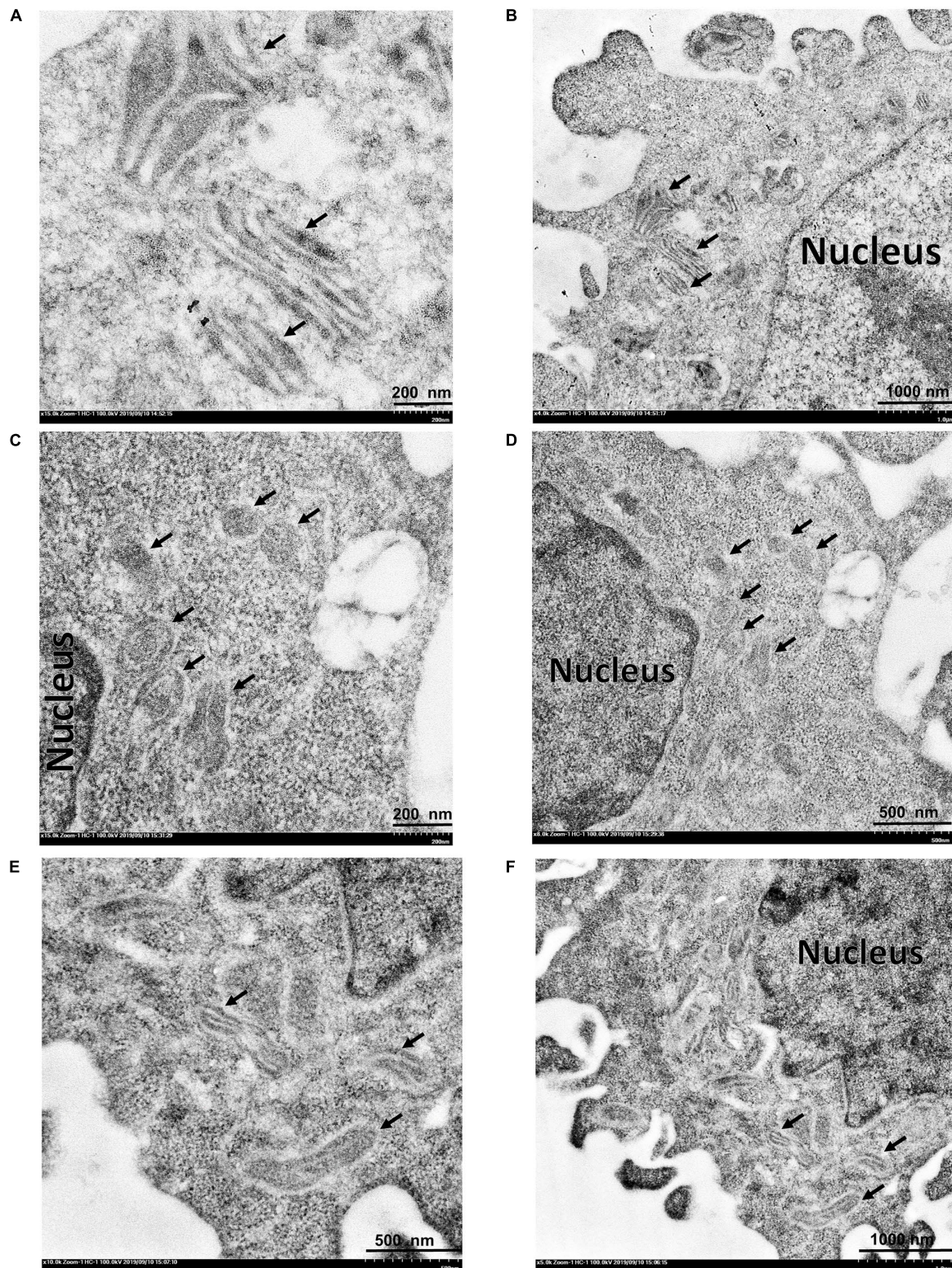


FIGURE 8 | Transmission electron micrographs of mitochondrial ultrastructure. **(A,B)** normal mitochondria of HeLa cells. **(C,D)** HeLa cells treated with 30-C12-HSL (50 μ M). **(E,F)** HeLa cells treated with a mixture of 50 μ M 30-C12-HSL and 2 μ M HuscFv-F19. Black arrows indicate mitochondria of the HeLa cells. Mitochondria of the cells exposed to the 30-C12-HSL were swollen, characterized by a size increment with decreased electron density of the crista-free matrix.

Tapryal et al., 2013). A repertoire of *E. coli* clones carrying recombinant *huscFv*-phagemids was previously retrieved from a HuscFv phage display library (Kulkeaw et al., 2009) by panning with *P. aeruginosa* exotoxin A (Santajit et al., 2019). Moreover, because the previously produced murine mAb, RS2-1G9, has been known as the *P. aeruginosa* quorum quencher, we used computerized antibody structure superimposition to select the bacterial derived-HuscFvs that shared structural homology with the murine mAb RS2-1G9 antigen-binding site. Using this method, the HuscFvs of three phagemid-transformed *E. coli* clones (E44, F15, and F19) showed high and satisfactory degrees of molecular similarity to the mAb RS2-1G9 antigen-binding site. Besides, these HuscFvs could neutralize the cytotoxic effects of the 3O-C12-HSL in the induction of cellular apoptosis. The HuscFv bound-3O-C12-HSL had a reduced capacity to mediate mitochondrial swelling, diminishing DNA damage and reducing sub-G1 arrest population of exposed cells. Unfortunately, the amount of C12-HSL inside the HeLa cells with and without HuscFv treatments were not measured; therefore, it is not known whether the HuscFvs could prevent HSL from entering the cells. Although the actual 3O-C12-HSL neutralizing mechanism of the HuscFvs needs laboratory investigation, the predicted structural complexes between the QS (ligand) and the HuscFvs (receptors) indicated that the latter used several residues in different CDRs and FRs to interact non-covalently with the target, including van der Waals' forces, hydrophobic interactions, and hydrogen bonds. These interactions might render the disarming of the bacterial toxic molecule through C12-HSL signal interference, which would mitigate bacterial disease severity. This perspective needs further testing of the HuscFvs on *P. aeruginosa* phenotypes both *in vitro* (bacterial culture), such as expression of the QS controlled virulence factors, as well as in the *in vivo* model of bacterial infection.

CONCLUSION

The engineered human single-chain variable fragments that attenuated the potent cytotoxicity of the *P. aeruginosa* quorum sensing molecule, 3O-C12-HSL, were generated successfully through the molecular basis of antibody polyspecificity and antigenic mimicry. The fully human antibody fragments rescued mammalian cells from the 3O-C12-HSL-mediated mitochondrial injuries, DNA damage, and cellular apoptosis *in vitro*. They should be tested further by step-by-step *in vivo* toward the

clinical application as a sole or an adjunct therapy for the failing antibiotic treatment of *P. aeruginosa* infections.

DATA AVAILABILITY STATEMENT

All datasets generated for this study are included in the article/Supplementary Material.

AUTHOR CONTRIBUTIONS

NI and WC conceived the project, analyzed the data, and edited the manuscript. SS did most of the experiments, drafted the manuscript, and prepared the figures. KM helped SS with flow cytometric analysis. WS advised SS on recombinant HuscFv production. PP supervised SS on fluorescence staining and confocal microscopy. SA performed the electron microscopy. NS, OR, and MC-N helped NI and WC to analyze the data and made comments. All authors critically reviewed the manuscript and gave final approval for publication.

FUNDING

This work was co-supported by the RSA scholar grant (RSA5980048) to NI, NSTDA Chair Professor grant (P-1450624) funded by the Crown Property Bureau of Thailand to WC, and Royal Golden Jubilee Ph.D. scholarship grant (PHD/0073/2558) to SS from the Thailand Research Fund.

ACKNOWLEDGMENTS

We acknowledge the Center of Research Excellence on Therapeutic Proteins and Antibody Engineering, Department of Parasitology, and Biomedical Research Unit, Department of Research, Faculty of Medicine Siriraj Hospital, for their technical support.

SUPPLEMENTARY MATERIAL

The Supplementary Material for this article can be found online at: <https://www.frontiersin.org/articles/10.3389/fmicb.2020.01172/full#supplementary-material>

REFERENCES

- Abhinandan, K. R., and Martin, A. C. (2008). Analysis and improvements to Kabat and structurally correct numbering of antibody variable domains. *Mol. Immunol.* 45, 3832–3839. doi: 10.1016/j.molimm.2008.05.022
- Ahmed, S. A. K. S., Rudden, M., Smyth, T. J., Dooley, J. S., Marchant, R., and Banat, I. M. (2019). Natural quorum sensing inhibitors effectively downregulate gene expression of *Pseudomonas aeruginosa* virulence factors. *Appl. Microbiol. Biotechnol.* 103, 3521–3535. doi: 10.1007/s00253-019-09618-0
- Blevess, S., Soscia, C., Nogueira-Orlandi, P., Lazdunski, A., and Filloux, A. (2005). Quorum sensing negatively controls type III secretion regulon expression in *Pseudomonas aeruginosa* PAO1. *J. Bacteriol.* 187, 3898–3902. doi: 10.1128/jb.187.11.3898-3902.2005
- Boontham, P., Robins, A., Chandran, P., Pritchard, D., Cámara, M., Williams, P., et al. (2008). Significant immunomodulatory effects of *Pseudomonas aeruginosa* quorum-sensing signal molecules: possible link in human sepsis. *Clin. Sci.* 115, 343–351. doi: 10.1042/cs20080018
- Chapa-Dubocq, X., Makarov, V., and Javadov, S. (2018). Simple kinetic model of mitochondrial swelling in cardiac cells. *J. Cell. Physiol.* 233, 5310–5321. doi: 10.1002/jcp.26335
- Cummings, B. S., and Schnellmann, R. G. (2004). Measurement of cell death in mammalian cells. *Curr. Protoc. Pharmacol.* 25, 12–18.

- Debler, E. W., Kaufmann, G. F., Kirchdoerfer, R. N., Mee, J. M., Janda, K. D., and Wilson, I. A. (2007). Crystal structures of a quorum-quenching antibody. *J. Mol. Biol.* 368, 1392–1402. doi: 10.1016/j.jmb.2007.02.081
- Defoirdt, T., Boon, N., and Bossier, P. (2010). Can bacteria evolve resistance to quorum sensing disruption? *PLoS Pathog.* 6:e1000989. doi: 10.1371/journal.ppat.1000989
- Duan, K., and Surette, M. G. (2007). Environmental regulation of *Pseudomonas aeruginosa* PAO1 Las and Rhl quorum-sensing systems. *J. Bacteriol.* 189, 4827–4836. doi: 10.1128/jb.00043-07
- Eberhard, A., Burlingame, A. L., Eberhard, C., Kenyon, G. L., Nealson, K. H., and Oppenheimer, N. J. (1981). Structural identification of autoinducer of *Photobacterium fischeri* luciferase. *Biochemistry* 20, 2444–2449. doi: 10.1021/bi00512a013
- El-Wafay, S. A., El Galil, K. H. A., El-Messery, S. M., and Shaaban, M. I. (2014). Aspirin is an efficient inhibitor of quorum sensing, virulence and toxins in *Pseudomonas aeruginosa*. *Microb. Pathog.* 74, 25–32. doi: 10.1016/j.micpath.2014.07.008
- Fong, J., Mortensen, K. T., Nørskov, A., Qvortrup, K., Yang, L., Tan, C. H., et al. (2018). Itaconimides as novel quorum sensing inhibitors of *Pseudomonas aeruginosa*. *Front. Cell. Infect. Microbiol.* 8:443. doi: 10.3389/fcimb.2018.00443
- Forli, S., Huey, R., Pique, M. E., Sanner, M. F., Goodsell, D. S., and Olson, A. J. (2016). Computational protein–ligand docking and virtual drug screening with the AutoDock suite. *Nat. Protoc.* 11, 905–919. doi: 10.1038/nprot.2016.051
- Geske, G. D., Mattmann, M. E., and Blackwell, H. E. (2008). Evaluation of a focused library of N-aryl L-homoserine lactones reveals a new set of potent quorum sensing modulators. *Bioorg. Med. Chem. Lett.* 18, 5978–5981. doi: 10.1016/j.bmcl.2008.07.089
- Givskov, M., de Nys, R., Manefield, M., Gram, L., Maximilien, R. I. A., Eberl, L. E. O., et al. (1996). Eukaryotic interference with homoserine lactone-mediated prokaryotic signalling. *J. Bacteriol.* 178, 6618–6622. doi: 10.1128/jb.178.22.6618-6622.1996
- Glab-Ampai, K., Chulanetra, M., Malik, A. A., Juntadech, T., Thanongsaksrikul, J., Srimanote, P., et al. (2017). Human single chain-transbodies that bound to domain-I of non-structural protein 5A (NS5A) of hepatitis C virus. *Sci. Rep.* 7:15042.
- Hentzer, M., Riedel, K., Rasmussen, T. B., Heydorn, A., Andersen, J. B., Parsek, M. R., et al. (2002). Inhibition of quorum sensing in *Pseudomonas aeruginosa* biofilm bacteria by a halogenated furanone compound. *Microbiology* 148, 87–102. doi: 10.1099/00221287-148-1-87
- Hentzer, M., Wu, H., Andersen, J. B., Riedel, K., Rasmussen, T. B., Bagge, N., et al. (2003). Attenuation of *Pseudomonas aeruginosa* virulence by quorum sensing inhibitors. *EMBO J.* 22, 3803–3815. doi: 10.1093/emboj/cdg366
- Ishida, T., Ikeda, T., Takiguchi, N., Kuroda, A., Ohtake, H., and Kato, J. (2007). Inhibition of quorum sensing in *Pseudomonas aeruginosa* by N-acyl cyclopentylamides. *Appl. Environ. Microbiol.* 73, 3183–3188. doi: 10.1128/aem.02233-06
- Jacobi, C. A., Schiffner, F., Henkel, M., Waibel, M., Stork, B., Daubrawa, M., et al. (2009). Effects of bacterial N-acyl homoserine lactones on human Jurkat T lymphocytes—O₂DHL induces apoptosis via the mitochondrial pathway. *Int. J. Med. Microbiol.* 299, 509–519. doi: 10.1016/j.ijmm.2009.03.005
- Jakobsen, T. H., van Gennip, M., Phipps, R. K., Shanmugham, M. S., Christensen, L. D., Alhede, M., et al. (2012). Ajoene, a sulfur-rich molecule from garlic, inhibits genes controlled by quorum sensing. *Antimicrob. Agents Chemother.* 56, 2314–2325. doi: 10.1128/aac.05919-11
- Jittavisuthikul, S., Seesua, W., Thanongsaksrikul, J., Thueng-in, K., Srimanote, P., Werner, R. G., et al. (2016). Human transbodies to HCV NS3/4A protease inhibit viral replication and restore host innate immunity. *Front. Immunol.* 7, 318. doi: 10.3389/fimmu.2016.00318
- Kalia, V. C., Wood, T. K., and Kumar, P. (2014). Evolution of resistance to quorum-sensing inhibitors. *Microb. Ecol.* 68, 13–23.
- Kaufmann, G. F., Park, J., Mee, J. M., Ulevitch, R. J., and Janda, K. D. (2008). The quorum quenching antibody RS2-1G9 protects macrophages from the cytotoxic effects of the *Pseudomonas aeruginosa* quorum sensing signaling molecule N-3-oxo-dodecanoyl-homoserine lactone. *Mol. Immunol.* 45, 2710–2714. doi: 10.1016/j.molimm.2008.01.010
- Kaufmann, G. F., Sartorio, R., Lee, S. H., Mee, J. M., Altobelli, L. J., Kujawa, D. P., et al. (2006). Antibody interference with N-acyl homoserine lactone-mediated bacterial quorum sensing. *J. Am. Chem. Soc.* 128, 2802–2803. doi: 10.1021/ja0578698
- Keller, M. A., and Stiehm, E. R. (2000). Passive immunity in prevention and treatment of infectious diseases. *Clin. Microbiol. Rev.* 13, 602–614. doi: 10.1128/cmr.13.4.602
- Kim, C., Kim, J., Park, H. Y., Park, H. J., Lee, J. H., Kim, C. K., et al. (2008). Furanone derivatives as quorum-sensing antagonists of *Pseudomonas aeruginosa*. *Appl. Microbiol. Biotechnol.* 80, 37–47.
- Kim, S., Thiessen, P. A., Bolton, E. E., Chen, J., Fu, G., Gindulyte, A., et al. (2015). PubChem substance and compound databases. *Nucleic Acids Res.* 44, D1202–D1213.
- Kravchenko, V. V., Kaufmann, G. F., Mathison, J. C., Scott, D. A., Katz, A. Z., Wood, M. R., et al. (2006). N-(3-oxo-acyl) homoserine lactones signal cell activation through a mechanism distinct from the canonical pathogen-associated molecular pattern recognition receptor pathways. *J. Biol. Chem.* 281, 28822–28830. doi: 10.1074/jbc.m606613200
- Krzyżek, P. (2019). Challenges and limitations of anti-quorum sensing therapies. *Front. Microbiol.* 10:2473. doi: 10.3389/fmicb.2019.02473
- Kulkeaw, K., Sakolvaree, Y., Srimanote, P., Tongtawe, P., Maneewatch, S., Sookkrung, N., et al. (2009). Human monoclonal ScFv neutralize lethal Thai cobra. *Naja kaouthia*, neurotoxin. *J. Proteomics* 72, 270–280.
- Laskowski, R. A., MacArthur, M. W., Moss, D. S., and Thornton, J. M. (1993). PROCHECK: a program to check the stereochemical quality of protein structures. *J. Appl. Crystallogr.* 26, 283–291. doi: 10.1107/s0021889892009944
- Li, L., Hooi, D., Chhabra, S. R., Pritchard, D., and Shaw, P. E. (2004). Bacterial N-acylhomoserine lactone-induced apoptosis in breast carcinoma cells correlated with down-modulation of STAT3. *Oncogene* 23, 4894–4902. doi: 10.1038/sj.onc.1207612
- Liu, Y. C., Chan, K. G., and Chang, C. Y. (2015). Modulation of host biology by *Pseudomonas aeruginosa* quorum sensing signal molecules: messengers or traitors. *Front. Microbiol.* 6:1226. doi: 10.3389/fmicb.2015.01226
- López-Jácome, L. E., Garza Ramos-Martínez, G., Hernández-Durán, M., Franco-Cendejas, R., Loarca, D., Romero-Martínez, D., et al. (2019). AiiM lactonase strongly reduces quorum sensing controlled virulence factors in clinical strains of *Pseudomonas aeruginosa* isolated from burned patients. *Front. Microbiol.* 10:2657. doi: 10.3389/fmicb.2019.02657
- Maeda, T., García-Contreras, R., Pu, M., Sheng, L., García, L. R., Tomás, M., et al. (2012). Quorum quenching quandary: resistance to antivirulence compounds. *ISME J.* 6, 493–501. doi: 10.1038/ismej.2011.122
- Malhotra, S., Hayes, D., and Wozniak, D. J. (2019). Cystic fibrosis and *Pseudomonas aeruginosa*: the host-microbe interface. *Clin. Microbiol. Rev.* 32:e00138-18.
- Miyairi, S., Tateda, K., Fuse, E. T., Ueda, C., Saito, H., Takabatake, T., et al. (2006). Immunization with 3-oxododecanoyl-L-homoserine lactone-protein conjugate protects mice from lethal *Pseudomonas aeruginosa* lung infection. *J. Med. Microbiol.* 55, 1381–1387. doi: 10.1099/jmm.0.46658-0
- Moradali, M. F., Ghods, S., and Rehm, B. H. (2017). *Pseudomonas aeruginosa* lifestyle: a paradigm for adaptation, survival, and persistence. *Front. Cell. Infect. Microbiol.* 7:39. doi: 10.3389/fcimb.2017.00039
- Nguyen, M. N., Tan, K. P., and Madhusudhan, M. S. (2011). CLICK—topology-independent comparison of biomolecular 3D structures. *Nucleic Acids Res.* 39, W24–W28.
- Ni, N., Li, M., Wang, J., and Wang, B. (2009). Inhibitors and antagonists of bacterial quorum sensing. *Med. Res. Rev.* 29, 65–124. doi: 10.1002/med.20145
- O'Connor, G., Knecht, L. D., Salgado, N., Strobel, S., Pasini, P., and Daunert, S. (2015). Whole-cell biosensors as tools for the detection of quorum-sensing molecules: uses in diagnostics and the investigation of the quorum-sensing mechanism. *Adv. Biochem. Eng. Biotechnol.* 154, 181–200. doi: 10.1007/10_2015_337
- Palliyil, S., and Broadbent, I. D. (2009). Novel immunotherapeutic approaches to the treatment of infections caused by Gram-negative bacteria. *Curr. Opin. Pharmacol.* 9, 566–570. doi: 10.1016/j.coph.2009.07.007
- Palliyil, S., Downham, C., Broadbent, I., Charlton, K., and Porter, A. J. (2014). High-sensitivity monoclonal antibodies specific for homoserine lactones protect mice from lethal *Pseudomonas aeruginosa* infections. *Appl. Environ. Microbiol.* 80, 462–469. doi: 10.1128/aem.02912-13

- Pearson, J. P., Gray, K. M., Passador, L., Tucker, K. D., Eberhard, A., Iglewski, B. H., et al. (1994). Structure of the autoinducer required for expression of *Pseudomonas aeruginosa* virulence genes. *Proc. Natl. Acad. Sci. U.S.A.* 91, 197–201. doi: 10.1073/pnas.91.1.197
- Pearson, J. P., Passador, L., Iglewski, B. H., and Greenberg, E. P. (1995). A second N-acylhomoserine lactone signal produced by *Pseudomonas aeruginosa*. *Proc. Natl. Acad. Sci. U.S.A.* 92, 1490–1494. doi: 10.1073/pnas.92.5.1490
- Penesyan, A., Gillings, M., and Paulsen, I. T. (2015). Antibiotic discovery: combatting bacterial resistance in cells and in biofilm communities. *Molecules* 20, 5286–5298. doi: 10.3390/molecules20045286
- Petronilli, V., Penzo, D., Scorrano, L., Bernardi, P., and Di Lisa, F. (2001). The mitochondrial permeability transition, release of cytochrome *c* and cell death correlation with the duration of pore openings *in situ*. *J. Biol. Chem.* 276, 12030–12034. doi: 10.1074/jbc.m010604200
- Preston, M. J., Seed, P. C., Toder, D. S., Iglewski, B. H., Ohman, D. E., Gustin, J. K., et al. (1997). Contribution of proteases and LasR to the virulence of *Pseudomonas aeruginosa* during corneal infections. *Infect. Immun.* 65, 3086–3090. doi: 10.1128/iai.65.8.3086-3090.1997
- Rasamiravaka, T., and El Jaziri, M. (2016). Quorum-sensing mechanisms and bacterial response to antibiotics in *P. aeruginosa*. *Curr. Microbiol.* 73, 747–753. doi: 10.1007/s00284-016-1101-1
- Rasmussen, T. B., and Givskov, M. (2006). Quorum-sensing inhibitors as anti-pathogenic drugs. *Int. J. Med. Microbiol.* 296, 149–161. doi: 10.1016/j.ijmm.2006.02.005
- Rasmussen, T. B., Skindersoe, M. E., Bjarnsholt, T., Phipps, R. K., Christensen, K. B., Jensen, P. O., et al. (2005). Identity and effects of quorum-sensing inhibitors produced by *Penicillium* species. *Microbiology* 151, 1325–1340. doi: 10.1099/mic.0.27715-0
- Riccardi, C., and Nicoletti, I. (2006). Analysis of apoptosis by propidium iodide staining and flow cytometry. *Nat. Protoc.* 1, 1458–1461. doi: 10.1038/nprot.2006.238
- Ritchie, A. J., Whittall, C., Lazenby, J. J., Chhabra, S. R., Pritchard, D. I., and Cooley, M. A. (2007). The immunomodulatory *Pseudomonas aeruginosa* signalling molecule N-(3-oxododecanoyl)-l-homoserine lactone enters mammalian cells in an unregulated fashion. *Immunol. Cell. Biol.* 85, 596–602. doi: 10.1038/sj.icb.7100090
- Rutherford, S. T., and Bassler, B. L. (2012). Bacterial quorum sensing: its role in virulence and possibilities for its control. *Cold Spring Harb. Perspect. Med.* 2:a012427. doi: 10.1101/cshperspect.a012427
- Sadikot, R. T., Blackwell, T. S., Christman, J. W., and Prince, A. S. (2005). Pathogen-host interactions in *Pseudomonas aeruginosa* pneumonia. *Am. J. Respir. Crit. Care Med.* 171, 1209–1223.
- Santajit, S., Seesay, W., Mahasongkram, K., Sookrung, N., Ampawong, S., Reamtong, O., et al. (2019). Human single-chain antibodies that neutralize *Pseudomonas aeruginosa*-exotoxin A-mediated cellular apoptosis. *Sci. Rep.* 9, 1–15.
- Sarabhai, S., Sharma, P., and Capalash, N. (2013). Ellagic acid derivatives from *Terminalia chebula* Retz. downregulate the expression of quorum sensing genes to attenuate *Pseudomonas aeruginosa* PAO1 virulence. *PLoS One* 8:e53441. doi: 10.1371/journal.pone.0053441
- Schwarzer, C., Fu, Z., Patanwala, M., Hum, L., Lopez-Guzman, M., Illek, B., et al. (2012). *Pseudomonas aeruginosa* biofilm-associated homoserine lactone C12 rapidly activates apoptosis in airway epithelia. *Cell. Microbiol.* 14, 698–709. doi: 10.1111/j.1462-5822.2012.01753.x
- Shiner, E. K., Terentyev, D., Bryan, A., Sennoune, S., Martinez-Zaguilan, R., Li, G., et al. (2006). *Pseudomonas aeruginosa* autoinducer modulates host cell responses through calcium signalling. *Cell. Microbiol.* 8, 1601–1610. doi: 10.1111/j.1462-5822.2006.00734.x
- Shreaz, S., Wani, W. A., Behbehani, J. M., Raja, V., Irshad, M., Karched, M., et al. (2016). Cinnamaldehyde and its derivatives, a novel class of antifungal agents. *Fitoterapia* 112, 116–131. doi: 10.1016/j.fitote.2016.05.016
- Silva Filho, L. V. R. F., Ferreira, F. D. A., Reis, F. J. C., Britto, M. C. A. D., Levy, C. E., Clark, O., et al. (2013). *Pseudomonas aeruginosa* infection in patients with cystic fibrosis: scientific evidence regarding clinical impact, diagnosis, and treatment. *J. Bras. Pneumol.* 39, 495–512. doi: 10.1590/s1806-37132013000400015
- Smith, G. P. (1985). Filamentous fusion phage: novel expression vectors that display cloned antigens on the virion surface. *Science* 228, 1315–1317. doi: 10.1126/science.4001944
- Smith, R. S., Harris, S. G., Phipps, R., and Iglewski, B. (2002). The *Pseudomonas aeruginosa* quorum-sensing molecule N-(3-oxododecanoyl) homoserine lactone contributes to virulence and induces inflammation *in vivo*. *J. Bacteriol.* 184, 1132–1139. doi: 10.1128/jb.184.4.1132-1139.2002
- Soto-Aceves, M. P., Cocotl-Yañez, M., Merino, E., Castillo-Juárez, I., Cortés-López, H., González-Pedraja, B., et al. (2019). Inactivation of the quorum-sensing transcriptional regulators LasR or RhlR does not suppress the expression of virulence factors and the virulence of *Pseudomonas aeruginosa* PAO1. *Microbiology* 165, 425–432. doi: 10.1099/mic.0.000778
- Sultan, A., and Sokolove, P. M. (2001). Free fatty acid effects on mitochondrial permeability: an overview. *Arch. Biochem. Biophys.* 386, 52–61. doi: 10.1006/abbi.2000.2195
- Tang, H. B., DiMango, E., Bryan, R., Gambello, M., Iglewski, B. H., Goldberg, J. B., et al. (1996). Contribution of specific *Pseudomonas aeruginosa* virulence factors to pathogenesis of pneumonia in a neonatal mouse model of infection. *Infect. Immun.* 64, 37–43. doi: 10.1128/iai.64.1.37-43.1996
- Tao, S., Luo, Y., He, B., Liu, J., Qian, X., Ni, Y., et al. (2016). Paraoxonase 2 modulates a proapoptotic function in LS174T cells in response to quorum sensing molecule N-(3-oxododecanoyl)-L-homoserine lactone. *Sci. Rep.* 6:28778.
- Tao, S., Niu, L., Cai, L., Geng, Y., Hua, C., Ni, Y., et al. (2018). N-(3-oxododecanoyl)-l-homoserine lactone modulates mitochondrial function and suppresses proliferation in intestinal goblet cells. *Life Sci.* 201, 81–88. doi: 10.1016/j.lfs.2018.03.049
- Tapryal, S., Gaur, V., Kaur, K. J., and Salunke, D. M. (2013). Structural evaluation of a mimicry-recognizing paratope: plasticity in antigen-antibody interactions manifests in molecular mimicry. *J. Immunol.* 191, 456–463. doi: 10.4049/jimmunol.1203260
- Tateda, K., Ishii, Y., Horikawa, M., Matsumoto, T., Miyairi, S., Pechere, J. C., et al. (2003). The *Pseudomonas aeruginosa* autoinducer N-3-oxododecanoyl homoserine lactone accelerates apoptosis in macrophages and neutrophils. *Infect. Immun.* 71, 5785–5793. doi: 10.1128/iai.71.10.5785-5793.2003
- Trott, O., and Olson, A. J. (2010). AutoDock Vina: improving the speed and accuracy of docking with a new scoring function, efficient optimization, and multithreading. *J. Comput. Chem.* 31, 455–461.
- Venturi, V. (2006). Regulation of quorum sensing in *Pseudomonas*. *FEMS Microbiol. Rev.* 30, 274–291.
- Wagner, V. E., Bushnell, D., Passador, L., Brooks, A. I., and Iglewski, B. H. (2003). Microarray analysis of *Pseudomonas aeruginosa* quorum-sensing regulons: effects of growth phase and environment. *J. Bacteriol.* 185, 2080–2095. doi: 10.1128/jb.185.7.2080-2095.2003
- Waters, C. M., and Goldberg, J. B. (2019). *Pseudomonas aeruginosa* in cystic fibrosis: a chronic cheater. *Proc. Natl. Acad. Sci. U.S.A.* 116, 6525–6527.
- Wing, M. G. (1995). The molecular basis for a polyspecific antibody. *Clin. Exp. Immunol.* 99, 313–315. doi: 10.1111/j.1365-2249.1995.tb05551.x
- Wyllie, A. H., Kerr, J. R., and Currie, A. R. (1980). Cell death: the significance of apoptosis. *Int. Rev. Cytol.* 68, 251–306. doi: 10.1016/s0074-7696(08)62312-8
- Xu, D., and Zhang, Y. (2011). Improving the physical realism and structural accuracy of protein models by a two-step atomic-level energy minimization. *Biophys. J.* 101, 2525–2534. doi: 10.1016/j.bpj.2011.10.024
- Yang, J., Yan, R., Roy, A., Xu, D., Poisson, J., and Zhang, Y. (2015). The I-TASSER suite: protein structure and function prediction. *Nat. Methods* 12, 7–8. doi: 10.1038/nmeth.3213
- Zhang, J. H., and Ming, X. U. (2000). DNA fragmentation in apoptosis. *Cell Res.* 10, 205–211.

Conflict of Interest: The authors declare that the research was conducted in the absence of any commercial or financial relationships that could be construed as a potential conflict of interest.

Copyright © 2020 Santajit, Seesay, Mahasongkram, Sookrung, Pumirat, Ampawong, Reamtong, Chongsa-Nguan, Chaicumpa and Indrawattana. This is an open-access article distributed under the terms of the Creative Commons Attribution License (CC BY). The use, distribution or reproduction in other forums is permitted, provided the original author(s) and the copyright owner(s) are credited and that the original publication in this journal is cited, in accordance with accepted academic practice. No use, distribution or reproduction is permitted which does not comply with these terms.



Synergistic Effect of Berberine Hydrochloride and Fluconazole Against *Candida albicans* Resistant Isolates

Jiangyan Yong^{1,2}, Ruiling Zu³, Xiaoxue Huang¹, Yiman Ge² and Yan Li^{1*}

¹ Chengdu University of Traditional Chinese Medicine, Chengdu, China, ² Hospital of Chengdu University of Traditional Chinese Medicine, Chengdu, China, ³ Sichuan Cancer Hospital and Institute, Chengdu, China

OPEN ACCESS

Edited by:

Marco Rinaldo Oggioni,
University of Leicester,
United Kingdom

Reviewed by:

Mihai Mares,
Ion Ionescu de la Brad University
of Agricultural Sciences
and Veterinary Medicine of Iasi,
Romania
Ayse Kalkanci,
Gazi University, Turkey

*Correspondence:

Yan Li
liliana@cdutcm.edu.cn

Specialty section:

This article was submitted to
Antimicrobials, Resistance
and Chemotherapy,
a section of the journal
Frontiers in Microbiology

Received: 26 January 2020

Accepted: 09 June 2020

Published: 02 July 2020

Citation:

Yong J, Zu R, Huang X, Ge Y and
Li Y (2020) Synergistic Effect
of Berberine Hydrochloride
and Fluconazole Against *Candida*
albicans Resistant Isolates.
Front. Microbiol. 11:1498.
doi: 10.3389/fmicb.2020.01498

The emergence of resistant *Candida albicans* has made clinical fluconazole (FLC) treatment difficult. Improving sensitivity to FLC is an effective way to treat resistant isolates. Berberine hydrochloride (BBH) is a commonly used traditional Chinese medicine with antimicrobial effects, especially in resistant isolates. We investigated the molecular mechanisms underlying BBH and FLC synergism on biofilm-positive FLC-resistant *C. albicans* inhibition. Checkerboard microdilution assays and time-kill assays showed a strong synergistic effect between BBH and FLC in resistant *C. albicans* isolates, causing a significant 32–512-fold reduction in minimum inhibitory concentrations. BBH combined with FLC inhibited intracellular FLC efflux due to key efflux pump gene *CDR1* downregulation, whereas FLC alone induced high *CDR1* transcription in resistant strains. Further, BBH + FLC inhibited yeast adhesion, morphological hyphae transformation, and biofilm formation by downregulating the hyphal-specific genes *ALS3*, *HWP1*, and *ECE1*. BBH caused cytoplasmic Ca^{2+} influx, while FLC alone did not induce high intracellular Ca^{2+} levels. The vacuolar calcium channel gene *YVC1* was upregulated, while the vacuolar calcium pump gene *PMC1* was downregulated in the BBH + FLC and BBH alone groups. However, vacuolar calcium gene expression after FLC treatment was opposite in biofilm-positive FLC-resistant *C. albicans*, which might explain why BBH induces Ca^{2+} influx. These results demonstrate that BBH + FLC exerts synergistic effects to increase FLC sensitivity by regulating multiple targets in FLC-resistant *C. albicans*. These findings further show that traditional Chinese medicines have multi-target antimicrobial effects that may inhibit drug-resistant strains. This study also found that the vacuolar calcium regulation genes *YVC1* and *PMC1* are key BBH + FLC targets which increase cytoplasmic Ca^{2+} in resistant isolates, which might be critical for reversing biofilm-positive FLC-resistant *C. albicans*.

Keywords: berberine hydrochloride, fluconazole, *Candida albicans*, synergism, multiple targets

INTRODUCTION

Candida is a common pathogen of nosocomial bloodstream infections, causing high-mortality invasive candidiasis. The SENTRY antifungal surveillance program showed that 46.4–57.4% of invasive candidiasis cases from 1997 to 2016 were caused by *Candida albicans* infection (Pfaller et al., 2019). Fluconazole (FLC) is a commonly used antifungal drug with a broad drug spectrum, high efficiency, and safety. However, widespread medication use has caused increased resistance annually (Xiao et al., 2018) making most FLC therapy ineffective. Thus, antifungal treatments face enormous challenges.

Berberine, an active component extracted from *Coptis chinensis*, which is a common traditional Chinese medicinal (TCM) herb, has a wide range of pharmacological effects and multiple-target therapeutic effects on several diseases. In particular, berberine is widely used to treat bacterial diarrhea in China. Additionally, berberine has anti-arrhythmic and anti-inflammatory activity (Lau et al., 2001; Kuo et al., 2004), reduces colorectal adenoma recurrence after polypectomy (Chen et al., 2019), decreases total cholesterol, improves insulin-resistance *in vivo*, and prevents or delays Alzheimer's disease development associated with atherosclerosis (Cai et al., 2016; Imenshahidi and Hosseinzadeh, 2019). Furthermore, this compound exerts DNA damage-mediated antimicrobial effects on various microorganisms, including *Staphylococcus aureus*, *Pseudomonas aeruginosa*, *Escherichia coli*, *Candida albicans*, *Cryptococcus*, and *Vibrio cholerae* (Čerňáková and Košťálová, 2002; Tillhon et al., 2012). Modern medicine indicates that Chinese herbal monomers or phytocompounds inhibit *C. albicans* growth by regulating multiple targets while inducing little drug resistance. Previous studies show that TCMs target several cellular pathways to exert antifungal effects, such as ergosterol biosynthesis suppression (Sun L. M. et al., 2015) intracellular reactive oxygen species (ROS) production (Sharma et al., 2010) inhibition of efflux pump Cdr1p and Mdr1p overexpression (Garcia-Gomes et al., 2012), biofilm inhibition (Sharma et al., 2010; Sun L. et al., 2015), and yeast apoptosis induced by intracellular or mitochondrial high Ca^{2+} levels (Yun and Lee, 2016; Tian et al., 2017). Previous studies revealed that ergosterol synthesis inhibition and apoptosis induced by endogenous ROS augmentation contribute to the synergistic effect of berberine plus FLC against *C. albicans* (Xu et al., 2009; Xu et al., 2017; Yang et al., 2018). Furthermore, this combination could also downregulate efflux pump genes *CDR1* and *CDR2* overexpression (Zhu et al., 2014).

Biofilm formation and calcium homeostasis are also important antifungal mechanisms against FLC-resistant *C. albicans*. However, there is no relevant literature exploring the synergistic antifungal effects of berberine and FLC on these two processes. Therefore, berberine hydrochloride (BBH) combined with FLC was tested to explore the molecular mechanism underlying the synergistic effect on efflux pump activity, biofilm formation, and intracellular calcium homeostasis. Synergistic molecular targets were investigated using multiple approaches to provide an effective solution for clinical treatment of drug-resistant strains.

MATERIALS AND METHODS

Strains and Media

Fluconazole-resistant *C. albicans*, CA 0253, CA 1460, CA 2119, CA 12038, and CA 21065 (Table 1), were isolated and identified by the clinical laboratory of Chengdu University of Traditional Chinese Medicine Hospital, Chengdu, China. *C. albicans* ATCC10231 was purchased from the Guangdong Microbial Culture Collection Center Co., Ltd., China. All strains were stored in yeast extract peptone dextrose (YPD) (Hope, China) medium containing glycerol at -80°C and subcultured twice with YPD medium at 35°C for 24 h before experiments.

Antimicrobial Agents

Berberine hydrochloride and FLC were purchased from Chengdu Pufei De Biotech Co., Ltd., China, dissolved with dimethyl sulfoxide to achieve stock solutions of 12.8 and 20.48 mg/L, respectively, filtered using 0.22 μm filters, and stored at -20°C .

Checkerboard Microdilution Assay

The BBH and FLC minimum inhibitory concentrations (MICs) against *C. albicans* were determined by broth microdilution assay. Drug interactions were evaluated using checkerboard microdilution assays according to CLSI (M27-A3) (CLSI, 2008). Briefly, yeast cell suspension was diluted in RPMI-1640 medium (Gibco, United States) buffered with morpholino propanesulfonic acid (MOPS) (Saigu, China), and added to 96-well microtiter plates at a final concentration of 2×10^3 CFU/mL. The serially diluted agents were subsequently added to each well. The final drug concentrations were 128–0.25 $\mu\text{g/mL}$ for BBH and 32–0.5 $\mu\text{g/mL}$ for FLC. Blank controls were prepared without yeast. Drug-free wells were set as growth controls. After incubation at 35°C for 24 h, prepared 2,3-bis(2-methoxy-4-nitro-5-sulfophenyl)-2H-tetrazolium-5-carboxanilide (XTT) (KeyGen, China) working solution was added to the wells and incubated in the dark for 2 h at 35°C . Finally, absorbance was measured with a microplate reader (Kehua, China) at 450 nm. MICs were defined

TABLE 1 | Interactions of BBH with FLC against *Candida albicans*.

Isolate	Drugs	MIC ₈₀ ($\mu\text{g/mL}$)		Interactions	
		Alone	Combined	FICI	IN
CA 0253	FLC	512	1	0.03	SYN
	BBH	64	2		
CA 1460	FLC	>512	1	<0.06	SYN
	BBH	64	4		
CA 2119	FLC	>512	1	<0.03	SYN
	BBH	64	2		
CA 12038	FLC	>512	1	<0.03	SYN
	BBH	64	2		
CA 21065	FLC	512	1	0.03	SYN
	BBH	64	2		

CA, *C. albicans*; MIC₈₀, minimum inhibitory concentration inhibiting 80% *C. albicans* growth in the control group; FICI, fractional inhibitory concentration index; IN, Interactions; SYN, synergism.

as the lowest drug concentration inhibiting 80% *C. albicans* growth in the growth control group. The fractional inhibitory concentration index (FICI) was calculated by the following equation: $FICI = MIC(A \text{ combo}) / MIC(A \text{ alone}) + MIC(B \text{ combo}) / MIC(B \text{ alone})$. FICI was used to identify whether the two drugs had a synergistic antifungal effect, where $FICI \leq 0.5$ indicated synergy, no synergism when FICI was between 0.5–4, and $FICI \geq 4$ indicated antagonism.

Time-Kill Curve Assay

Time-kill curve assays were performed to monitor the dynamic antifungal effect of BBH and FLC against *C. albicans* (Liu et al., 2016). The final concentrations were 2 µg/mL for BBH, 1 µg/mL for FLC, and 2×10^3 CFU/mL for *C. albicans* (CA 0253). A drug-free group served as the negative control. The cells were incubated at 35°C with constant shaking (200 rpm) after different treatments. 100 µL was sampled at 0, 6, 12, 24, and 48 h in each group, and drug effects were detected with XTT tests ($\lambda = 450$ nm).

Rh6G Efflux Assay

To evaluate the combined BBH and FLC effect on resistant *C. albicans* drug efflux, Rh6G assays were performed as previously described, with some modifications (Xu et al., 2019). The cells were first incubated with constant shaking (200 rpm) in fresh RPMI 1640 at 35°C for 2 h to exhaust cellular energy stores. A fungal suspension was added with Rh6G (Acros Organics, United States) at a final concentration of 10 µM, cultured at 35°C with constant shaking (200 rpm) for 1 h, washed three times with PBS, and resuspended in PBS containing 5% glucose to 4×10^7 CFU/mL. Drugs were then added, and the cells were incubated for 0, 10, 30, 60, and 120 min at 35°C in a shaker. After incubation, the supernatant was collected by centrifugation at 12,000 rpm for 1 min at room temperature. The 530 nm fluorescence of the centrifuged supernatant was detected at designated time points by a microplate reader.

Hyphal Growth Assay

The effect of combined treatment on *C. albicans* hyphal formation was assessed using hyphal growth assays according to previous protocols, with a few modifications (Haque et al., 2016). Briefly, the cells (1×10^5 CFU/mL) were treated with different drugs and incubated at 35°C with agitation (200 rpm) for 16–17 h. Unstained samples and Gram-stained samples were observed under an optical microscope and photographed (Olympus, Japan). Three random visual fields for each well and three duplicate wells for each group were also observed.

Biofilm Information Assay

Berberine hydrochloride and FLC inhibition of *C. albicans* biofilm formation was assessed as previously described (Haque et al., 2016). Biofilm formation assays were carried out in 6-well plates incubated overnight with 10% fetal bovine serum (Tianhang, China). Cell suspensions (1×10^5 CFU/mL) and drugs were added to the wells and incubated overnight at 35°C. The biofilm was washed with PBS and photographed under bright

field using an inverted fluorescence microscope (Olympus, Japan) after culture (6, 12, 24, 48, and 72 h). The visual fields were photographed as described above.

Cytoplasmic Calcium Assays

Cytoplasmic calcium assays were performed to detect intracellular calcium concentration after combination therapy (Liu et al., 2016). Briefly, overnight-cultured cells were washed and diluted with HBSS.D-Hanks buffer (Thermo Fisher, United States) (final concentration 1×10^7 CFU/mL), and then mixed with 5 µM calcium indicator Fluo-3-AM (Solarbio, China) and 20% Pluronic F-127 (Meilun, China). The suspensions were incubated with agitation (200 rpm) at 35°C for 30 min, washed three times with HBSS buffer, and diluted to 1×10^7 CFU/mL. After drug treatment, the cells were shaken at 35°C in the dark. Fluorescence was detected by inverted fluorescence microscopy and flow cytometry (Beckman, United States) at 0, 2, and 3 h.

Quantitative Reverse Transcription PCR

To explore the molecular mechanism underlying the BBH and FLC synergistic effect, quantitative reverse transcription PCR (qRT-PCR) experiments were performed (Haque et al., 2016). *C. albicans* cells were cultured in YPD medium and diluted to 1×10^5 CFU/mL with RPMI 1640 medium. Cells were incubated overnight with agitation (200 rpm) at 35°C with 2 µg/mL BBH and 1 µg/mL FLC. Then cells were washed and harvested for RNA extraction. Total RNA was isolated using a TRIzol RNA isolation kit (Invitrogen, United States). cDNA was synthesized using TransScript First-Strand cDNA Synthesis SuperMix (Transgen, China) for qPCR. Target gene and endogenous control (actin1) primers were designed and synthesized by Shanghai Biotech (Supplementary Table S1). The qRT-PCR reaction system was mixed with cDNA, gene primers, and TransStart Green qPCR SuperMix kit (Transgen, China) in 20 µL reaction. qRT-PCR was carried on a qTower real-time PCR system (Analytik Jena, Germany) with an initial denaturation at 94°C for 30 s, followed by 40 cycles of 94°C for 5 s, annealing at 59°C for 15 s, and extension 72°C for 10 s. Primer specificity and optimal annealing temperature were determined using melt-curve analysis. Relative target gene expression fold changes were calculated by the $2^{-\Delta\Delta Ct}$ method.

Statistical Analysis

Three independent experiments were performed and a drug-free group served as the negative control in all experiments. Statistical differences were analyzed by ANOVA using SPSS Statistics version 21.0 software. Data are presented as mean \pm the standard error of the mean (SEM). $P < 0.05$ was considered significant.

RESULTS

BBH Enhances the Susceptibility of Resistant *C. albicans* to FLC

The interactions between BBH and FLC, and treatment MICs were assessed using five *C. albicans* isolates (Table 1). The clinical

isolates showed distinct biofilm formation capacity compared with biofilm-positive *C. albicans* ATCC10231. The five isolates were all FLC-resistant strains with MIC ≥ 512 $\mu\text{g/mL}$. The BBH MICs were 64 $\mu\text{g/mL}$, indicating insensitivity to both drugs. The FICI values were 0.03–0.06, indicating that BBH + FLC has strong synergistic effects. Combined use could increase *C. albicans* sensitivity to FLC and BBH, causing decreased FLC MIC from ≥ 512 to 1 $\mu\text{g/mL}$ and reduced BBH MIC from 64 to 2–4 $\mu\text{g/mL}$. These results demonstrate that the FLC MIC is decreased by 256–512-fold with minute BBH addition. Further, these results show that BBH combined with FLC synergistically inhibits FLC-resistant *C. albicans* and significantly enhances FLC antifungal activity. Subsequent experiments were carried out with the CA 0253 strain using 2 $\mu\text{g/mL}$ BBH and 1 $\mu\text{g/mL}$ FLC.

The combined BBH and FLC antifungal effect was first investigated by a 48-h dynamic time-kill study (Figure 1). Compared with the control group, growth was delayed in the other groups. However, much lower cell viability was observed in the BBH + FLC group than in the drug-monotherapy groups, especially at 0–24 h, indicating BBH + FLC treatment effectively inhibits FLC-resistant *C. albicans* growth ($p < 0.05$). A weak antifungal effect was observed in the FLC group, which was significantly lower than the combined group ($p < 0.05$). BBH alone had a poor antifungal effect, instead promoting growth at 24–48 h. These data indicate that BBH increases resistant isolate drug sensitivity, and that BBH combined with FLC synergistically inhibits *C. albicans* with a significantly dynamic antifungal effect.

Combination of BBH and FLC Reduces Rh6G Efflux

Rh6G fluorescent substrate was used to evaluate the effect of drug combinations on drug efflux pumps. *C. albicans* actively transported the absorbed Rh6G out of the cells, indicated by gradually increased fluorescence in the supernatant over time. Compared with the control group, lower supernatant fluorescence was observed in the BBH + FLC group, FLC group, and BBH group ($p < 0.05$), showing inhibited Rh6G efflux after

drug treatments (Table 2). When BBH + FLC was applied for 2 h, the extracellular Rh6G concentration was 1.43-fold lower than the FLC alone group and 1.28-fold lower than the BBH alone group ($p < 0.05$). These data indicate that BBH plus FLC significantly reduce the FLC efflux effect. Moreover, there was no significant difference between FLC or BBH treatment alone ($p > 0.05$).

BBH Combined With FLC Inhibits Hyphae and Biofilm Formation

The biofilm-producing strain CA 0253 was used to detect the effect of BBH combined with FLC on yeast-to-hyphae conversion (Figure 2) and biofilm formation (Figure 3). Hyphal growth was absent in the presence of BBH + FLC, with very few spherical yeast cells. FLC monotherapy significantly increased the number of fungal cells, and yeast-to-hyphae conversion occurred in a portion of cells, accompanied with pseudohyphae formation. The number of fungal cells in the BBH alone group and the control group significantly increased with extensive hyphae forming a network.

Berberine hydrochloride combined with FLC completely inhibited biofilm production within 6–72 h. Only a few cells remained in the yeast form without obvious hyphae. Notably, BBH plus FLC significantly reduced yeast cell surface adherence, especially in the biofilm adhesion stage (0–12 h). Pseudohyphae growth (ellipsoidal cells joined end to end) was observed in FLC alone group, and numerous pseudohyphae formed and adhered to the surface at 24–72 h, forming an aggregated cell population. The BBH alone and the control group contained complex biofilm structure with hyphae (chains of cylindrical cells), pseudohyphae, and yeast-form cells. Hyphae growth appeared at 6 h. Hyphal cells continued to elongate at 12 h. Numerous long hyphae formed and adhered to the surface at 24–48 h, accompanied with yeast-form cells and pseudohyphae that accumulated around the hyphal cells. These data indicate that BBH combined with FLC inhibits yeast adherence and hyphae development, causing biofilm formation defects.

BBH Plus FLC Increases Cytoplasmic Calcium

Inverted fluorescence microscopy was used to observe cellular calcium levels (Figure 4). The BBH plus FLC and BBH alone groups showed pale green fluorescence at 2 and 3 h, indicating Ca^{2+} influx. However, no fluorescence was observed in the FLC monotherapy or control groups, indicating no Ca^{2+} influx.

Flow cytometry was performed to compare the cytoplasmic Ca^{2+} concentration (Table 3). Compared with control and drug-monotherapy groups, higher fluorescence was observed in the BBH + FLC group at 0, 2, and 3 h ($p < 0.05$). Further, the fluorescence of BBH + FLC group at 2 h was 1.17-, 1.07-, and 1.18-fold higher than the FLC monotherapy, BBH alone, and control groups, respectively ($p < 0.05$). The fluorescence after BBH treatment alone was higher than after FLC alone ($p < 0.05$), but there was no significant difference between the FLC alone and control groups ($p > 0.05$). These observations indicate that BBH

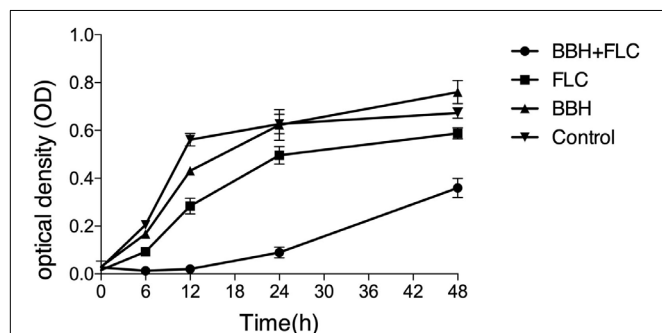


FIGURE 1 | Synergistic BBH and FLC antifungal effect. CA 0253 were treated with BBH (2 $\mu\text{g/mL}$) plus FLC (1 $\mu\text{g/mL}$), FLC (1 $\mu\text{g/mL}$), BBH (2 $\mu\text{g/mL}$), and RPMI-1640 medium. The optical density (OD) was measured at 0, 6, 12, 24, and 48 h after drug treatment. Three independent experiments were performed, with eight replicates in each group ($n = 8$). Values represent means \pm SEM. ANOVA tested statistical differences.

TABLE 2 | Rhodamine 6G efflux in BBH and FLC-treated *C. albicans*.

CA 0253	Time of drug action				
	0 min	10 min	30 min	60 min	2 h
BBH + FLC◆★★▲	1069 ± 131	2472 ± 117	8596 ± 305	16892 ± 310	26019 ± 663
FLC*▲	1107 ± 169	2172 ± 101	12761 ± 69	21579 ± 982	38365 ± 1132
BBH▲	1466 ± 242	2946 ± 170	15366 ± 902	20047 ± 696	33294 ± 293
Control	932 ± 15	2782 ± 143	16502 ± 813	26887 ± 153	39751 ± 705

CA 0253 were treated with BBH (2 μ g/mL) plus FLC (1 μ g/mL), FLC (1 μ g/mL), BBH (2 μ g/mL), or RPMI-1640 medium. After drug treatment, fluorescence intensity was detected (emission wavelength 530 nm) at 0, 10, 30, 60, and 120 min. Three independent experiments were performed, with eight replicates in each group ($n = 8$). Values represent means \pm SEM. ANOVA tested statistical differences. ◆ compared with the FLC group, $p < 0.05$; ★ compared with the BBH group, $p < 0.05$; ▲ compared with the control group, $p < 0.05$; * compared with the BBH group, $p > 0.05$.

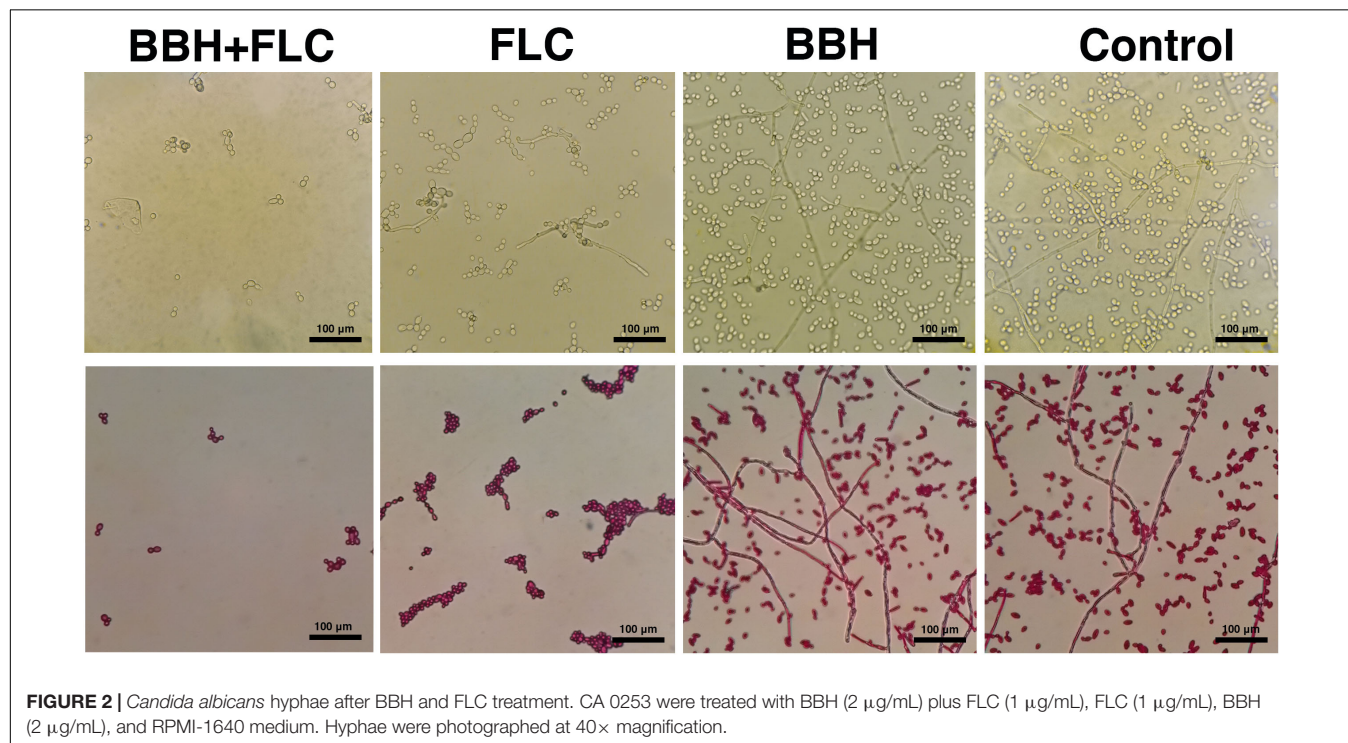


FIGURE 2 | *Candida albicans* hyphae after BBH and FLC treatment. CA 0253 were treated with BBH (2 μ g/mL) plus FLC (1 μ g/mL), FLC (1 μ g/mL), BBH (2 μ g/mL), and RPMI-1640 medium. Hyphae were photographed at 40 \times magnification.

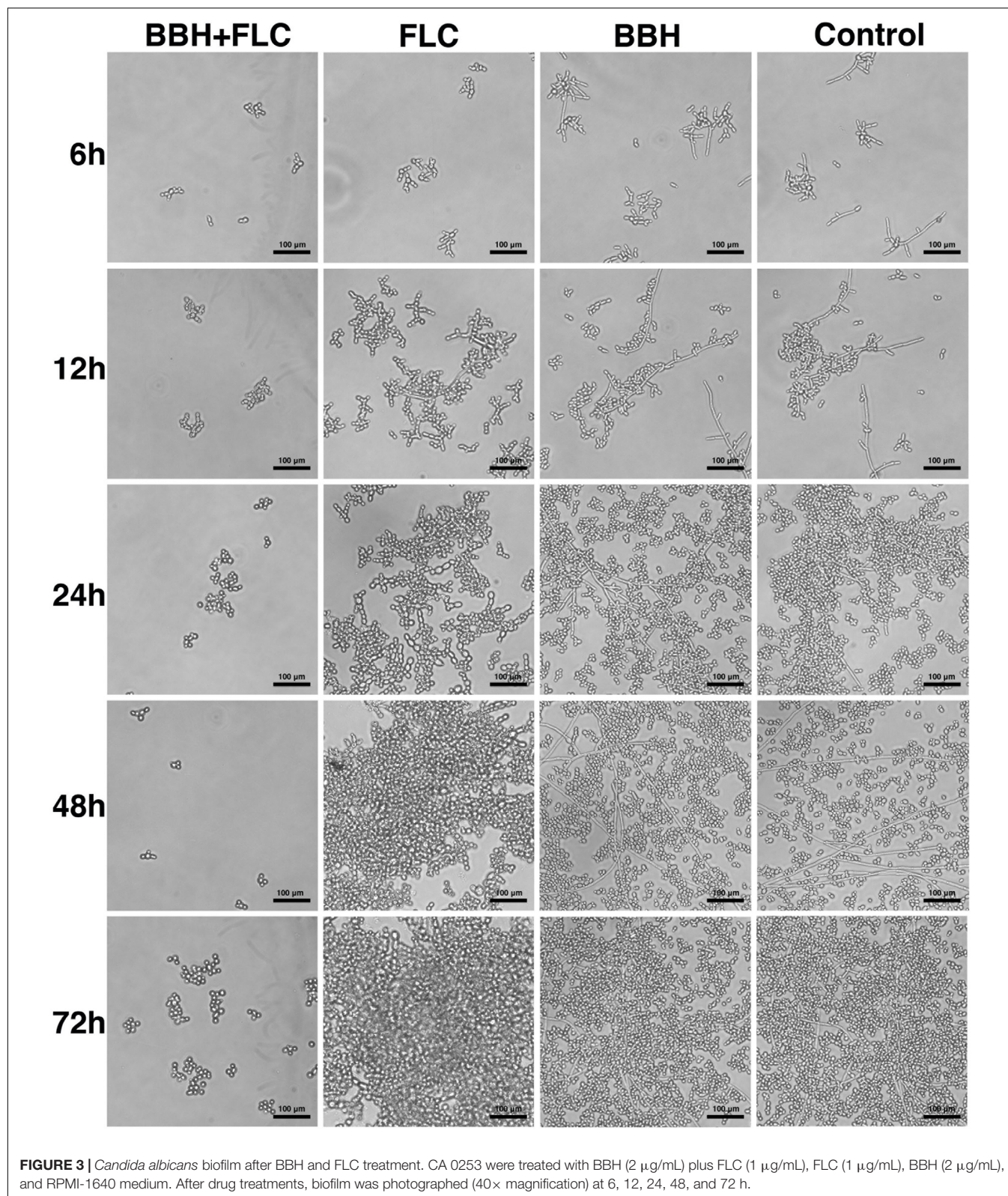
further increases intracellular calcium concentration, disrupting *C. albicans* calcium homeostasis.

BBH Combined With FLC Induces Expression of Multiple Genes

qRT-PCR was conducted to explore the effect of BBH + FLC on drug-resistance, biofilm-related, and calcium-related genes (Figure 5). Compared with the control and drug-monotherapy groups, *CDR1* transcription in the BBH + FLC group was downregulated 3-to-5-fold ($p < 0.05$). However, FLC alone caused 1.52-fold *CDR1* upregulation ($p < 0.05$). Although BBH plus FLC significantly downregulated *CDR2* by 3.58-fold, much lower *CDR2* expression was observed in the FLC alone group than in the other groups ($p < 0.05$). *MDR1* expression in the combined group was almost 1.70-fold lower than in the drug-monotherapy groups ($p < 0.05$). No significant difference was detected between FLC or BBH treatment alone.

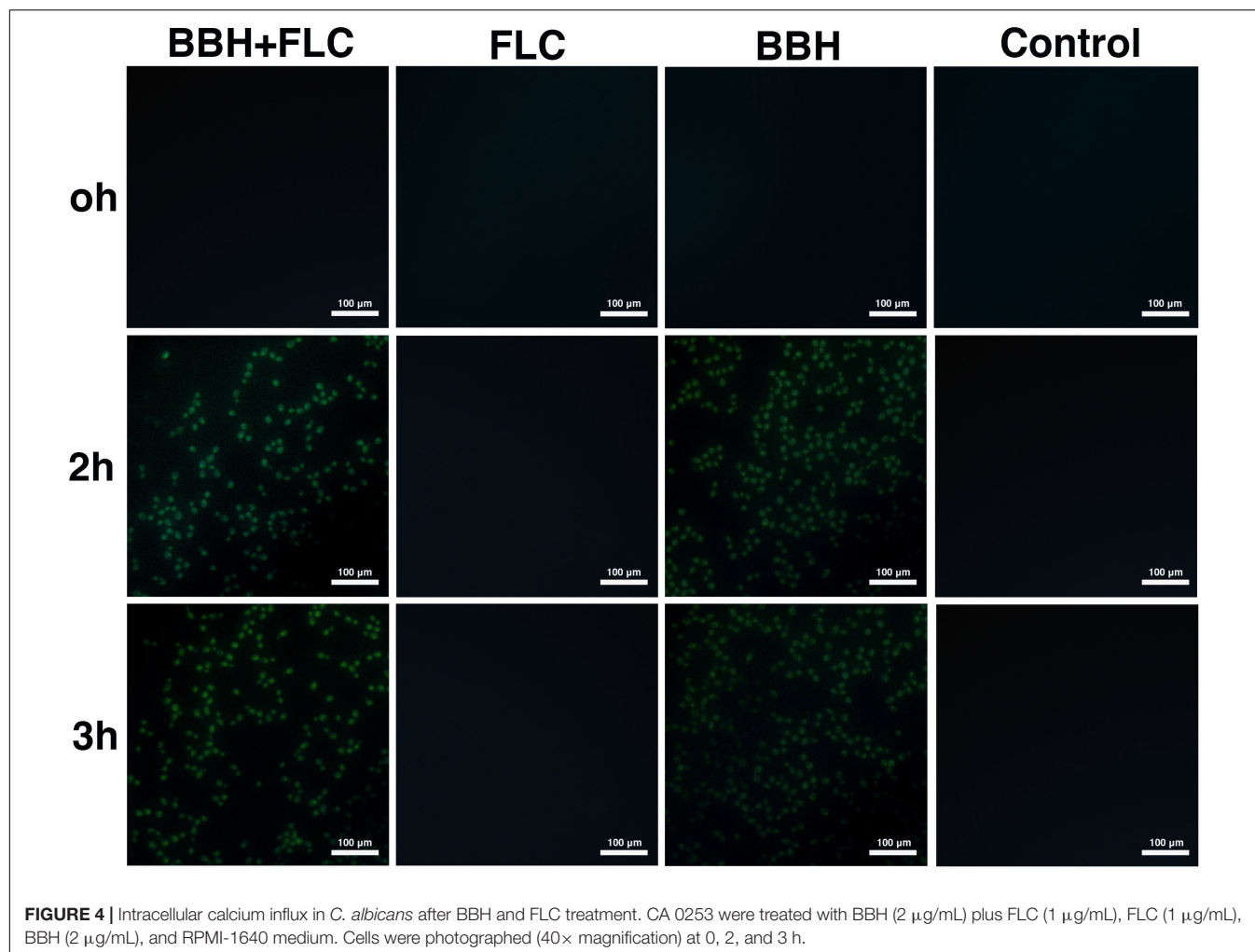
HWPI, *ECE1*, and *ALS3* expression in the BBH + FLC group was significantly decreased by 7.26-, 12.20-, and 3.73-fold, respectively, compared to FLC alone ($p < 0.05$). Further, their expression was substantially reduced by 54.11-, 34.20-, and 13.62-fold, respectively, compared with BBH alone ($p < 0.05$). There was no significant difference in *HWPI* ($p = 0.499$) or *ALS3* ($p = 0.396$) expression between the FLC alone and control groups, while *ECE1* expression was increased 5.68-fold after FLC treatment alone ($p < 0.05$).

Compared with the control group, FLC alone downregulated *YVC1* expression. However, *YVC1* was upregulated after BBH + FLC therapy and BBH monotherapy ($p < 0.05$). Nonetheless, *YVC1* expression in the combined group was 1.62- and 6.47-fold higher than in the BBH alone and FLC alone groups, respectively ($p < 0.05$). Compared with the control group, *PMC1* expression increased when exposed to FLC alone, and decreased when exposed to BBH + FLC or BBH alone ($p < 0.05$). BBH + FLC significantly downregulated *PMC1*



by 5.28-fold compared with FLC alone ($p < 0.05$). There was no significant difference between the combined group and the BBH alone group. BBH + FLC and FLC alone significantly

downregulated *VCX1* and *PMR1* expression, but the difference between the groups was not significant difference. Combined BBH and FLC significantly downregulated *VCX1* and *PMR1*



expression by 8.89- and 1.69-fold, respectively, compared with BBH alone ($P < 0.05$). These results indicate that BBH combined with FLC significantly downregulates genes for the efflux pump *CDR1*, hyphal-associated *ALS3*, *HWP1*, and *ECE1*, and the calcium pump *PMC1*.

DISCUSSION

Berberine has multiple antibacterial and antifungal activities, which suppress Gram-positive and Gram-negative bacteria, and also suppress FLC-resistant *Candida* and *Cryptococcus neoformans* (Čerňáková and Košťálová, 2002; Tillhon et al., 2012; da Silva et al., 2016). Previous studies have shown that berberine induces a significant increase in DNA strand break and DNA damage. Berberine not only destroys the cell wall integrity in *C. albicans*, but also targets the cell membrane by affecting ergosterol synthesis, resulting in increased membrane permeability (da Silva et al., 2016; Zorić et al., 2017). In our study, BBH treatment alone exerted weak antifungal effects for all resistant isolates. However, it has been reported that high doses of berberine can cause functional damage to the lungs, liver,

and intestines of experimental animals. Therefore, combination therapy will be an effective strategy to reduce the toxic side effects of berberine. Because BBH + FLC will produce synergistic effect and enhance drug sensitivity, thereby significantly reducing

TABLE 3 | Intracellular Ca^{2+} fluorescence in *C. albicans* after BBH and FLC treatment.

CA 0253	Time of drug action		
	0 h	2 h	3 h
BBH + FLC $\blacklozenge\star\blacktriangle$	4364.70 \pm 44.33	5623.23 \pm 41.16	5492.60 \pm 11.00
FLC $\star\Delta$	3389.07 \pm 4.18	4793.57 \pm 9.49	4679.17 \pm 24.69
BBH \blacktriangle	4158.93 \pm 53.24	5266.37 \pm 14.98	5080.40 \pm 16.00
Control	3169.30 \pm 54.53	4773.53 \pm 45.29	4736.17 \pm 16.4

CA 0253 were treated with BBH (2 $\mu\text{g/mL}$) plus FLC (1 $\mu\text{g/mL}$), FLC (1 $\mu\text{g/mL}$), BBH (2 $\mu\text{g/mL}$), and RPMI-1640 medium. Fluorescence was measured (emission: 530 nm) at 0, 2, and 3 h. Three independent experiments were performed, with eight replicates in each group ($n = 8$). Values represent means \pm SEM. ANOVA tested statistical differences. \blacklozenge compared with the FLC group, $p < 0.05$; \star compared with the BBH group, $p < 0.05$; \blacktriangle compared with the control group, $p < 0.05$; Δ compared with the control group, $p > 0.05$.

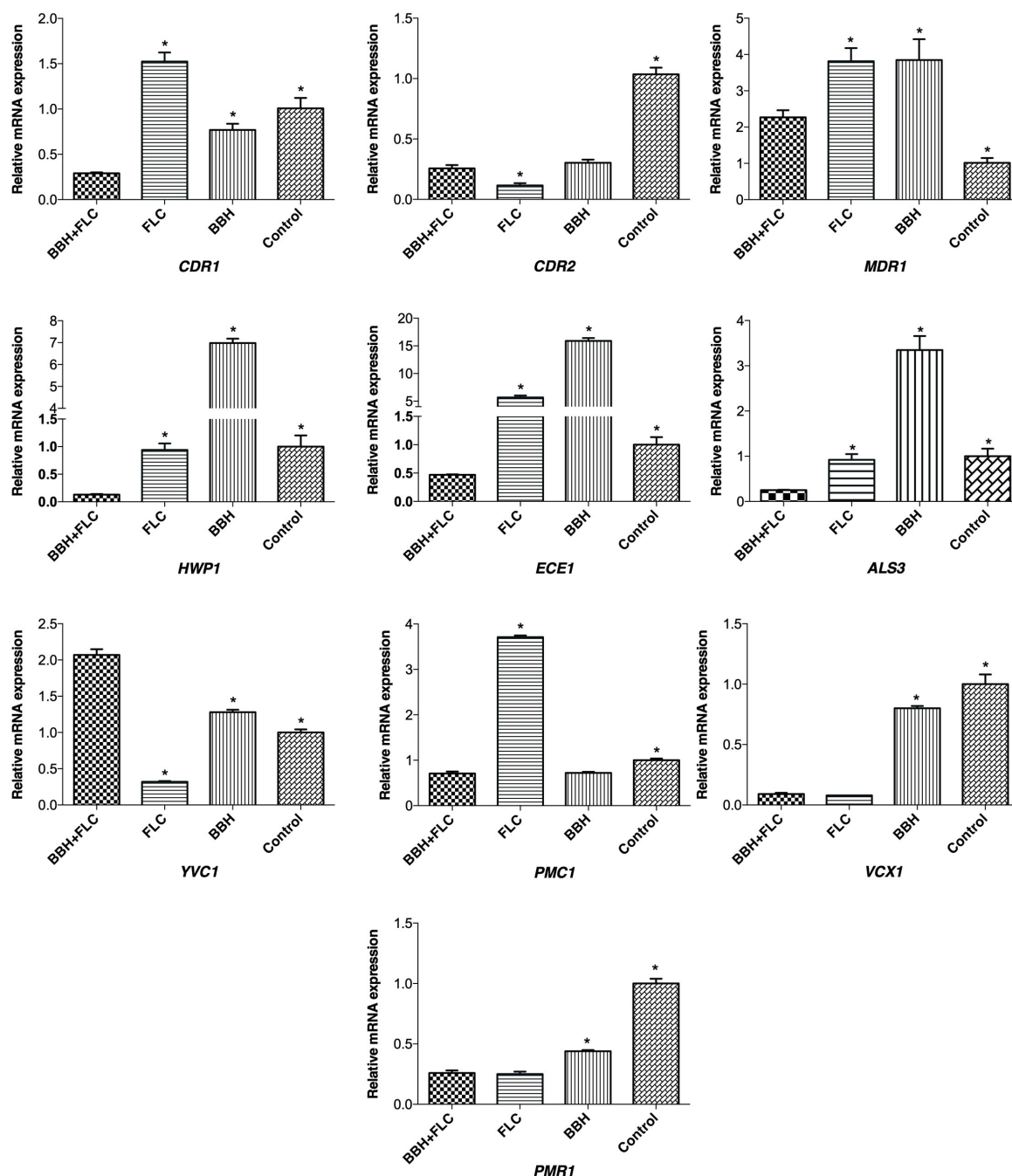


FIGURE 5 | Genes expression in *C. albicans* after BBH and FLC treatment. CA 0253 were treated with BBH (2 $\mu\text{g/mL}$) plus FLC (1 $\mu\text{g/mL}$), FLC (1 $\mu\text{g/mL}$), BBH (2 $\mu\text{g/mL}$), and RPMI-1640 medium. Three independent experiments were performed, with 8 replicates in each group ($n = 8$). * $p < 0.05$, compared to the BBH + FLC groups, ANOVA.

effective drug concentration and reducing the possibility of toxic and side effects (Singh et al., 2018). Time-kill curve assays further demonstrated that the dynamic antifungal effect of combined BBH and FLC was significantly better than the drug-monotherapy groups within 48 h. Efflux pump, biofilm, and calcium-signaling pathways are important factors underlying *C. albicans* FLC resistance. Importantly, these cellular processes

are not independent, but interact with each other in the fungus. Constitutive efflux pump upregulation, including CDR1, CDR2, and MDR1, is a key contributor to early biofilm resistance in *C. albicans* (Nobile and Johnson, 2015). Luna-Tapia et al. (2019) demonstrated that the calcium pump Pmc1p is essential for transformation from yeast-to-hyphae and biofilm formation. Previous work indicated that the vacuolar calcium channel Yvc1p

participates in hyphal elongation and maintenance by regulating hyphal-associated gene expression (Yu et al., 2014). In this study, the effects of combined BBH and FLC on mechanisms leading to FLC resistance were assessed to investigate possible mechanisms for increasing drug sensitivity of FLC-resistant strains.

One important reason for FLC resistance in *C. albicans* is enhanced efflux pump activity (Cdr1p, Cdr2p, and Mdr1p), causing FLC to be pumped out of the cell (Cannon et al., 2009; Dhamgaye et al., 2014; Prasad and Rawal, 2014). Antifungal agents such as farnesol or clorgyline are ATP-binding cassette superfamily (ABC) and major facilitator class (MFS) transporter inhibitors, which could reverse *C. albicans* azole resistance (Holmes et al., 2012; Černáková et al., 2019). Therefore, regulating drug transporter activity would increase FLC sensitivity. According to our results, BBH + FLC, BBH alone and FLC alone reduce Rh6G excretion by decreasing *CDR1* and *CDR2* mRNA expression. Previous studies reported that Eucalyptal D (Xu et al., 2019) geraniol (Singh and Sharma, 2018) and magnolol (Sun L. M. et al., 2015) which are substrates for Cdr1p efflux pumps, exert synergistic effects by simultaneously upregulating *CDR1* and *CDR2* expression, while competitively inhibiting FLC efflux. Numerous studies suggest that synergy results from increased intracellular drug accumulation caused by downregulated efflux pump genes in FLC-resistant strains (Garcia-Gomes et al., 2012; Zhu et al., 2014; Shao et al., 2016). Although Rh6G efflux gradually increased in all groups, much lower Rh6G efflux and *CDR1* expression were detected in the BBH + FLC group, confirming previous results. In addition, *CDR1* inhibition in the BBH + FLC group was higher than *CDR2*, because the FLC-resistant strain treated with BBH + FLC revealed considerably decreased *CDR1* mRNA expression compared with the drug-monotherapy groups. However, the inhibitory effect on *CDR2* in the BBH + FLC group was not significantly superior. Previous studies showed that deleting the *CDR1* gene significantly reduces FLC resistance, while deleting *CDR2* has a relatively weak effect (Tsao et al., 2009). Based on efflux function, both Holmes et al. (2008) and Tsao et al. (2009) demonstrated that *Cdr1p* plays the most important role in inducing azole resistance. Therefore, *CDR1* mRNA expression decreased after BBH + FLC therapy, whereas *CDR1* upregulation with FLC treatment was observed in resistant strains. These results might be a crucial reason for increasing FLC sensitivity.

Candida albicans biofilm formation can significantly enhance antifungal drug resistance, causing increased azole MIC values by more than 1,000-fold. However, no biofilm-specific drugs exist today (Nobile and Johnson, 2015). *C. albicans* is polymorphic and capable of undergoing reversible morphological transformation between yeast, pseudohyphae, and hyphae (Sudbery et al., 2004; Noble et al., 2017). Inhibiting the yeast-to-hyphae transition can lead to biofilm formation defects, which is a new target for biofilm-specific therapeutics (Romo et al., 2017; Vila et al., 2017). We found that hyphae formation in *C. albicans* was effectively inhibited by combined BBH + FLC treatment, with very few yeast cells remaining after treatment. However, hyphae formation was not inhibited in the drug-monotherapy groups and was accompanied by numerous hyphae and pseudohyphae. The formation of hyphae upregulates the

expression of the hyphal-specific genes *HWPI*, *ALS3*, and *ECE1* in the core filamentation response network, maintaining filament morphology and function (Finkel and Mitchell, 2011; Koch et al., 2018). Our results showed that BBH + FLC causes *C. albicans* hyphal structure formation failure by inhibiting *HWPI*, *ECE1*, and *ALS3* expression. The drug-monotherapy groups could not effectively inhibit hyphal-specific gene expression, such as *ECE1* upregulation after FLC exposure, or *HWPI*, *ALS3*, and *ECE1* upregulation after BBH exposure, indicated by numerous hyphae or pseudohyphae. Hyphae are physical scaffolds for yeast cell adhesion and aggregation, which enable increased biofilm strength, integrity, and maturation (Haque et al., 2016; Lee et al., 2019). *HWPI* mutants produce a thin biofilm with less hyphae *in vitro*, but display serious biofilm defects *in vivo*, only forming yeast microcolonies (Nobile et al., 2006b). *ALS3* mutants are able to form hyphae, but exhibit defects in biofilm formation (Nobile et al., 2006a, 2008). Our results support this observation. Indeed, only the combined BBH + FLC group had biofilm defects, which might be related to hyphae-specific gene inhibition. In addition, *ALS3* and *HWPI* are also capable of regulating the initial adhesion of yeast cells to surfaces, which is essential for all stages of biofilm development (Nobile et al., 2006a; Nobile and Johnson, 2015). Compared with other groups, the BBH + FLC group had significantly reduced yeast cell surface adherence, which inhibited the development of the initial basal cell layer of biofilm formation (0–12 h), thereby suppressing biofilm formation. This inhibition might be associated with downregulated *HWPI* and *ALS3* expression.

Intracellular calcium is closely related to the regulation of stress responses, antifungal drug resistance, and morphogenetic filament conversion in *C. albicans* (Juvvadi et al., 2014; Liu et al., 2015). Cytoplasmic Ca^{2+} in *C. albicans* is usually low, and calcium hypersensitivity induced by high cytoplasmic Ca^{2+} leads to toxicity and cell death (Li et al., 2018). Based on cytoplasmic calcium assay results, FLC alone failed to disrupt Ca^{2+} homeostasis in FLC-resistant *C. albicans*, but BBH + FLC and BBH monotherapy increased cytoplasmic Ca^{2+} . These results indicate that BBH might be a key factor in inducing high cytoplasmic Ca^{2+} . The calcium cell survival (CCS) pathway is the major calcium-signaling pathway maintaining Ca^{2+} homeostasis in *C. albicans* (Li et al., 2018). Indeed, CCS pathway activation induces calcium-related gene expression in response to increased Ca^{2+} , which decreases the intracellular Ca^{2+} concentration by transporting excess cytoplasmic Ca^{2+} into internal compartments, including vacuoles, endoplasmic reticulum, and the Golgi apparatus (Juvvadi et al., 2014; Liu et al., 2016). RT-qPCR results showed that BBH + FLC and BBH monotherapy significantly upregulates *YVC1* and downregulates *PMC1*, while FLC monotherapy had the opposite effect. Vacuoles serve as the major storage site for excess Ca^{2+} in *C. albicans*. *Yvc1p* localized on the vacuolar membrane mediates Ca^{2+} release from the vacuole into the cytoplasm, while the P-type ATPase *Pmc1p* translocates Ca^{2+} from cytoplasm into the vacuole using ATP hydrolysis (Bouillet et al., 2012; Luna-Tapia et al., 2019). According to these previous studies and our results, BBH + FLC and BBH monotherapy promote Ca^{2+} release from the vacuole into the cytoplasm by upregulating

YVC1 and reduce excess cytoplasmic Ca^{2+} transport into the vacuole by downregulating *PMC1*. Together, this causes increased cytoplasmic Ca^{2+} , which enhances drug sensitivity in FLC-resistant *C. albicans*. However, *YVC1* could be downregulated to prevent Ca^{2+} transport into the cytoplasm after FLC treatment. In addition, upregulated *PMC1* promotes Ca^{2+} transport into the vacuole and effectively prevents increased cytoplasmic Ca^{2+} , which might be an important cause of FLC resistance. The $\text{H}^+/\text{Ca}^{2+}$ exchanger *Vcx1p* transports Ca^{2+} into the vacuole using the proton-motive force across the vacuolar membrane. The calcium pump *Pmr1p* transfers Ca^{2+} to the Golgi apparatus (Förster and Kane, 2000; Jiang et al., 2018). In our study, both FLC monotherapy and BBH + FLC downregulated *Vcx1* and *PMR1*, but there was no statistical difference. Luna-Tapia et al. (2019) reported that *pmc1* Δ/Δ mutants are severely impaired by high Ca^{2+} concentration in the medium, because they are unable to transport Ca^{2+} from the cytoplasm into the vacuole. However, *vcx1* Δ/Δ mutants are unaffected by high Ca^{2+} , demonstrating that *Pmc1p* is required for *C. albicans* pathogenicity, FLC tolerance, and hyphal growth (Luna-Tapia et al., 2019). Thus, *YVC1* and *PMC1* might be the most important calcium-related genes to maintain cellular calcium homeostasis in FLC-resistant *C. albicans*, and may be antifungal therapy targets. The flow cytometry results showed that the cytoplasmic Ca^{2+} in the BBH + FLC group was higher than in the BBH monotherapy group, indicating that their combined use further enhances cytoplasmic Ca^{2+} . Although there was no significant difference in *PMC1* expression, *YVC1* expression in the BBH + FLC group was higher than in the BBH monotherapy group, which might explain the higher cytoplasmic Ca^{2+} in the BBH + FLC group.

Our study found that BBH + FLC treatment exerts a synergistic antifungal effect by regulating efflux pumps, hyphae, and calcium-related pathways. One limitation of this study is that additional synergistic regulatory sites need to be further explored. Hyphae are a key factor for *C. albicans* virulence and invasiveness, and some researchers observed that Ca^{2+} -regulated genes *YVC1* and *PMC1* deletion cause hyphae defects in *C. albicans* (Yu et al., 2014; Luna-Tapia et al., 2019). We found that combined BBH + FLC simultaneously regulates vacuolar Ca^{2+} -regulated genes and significantly inhibits yeast-to-hyphae conversion. Therefore, how BBH + FLC modulates vacuolar Ca^{2+} regulation and hyphae formation in biofilm-positive FLC-resistant *C. albicans* will be explored in future studies. We also found that the Ca^{2+} channel, *YVC1*, and the Ca^{2+} pump, *PMC1*, increase cytoplasmic Ca^{2+} in *C. albicans*, and gene transcription level of resistant isolate treated with BBH + FLC and FLC alone were completely opposite. This finding informs further study of key targets to inhibit biofilm-positive FLC-resistant *C. albicans*.

CONCLUSION

Berberine hydrochloride synergistically suppresses FLC efflux, hyphae and biofilm formation, and induces high cytoplasmic Ca^{2+} , indicating that the combination could restore FLC antifungal activity in FLC-resistant *C. albicans* by regulating multiple targets. This paper provides state-of-the-art TCM

antimicrobial research, demonstrates that TCMs have multi-target antimicrobial effects, and suggests new ideas for resistant strain treatments. These findings clearly suggest that BBH + FLC may be an effective therapeutic option for infections related to FLC-resistant *C. albicans*, especially biofilm-positive resistant isolates. Future experiments will explore the relationship between hyphae formation and Ca^{2+} signaling pathways, and further study the key nodes inhibiting biofilm-positive FLC-resistant *C. albicans*.

DATA AVAILABILITY STATEMENT

The datasets generated for this study are available on request to the corresponding author.

ETHICS STATEMENT

This study was carried out in accordance with the recommendations of Specimen Collection and Transport in Clinical Microbiology (WS/T640-2018), People's Republic of China Health Industry Standard. The protocol was approved by the National Health Commission of the People's Republic of China. Informed consent was not needed as this study was retrospective without involving any information from patients.

AUTHOR CONTRIBUTIONS

JY and YL conceived and designed the experiments. JY performed the experiments. JY, RZ, XH, YG, and YL contributed to reagents, data analysis, and interpretation. JY and YL wrote the manuscript. All authors approved the manuscript for publication.

FUNDING

This work was supported by the Science and Technology Innovation Project of Sichuan Educational Committee, People's Republic of China (17TD0013) and the "Xinglin Scholar" Scientific Research Project of Chengdu University of TCM (JSZX2018006).

ACKNOWLEDGMENTS

We are grateful to the clinical laboratory of Chengdu University of Traditional Chinese Medicine Hospital, China for providing clinical isolates. We also would like to thank Editage [www.editage.cn] for English language editing.

SUPPLEMENTARY MATERIAL

The Supplementary Material for this article can be found online at: <https://www.frontiersin.org/articles/10.3389/fmicb.2020.01498/full#supplementary-material>

TABLE S1 | Primer sequences used in this study.

REFERENCES

- Bouillet, L., Cardoso, A. S., Perovano, E., Pereira, R., Ribeiro, E. M., Trópia, M. J. M., et al. (2012). The involvement of calcium carriers and of the vacuole in the glucose-induced calcium signaling and activation of the plasma membrane H⁺-ATPase in *Saccharomyces cerevisiae* cells. *Cell Calcium* 51, 72–81. doi: 10.1016/j.ceca.2011.10.008
- Cai, Z., Wang, C., and Yang, W. (2016). Role of berberine in Alzheimer's disease. *Neuropsychiatr. Dis. Treat.* 12:2509. doi: 10.2147/ndt.s114846
- Cannon, R. D., Lamping, E., Holmes, A. R., Niimi, K., Baret, P. V., Keniya, M. V., et al. (2009). Efflux-mediated antifungal drug resistance. *Clin. Microbiol. Rev.* 22, 291–321.
- Černáková, L., Dižová, S., Gášková, D., Jančíková, I., and Bujdaková, H. (2019). Impact of farnesol as a modulator of efflux pumps in a fluconazole-resistant strain of *Candida albicans*. *Microb. Drug Resist.* 25, 805–812. doi: 10.1089/mdr.2017.0332
- Černáková, M., and Košťálová, D. (2002). Antimicrobial activity of berberine—A constituent of *Mahonia aquifolium*. *Folia Microbiol.* 47, 375–378. doi: 10.1007/bf02818693
- Chen, Y.-X., Gao, Q.-Y., Zou, T.-H., Wang, B.-M., Liu, S.-D., Sheng, J.-Q., et al. (2019). Berberine Hydrochloride For The Prevention Of Colorectal Adenomas: A Double-Blind, Randomised Controlled Multicenter Clinical Trial. Available online at: <https://ssrn.com/abstract=3414428>
- CLSI (2008). *Reference Methods for Broth Dilution Antifungal Susceptibility Testing Of Yeast; Approved Standard-Third Edition, CLSI Document M27-A3*. Wayne, PA: CLSI.
- da Silva, A. R., de Andrade Neto, J. B., da Silva, C. R., de Sousa Campos, R., Silva, R. A. C., Freitas, D. D., et al. (2016). Berberine antifungal activity in fluconazole-resistant pathogenic yeasts: action mechanism evaluated by flow cytometry and biofilm growth inhibition in *Candida* spp. *Antimicrob. Agents Chemother.* 60, 3551–3557. doi: 10.1128/aac.01846-15
- Dhangay, S., Devaux, F., Vandeputte, P., Khandelwal, N. K., Sanglard, D., Mukhopadhyay, G., et al. (2014). Molecular mechanisms of action of herbal antifungal alkaloid berberine, in *Candida albicans*. *PLoS One* 9:e104554. doi: 10.1371/journal.pone.0104554
- Finkel, J. S., and Mitchell, A. P. (2011). Genetic control of *Candida albicans* biofilm development. *Nat. Rev. Microbiol.* 9:109. doi: 10.1038/nrmicro2475
- Förster, C., and Kane, P. M. (2000). Cytosolic Ca²⁺ homeostasis is a constitutive function of the V-ATPase in *Saccharomyces cerevisiae*. *J. Biol. Chem.* 275, 38245–38253. doi: 10.1074/jbc.m006650200
- Garcia-Gomes, A., Curvelo, J., Soares, R. A., and Ferreira-Pereira, A. (2012). Curcumin acts synergistically with fluconazole to sensitize a clinical isolate of *Candida albicans* showing a MDR phenotype. *Med. Mycol.* 50, 26–32. doi: 10.3109/13693786.2011.578156
- Haque, F., Alfatah, M., Ganesan, K., and Bhattacharyya, M. S. (2016). Inhibitory effect of sophorolipid on *Candida albicans* biofilm formation and hyphal growth. *Sci. Rep.* 6:23575.
- Holmes, A. R., Keniya, M. V., Ivnitki-Steele, I., Monk, B. C., Lamping, E., Sklar, L. A., et al. (2012). The monoamine oxidase A inhibitor clorgyline is a broad-spectrum inhibitor of fungal ABC and MFS transporter efflux pump activities which reverses the azole resistance of *Candida albicans* and *Candida glabrata* clinical isolates. *Antimicrob. Agents Chemother.* 56, 1508–1515. doi: 10.1128/aac.05706-11
- Holmes, A. R., Lin, Y.-H., Niimi, K., Lamping, E., Keniya, M., Niimi, M., et al. (2008). ABC transporter Cdr1p contributes more than Cdr2p does to fluconazole efflux in fluconazole-resistant *Candida albicans* clinical isolates. *Antimicrob. Agents Chemother.* 52, 3851–3862. doi: 10.1128/aac.00463-08
- Imenshahidi, M., and Hosseinzadeh, H. (2019). Berberine and barberry (*Berberis vulgaris*): a clinical review. *Phytother. Res.* 33, 504–523. doi: 10.1002/ptr.6252
- Jiang, L., Wang, J., Asghar, F., Snyder, N., and Cunningham, K. W. (2018). CaGdt1 plays a compensatory role for the calcium pump CaPmr1 in the regulation of calcium signaling and cell wall integrity signaling in *Candida albicans*. *Cell Commun. Signal.* 16:33.
- Juvvadi, P. R., Lamothe, F., and Steinbach, W. J. (2014). Calcineurin as a multifunctional regulator: unraveling novel functions in fungal stress responses, hyphal growth, drug resistance, and pathogenesis. *Fungal Biol. Rev.* 28, 56–69. doi: 10.1016/j.fbr.2014.02.004
- Koch, B., Barugahare, A. A., Lo, T. L., Huang, C., Schittenhelm, R. B., Powell, D. R., et al. (2018). A metabolic checkpoint for the yeast-to-hyphae developmental switch regulated by endogenous nitric oxide signaling. *Cell Rep.* 25, 2244–2258.
- Kuo, C.-L., Chi, C.-W., and Liu, T.-Y. (2004). The anti-inflammatory potential of berberine in vitro and in vivo. *Cancer Lett.* 203, 127–137. doi: 10.1016/j.canlet.2003.09.002
- Lau, C. W., Yao, X. Q., Chen, Z. Y., Ko, W. H., and Huang, Y. (2001). Cardiovascular actions of berberine. *Cardiovasc. Drug. Rev.* 19, 234–244. doi: 10.1111/j.1527-3466.2001.tb00068.x
- Lee, J.-H., Kim, Y.-G., Khadke, S. K., Yamano, A., Watanabe, A., and Lee, J. (2019). Inhibition of biofilm formation by *Candida albicans* and polymicrobial microorganisms by nepodin via hyphal-growth suppression. *ACS Infect. Dis.* 5, 1177–1187. doi: 10.1021/acsinfecdis.9b00033
- Li, Y., Sun, L., Lu, C., Gong, Y., Li, M., and Sun, S. (2018). Promising antifungal targets against *Candida albicans* based on ion homeostasis. *Front. Cell. Infect. Microbiol.* 8:286. doi: 10.3389/fcimb.2018.00286
- Liu, S., Hou, Y., Liu, W., Lu, C., Wang, W., and Sun, S. (2015). Components of the calcium-calcineurin signaling pathway in fungal cells and their potential as antifungal targets. *Eukaryot. Cell* 14, 324–334. doi: 10.1128/ec.00271-14
- Liu, S., Yue, L., Gu, W., Li, X., Zhang, L., and Sun, S. (2016). Synergistic effect of fluconazole and calcium channel blockers against resistant *Candida albicans*. *PLoS One* 11:e0150859. doi: 10.1371/journal.pone.0150859
- Luna-Tapia, A., DeJarnette, C., Sansevere, E., Reitler, P., Butts, A., Hevener, K. E., et al. (2019). The vacuolar Ca²⁺ ATPase Pump Pmc1p is required for *Candida albicans* pathogenesis. *mSphere* 4:e00715-18.
- Nobile, C. J., and Johnson, A. D. (2015). *Candida albicans* biofilms and human disease. *Annu. Rev. Microbiol.* 69, 71–92.
- Nobile, C. J., Andes, D. R., Nett, J. E., Smith, F. J. Jr., Yue, F., Phan, Q.-T., et al. (2006a). Critical role of Bcr1-dependent adhesins in *C. albicans* biofilm formation in vitro and in vivo. *PLoS Pathog.* 2:e63. doi: 10.1371/journal.pone.0000063
- Nobile, C. J., Nett, J. E., Andes, D. R., and Mitchell, A. P. (2006b). Function of *Candida albicans* adhesin Hwp1 in biofilm formation. *Eukaryot. Cell* 5, 1604–1610. doi: 10.1128/ec.00194-06
- Nobile, C. J., Schneider, H. A., Nett, J. E., Sheppard, D. C., Filler, S. G., Andes, D. R., et al. (2008). Complementary adhesin function in *C. albicans* biofilm formation. *Curr. Biol.* 18, 1017–1024. doi: 10.1016/j.cub.2008.06.034
- Noble, S. M., Gianetti, B. A., and Witchley, J. N. (2017). *Candida albicans* cell-type switching and functional plasticity in the mammalian host. *Nat. Rev. Microbiol.* 15:96. doi: 10.1038/nrmicro.2016.157
- Pfaller, M. A., Diekema, D. J., Turnidge, J. D., Castanheira, M., and Jones, R. N. (2019). Twenty years of the SENTRY antifungal surveillance program: results for *Candida* species from 1997–2016. *Open Forum Infect. Dis.* 6, S79–S94.
- Prasad, R., and Rawal, M. K. (2014). Efflux pump proteins in antifungal resistance. *Front. Pharmacol.* 5:202. doi: 10.3389/fcimb.2018.00202
- Romo, J. A., Pierce, C. G., Chaturvedi, A. K., Lazzell, A. L., McHardy, S. F., Saville, S. P., et al. (2017). Development of anti-virulence approaches for candidiasis via a novel series of small-molecule inhibitors of *Candida albicans* filamentation. *mBio* 8:e01991-17.
- Shao, J., Zhang, M., Wang, T., Li, Y., and Wang, C. (2016). The roles of CDR1, CDR2, and MDR1 in kaempferol-induced suppression with fluconazole-resistant *Candida albicans*. *Pharm. Biol.* 54, 984–992. doi: 10.3109/13880209.2015.1091483
- Sharma, M., Manoharlal, R., Puri, N., and Prasad, R. (2010). Antifungal curcumin induces reactive oxygen species and triggers an early apoptosis but prevents hyphae development by targeting the global repressor TUP1 in *Candida albicans*. *Biosci. Rep.* 30, 391–404. doi: 10.1042/bsr20090151
- Singh, N., and Sharma, B. (2018). Toxicological Effects of berberine and sanguinarine. *Front. Mol. Biosci.* 5:21. doi: 10.3389/fcimb.2018.0021
- Singh, S., Fatima, Z., Ahmad, K., and Hameed, S. (2018). Fungicidal action of geraniol against *Candida albicans* is potentiated by abrogated CaCdr1p drug efflux and fluconazole synergism. *PLoS One* 13:e0203079. doi: 10.1371/journal.pone.0203079
- Sudbery, P., Gow, N., and Berman, J. (2004). The distinct morphogenic states of *Candida albicans*. *Trends Microbiol.* 12, 317–324. doi: 10.1016/j.tim.2004.05.008

- Sun, L., Liao, K., and Wang, D. (2015). Effects of magnolol and honokiol on adhesion, yeast-hyphal transition, and formation of biofilm by *Candida albicans*. *PLoS One* 10:e0117695. doi: 10.1371/journal.pone.0117695
- Sun, L. M., Liao, K., Liang, S., Yu, P. H., and Wang, D. Y. (2015). Synergistic activity of magnolol with azoles and its possible antifungal mechanism against *Candida albicans*. *J. Appl. Microbiol.* 118, 826–838. doi: 10.1111/jam.12737
- Tian, H., Qu, S., Wang, Y., Lu, Z., Zhang, M., Gan, Y., et al. (2017). Calcium and oxidative stress mediate perillaldehyde-induced apoptosis in *Candida albicans*. *Appl. Microbiol. Biotechnol.* 101, 3335–3345. doi: 10.1007/s00253-017-8146-3
- Tillhon, M., Ortiz, L. M. G., Lombardi, P., and Scovassi, A. I. (2012). Berberine: new perspectives for old remedies. *Biochem. Pharmacol.* 84, 1260–1267. doi: 10.1016/j.bcp.2012.07.018
- Tsao, S., Rahkhoodae, F., and Raymond, M. (2009). Relative contributions of the *Candida albicans* ABC transporters Cdr1p and Cdr2p to clinical azole resistance. *Antimicrob. Agents Chemother.* 53, 1344–1352. doi: 10.1128/aac.00926-08
- Vila, T., Romo, J. A., Pierce, C. G., McHardy, S. F., Saville, S. P., and Lopez-Ribot, J. L. (2017). Targeting *Candida albicans* filamentation for antifungal drug development. *Virulence* 8, 150–158. doi: 10.1080/21505594.2016.1197444
- Xiao, M., Sun, Z.-Y., Kang, M., Guo, D.-W., Liao, K., Chen, S. C.-A., et al. (2018). Five-year national surveillance of invasive candidiasis: species distribution and azole susceptibility from the China Hospital Invasive Fungal Surveillance Net (CHIF-NET) study. *J. Clin. Microbiol.* 56:e0577-18.
- Xu, J., Liu, R., Sun, F., An, L., Shang, Z., Kong, L., et al. (2019). Eucalyptal D enhances the antifungal effect of fluconazole on fluconazole-resistant *Candida albicans* by competitively inhibiting efflux pump. *Front. Cell. Infect. Microbiol.* 9:211. doi: 10.3389/fcimb.2018.00211
- Xu, Y., Quan, H., Wang, Y., Zhong, H., Sun, J., Xu, J., et al. (2017). Requirement for ergosterol in berberine tolerance underlies synergism of fluconazole and berberine against fluconazole-resistant *Candida albicans* isolates. *Front. Cell. Infect. Microbiol.* 7:491. doi: 10.3389/fcimb.2018.00491
- Xu, Y., Wang, Y., Yan, L., Liang, R.-M., Dai, B.-D., Tang, R.-J., et al. (2009). Proteomic analysis reveals a synergistic mechanism of fluconazole and berberine against fluconazole-resistant *Candida albicans*: endogenous ROS augmentation. *J. Proteome Res.* 8, 5296–5304. doi: 10.1021/pr9005074
- Yang, Z., Wang, Q., Ma, K., Shi, P., Liu, W., and Huang, Z. (2018). Fluconazole inhibits cellular ergosterol synthesis to confer synergism with berberine against yeast cells. *J. Glob. Antimicrob. Resist.* 13, 125–130. doi: 10.1016/j.jgar.2017.12.011
- Yu, Q., Wang, F., Zhao, Q., Chen, J., Zhang, B., Ding, X., et al. (2014). A novel role of the vacuolar calcium channel Yvc1 in stress response, morphogenesis and pathogenicity of *Candida albicans*. *Int. J. Med. Microbiol.* 304, 339–350. doi: 10.1016/j.ijmm.2013.11.022
- Yun, D. G., and Lee, D. G. (2016). Silibinin triggers yeast apoptosis related to mitochondrial Ca²⁺ influx in *Candida albicans*. *Intern. J. Biochem. Cell Biol.* 80, 1–9. doi: 10.1016/j.biocel.2016.09.008
- Zhu, S.-L., Yan, L., Zhang, Y.-X., Jiang, Z.-H., Gao, P.-H., Qiu, Y., et al. (2014). Berberine inhibits fluphenazine-induced up-regulation of CDR1 in *Candida albicans*. *Biol. Pharm. Bull.* 37, 268–273. doi: 10.1248/bpb.b13-00734
- Zorić, N., Kosalec, I., Tomić, S., Bobnjarić, I., Jug, M., Vlajnić, T., et al. (2017). Membrane of *Candida albicans* as a target of berberine. *BMC Complement. Altern. Med.* 17:268. doi: 10.1186/s12906-017-1773-5

Conflict of Interest: The authors declare that the research was conducted in the absence of any commercial or financial relationships that could be construed as a potential conflict of interest.

Copyright © 2020 Yong, Zu, Huang, Ge and Li. This is an open-access article distributed under the terms of the Creative Commons Attribution License (CC BY). The use, distribution or reproduction in other forums is permitted, provided the original author(s) and the copyright owner(s) are credited and that the original publication in this journal is cited, in accordance with accepted academic practice. No use, distribution or reproduction is permitted which does not comply with these terms.



Toxoplasma gondii Dense Granule Proteins 7, 14, and 15 Are Involved in Modification and Control of the Immune Response Mediated via NF- κ B Pathway

Fumiaki Ihara¹, Ragab M. Fereig^{1,2}, Yuu Himori¹, Kyohko Kameyama¹, Kosuke Umeda¹, Sachi Tanaka^{1,3}, Rina Ikeda¹, Masahiro Yamamoto^{4,5} and Yoshifumi Nishikawa^{1*}

OPEN ACCESS

Edited by:

Marco Rinaldo Oggioni,
University of Leicester,
United Kingdom

Reviewed by:

Christopher Michael Reilly,
Edward Via College of Osteopathic
Medicine, United States
Young-Ha Lee,
School of Medicine, Chungnam
National University, South Korea

*Correspondence:

Yoshifumi Nishikawa
nishikawa@obihiro.ac.jp

Specialty section:

This article was submitted to
Microbial Immunology,
a section of the journal
Frontiers in Immunology

Received: 12 February 2020

Accepted: 26 June 2020

Published: 31 July 2020

Citation:

Ihara F, Fereig RM, Himori Y,
Kameyama K, Umeda K, Tanaka S,
Ikeda R, Yamamoto M and
Nishikawa Y (2020) *Toxoplasma gondii*
Dense Granule Proteins 7, 14, and 15
Are Involved in Modification and
Control of the Immune Response
Mediated via NF- κ B Pathway.
Front. Immunol. 11:1709.
doi: 10.3389/fimmu.2020.01709

¹ National Research Center for Protozoan Diseases, Obihiro University of Agriculture and Veterinary Medicine, Obihiro, Japan, ² Department of Animal Medicine, Faculty of Veterinary Medicine, South Valley University, Qena City, Egypt, ³ Division of Animal Science, Department of Agricultural and Life Sciences, Faculty of Agriculture, Shinshu University, Nagano, Japan, ⁴ Department of Immunoparasitology, Research Institute for Microbial Diseases, Osaka University, Osaka, Japan, ⁵ Laboratory of Immunoparasitology, WPI Immunology Frontier Research Center, Osaka University, Osaka, Japan

Toxoplasma gondii infects almost all warm-blooded animals, including humans, leading to both cellular and humoral immune responses in the host. The virulence of *T. gondii* is strain specific and is defined by secreted effector proteins that disturb host immunity. Here, we focus on nuclear factor-kappa B (NF κ B) signaling, which regulates the induction of T-helper type 1 immunity. A luciferase assay for screening effector proteins, including ROPs and GRAs that have biological activity against an NF κ B-dependent reporter plasmid, found that overexpression of GRA7, 14, and 15 of a type II strain resulted in a strong activity. Thus, our study was aimed at understanding the involvement of NF κ B in the pathogenesis of toxoplasmosis through a comparative analysis of these three molecules. We found that GRA7 and GRA14 were partially involved in the activation of NF κ B, whereas GRA15 was essential for NF κ B activation. The deletion of GRA7, GRA14, and GRA15 in the type II Prugniaud (Pru) strain resulted in a defect in the nuclear translocation of RelA. Cells infected with the Pru Δ gra15 parasite showed reduced phosphorylation of inhibitor- κ B α . GRA7, GRA14, and GRA15 deficiency decreased the levels of interleukin-6 in RAW246.7 cells, and RNA-seq analysis revealed that GRA7, GRA14, and GRA15 deficiency predominantly resulted in downregulation of gene expression mediated by NF κ B. The virulence of all mutant strains increased, but Pru Δ gra14 only showed a slight increase in virulence. However, the intra-footpad injection of the highly-virulent type I RH Δ gra14 parasites in mice resulted in increased virulence. This study shows that GRA7, 14, and 15-induced host immunity via NF κ B limits parasite expansion.

Keywords: *Toxoplasma gondii*, dense granule protein, NF κ B, immune response, host-pathogen interaction

INTRODUCTION

The obligate intracellular protozoan parasite *Toxoplasma gondii* can cause congenital toxoplasmosis, opportunistic infections in immunocompromised patients, and ocular disease (1–3). Epidemiological investigation of toxoplasmosis revealed that the majority of European and North American strains of the parasite belong to three distinct clonal lineages: type I, II, and III (4). These strains differ in virulence in mice: type I strains are the most virulent with a lethal dose (LD₁₀₀) of one parasite, whereas the LD₅₀ of type II and III strains are $\sim 10^3$ and 10^5 , respectively (5). Previous studies demonstrated that virulence is largely mediated by several families of secretory pathogenesis determinants (6). These secreted effector proteins originate from different organelles, namely the rhoptries, known as rhoptry proteins (ROPs), and dense granules, known as dense granule proteins (GRAs) (7). Recently, it has become clear that *T. gondii* manipulates and modulates host resistance mechanisms at multiple points along pro-inflammatory pathways, which in turn dictates parasite burden and disease (8).

Nuclear factor-kappa B (NF κ B), the central mediator of inflammatory responses and immune function, comprises homo- and heterodimers of five members: NF κ B1 (p50), NF κ B2 (p52), RelA (p65), RelB, and c-Rel (9, 10). The NF κ B complex structure resides in the cytoplasm of unstimulated cells, where it is complexed with the inhibitor- κ B (I κ B) family of proteins, such as I κ B α , I κ B β , and I κ B ϵ , which bind to the NF κ B DNA binding domain and dimerization domain, the Rel homology domain, and thereby interfere with the function of the nuclear localization signal (11). Upon exposure to various infectious and inflammatory stimuli, the inhibitor proteins are phosphorylated, resulting in their ubiquitination and degradation, allowing the nuclear translocation of NF κ B dimers to regulate gene expression (10). Many pathogens, including viruses, bacteria, and protozoa, have been reported to modulate the host NF κ B pathway to optimize survival in the host (12).

Mice lacking c-Rel and RelB are highly susceptible to intraperitoneally infection with *T. gondii* and die within 10–15 days of infection, indicating the importance of the NF κ B pathway for an adequate response to *T. gondii* infection (13, 14). C-Rel^{-/-} mice show an early defect in the number of IL-12p40-producing cells among the peritoneal exudates cells collected at 12, 24, and 48 h post-infection, although within 2–3 days this defect is no longer apparent (14). Moreover, increased susceptibility of c-Rel^{-/-} mice can be rescued by administration of IL-12 until 2 days post-infection, indicating that delayed production of IL-12 up to 2 days post-infection causes decreased production of IFN- γ and a failure to control the parasite burden (14). Despite these findings, modulation of the NF κ B pathway by *T. gondii* remains to be further elucidated.

In this study, we used an NF κ B-luciferase assay to screen candidates for their ability to regulate NF κ B activity. We found that overexpression of GRA7, 14, and 15 in a type II strain resulted in strong NF κ B activity; thus, we focused on these proteins. *Toxoplasma* GRA15 accounts for differences in NF κ B activation among different strains (15). Recombinant GRA7 protein also has potent activity against the NF κ B

pathway; however, it is unclear whether endogenous GRA7 is capable of affecting the NF κ B pathway (16). GRA14, which is secreted into the vacuole, can be transferred to both the parasitophorous vacuole (PV) membrane (PVM) and the intravacuolar network (17). However, the molecular function of this protein remains unknown. Thus, the aim of this study was to gain a comprehensive understanding of the involvement of NF κ B in the pathogenesis of toxoplasmosis by comparative analysis of three molecules that modulate inflammatory cytokines and chemokines, to ultimately aid the development of strategies to control chronic *Toxoplasma* infections.

MATERIALS AND METHODS

Reagents

Anti-RelA (Sc-109) antibody was obtained from Santa Cruz Biotechnology (Santa Cruz, CA, USA). Anti-total I κ B α (#9242), anti-phospho-I κ B α (#2859), and anti-glyceraldehyde-3-phosphate dehydrogenase (GAPDH, #2118) were purchased from Cell Signaling Technology (Beverly, MA, USA).

Ethics Statement

The use and care of animals complied with the Guide for the Care and Use of Laboratory Animals from the Ministry of Education, Culture, Sports, Science, and Technology, Japan. The experimental protocol was approved by the Committee on the Ethics of Animal Experiments at the Obihiro University of Agriculture and Veterinary Medicine (permit number: 19-50). All efforts were made to minimize animal suffering.

Experimental Design

First, we constructed 17 GRAs and 21 ROPs expressing vectors. Then they were transiently transfected into 293T cells for monitoring NF κ B activity. Next, 293T cells were infected with the parental Pru, Pru Δ gra7, Pru Δ gra14, and Pru Δ gra15 parasite strains and assessed their effect on NF κ B activity. We evaluated the nuclear translocation of RelA in 293T cells overexpressing GRA7, GRA14, and GRA15 alone. Moreover, we also examined it in HFF cells infected with each parasite strain. Then, level of phosphorylated-I κ B α in HFF cells infected with parasite strains were quantified. After that, we measured level of secreted IL-6 in Raw246.7 mouse macrophage cells infected with parasite strains, and then their RNA samples were supplied for transcriptome analysis. Lastly, we conducted survival test of both mice infected with type II *T. gondii* strains and mice infected with type I *T. gondii* strains.

Parasites and Cell Culture

Toxoplasma gondii (type II, Pru Δ ku80 Δ hxgprrt and type I, RH Δ hxgprrt, RH Δ hxgprrt Δ gra7, and RH Δ hxgprrt Δ gra14) was maintained in monkey kidney adherent epithelial (Vero) cells in Eagle's minimum essential medium (MEM, Sigma, St. Louis, MO, USA) with 8% fetal bovine serum (FBS) and the appropriate antibiotics. RH Δ hxgprrt Δ gra7 and RH Δ hxgprrt Δ gra14 were kindly gifted by Prof. John Boothroyd (Stanford University School of Medicine) and Prof. Peter Bradley (University of California), respectively. Human embryonic kidney (293T) cells,

human foreskin fibroblast (HFF) cells, and Raw264.7 mouse macrophages were cultured in Dulbecco's modified Eagle's medium (DMEM; Sigma) supplemented with 10% FBS and the appropriate antibiotics. For the purification of tachyzoites, infected cells were syringe-lysed using a 27-gauge needle to release the tachyzoite-stage parasites into the medium, which was then filtered using a 5.0- μ m pore-sized filter (Millipore, Bedford, MA, USA).

Plasmid Construction

All of the plasmids and primers used in this study are listed in **Tables 1, 2**. Further details of the plasmid construction can be found in the **Supplemental Methods**.

Luciferase Assay in 293T Cells Expressing *Toxoplasma* Genes

293T cells in a 96-well plate were transfected with pGL4.32[luc2P/NF- κ B-RE/Hygro] (Promega, Madison, WI, USA), together with the pGL4.74[hRluc/TK] vectors (Promega) and the mammalian expression plasmids of each parasite molecule, respectively, using Fugene HD (Promega). The empty p3 \times FLAG-cmv14 vector was used as a negative (empty) control. At 18 h post-transfection, the luciferase activities of the total cell lysates were measured with the Dual-Glo luciferase assay system (Promega).

Generation of Pru Δ gra7 Pru Δ gra14, and Pru Δ gra15 Deletion Mutants, and GRA7- and GRA14-Complemented Strains

The knock-out plasmid (pBS/GFP/TgGRA7KO/HX) was transfected into parental Pru strains, and selected with 25 μ g/ml 3-mercaptopyruvate and 50 μ g/ml xanthine. The electroporation of tachyzoites was performed as described previously (18). The drug-resistant parasites were cloned by limiting dilution and tested by PCR (**Supplemental Figure 1**). PCR-positive clones were further analyzed with western blotting and indirect fluorescent antibody test (IFAT) to confirm the protein expression. To disrupt GRA14 and GRA15 in Pru, we cotransfected the parasite with 50 μ g of the CRISPR plasmid (pSAG1::CAS9-U6::sgTgGRA14 and pSAG1::CAS9-U6::sgTgGRA15), along with an amplicon containing homologous regions of GRA14 and GRA15 surrounding a pyrimethamine-resistant dihydrofolate reductase (DHFR*) cassette (5 μ g), respectively. Insert fragments were prepared by PCR amplification using the primers listed in **Table 2**. Selection by growth for 10 to 14 days in pyrimethamine (1 μ M) was used to obtain stably resistant parasite clones that were subsequently screened by PCR to ensure the correct integration of DHFR* into the GRA14 and GRA15 gene loci (**Supplemental Figure 1**). PCR-positive clones were further analyzed by western blotting and IFAT to confirm the loss of GRA14 expression (**Supplemental Figure 3**). To complement the GRA7 and GRA14 genes, we transfected GRA7- and GRA14-deficient parasites with pSAG1::CAS9-U6::sgUPRT (50 μ g) to target integration to the UPRT locus, along with an amplicon containing the TgGRA7 and TgGRA14 genes containing the

5'- and 3'-untranslated regions (UTRs) (5 μ g), respectively. Stably resistant clones were selected by growth on fluorouracil (10 μ M) for 10 to 14 days and were subsequently screened by PCR to ensure the correct integration into the UPRT gene locus (**Supplemental Figure 1**). PCR-positive clones were further analyzed by western blotting and IFAT to confirm the protein expression (**Supplemental Figure 2**).

Cytokine ELISA

Raw246.7 mouse macrophage cells in a 12-well plate were infected with parasite lines (multiplicity of infection = 0.5) for 24 h, along with control uninfected cells. Then, supernatants were collected and IL-6 levels were determined using a cytokine enzyme-linked immunosorbent assay (ELISA) kit (Mouse OptEIA ELISA set; BD Biosciences, San Jose, CA, USA).

RNA Sequencing and KEGG Pathway Enrichment Analysis

Raw246.7 mouse macrophage cells were infected with parasite lines for 24 h, then cells were lysed and total RNA was extracted using TRI reagent (Sigma). Library preparation was performed using a TruSeq stranded mRNA sample prep kit (Illumina, San Diego, CA, USA). Sequencing was performed on an Illumina HiSeq 2500 platform in a 75-base single-end mode. Illumina Casava1.8.2 software was used for base calling and raw sequence reads were subjected to quality control, then the cleaned reads were mapped to the reference mouse genome (mm10) with CLC Genomics Workbench version 10 (GWB; CLC bio, Aarhus, Denmark) (read mapping parameters: minimum fraction length of read overlap = 0.95 and minimum sequence similarity = 0.95). Only uniquely mapped reads were retained for further analysis. We identified differentially expressed genes (DEGs) as described in detail previously (19). The expression of each gene was compared among parasite lines using the differential expression for RNA-seq function in CLC GWB. DEGs were identified as genes with a fold change in expression of >2 , and a max group mean of >1 . KEGG pathway analysis was also conducted as described in detail in a previous article (19). The list of DEGs was subjected to a KEGG pathway enrichment analysis using the clusterProfiler package (20) in the statistical environment R to assess their overarching function. Following CPM normalization, the expression of each gene in the enriched pathways was normalized with Z-score normalization and visualized. Normalized gene expression was visualized in a heatmap using the heatmap.2 function (21) in the gplots package in R. The genes were hierarchically clustered based on the Pearson correlation distance and the group average method.

IFAT in *T. gondii*-Infected Cells

HFF cells in a 12-well plate were infected with parasites (multiplicity of infection = 1) for 24 h, along with uninfected control cells. The cells were then fixed with 4% (vol/vol) paraformaldehyde in PBS for 15 min at room temperature, permeabilized with 0.1% (vol/vol) Triton X-100 and blocked in PBS with 3% (wt/vol) bovine serum albumin. Cover slips were incubated with primary antibody for 1 h at room temperature, and fluorescent secondary antibody for 1 h at room temperature.

TABLE 1 | Plasmids used in this study.

Plasmid	Description	Use	Source or reference
pBS/GFP/HX		Plasmid for cloning TgGRA7 knock-out vector	This study
pBS/GFP/TgGRA7KO/HX	HXGPRT cassette flanked by two homology arms from the 5'- and 3'- UTR of TgGRA7 gene	The knock-out vector targeting TgGRA7 gene	This study
pSAG1::CAS9-U6::sgUPRT	CAS9 expressed from the <i>Toxoplasma</i> SAG1 promoter and CRISPR gRNA targeting <i>Toxoplasma</i> UPRT produced from the U6 promoter	CRISPR plasmid targeting <i>Toxoplasma</i> UPRT	Addgene
pSAG1::CAS9-U6::sgTgGRA14	CAS9 expressed from the <i>TgSAG1</i> promoter and CRISPR gRNA targeting <i>TgGRA14</i> produced from the U6 promoter	CRISPR plasmid targeting between nucleotides 488 and 489 in <i>TgGRA14</i> gene	This study
pSAG1::CAS9-U6::sgTgGRA15	CAS9 expressed from the <i>TgSAG1</i> promoter and CRISPR gRNA targeting <i>TgGRA15</i> produced from the U6 promoter	CRISPR plasmid targeting between nucleotides 146 and 147 in <i>TgGRA14</i> gene	This study
pUPRT::DHFR-D	DHFR* cassette flanked by two homology arms from the 5'- and 3'-UTR of UPRT gene, respectively	Knockin the DHFR* expressed cassette into targeting gene	Addgene
p3XFLAG-CMV-14		Plasmid for cloning of FLAG tag fused gene	Sigma-Aldrich
p3XFLAG-CMV- <i>TgGRA1</i>	FLAG tag-fused <i>Tg(GOI)</i>	Luciferase reporter assay	This study
p3XFLAG-CMV- <i>TgGRA2</i>			This study
p3XFLAG-CMV- <i>TgGRA3</i>			This study
p3XFLAG-CMV- <i>TgGRA4</i>			This study
p3XFLAG-CMV- <i>TgGRA5</i>			This study
p3XFLAG-CMV- <i>TgGRA6</i>			This study
p3XFLAG-CMV- <i>TgGRA7</i>			This study
p3XFLAG-CMV- <i>TgGRA8</i>			This study
p3XFLAG-CMV- <i>TgGRA9</i>			This study
p3XFLAG-CMV-TgGRA11			This study
p3XFLAG-CMV-TgGRA12			This study
p3XFLAG-CMV-TgGRA14			This study
p3XFLAG-CMV-TgGRA15			This study
p3XFLAG-CMV-TgGRA16			This study
p3XFLAG-CMV-TgGRA23			This study
p3XFLAG-CMV-TgGRA24			This study
p3XFLAG-CMV-TgGRA25			This study
p3XFLAG-CMV-TgROP5			This study
p3XFLAG-CMV-TgROP8			This study
p3XFLAG-CMV-TgROP9			This study
p3XFLAG-CMV-TgROP10			This study
p3XFLAG-CMV-TgROP11			This study
p3XFLAG-CMV-TgROP12			This study
p3XFLAG-CMV-TgROP13			This study
p3XFLAG-CMV-TgROP14			This study
p3XFLAG-CMV-TgROP15			This study
p3XFLAG-CMV-TgROP16			This study
p3XFLAG-CMV-TgROP17			This study
p3XFLAG-CMV-TgROP18			This study
p3XFLAG-CMV-TgROP19A			This study
p3XFLAG-CMV-TgROP20			This study
p3XFLAG-CMV-TgROP23			This study
p3XFLAG-CMV-TgROP24			This study
p3XFLAG-CMV-TgROP26			This study
p3XFLAG-CMV-TgROP34			This study
p3XFLAG-CMV-TgROP35			This study
p3XFLAG-CMV-TgROP38			This study
p3XFLAG-CMV-TgROP39			This study

(Continued)

TABLE 1 | Continued

Plasmid	Description	Use	Source or reference
pGL4.32	Nuclear factor- κ B response element (NF- κ B)	Luciferase reporter assay for NF- κ B signal	Promega
pGL4.74	Control Renilla luciferase expression vector		Promega
pBluescript SK (+)		Plasmid for cloning of <i>TgGRA14</i> +UTR gene	Add gene
pBluescript SK (+)- <i>TgGRA7</i> +UTR	<i>TgGRA14</i> expressed from the <i>TgGRA7</i> 5'UTR and 3' UTR	Replacing the UPRT gene by <i>TgGRA7</i>	This study
pBluescript SK (+)- <i>TgGRA14</i> +UTR	<i>TgGRA14</i> expressed from the <i>TgGRA14</i> 5'UTR and 3' UTR	Replacing the UPRT gene by <i>TgGRA14</i>	This study

Nuclei were counterstained with Hoechst dye. Coverslips were then mounted onto the glass slide with Mowiol 4-88 (Sigma), and photographs were taken using All-in-One microscopy (BZ-9000, Keyence, Itasca, IL, USA). Quantification of the nuclear signal was performed by randomly selecting at least 20 infected cells per *T. gondii* strain and measuring the mean signal intensity per nucleus using the BZ analyzer II (Keyence).

IFAT in 293T Cells With Forced Expression of GRA Proteins

The 293T cells in a collagen 1-coated 12-well plate were transiently transfected with expression vectors of GRA7, GRA14, or GRA15, or the empty p3 \times FLAG-cmv14 vector as a negative (empty) control, using Fugene HD. After 24 h, IFAT and quantification of the nuclear signal were performed as described above.

Western Blotting

HFF cells were infected with parasites (multiplicity of infection = 3) for 24 h, then lysed using the LysoPureTM Nuclear and Cytoplasmic Extractor Kit (Wako, Osaka, Japan) supplemented with complete mini protease inhibitors and Phos stop (Roche, Mannheim, Germany). The cell lysates were separated by SDS-polyacrylamide gel electrophoresis and transferred to a Poly Vinylidene Di-Fluoride membrane (Millipore), which was blocked in TBS/0.1% Tween-20/2% ECL Prime Blocking Reagent (GE Healthcare, Buckinghamshire, UK) and incubated with primary and secondary antibodies. The protein bands were visualized by ECL Prime Western Blotting Detection reagent (GE Healthcare), and analyzed by Versa Doc with Quantity One (Bio-Rad, Munich, Germany). Band intensity was quantified using ImageJ software developed by the US National Institutes of Health.

Survival of Mice Infected With *Toxoplasma gondii*

Male C57BL/6J mice, of 8 weeks of age, were obtained from Clea Japan (Tokyo, Japan). Mice were infected intraperitoneally with 500 tachyzoites of the parental strain Pru, or mutant strains Pru Δ *gra7*, Pru Δ *gra14*, or Pru Δ *gra15*. Mice were also infected intraperitoneally with 10,000 parental Pru or Pru Δ *gra14* parasites. To determine the survival rates to the type I RH strain, 500 tachyzoites the RH Δ *gra14*, RH Δ *gra7*, or their parental parasites were injected into the right footpads of mice and their survival was monitored for up to 30 days.

Statistical Analyses

Statistical analyses were performed using GraphPad Prism (version 6.0) software (GraphPad Software, San Diego, CA, USA). Statistically significant differences among groups were determined using one-way ANOVA with Tukey's *post-hoc* test. *P*-values of < 0.05 represent statistically significant differences. The survival rate was compared between groups using the log-rank test.

RESULTS

Ectopic Expression of Type II GRA14 Activates NF κ B Signaling in 293T Cells

To investigate which molecules modulate the NF κ B pathway in *Toxoplasma*, we constructed mammalian expression vectors for 17 GRAs and 21 ROPs of a *Toxoplasma* type II strain. Then, we assessed whether their overexpression, together with luciferase reporter plasmids carrying an element dependent on the NF κ B promoter, activated the reporter. Overexpression of GRA7, GRA14, and GRA15 activated NF κ B (Figure 1A). Overexpression of GRA14 stimulated the NF κ B promoter to a similar level as that of GRA7, whereas GRA15 produced much higher levels of NF κ B-dependent luciferase activity than GRA7 and GRA14 (Figure 1B). The expression of these molecules in 293T cells was confirmed by western blotting (Supplemental Figure 3). Thus, we focused on GRA7, GRA14, and GRA15 for further analysis.

Next, we generated Pru Δ *gra7*, Pru Δ *gra14*, and Pru Δ *gra15* parasites based on the gene-editing strategies depicted in Supplemental Figure 2. We isolated single clones of drug-resistant parasites and performed diagnostic PCR to check for correct integration (Supplemental Figure 1). Moreover, we established complementation of GRA7 and GRA14. The GRA7 and GRA14 expression cassettes containing the 5' UTR and 3'UTR were inserted into the UPRT gene locus. Drug-resistant clones were isolated and correct integration into the UPRT locus was confirmed (Supplemental Figure 1). Clones, with the exception of Pru Δ *gra15*, were further analyzed by an IFAT and western blotting to confirm the protein expression (Supplemental Figure 2). The Pru Δ *gra15* mutant was excluded because of the lack of an anti-GRA15 antibody. We then assessed the physiological changes in the transgenic lines *in vitro*. The infection rates and egress rates of the Pru Δ *gra7* and Pru Δ *gra14* strains in Vero cells were similar to those of the parental strain (Supplemental Figures 5A–D). Whereas, the *in vitro* replication

TABLE 2 | Primers used in this study.

Primer	Sequence (5'-3')	Use
TgGRA1_cDNA_1F	ACC AGT CGA CTC TAG ATG GTG CGT GTG AGC GCT AT	To clone full length of the gene into XbaI and BamHI sites of the p3XFLAG-CMV-14 plasmid by In-Fusion cloning
TgGRA1_cDNA_2R	AGT CAG CCC GGG ATC TCT CTC TCT CTC CTG TTA AGA	
TgGRA2_cDNA_1F	ACC AGT CGA CTC TAG ATG TTC GCC GTA AAA CAT TG	
TgGRA2_cDNA_2R	AGT CAG CCC GGG ATC TCT GC GAA AAG TCT GGG ACG G	
TgGRA3_cDNA_1F	ACCA GTC GAC TCT AGA TGG ACC GTA CCA TAT GTC C	
TgGRA3_cDNA_2R	AGT CAG CCC GGG ATC TTT TCT TGG AGG CTT TGT CCA	
TgGRA4_cDNA_1F	ACC AGT CGA CTC TAG ATG CAG GGC ACT TGG TTT TC	
TgGRA4_cDNA_2R	AGT CAG CCC GGG ATC TCT CTT TGC GCA TTC TTT CCA	
TgGRA5_cDNA_1F	ACC AGT CGA CTC TAG ATG GCG TCT GTA AAA CGC GT	
TgGRA5_cDNA_2R	AGT CAG CCC GGG ATC TCT CTT CCT CGG CAA CTT CTT	
TgGRA6_cDNA_1F	ACC AGT CGA CTC TAG ATG GCA CAC GGT GGC ATC TA	
TgGRA6_cDNA_2R	AGT CAG CCC GGG ATC TAA AAT CAA ACT CAT TCA CAC	
TgGRA7_cDNA_1F	ACC AGT CGA CTC TAG ATG GCC CGA CAC GCA ATT TT	
TgGRA7_cDNA_2R	AGT CAG CCC GGG ATC TCT GGC GGG CAT CCT CCC CAT	
TgGRA8_cDNA_1F	ACC AGT CGA CTC TAG ATG GCT TTA CCA TTG CGT GT	
TgGRA8_cDNA_2R	AGT CAG CCC GGG ATC TAT TCT GCG TCG TTT GGA CGG	
TgGRA9_cDNA_1F	ACC AGT CGA CTC TAG ATG TGC GGT CAC TCA AGT CAA T	
TgGRA9_cDNA_2R	AGT CAG CCC GGG ATC TGA GTC CTC GGT CTT CCT GCG	
TgGRA11_212410_cDNA_1F	ACC AGT CGA CTC TAG ATG TCC CGC CGC ATG GCA TC	
TgGRA11_212410_cDNA_2R	AGT CAG CCC GGG ATC TTG GCT TCA ACT CGT CCT CTT	
TgGRA12_275850_cDNA_1F	ACC AGT CGA CTC TAG ATG GAG ACT GGC CTA AAG GA	
TgGRA12_275850_cDNA_2R	AGT CGC CCG GGA TCT CTT CTT TTG TGA AGG TTT C	
TgGRA14_cDNA_1F	ACC AGT CGA CTC TAG ATG CAG GCG ATA GCG CGG GG	
TgGRA14_cDNA_2R	AGT CAG CCC GGG ATC TTT CGC TTG GTC TCT GGT AGC	
TgGRA15_cDNA_1F	ACC AGT CGA CTC TAG ATG GTG ACA ACA ACC ACG CC	
TgGRA15_cDNA_2R	AGT CAG CCC GGG ATC TTG GAG TTA CCG CTG ATT GT	
TgGRA16_cDNA_1F	ACC AGT CGA CTC TAG ATG TAT CGA AAC CAC TCA GG	
TgGRA16_cDNA_2R	AGT CAG CCC GGG ATC TCA TCT GAT CAT TTT TCC GC	
TgGRA23_cDNA_1F	ACC AGT CGA CTC TAG ATG GCA GCG CGT GCG GGA AG	
TgGRA23_cDNA_2R	AGT CAG CCC GGG ATC TGT TCT TTC GCG CAA GGG GT	
TgGRA24_cDNA_1F	ACC AGT CGA CTC TAG ATG CTC CAG ATG GCA CGA TA	
TgGRA24_cDNA_2R	AGT CAG CCC GGG ATC TAT TAC CCT TAG TGG GTG GT	
TgGRA25_cDNA_1F	ACC AGT CGA CTC TAG ATG AAG CGT TTC TGG TTG TG	
TgGRA25_cDNA_2R	AGT CAG CCC GGG ATC TGT TTC TAT CGA ATT CCG GG	
TgROP5_cDNA_1F	ACC AGT CGA CTC TAG ATG GCG ACG AAG CTC GCT AG	
TgROP5_cDNA_2R	AGT CAG CCC GGG ATC TAG CGA CTG AGG GCG CAG CA	
TgROP8_cDNA_1F	ACC AGT CGA CTC TAG ATG TTT TCT GTG TTA CGT AA	
TgROP8_cDNA_2R	AGT CAG CCC GGG ATC TTG CCG GTT CTC CAT CAG TT	
TgROP9_cDNA_1F	ACC AGT CGA CTC TAG ATG ACG CAC CCA AAT CCC CT	
TgROP9_cDNA_2R	AGT CAG CCC GGG ATC TCT GCA TGA TCA ACG AGG GC	
TgROP10_cDNA_1F	ACC AGT CGA CTC TAG ATG GGA CGA CCC AGG TGG CC	
TgROP10_cDNA_2R	AGT CAG CCC GGG ATC TGT TGG GCG CAT CTT CCG TA	
TgROP11_cDNA_1F	ACC AGT CGA CTC TAG ATG TCG TCA TCC AGA TTG GT	
TgROP11_cDNA_2R	AGT CAG CCC GGG ATC TCC CCG TGA CGG GGA AGT AC	
TgROP12_cDNA_1F	ACC AGT CGA CTC TAG ATG GCA GCG GTT CTT CCT TG	
TgROP12_cDNA_2R	AGT CAG CCC GGG ATC TGA ACC GCC TCA AGA GAA AA	
TgROP13_cDNA_1F	ACC AGT CGA CTC TAG ATG AAG AGA ACA GAG CTT TG	
TgROP13_cDNA_2R	AGT CAG CCC GGG ATC TCA ATA GCC TCA AGG AAT TC	
TgROP14_cDNA_1F	ACC AGT CGA CTC TAG ATG TAT TCC TCC CCT CAG TC	
TgROP14_cDNA_2R	AGT CAG CCC GGG ATC TCA GCG CTT GCT TCT TCC TA	

(Continued)

TABLE 2 | Continued

Primer	Sequence (5'-3')	Use
TgROP15_cDNA_1F	ACC AGT CGA CTC TAG ATG CTG AAA ACG ACA CCT GC	
TgROP15_cDNA_2R	AGT CAG CCC GGG ATC TGA AAG GTG AGC TAT GAG GT	
TgROP16_cDNA_1F	ACC AGT CGA CTC TAG ATG AAA GTG ACC ACG AAA GG	
TgROP16_cDNA_2R	AGT CAG CCC GGG ATC TCA TCC GAT GTG AAG AAA GT	
TgROP17_cDNA_1F	ACC AGT CGA CTC TAG ATG GAG TTG GTG TTG TGC TT	
TgROP17_cDNA_2R	AGT CAG CCC GGG ATC TCT CCT TCT GTA ATA AAG CC	
TgROP18_cDNA_1F	ACC AGT CGA CTC TAG ATG TTT TCG GTA CAG CGG CC	
TgROP18_cDNA_2R	AGT CAG CCC GGG ATC TTT CTG TGT GGA GAT GTT CC	
TgROP19A_cDNA_1F	ACC AGT CGACTC TAG ATG AGA AGG CGC TGC TTT C	
TgROP19A_cDNA_2R	AGT CAG CCC GGG ATC TCT GAG ATC TGG ATG CGC GC	
TgROP20_cDNA_1F	ACC AGT CGA CTC TAG ATG CGC CTG GAT GCT GTG TA	
TgROP20_cDNA_2R	AGT CAG CCC GGG ATC TGT CAC TTG AAC TTG GCT CC	
TgROP23_cDNA_1F	ACC AGT CGA CTC TAG ATG GAA AAG ATC CTG TGG GC	
TgROP23_cDNA_2R	AGT CAG CCC GGG ATC TCT TGA TGC CTT TCA ACA GG	
TgROP24_cDNA_1F	ACC AGT CGA CTC TAG ATG GCA ACG CGT TCA TTC CT	
TgROP24_cDNA_2R	AGT CAG CCC GGG ATC TGG GAT TAC GGG AGA GTG TT	
TgROP26_cDNA_1F	ACC AGT CGA CTC TAG ATG TTG TTA AGC ATA TCT GC	
TgROP26_cDNA_2R	AGT CAG CCC GGG ATC TTA ATG GGG TAA ACA ACT GC	
TgROP34_cDNA_1F	ACC AGT CGA CTC TAG ATG ATG TTT CCT GCC GTC GC	
TgROP34_cDNA_2R	AGT CAG CCC GGG ATC TGC TCT CCT GTG CGT CTT CC	
TgROP35_cDNA_1F	ACC AGT CGA CTC TAG ATG CCG GAA CAA GAT CTT GC	
TgROP35_cDNA_2R	AGT CAG CCC GGG ATC TTT CGT TTT CCT GTT CAT GG	
TgROP38_cDNA_1F	ACC AGT CGA CTC TAG ATG AAA AAT ACT CTG TTG TC	
TgROP38_cDNA_2R	AGT CAG CCC GGG ATC TAA ATT GAT GCG TTC TTA TC	
TgROP39_cDNA_1F	ACC AGT CGA CTC TAG ATG AGC AAA CCT TTT TTC CC	
TgROP39_cDNA_2R	AGT CAG CCC GGG ATC TAA CAA TTG ACT CCC GAA GA	
TgROP41_cDNA_1F	ACC AGT CGA CTC TAG ATG CGT CAC GTG TTC AAC TC	
TgROP41_cDNA_2R	AGT CAG CCC GGG ATC TGG AAA GCA CTT GT GAG GTC	
TgGRA7_5UTR_1F	GTG GAT CCC ATG GAG ACA CAC GGT CAA CA	To clone 5'UTR of the TgGRA7 gene into pBS/GFP/HX
TgGRA7_5UTR_2R	CGA AGC TTT AAT GCA GCT GTC ATG TCT CG	
TgGRA7_3UTR_1F	ATGGGCCCGGTTGAAAAGGACCCGTATG	To clone 3'UTR of the TgGRA8 gene into pBS/GFP/HX
TgGRA7_3UTR_2R	ATGGGCCACGGAGACTGCCTTGTCTTTC	
TgGRA14II_484-gRNA	GAA GTT CTG AGC CGT TTC CTG TTT TAG AGC TAG AAA TAG C	Primer for CRISPR/CAS9 plasmids targeting the TgGRA14 gene (pSAG1::CAS9-U6::sgTgGRA14)
TgGRA15(II)_146-gRNA	GCT CGA TAA TTC GGT GGC TTG GGG TTT TAG AGC TAG AAA TAG C	Primer for CRISPR/CAS9 plasmids targeting the TgGRA15 gene (pSAG1::CAS9-U6::sgTgGRA15)
Common CAS9-U6-Rv	AAC TTG ACA TCC CCA TTT AC	Common primer for CRISPR/CAS9 plasmids targeting <i>Toxoplasma</i> genes
DHFR_GRA14_484_1F	AGG TTC AAG AAG TTC TGA GCC GTT TAA GCT TCG CCA GGC TGT AAA	To amplify an amplicon containing TgGRA14 homology regions surrounding a pyrimethamine-resistant DHFR* cassette
DHFR_GRA14_484_2R	CAG ACG CAA CAG AAC CAA GGG GAA TTC ATC CTG CAA GTG CAT AG	
DHFR-25ntTgGRA15(II)_146_1F	CAA GTC ACG CTC GAT AAT TCG GTG GAA GCT TCG CCA GGC TGT AAA	To amplify an amplicon containing TgGRA15 homology regions surrounding a pyrimethamine-resistant DHFR* cassette
DHFR-21ntTgGRA15(II)_146_2R	GAG CAC CGT AAG ATA CCC AAG GGA ATT CAT CCT GCA AGT GCA TAG	
TgGRA7-KOS-1F	CGT CAT GAG TAC CGG GAC AT	To confirm the correct homologous recombination of HXGPRT cassette with the TgGRA7 gene
TgGRA7-KOS-2R	ATT CAG ACC TGC TGC GAG CC	
TgGRA7-KOS-3R	GCA AGG AAC GAT CAT GCG TG	

(Continued)

TABLE 2 | Continued

Primer	Sequence (5'-3')	Use
HXGPRT-KOS-1F TgGRA7_RT_1F	CTTGTCGGGAGCAACAGCC TCA CCA CCA GCA TGG ATA AGG	To confirm the insertion of TgGRA7+UTR cassette into the TgUPRT gene
TgGRA7_RT_2R TgGRA7+UTR_467-2R	GCC TCG CTT CCT GAA ATG AAC GAT TTT CAG CCA CGC CTG TC	
TgGRA7+UTR_467-1F TgGRA14screen-1Fv3	AAG GAC CCG TAT GCA GGT AGC T CGA GTT GTA GCT GG CTT TTC	To confirm the insertion of TgGRA7+UTR cassette into the TgUPRT gene
TgGRA14screen-1Rv3 TgGRA15(II)_screen_1F	TGT CAC GGG GAG ACT AGC GT TTT CCA GGA GGA ATC GCG CC	
TgGRA15 (II)_screen_2R DHFR2-1F	CTG CCT CGT CGT GTT TCC CG CCA TTG TGA ACA TCC TCA AC	To confirm the insertion of DHFR* cassette into the TgGRA14 gene
TgDHFR-TS_screen_2R TgGRA7(II)+UTR_1F	CAG ACA CAC CGG TTT CTG CAT ATG CGG CCG CAG GAA AAC AGT GTT TCC GAA	
TgGRA7(II)+UTR_2R TgGRA14(II)+UTR_1Fv2	ACG ATA TCA TGC GTC TTT TGT AGT GAA T ATT CTA GAA AAT AAT GTG CGC ACA CAA C	To confirm the insertion of DHFR* cassette into the target gene
TgGRA14(II)+UTR_2Rv2 pBlue_UPRT_1F	TCA TCG ATT GCC AGC TCC TTT CAG CTT C TGT GGC GTC TCG ATT GTG AGA TAG GGC GAA TTG GAG CTC C	
pBlue_UPRT_2R UpgRNA-1F	TTT CCA TCG ACT CGC CAG CTA GGG AAC AAA AGC TGG GTA C GAT CCG CTT CTC TTG TAC TGC	To clone full length of the TgGRA7 containing UTR region into Not1 and EcoR5 sites of the pBluescript+SK plasmid by ligation cloning (pBluescript-TgGRA7+UTR)
DngRNA-2R CXCL1_RT_1F	AAG CAG GTG CAG CGG ACA AG CAA TGA GCT GCG CTG TCA GT	
CXCL1_RT_2R CXCL5_RT_1F	TTG AGG TGA ATC CCA GCC AT CGC TAA TTT GGA GGT GAT CCC	To clone full length of the TgGRA14 containing UTR region into Not1 and EcoR5 sites of the pBluescript+SK plasmid by ligation cloning (pBluescript-TgGRA14+UTR)
CXCL5_RT_2R IL1-beta-RT-F1	ACT TCC ACC GTA GGG CAC TG CCA AAA GATGAA GGG CTG CT	
IL1-beta-RT-R1 IL6-RT-F1	TCA TCT GGA CAG CCC AGG TC TTC CAT CCA GTT GCC TTC TTG	To amplify an amplicon containing TgUPRT homology region surrounding TgGRA14+UTR expressed cassette
IL6-RT-R2 CCL17_RT_1F	GAA GGC CGT GGT TGT CAC C ATG TAG GCC GAG AGT GCT GC	
CCL17_RT_2R CCL7_RT_1F	TGA TAG GA ATG GCC CCT TTG GGA TCT CTG CCA CGC TTC TG	To confirm the insertion of TgGRA14+UTR cassette into the TgUPRT gene
CCL7_RT_2R LCN2-RT-F1	GGC CCA CAC TTG GAT GCT CCA GTT CGC CAT GGT ATT TTT C	
LCN2-RT-R1 CSF3-RT-F1	CAC ACT CAC CAC CCA TTC AGT T CTG GCA GCA GAT GGA AAA CC	Real-time PCR for expression of mouse CXCL1 mRNA
CSF3-RT-R2 Ptgs2_RT_1F	TGT GTG GGC TGC ACA GTA GG ATG TAG GCC GAG AGT GCT GC	
Ptgs2_RT_2R GAPDH-RT-1F	CCA GCA CTT CAC CCA TCA GTT CCC AGG TCC TCG CTT ATG ATC	Real-time PCR for expression of mouse CXCL5 mRNA
GAPDH-RT-2R	CCT GCT TCA CCA CC TTC TTG AT	

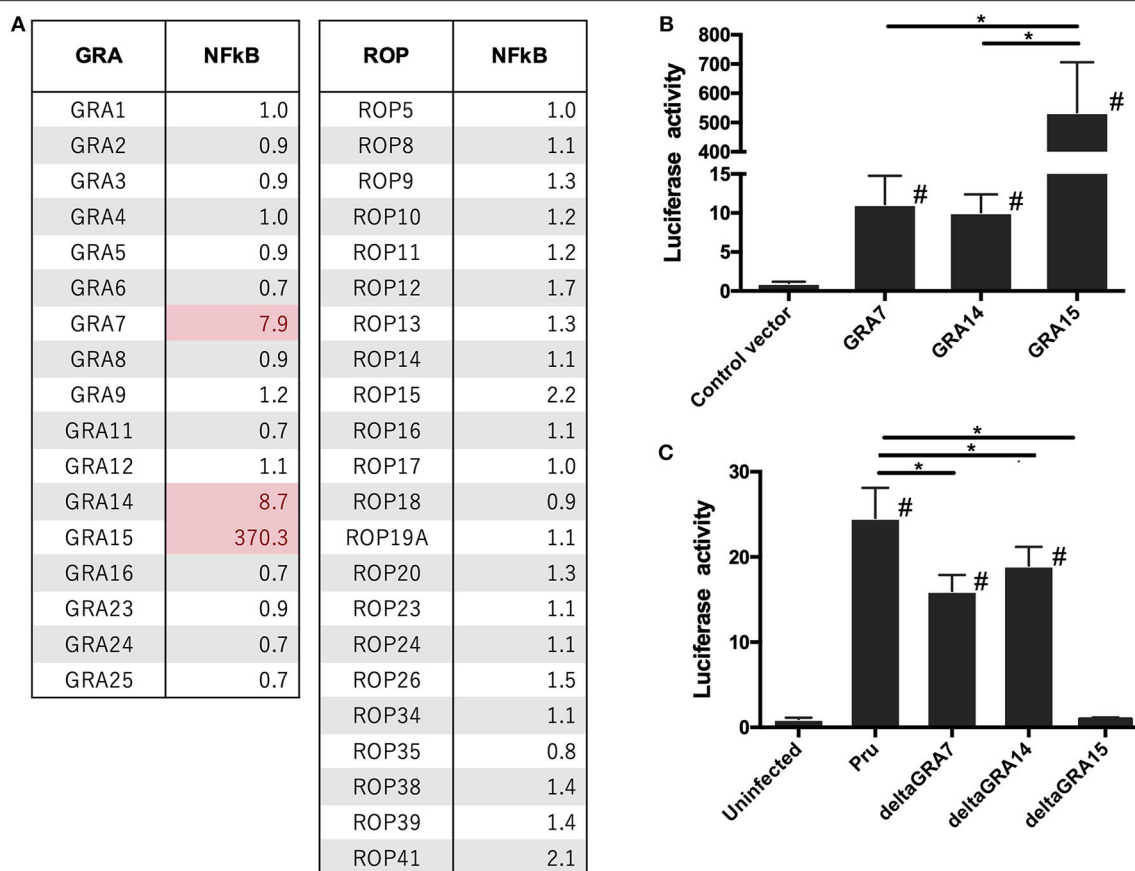


FIGURE 1 | Luciferase activities in 293T cells transfected with NF κ B reporter plasmid. 293T cells were transiently transfected with pGL4.32 expressing firefly luciferase and pGL4.74 expressing renilla luciferase. **(A,B)** Cells were immediately transfected with the expression vectors of GRAs and ROPs, and the empty p3 \times FLAG-cmv14 vector used as a negative (empty) control. The promoter activity was determined and is shown as a fold-increase in the luciferase activity normalized for Renilla luciferase activity. **(C)** Pru, Pru Δ gra7 (deltaGRA7), Pru Δ gra14 (deltaGRA14), or Pru Δ gra15 (deltaGRA15) lines were added to the cells. After 12 h, parasites were added to the host cells, lysates were prepared, and luciferase activity was measured. The promoter activity was determined and is shown as a fold-increase in the luciferase activity normalized for Renilla luciferase activity. Values are the means \pm SD of triplicate samples, $^*p < 0.05$. #a significant difference with the control vector and/or uninfected cells ($p < 0.05$). Differences were tested by one-way ANOVA with turkey's *post-hoc* test in **(B,C)**. Data are representative of two independent experiments.

rate of Pru Δ gra7 parasites was significantly higher than that of the parental parasites (**Supplemental Figure 5E**). The replication rate of Pru Δ gra14 was comparable to that of the parental parasites (**Supplemental Figure 5F**).

Next, we analyzed how each GRA contributes to NF κ B activation because it is known that GRA15 plays a dominant role in NF κ B activation by type II *T. gondii*. Cells infected with the Pru Δ gra7 and Pru Δ gra14 mutants showed a partial decrease in luciferase activity compared with cells infected with the parental Pru (**Figure 1C**). However, for Pru Δ gra15, NF κ B activity was abolished in the infected cells (**Figure 1C**).

Each GRA Expression Alone Is Sufficient to Activate NF κ B in 293T Cells

We assessed whether each GRA protein alone is sufficient to activate the process of NF κ B signal transduction. The level of nuclear RelA in GRA7- or GRA14-expressing cells was significantly higher than the level in control cells (**Figure 2**).

Moreover, the level of RelA nuclear translocation in cells expressed GRA15 was even higher than that in cells expressing GRA7 and GRA14 (**Figure 2**). First, we performed transient expression of each GRA gene. However, it is uncertain whether the function of ectopic single parasite molecule is the same as that of its native molecule. In addition, western blotting in the **Supplemental Figure 3** indicated different expression levels among the transfection with GRA genes. Thus, we conducted similar experiments using deficient parasite strains.

Cells infected with the parental Pru strain revealed a higher level of nuclear RelA than cells infected with Pru Δ gra7 or Pru Δ gra14, whereas the complemented strain showed a similar level of RelA signal to the parental parasite (**Figures 3A,B**). Moreover, GRA15 deletion almost abolished the nuclear translocation of RelA (**Figure 3C**). Representative images from these experiments are shown in **Figure 3D**. Next, we assessed whether each GRA affects the phosphorylation of I κ B α by western blotting. The phosphorylated I κ B α levels were

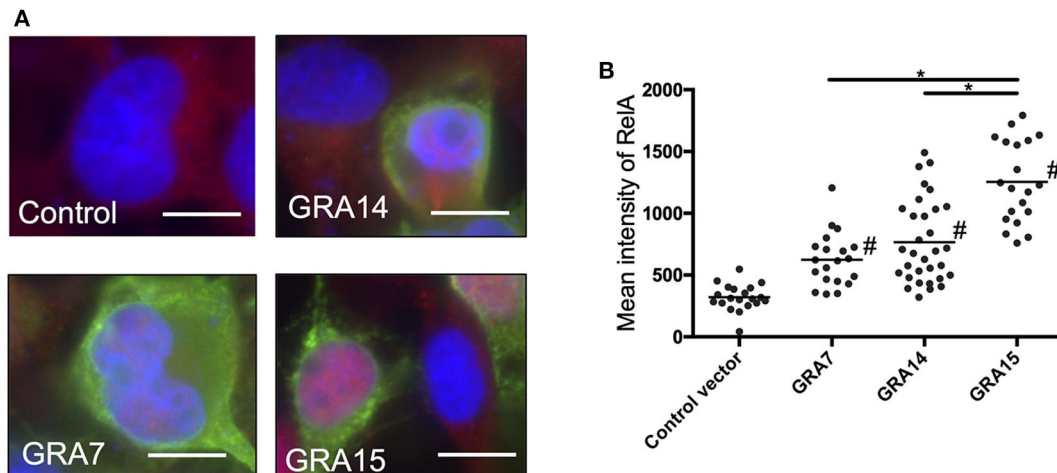


FIGURE 2 | GRA expression activates nuclear translocation of NF- κ B RelA in 293T cells. **(A)** 293T cells were transfected with the expression vectors for GRA7, GRA14, or GRA15, or the empty p3 \times FLAG-cmv14 vector used as a negative (empty) control. Cells were then fixed and stained with α -NF κ B RelA (red), α -FLAG (green), or Hoechst dye (blue). Bars, 10 μ m. **(B)** The mean intensity of RelA in the nucleus was measured for at least 20 cells per group. Bar indicates the mean of each group, * $p < 0.05$. #a significantly higher level of nuclear RelA compared with the control cells ($p < 0.05$). Differences were tested by one-way ANOVA with turkey's *post-hoc* test. Experiments were performed twice.

comparable between cells infected with the parental, Pru Δ *gra14* and Pru Δ *gra7* strains, whereas GRA15 deficiency obviously reduced phosphorylated I κ B (Figure 4). The relative levels of phosphorylated I κ B α compared with the parental Pru-infected cells were 89, 105, and 38% in cells infected with Pru Δ *gra7*, Pru Δ *gra14*, and Pru Δ *gra15* strains, respectively (Figure 4).

Deficiency of GRA7, GRA14, and GRA15 Predominantly Results in Downregulation of Gene Expression Mediated by NF κ B in Macrophages Infected With *T. gondii*

We next analyzed the levels of interleukin-6 (IL-6) in mouse macrophage Raw246.7 cells infected with parasites, and found that not only GRA15 deficiency but also GRA7 and GRA14 deficiency decreased the level of secreted IL-6 in the culture supernatant (Figure 5). This result indicated that all of these GRAs affect the induction of the host immune response. To determine the host gene expression profiles relevant to these GRAs, we conducted transcriptome analysis of Raw246.7 cells infected with each strain and the uninfected cells. In total, 49, 103, and 338 genes were downregulated and 24, 15, and 111 genes were upregulated by GRA7, GRA14, and GRA15 deficiency, respectively (Figure 6A, the complete sets of genes are listed in Supplemental Data Sheet 1). A Venn diagram was created to illustrate the similarities and differences among the genes regulated by these three GRAs (Figure 6A). This indicated that a number of common genes were regulated by these GRAs, and that GRA15 deficiency had more diverse effects than GRA7 and GRA14 deficiency.

To gain greater insight into the pathways regulated by each GRA in host cells, we conducted Kyoto Encyclopedia of Genes and Genomes (KEGG) pathway analysis on the relevant genes. This analysis primarily identified immune-response-related

pathways, such as the cytokine-cytokine receptor interaction pathway, the IL-17 signaling pathway, and the tumor necrosis factor (TNF) signaling pathway, that were significantly enriched in the DEGs downregulated in macrophage cultures infected with deficient parasites compared with their expression in cell cultures infected by Pru and the complemented parasites (Supplemental Data Sheet 2). A heatmap of the gene expression associated with the cytokine-cytokine receptor interactions illustrated that GRA14, similar to GRA15, regulated some cytokines and chemokines (Figure 6B). In addition, a heatmap of the gene expression associated with the IL-17 signaling pathway defined several cytokines and chemokines as GRA7-regulated genes (Figure 6C, the complete sets of genes are available in Supplemental Data Sheet 3). To confirm the host genes whose expression is regulated by GRAs, we quantified the expression levels of several genes: IL-1 β , IL-6, Cxcl1, Cxcl5, and Ccl17 for GRA14 and GRA15; and IL-6, Ccl7, Lcn2, Csf3, and Ptgs2 for GRA7. These genes were selected because their expression appeared to be regulated by GRAs according to the heatmaps (Supplemental Data Sheet 3). In most cases, the gene expression profiles were consistent between the transcriptome and the real-time PCR data (Supplemental Figure 6). Collectively, these results indicated that GRA7, GRA14, and GRA15 deficiency robustly downregulated the immune response-related pathways induced by *T. gondii* infection.

GRA7, GRA14, and GRA15 Deficiency Increased Parasite Virulence in Mice

Next, we assessed the *in vivo* effects of each GRA on parasite virulence. Almost all mice intraperitoneally injected with 500 tachyzoites of the parental Pru parasites survived (15/16, 15/16, 12/14), whereas approximately 20% (3/16), 60% (10/16), and 0% (0/14) of mice survived after infection with Pru Δ *gra7*,

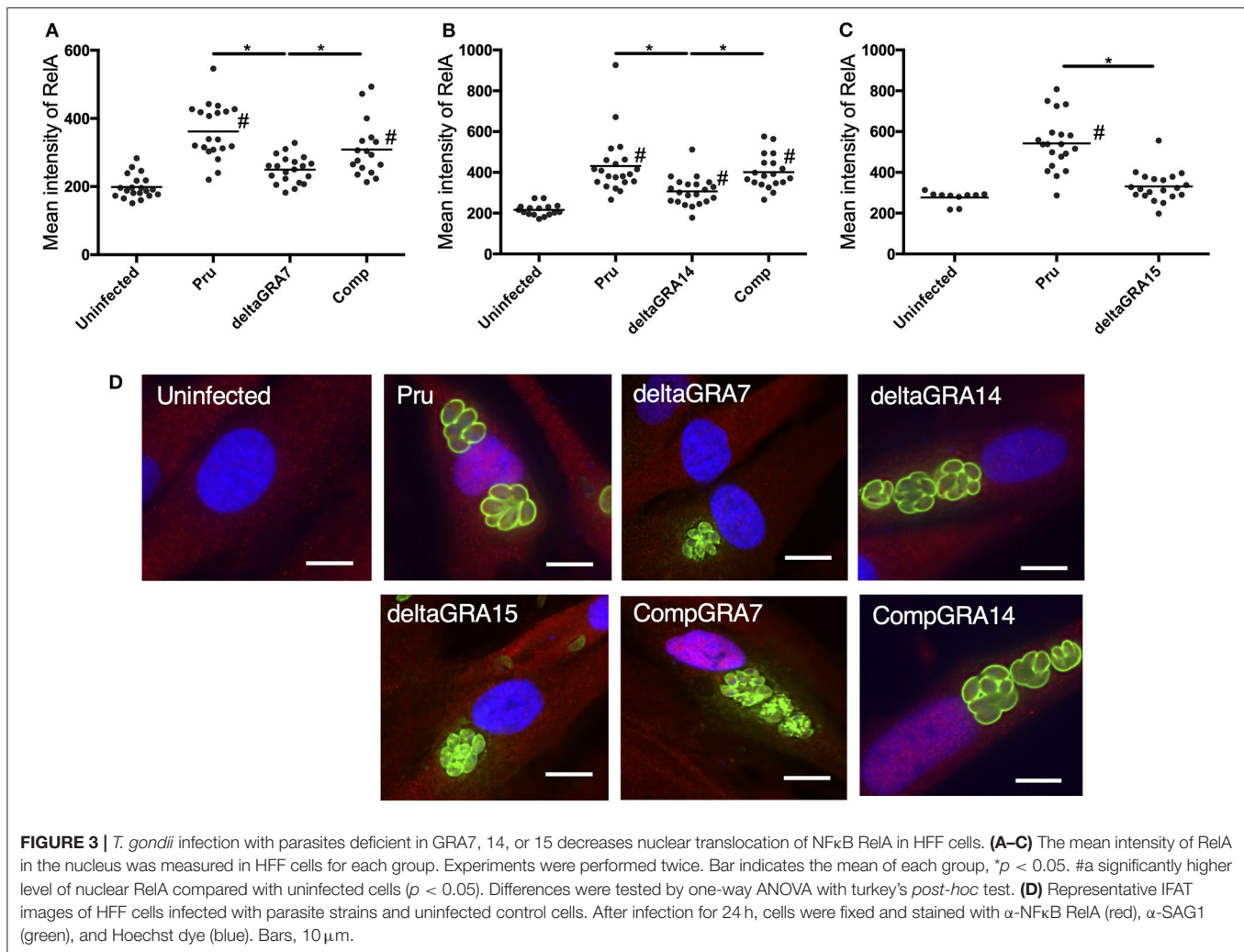


FIGURE 3 | *T. gondii* infection with parasites deficient in GRA7, 14, or 15 decreases nuclear translocation of NF κ B RelA in HFF cells. **(A–C)** The mean intensity of RelA in the nucleus was measured in HFF cells for each group. Experiments were performed twice. Bar indicates the mean of each group, * $p < 0.05$. #a significantly higher level of nuclear RelA compared with uninfected strains ($p < 0.05$). Differences were tested by one-way ANOVA with turkey's *post-hoc* test. **(D)** Representative IFAT images of HFF cells infected with parasite strains and uninfected control cells. After infection for 24 h, cells were fixed and stained with α -NF κ B RelA (red), α -SAG1 (green), and Hoechst dye (blue). Bars, 10 μ m.

Pru Δ gra14, and Pru Δ gra15 strains, respectively (Figures 7A–C). To further confirm the role of GRA14 in virulence, we infected mice by intraperitoneal injection with 10,000 tachyzoites of the parental Pru and Pru Δ gra14 parasites, and monitored mouse survival until 30 days post-infection. There was no significant difference in survival between mice infected with 10,000 parasites of the parental Pru and Pru Δ gra14 strains (Figure 7D).

Next, to determine the effect of GRA14 on *in vivo* parasite growth and the immune response at the site of infection, mice were infected with 500 tachyzoites of the parental Pru, Pru Δ gra14, and GRA14-complemented lines. At 5 days after infection, mice were euthanized and the parasite burden and levels of cytokine secretion, including IL-12p40 and interferon- γ (IFN- γ), were examined. Mice infected with each strain showed no significant difference in parasite burden in the spleen or the peritoneal exudate cells (Supplemental Figures 7A,B). Although the differences in IL-12p40 and IFN- γ secretion by the peritoneal exudate cells were not significant, the average level of IFN- γ in Pru Δ gra14 mutant-infected mice was higher than that in the parental Pru and

complemented strains (Supplemental Figures 7C,D). Moreover, no significant difference was detected in the level of serum IFN- γ on either day 3 or day 5 among these mouse groups (Supplemental Figures 7E,F).

To investigate how the deficiency of each GRA affects host immunity at an earlier time, we conducted a time-course experiment using thioglycolate-induced peritoneal macrophages (Supplemental Figure 8). Supernatants were collected every 6 h for 24 h and measured the production of IL-12p40. IL-12p40 production was abolished in the macrophages infected with Pru Δ gra7, Pru Δ gra14, and Pru Δ gra15 strains until 18 hours post-infection. However, the IL-12p40 production at 24 h post-infection decreased in the macrophages infected with the deficient parasite lines, with the highest decrease from Pru Δ gra15, followed by Pru Δ gra7, and then Pru Δ gra14.

Lastly, we examined the effect of GRA7 and GRA14 on type I RH parasites. Mice were infected by intra-footpad injection with 500 parasites of the RH Δ gra7, RH Δ gra14, and parental RH parasite strains, respectively. Survival was monitored for 30 days and 86% (13/15) of mice infected with the parental

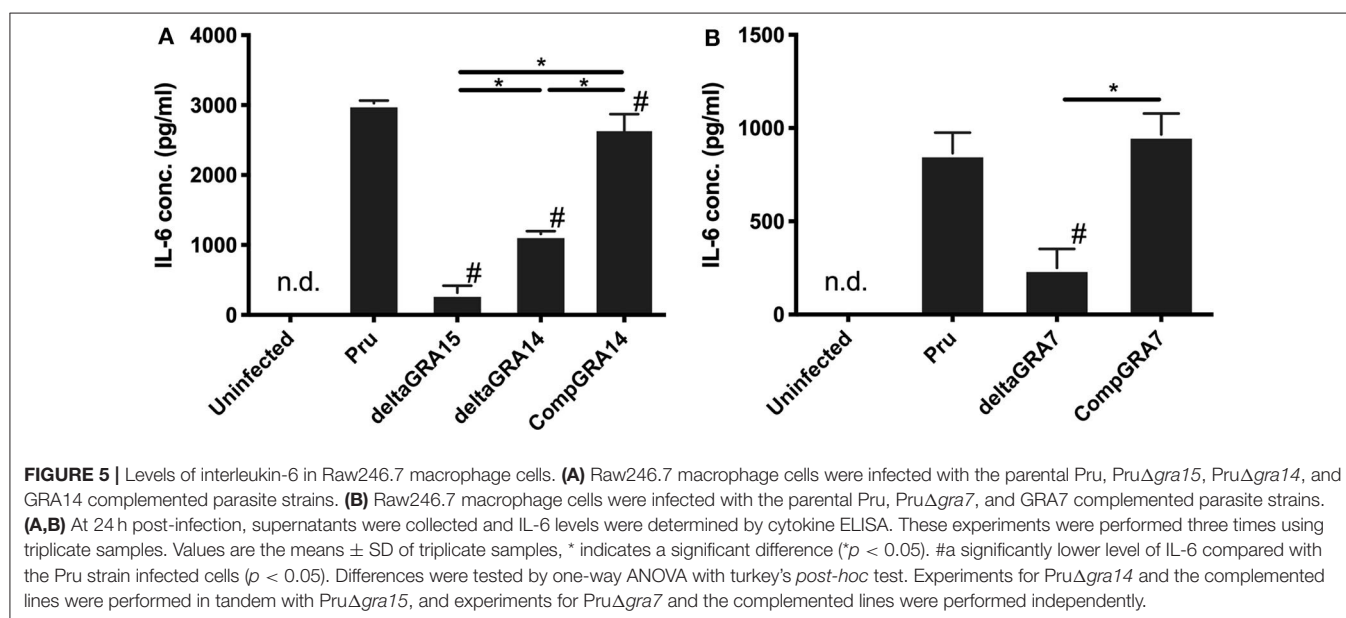
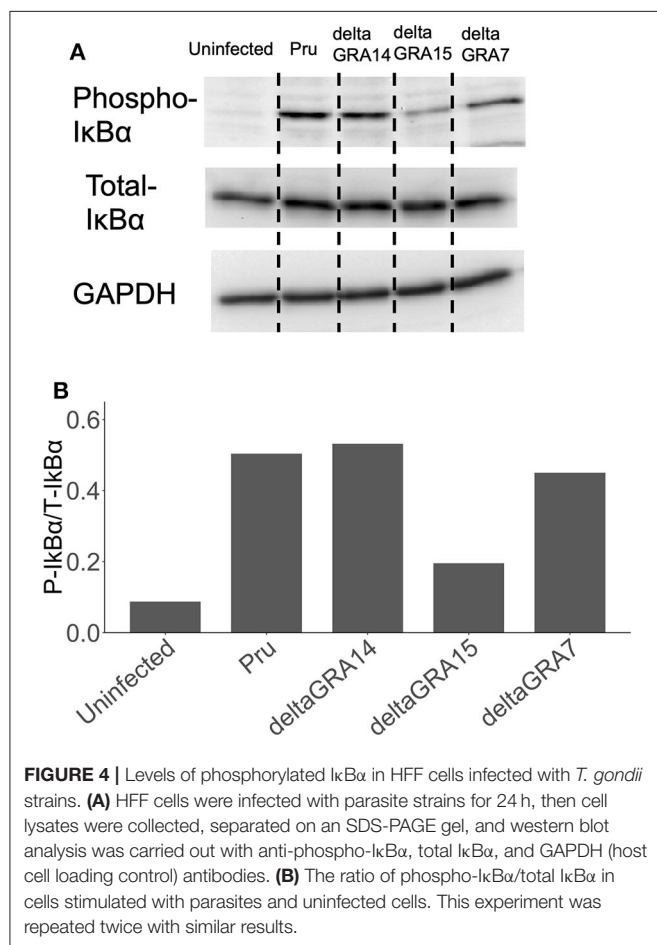
RH strain survived, whereas all RH Δ *gra14* mutant-infected mice succumbed to the infection between 15 and 26 days after infection (Figure 7E). By contrast, when challenged with the

parental RH and RH Δ *gra7* parasites, 0% (0/8) and 25% (2/8) of mice survived after infection with the parental RH and RH Δ *gra7* parasites, respectively (Figure 7F).

DISCUSSION

Secreted GRA15 has been identified as a major factor that contributes to the strain-specific differences in NF κ B activation (15). Meanwhile, GRA7 produces a strong antibody response in the acute phase of infection (22) and has been tested as a candidate for vaccine development (23). Recent studies have revealed that GRA7 associates with ROP2 and ROP4, and functions in concert with ROP18 protein complexes that resist IFN- γ -activated host immune-related GTPase (24–26). Moreover, recombinant GRA7 interacts with inflammasome-related molecules, such as an apoptosis-associated speck-like protein that contains a caspase recruitment domain (ASC) and phospholipase D1 (PLD1) (27). However, few studies have investigated the role of GRA7 in the pathogenesis of type II *T. gondii* strains. In the present study, we demonstrated that GRA14 is involved with NF κ B activation by *T. gondii*. GRA14 seems to be implicated in the interaction with host molecules because secreted GRA14 localizes to PVs containing membranous strand-like extensions (called PVM extensions) similar to other GRA proteins such as GRA3 and GRA7 (17). Furthermore, GRA14 is anchored in the PVM with its C terminus facing the host cell cytosol (17). GRA14 has also been reported as a potential vaccine candidate against *T. gondii* infection. Several studies have reported the protective immunity induced by vaccination with GRA14 antigen (28–32). However, there have been no previous reports regarding the modification of host cell function by GRA14. Thus, we targeted GRA7, GRA14, and GRA15 in this study.

Although we focused on NF κ B signaling pathway, reporter activity by GRA was also evaluated in this study using reporter



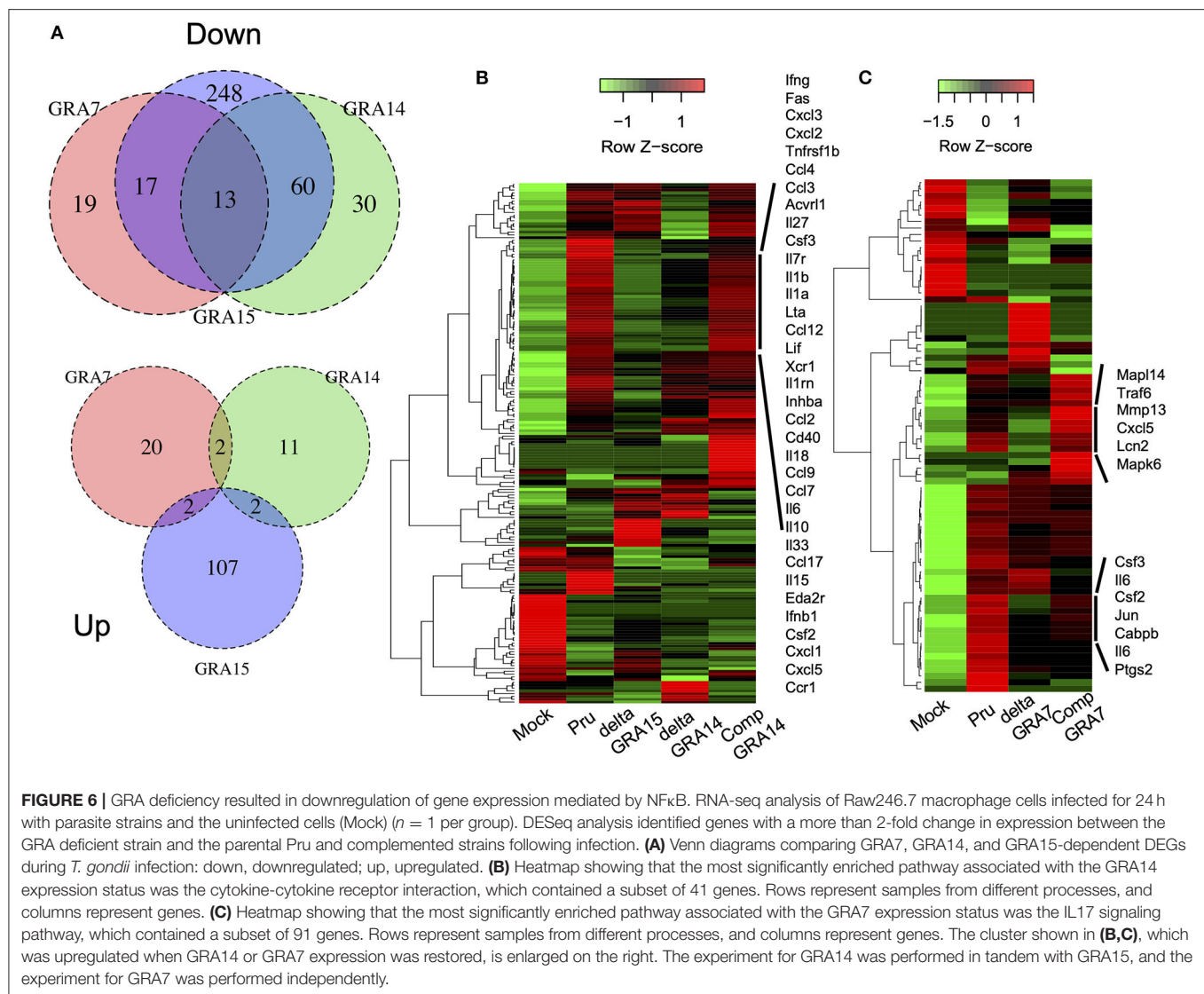
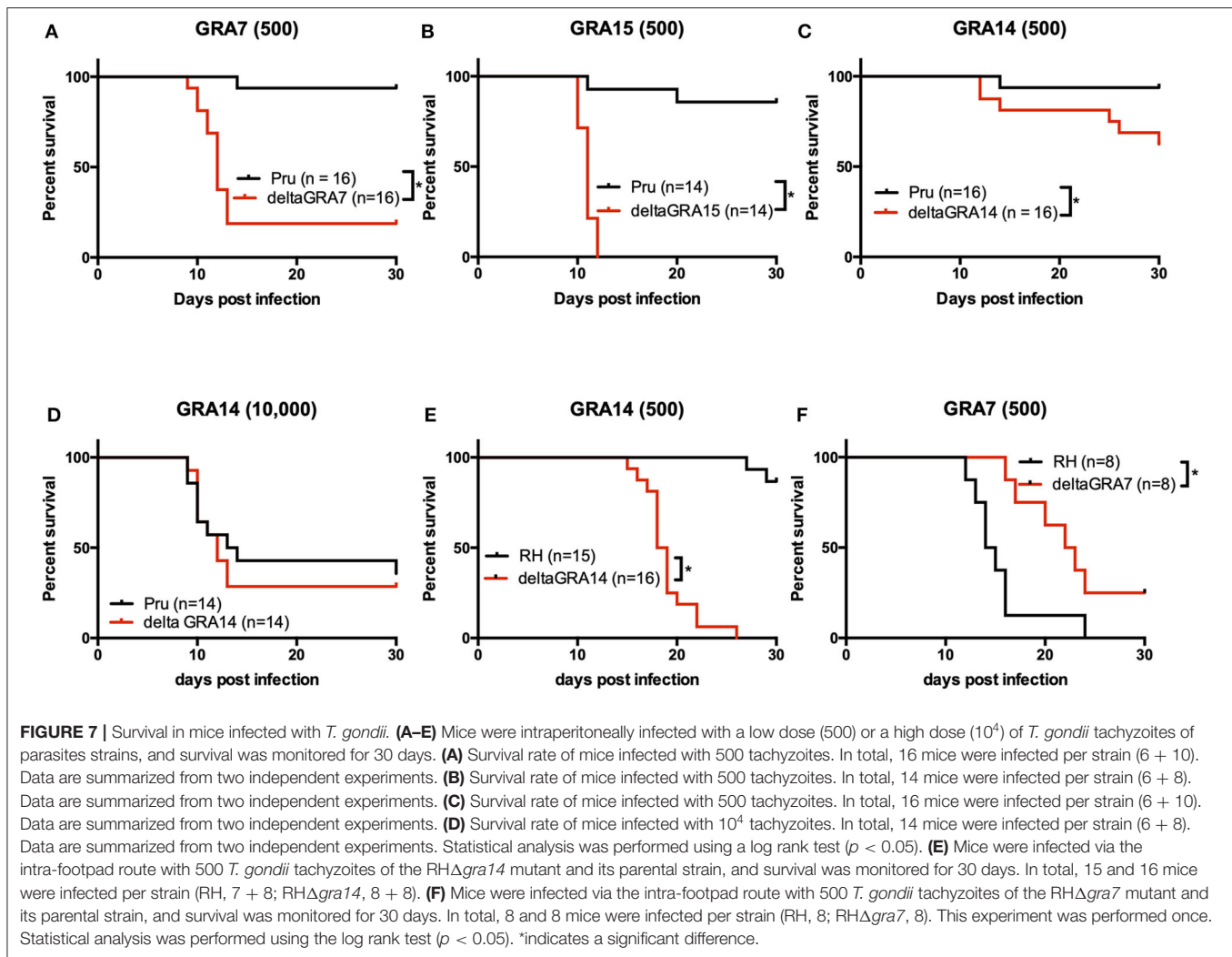


FIGURE 6 | GRA deficiency resulted in downregulation of gene expression mediated by NF κ B. RNA-seq analysis of Raw264.7 macrophage cells infected for 24 h with parasite strains and the uninfected cells (Mock) ($n = 1$ per group). DESeq analysis identified genes with a more than 2-fold change in expression between the GRA deficient strain and the parental Pru and complemented strains following infection. **(A)** Venn diagrams comparing GRA7, GRA14, and GRA15-dependent DEGs during *T. gondii* infection: down, downregulated; up, upregulated. **(B)** Heatmap showing that the most significantly enriched pathway associated with the GRA14 expression status was the cytokine-cytokine receptor interaction, which contained a subset of 41 genes. Rows represent samples from different processes, and columns represent genes. **(C)** Heatmap showing that the most significantly enriched pathway associated with the GRA7 expression status was the IL17 signaling pathway, which contained a subset of 91 genes. Rows represent samples from different processes, and columns represent genes. The cluster shown in **(B,C)**, which was upregulated when GRA14 or GRA7 expression was restored, is enlarged on the right. The experiment for GRA14 was performed in tandem with GRA15, and the experiment for GRA7 was performed independently.

plasmids having response elements such as cAMP-responsive element, nuclear factor of activated T cells (NFAT), serum responsive element, serum responsive factor (SRF), and activated protein 1. As shown in **Supplemental Figure 4**, GRA14 and GRA15 activated all of them, while GRA7 activated NFAT and SRF other than NF κ B. However, the main activities of GRAs were observed in NF κ B activation. Interacting host factor of GRA14 is unknown, while GRA7 and GRA15 activate NF κ B via TNF receptor-associated protein (TRAF). TRAF participates in the activation of the transcription factor NF κ B and members of the mitogen-activated protein kinase (MAPK) family, including MAPK, c-jun N-terminal kinase, and p38. It remains possible that each GRA regulates host immunity via signaling pathway other than NF κ B, but we believe that one of the primary sites of action is the NF κ B pathway. Interestingly, although the levels of nuclear translocation of RelA in GRA7- and GRA14-expressing cells were significantly lower than in GRA15-expressing cells, expression alone was adequate for nuclear

translocation. Moreover, cells infected with Pru Δ gra7 parasites showed no significant difference in the intensity of nuclear translocation compared with uninfected cells. In addition, GRA14 deficiency partially attenuated the intensity of nuclear RelA in cells infected with *T. gondii*. Collectively, these results suggest that GRA15 is the main player for NF κ B activation by type II *T. gondii*. Additionally, GRA7 and GRA14 play a certain role in modulation of the NF κ B pathway by type II *T. gondii*. By contrast, the levels of phosphorylated I κ B α were comparable among cells infected with the parental Pru strain and mutant strains Pru Δ gra7 and Pru Δ gra14. It was reported that GRA15-mediated NF κ B activation was dependent on TRAF6, and GRA15 deficiency caused a decrease in the levels of phosphorylated-I κ B α (15), which was consistent with our results. Contrary to this, another study showed that recombinant GRA7 also interacted with TRAF6, and recombinant GRA7 protein stimulated the phosphorylation of I κ B α (16). However, in the present study, GRA7 deficiency showed no clear change in



the phosphorylation level of I κ B α . It may be that due to the higher activity of GRA15 compared with that of GRA7 and GRA14, GRA15 compensates for the loss of GRA7 and GRA14 function.

Pru Δ gra7, Pru Δ gra14, and Pru Δ gra15 strains induced significantly less cytokine secretion from infected macrophages than the parental Pru strain-infected cells. NF κ B activation leads to the transcription of pro-inflammatory genes, such as those encoding IL-1 β and IL-12 (15, 33). In addition, our transcriptome analysis revealed that these GRAs regulated the gene expression levels of similar inflammatory cytokines and chemokines by macrophages, in turn stimulating the development of a T-helper type 1 (Th1) immune response (33). Our data suggested that either GRA7 or GRA15 deficiency is sufficient for the increase in acute virulence in infected mice. Mice infected with a type II GRA15-deficient strain had a significantly higher parasite burden than mice infected with a parental type II strain (15). GRA15 activates NF κ B in host cells and induces early IL-12 secretion (15). IL-12 stimulates NK cells and T cells to secrete IFN- γ (34). On day 2 after infection, mice infected with a type II GRA15-deficient strain had significantly less IFN- γ in their

intraperitoneal cavities than mice infected with a parental type II strain (15). IFN- γ is the primary cytokine of host resistance to intracellular pathogens (35). Thus, this difference in IFN- γ levels was the likely cause of the virulence differences. It has been demonstrated that GRA7 interacts with TRAF6, inducing innate immune responses via the NF κ B pathway in macrophages (16). Our results suggested that the GRA7-induced reporter activity of the NF κ B promoter was less than that of GRA15. However, GRA7 also interacts with a number of host cell proteins, including ASC and PLD1, revealing a new facet of the role of GRA7 in the regulation of innate immune responses (36). Thus, GRA7 deficiency might result in increased mortality comparable to that of GRA15.

GRA14 deficiency also resulted in a slight but significant increase in virulence compared with the parental strain in mice after the injection of 500 parasites. Whereas, consistent with recent research involving 2×10^5 parental type II Δ gra14 parasites, such a difference was no longer detectable when 10,000 parasites were injected, which furthermore had the potential to cause lethal tissue damage (37). However, after 5 days of

intraperitoneal infection, GRA14 did not affect the parasite burden or the level of cytokine secretion, including IL-12p40 and IFN- γ , from the peritoneal cavity. Moreover, no significant difference was detected in the levels of serum IFN- γ on days 3 or 5 among the groups of mice. The attenuated signal output caused by GRA14-deficiency may impair the proper immune response, resulting in an increased parasite burden in mice infected with Pru Δ gra14 parasites at an early stage (days 1–4), explaining the slight difference in virulence of this strain. The GRA-induced protective immune response against *T. gondii* in mice requires activation of antigen-presenting cells such as IL-12 production in the early stages of infection. If the parasites were controlled by the protective immune response in the early stage of infection, the level of the inflammatory marker IFN- γ would be suppressed. Therefore, the increased activity of Pru Δ gra14 at the initial stage of infection might increase IFN- γ level compared to the parental and complemented lines. Overall, our results suggest that GRA7 and GRA15 are the major contributors to *in vivo* virulence, whereas GRA14 has a relatively low impact on mice virulence. Furthermore, parasites deficient in GRA7 but not in GRA14 affect parasite growth *in vitro*. Moreover, a previous study reported that a type II Δ gra15 mutant formed significantly larger plaques than a type II strain in HFF cells, but this was not apparent in mouse embryo fibroblast cells (15). These data indicate that growth differences in GRA7 and GRA15-deficient strains may affect their virulence in mice.

In this study, our experiments had focused on type II strains; however, we conjectured that the GRA14 proteins of type I strains are functional because there are few amino acid differences between the type I and II proteins (P43S, D323G, and S356V). The GRA15 proteins from type II and type III strains activate NF κ B. Type II strains activate NF κ B more strongly than type III strains, whereas the type I RH strain does not induce NF κ B activation because it has a mutation in GRA15, leading to a frameshift and an early stop codon (15, 38). Therefore, because GRA15 of type I strains lacks activity, it is easy to evaluate the effect of GRA14 deficiency. Thus, we hypothesized that GRA14 might be involved with the mechanisms of NF κ B activation by type I *T. gondii*. Previous studies have shown that type I strains interfere with the host NF κ B pathway to promote their survival. ROP18, a key serine/threonine kinase that phosphorylates host proteins to modulate acute virulence, is associated with phosphorylation of RelA at Ser-468 and promotes the degradation of RelA to inhibit the NF κ B pathway (39). Moreover, polymorphic kinase ROP16 of type I strains is capable of suppressing the IL-12 response of infected macrophages stimulated with lipopolysaccharide, thereby inhibiting NF κ B transcriptional activity (15, 40). Whereas, other studies have shown that NF κ B is activated by a type I strain of *T. gondii*, and that its activation is necessary for the inhibition of apoptosis (41–43). However, it is not known what effect GRAs have on the NF κ B pathway.

Therefore, we lastly evaluated the effects of GRA7 and GRA14 deficiency in the type I RH strain on the survival of mice. Surprisingly, unlike type II parasites, all mice infected with RH Δ gra14 parasites died within 26 days of footpad inoculation. Previous studies showed that GRA14 did not affect the growth

and virulence of parasites following intraperitoneal injection of mice (17, 44). Unlike intraperitoneal inoculation, which results in a rapid, acute systemic infection, intra-footpad inoculation allows us to observe the gradual spread of *T. gondii* *in vivo* (45). Generally, intraperitoneal infection by RH tachyzoites was lethal. However, intra-footpad infection led to survival or, at least, a prolonged survival time in the present study. Therefore, deleting GRA14 may result in a lethal parasitic load in mice. By contrast, mice infected with RH Δ gra7 parasites experienced a significant delay in death compared with the parental RH strain. A previous study reported that outbred CD-1 mice infected with RH Δ gra7 parasites exhibited a similar phenotype (25). GRA7 binds to the GTP-bound immunity-related GTPase a6 and acts synergistically with ROP18 to block immunity-related GTPases (25, 26). Thus, these results suggest that GRA14 plays an important role in the control of parasite infection, creating a paradigm that protects the host animals from acute infection and death.

In conclusion, the present study demonstrated new molecular functions for GRA7 and GRA14 and confirmed their role in the induction of NF κ B during a type II strain infection. NF κ B activation mediated via GRA7, GRA14, and GRA15 was closely related to the Th1 response promoted by inflammatory cytokines following the activation of macrophages. This immune response limits the tissue invasion of the parasite, ensuring the survival of the host but, paradoxically, also aiding the survival of the parasite by converting it into a bradyzoite form able to persist in the muscle and brain tissues (46). GRA7 has multiple target components within the host cell that cause different virulence phenotypes dependent on the type of parasite. Whereas, the GRA14 protein has a low polymorphic phenotype and is potentially functional throughout type I, II, and III strains. Moreover, the suppressive control of virulence by early immune activation after infection, which has been regarded as a unique event to type II strains, is a conserved strategy across parasite strains. This may contribute to the high prevalence and wide distribution of this protozoan parasite. Thus, further insight into the precise role of these GRAs may help delineate the mechanism of NF κ B modulation by *T. gondii*.

DATA AVAILABILITY STATEMENT

The original contributions presented in the study are publicly available. This data can be found in NCBI SRA: <https://www.ncbi.nlm.nih.gov/sra/?term=DRA010408>, accession number DRA010408.

ETHICS STATEMENT

The experimental protocol was approved by the Committee on the Ethics of Animal Experiments at the Obihiro University of Agriculture and Veterinary Medicine (permit number: 19-50).

AUTHOR CONTRIBUTIONS

FI, RE, YH, KK, KU, ST, and RI conducted the experiments. FI, MY, and YN designed the experiments. FI and YN performed the

data analyses and wrote the manuscript. All authors revised the manuscript and approved the final version.

FUNDING

This research was supported by the Japan Society for the Promotion of Science (JSPS) through the Funding Program for Next Generation World-Leading Researchers (NEXT Program), initiated by the Council for Science and Technology Policy (2011/LS003) (to YN), Grant-in-Aid for Exploratory Research (JP15K15118) (to YN) by a grant-in-Aid for Young Scientists (18K14577) (to FI), Challenging Research (Exploratory) JP17K19538 (to YN), and a research fellowship (15J03171) (to FI) from the Japan Society for the Promotion of Science, Japan. This study was supported by the Research Program on Emerging and Re-emerging Infectious Diseases (JP17fk0108120 and JP20fk0108137) (to MY) from the Agency for Medical Research and Development. This study was supported by a Grant for a Joint Research Project from the Research Institute for Microbial Diseases, Osaka University (to YN).

ACKNOWLEDGMENTS

We acknowledge the NGS core facility of the Genome Information Research Center at the Research Institute for Microbial Diseases of Osaka University for their support in RNA sequencing and data analysis. We express our gratitude to Prof. John Boothroyd (Stanford University School of Medicine) and Prof. Peter Bradley (University of California, Los Angeles) for providing us with RH $\Delta ku80\Delta hxpgrt\Delta gra7$ parasites and RH $\Delta ku80\Delta hxpgrt\Delta gra14$ parasites, respectively. The authors would like to thank Kate Fox, DPhil, from Edanz Group (www.edanzediting.com/ac) and Rochelle Haidee D. Ybanez for editing a draft of this manuscript.

SUPPLEMENTARY MATERIAL

The Supplementary Material for this article can be found online at: <https://www.frontiersin.org/articles/10.3389/fimmu.2020.01709/full#supplementary-material>

Supplemental Data Sheet 1 | Detailed expression data for GRA-dependently regulated genes.

Supplemental Data Sheet 2 | Results of KEGG pathway analysis.

Supplemental Data Sheet 3 | Heat map.

Supplemental Figure 1 | GRA knockout and the complementation strategies. **(A)** Schematic genomic representation of the GRA7 locus and the plasmid construct used to target the GRA7 gene. The drug-resistant hypoxanthine-xanthine-guanine phosphoribosyl transferase (HXGPRT) cassette was surrounded by the 5' and 3' untranslated regions (UTR) of GRA7. **(B)** Schematic representation of the CRISPR/CAS9 strategy used to inactivate the target genes by inserting the pyrimethamine-resistance DHFR cassette (DHFR*). Transfection of the CRISPR plasmid targeting TgGRA (G01), together with an amplicon containing the DHFR*-expressing cassette flanked by regions homologous to the target gene, was used to disrupt the corresponding target gene by insertion. **(C)** Transfection of the CRISPR plasmid targeting the TgUPRT gene, together with an amplicon containing 1,000 bp of the 5' and 3' untranslated regions (5' UTR and 3' UTR) flanked by regions homologous to the TgUPRT gene, was used.

Supplemental Figure 2 | IFAT and western blotting to confirm the expression of TgGRA7 and TgGRA14. **(A)** IFAT analysis of Vero cells infected with Pm, PruAgra7 (deltaGRA7), PruAgra14 (deltaGRA14), and complemented (CompGRA7 and CompGRA14) parasites at 24 h post-infection. Cells were fixed and stained with a-TgSAG1 (green), a-TgGRA7 (red), a-TgGRA14 (red), and Hoechst dye (blue). Bars, 10 μ m. **(B)** Western blots of the parasite strains. Into each lane, 1×10^6 parasites were loaded. Anti-TgGRA7 and anti-GRA14 antibodies detected 25.9 and 42 kDa proteins in the parental Pru and complemented parasites, respectively, but not in the deficient mutant parasites.

Supplemental Figure 3 | Forced expression of GRA7, GRA14, and GRA15 in 293T cells. 293T cells were transiently transfected with the expression vectors for GRA7, GRA14, and GRA15. Cells lysates were then separated by SDS-PAGE, and western blot analysis was carried out using an anti-FLAG antibody. The estimated sizes of the FLAG-tag fused to GRA7, GRA14, and GRA15 were 29.9, 48.7, and 61.8 kDa, respectively. However, the observed molecular weight of the FLAG-tag fused to GRA15 (~75 kDa), was higher than the expected predicted size (61.8 kDa). It has been shown that this is not caused by parasite-mediated modification of GRA15. Most likely, it is the particular amino acid composition of GRA15, which is enriched in Pro, Ser, and Thr, that makes it run slower than expected on an SDS-PAGE gel. Black arrows indicate the estimated band sizes of the target proteins.

Supplemental Figure 4 | Luciferase activities in 293T cells transfected with various reporter plasmids. 293T cells were transiently transfected with pGL4.29 (CRE), pGL4.30 (NFAT), pGL4.32 (NF κ B1), pGL4.33 (SRE), pGL4.34 (SRF), and pGL4.44 (AP1) expressing firefly luciferase and pGL4.74 expressing renilla luciferase. Cells were immediately transfected with the expression vectors of GRA7, GRA14, GRA15, and the empty p3 \times FLAG-cmv14 vector used as a negative (empty) control. The promoter activity was shown as relative fold-increase as compared to control cells in the luciferase activity normalized for Renilla luciferase activity. Values are the means of triplicate samples.

Supplemental Figure 5 | Infection rate, growth, and egress assay. **(A)** Infection rates of the different parasite lines in Vero cells at 24 h post-infection. **(B)** Egress rates of the different parasite lines in Vero cells at 72 h post-infection. **(C)** Intracellular replication assay of the parasite lines in Vero cells at 48 h post-infection. Each bar represents the means \pm the standard deviation ($n = 4$ for all groups), and the results represent two independent experiments with similar results. Statistical analysis was performed using one-way ANOVA, *a significant difference ($p < 0.05$).

Supplemental Figure 6 | Expression levels of chemokines and cytokines in Raw246.7 macrophage cells. **(A,B)** Raw246.7 macrophage cells were infected with parasite strains for 24 h, then cells were lysed, and total RNA was extracted. RNA was used to synthesize cDNA. Real-time RT-qPCR amplification was carried out for CXCL1, CXCL5, IL-1 β , IL-6, and Cc117. Each bar represents the mean \pm the standard deviation ($n = 3$ for all groups), and the results are from a single experiment. Statistical analysis was performed using one-way ANOVA with *post-hoc* Tukey's test, *a significant difference ($p < 0.05$).

Supplemental Figure 7 | *In vivo* cytokine ELISA and parasite burden. Mice were infected with 500 tachyzoites of the parasites and then euthanized to examine the parasite burden and level of cytokine secretion, including IL-12p40 and IFN- γ , 5 days after infection. **(A,B)** Parasite burden in the spleen and peritoneal cavity in mice infected with parental Pru, PruLgra14 (deltaGRA14), and the complemented parasites (Comp). **(C,D)** Levels of serum IFN- γ and IL-12p40 in mice. **(E,F)** Cytokine levels in the peritoneal cavity in mice. Each plot represents data from one mouse. Statistically significant differences were analyzed by one-way ANOVA with *post-hoc* Tukey's test but no significant difference was found. Data were collected from one experiment.

Supplemental Figure 8 | Levels of interleukin-12p40 in thioglycolate-elicited macrophage cells. Macrophages were infected with the parental Pru, PruAgra7, PruAgra14, and PruAgra15 parasite strains. At every 6 h for 24 h post-infection, supernatants were collected, and IL-12p40 levels were determined by cytokine ELISA. Values are the means \pm SD of four samples, *a significant difference ($p < 0.05$). #a significantly lower level of IL-12p40 compared with the Pm strain infected cells ($p < 0.05$). Differences were tested by one-way ANOVA with Turkey's *post-hoc* test.

REFERENCES

- Luft BJ, Brooks RG, Conley FK, McCabe RE, Remington JS. Toxoplasmic encephalitis in patients with acquired immune deficiency syndrome. *JAMA*. (1984) 252:913–17. doi: 10.1001/jama.1984.03350070031018
- Luft BJ, Remington JS. Toxoplasmic encephalitis in AIDS. *Clin Infect Dis*. (1992) 15:211–22. doi: 10.1093/clinids/15.2.211
- Kravetz JD, Federman DG. Toxoplasmosis in pregnancy. *Am J Med*. (2005) 118:212–16. doi: 10.1016/j.amjmed.2004.08.023
- Saeij JPJ, Boyle JP, Boothroyd JC. Differences among the three major strains of *Toxoplasma gondii* and their specific interactions with the infected host. *Trends Parasitol*. (2005) 21:476–81. doi: 10.1016/j.pt.2005.08.001
- Sibley LD, Boothroyd JC. Virulent strains of *Toxoplasma gondii* comprise a single clonal lineage. *Nature*. (1992) 359:82–85. doi: 10.1038/359082a0
- Lorenzi H, Khan A, Behnke MS, Namasivayam S, Swapna LS, Hadjithomas M, et al. Local admixture of amplified and diversified secreted pathogenesis determinants shapes mosaic *Toxoplasma gondii* genomes. *Nat Commun*. (2016) 7:10147. doi: 10.1038/ncomms10147
- Hakimi M-A, Boudgour A. *Toxoplasma*'s ways of manipulating the host transcriptome via secreted effectors. *Curr Opin Microbiol*. (2015) 26:24–31. doi: 10.1016/j.mib.2015.04.003
- Melo MB, Jensen KDC, Saeij JPJ. *Toxoplasma gondii* effectors are master regulators of the inflammatory response. *Trends Parasitol*. (2011) 27:487–95. doi: 10.1016/j.pt.2011.08.001
- Ghosh S, May MJ, Kopp EB. NF- κ B and rel proteins: evolutionarily conserved mediators of immune responses. *Annu Rev Immunol*. (1998) 16:225–60. doi: 10.1146/annurev.immunol.16.1.225
- Karin M, Ben-Neriah Y. Phosphorylation meets ubiquitination: the control of NF- κ B activity. *Annu Rev Immunol*. (2000) 18:621–63. doi: 10.1146/annurev.immunol.18.1.621
- Li Q, Verma IM. NF- κ B regulation in the immune system. *Nat Rev Immunol*. (2002) 2:725–34. doi: 10.1038/nri910
- Tato CM, Hunter CA. Host-pathogen interactions: subversion and utilization of the NF- κ B pathway during infection. *Infect Immun*. (2002) 70:3311–17. doi: 10.1128/IAI.70.7.3311-3317.2002
- Caamaño J, Alexander J, Craig L, Bravo R, Hunter CA. The NF- κ B family member RelB is required for innate and adaptive immunity to *Toxoplasma gondii*. *J Immunol*. (1999) 163:4453–61.
- Mason NJ, Artis D, Hunter CA. New lessons from old pathogens: what parasitic infections have taught us about the role of nuclear factor- κ B in the regulation of immunity. *Immunol Rev*. (2004) 201:48–56. doi: 10.1111/j.0105-2896.2004.00189.x
- Rosowski EE, Lu D, Julien L, Rodda L, Gaiser RA, Jensen KDC, et al. Strain-specific activation of the NF- κ B pathway by GRA15, a novel *Toxoplasma gondii* dense granule protein. *J Exp Med*. (2011) 208:195–212. doi: 10.1084/jem.20100717
- Yang C-S, Yuk J-M, Lee Y-H, Jo E-K. *Toxoplasma gondii* GRA7-induced TRAF6 activation contributes to host protective immunity. *Infect Immun*. (2016) 84:339–50. doi: 10.1128/IAI.00734-15
- Rome ME, Beck JR, Turetzky JM, Webster P, Bradley PJ. Intervacuolar transport and unique topology of GRA14, a novel dense granule protein in *Toxoplasma gondii*. *Infect Immun*. (2008) 76:4865–75. doi: 10.1128/IAI.00782-08
- Sibley LD, Messina M, Niesman IR. Stable DNA transformation in the obligate intracellular parasite *Toxoplasma gondii* by complementation of tryptophan auxotrophy. *Proc Natl Acad Sci USA*. (1994) 91:5508–12. doi: 10.1073/pnas.91.12.5508
- Nishikawa Y, Shimoda N, Fereig RM, Moritaka T, Umeda K, Nishimura M, et al. *Neospora caninum* dense granule protein 7 regulates the pathogenesis of neosporosis by modulating host immune response. *Appl Environ Microbiol*. (2018) 84:e01350–18. doi: 10.1128/AEM.01350-18
- Yu G, Wang L-G, Han Y, He Q-Y. clusterProfiler: an R package for comparing biological themes among gene clusters. *OMICS*. (2012) 16:284–7. doi: 10.1089/omi.2011.0118
- Warnes GR, Bolker B, Bonebakker L, Gentleman R, Huber W, Liaw A, et al. *gplots: Various R Programming Tools for Plotting Data*. R package version 2:1 (2009).
- Jacobs D, Dubremetz JF, Loyens A, Bosman F, Saman E. Identification and heterologous expression of a new dense granule protein (GRA7) from *Toxoplasma gondii*. *Mol Biochem Parasitol*. (1998) 91:237–49. doi: 10.1016/S0166-6851(97)00204-1
- Rezaei F, Sharif M, Sarvi S, Hejazi SH, Aghayan S, Pagheh AS, et al. A systematic review on the role of GRA proteins of *Toxoplasma gondii* in host immunization. *J Microbiol Methods*. (2019) 165:105696. doi: 10.1016/j.mimet.2019.105696
- Dunn JD, Ravindran S, Kim S-K, Boothroyd JC. The *Toxoplasma gondii* dense granule protein GRA7 is phosphorylated upon invasion and forms an unexpected association with the rhoGTPase proteins ROP2 and ROP4. *Infect Immun*. (2008) 76:5853–61. doi: 10.1128/IAI.01667-07
- Alagunan A, Fentress SJ, Tang K, Wang Q, Sibley LD. *Toxoplasma* GRA7 effector increases turnover of immunity-related GTPases and contributes to acute virulence in the mouse. *Proc Natl Acad Sci USA*. (2014) 111:1126–31. doi: 10.1073/pnas.1313501111
- Hermanns T, Müller UB, Könen-Waisman S, Howard JC, Steinfeldt T. The *Toxoplasma gondii* rhoGTPase protein ROP18 is an Irga6-specific kinase and regulated by the dense granule protein GRA7. *Cell Microbiol*. (2016) 18:244–59. doi: 10.1111/cmi.12499
- Koh H-J, Kim Y-R, Kim J-S, Yun J-S, Jang K, Yang C-S. *Toxoplasma gondii* GRA7-targeted ASC and PLD1 promote antibacterial host defense via PKC α . *PLoS Pathog*. (2017) 13:e1006126. doi: 10.1371/journal.ppat.1006126
- Ahmadpour E, Sarvi S, Hashemi Soteh MB, Sharif M, Rahimi MT, Valadan R, et al. Evaluation of the immune response in BALB/c mice induced by a novel DNA vaccine expressing GRA14 against *Toxoplasma gondii*. *Parasite Immunol*. (2017) 39. doi: 10.1111/pim.12419
- Ahmadpour E, Sarvi S, Hashemi Soteh MB, Sharif M, Rahimi MT, Valadan R, et al. Enhancing immune responses to a DNA vaccine encoding *Toxoplasma gondii* GRA14 by calcium phosphate nanoparticles as an adjuvant. *Immunol Lett*. (2017) 185:40–47. doi: 10.1016/j.imlet.2017.03.006
- Rahimi MT, Sarvi S, Sharif M, Abediankenari S, Ahmadpour E, Valadan R, et al. Immunological evaluation of a DNA cocktail vaccine with co-delivery of calcium phosphate nanoparticles (CaPNs) against the *Toxoplasma gondii* RH strain in BALB/c mice. *Parasitol Res*. (2017) 116:609–16. doi: 10.1007/s00436-016-5325-6
- Ahady MT, Hoghooghi-Rad N, Madani R, Esmaili Rastaghi AR. Identification of antigenic and immunogenic proteins of *Toxoplasma gondii* in human and sheep by immunoproteomics. *Iran J Parasitol*. (2018) 13:39–48.
- Pagheh AS, Sarvi S, Gholami S, Asgarian-Omran H, Valadan R, Hassannia H, et al. Protective efficacy induced by DNA prime and recombinant protein boost vaccination with *Toxoplasma gondii* GRA14 in mice. *Microb Pathog*. (2019) 134:103601. doi: 10.1016/j.micpath.2019.103601
- Jensen KDC, Wang Y, Wojno EDT, Shastri AJ, Hu K, Cornel L, et al. *Toxoplasma* polymorphic effectors determine macrophage polarization and intestinal inflammation. *Cell Host Microbe*. (2011) 9:472–83. doi: 10.1016/j.chom.2011.04.015
- Sher A, Collazzo C, Scanga C, Jankovic D, Yap G, Aliberti J. Induction and regulation of IL-12-dependent host resistance to *Toxoplasma gondii*. *Immunol Res*. (2003) 27:521–7. doi: 10.1385/IR.27.2.3.521
- Boehm U, Klamp T, Groot M, Howard JC. Cellular responses to interferon- γ . *Annu Rev Immunol*. (1997) 15:749–95. doi: 10.1146/annurev.immunol.15.1.749
- Yang C-S. Advancing host-directed therapy for tuberculosis: new therapeutic insights from the *Toxoplasma gondii*. *Microb Cell*. (2007) 4:105–7. doi: 10.15698/mic2017.03.565
- Fox BA, Guevara RB, Rommereim LM, Falla A, Bellini V, Pètre G, et al. *Toxoplasma gondii* Parasitophorous vacuole membrane-associated dense granule proteins orchestrate chronic infection and GRA12 underpins resistance to host gamma interferon. *mBio*. (2019) 10:e00589–19. doi: 10.1128/mBio.00589-19
- Sangaré LO, Yang N, Konstantinou EK, Lu D, Mukhopadhyay D, Young LH, et al. *Toxoplasma* GRA15 activates the NF- κ B pathway through interactions with TNF receptor-associated factors. *mBio*. (2019) 10:e00808–19. doi: 10.1128/mBio.00808-19

39. Du J, An R, Chen L, Shen Y, Chen Y, Cheng L, et al. *Toxoplasma gondii* virulence factor ROP18 inhibits the host NF- κ B pathway by promoting p65 degradation. *J Biol Chem.* (2014) 289:12578–92. doi: 10.1074/jbc.M113.544718
40. Saeij JPJ, Collier S, Boyle JP, Jerome ME, White MW, Boothroyd JC. *Toxoplasma* co-opts host gene expression by injection of a polymorphic kinase homologue. *Nature.* (2007) 445:324–7. doi: 10.1038/nature05395
41. Molestina RE, Payne TM, Coppens I, Sinai AP. Activation of NF- κ B by *Toxoplasma gondii* correlates with increased expression of antiapoptotic genes and localization of phosphorylated I κ B to the parasitophorous vacuole membrane. *J Cell Sci.* (2003) 116:4359–71. doi: 10.1242/jcs.00683
42. Payne TM, Molestina RE, Sinai AP. Inhibition of caspase activation and a requirement for NF-kappaB function in the *Toxoplasma gondii*-mediated blockade of host apoptosis. *J Cell Sci.* (2003) 116:4345–58. doi: 10.1242/jcs.00756
43. Molestina RE, Sinai AP. Host and parasite-derived IKK activities direct distinct temporal phases of NF-kappaB activation and target gene expression following *Toxoplasma gondii* infection. *J Cell Sci.* (2005) 118:5785–96. doi: 10.1242/jcs.02709
44. Bai M-J, Wang J-L, Elsheikha HM, Liang Q-L, Chen K, Nie L-B, et al. Functional characterization of dense granule proteins in *Toxoplasma gondii* RH strain using CRISPR-Cas9 system. *Front Cell Infect Microbiol.* (2018) 8:300. doi: 10.3389/fcimb.2018.00300
45. Ma JS, Sasai M, Ohshima J, Lee Y, Bando H, Takeda K, et al. Selective and strain-specific NFAT4 activation by the *Toxoplasma gondii* polymorphic dense granule protein GRA6. *J Exp Med.* (2014) 211:2013–32. doi: 10.1084/jem.20131272
46. Filisetti D, Candolfi E. Immune response to *Toxoplasma gondii*. *Ann Super Sanita.* (2004) 40:71–80.

Conflict of Interest: The authors declare that the research was conducted in the absence of any commercial or financial relationships that could be construed as a potential conflict of interest.

Copyright © 2020 Ihara, Fereig, Himori, Kameyama, Umeda, Tanaka, Ikeda, Yamamoto and Nishikawa. This is an open-access article distributed under the terms of the Creative Commons Attribution License (CC BY). The use, distribution or reproduction in other forums is permitted, provided the original author(s) and the copyright owner(s) are credited and that the original publication in this journal is cited, in accordance with accepted academic practice. No use, distribution or reproduction is permitted which does not comply with these terms.



Liposomes Loaded With Phosphatidylinositol 5-Phosphate Improve the Antimicrobial Response to *Pseudomonas aeruginosa* in Impaired Macrophages From Cystic Fibrosis Patients and Limit Airway Inflammatory Response

OPEN ACCESS

Edited by:

Luigina Romani,
University of Perugia, Italy

Reviewed by:

Karlhans Fru Che,
Karolinska Institutet (KI), Sweden
Dwayne R. Roach,
San Diego State University,
United States

*Correspondence:

Maurizio Fraziano
fraziano@bio.uniroma2.it

Specialty section:

This article was submitted to
Microbial Immunology,
a section of the journal
Frontiers in Immunology

Received: 03 February 2020

Accepted: 10 September 2020

Published: 02 October 2020

Citation:

Poerio N, De Santis F, Rossi A, Ranucci S, De Fino I, Henriquez A, D'Andrea MM, Ciciriello F, Lucidi V, Nisini R, Bragonzi A and Fraziano M (2020) Liposomes Loaded With Phosphatidylinositol 5-Phosphate Improve the Antimicrobial Response to *Pseudomonas aeruginosa* in Impaired Macrophages From Cystic Fibrosis Patients and Limit Airway Inflammatory Response. *Front. Immunol.* 11:532225. doi: 10.3389/fimmu.2020.532225

Noemi Poerio¹, Federica De Santis¹, Alice Rossi², Serena Ranucci², Ida De Fino², Ana Henriquez¹, Marco M. D'Andrea¹, Fabiana Ciciriello³, Vincenzina Lucidi³, Roberto Nisini⁴, Alessandra Bragonzi² and Maurizio Fraziano^{1*}

¹ Dipartimento di Biologia, Università degli Studi di Roma "Tor Vergata", Roma, Italy, ² Unità di Infezioni e Fibrosi Cistica, Istituto Scientifico San Raffaele, Milano, Italy, ³ Unità Operativa Complessa Fibrosi Cistica, Dipartimento di Medicina Pediatrica, Ospedale Pediatrico Bambino Gesù, Roma, Italy, ⁴ Dipartimento di Malattie Infettive, Istituto Superiore di Sanità, Roma, Italy

Despite intensive antimicrobial and anti-inflammatory therapies, cystic fibrosis (CF) patients are subjected to chronic infections due to opportunistic pathogens, including multidrug resistant (MDR) *Pseudomonas aeruginosa*. Macrophages from CF patients show many evidences of reduced phagocytosis in terms of internalization capability, phagosome maturation, and intracellular bacterial killing. In this study, we investigated if apoptotic body-like liposomes (ABLs) loaded with phosphatidylinositol 5-phosphate (PI5P), known to regulate actin dynamics and vesicular trafficking, could restore phagocytic machinery while limiting inflammatory response in *in vitro* and *in vivo* models of MDR *P. aeruginosa* infection. Our results show that the *in vitro* treatment with ABL carrying PI5P (ABL/PI5P) enhances bacterial uptake, ROS production, phagosome acidification, and intracellular bacterial killing in human monocyte-derived macrophages (MDMs) with pharmacologically inhibited cystic fibrosis transmembrane conductance regulator channel (CFTR), and improve uptake and intracellular killing of MDR *P. aeruginosa* in CF macrophages with impaired bactericidal activity. Moreover, ABL/PI5P stimulation of CFTR-inhibited MDM infected with MDR *P. aeruginosa* significantly reduces NF- κ B activation and the production of TNF- α , IL-1 β , and IL-6, while increasing IL-10 and TGF- β levels. The therapeutic efficacy of ABL/PI5P given by pulmonary administration was evaluated in a murine model of chronic infection with MDR *P. aeruginosa*. The treatment with ABL/PI5P significantly reduces pulmonary neutrophil infiltrate and the levels of KC and MCP-2 cytokines in the lungs, without affecting pulmonary bacterial load. Altogether,

these results show that the ABL/PI5P treatment may represent a promising host-directed therapeutic approach to improve the impaired phagocytosis and to limit the potentially tissue-damaging inflammatory response in CF.

Keywords: phosphatidylinositol 5-phosphate, host-directed therapy, cystic fibrosis, innate immunity, *Pseudomonas aeruginosa*, liposome

INTRODUCTION

Cystic fibrosis (CF) is an autosomal recessive genetic disease caused by a mutation in the gene encoding the cystic fibrosis transmembrane conductance regulator channel (CFTR) (1). The CFTR is usually expressed on the apical membrane of epithelia, and its dysfunction causes a defective chloride secretion leading to a modification in the airway surface liquid (2). The pathophysiological changes in CF result in a systemic disease, which affects the pancreas, liver, reproductive tract, and mainly the lungs (3). Here, the loss of function of CFTR causes a defective mucociliary clearance and a dramatic production of sticky mucus, which is associated with chronic infection by opportunistic pathogens, such as *P. aeruginosa* (4). Infections sustained by MDR *P. aeruginosa* in CF are increasing, reflecting cumulative exposure to antibiotic treatment (5). Moreover, the chronic bacterial infections associated with the persistent inflammation, leading to pulmonary insufficiency, represent the main cause of mortality and morbidity in CF patients (6). Today, the identification of novel host- and/or pathogen-directed therapeutic tools represents an urgent challenge for the scientific community to fight the emergence of MDR pathogens, as well as a priority also at the global level.

The defective antimicrobial response exerted by innate immune cells in CF patients has been documented and depends, at least in part, on a dysfunctional phagocytosis process (7, 8). Phagocytosis is an important innate effector mechanism deputed to the intracellular elimination of invading pathogen by the generation of highly microbicidal organelles called phagolysosomes. These organelles originate from a phagosome, generated by the invagination of plasma membrane, which matures to a fully microbicidal phagolysosome, through sequential events of fusion with early endosomes, late endosomes, and, ultimately, lysosomes. This process is driven by a topologically and timely coordinated expression of second lipid messengers, which recruit signal proteins, on the nascent or maturing phagosome, through specific lipid-binding domains (9, 10), and may be target of bacterial interference (11).

The second lipid messenger phosphatidylinositol 5-phosphate (PI5P) is a minor phosphoinositide representing less than 10% of the total lipids (12). PI5P can be directly produced from phosphatidyl inositol (PI) by the activity of phosphoinositide 5-kinase (PIKfyve) or by the dephosphorylation of phosphatidylinositol 3,5-bisphosphate (PI3,5P₂) by myotubularin 3-phosphatases (13). PI5P is present at the cellular membrane and at the early phagosome (14), and its level result increased during the late stages of the phagocytosis process (15). Moreover, it can

regulate endosome vesicle trafficking (16), cellular actin remodeling, and bacterial invasion (14), and can be involved in class III phosphatidylinositol 3-kinase (Vps34)-independent autophagy activation (17).

In this study, we have generated asymmetric apoptotic body-like liposomes (ABLs) composed by phosphatidylserine (PS) at the outer membrane surface resembling an apoptotic body, to target macrophages and to downmodulate inflammatory reaction (18), and by the bioactive lipid PI5P at the inner membrane surface to enhance the phagocytosis process. In particular, this study evaluates the immunotherapeutic value of ABL/PI5P *in vitro* in impaired macrophages from CF patients and *in vivo* in models of *P. aeruginosa* infection, assessed in terms of i) uptake and intracellular bacterial killing, ii) mechanisms of bactericidal activity, and iii) potentially tissue-damaging inflammatory response.

MATERIAL AND METHODS

Liposome Preparation

Apoptotic body-like liposomes (ABLs) were produced as previously described (19). Briefly, the inner monolayer lipids composed by 1,2-dioleoyl-*sn*-glycero-3-phospho-(1'-myo-inositol-5'-phosphate) (PI5P, Avanti Polar Lipids) were suspended in anhydrous dodecane (Sigma) at a concentration of 0.05 mg/ml. L- α -phosphatidylserine (PS, Avanti Polar Lipids) was used as outer monolayer lipid and was added to a 99:1 dodecane:silicone solution to obtain a final concentration of 0.05 mg/ml. Asymmetric liposomes were prepared by adding 2 ml of outer monolayer lipid suspension over 3 ml of cell culture medium (for *in vitro* experiments) or saline (for *in vivo* experiments). Finally, 100 μ l of the inner monolayer lipid suspensions were added over the 2-ml lipid phase, and the samples were centrifuged at 120 \times g for 10 min. After the centrifugation, ABLs were collected in the aqueous phase using a 5-ml syringe with a 16-gauge stainless steel needle, in order to produce PS outside/PI5P inside liposomes (ABL/PI5P). Liposomes were then quantified by a flow cytometer FACSCalibur (Becton Dickinson), allowing quantification of monodispersed vesicles >0.2 μ m in diameter.

Cell Culture

Primary monocyte-derived macrophages (MDMs) were prepared as previously described (17). Briefly, peripheral blood mononuclear cells (PBMCs) from healthy donors and CF patients were isolated by Ficoll density gradient, and monocytes were then positively sorted using anti-CD14

monoclonal antibodies conjugated to magnetic microbeads (Miltenyi Biotec), according to manufacturer's instructions. Monocytes were then suspended in complete medium and incubated for a further 5 days in 96-well plates at a concentration of 10^6 cells/ml in the presence of M-CSF (50 ng/ml, Miltenyi Biotec) to get differentiated macrophages.

Bacteria

MDR *P. aeruginosa* strain (ATCC[®] BAA-2113) was used in *in vitro* experiments and MDR-RP73 *P. aeruginosa* clinical isolate (20) was used in an *in vivo* mouse model of chronic *P. aeruginosa* infection (21, 22). The BAA-2113 single colony was collected by streaking on Trypticase soy agar (TSA, BD Difco[™]) and then suspended in 15 ml of Trypticase soy broth (TSB, BD Difco[™]). Bacteria were grown in Erlenmeyer flask at 37°C under stirring for 18 h, and their growth was monitored by measuring the optical density at a wavelength of 600 nm by Varioskan LUX Multimode Microplate Reader (Thermo Fisher Scientific). BAA-2113 was stored at -80°C until use after suspension in TSB and 30% glycerol.

For *in vivo* experiments, an aliquot of RP73 strain from glycerol stocks (TSB + 25% glycerol) was streaked for isolation on TSA and incubated at 37°C O/N. One colony was picked from the plate and used to inoculate 10 ml of TSB and placed overnight in a shaking incubator at 37°C 200 rpm. Thereafter, bacterial suspension was diluted to 0.15 OD/ml in 20 ml of TSB/flask and grown for 4 h at 37°C at 200 rpm, to reach the log phase.

Patients

CF patients (n = 19) were enrolled at “Bambino Gesù” Children's Hospital in Rome, Italy. All of the CF patients were clinically

stable at the time of blood donation (5 ml). Controls (n = 20) were represented by buffy coats from healthy blood donors, attending at the Blood Transfusion Unit of Policlinico “Umberto I” in Rome, Italy. Clinical and demographic features of CF patients as well as healthy controls are summarized in **Table 1**.

Evaluation of *In Vitro* Bacterial Uptake and Intracellular Growth

To assess bacterial uptake, MDMs from healthy donors or from CF patients were distributed in 96-well plates at a concentration of 2×10^5 cells/well and were stimulated with ABL/PI5P used at a ratio of 1:1 (ABL:MDM), for 30 min before infection and/or simultaneously with the infection, in the presence or absence of the CFTR inhibitor INH172 (Sigma), used at a concentration of 10 μ M. Then cells were washed once and infected with MDR *P. aeruginosa* for 1 h at 37°C at an MOI of 30 in the presence or absence of INH172. Thereafter, extracellular bacilli were killed at 1 h of incubation with 400 μ g/ml amikacin. Finally, cells were lysed with 1% deoxycholate (Sigma), samples were diluted in PBS-tween 80, and colony-forming units (CFUs) were quantified by plating bacilli in triplicate on TSA.

To assess intracellular bacterial growth, MDMs from healthy donors or from CF patients were distributed in 96-well plates at a concentration of 2×10^5 cells/well and were infected with MDR *P. aeruginosa*, for 1 h at 37°C at an MOI of 30, in the presence or absence of INH172, used at a concentration of 10 μ M. Thereafter, extracellular bacilli were killed at 1 h of incubation with 400 μ g/ml amikacin. Cells were then washed and incubated with ABL/PI5P, added to a ratio of 1:1 (ABL:MDM) for a further 2 h, in the presence or absence of INH172. Finally, cells were lysed with 1% deoxycholate (Sigma), samples were diluted in PBS-tween 80, and CFUs were quantified by plating bacilli in triplicate on TSA.

TABLE 1 | Demographic and clinical characteristics of cystic fibrosis (CF) patients and healthy donors (HD).

CF	Age (range)	Genotype	Microbiology	FEV-1 (%)	HD	Age (range)
1	26–30	F508del/N1303K	<i>S.a.</i> , <i>A.x.</i> , <i>S.m.</i>	44	1	36–40
2	16–20	F508del/P5L	<i>S.a.</i>	79	2	21–25
3	11–15	G576A/R668C	<i>S.a.</i> , <i>En.c.</i> , <i>E.a.</i>	106	3	51–55
4	21–25	F508del/F508del	<i>S.a.</i> , <i>B.b.</i>	85	4	56–60
5	31–35	F508del/f508del	<i>S.a.</i> , <i>Bu.c.</i>	72	5	41–45
6	21–25	F508del/621+1G>T	<i>P.a.</i> , <i>Bu.c.</i>	50	6	36–40
7	41–45	F508del/F508del	<i>S.m.</i> , <i>Bu.c.</i>	91	7	56–60
8	31–35	F508del/W1282X	<i>S.a.</i> , <i>P.a.</i>	109	8	56–60
9	26–30	F508del/F508del	<i>S.a.</i> , <i>Es.c.</i>	115	9	41–45
10	21–25	F508del/G1244E	<i>S.a.</i>	97–103	10	56–60
11	26–30	F508del/G542X	<i>E.f.</i> , <i>S.a.</i> , <i>C.g.</i> , <i>S.m.</i>	65	11	51–55
12	26–30	DeltaF508/G85E	<i>S.a.</i> , <i>P.m.</i> , <i>S.m.</i> , <i>A.f.</i>	82	12	46–50
13	6–10	DeltaF508/R334L	<i>S.p.</i> , <i>S.a.</i> , <i>H.i.</i>	95–104	13	21–25
14	11–15	R553X/3272-26A->G	<i>S.a.</i>	88	14	41–45
15	6–10	G85E/621+1G->T	<i>A.f.</i> , <i>H.i.</i>	86	15	56–60
16	21–25	G1244E/T338I	<i>H.i.</i>	102	16	51–55
17	6–10	1717-1G->A/E831X	<i>GAS</i> , <i>Br.c.</i> , <i>H.i.</i>	119	17	41–45
18	16–20	W1282X/2789+5G>A	<i>S.a.</i> , <i>Sc.a.</i>	85	18	31–35
19	26–30	DeltaF508/DeltaF508	<i>S.a.</i> , <i>P.a.</i>	25	19	21–25
					20	26–30

S.a., *Staphylococcus aureus*; *A.x.*, *Achromobacter xylosoxidans*; *S.m.*, *Stenotrophomonas maltophilia*; *En.c.*, *Enterobacter cloacae*; *E.a.*, *Enterobacter asburiae*; *B.b.*, *Bordetella bronchiseptica*; *Bu.c.*, *Burkholderia cepacia*; *P.a.*, *Pseudomonas aeruginosa*; *Es.c.*, *Escherichia coli*; *E.f.*, *Enterococcus faecalis*; *C.g.*, *Candida glabrata*; *P.m.*, *Proteus mirabilis*; *A.f.*, *Aspergillus fumigatus*; *S.p.*, *Streptococcus pneumoniae*; *H.i.*, *Haemophilus influenzae*; *GAS*, Group A *Streptococcus*; *Br.c.*, *Branhamella catarrhalis*; *S.a.*, *Scedosporium apiospermum*.

In order to evaluate the role of ROS and of phagosome acidification in intracellular bacterial killing, *P. aeruginosa*-infected cells were treated simultaneously with ABL/PI5P with either PEG-Catalase (100 U/ml) or Concanamycin A (10 nM), respectively.

Fluorimetric Analysis

Phagosome acidification was assessed by using the fluorescent probe Lysosensor green DND 189 (Molecular Probes) (23), which measures the pH of acidic organelles, such as phagolysosomes. Briefly, MDM from healthy donors were pretreated or not for 1 h with 10 μ M INH172 and then exposed or not to Crimson fluorescent microbeads (1 μ m FluoSpheres[®] carboxylate-modified microspheres, Life Technologies), for 1 h at 37°C at a ratio of 5:1 in the presence or absence of 10 μ M of INH172, in order to exclude possible differences in microbead internalization among experimental groups. Then cells were washed and incubated for a further 90 min with ABL/PI5P, added to a ratio of 1:1 (ABL:MDM), in the presence or absence of INH172. Cells were stained for 15 min at 37°C with 1 μ M of Lysosensor green DND 189. pH calibration curve was obtained by incubating macrophages in calibration buffers at pH 4.5, 5.5, 6.5, and 7.5 (Intracellular pH Calibration Buffer Kit, Molecular Probes), and by labeling cells for 15 min at 37°C with 1 μ M of Lysosensor green DND 189 according to the manufacturer's instructions. pH was evaluated by fluorimetry by setting the wavelength of excitation at 443 or 625 nm and emission at 505 or 645 nm, for Lysosensor green DND 189 and Crimson fluorescent microbeads, respectively.

ROS generation was analyzed by loading MDM isolated from healthy donors with the fluorescent indicator 20,70-dichlorofluorescein diacetate (DCF, Molecular Probes), used at a concentration of 10 μ M, for 40 min at 37°C in the dark. Thereafter, MDM isolated from healthy donors were pretreated or not for 1 h with 10 μ M INH172 and then exposed or not to Crimson fluorescent microbeads (1 μ m FluoSpheres[®] carboxylate-modified microspheres, Life Technologies), for 1 h at 37°C at a ratio of 5:1 in the presence or absence of 10 μ M of INH172, in order to exclude possible differences in microbead internalization among experimental groups. Cells were then washed and incubated for a further 90 min in the presence or absence of INH172 with ABL/PI5P, added to a ratio of 1:1 (ABL:MDM). The production of ROS was evaluated by fluorimetry by setting the wavelength of excitation at 443 or 625 nm and emission at 505 or 645 nm, for DCF and Crimson fluorescent microbeads, respectively. Fluorescence has been evaluated by the use of a Varioskan LUX Multimode Microplate Reader (Thermo Fisher Scientific).

Mouse Model of Chronic Infection

Immunocompetent C57Bl/6NCrIBR male mice (8–10 weeks, Charles River) ($n = 16$ treated with 3×10^5 ABL/PI5P and $n = 16$ treated with vehicle) were challenged with $3\text{--}4 \times 10^5$ CFUs of the *P. aeruginosa* MDR-RP73 embedded in agar beads for chronic infection by intratracheal (i.t.) administration. Agar beads were prepared following established procedures (21, 24). Local treatment by Penn-Century MicroSprayer[®] Aerosoliser

with 3×10^5 ABL/PI5P started soon (5 min) after infection and was repeated daily for 6 days. Body weight and health status were monitored daily. After 6 days postinfection, lung CFUs and cell counts in the bronchoalveolar lavage fluid (BALF) were analyzed as previously described (21, 24). Finally, 6 days after infection, murine lungs were excised aseptically and homogenized in 2 ml of PBS added with protease inhibitors (Complete[™] Protease Inhibitor cocktail—Roche) using the homogenizer GentleMACS[™] Octo Dissociator, and the levels of TNF- α , KC, JE, and MIP-2 in the supernatant of murine lungs were measured by ELISA kit (DuoSet[®] ELISA Development Systems).

Enzyme-Linked Immunosorbent Assay

MDMs were infected or not with *P. aeruginosa* (MOI 30) in the presence or absence of INH172 and stimulated or not with ABL/PI5P at a ratio of 1:1 (ABL:MDM) for 2 h. Thereafter, supernatants were collected, cells were lysed, and both stored at -20°C until analysis. The levels of tumor necrosis factor- α (TNF- α), interleukin-1 β (IL-1 β), IL-6, IL-10, and transforming growth factor-beta (TGF- β) in the supernatants of MDMs were measured by human TNF- α ELISA kit (BD Biosciences), human IL-6 DuoSet[®] ELISA Development Systems, human IL-1 β DuoSet[®] ELISA Development Systems, human IL-10 DuoSet[®] ELISA Development Systems, and human TGF- β DuoSet[®] ELISA Development Systems (all by R&D system) and used according to the manufacturer's instructions. The levels of murine TNF- α , KC, JE, and MIP-2 were measured by DuoSet[®] ELISA Development Systems (R&D system). The activation of NF- κ B transcription factor was assessed on lysed cells by "NF κ B p65 (Total/Phospho) Human InstantOne[™] ELISA Kit" (Invitrogen) and used according to the manufacturer's instructions.

Statistics

Comparison between groups was done using Student's *t* test, as appropriate, for normally distributed data. The Wilcoxon rank test sum or Mann-Whitney test was performed for data that were not normally distributed.

Ethics Statement

Buffly coats from anonymized healthy donors, who gave their written informed consent to donate the nonclinically usable components of their blood for scientific research, were obtained from the Blood Transfusion Unit of Policlinico "Umberto I" in Rome. The present study, which is based on nonclinical *in vitro* research, did not require any specific approval from an ethical committee, according to the Italian law (decree by Ministero della Salute by February 8, 2013, published on Gazzetta Ufficiale della Repubblica Italiana no. 96 of April 24, 2013, and legislative decree no. 211 of June 24, 2003, published on Gazzetta Ufficiale della Repubblica Italiana no. 184 of August 9, 2003). Cystic fibrosis patients, giving their (or parental) informed consent to participate in the study, were enrolled at "Bambino Gesù" Children's Hospital in Rome after having received detailed information on the scope and objectives of the study by a sanitary personnel who explained the patient

information leaflet (ethics approval #738/2017 of “Bambino Gesù” Children’s Hospital, Rome).

Animal studies adhered to the Italian Ministry of Health guidelines for the use and care of experimental animals (IACUC #733).

Research with *P. aeruginosa* RP73 clinical isolate from CF patient has been approved by the Ethics Commission of Hannover Medical School, Germany. The patient and parent gave informed consent before the sample collection.

RESULTS

ABL Loaded With PI5P Improve Dysfunctional Bacterial Uptake in CF and INH172 Treated Macrophages

CF macrophages show defective *P. aeruginosa* internalization (25–27). Hence, we tested the capability of ABL carrying PI5P to improve phagocytosis of MDR *P. aeruginosa* in macrophages with disabled CFTR. Results confirmed that the bacterial uptake of MDM from CF patients or INH172-treated MDM from healthy donors was dysfunctional compared to that of untreated MDM (**Figure 1A**). The dysfunctional bacterial uptake capacity was significantly improved by the preventive treatment with ABL/PI5P of INH172-treated dTHP-1 cells, infected with MDR *P. aeruginosa* at an MOI of 30 and 10, and resulted completely restored at an MOI of 30 (**Figure S1A**). Moreover, this effect was specific for ABL/PI5P, as any effect was not observed when liposomes composed by either PS or PI5P only were used (**Figure S1B**). Bacterial internalization was also improved by the pretreatment with ABL/PI5P of primary MDM, with pharmacologically inhibited CFTR (**Figure S2**), and of CF MDM (**Figures 1B, C**). No modification of the bacterial uptake was observed when ABL/PI5P was used simultaneously with MDR *P. aeruginosa* infection, excluding that liposomes exerted their effect interacting with the pathogen (**Figure S2**).

Treatment With ABL/PI5P Rescues Impaired Phagosome Maturation and ROS Generation in Macrophages With Pharmacologically Inhibited CFTR

Dysfunctional activity of CFTR leads to impaired phagosome maturation due to unbalanced influx of chloride ions (Cl^-) that does not allow intraphagosomal acidification (8). In this context, we determined basal intracellular pH and ROS production, both in the normal and CFTR-pharmacologically inhibited macrophages. MDMs with CFTR functionally inhibited by INH172 had a more basic intracellular pH than untreated MDM and, after exposure to microbeads, showed an impaired phagosome acidification (**Figure 2A**), which could be completely restored after 90 min of treatment with ABL/PI5P (**Figure 2A**). This result was confirmed by using microbeads labeled with NHS, a pH-sensitive fluorochrome, whose fluorescence decreases proportionally to acidification of phagosome microenvironment: MDMs with CFTR functionally inhibited by INH172 and treated

with ABL/PI5P showed a reduction of NHS fluorescence at levels comparable to that of control MDMs (**Figure S3**).

Phagosome acidification and ROS generation are sequential steps leading to intracellular bacterial killing and type II NADPH oxidase (NOX-2) assemblies from component subunits on maturing phagosomes (28). On these grounds, we monitored ROS generation in MDM with or without pharmacologically inhibited CFTR following exposure to microbeads and after 90 min of treatment with ABL/PI5P. As expected, the exposure to microbeads induced a significant ROS generation in control cells (**Figure 2B**). On the contrary, the exposure to microbeads provoked an impaired ROS production in MDM with INH172-inhibited CFTR, which was significantly restored by the ABL/PI5P treatment (**Figure 2B**). Together, these results show that the inhibition of CFTR by INH172 causes an impaired phagosome acidification and a reduced ROS production that could be significantly recovered by the treatment with ABL/PI5P.

ABL/PI5P Promote Intracellular Bacterial Killing of INH172-inhibited Control Macrophages and CF Macrophages

Since ABLs/PI5Ps were shown to restore the functional intraphagosomal acidification and oxidative burst of macrophages with pharmacologically inhibited CFTR, we investigated whether an increased bactericidal activity against MDR *P. aeruginosa* strains could also represent a functional consequence of ABL/PI5P treatment of cells with altered CFTR function. In this context, we preliminarily tested the capability of ABL/PI5P to improve intracellular bacterial killing in dTHP-1 cells with disabled CFTR infected with MDR *P. aeruginosa* (BAA-2113 strain) at the MOI of 30 and 10. Results expressed in **Figure S4A** show a significant reduction in intracellular bacterial viability after exposure to ABL/PI5P, which was higher at an MOI of 30. Moreover, such effect was specific for ABL/PI5P, as any effect was not observed when liposomes composed by either PS or PI5P only were used (**Figure S4B**). Thereafter, we investigated the effect of ABL/PI5P on primary MDMs with pharmacologically inhibited CFTR. Our results show that 2 h of ABL/PI5P treatment on INH172-treated MDM significantly enhances the intracellular killing of MDR *P. aeruginosa* strain (BAA-2113) (**Figure 3A**) as well as of a panel of additional three MDR *P. aeruginosa* strains (BAA-2108, BAA-2111, and BAA-2112) (**Figure S5**).

In order to evaluate the role of phagosome acidification and/or of ROS generation in intracellular killing of MDR *P. aeruginosa* induced by ABL/PI5P, we exposed *P. aeruginosa*-infected cells to either Concanamycin A (ConcA), a specific inhibitor of V-ATPases blocking phagosome acidification, or polyethylene glycol-Catalase (PEG-Cat), which reduces hydrogen peroxide to water. Results show that intracellular killing of MDR *P. aeruginosa*, induced by ABL/PI5P stimulation of MDM with pharmacologically inhibited CFTR, is ROS mediated and phagosome acidification dependent, as it results ineffective in the presence of Peg-Cat and Conc A, respectively (**Figure 3B**).

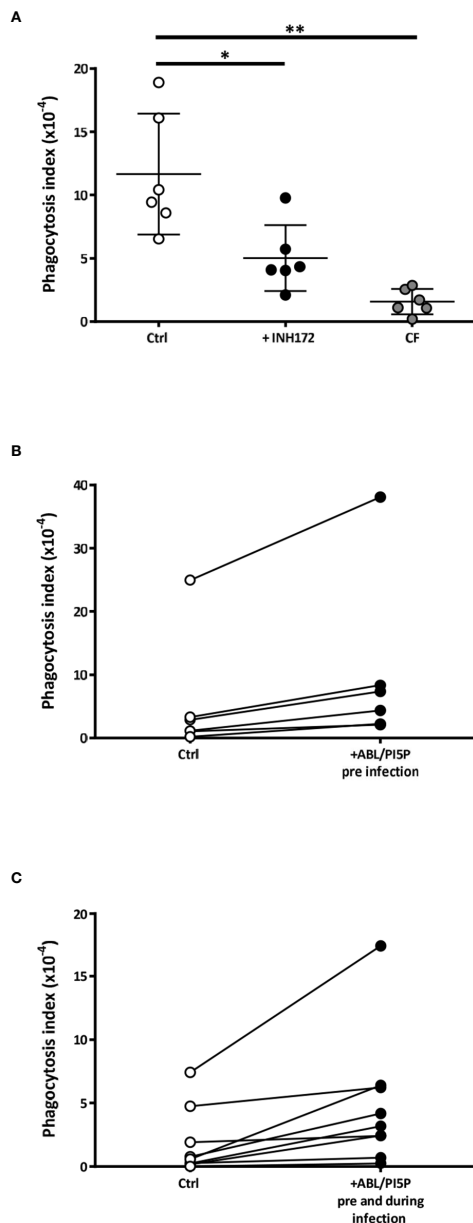


FIGURE 1 | Dysfunctional *Pseudomonas aeruginosa* uptake in macrophages with pharmacologically inhibited or naturally mutated cystic fibrosis transmembrane conductance regulator channel (CFTR) and its enhancement by apoptotic body-like liposome/phosphatidylinositol 5-phosphate (ABL/PI5P) stimulation. **(A)** Monocyte-derived macrophages (MDMs) from healthy donors, treated or not with INH172, or from cystic fibrosis (CF) patients were infected with multidrug-resistant (MDR) *P. aeruginosa* (BAA-2113 strain) at an MOI of 30. **(B, C)** CF MDMs were stimulated or not with ABL/PI5P for 30 min before infection **(B)** or before and during infection **(C)**. Cells were then infected with MDR *P. aeruginosa* (BAA-2113 strain) at an MOI of 30. The bacterial uptake was quantified by colony-forming unit (CFU) assay and indicated as phagocytosis index, calculated as the ratio between the CFUs obtained immediately after the infection and the inoculum. **(A)** Statistical analysis was performed by using the two-sided Mann-Whitney test and * $p < 0.05$; ** $p < 0.01$ in comparison with control cells (healthy donors, $n = 6$; CF patients, $n = 6$). **(B, C)** Statistical analysis was performed by using the two-sided Wilcoxon rank sum test **(B)**, $n = 6$ $p = 0.03$ and **(C)**, $n = 9$ $p = 0.004$.

Finally, we tested the efficacy of ABL/PI5P in MDMs from CF patients. On the basis of the efficacy of freshly isolated and nontreated CF macrophages to limit intracellular bacterial growth, we could divide patients in two groups: “impaired” and “controller,” according to intracellular bacterial replication index higher or lower than 1, respectively (**Figure 4A**). Notably, MDM isolated from patients of the “impaired” group were susceptible to ABL/PI5P stimulation (**Figure 4C**), increasing significantly their intracellular killing upon liposome treatment, whereas ABL/PI5P did not further increase the intracellular killing of MDM isolated from patients belonging to the “controller” group (**Figure 4B**) or from healthy donors (**Figure S6**).

ABL/PI5P Treatment Modulates Anti- and Pro- Inflammatory Cytokine Production in Macrophages With Pharmacologically Inhibited CFTR

Chronic infection, mainly due to *P. aeruginosa*, and unresolved acute inflammation are key mechanisms responsible for progressive lung destruction in CF (29) and an effective host-directed therapeutic strategy should also limit the inflammation-based immunopathology. On the basis of previous results showing the anti-inflammatory effect of ABL (18), we wanted to investigate the effect of ABL/PI5P treatment of MDM incubated or not with INH172 on NF- κ B activation and on the production of a panel of pro- and anti-inflammatory cytokines after infection with MDR *P. aeruginosa*. In this model, we could show high basal levels of NF- κ B activation after CFTR inhibition, which further increased following infection with MDR *P. aeruginosa*. Interestingly, the same NF- κ B activation levels were significantly reduced by the treatment with ABL/PI5P (**Figure 5A**). The reduced activation of NF- κ B was confirmed by the comparative *in vitro* measure of cytokines whose transcription depends upon NF- κ B activity (TNF- α , IL-1 β , and IL-6). In fact, infected macrophages with dysfunctional CFTR showed a significant increase in TNF α , IL-1 β , and IL-6 secretion in comparison with control infected macrophages, and ABL/PI5P treatment reduced the levels of the same inflammatory cytokines in infected macrophages irrespective of CFTR inhibition (**Figures 5B–D**). On the contrary, the secretion of anti-inflammatory cytokines, such as IL-10 and TGF- β , was significantly increased in ABL/PI5P-treated MDMs (**Figures 5E, F**).

ABL/PI5P Therapeutic Treatment Reduces Inflammatory Reaction in a Murine Model of MDR *P. aeruginosa* Chronic Infection

We wanted to test in an *in vivo* model the functional consequences of the *in vitro* observed anti-inflammatory functions of ABL/PI5P in addition to the promotion of intracellular killing of pathogens. This is particularly interesting since massive neutrophil infiltration is the main cause of chronic damage to the epithelial lung structure in the CF lung (30). Thus, we tested the efficacy of ABL/PI5P administrated by Penn-Century MicroSprayer® Aerosoliser in mice, 5 min after infection with MDR *P. aeruginosa* embedded in agar beads. An evaluation of the inflammatory response and bacterial burden in lung and in BALFs was considered as read-

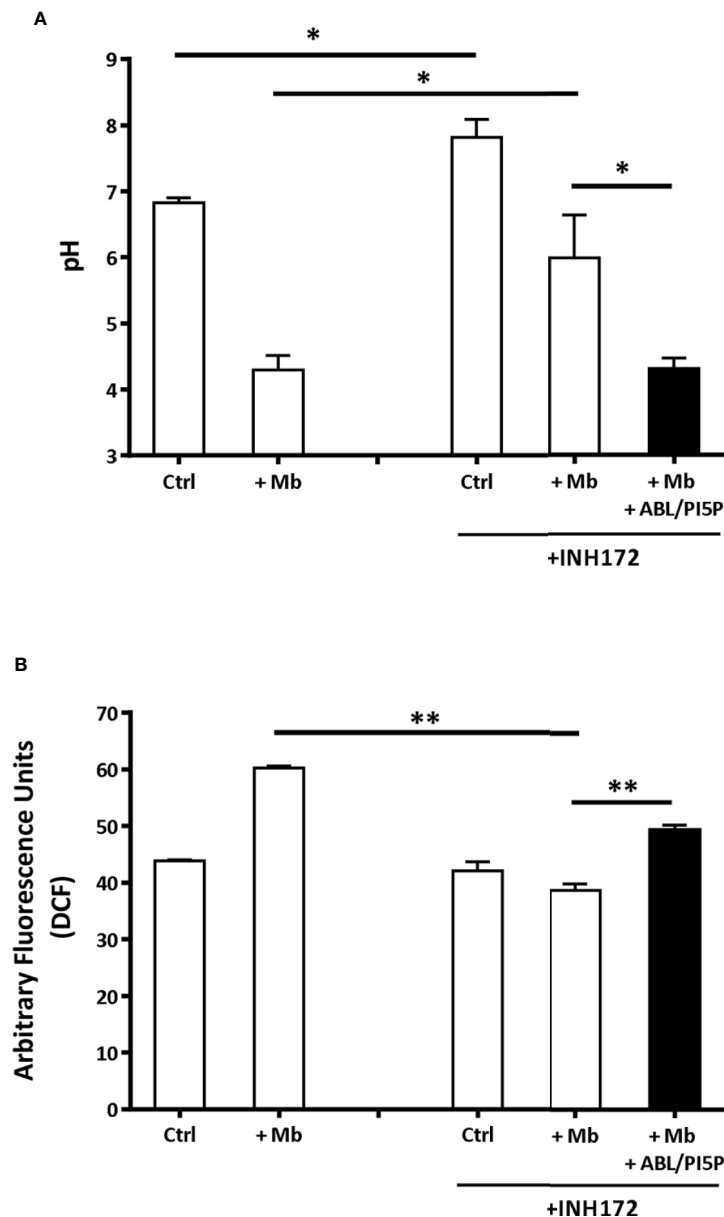


FIGURE 2 | Treatment with ABL/PI5P rescues impaired phagosome acidification and ROS production in MDM with pharmacologically inhibited CFTR. Primary MDMs, treated or not with INH172, were exposed for 1 h to 1- μ m microbeads (Mb). Phagosomal pH (**A**) and ROS (**B**) were assessed, by staining with Lysosensor green DND 189 or DCF, after 90 min of stimulation with ABL/PI5P, respectively. Results are shown as mean + standard deviation of the values obtained from triplicate cultures and are representative of experiments with cells by two different donors. * $p < 0.05$; ** $p < 0.01$, in comparison with INH172-unstimulated cells and in comparison with untreated cells by one-sided Student's *t* test.

out measures of ABL/PI5P treatment efficacy. Results showed a significant reduction of both KC and MIP-2 (**Figures 6A, B**) and no significant variations in the levels of TNF- α and MCP-1 (**Figures 6C, D**) in the lungs of ABL/PI5P-treated mice in comparison with vehicle-treated mice. Results also showed a significant reduction in neutrophil count in BALF (**Figure 7B**) of ABL/PI5P-treated mice in comparison with vehicle-treated mice. A reduction, although not significant, of BALF total cells (**Figure 7A**) and macrophages (**Figure 7C**) was observed. Of note, the

significant reduction in BALF neutrophils observed in ABL/PI5P-treated mice did not significantly interfere with pulmonary bacterial burden (**Figure 7D**).

DISCUSSION

CF is a genetic disorder that leads to a progressive dysfunction of lung activity by predisposing patients to colonization by

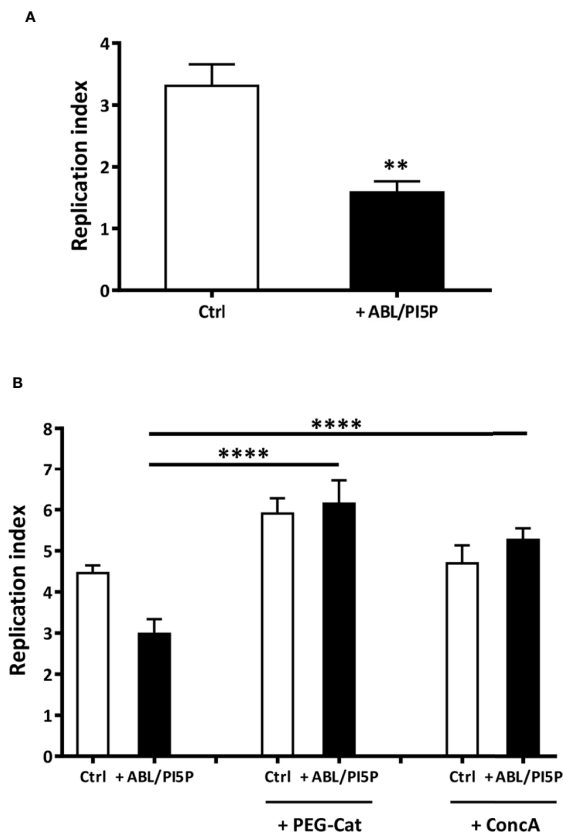


FIGURE 3 | ABL/PI5P promotes both ROS and phagolysosome acidification-dependent intracellular *P. aeruginosa* killing in MDM with pharmacologically inhibited CFTR. **(A)** Primary MDMs were exposed to the CFTR inhibitor INH172 at a concentration of 10 μ M, infected with MDR *P. aeruginosa* (BAA-2113 strain) and then stimulated for further 2 h with ABL/PI5P. **(B)** Primary MDMs were exposed to the CFTR inhibitor INH172 at a concentration of 10 μ M, infected with MDR *P. aeruginosa* (BAA-2113 strain), and then stimulated for a further 2 h with ABL/PI5P in the presence or absence of catalase (PEG-Cat) or Concanamycin A (Conc A), at a concentration of 100 U/ml or 10 nM, respectively. Bacterial growth was assessed by CFU assay, and replication index was calculated as the ratio between the CFU obtained after 2 h of infection, in the presence or absence of ABL/PI5P, and the CFU was obtained before the addition of liposomes. The results are shown as mean + standard deviation of the values obtained from triplicate of each condition. ** $p < 0.01$; **** $p < 0.0001$ by two-sided Student's test.

opportunistic bacterial pathogens. Infections caused by *P. aeruginosa*, particularly because of the emergence of MDR strains, represent the major cause of morbidity and mortality in CF patients (31). These evidences highlight the urgency to develop novel therapeutic approaches, which may contribute to the control of MDR pathogens, including *P. aeruginosa*. Phagocytosis and intracellular killing of extracellular pathogens are the most important effector mechanisms of innate immune cells that can be hampered in CF patients (26). Hence, strategies aimed at improving the capacity of lung resident innate immune cells to phagocytose and kill pathogens may represent a

promising host-directed approach to combat bacterial lung infections in CF patients.

In the present manuscript, we show that ABLs carrying PI5Ps are able to increase, both *in vitro* and *ex vivo*, the capacity of INH172-treated and CF macrophages to internalize and kill MDR strains of *P. aeruginosa*. Moreover, in a murine model of *in vivo* *P. aeruginosa* infection, we show that ABLs carrying PI5Ps are capable of reducing neutrophil recruitment and lung inflammation, without promoting bacterial growth. In particular, we show that treatment with ABL/PI5P enhance nonopsonic *P. aeruginosa* phagocytosis in CF and INH172-treated macrophages. Several not mutually exclusive mechanisms may explain this observation. PI5P may promote actin dynamics and bacterial phagocytosis i) *via* recruitment and activation of the exchange factor Tiam1 and Rac1 (14), ii) by directly activating PI3K/Akt signaling pathway (32), or iii) by participating as substrate to the PI(4,5)P₂ production (33), which may directly induce membrane remodeling (34) or be converted, by means of phosphoinositide 3-kinase (PI3K), in 3,4,5-tris phosphate [PI(3,4,5)P₃], which in turn is able to activate Akt signaling pathway (35).

We then showed that ABL/PI5P treatment restores intracellular acidification and ROS production of human macrophages, whose CFTR was pharmacologically inhibited. Following phagocytosis, phagosome maturation requires the sequential interaction with early endosomes, late endosomes, and ultimately, with lysosomes, leading to the generation of a highly microbicidal organelle called phagolysosome. In pharmacologically inhibited- or CF-macrophages, the altered CFTR function leads to a limited phagosome acidification because of the unbalanced Cl⁻ ion distribution, which alters phagolysosome maturation and causes a defective intracellular bacterial clearance (8, 36). Together, our data indicate that ABL/PI5P treatment may rescue the impaired bactericidal mechanisms of macrophages with dysfunctional CFTR by restoring phagosome acidification and enhancing ROS production. Finally, the effect was specific to PI5P, as ABL loaded with PI3P, a second lipid messenger involved in membrane trafficking and autophagy (12), did not result in any modulation of intracellular *P. aeruginosa* killing (18).

The *ex vivo* analysis of MDM from CF patients indicated the presence of two groups of patients that we classified as “impaired” or “controller,” based on their different capability to control *in vitro* *P. aeruginosa* infection (bacterial replication index >1 or <1, respectively). It has been reported that host-genotypic traits have a critical role in the outcome of *P. aeruginosa* infection (37). In particular, the host susceptibility and the severity of infections caused by *P. aeruginosa* also depend upon a wide complex arrangement of genes, which is highly variable among immunocompromised individuals, including CF patients (38). Changes in clinical disease signs are mostly dependent on secondary gene variants that affect the outcome of the infection. These genes are identified as “modifier genes,” some of which play a role in innate immune response (39–41). Importantly, we observed that ABL/PI5P *ex vivo* treatment of macrophages induced a significant intracellular bacterial killing in the “impaired” group, highlighting the immunostimulant properties of ABL/PI5P, which

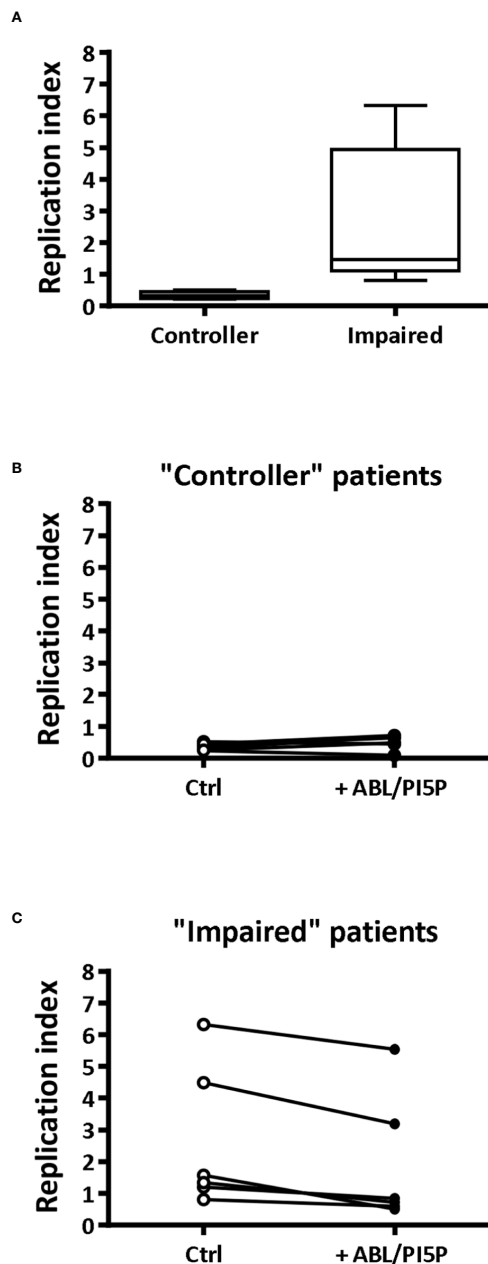


FIGURE 4 | ABL/PI5P enhances intracellular bacterial killing in CF macrophages characterized by impaired antimicrobial activity. MDM isolated from CF patients ($n = 12$) were infected with MDR *P. aeruginosa* (BAA-2113 strain) and then stimulated for another 2 h with ABL/PI5P. Bacterial growth was assessed by CFU assay, and replication index was calculated as the ratio between the CFU obtained after 2 h of infection in the presence or absence of ABL/PI5P and the CFU obtained before the addition of liposomes. **(A)** CF patients have been defined as “functional” or “controller” on the basis of bacterial replication index, less or higher than 1, respectively. Bacterial replication index is shown in “controller” **(B, $n = 6$)** and “impaired” **(C, $n = 6$)** macrophages from CF patients following ABL/PI5P stimulation. Statistical analysis was performed by using the two-sided Mann–Whitney test **(A)** and two-sided Wilcoxon matched-pairs signed rank test **(B, C)**. **(A)** $p = 0.0022$; **(B)** $p =$ not significant; **(C)** $p = 0.0313$.

restores the dysfunctional CF bactericidal response. On the contrary, the same treatment did not further increase the intracellular *P. aeruginosa* killing of macrophages from the “controller” group or from functional MDM by healthy donors. In agreement with these observations *in vitro*, we did not observe variations in terms of pulmonary bacterial burden in an *in vivo* model of *P. aeruginosa* chronic infection in immunocompetent mice. Together, these data support the hypothesis that ABL/PI5P treatment has no general and broad-spectrum immunoenhancing effect, but it is endowed with the potential to rescue impaired microbicidal innate immune function.

Airway inflammation is a hallmark of CF disease that leads to the decline in lung function (26) and is characterized by elevated levels of NF- κ B activation and proinflammatory cytokine and chemokine production (30), resulting in chronic inflammation, neutrophil recruitment, and progressive airway destruction. It is still a matter of debate on whether excessive inflammation in CF is the result of either underlying chronic bacterial infection(s) in the lungs or of exaggerated NF- κ B signaling (42). Results reported herein show that the levels of NF- κ B activation increase in macrophages following *P. aeruginosa* infection, and such an increase is significantly higher following pharmacological inhibition of CFTR, both in uninfected and in infected macrophages in comparison with the control cells. However, despite higher basal NF- κ B activation in the cells with pharmacologically inhibited CFTR, differences in TNF- α , IL-1 β , IL-6 levels were observed in *P. aeruginosa*-infected macrophages only, suggesting that the presence of the pathogen is necessary to NF- κ B-dependent proinflammatory cytokine production. These results support the hypothesis of a higher, NF- κ B dependent, predisposition to a hyperinflammatory response by the macrophages with dysfunctional CFTR, which requires the presence of bacterial pathogens to over-express proinflammatory cytokines (30).

PS exposure at the outer surface of the cell membrane is a physiologically relevant signal for phagocytic cells, for which it represents the “eat me” signal provided by apoptotic bodies generated by cells undergoing apoptosis (43). This process is an anti-inflammatory/tolerogenic signal with immunomodulatory properties (44), which have been previously exploited for the treatment of autoimmune diseases (45). Furthermore, PI5P is involved in the activation of PI3K/Akt pathway that is crucial in restricting proinflammatory and promoting anti-inflammatory response (32, 46). The results reported herein support the anti-inflammatory and protolerogenic role of PS and PI5P even when they are delivered as a single liposome formulation. Based on these *in vitro* experimental results, we moved to the *in vivo* murine model of chronic *P. aeruginosa* infection and assessed the effects of ABL/PI5P treatment in terms of lung KC, MIP-2, JE and TNF- α production, leukocyte infiltrates, and pulmonary bacterial burden. Results show that in ABL-/PI5P-treated mice, the number of BALF neutrophils was significantly reduced, and such reduction paralleled with KC and MIP-2 levels, whereas any reduction of TNF- α and JE levels was not observed. The different results obtained following *in vitro* and *in vivo* infection, in terms of TNF- α production, may be explained by the activation of different cell types, such as antigen-specific Th1, Th17,

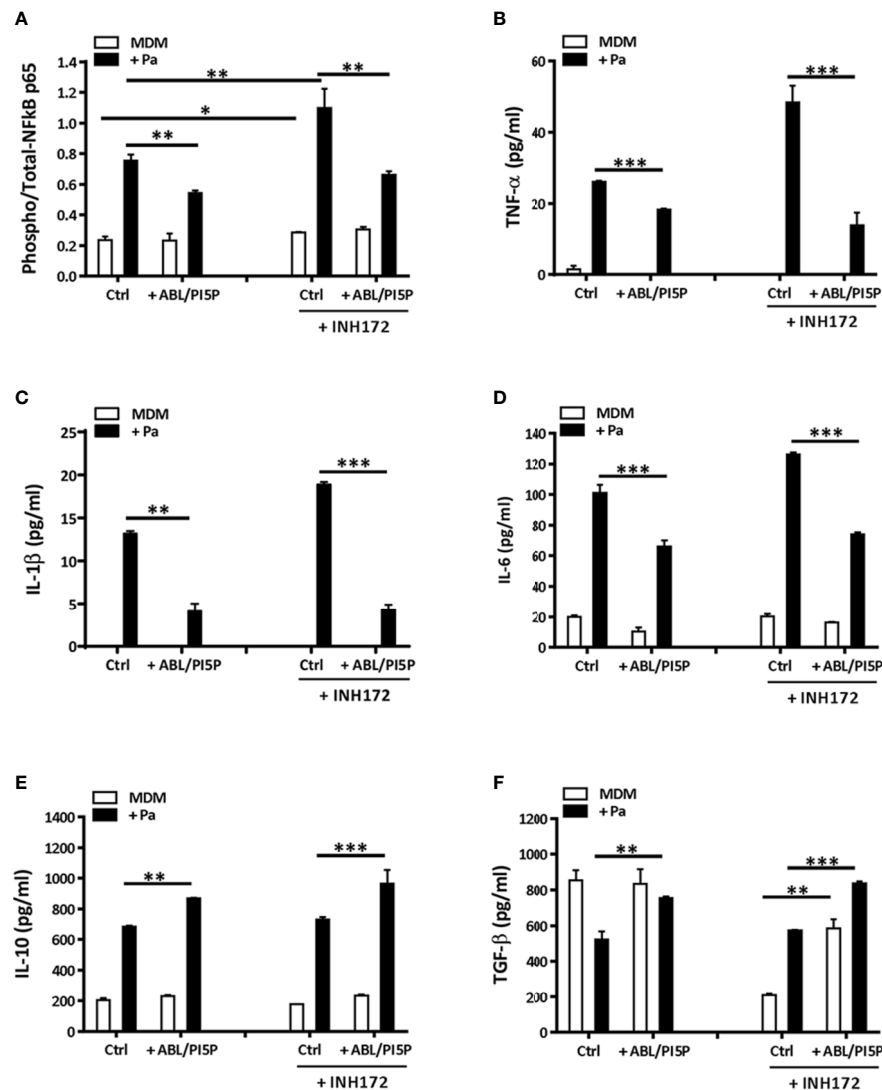


FIGURE 5 | ABL/PI5P stimulation modulates NF-κB and cytokine production in MDM with pharmacologically inhibited CFTR. MDMs were treated or not with INH172, infected or not with MDR *P. aeruginosa* (Pa, BAA-2113 strain), and then stimulated or not with ABL/PI5P for 2 h. Thereafter, cells were lysed (A) or supernatants were collected (B–F), and both were stored at -20°C until analysis. (A) Cell lysates were analyzed by NF-κB p65 (Total/Phospho) Human InstantOne™ ELISA kit, and results are shown as the ratio between phosphorylated and total NF-κB p65. The production of TNF-α (B), IL-1β (C), IL-6 (D), IL-10 (E), and TGF-β (F) was analyzed by ELISA. The results are shown as mean + standard deviation of the values obtained from triplicate of each conditions and are representative of experiments with cells from at least three different donors. * $p < 0.05$; ** $p < 0.01$; *** $p < 0.001$ one-sided *t* test.

and Th22 cells that may be involved and recruited to the lung during *in vivo* infections (47). Anti-inflammatory therapies, such as corticosteroids or biotechnologicals, may cause immunosuppression, which in turn is associated with the emergence of latent or opportunistic infections, and for this reason, they are often administered in combination with antibiotics (48). A clinical study to investigate the leukotriene B(4) (LTB(4)-receptor antagonist BIIL284 in CF patients was prematurely terminated due to a significant increased risk of adverse pulmonary events (49). Subsequent *in vivo* models showed that decreased airway neutrophils induced lung proliferation and severe bacteremia in a murine model of *P. aeruginosa* lung infection (50), indicating that

strategies that interfere with neutrophil mechanisms have to be implemented with great caution. Of note, the reduction in inflammatory reactions in the lung of infected mice treated with ABL/PI5P was not associated with a significant increase in bacterial burden, suggesting that the *in vivo* administration of ABL/PI5P, by activating the macrophage component, may compensate for the reduction in neutrophil response and may have a therapeutic value also in critical conditions such as neutropenia.

Altogether, our data support the possibility that PI5P conveyed by ABL represents a novel therapeutic strategy devoid of immunosuppressive side effects, aimed at improving the efficiency of phagocytosis of mononuclear phagocytes and at reducing the

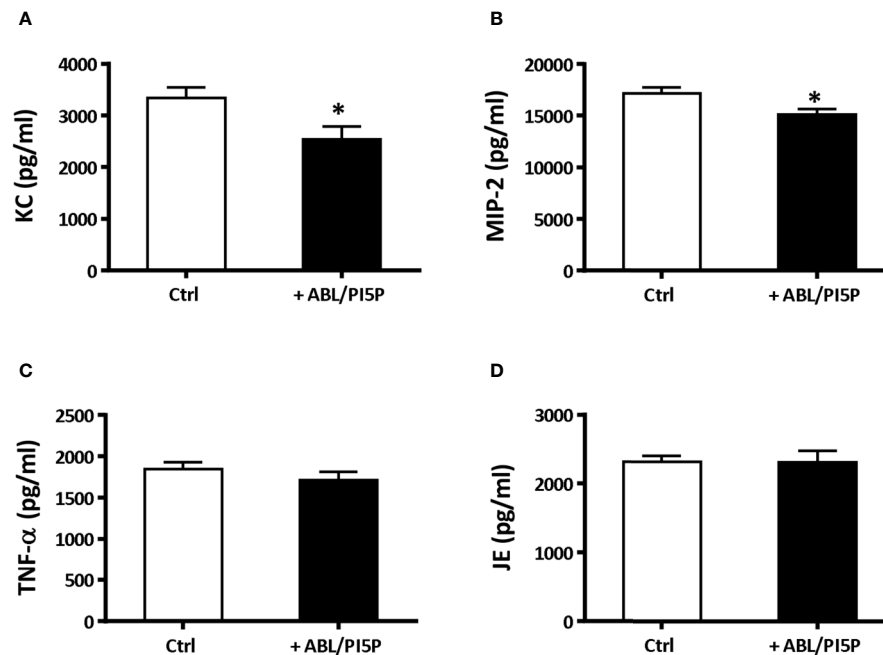


FIGURE 6 | ABL/PI5P treatment modulates KC and MIP-2 production in a murine model of MDR *P. aeruginosa* chronic lung infection. C57Bl/6NCrIBR mice were infected with MDR *P. aeruginosa* (RP73 strain) and then treated with ABL/PI5P (n = 16) or vehicle (n = 16), as described in the *Material and Methods* section. At day 6 post-infection, mice were sacrificed. Levels of KC (A), MIP-2 (B), TNF-α (C), and JE (D) upon treatment with ABL/PI5P or vehicle in the supernatants of lung homogenates were measured by ELISA. Data are shown as mean values + standard error. The data are pooled from two independent experiments. Statistical analysis was performed by using the two-sided Mann-Whitney test. Statistical significance is indicated: *p < 0.05. Outlier data, identified by Grubbs' test, were excluded by the analysis.

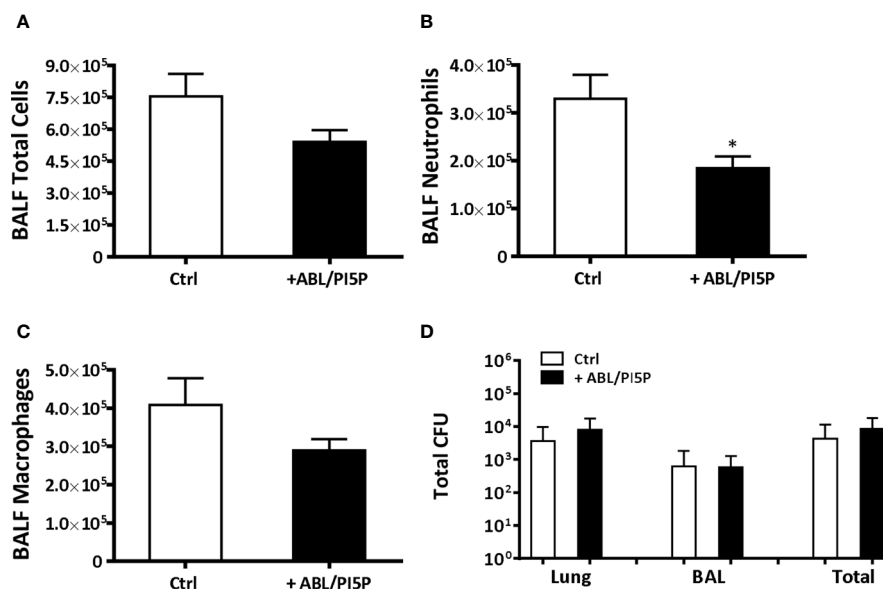


FIGURE 7 | ABL/PI5P treatment reduces neutrophilic recruitment in a murine model of MDR *P. aeruginosa* chronic lung infection. C57Bl/6NCrIBR mice were infected with MDR *P. aeruginosa* (RP73 strain) and then treated with ABL/PI5P (n = 16) or vehicle (n = 16), as described in the *Materials and Methods* section. At day 6 postinfection, mice were sacrificed, BALF was collected, and lungs were excised, homogenized, and plated onto TSA to determine bacterial burden. Counts of total number of cells (A), neutrophils (B), and macrophages (C) were performed in BALF. (D) The bacterial burden and was assessed by CFU assay. Data are shown as mean values + standard error. The data are pooled from two independent experiments. Statistical analysis was performed by using two-sided Mann-Whitney test. Statistical significance is indicated: *p < 0.05. Outlier data, identified by Grubbs' test, were excluded by the analysis.

damage of chronic inflammation. In conclusion, the ABL-/PI5P-based immunomodulatory strategy may represent an additional therapeutic tool in the fight against MDR opportunistic pathogens, such as *P. aeruginosa*, with the added value of the capacity to reduce the hyperinflammatory reactions in chronic lung infections that are particularly invalidating in CF patients.

DATA AVAILABILITY STATEMENT

All datasets generated for this study are included in the article/**Supplementary Material**.

ETHICS STATEMENT

The studies involving human participants were reviewed and approved by Ethics Committee of “Bambino Gesù” Children’s Hospital, Rome, Italy. Ethics approval #738/2017. Written informed consent to participate in this study was provided by the participants’ legal guardian/next of kin. The animal study was reviewed and approved by Institutional Animal Care and Use Committee (IACUC) #733.

AUTHOR CONTRIBUTIONS

VL, RN, AB, and MF contributed to the conception and design of the study. NP, FDS, AR, SR, IDF, AH, and FC contributed to data

acquisition. NP, MMDA, RN, AB, and MF participated in data analysis and manuscript writing. All authors contributed to the article and approved the submitted version.

FUNDING

Research was supported by i) the Horizon 2020 Programme of European Commission, grant “EMI-TB”; Eliciting Mucosal Immunity against Tuberculosis—grant # 643558; ii) the Italian Cystic Fibrosis Research Foundation, FFC #14/2017, FFC#19/2019, and CFAaCore; iii) the Italian Foundation for multiple sclerosis, grant #2016/R/22; and iv) Regione Lazio, grant # E56C18000460002.

ACKNOWLEDGMENTS

The authors thank B. Tümmeler (Medizinische Hochschule Hannover, Germany) for supplying the *P. aeruginosa* strains from a CF patient. We thank Medede Melessike for technical support.

SUPPLEMENTARY MATERIAL

The Supplementary Material for this article can be found online at: <https://www.frontiersin.org/articles/10.3389/fimmu.2020.532225/full#supplementary-material>

REFERENCES

- Castellani C, Assael BM. Cystic fibrosis: a clinical view. *Cell Mol Life Sci* (2017) 74:129–40. doi: 10.1007/s00018-016-2393-9
- Perez A, Issler A, Cotton CU, Kelley TJ, Verkman AS, Davis PB. CFTR inhibition mimics the cystic fibrosis inflammatory profile. *Am J Physiol Lung Cell Mol Physiol* (2007) 292:383–95. doi: 10.1152/ajplung.00403.2005
- Ratjen F, Döring G. Cystic Fibrosis. *Lancet* (2003) 361:681–9. doi: 10.1016/S0140-6736(03)12567-6
- Ferrari E, Monzani R, Villella VR, Esposito S, Saluzzo F, Rossin F, et al. Cysteamine re-establishes the clearance of *Pseudomonas P. aeruginosa* by macrophages bearing the cystic fibrosis-relevant F508del-CFTR mutation. *Cell Death Dis* (2017) 8:e2544. doi: 10.1038/cddis.2016.476
- Cystic fibrosis foundation patient registry. *Annual data report*. C Bruce, MD Marshall, editors. Bethesda, Maryland: Cystic Fibrosis Foundation (2018).
- O’ Sullivan BP, Freedman SD. Cystic Fibrosis. *Lancet* (2009) 373:1891–904. doi: 10.1016/S0140-6736(09)60327-5
- Donnelly LE, Barnes PJ. Defective phagocytosis in airways disease. *Chest* (2012) 141:1055–62. doi: 10.1378/chest.11-2348
- Di A, Brown ME, Deriy LV, Li C, Szeto FL, Chen Y, et al. CFTR regulates phagosome acidification in macrophages and alters bactericidal activity. *Nat Cell Biol* (2006) 8:933–44. doi: 10.1038/ncb1456
- Yeung T, Ozdamar B, Paroutis P, Grinstein S. Lipid metabolism and dynamics during phagocytosis. *Curr Opin Cell Biol* (2006) 18:429–37. doi: 10.1016/j.ceb.2006.06.006
- Steinberg BE, Grinstein S. Pathogen destruction versus intracellular survival: the role of lipids as phagosomal fate determinants. *J Clin Invest* (2008) 118:2002–11. doi: 10.1172/JCI35433
- Nisini R, Poerio N, Mariotti S, De Santis F, Fraziano M. The Multirole of Liposomes in Therapy and Prevention of Infectious Diseases. *Front Immunol* (2018) 9:155. doi: 10.3389/fimmu.2018.00155
- De Craene J, Bertazzi DL, Bär S, Friant S. Phosphoinositides, major actors in membrane trafficking and lipid signaling pathways. *Int J Mol Sci* (2017) 18:634. doi: 10.3390/ijms18030634
- Oppelt A, Lobert VH, Haglund K, Mackey AM, Rameh LE, Liestøl K, et al. Production of phosphatidylinositol 5-phosphate via PIKfyve and MTMR3 regulates cell migration. *EMBO Rep* (2013) 14:57–64. doi: 10.1038/embor.2012.183
- Viaud J, Lagarrigue F, Ramel D, Allart S, Chicanne G, Ceccato L, et al. Phosphatidylinositol 5-phosphate regulates invasion through binding and activation of Tiam1. *Nat Commun* (2014) 5:4080. doi: 10.1038/ncomms5080
- Yeung T, Grinstein S. Lipid signaling and the modulation of surface charge during phagocytosis. *Immunol Rev* (2007) 219:17–36. doi: 10.1111/j.1600-065X.2007.00546.x
- Schaletzky J, Dove SK, Short B, Lorenzo O, Clague MJ, Barr FA. Phosphatidylinositol-5-phosphate activation and conserved substrate specificity of the myotubularin phosphatidylinositol 3-phosphatases. *Curr Biol* (2003) 13:504–9. doi: 10.1016/S0960-9822(03)00132-5
- Vicinanza M, Korolchuk VI, Ashkenazi A, Puri C, Menzies FM, Clarke JH, et al. PI(5)P regulates autophagosome biogenesis. *Mol Cell* (2015) 57:219–34. doi: 10.1016/j.molcel.2014.12.007
- Greco E, Quintiliani G, Santucci MB, Serafino A, Ciccaglione AR, Marcantonio C, et al. Janus-faced liposomes enhance antimicrobial innate immune response in *Mycobacterium tuberculosis* infection. *Proc Natl Acad Sci USA* (2012) 109:E1360–8. doi: 10.1073/pnas.1200484109
- Poerio N, Bugli F, Taus F, Santucci MB, Rodolfo C, Ceconi F, et al. Liposomes loaded with bioactive lipids enhance antibacterial innate immunity irrespective of drug resistance. *Sci Rep* (2017) 7:45120. doi: 10.1038/srep45120
- Jeukens J, Boyle B, Bianconi I, Kukavica-Ibrulj I, Tümmeler B, Bragonzi A, et al. Complete Genome Sequence of Persistent Cystic Fibrosis Isolate *Pseudomonas P. aeruginosa* Strain RP73. *Genome Announc* (2013) 1(4): e00568-13. doi: 10.1128/genomeA.00568-13

21. Facchini M, De Fino I, Riva C, Bragonzi A. Long term chronic *Pseudomonas P. aeruginosa* airway infection in mice. *JoVE* (2014) 85:51019. doi: 10.3791/51019
22. Cigana C, Ranucci S, Rossi A, De Fino I, Melessike M, Bragonzi A. Antibiotic efficacy varies based on the infection model and treatment regimen for *Pseudomonas aeruginosa*. *Eur Respir J* (2019) 55(3):1802456. doi: 10.1183/13993003.02456-2018
23. Zhang Y, Li X, Grassmé H, Döring G, Gulbins E. Alterations in ceramide concentration and pH determine the release of reactive oxygen species by Cfr-deficient macrophages on infection. *J Immunol* (2010) 184:5104–11. doi: 10.4049/jimmunol.0902851
24. Cigana C, Bernardini F, Facchini M, Alcalá-Franco B, Riva C, De Fino I, et al. Efficacy of the Novel Antibiotic POL7001 in Preclinical Models of *Pseudomonas P. aeruginosa* Pneumonia. *Antimicrob Agents Chemother* (2016) 60(8):4991–5000. doi: 10.1128/AAC.00390-16
25. Zhang S, Shrestha CL, Kopp BT. Cystic fibrosis transmembrane conductance regulator (CFTR) modulators have differential effects on cystic fibrosis macrophage function. *Sci Rep* (2018) 8:17066. doi: 10.1038/s41598-018-35151-7
26. Lévêque M, Le Trionnaire S, Del Porto P, Martin-Chouly C. The impact of impaired macrophage functions in cystic fibrosis disease progression. *J Cyst Fibros* (2017) 16:443–53. doi: 10.1016/j.jcf.2016.10.011
27. Sallenave JM. Phagocytic and signaling innate immune receptors: are they dysregulated in cystic fibrosis in the fight against *Pseudomonas aeruginosa*? *Int J Biochem Cell Biol* (2014) 52:103–7. doi: 10.1016/j.biocel.2014.01.013
28. Nunes P, Demareux N, Dinanier MC. Regulation of the NADPH oxidase and associated ion fluxes during phagocytosis. *Traffic* (2013) 14:1118–113. doi: 10.1111/tra.12115
29. Malhotra S, Hayes DJr, Wozniak DJ. Cystic Fibrosis and *Pseudomonas aeruginosa*: the Host-Microbe Interface. *Clin Microbiol Rev* (2019) 32(3):e00138–18. doi: 10.1128/CMR.00138-18
30. Cohen-Cymbarknoh M, Kerem E, Ferkol T, Elizur A. Airway inflammation in cystic fibrosis: molecular mechanisms and clinical implications. *Thorax* (2013) 68:1157–62. doi: 10.1136/thoraxjnl-2013-203204
31. Stefani S, Campana S, Cariani L, Carnovale V, Colombo C, Lleo MM, et al. Relevance of multidrug-resistant *Pseudomonas P. aeruginosa* infections in cystic fibrosis. *Int J Med Microbiol* (2017) 6:353–62. doi: 10.1016/j.ijmm.2017.07.004
32. Pendaries C, Tronchère H, Arbibe L, Mounier J, Gozani O, Cantley L, et al. PtdIns5P activates the host cell PI3-kinase/Akt pathway during *Shigella flexneri* infection. *EMBO J* (2006) 25:1024–34. doi: 10.1038/sj.emboj.7601001
33. Hasegawa J, Iwamoto R, Otomo T, Nezu A, Hamasaki M, Yoshimori T. Autophagosome-lysosome fusion in neurons requires INPP5E, a protein associated with Joubert syndrome. *EMBO J* (2016) 35:1853–67. doi: 10.15252/embj.201593148
34. Janmey PA, Lindberg U. Cytoskeletal regulation: rich in lipids. *Nat Rev Mol Cell Biol* (2004) 5:658–66. doi: 10.1038/nrm1434
35. Lovewell RR, Hayes SM, O'Toole GA, Berwin B. *Pseudomonas P. aeruginosa* flagellar motility activates the phagocyte PI3K/Akt pathway to induce phagocytic engulfment. *Am J Physiol Lung Cell Mol Physiol* (2014) 306:698–707. doi: 10.1152/ajplung.00319.2013
36. Del Porto P, Cifani N, Guarnieri S, Di Domenico EG, Mariggiò MA, Spadaro F, et al. Dysfunctional CFTR alters the bactericidal activity of human macrophages against *Pseudomonas aeruginosa*. *PLoS One* (2011) 6:e19970. doi: 10.1371/journal.pone.0019970
37. Lorè NI, Iraqi FA, Bragonzi A. Host genetic diversity influences the severity of *Pseudomonas P. aeruginosa* pneumonia in the Collaborative Cross mice. *BMC Genet* (2015) 16:106. doi: 10.1186/s12863-015-0260-6
38. Gellatly SL, Hancock RE. *Pseudomonas aeruginosa*: new insights into pathogenesis and host defenses. *Pathog Dis* (2013) 67:159–73. doi: 10.1111/2049-632X.12033
39. Weiler CA, Drumm ML. Genetic influences on cystic fibrosis lung disease severity. *Front Pharmacol* (2013) 4:40. doi: 10.3389/fphar.2013.00040
40. Bruscia EM, Bonfield TL. Cystic Fibrosis Lung Immunity: The Role of the Macrophage. *J Innate Immun* (2016) 8:550–63. doi: 10.1159/000446825
41. Cutting GR. Cystic fibrosis genetics: from molecular understanding to clinical application. *Nat Rev Genet* (2015) 16:45–56. doi: 10.1038/nrg3849
42. Roesch EA, Nichols DP, Chmiel JF. Inflammation in cystic fibrosis: An update. *Pediatr Pulmonol* (2018) 53:S30–50. doi: 10.1002/ppul.24129
43. Segawa K, Nagata S. An Apoptotic 'Eat Me' Signal: Phosphatidylserine Exposure. *Trends Cell Biol* (2015) 25:639–50. doi: 10.1016/j.tcb.2015.08.003
44. Birge RB, Ucker DS. Innate apoptotic immunity: The calming touch of death. *Cell Death Differ* (2008) 15:1096–102. doi: 10.1038/cdd.2008.58
45. Pujol-Autonell I, Mansilla MJ, Rodríguez-Fernández S, Cano-Sarabia M, Navarro-Barriuso J, Ampudia RM, et al. Liposome-based immunotherapy against autoimmune diseases: therapeutic effect on multiple sclerosis. *Nanomedicine (Lond)* (2017) 12:1231–42. doi: 10.2217/nnm-2016-0410
46. Vergadi E, Ieronymaki E, Lyroni K, Vaporidi K, Tsatsanis C. Akt Signaling Pathway in Macrophage Activation and M1/M2 Polarization. *J Immunol* (2017) 198:1006–14. doi: 10.4049/jimmunol.1601515
47. Bayes HK, Bicknell S, MacGregor G, Evans TJ. T helper cell subsets specific for *Pseudomonas P. aeruginosa* in healthy individuals and patients with cystic fibrosis. *PLoS One* (2014) 9:e90263. doi: 10.1371/journal.pone.0090263
48. Vozoris NT, Seemungal J, Batt J. Prevalence, screening and treatment of latent tuberculosis among oral corticosteroid recipients. *Eur Respir J* (2014) 44:1373–5. doi: 10.1183/09031936.00076714
49. Konstan M, Döring G, Heltshe SL, Lands LC, Hilliard KA, Koker P, et al. Investigators and Coordinators of BI Trial 543.45. A randomized double blind, placebo controlled phase 2 trial of BIIL 284 BS (an LTB4 receptor antagonist) for the treatment of lung disease in children and adults with cystic fibrosis. *J Cyst Fibros* (2014) 13:148–55. doi: 10.1016/j.jcf.2013.12.009
50. Döring G, Bragonzi A, Paroni M, Aktürk FF, Cigana C, Schmidt A, et al. BIIL 284 reduces neutrophil numbers but increases *P. aeruginosa* bacteremia and inflammation in mouse lungs. *J Cyst Fibros* (2014) 13:156–63. doi: 10.1016/j.jcf.2013.10.007

Conflict of Interest: The authors declare that the research was conducted in the absence of any commercial or financial relationships that could be construed as a potential conflict of interest.

Copyright © 2020 Poerio, De Santis, Rossi, Ranucci, De Fino, Henriquez, D'Andrea, Ciciriello, Lucidi, Nisini, Bragonzi and Fraziano. This is an open-access article distributed under the terms of the Creative Commons Attribution License (CC BY). The use, distribution or reproduction in other forums is permitted, provided the original author(s) and the copyright owner(s) are credited and that the original publication in this journal is cited, in accordance with accepted academic practice. No use, distribution or reproduction is permitted which does not comply with these terms.



Etiopathogenesis, Challenges and Remedies Associated With Female Genital Tuberculosis: Potential Role of Nuclear Receptors

Shalini Gupta and Pawan Gupta*

Department of Molecular Biology, CSIR-Institute of Microbial Technology, Chandigarh, India

OPEN ACCESS

Edited by:

Marco Rinaldo Oggioni,
University of Leicester,
United Kingdom

Reviewed by:

Sunil Joshi,
University of Miami, United States
Jiezuan Yang,
Zhejiang University, China
Marielle C. Haks,
Leiden University Medical Center,
Netherlands

Yean Kong Yong,

Xiamen University, Malaysia

*Correspondence:

Pawan Gupta
pawan@imtech.res.in

Specialty section:

This article was submitted to
Microbial Immunology,
a section of the journal
Frontiers in Immunology

Received: 29 January 2020

Accepted: 07 August 2020

Published: 15 October 2020

Citation:

Gupta S and Gupta P (2020)
Etiopathogenesis, Challenges and
Remedies Associated With Female
Genital Tuberculosis: Potential Role of
Nuclear Receptors.
Front. Immunol. 11:02161.
doi: 10.3389/fimmu.2020.02161

Extra-pulmonary tuberculosis (EPTB) is recognized mainly as a secondary manifestation of a primary tuberculosis (TB) infection in the lungs contributing to a high incidence of morbidity and mortality. The TB bacilli upon reactivation maneuver from the primary site disseminating to other organs. Diagnosis and treatment of EPTB remains challenging due to the abstruse positioning of the infected organs and the associated invasiveness of sample acquisition as well as misdiagnosis, associated comorbidities, and the inadequacy of biomarkers. Female genital tuberculosis (FGTB) represents the most perilous form of EPTB leading to poor uterine receptivity (UR), recurrent implantation failure and infertility in females. Although the number of TB cases is reducing, FGTB cases are not getting enough attention because of a lack of clinical awareness, nonspecific symptoms, and inappropriate diagnostic measures. This review provides an overview for EPTB, particularly FGTB diagnostics and treatment challenges. We emphasize the need for new therapeutics and highlight the need for the exaction of biomarkers as a point of care diagnostic. Nuclear receptors have reported role in maintaining UR, immune modulation, and TB modulation; therefore, we postulate their role as a therapeutic drug target and biomarker that should be explored in FGTB.

Keywords: nuclear receptors, uterine receptivity, cytokine modulation, female genital tuberculosis, recurrent implantation failure, endometrium regeneration, extrapulmonary tuberculosis

INTRODUCTION

Mycobacterium tuberculosis (*M. tuberculosis*) is an etiological agent that causes tuberculosis (TB), which is a health issue of global importance. TB profoundly exists in two forms, i.e., pulmonary and extrapulmonary. The most prevalent site of TB infection is the lungs; this is called pulmonary TB (PTB), where the bacilli are phagocytosed in alveolar macrophages and are contagious *via*

Abbreviations: EPTB, Extrapulmonary Tuberculosis; PTB, Pulmonary Tuberculosis; TB, Tuberculosis; FGTB, Female Genital Tuberculosis; RIF, Recurrent Implantation Failure; UR, Uterine Receptivity; ER, Endometrium regeneration; CM, Cytokine modulation; LIF, Leukemia inhibitory factor; VEGF, Vascular endothelial growth factor; NR, Nuclear Receptors; TR4, Testicular receptor; PPAR, Peroxisome Proliferator Activated Receptor; PXR, Pregnane X Receptor; VDR, Vitamin D Receptor; LXR, Liver X Receptor; PR, Progesterone receptor; LHR1, Liver receptor homolog 1; Nurr, Nuclear receptor related; AR, Androgen receptor; COUP-TF, Chicken Ovalbumin Upstream Promoter; SF-1, Steroidogenic Factor; FXR, Farnesoid X Receptor; IL, Interleukin.

aerosol dissemination. TB bacilli can also disseminate to other organs and causes extrapulmonary tuberculosis (EPTB). The genital organs are also an important site for dissemination. **Table 1** shows the distribution of TB cases at extrapulmonary sites (1). EPTB is mainly considered to be a secondary manifestation of the primary infection, which is rarely contagious; however, extrapulmonary involvement can occur with or without PTB. The World Health Organization (WHO) reported 7 million TB cases in 2018 of which 15% were EPTB (2). Additionally, approximately, 10%–50% of EPTB cases are reported to also have pulmonary manifestation (3). The prevalence of EPTB significantly contributes to TB-related morbidity and mortality and is a leading cause of maternal mortality. In a case study, the highest mortality rates are reported for meningitis TB (9.6%) and peritoneal TB (8.5%) (4). Peritoneal TB and female genital TB (FGTB) are a threat to human species propagation (5). Bacterial dissemination leading to EPTB occurs majorly *via* three different channels, i.e., hematogenous, lymphatic, and direct spread (6). Additionally, producing new blood vessels through vascular endothelial growth factor (VEGF) can assist in bacterial dissemination (7). Some rare modes of transmission include congenital transmission, accidental inoculation, therapeutic instillation, and vaccination (8). The atypical presentation, paucibacillary nature, arduousness in procuring appropriate clinical sample, lack of awareness among clinicians, and poor sensitivity of conventional microbiological techniques in EPTB, particularly FGTB, are challenges in diagnosis that further raise the cost due to disability. EPTB cases are on the rise; however, there is still a very extensive awareness gap compared to PTB (15% vs. 86%) (9). The aim of the WHO's "end TB strategy" highlights the need for patient TB care and awareness programs in PTB (10). However, the information on EPTB needs to be adequately addressed. FGTB, which represents the most perilous form of EPTB, is steadily rising as one of the major causes of infertility in females. Globally, about 5%–10% of infertile women are reported to have FGTB (11). FGTB demands immediate attention because of its low recovery rates and the increased abortion rates observed during recent years. Primary infection of TB in the genital tract of females, albeit rare, may occur if the partner has active genitourinary TB. Despite our current understanding, it is vital that research into EPTB and especially FGTB is increased as it is critical to enhance our knowledge of this disease in order to effectively combat it.

TABLE 1 | The bacterial manifestation reported at the surplus site and the prepotency.

Extrapulmonary forms	Occupied site of EPTB (%)	Mode of spread
Lymph node TB	35%	Direct
Pleural TB	20%	Hematogenous
Meningitis TB	5%	Hematogenous
Abdomen TB	3%	Direct
Miliary TB	8%	Hematogenous
Bone and joint TB	10%	Hematogenous
Genitourinary TB	9%	Hematogenous
Others	10%	

This review highlights the major challenges of EPTB, especially FGTB, and necessitates the need for research efforts for effective biomarker discovery in FGTB. The objective of this review is to introduce the diagnostic, treatment, and comorbidity challenges associated with EPTB and, in particular, FGTB and to raise fundamental biological questions regarding the impact of FGTB on female fertility and on the major issues of endometrium regeneration (ER), uterine receptivity (UR), and cytokine modulation (CM). This review covers the current knowledge of nuclear receptors (NRs), reported in regeneration, female reproduction, and in the maintenance of pregnancy with the aim of conceptually postulating that NRs should be explored in the diagnosis and combating of FGTB-associated female infertility.

EPIDEMIOLOGY AND CLINICAL PRESENTATION OF FGTB: THE SILENT RISE

FGTB is the most enigmatic form of EPTB, representing 15%–20% of EPTB cases (12, 13), and is responsible for poor UR, poor endometrial adhesions, and recurrent implantation failure (RIF) in females (14). However, the exact proportion of FGTB is not known due to underreporting of cases, nonspecific symptoms, misleading clinical appearance, and lack of diagnostic measures. Additionally, in a case study, approximately 75.6% of patients' cases evaluated for infertility were diagnosed with FGTB (15). It is highly concerning because the manifestations are asymptomatic, and by the time FGTB is diagnosed, it has already left an impact on female fertility and morbidity. There is also a social stigma attached to FGTB that causes it to be difficult for women to talk openly about it. FGTB is known to mainly cause primary infertility rather than secondary infertility (16); therefore, even after successful treatment, conception rates are very low (19.2%), the success of pregnancy is very low (16.6%), and the birth rate is also extremely low (7.2%) (17, 18). The TB bacilli break out from the primary site of infection and reach the genital area generally through hematogenous spread (19). The most prevalent site of bacterial infection for FGTB includes the endometrium (50%–60%), fallopian tubes (95%–100%), ovaries (20%–30%), cervix (5%–15%), myometrium (2.5%), and vagina/vulva (1%) (19, 20). FGTB causes caseation, adhesions, ulcerations, and complete distortion of the cavity causing Asherman syndrome. The clinical appearance of FGTB is generally called "the considerable pretender" because it mimics ovarian carcinoma (21). FGTB represent various clinical symptoms of infertility (43%–74%), oligomenorrhea (54%), amenorrhea (14%), dysmenorrhea (12%–30%), abdominal pain (42.5%), menorrhagia (19%), dyspareunia (5%–12%), and postmenopausal bleeding (2%) (19, 22–25). The abovementioned clinical presentations arise because the ER capability is compromised, which contributes to recurrent pregnancy loss and infertility (**Table 2**). All these symptoms pertain to the endometrium, and its regeneration needs to be addressed and investigated. The key factors that modulate and exacerbate FGTB need to be identified.

TABLE 2 | Various forms of clinical presentations of FG TB are shown along with signs and symptoms.

Extrapulmonary infection	Clinical presentation	Signs and Symptoms
TB of endometrium	Uterine leiomyoma Postmenopausal TB Oligomenorrhoea Amenorrhoea Menorrhagia	Pyometra Irregular vaginal bleeding and persistent leucorrhoea Menstrual disturbance Menstrual disturbance Abnormal vaginal discharge
TB of cervix	Ovarian carcinoma	Postcoital bleeding
TB of vulva	Tumor	Bloodstained discharge
TB of ovary	Perioophoritis	Tubo-ovarian masses
TB of fallopian tube	Salpingitis and tubal block	Ectopic pregnancy
	Infertility	Implantation failure
TB of pelvic	Fistula formation	Rupture of a tuberculous pyosalpinx
	Malaise	Pelvic inflammatory disease

THE DIAGNOSTIC CHALLENGES OF EPTB WITH AN EMPHASIS ON FG TB

The diagnostic tools for EPTB include the nucleic acid amplification test (Gene-Xpert), immunological test, biopsy, body fluid examination, and sputum acid-fast bacillus (AFB) smear. Gene-Xpert shows high sensitivity in EPTB samples but is less in cerebrospinal fluid (CSF), i.e., 29% (26). The antibody-based serological test has poor sensitivity and is not applicable to EPTB samples (27). Blood transcriptomic biomarkers are identified in TB, which can easily discriminate between healthy and infected persons (28–31). The onset of TB can be predicted through metabolite changes in blood (32). Blood transcriptomic and metabolic signatures have improved diagnosis in TB and are being explored as probable diagnosis for EPTB (8, 33, 34). Systematic reviews on TB biomarkers, including antibodies, cytokines, chemokines, proteins, and metabolic activity markers have already been published (35). These biomarkers, to some extent, have also been studied in EPTB (36, 37). EPTB is largely undiagnosed in patients, especially when visceral sites are involved. The detection of EPTB, particularly FG TB, poses a major challenge with conventional methods. EPTB diagnosis is challenging because of misdiagnosis, arduousness in acquiring of clinical samples, being asymptomatic, and poor sensitivity of existing diagnostic (**Figure 1**). Generally, miliary TB is misdiagnosed with systemic lupus erythematosus (SLE) (38). EPTB, particularly peritoneal TB, may also be misinterpreted as ovarian cancer and peritoneal carcinomatosis (5, 39). Intestinal TB is misdiagnosed with Crohn disease (40). Bone and joint TB are misdiagnosed as rheumatoid arthritis, traumatism, and gout. Vulva and vaginal TB is misdiagnosed with malignancy (41). Invasiveness and constraints in obtaining biopsies prevent the early diagnosis of EPTB, and in addition, these diagnostic tests can cause incidental damages and infection; for instance, in the case of meningitis TB, extraction of CSF can possibly harm the nerves around the site of insertion. Biopsy, endoscopy, cystoscopy, and lumbar puncture are all performed depending on the case for other EPTBs (8). Meningitis TB is suspected when

the patient is diagnosed with mental disturbance or is found to have lymphocytic pleocytosis (42). Due to the nonparticular symptoms, miliary TB and urogenital TB are often diagnosed at an autopsy (8, 43–46).

Being a paucibacillary disease, the diagnostic measures of FG TB involve a combination of bacteriological confirmatory measures. FG TB patients exhibit features of dysfunction of genital organs rather than any symptoms of infection. Repeatedly invasive techniques are utilized to acquire sufficient samples of body fluids, tissues, or biopsies. FG TB diagnosis is mainly done through endometrial samples using microscopy (AFB), histopathological detection of epithelioid granuloma on biopsy, and Gene-Xpert (41). Peritoneal fluid or biopsy for culture, endoscopy, and cervical cytology are also performed for diagnosis. However, histopathological findings are not specific for FG TB because of shedding of the endometrium. Magnetic resonance imaging and positron emission tomography have been used for detecting tubo-ovarian masses (47, 48). Loop-mediated isothermal amplification is the most convenient technique used for diagnosing FG TB (49). A laparoscopy combined with hysteroscopy is the most reliable tool to diagnose FG TB; however, this is associated with perioperative complications. Laparoscopy is risky because of the presence of many adhesions, which cover the pelvic organs and may hinder the diagnosis and can increase the risk of bleeding (41, 50). Hysteroscopy is associated with various complications, such as excessive bleeding, perforation, inability to distinguish and distend cavity, and flare-up of genital TB, which can cause abortions and infertility (51). FG TB, specifically endometrial TB, represents ulceration, caseous necrosis, and hemorrhage; this necessitates careful macroscopic sampling (51, 52). FG TB is a silent disease; rarely, it presents as abdominal pain, abnormal genital bleeding, and dyspareunia (53). The misdiagnosis rate is very high among FG TB patients and is associated with several complications. The disease is mistaken for other gynecological conditions or malignancy; for example, FG TB is misdiagnosed as ovarian cancer or chocolate cyst or pelvic inflammatory disease (PID) (54), and FG TB patients who are reported to have cervical TB may masquerade as cervical cancer (41, 55). Additionally, FG TB patients may be mistaken or coexist with acute appendicitis or ectopic pregnancy (52). TB of the vulva and cervix is very arduous to distinguish as it appears as brucellosis, schistosomiasis, tularemia, cervical amoebiasis, sarcoidosis, syphilis, or chancroid (56). Furthermore, a high level of drug resistance is witnessed in FG TB (57). Given the above challenges with FG TB diagnosis, including exceptional positioning of organs, associated invasiveness of sample collections, misdiagnosis, being asymptomatic, poor sensitivity, the emergence of drug resistance, and the lack of point of care, there is a strong need to identify FG TB-specific biomarkers. The biosignatures emanating from the pathogen have been reported for FG TB diagnosis (58). However, the sensitivity of detection in FG TB patient samples is very low because the infected sites are missed due to the paucibacillary nature of *M. tuberculosis*. We are focusing on the host-derived biomarkers for the prompt and accurate diagnosis of FG TB from easily accessible samples without utilizing any invasive procedure.

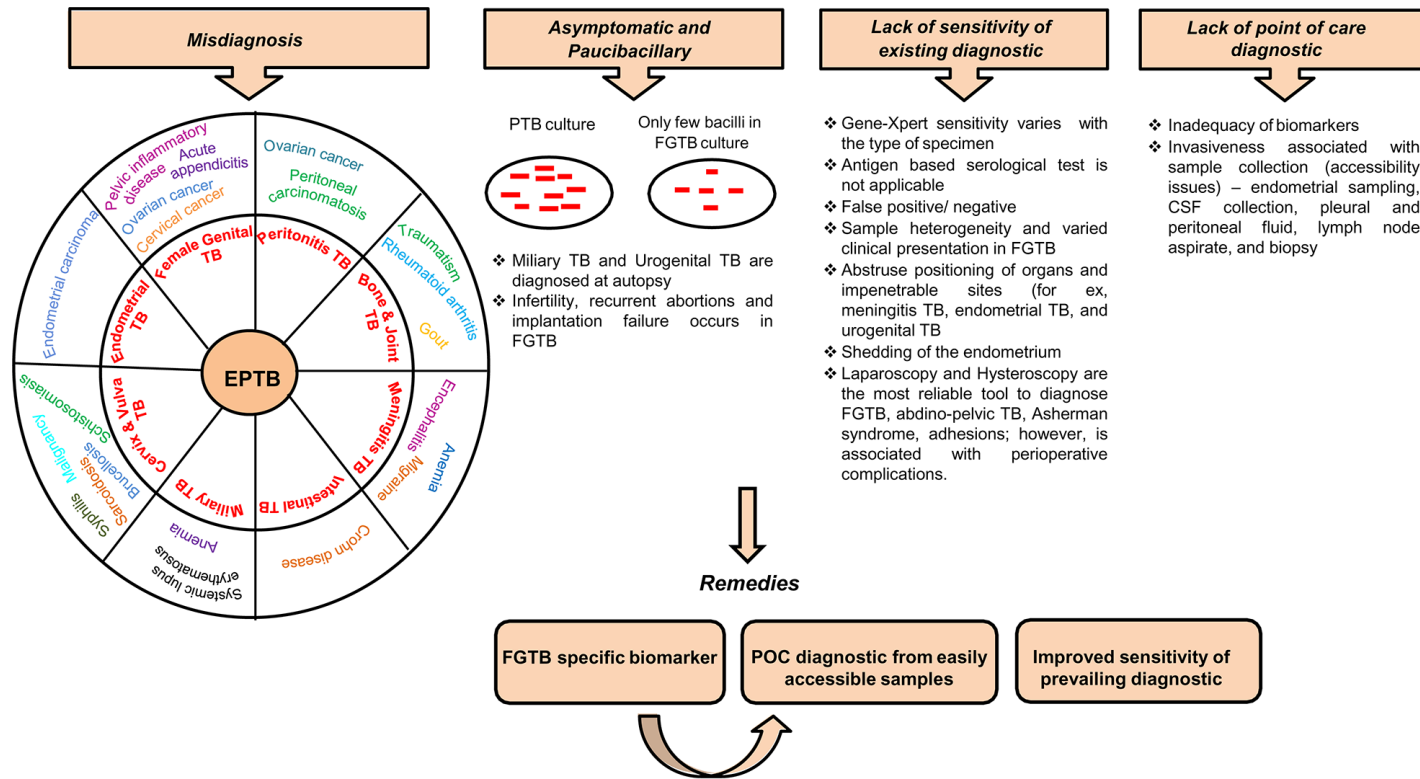


FIGURE 1 | Diagnostic challenges and remedies for EPTB, in particular FGTB. Various challenges associated with EPTB diagnosis, such as misdiagnosis, often asymptomatic and paucibacillary nature of bacilli, lack of sensitivity of existing conventional methods, and lack of point-of-care diagnostics, lead to loss due to disability.

TREATMENT CHALLENGES OF EPTB WITH AN EMPHASIS ON FGTB

Treatment of EPTB faces major challenges from comorbidities (e.g., HIV coinfection or renal failure), drug sovereignty, misdiagnosis, drug disposition, and unusual positioning of a few organs, i.e., endometrium, central nervous system (CNS) (**Figure 2**). Chronic renal failure exacerbates EPTB more than TB (59). During renal impairment, DOTS therapy is eliminated by nonrenal routes; for example, by biliary secretion or through metabolism. Coadministration of anti-HIV and anti-TB drugs in a comorbid condition leads to absorption issues due to a reduction in the assimilation of the two key anti-TB drugs (rifampin and isoniazid) (60). Likewise, TB drugs also lower the levels of antiretroviral drugs; as soon as the antiretroviral therapy is initiated, it paradoxically results in worsening of symptoms or causes immune reconstitution inflammatory syndrome (1, 61). A high proportion of drug-induced liver injuries are observed in cirrhosis patients coinfecting with TB (62). Ascites formed in the body in peritonitis TB present a problem for anti-TB drug disposition (63). Approximately 10%–20% of patients consuming ATT (anti-TB drugs; Ethambutol, Pyrazinamide, Isoniazid, and Rifampicin) either in a single or combinatorial therapy are at a risk of evolving hepatotoxicity (64–66). When EPTB is misdiagnosed as another disease, the treatment for the erroneous disease may exacerbate EPTB; for example, immunosuppressant therapy given when EPTB is misdiagnosed as chronic kidney disease exacerbates the actual case of EPTB (67, 68). A case was reported in which immunosuppressant therapy given for SLE in a patient coinfecting with disseminated TB led to respiratory failure (69). Meningitis TB treatment is challenging because of the poor penetration of drugs (e.g., rifampin and streptomycin) into the CSF due to the impervious blood–brain barrier (70). EPTB is curable with ATT drugs only to an extent and may result in several complications; for example, patients on ATT treatment may develop acute kidney injuries and increase the risk for nephrotoxicity neuropathy and CNS toxicity (71–73). EPTB treatment also has some exclusion criterion; i.e., chemotherapy is detrimental during the first trimester of pregnancy as it prompts pregnancy termination. Specific adjuvant therapy, chemotherapy, and major surgery are suggested in some uncommon types of EPTB to avoid the complications of TB dissemination (**Figure 2**). Chemotherapy is required for genitourinary TB with surgery being substantial and reconstructive surgery required to repair the ureteral strictures (3).

The treatment of FGTB faces formidable challenges from coinfection (HIV, etc.); drug toxicity; obstetric, perioperative, and postoperative complications; reactivation; and emergence of drug-resistant bacteria (**Figure 2**). FGTB and HIV coinfection make the most deadly combination and is the leading cause of maternal mortality. Moreover, reactivation of bacilli has been observed in FGTB and HIV coinfection (12). HIV-induced immunosuppression in FGTB patients may also cause PID (74). ATT drugs can cause several complications in FGTB (41). Stem cells, nanotechnology, and colostrum are being used as a

regenerative therapy to treat damaged endometrium, fallopian tubes, and ovaries (41). Vitamin D plays a crucial role in the treatment of FGTB (75). The use of steroids and immunotherapy is observed to a large extent among infertile patients and leads to resurgence of *M. tuberculosis* (76). Surgery in FGTB is performed as an adjunctive therapy during persistent or recurrent infection, the presence of nonhealing fistulae, and for multi-drug-resistant TB; however, reactivation of bacilli has been observed during surgery and has been detected after hysterosalpingography, laparoscopy, hysteroscopy, and laparotomy (77). Obstetric complications, such as preterm labor, increased rate of abortions, and neonatal mortality is high in FGTB. Perioperative complications, such as extreme hemorrhage with huge risk of damage to the pelvic and abdominal organs and the bowel, have been discerned during laparotomy (41). FGTB with pervasive adhesions in the uterus and blocked tubes and pelvis is not treatable even after successful treatment (41). Hysteroscopy is used to diagnose the adhesions and Asherman syndrome (78); however, it is associated with several complications in FGTB, such as, inability to visualize the cavity, excessive bleeding, perforation, bowel injury, peritonitis, and flare-up of genital TB (51, 79). Postoperative complications, such as bowel fistula and mortality rate are high in FGTB. Repeated invasive measures are required after ATT treatment for proper prognosis for fertility. The conception rate after ATT is only 12.8%, and the outcome of pregnancy could still be a live birth, spontaneous abortion, or ectopic pregnancy (80, 81). Furthermore, if patients are considered cured, their chances of pregnancy drop due to the irreversible damage of the fallopian tube and endometrium. Moreover, FGTB, if not properly treated, can cause permanent sterility through endometrial destruction and tubal damage (41). In vitro fertilization (IVF) is considered to be the successful modality for pregnancy in FGTB patients; however, a pregnancy rate of only 17.3% is observed even after successful treatment (82, 83).

The emergence of drug resistance among EPTB, particularly FGTB patients, is on the rise, and it poses a further threat to TB control. EPTB patients have a higher proportion of drug resistance compared to PTB patients (84). Furthermore, a high proportion of drug resistance is witnessed among the treatment failure cases of EPTB (52.7%) and PTB (48.1%) (85). The emergence of a multi-drug-resistant strain has been reported in FGTB (57). Engineered bacteriophages (Muddy, BPs33ΔHTH-HRM10, and ZoeJΔ45) are used as an adjunctive therapy against drug-resistant disseminated *Mycobacterium abscessus* (86). Antitubercular peptides, such as cathelicidins, defensins, granulysin, and hepcidin, are developed as novel TB therapeutics against drug-resistant TB (87).

GENITAL TUBERCULOSIS: ADEPTNESS IN IMMUNE MODULATION

Various molecules that are essential for implantation are being identified as potential players of uterine receptivity, such as growth factors, i.e., VEGF; cytokines, i.e., leukemia inhibitory factor (LIF) (88, 89); and cell adhesion molecules, i.e., CDH1 (E cadherin),

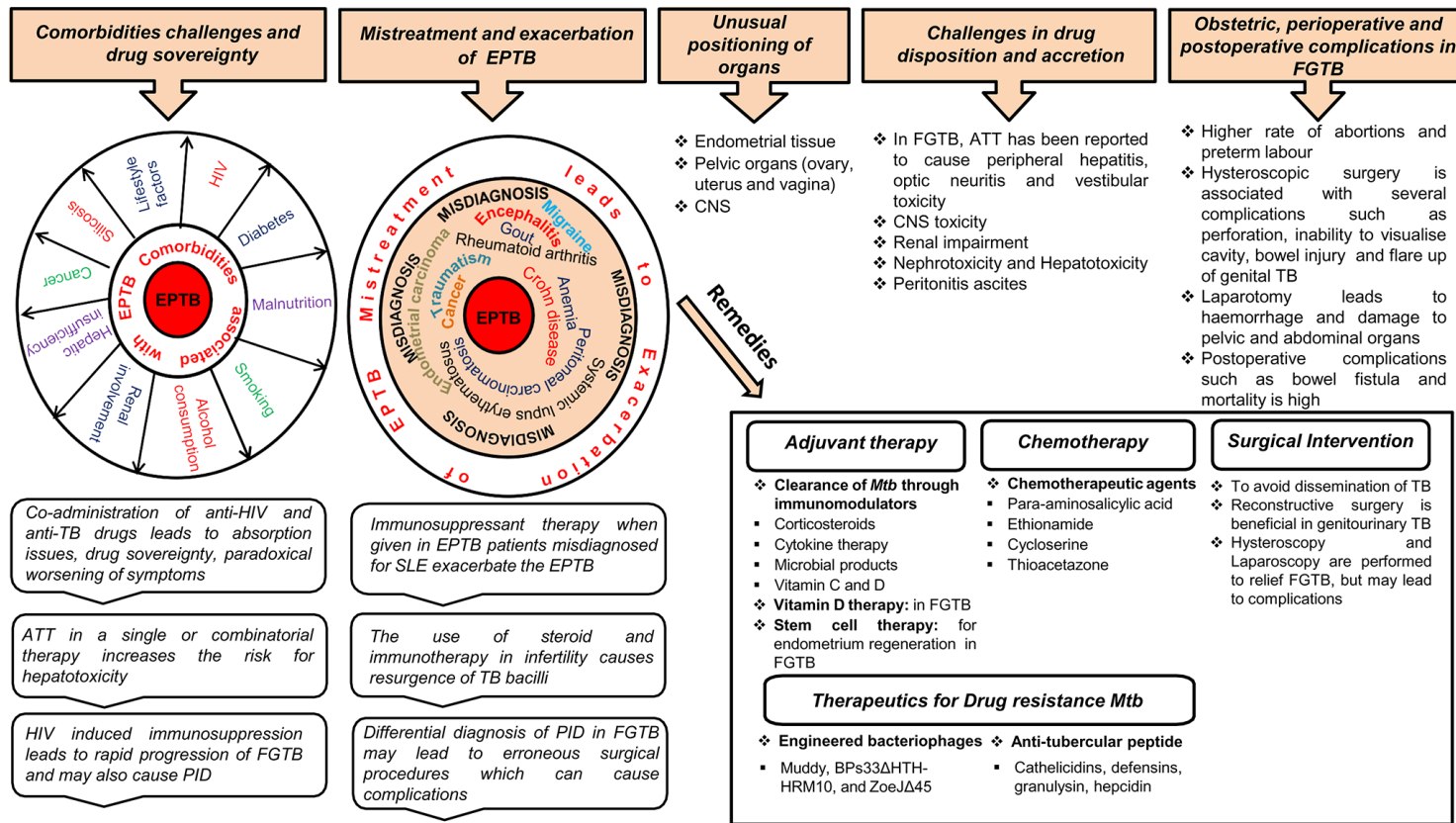


FIGURE 2 | Treatment challenges and remedies for EPTB, in particular, FGTB. Various comorbidity challenges associated with EPTB are depicted. The risk of EPTB, particularly FGTB, occurrence increases in a comorbid condition depending on the severity of immunosuppression associated with these diseases. Coadministration of drugs results in drug sovereignty, toxicity, absorption issues, and paradoxical reactions in the body, which can further exacerbate the condition. EPTB misdiagnosis and subsequent mistreatment suppress the immune system to such an extent that it increases the bacterial prepotency of spreading to other organs (example genital organs) and exacerbation. Differential diagnosis in FGTB leads to erroneous surgical procedures, which can cause complications. ATT treatment in EPTB, in particular FGTB, faces drug disposition and accretion challenges. The unusual positioning of infected organs in EPTB illustrate treatment challenges, especially in meningitis TB, ovarian TB, urogenital TB, and endometrial TB. Due to the inaccessibility of organs in FGTB, surgical interventions are required to avoid dissemination of *M. tuberculosis*; however, several perioperative complications have been observed during surgery. Erroneous surgical procedures and mistreatment lead to obstetric and postoperative complications. Stem cell therapy, chemotherapy, vitamin D therapy, and surgical interventions can be beneficial in FGTB, whereas adjuvant therapy is known to be effective in EPTB, and engineered bacteriophages and antitubercular peptides are used for drug-resistant TB.

ITGAVB3 ($\alpha v\beta 3$), MUC-1 (Mucin-1), and MECA79, as well as hormones expressed during implantation (90, 91) (**Figure 3**). FG TB infection is found to alter the endometrial milieu and, thus, the UR, by causing immune modulation, endocrine disruption, activation of antiphospholipids antibodies, and microthrombosis, which leads to RIF, a major cause of infertility (92). FG TB significantly alters the level of ITGAVB3, MECA79, CDH1, MUC-1, and VEGF, leading to RIF (90). ITGAVB3 is essential for implantation, and its expression is reduced in both FG TB and unexplained recurrent pregnancy loss (90, 91). Additionally, an aberrant (reduced) expression of LIF has been reported in the endometrium in FG TB. The concentration of LIF is higher in fertile women compared to infertile females (93). LIF can activate signal transducers and activators of transcription 3 (STAT3) through a signaling cascade mechanism, which regulates UR and is further required for the transcription of VEGF, an angiogenic factor whose role during pregnancy is well studied (88, 90, 94, 95). FG TB lowers VEGF expression; thus creating an unfavorable environment for embryonic implantation (90). On the contrary, high VEGF levels

contribute to the pathogenesis of EPTB; therefore, anti-VEGF agents are used in TB to prevent bacterial dissemination (96, 97). TB bacilli show an antigonadotropic effect in FG TB, impeding the production of progesterone and human chorionic gonadotropin (98). In FG TB, luteinizing hormone (LH) and follicle stimulating hormone (FSH) levels are high, and inhibin levels are very low (99). Inhibin is considered to be a more sensitive marker of ovarian reserve in FG TB compared to FSH (99, 100). Latent FG TB not only interferes with implantation in the basal endometrial layer, but also lowers the level of two ovarian markers, i.e., antimüllerian hormone and antral follicle count (101). Furthermore, it has been observed that FG TB lowers the oocyte yield and the ovarian reserve (101).

Cytokine production differs in PTB and EPTB patients; females with normal pregnancy have been observed to have Th2-type cytokine milieu, whereas there has been shown to be an increased production of Th1-type cytokines in unexplained recurrent abortions (102, 103). The inflammatory environment in the endometrium prompts the preponderance of adverse cytokines and antibodies of the Th1 repertoire, making it nonreceptive to

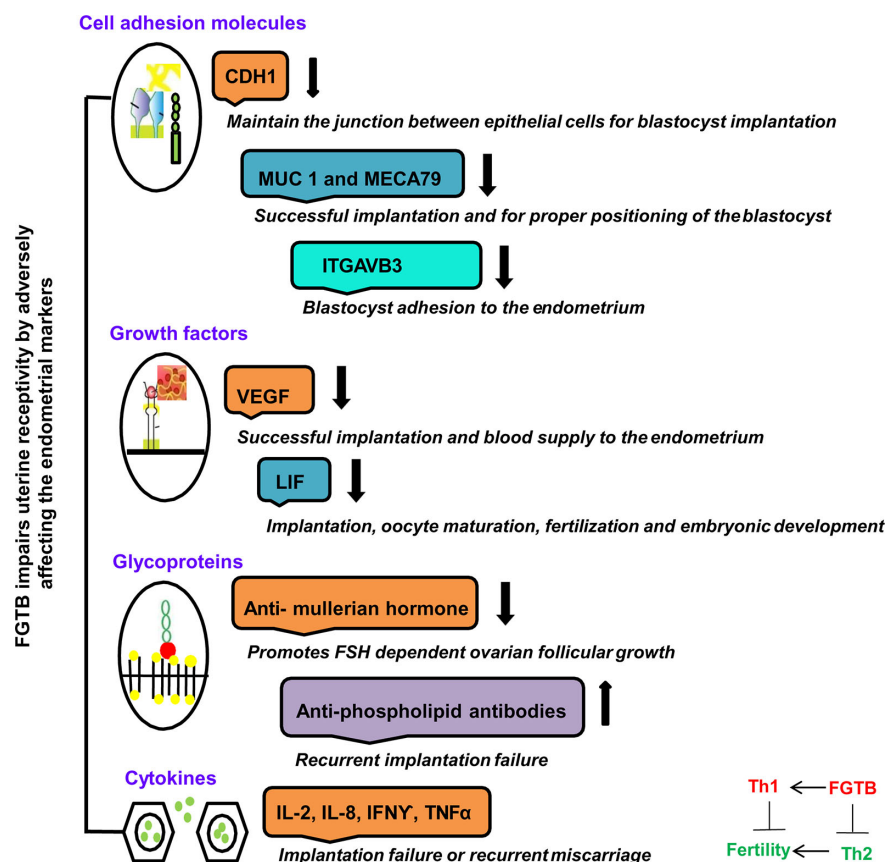


FIGURE 3 | FG TB: Immune dysregulation compromises female fertility. The impact of FG TB on female fertility is depicted. FG TB adversely affects uterine receptivity through immune dysregulation. Various cell adhesion molecules, growth factors, glycoproteins, and cytokines mentioned here are potential biomarkers of uterine receptivity and for successful placentation. FG TB lowers the level of CDH1, MUC1, MECA79, and ITGAVB3, leading to recurrent implantation failure. Similarly, FG TB pares down the levels of VEGF and LIF, which are required for successful placentation, thus creating an unfavorable environment for embryonic implantation. Glycoproteins and cytokines are also required for embryonic development. FG TB also affects embryonic development through upregulating proinflammatory cytokine expression and antiphospholipid antibodies as well as by lowering anti-inflammatory cytokine expression and ovarian reserve markers, such as the antimüllerian hormone.

the embryo, thereby causing an implantation failure (92). However, T regulatory cells, a subset of CD4⁺ T cells limit the adaptive immune response and contribute to the persistence of chronic infection. Immune dysregulation has been reported in patients who have a past or present history of EPTB as observed by an increased production of T regulatory cells, high levels of IL-17, and CD4⁺ lymphocyte activation (104, 105).

NRS AND FGTB: POTENTIAL MARKERS AND DRUG TARGETS

This review aims to accentuate three major points: (i) the diagnostic and treatment challenges of EPTB, particularly FGTB; (ii) the need for new therapeutics and diagnostics of EPTB, particularly FGTB; and (iii) the demand for FGTB biomarkers as a point-of-care diagnostic. NRs appear to be major potential therapeutic targets owing to their roles being reported as both pro-TB and anti-TB

(Figure 4). NRs are ligand-activated transcriptional factors that act as molecular switches and can govern many physiological processes, such as metabolism, reproduction, and development. The superfamily of NRs shares a common structure containing an amino terminal domain, a conserved DNA-binding domain (DBD), a hinge region, and a ligand-binding domain (LBD) at the carboxy terminal. The amino terminal domain includes the activator function-1 region (AF-1), which interacts with several coregulatory proteins and is also a site for various posttranslational modification. The DBD is conserved and has two subdomains (for DNA binding and receptor dimerization), each containing 4 cysteine residues that coordinate with a zinc ion to form zinc finger motif. The hinge region consists of a nuclear localization signal, and the LBD harbors another activation function domain (AF-2) that can interact directly with coregulator proteins (106). NRs can exist as monomer, homodimer, and heterodimer that recognize a specific DNA sequence on the target genes known as response elements. NRs are classified into three categories based on

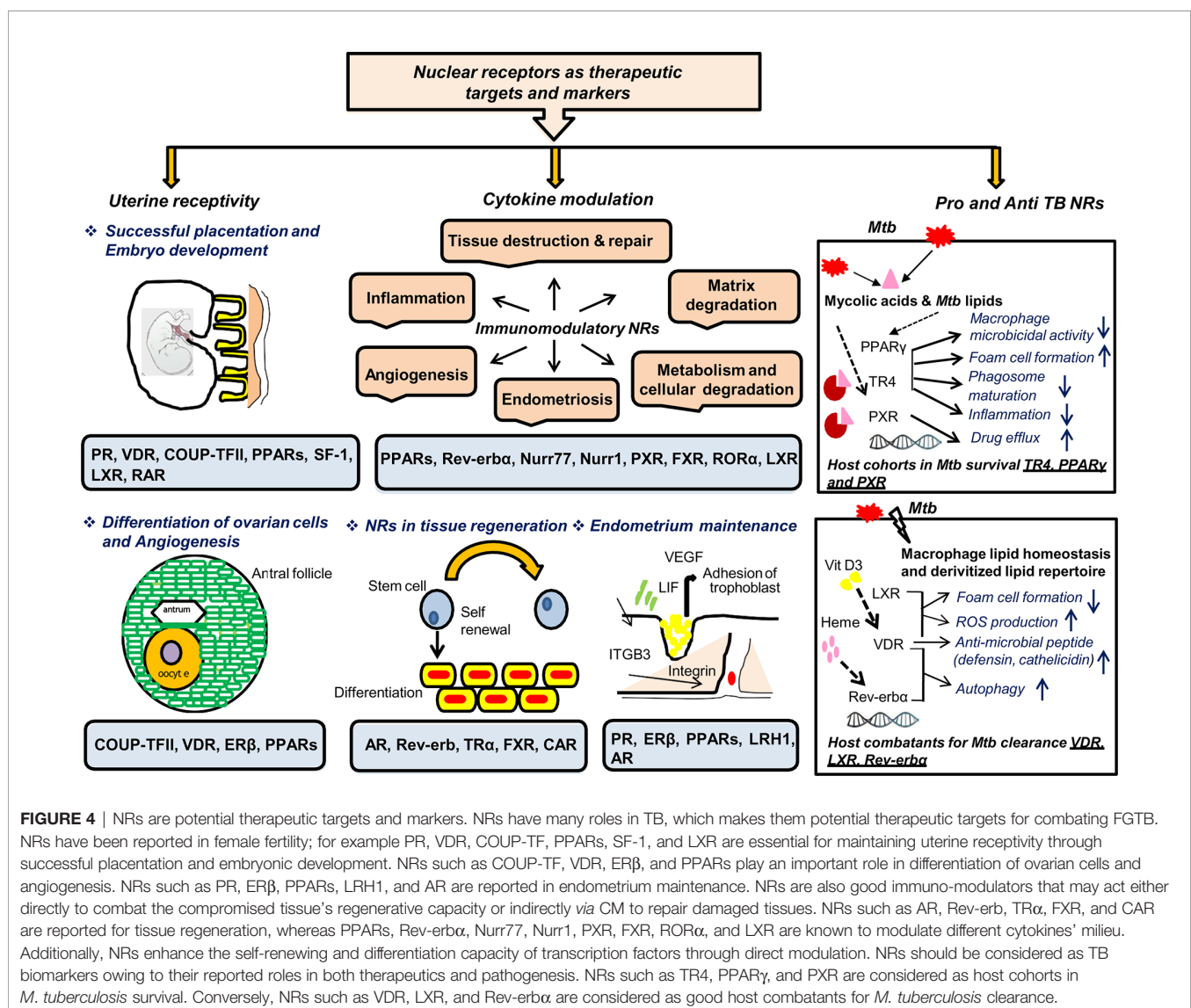


FIGURE 4 | NRs are potential therapeutic targets and markers. NRs have many roles in TB, which makes them potential therapeutic targets for combating FGTB. NRs have been reported in female fertility; for example PR, VDR, COUP-TF, PPARs, SF-1, and LXR are essential for maintaining uterine receptivity through successful placenta and embryonic development. NRs such as COUP-TF, VDR, ERβ, and PPARs play an important role in differentiation of ovarian cells and angiogenesis. NRs such as PR, ERβ, PPARs, LRH1, and AR are reported in endometrium maintenance. NRs are also good immuno-modulators that may act either directly to combat the compromised tissue's regenerative capacity or indirectly via CM to repair damaged tissues. NRs such as AR, Rev-erb, TRα, FXR, and CAR are reported for tissue regeneration, whereas PPARs, Rev-erbα, Nurr77, Nurr1, PXR, FXR, RORα, and LXR are known to modulate different cytokines' milieu. Additionally, NRs enhance the self-renewing and differentiation capacity of transcription factors through direct modulation. NRs should be considered as TB biomarkers owing to their reported roles in both therapeutics and pathogenesis. NRs such as TR4, PPARγ, and PXR are considered as host cohorts in *M. tuberculosis* survival. Conversely, NRs such as VDR, LXR, and Rev-erbα are considered as good host combatants for *M. tuberculosis* clearance.

the ligand variability: class I constitutes the endocrine receptors, class II includes orphan receptors, and class III comprises adopted orphan receptors. The endocrine receptors recognize steroid molecules and vitamins as their ligands and possess a high affinity toward them. The orphan receptors are those for which no endogenous ligand has been deciphered, and the adopted orphans are those whose ligands have been recently identified, and they bind to low-affinity dietary lipids. As various biological processes are regulated by NRs, pharmacological inhibition or dysregulation of them can lead to various diseases, including cancer, metabolic disorders, infertility, and neurodegeneration. They also play a significant role in infectious disease biology as many pathogens, for their own advantage, can modulate NRs either by interfering with their transcriptional activity or by changing their function. NRs have been studied in macrophage response to infectious disease, which also shows the potential role of NRs in combating infectious disease (107). Our earlier studies show a heterologous and noncanonical ligand receptor pairing, which clearly demonstrates that *M. tuberculosis* engage NRs (108–110). NRs, such as testicular receptor (TR4), peroxisome proliferator activated receptor (PPAR γ), and pregnane X receptor (PXR), enhance *M. tuberculosis* survival by subverting the host innate immune defense mechanism and may increase the risk of dissemination (108, 109, 111). Our group has shown that *M. tuberculosis* cell wall lipids can crosstalk with NRs, such as PPAR γ , TR4, and PXR. These NRs are involved in the formation of lipid-enriched foamy macrophages inside the host cell, which further enhances *M. tuberculosis* survival and subverts the immune response by abrogating the phagolysosomal fusion, inhibiting the secretion of proinflammatory cytokines and abating apoptosis. Furthermore, our group also reports that PXR causes TB drug nonresponsiveness in human macrophages by virtue of modulating drug efflux transporters (111). It has been observed that knockout of PPAR γ in a mouse model reduces the growth of *M. tuberculosis*, lowers granulomatous infiltration, and enhances secretion of the proinflammatory cytokines (112). Moreover, NRs, such as vitamin D receptor (VDR) (113), Rev-erb α (114), and liver X receptor (LXR) (115), help with *M. tuberculosis* clearance. Interestingly, EPTB patients with multidrug-resistant TB have lower vitamin D levels (116). TR4 is identified as a marker for early TB detection in rhesus macaques, demonstrating that NRs are likely to make good biomarkers for TB (117). The expression level of TR4 is linked with severity of disease progression in the PBMCs of *M. tuberculosis*-infected rhesus macaques. Correspondingly, NRs can be modulated by small molecules, which allows them to be a potential therapeutic drug target. NRs also may have a role in EPTB, particularly FG TB which needs to be addressed further.

The three chief challenges pertaining to FG TB are UR, ER, and CM. These three factors are required for maintaining female fertility; their dysregulation, either directly or indirectly, leads to fertility issues. FG TB, either directly or indirectly, modulates UR and ER or CM, respectively; thereby, causing RIF. As mentioned before, NRs also play multifarious roles in female reproduction and in sustaining viable pregnancies (Table 3). Any perturbations in the expression of NRs could lead to spontaneous abortions. NRs, such as liver receptor homolog 1

(LRH1), retinoic acid receptor (RAR), chicken ovalbumin upstream promoter (COUP-TFII), steroidogenic factor (SF-1), androgen receptor (AR), LXR, VDR, progesterone receptor (PR), estrogen receptor (ER β), and PPARs have been reported for successful uterine implantation and endometrium maintenance. VDR has also been reported to be important for the differentiation of granulosa cells. The NR LRH1 is reported to be important for mouse fertility (118), ovulation, and ovarian steroidogenesis (119, 120). RAR is involved in early embryonic development (121). COUP-TFII is required for placental development and angiogenesis (122, 123). SF-1 is reported for folliculogenesis and in the process of ovulation with its absence in granulosa cells leading to impaired ovulation (124, 125). AR signaling is essential for endometrial function, whereas its perturbation leads to reproductive failure (126). LXR modulates ovarian endocrine and exocrine function and uterus contractility (127). VDR expression increases during pregnancy and helps with reproductive function (128). Vitamin D has roles in folliculogenesis, differentiation, luteinization, and steroidogenesis as well as altering antimüllerian hormone signaling and progesterone production (129). Vitamin D deficiency in pregnancy increases the fortuity of preterm birth and preeclampsia (130, 131). PR signaling is essential for the initiation and maintenance of pregnancy (132). ER β is essential for maintaining the endometrium quiescence and vasculature (133). PPARs are essential for trophoblast invasion, decidualization, tissue remodeling, ovarian function, and placental formation (134–136). Additionally, circadian rhythm disturbance is reported to affect female fertility (137). Rev-erb is a circadian NR, which maintains the circadian rhythm (138) and may have a role in female fertility. Because NRs play crucial roles in female reproduction, they could make good therapeutic targets to combat female infertility.

RIF occurs due to compromised ER capacity; therefore, stem cell therapy for ER could be helpful. Many NRs have gained

TABLE 3 | Role of Nuclear receptors in female reproduction.

Nuclear Receptors	Functions in Female Reproduction
LRH1	Essential for ovarian steroidogenesis and ovulation
PR	Implantation, decidualization, and preventing endometriosis
ER α	Endometriosis progression
ER β	Maintenance of endometrium quiescence and vasculature
SF-1	Development of reproductive tissue, ovulation, and folliculogenesis
VDR	Differentiation of granulosa cells, folliculogenesis, luteinization, and steroidogenesis
PPAR α	Proliferation and differentiation of ovarian cells
PPAR β	Implantation and decidualization
PPAR γ	Trophoblast invasion and placental formation, decidualization, and preventing endometriosis
AR	Maintenance of endometrium physiology
RAR	Embryonic development, growth, and reproduction
Rev-erb	Regulating the circadian rhythm
COUP-TFII	Placental development and angiogenesis
LXR	Control ovarian endocrine and exocrine function and uterine contractility

attention in stem cell biology (139–142); estrogen receptor (ER α), PR, and PPAR γ are all implicated in endometriosis (143–146); and AR, thyroid receptor (TR), farnesoid X receptor (FXR), Rev-erb, and constitutive androstane receptor (CAR) are reported in tissue regeneration (147–152). Female fertility is compromised due to endometriosis. NRs are known to modulate endometriosis; for example, loss of PR expression leads to endometriotic tissue becoming resistant to progesterone, leading to endometriosis (146). PR helps to relieve pain in endometriosis by limiting inflammation and the growth of endometriotic tissue. PPARs and retinoid X receptor alpha are expressed in abortive trophoblastic tissue and are upregulated in extra villous trophoblast in recurrent miscarriages (153, 154).

M. tuberculosis modulates various cytokines' milieu, such as interferon γ (IFN γ) and interleukin- (IL2) in the endometrium and TNF α , IL-6, IL-4, and IL-8 in the blood (155, 156). Additionally, administration of IFN γ , TNF α , and IL-2 is reported to cause abortions in pregnant mice (102, 157, 158). Moreover, IL-1 β is shown to promote endometriosis and angiogenesis (159, 160). Conversely, IL-6 and IL-10 are reported to have increased production in normal pregnancy compared to spontaneous abortion (103). Various proinflammatory, anti-inflammatory, and pleiotropic NRs, such as retinoic acid receptor-related orphan receptor, nuclear receptor related (Nurr) 77, Nurr1, ROR α , PXR, FXR, PPAR α , LXR, Rev-erb α , and PPARs, are known as immune modulators as they can modulate different cytokines' milieu (114, 161–167). LXR is known to inhibit proinflammatory cytokine expression and is also responsible for maternal-fetal cholesterol transport; there is also a reduction in LXR expression in miscarriages (168, 169). Additionally, FGTB modulates pregnancy-related hormones, such as human chorionic gonadotropin and progesterone, which are known to function *via* their cognate endocrine receptors (98). Taken together, NRs seem to be a promising target to combat FGTB by addressing the issues of UR, ER, and CM. Extensive knowledge about the expression and function of the NRs in FGTB is lacking and needs to be addressed.

FGTB modulates the localized endometrial immune repertoire, which has been reported to modulate UR. There are various reports illustrating the function of the endometrial immune repertoire in recurrent spontaneous miscarriage (170), polycystic ovarian syndrome (171), endometriosis (172), and unexplained infertility (173). Given the reported role of NRs in the regulation of uterine implantation and CM as well as being cognate to pregnancy-related hormones, for example, estrogen, progesterone, human chorionic gonadotropin, and human placental lactogen, which function *via* estrogen receptor, PR, and VDR, respectively (174–178), they are good potential targets to alleviate the disease. NRs could be excellent host-directed targets in FGTB as evident from previous reports of NRs in TB. *M. tuberculosis* can modulate the expression of NRs by certain crosstalk with its lipid repertoire. It would be interesting to see whether *M. tuberculosis* components interfere or modulate the interaction of pregnancy-related hormones with their cognate endocrine receptors. It would be interesting to decipher whether

the *M. tuberculosis* components also relay their effect through orphan or adopted orphan receptors.

DISCUSSION

Globally, EPTB and, in particular, FGTB are growing problems with increasing rates of morbidity and mortality worldwide. FGTB represents the most perilous form of EPTB and is the leading cause of infertility and recurrent implantation failure in females. FGTB cases are asymptomatic in early stages, and untreated FGTB can cause permanent sterility through endometrial destruction and tubal damage. FGTB diagnosis is arduous because of varied clinical presentations, misdiagnosis, associated comorbidities, arduousness in acquiring of clinical samples, poor sensitivity, it is often asymptomatic and paucibacillary, emergence of drug resistance, lack of point of care, impenetrable sites, and abstruse positioning of the organs. Likewise, the treatment of FGTB faces formidable challenges due to drug toxicity; HIV coinfection; obstetric, perioperative, and postoperative complications; reactivation; and emergence of drug-resistant bacteria. Our review rolls out the possible remedies to prevent FGTB by precluding several of these challenges and also highlights the need for exaction of biomarkers in FGTB.

It is imperative to understand that FGTB adversely affects UR and causes immune modulation, which promptly leads to abortions and also reduces the chances of conception. We emphasize the imperative mechanism of FGTB-associated female infertility by highlighting the three major challenges, i.e., UR, ER, and CM. FGTB adversely affects various endocrine hormones (progesterone, estrogen, and human chorionic gonadotropin), cytokines, growth factors (LIF and VEGF), and cell adhesion molecules (ITGAVB3, MECA79, CDH1 and MUC-1), which are responsible for the maintenance of successful pregnancy. We epitomize the need to identify the molecular switches at the interface of FGTB and mechanisms associated with female infertility.

Given the above challenges in FGTB, there is an exigent need to identify FGTB-specific biomarkers from accessible samples. NRs have been reported as both pro- and anti-TB but have gained less attention in FGTB. They are reported to modulate female fertility and stem cell plasticity and are also known as immune modulators. We attempt to invoke interest in the exploration of NRs as a novel therapeutic target in FGTB-associated female infertility and as a potential biomarker. NRs, which are cognate to pregnancy-related hormones (estrogen, progesterone, and human chorionic gonadotropin) and have been cited in female reproduction and regeneration, prompt us to postulate them as a potential player and target to combat FGTB-associated female infertility by addressing the issues of UR, ER, and CM.

The topic is of immediate importance because of the abrupt increase in disease severity, drug resistance, and lack of a knowledge base of the major diagnostic and treatment challenges, which leads to exacerbation in FGTB. Although a

large number of biosignatures and mechanisms have been reported in FG TB, there is a paucity of specific targets and biomarkers. Our review provides the conceptual advance; it postulates the role of NRs as a potential target and biomarker in FG TB. The description is comprehensive and is factual. Fostering innovative research is required to (i) develop highly permeable, safe, and nontoxic drugs with a novel mechanism of action and target; (ii) identify biomarkers and point-of-care diagnostics; and (iii) develop a strategy to shorten the treatment regimens and reduce treatment-related functional disability.

AUTHOR CONTRIBUTIONS

SG and PG designed the study. SG and PG wrote the review. PG contributed to the overall supervision of the manuscript. All authors contributed to the article and approved the submitted version.

REFERENCES

- Sharma S, Mohan A. Extrapulmonary tuberculosis. *Indian J Med Res* (2004) 120:316–353.
- World Health Organization *Global Tuberculosis Report*. (2019) 1–297.
- Lee JY. Diagnosis and treatment of extrapulmonary tuberculosis. *Tuberc Respir Dis* (2015) 78:47–55. doi: 10.4046/trd.2015.78.2.47
- Qian X, Nguyen DT, Lyu J, Albers AE, Bi X, Graviss EA. Risk factors for extrapulmonary dissemination of tuberculosis and associated mortality during treatment for extrapulmonary tuberculosis. *Emerg Microbes Infect* (2018) 7:1–14. doi: 10.1038/s41426-018-0106-1
- Jalali SM, Mashuri N, Tamannaie Z, Jesmi F, Pazouki A. Peritoneal Tuberculosis: An Uncommon Disease Calling for Close Scrutiny. *Arch Clin Infect Dis* (2013) 8:e16672. doi: 10.5812/archcid.16672
- Hopewell PC. Overview of clinical tuberculosis in Tuberculosis. in: Bloom B.R, editor. *Pathogenesis, Protection, and Control*. Washington DC: American Society for Microbiology (1994) 25–46. doi: 10.1128/9781555818357.ch3
- Polena H, Boudou F, Tilleul S, Dubois-Colas N, Lecoine C, Rakotosamimanana N, et al. Mycobacterium tuberculosis exploits the formation of new blood vessels for its dissemination. *Sci Rep* (2016) 6:33162. doi: 10.1038/srep33162
- Muneer A, Macrae B, Krishnamoorthy S, Zumla A. Urogenital tuberculosis — epidemiology, pathogenesis and clinical features. *Nat Rev Urol* (2019) 16:573–98. doi: 10.1038/s41585-019-0228-9
- Purohit MR, Purohit R, Mustafa T. Patient Health Seeking and Diagnostic Delay in Extrapulmonary Tuberculosis: A Hospital Based Study from Central India. *Tuberc Res Treat* (2019) 2019:4840561. doi: 10.1155/2019/4840561
- Mirsaeidi M, Sadikot RT. Patients at high risk of tuberculosis recurrence. *Int J Mycobacteriol* (2018) 7:1–6. doi: 10.4103/ijmy.ijmy_164_17
- Eftekhari M, Pourmasumi S, Sabeti P, Aflatoonian A, Sheikhha MH. Mycobacterium tuberculosis infection in women with unexplained infertility. *Int J Reprod BioMed* (2015) 13:749–54. doi: 10.29252/ijrm.13.12.749
- Duggal S, Duggal N, Hans C, Mahajan R. Female genital TB and HIV co-infection. *Indian J Med Microbiol* (2009) 27:361–363. doi: 10.4103/0255-0857.55461
- Al-Hakeem M, Schneider A. Genital tuberculosis: A rare cause of vulvovaginal discharge and swelling. *J Microbiol Infect Dis* (2013) 03:141–3. doi: 10.5799/ahinjs.02.2013.03.0097
- Sharma JB, Sneha J, Singh UB, Kumar S, Roy KK, Singh N, et al. Comparative Study of Laparoscopic Abdominopelvic and Fallopian Tube Findings Before and After Antitubercular Therapy in Female Genital Tuberculosis With Infertility. *J Minim Invasive Gynecol* (2016) 23:215–22. doi: 10.1016/j.jmig.2015.09.023

FUNDING

This work was supported by the Council of Scientific and Industrial Research (CSIR) RC project (OLP115) to PG. This work is also supported by the Department of Biotechnology, Ministry of Science and Technology, National Bioscience Award project (GAP-0162) to PG. We thank IMTECH, a CSIR laboratory, for the facilities and financial support. The funders had no role in study design, data collection, or interpretation or in any decision to submit the work for publication.

ACKNOWLEDGMENTS

We express regret for not citing the work of many our colleagues due to space constraints.

- Namavar Jahromi B, Parsanezhad ME, Ghane-Shirazi R. Female genital tuberculosis and infertility. *Int J Gynecol Obstet* (2001) 75:269–72. doi: 10.1016/S0020-7292(01)00494-5
- Shahzad S. Investigation of the prevalence of female genital tract tuberculosis and its relation to female infertility: An observational analytical study. *Iran J Reprod Med* (2012) 10:581–8.
- Parikh FR, Nadkarni SG, Kamat SA, Naik N, Soonawala SB, Parikh RM. Genital tuberculosis—a major pelvic factor causing infertility in Indian women. *Fertil Steril* (1997) 67:497–500. doi: 10.1016/S0015-0282(97)80076-3
- Tripathy SN, Tripathy SN. Infertility and pregnancy outcome in female genital tuberculosis. *Int J Gynecol Obstet* (2002) 76:159–63. doi: 10.1016/S0020-7292(01)00525-2
- Gatongi DK, Gitau G, Kay V, Ngwenya S, Lafong C, Hasan A. Female genital tuberculosis. *Obstet Gynaecol* (2005) 7:75–9. doi: 10.1576/toag.7.2.075.27000
- Das P, Ahuja A, Gupta SD. Incidence, etiopathogenesis and pathological aspects of genitourinary tuberculosis in India: A journey revisited. *Indian J Urol* (2008) 24:356–61. doi: 10.4103/0970-1591.42618
- Hasanzadeh M, Naderi HR, Hoshyar AH, Shabane S, Shahidsales S. Female genital tract tuberculosis presenting as ovarian cancer. *J Res Med Sci Off J Isfahan Univ Med Sci* (2014) 19:184–9.
- Gungorduk K, Ulker V, Sahbaz A, Ark C, Ismet Tekirdag A. Postmenopausal Tuberculosis Endometritis. *Infect Dis Obstet Gynecol* (2007) 2007:27028. doi: 10.1155/2007/27028
- Margolis K, Wranz P, Kruger T, Joubert J, Odendaal H. Genital tuberculosis at Tygerberg Hospital—prevalence, clinical presentation and diagnosis. *South Afr Med J Suid-Afr Tydskr Vir Geneeskde* (1992) 81:12–15.
- Qureshi R, Samad S, Hamid R, Lakha S. Female genital tuberculosis revisited. *JPMA J Pak Med Assoc* (2001) 51:16–18.
- Samal S, Gupta U, Agarwal P. Menstrual disorders in genital tuberculosis. *J Indian Med Assoc* (2000) 98:126–7, 129.
- Vadwai V, Boehme C, Nabeta P, Shetty A, Alland D, Rodrigues C. Xpert MTB/RIF: a new pillar in diagnosis of extrapulmonary tuberculosis? *J Clin Microbiol* (2011) 49:2540–5. doi: 10.1128/JCM.02319-10
- Bartoloni A, Strohmeier M, Bartalesi F, Messeri D, Tortoli E, Farese A, et al. Evaluation of a rapid immunochromatographic test for the serologic diagnosis of tuberculosis in Italy. *Clin Microbiol Infect* (2003) 9:632–9. doi: 10.1046/j.1469-0691.2003.00574.x
- Maertzdorf J, Kaufmann SH, Weiner J. Toward a Unified Biosignature for Tuberculosis. *Cold Spring Harb Perspect Med* (2015) 5:a018531. doi: 10.1101/cshperspect.a018531
- Berry MPR, Graham CM, McNab FW, Xu Z, Bloch SAA, Oni T, et al. An Interferon-Inducible Neutrophil-Driven Blood Transcriptional Signature in Human Tuberculosis. *Nature* (2010) 466:973–7. doi: 10.1038/nature09247
- Maertzdorf J, Ota M, Repsilber D, Mollenkopf HJ, Weiner J, Hill PC, et al. Functional Correlations of Pathogenesis-Driven Gene Expression Signatures

- in Tuberculosis. *PLoS One* (2011) 6:e26938. doi: 10.1371/journal.pone.0026938
31. Duffy FJ, Weiner JI, Hansen S, Tabb DL, Suliman S, Thompson E, et al. Immunometabolic Signatures Predict Risk of Progression to Active Tuberculosis and Disease Outcome. *Front Immunol* (2019) 10:527. doi: 10.3389/fimmu.2019.00527
 32. Weiner J, Maertzdorf J, Sutherland JS, Duffy FJ, Thompson E, Suliman S, et al. Metabolite changes in blood predict the onset of tuberculosis. *Nat Commun* (2018) 9:5208. doi: 10.1038/s41467-018-07635-7
 33. Walzl G, Mcnerney R, de Plessis N, Bates M, McHugh TD, Chegou NN, et al. Tuberculosis: advances and challenges in development. *Lancet Infect Dis* (2018) 18:e119–e210. doi: 10.1016/S1473-3099(18)30111-7
 34. Roe JK, Thomas N, Gil E, Best K, Tsaliki E, Morris-Jones S, et al. Blood transcriptomic diagnosis of pulmonary and extrapulmonary tuberculosis. *JCI Insight* (2016) 1:e87238. doi: 10.1172/jci.insight.87238
 35. MacLean E, Broger T, Yerlikaya S, Fernandez-Carballo BL, Pai M, Denkinger CM. A systematic review of biomarkers to detect active tuberculosis. *Nat Microbiol* (2019) 4:748–58. doi: 10.1038/s41564-019-0380-2
 36. Fortún J, Martín-Dávila P, Gómez-Mampaso E, Vallejo A, Cuartero C, González-García A, et al. Extra-pulmonary tuberculosis: a biomarker analysis. *Infection* (2014) 42:649–54. doi: 10.1007/s15010-014-0602-8
 37. Kumar NP, Anuradha R, Andrade BB, Suresh N, Ganesh R, Shankar J, et al. Circulating Biomarkers of Pulmonary and Extrapulmonary Tuberculosis in Children. *Clin Vaccine Immunol* (2013) 20:704–11. doi: 10.1128/CI.00038-13
 38. Elzein F, Elzein A, Mohammed N, Alswailem R. Miliary tuberculosis mimicking systemic lupus erythematosus flare. *Respir Med Case Rep* (2018) 25:216–9. doi: 10.1016/j.rmcr.2018.09.005
 39. Boss JD, Shah CT, Oluwole O, Sheagren JN. TB Peritonitis Mistaken for Ovarian Carcinomatosis Based on an Elevated CA-125. *Case Rep Med* (2012) 2012:215293–3. doi: 10.1155/2012/215293
 40. Seo H, Lee S, So H, Kim S-O, Soh JS, et al. Temporal trends in the misdiagnosis rates between Crohn's disease and intestinal tuberculosis. *World J Gastroenterol* (2017) 23:6306–14. doi: 10.3748/wjg.v23.i34.6306
 41. Sharma JB. Current Diagnosis and Management of Female Genital Tuberculosis. *J Obstet Gynaecol India* (2015) 65:362–71. doi: 10.1007/s13224-015-0780-z
 42. Khanna SR, Kralovic SM, Prakash R. Tuberculous Meningitis in an Immunocompetent Host: A Case Report. *Am J Case Rep* (2016) 17:977–81. doi: 10.12659/ajcr.900762
 43. Chapman CB, Whorton CM. Acute Generalized Miliary Tuberculosis in Adults. *N Engl J Med* (1946) 235:239–48. doi: 10.1056/NEJM194608222350801
 44. Sharma SK, Mohan A, Sharma A. Miliary tuberculosis: A new look at an old foe. *J Clin Tuberc Mycobact Dis* (2016) 3:13–27. doi: 10.1016/j.jctube.2016.03.003
 45. Vasankari T, Liippo K, Tala E. Overt and Cryptic Miliary Tuberculosis Misdiagnosed until Autopsy. *Scand J Infect Dis* (2003) 35:794–6. doi: 10.1080/00365540310016961
 46. Schubert GE, Haltaufderheide T, Golz R. Frequency of Urogenital Tuberculosis in an Unselected Autopsy Series from 1928 to 1949 and 1976 to 1989. *Eur Urol* (1992) 21:216–23. doi: 10.1159/000474841
 47. Sharma JB, Karmakar D, Kumar R, Shamim SA, Kumar S, Singh N, et al. Comparison of PET/CT with other imaging modalities in women with genital tuberculosis. *Int J Gynecol Obstet* (2012) 118:123–8. doi: 10.1016/j.ijgo.2012.02.020
 48. Sharma JB, Karmakar D, Hari S, Singh N, Singh SP, Kumar S, et al. Magnetic resonance imaging findings among women with tubercular tubo-ovarian masses. *Int J Gynecol Obstet* (2011) 113:76–80. doi: 10.1016/j.ijgo.2010.10.021
 49. Sethi S, Dhaliwal L, Dey P, Kaur H, Yadav R, Sethi S. Loop-mediated isothermal amplification assay for detection of Mycobacterium tuberculosis complex in infertile women. *Indian J Med Microbiol* (2016) 34:322–7. doi: 10.4103/0255-0857.188323
 50. Efed B, Sidibé IS, Erregad F, Hammam N, Chbani L, El Fatemi H. Female genital tuberculosis: a clinicopathological report of 13 cases. *J Surg Case Rep* (2019) 3:rjz083. doi: 10.1093/jscr/rjz083
 51. Sharma JB, Roy KK, Pushparaj M, Karmakar D, Kumar S, Singh N. Increased Difficulties and Complications Encountered During Hysteroscopy in Women with Genital Tuberculosis. *J Minim Invasive Gynecol* (2011) 18:660–5. doi: 10.1016/j.jmig.2011.05.008
 52. Grace GA, Devaleenal DB, Natrajan M. Genital tuberculosis in females. *Indian J Med Res* (2017) 145:425–36. doi: 10.4103/ijmr.IJMR_1550_15
 53. Neonakis IK, Spandidos DA, Petinaki E. Female genital tuberculosis: A review. *Scand J Infect Dis* (2011) 43:564–72. doi: 10.3109/00365548.2011.568523
 54. Sah SK, Shi X, Du S, Li X, Li CH, Shah S, et al. CT findings and analysis for misdiagnosis of female pelvic tuberculosis. *Radiol Infect Dis* (2017) 4:19–25. doi: 10.1016/j.rid.2016.04.001
 55. Sharma S, Dutta S, Yadav A, K, Mandal A. A Rare Case of Cervical Tuberculosis Masquerading as Carcinoma Cervix. *Ann Woman Child Health* (2016) 2:C20–3.
 56. Gupta B, Shree S, Rajaram S, Goel N. Genital tuberculosis: Unusual presentations. *Int J Mycobacteriol* (2016) 5:357–9. doi: 10.1016/j.ijmyco.2016.06.017
 57. Sharma JB, Kriplani A, Sharma E, Sharma S, Dharmendra S, Kumar S, et al. Multi drug resistant female genital tuberculosis: A preliminary report. *Eur J Obstet Gynecol Reprod Biol* (2017) 210:108–15. doi: 10.1016/j.ejogrb.2016.12.009
 58. Bhanothu V, Theophilus JP, Rozati R. Use of Endo-Ovarian Tissue Biopsy and Pelvic Aspirated Fluid for the Diagnosis of Female Genital Tuberculosis by Conventional versus Molecular Methods. *PLoS One* (2014) 9:e98005. doi: 10.1371/journal.pone.0098005
 59. Yousef AI, Ismael MF, Elshora AE, Abdou HE. Pulmonary tuberculosis in patients with chronic renal failure at Zagazig University Hospitals. *Egypt J Chest Dis Tuberc* (2014) 63:187–92. doi: 10.1016/j.ejcd.2013.11.002
 60. Gurumurthy P, Ramachandran G, Kumar AKH, Rajasekaran S, Padmapriyadarsini C, Swaminathan S, et al. Malabsorption of Rifampin and Isoniazid in HIV-Infected Patients With and Without Tuberculosis. *Clin Infect Dis* (2004) 38:280–3. doi: 10.1086/380795
 61. Rajasekaran S, Khandelwal G. Drug therapy in spinal tuberculosis. *Eur Spine J Off Publ Eur Spine Soc Eur Spinal Deform Soc Eur Sect Cerv Spine Res Soc* (2013) 22 Suppl 4:587–93. doi: 10.1007/s00586-012-2337-5
 62. Sharma P, Tyagi P, Singla V, Bansal N, Kumar A, Arora A. Clinical and biochemical profile of tuberculosis in patients with liver cirrhosis. *J Clin Exp Hepatol* (2015) 5:8–13. doi: 10.1016/j.jceh.2015.01.003
 63. Jullien S, Jain S, Ryan H, Ahuja V. Six-month therapy for abdominal tuberculosis. *Cochrane Database Syst Rev* (2016) 11:CD012163. doi: 10.1002/14651858.CD012163.pub2
 64. Scharer L, JP S. Serum Transaminase Elevations and Other Hepatic Abnormalities in Patients Receiving Isoniazid. *Ann Intern Med* (1969) 71:1113–20. doi: 10.7326/0003-4819-71-6-1113
 65. Mitchell JR, Zimmerman HJ, Ishak KG, Thorgeirsson UP, Timbrell JA, Snodgrass WR, et al. Isoniazid Liver Injury: Clinical Spectrum, Pathology, and Probable Pathogenesis. *Ann Intern Med* (1976) 84:181–92. doi: 10.7326/0003-4819-84-2-181
 66. Ramappa V, Aithal GP. Hepatotoxicity Related to Anti-tuberculosis Drugs: Mechanisms and Management. *J Clin Exp Hepatol* (2013) 3:37–49. doi: 10.1016/j.jceh.2012.12.001
 67. Amedia C, Oettinger C. Unusual presentation of tuberculosis in chronic hemodialysis patients. *Clin Nephrol* (1977) 8:363–6.
 68. Milburn H, Ashman N, Davies P, Doffman S, Drobniewski F, Khoo S, et al. Guidelines for the prevention and management of Mycobacterium tuberculosis infection and disease in adult patients with chronic kidney disease. *Thorax* (2010) 65:557–70. doi: 10.1136/thx.2009.133173
 69. Chen D, Yang Z, Yang Y, Zhan Z, Yang X. A Rare Case of Disseminated Tuberculosis of the Bone Marrow in Systemic Lupus Erythematosus: Case Report. *Med (Baltimore)* (2016) 95:e3552–2. doi: 10.1097/MD.00000000000003552
 70. Nau R, Sörgel F, Eiffert H. Penetration of Drugs through the Blood-Cerebrospinal Fluid/Blood-Brain Barrier for Treatment of Central Nervous System Infections. *Clin Microbiol Rev* (2010) 23:858–83. doi: 10.1128/CMR.00007-10
 71. Chang C-H, Chen Y-F, Wu V-C, Shu C-C, Lee C-H, Wang J-Y, et al. Acute kidney injury due to anti-tuberculosis drugs: a five-year experience in an

- aging population. *BMC Infect Dis* (2014) 14:23–3. doi: 10.1186/1471-2334-14-23
72. Pazhayattil GS, Shirali AC. Drug-induced impairment of renal function. *Int J Nephrol Renov Dis* (2014) 7:457–68. doi: 10.2147/IJNRD.S39747
 73. Beebe A, Seaworth B, Patil N. Rifampicin-induced nephrotoxicity in a tuberculosis patient. *J Clin Tuberc Mycobact Dis* (2015) 1:13–5. doi: 10.1016/j.jctube.2015.09.001
 74. Ilmer M, Bergauer F, Friese K, Mylonas I. Genital Tuberculosis as the Cause of Tuboovarian Abscess in an Immunosuppressed Patient. *Infect Dis Obstet Gynecol* (2010) 2009:745060. doi: 10.1155/2009/745060
 75. Gautam S, Jain A, Akhtar S, Priyadarshini A, Jaiswar SP. Serum Vitamin D Level as a Risk Factor for Female Genital Tuberculosis (FGTB). *J Clin Diagn Res* (2017) 11:DC18–DC20. doi: 10.7860/JCDR/2017/30084.10636
 76. Mahajan N, Naidu P, Kaur S. Insight into the diagnosis and management of subclinical genital tuberculosis in women with infertility. *J Hum Reprod Sci* (2016) 9:135–44. doi: 10.4103/0974-1208.192043
 77. Ballon SC, Clewell WH, Lamb EJ. Reactivation of silent pelvic tuberculosis by reconstructive tubal surgery. *Am J Obstet Gynecol* (1975) 122:991. doi: 10.1016/0002-9378(75)90363-4
 78. Sharma J, Roy K, Pushparaj M, Gupta N, Jain S, Malhotra N, et al. Genital tuberculosis: An important cause of Asherman's syndrome in India. *Arch Gynecol Obstet* (2008) 277:37–41. doi: 10.1007/s00404-007-0419-0
 79. Sharma JB, Mohanraj P, Jain SK, Roy KK. Increased complication rates in vaginal hysterectomy in genital tuberculosis. *Arch Gynecol Obstet* (2011) 283:831–5. doi: 10.1007/s00404-010-1463-8
 80. Al erylani AA, Abdelrub AS, Al Harazi AH. Genital tuberculosis is common among females with tubal factor infertility: Observational study. *Alex J Med* (2015) 51:321–4. doi: 10.1016/j.ajme.2014.11.004
 81. Kulshrestha V, Kriplani A, Agarwal N, Singh UB, Rana T. Genital tuberculosis among infertile women and fertility outcome after antitubercular therapy. *Int J Gynecol Obstet* (2011) 113:229–34. doi: 10.1016/j.ijgo.2010.12.014
 82. Jindal UN, Verma S, Bala Y. Favorable infertility outcomes following anti-tubercular treatment prescribed on the sole basis of a positive polymerase chain reaction test for endometrial tuberculosis. *Hum Reprod* (2012) 27:1368–74. doi: 10.1093/humrep/des076
 83. Sharma JB, Sharma E, Sharma S, Dharmendra S. Female genital tuberculosis: Revisited. *Indian J Med Res* (2018) 148:S71–83. doi: 10.4103/ijmr.IJMR_648_18
 84. Pang Y, An J, Shu W, Huo F, Chu N, Gao M, et al. Epidemiology of Extrapulmonary Tuberculosis among Inpatients, China, 2008–2017. *Emerg Infect Dis J* (2019) 25:457–64. doi: 10.3201/eid2503.180572
 85. Sethi S, Biswal M, Chatterjee S, Mewara A, Gupta D, Kumar S, et al. Susceptibility pattern among pulmonary and extrapulmonary isolates of *Mycobacterium tuberculosis* in north India. *Afr J Microbiol Res* (2012) 6:3696–9. doi: 10.5897/AJMR12.195
 86. Dedrick RM, Guerrero-Bustamante CA, Garlena RA, Russell DA, Ford K, Harris K, et al. Engineered bacteriophages for treatment of a patient with a disseminated drug-resistant *Mycobacterium abscessus*. *Nat Med* (2019) 25:730–3. doi: 10.1038/s41591-019-0437-z
 87. Khuroo A, Aarti C, Agastian P. Anti-tubercular peptides: A quest of future therapeutic weapon to combat tuberculosis. *Asian Pac J Trop Med* (2016) 9:1023–34. doi: 10.1016/j.apjtm.2016.09.005
 88. Vuorela P, Carpén O, Tulppala M, Halmesmäki E. VEGF, its receptors and the Tie receptors in recurrent miscarriage. *Mol Hum Reprod* (2000) 6:276–82. doi: 10.1093/molehr/6.3.276
 89. Marwood M, Visser K, Salomonsen LA, Dimitriadis E. Interleukin-11 and Leukemia Inhibitory Factor Regulate the Adhesion of Endometrial Epithelial Cells: Implications in Fertility Regulation. *Endocrinology* (2009) 150:2915–23. doi: 10.1210/en.2008-1538
 90. Subramani E, Madogwe E, Ray CD, Dutta SK, Chakravarty B, Bordignon V, et al. Dysregulated leukemia inhibitory factor and its receptor regulated signal transducers and activators of transcription 3 pathway: a possible cause for repeated implantation failure in women with dormant genital tuberculosis? *Fertil Steril* (2016) 105:1076–1084. doi: 10.1016/j.fertnstert.2015.12.015
 91. Casals G, Ordi J, Creus M, Fábregues F, Carmona F, Casamitjana R, et al. Osteopontin and $\alpha\text{v}\beta 3$ integrin as markers of endometrial receptivity: the effect of different hormone therapies. *Reprod BioMed Online* (2010) 21:349–59. doi: 10.1016/j.rbmo.2010.04.012
 92. Chowdhury R, Paine S, Bhattacharjee B, Chatterjee S. Infestation Of Endometrium By *Mycobacterium Tuberculosis* Bacilli-Cause Of Reproductive Failure. *Al Ameen J Med Sci* (2010) 3:322–31.
 93. Hambartsoumian E. Endometrial Leukemia Inhibitory Factor (LIF) as a Possible Cause of Unexplained Infertility and Multiple Failures of Implantation. *Am J Reprod Immunol* (1998) 39:137–43. doi: 10.1111/j.1600-0897.1998.tb00345.x
 94. Cheng J-G, Chen JR, Hernandez L, Alvord WG, Stewart CL. Dual control of LIF expression and LIF receptor function regulate Stat3 activation at the onset of uterine receptivity and embryo implantation. *Proc Natl Acad Sci* (2001) 98:6680–5. doi: 10.1073/pnas.151180898
 95. Fedorcsák P, Storeng R. Effects of Leptin and Leukemia Inhibitory Factor on Preimplantation Development and STAT3 Signaling of Mouse Embryos In Vitro. *Biol Reprod* (2003) 69:1531–8. doi: 10.1095/biolreprod.103.019034
 96. Invernizzi A, Franzetti F, Viola F, Meroni L, Staurengi G. Optic Nerve Head Tubercular Granuloma Successfully Treated with Anti-VEGF Intravitreal Injections in Addition to Systemic Therapy. *Eur J Ophthalmol* (2014) 25:270–2. doi: 10.5301/ejo.5000528
 97. Oehlers SH, Cronan MR, Scott NR, Thomas MI, Okuda KS, Walton EM, et al. Interception of host angiogenic signalling limits mycobacterial growth. *Nature* (2015) 517:612–5. doi: 10.1038/nature13967
 98. Kumar A, Rattan A. Antigonadotrophic effect of *Mycobacterium tuberculosis*. *Horm Metab Res Horm Stoffwechselforschung Horm Metab* (1997) 29:501–3. doi: 10.1055/s-2007-979088
 99. Malhotra N, Sharma V, Bahadur A, Sharma JB, Roy KK, Kumar S. The effect of tuberculosis on ovarian reserve among women undergoing IVF in India. *Int J Gynaecol Obstet Off Organ Int Fed Gynaecol Obstet* (2012) 117:40–4. doi: 10.1016/j.ijgo.2011.10.034
 100. Danforth DR, Arbogast LK, Mrroueh J, Kim MH, Kennard EA, Seifer DB, et al. Dimeric inhibin: a direct marker of ovarian aging. *Fertil Steril* (1998) 70:119–23. doi: 10.1016/S0015-0282(98)00127-7
 101. Jirge PR, Chougule SM, Keni A, Kumar S, Modi D. Latent genital tuberculosis adversely affects the ovarian reserve in infertile women. *Hum Reprod* (2018) 33:1262–9. doi: 10.1093/humrep/dey117
 102. Makhseed M, Raghupathy R, Azizieh F, Omu A, Al-Shamali E, Ashkanani L. Th1 and Th2 cytokine profiles in recurrent aborters with successful pregnancy and with subsequent abortions. *Hum Reprod* (2001) 16:2219–26. doi: 10.1093/humrep/16.10.2219
 103. Raghupathy R, Makhseed M, Azizieh F, Omu A, Gupta M, Farhat R. Cytokine production by maternal lymphocytes during normal human pregnancy and in unexplained recurrent spontaneous abortion. *Hum Reprod* (2000) 15:713–8. doi: 10.1093/humrep/15.3.713
 104. de Almeida AS, Fiske CT, Sterling TR, Kalams SA. Increased frequency of regulatory T cells and T lymphocyte activation in persons with previously treated extrapulmonary tuberculosis. *Clin Vaccine Immunol CVI* (2012) 19:45–52. doi: 10.1128/0152-0282.119.05263-11
 105. Hasan Z, Jamil B, Ashraf M, Islam M, Yusuf MS, Khan JA, et al. ESAT6-induced IFN γ and CXCL9 can differentiate severity of tuberculosis. *PLoS One* (2009) 4:e5158. doi: 10.1371/journal.pone.0005158
 106. Weikum ER, Liu X, Ortlund EA. The nuclear receptor superfamily: A structural perspective. *Protein Sci* (2018) 27:1876–92. doi: 10.1002/pro.3496
 107. Leopold Wager CM, Arnett E, Schlesinger LS. Macrophage nuclear receptors: Emerging key players in infectious diseases. *PLoS Pathog* (2019) 15:e1007585. doi: 10.1371/journal.ppat.1007585
 108. Bhagyaraj E, Nanduri R, Saini A, Dkhar HK, Ahuja N, Chandra V, et al. Human Xenobiotic Nuclear Receptor PXR Augments *Mycobacterium tuberculosis* Survival. *J Immunol Baltim Md 1950* (2016) 197:244–255. doi: 10.4049/jimmunol.1600203
 109. Dkhar HK, Nanduri R, Mahajan S, Dave S, Saini A, Somavarapu AK, Arora A, et al. *Mycobacterium tuberculosis* keto-mycolic acid and macrophage nuclear receptor TR4 modulate foamy biogenesis in granulomas: a case of a heterologous and noncanonical ligand-receptor pair. *J Immunol* (2014) 193:295–305. doi: 10.4049/jimmunol.1400092
 110. Saini A, Mahajan S, Ahuja N, Bhagyaraj E, Kalra R, Gupta P. An Accord of Nuclear Receptor Expression in *M. Tuberculosis* Infected Macrophages and Dendritic Cells. *Sci Rep* (2018) 8:2296. doi: 10.1038/s41598-018-20769-4

111. Bhagyaraj E, Tiwari D, Ahuja N, Nanduri R, Saini A, Kalra R, et al. A human xenobiotic nuclear receptor contributes to nonresponsiveness of *Mycobacterium tuberculosis* to the antituberculosis drug rifampicin. *J Biol Chem* (2018) 293:3747–57. doi: 10.1074/jbc.M117.818377
112. Guirado E, Rajaram MV, Chawla A, Daigle J, La Perle KM, Arnett E, et al. Deletion of PPAR γ in lung macrophages provides an immunoprotective response against *M. tuberculosis* infection in mice. *Tuberc Edinb Scotl* (2018) 111:170–7. doi: 10.1016/j.tube.2018.06.012
113. Liu PT, Stenger S, Li H, Wenzel L, Tan BH, Krutzik SR, et al. Toll-Like Receptor Triggering of a Vitamin D-Mediated Human Antimicrobial Response. *Science* (2006) 311:1770–3. doi: 10.1126/science.1123933
114. Chandra V, Mahajan S, Saini A, Dkhar HK, Nanduri R, Raj EB, et al. Human IL10 repression by Reverb α ameliorates *Mycobacterium tuberculosis* clearance. *J Biol Chem* (2013) 288:10692–702. doi: 10.1074/jbc.M113.455915
115. Korf H, Vander Beken S, Romano M, Steffensen KR, Stijlemans B, Gustafsson J-Å, et al. Liver X receptors contribute to the protective immune response against *Mycobacterium tuberculosis* in mice. *J Clin Invest* (2009) 119:1626–37. doi: 10.1172/JCI35288
116. Zhang Y, Zhu H, Yang X, Guo S, Liang Q, Lu Y, et al. Serum vitamin D level and vitamin D receptor genotypes may be associated with tuberculosis clinical characteristics: A case-control study. *Med (Baltimore)* (2018) 97:e11732. doi: 10.1097/MD.00000000000011732
117. Roodgar M, Ross CT, Tarara R, Lowenstein L, Dandekar S, Smith DG. Gene expression and TB pathogenesis in rhesus macaques: TR4, CD40, CD40L, FAS (CD95), and TNF are host genetic markers in peripheral blood mononuclear cells that are associated with severity of TB lesions. *Infect Genet Evol* (2015) 36:396–409. doi: 10.1016/j.meegid.2015.10.010
118. Bertolin K, Gossen J, Schoonjans K, Murphy B. The Orphan Nuclear Receptor Nr5a2 Is Essential for Luteinization in the Female Mouse Ovary. *Endocrinology* (2014) 155:1931–43. doi: 10.1210/en.2013-1765
119. Vasquez YM, DeMayo FJ. Role of nuclear receptors in blastocyst implantation. *Semin Cell Dev Biol* (2013) 24:724–35. doi: 10.1016/j.semcdb.2013.08.004
120. Duggavathi R, Volle DH, Matak C, Antal MC, Messaddeq N, Auwerx J, et al. Liver receptor homolog 1 is essential for ovulation. *Genes Dev* (2008) 22:1871–6. doi: 10.1101/gad.472008
121. Kam RKT, Deng Y, Chen Y, Zhao H. Retinoic acid synthesis and functions in early embryonic development. *Cell Biosci* (2012) 2:11. doi: 10.1186/2045-3701-2-11
122. Pereira FA, Qiu Y, Zhou G, Tsai MJ, Tsai SY. The orphan nuclear receptor COUP-TFII is required for angiogenesis and heart development. *Genes Dev* (1999) 13:1037–49. doi: 10.1101/gad.13.8.1037
123. Petit FG, Jamin SP, Kurihara I, Behringer RR, DeMayo FJ, Tsai M-J, et al. Deletion of the orphan nuclear receptor COUP-TFII in uterus leads to placental deficiency. *Proc Natl Acad Sci USA* (2007) 104:6293–8. doi: 10.1073/pnas.0702039104
124. Jeyasuria P, Ikeda Y, Jamin SP, Zhao L, de Rooij DG, Themmen APN, et al. Cell-Specific Knockout of Steroidogenic Factor 1 Reveals Its Essential Roles in Gonadal Function. *Mol Endocrinol* (2004) 18:1610–9. doi: 10.1210/me.2003-0404
125. Pelusi C, Ikeda Y, Zubair M, Parker KL. Impaired Follicle Development and Infertility in Female Mice Lacking Steroidogenic Factor 1 in Ovarian Granulosa Cells. *Biol Reprod* (2008) 79:1074–83. doi: 10.1095/biolreprod.108.069435
126. Cloke B, Christian M. The role of androgens and the androgen receptor in cycling endometrium. *Endocrinol Uterus Uterine-Relat Disord* (2012) 358:166–75. doi: 10.1016/j.mce.2011.06.031
127. Lobaccaro JMA, Gallot D, Lumbroso S, Mouzat K. Liver X Receptors and female reproduction: When cholesterol meets fertility! *J Endocrinol Invest* (2013) 36:55–60. doi: 10.3275/8765
128. Shahbazi M, Jeddi-Tehrani M, Zareie M, Salek-Moghaddam A, Akhondi MM, Bahmanpoor M, et al. Expression profiling of vitamin D receptor in placenta, decidua and ovary of pregnant mice. *Placenta* (2011) 32:657–64. doi: 10.1016/j.placenta.2011.06.013
129. Irani M, Merhi Z. Role of vitamin D in ovarian physiology and its implication in reproduction: a systematic review. *Fertil Steril* (2014) 102:460–8. doi: 10.1016/j.fertnstert.2014.04.046
130. Wei S-Q, Audibert F, Luo Z-C, Nuyt AM, Masse B, Julien P, et al. Maternal plasma 25-hydroxyvitamin D levels, angiogenic factors, and preeclampsia. *Am J Obstet Gynecol* (2013) 208:390.e1–6. doi: 10.1016/j.ajog.2013.03.025
131. Wei S-Q, Qi H-P, Luo Z-C, Fraser WD. Maternal vitamin D status and adverse pregnancy outcomes: a systematic review and meta-analysis. *J Matern-Fetal Neonatal Med Off J Eur Assoc Perinat Med Fed Asia Ocean Perinat Soc Int Soc Perinat Obstet* (2013) 26:889–899. doi: 10.3109/14767058.2013.765849
132. Wetendorf M, DeMayo FJ. The progesterone receptor regulates implantation, decidualization, and glandular development via a complex paracrine signaling network. *Mol Cell Endocrinol* (2012) 357:108–18. doi: 10.1016/j.mce.2011.10.028
133. Hapangama DK, Kamal AM, Bulmer JN. Estrogen receptor β : the guardian of the endometrium. *Hum Reprod Update* (2014) 21:174–93. doi: 10.1093/humupd/dmu053
134. Schaiff WT, Barak Y, Sadovsky Y. The pleiotropic function of PPAR γ in the placenta. *Mol Cell Endocrinol* (2006) 249:10–5. doi: 10.1016/j.mce.2006.02.009
135. Yessoufou A, Hichami A, Besnard P, Moutairou K, Khan NA. Peroxisome Proliferator-Activated Receptor α Deficiency Increases the Risk of Maternal Abortion and Neonatal Mortality in Murine Pregnancy with or without Diabetes Mellitus: Modulation of T Cell Differentiation. *Endocrinology* (2006) 147:4410–8. doi: 10.1210/en.2006-0067
136. Komar CM. Peroxisome proliferator-activated receptors (PPARs) and ovarian function—implications for regulating steroidogenesis, differentiation, and tissue remodeling. *Reprod Biol Endocrinol RBE* (2005) 3:41. doi: 10.1186/1477-7827-3-41
137. Goldstein CA, Smith YR. Sleep, Circadian Rhythms, and Fertility. *Curr Sleep Med Rep* (2016) 2:206–17. doi: 10.1007/s40675-016-0057-9
138. Bugge A, Feng D, Everett LJ, Briggs ER, Mullican SE, Wang F, et al. Rev-erba and Rev-erb β coordinately protect the circadian clock and normal metabolic function. *Genes Dev* (2012) 26:657–67. doi: 10.1101/gad.186858.112
139. Chute JP, Ross JR, McDonnell DP. Minireview: Nuclear receptors, hematopoiesis, and stem cells. *Mol Endocrinol Baltim Md* (2010) 24:1–10. doi: 10.1210/me.2009-0332
140. Purton L, Bernstein I, Collins S. All-trans retinoic acid enhances the long-term repopulating activity of cultured hematopoietic stem cells. *Blood* (2000) 95:470–7. doi: 10.1182/blood.V95.2.470
141. Mullen EM, Gu P, Cooney AJ. Nuclear Receptors in Regulation of Mouse ES Cell Pluripotency and Differentiation. *PPAR Res* (2007) 2007:61563. doi: 10.1155/2007/61563
142. Mullican SE, Zhang S, Konopleva M, Ruvolo V, Andreff M, Milbrandt J, et al. Abrogation of nuclear receptors Nr4a3 and Nr4a1 leads to development of acute myeloid leukemia. *Nat Med* (2007) 13:730–5. doi: 10.1038/nm1579
143. Han SJ, O'Malley BW. The dynamics of nuclear receptors and nuclear receptor coregulators in the pathogenesis of endometriosis. *Hum Reprod Update* (2014) 20:467–84. doi: 10.1093/humupd/dmu002
144. Lebovic DI, Kavoussi SK, Lee J, Banu SK, Arosh JA. PPAR γ Activation Inhibits Growth and Survival of Human Endometriotic Cells by Suppressing Estrogen Biosynthesis and PGE2 Signaling. *Endocrinology* (2013) 154:4803–13. doi: 10.1210/en.2013-1168
145. Pellegrini C, Gori I, Achdari C, Hornung D, Chardonnes E, Wunder D, et al. The expression of estrogen receptors as well as GREB1, c-MYC, and cyclin D1, estrogen-regulated genes implicated in proliferation, is increased in peritoneal endometriosis. *Fertil Steril* (2012) 98:1200–8. doi: 10.1016/j.fertnstert.2012.06.056
146. Bulun SE, Cheng Y-H, Yin P, Imir G, Utsunomiya H, Attar E, et al. Progesterone resistance in endometriosis: Link to failure to metabolize estradiol. *Int Workshop 11beta 17beta-Hydroxysteroid Dehydrogenases* (2006) 248:94–103. doi: 10.1016/j.mce.2005.11.041
147. Bielecki B, Mattern C, Ghoumari AM, Javadi S, Smietanka K, Abi Ghanem C, et al. Unexpected central role of the androgen receptor in the spontaneous regeneration of myelin. *Proc Natl Acad Sci* (2016) 113:14829–34. doi: 10.1073/pnas.1614826113
148. Chen W-D, Wang Y-D, Zhang L, Shiah S, Wang M, Yang F, et al. Farnesoid X receptor alleviates age-related proliferation defects in regenerating mouse livers by activating forkhead box m1b transcription. *Hepatology* (2010) 51:953–62. doi: 10.1002/hep.23390

149. Dierickx P, Van Laake LW, Geijsen N. Circadian clocks: from stem cells to tissue homeostasis and regeneration. *EMBO Rep* (2018) 19:18–28. doi: 10.15252/embr.201745130
150. Huang W, Ma K, Zhang J, Qatanani M, Cuvillier J, Liu J, et al. Nuclear Receptor-Dependent Bile Acid Signaling Is Required for Normal Liver Regeneration. *Science* (2006) 312:233–6. doi: 10.1126/science.1121435
151. Pantos C, Mourouzis I. Thyroid hormone receptor α 1 as a novel therapeutic target for tissue repair. *Ann Transl Med* (2018) 6:254. doi: 10.21037/atm.2018.06.12
152. Tschuor C, Kachaylo E, Limani P, Raptis DA, Linecker M, Tian Y, et al. Constitutive androstane receptor (Car)-driven regeneration protects liver from failure following tissue loss. *J Hepatol* (2016) 65:66–74. doi: 10.1016/j.jhep.2016.02.040
153. Pestka A, Toth B, Kuhn C, Hofmann S, Wiest I, Wypior G, et al. Retinoid X receptor α and retinoids are key regulators in apoptosis of trophoblasts of patients with recurrent miscarriages. *J Mol Endocrinol* (2011) 47:145–156. doi: 10.1530/jme-11-0002
154. Toth B, Bastug M, Scholz C, Arck P, Schulze S, Kunze S, et al. Leptin and peroxisome proliferator-activated receptors: impact on normal and disturbed first trimester human pregnancy. *Histol Histopathol* (2008) 23:1465–75. doi: 10.14670/hh-23.1465
155. Rose Ukibe N, Ukibe S, Ikechukwu Onwubuya E, Onyenekwe C, Nwamaka Monago I, Emelumadu O, et al. Possible impact of variations in some Cytokine levels during menstrual cycle in women of reproductive age infected with Pulmonary Tuberculosis at Nnewi, Nigeria. *Clin Invest* (2018) 08:63–73. doi: 10.4172/Clinical-Investigation.1000130
156. Datta A, Chaudhuri A, Chatterjee S, Chowdhury R, Bhattacharya B. Role of endometrial cytokines of the female genital tract tuberculosis in the context of infertility. *BLDE Univ J Health Sci* (2018) 3:24–30. doi: 10.4103/bjhs.bjhs_1_18
157. Chaouat G, Menu E, Clark DA, Dy M, Minkowski M, Wegmann TG. Control of fetal survival in CBA \times DBA/2 mice by lymphokine therapy. *J Reprod Fertil* (1990) 89:447–58. doi: 10.1530/jrf.0.0890447
158. Tezabwala BU, Johnson PM, Rees RC. Inhibition of pregnancy viability in mice following IL-2 administration. *Immunology* (1989) 67:115–9.
159. Fakih H, Baggett B, Holtz G, Tsang K-Y, Lee JC, Williamson HO. Interleukin-1: a possible role in the infertility associated with endometriosis. *Fertil Steril* (1987) 47:213–7. doi: 10.1016/S0015-0282(16)49993-0
160. Lebovic DI, Bentzien F, Chao VA, Garrett EN, Meng YG, Taylor RN. Induction of an angiogenic phenotype in endometriotic stromal cell cultures by interleukin-1 β . *Mol Hum Reprod* (2000) 6:269–75. doi: 10.1093/molehr/6.3.269
161. Straus DS, Glass CK. Anti-inflammatory actions of PPAR ligands: new insights on cellular and molecular mechanisms. *Trends Immunol* (2007) 28:551–8. doi: 10.1016/j.it.2007.09.003
162. Pourcet B, Gage MC, León TE, Waddington KE, Pello OM, Steffensen KR, et al. The nuclear receptor LXR modulates interleukin-18 levels in macrophages through multiple mechanisms. *Sci Rep* (2016) 6:25481. doi: 10.1038/srep25481
163. Lo Verme J, Fu J, Astarita G, La Rana G, Russo R, Calignano A, et al. The Nuclear Receptor Peroxisome Proliferator-Activated Receptor- α Mediates the Anti-Inflammatory Actions of Palmitoylethanolamide. *Mol Pharmacol* (2005) 67:15–19. doi: 10.1124/mol.104.006353
164. Sun M, Cui W, Woody SK, Staudinger JL. Pregnane X Receptor Modulates the Inflammatory Response in Primary Cultures of Hepatocytes. *Drug Metab Dispos* (2015) 43:335–43. doi: 10.1124/dmd.114.062307
165. Hollman DAA, Milona A, van Erpecum KJ, van Mil SWC. Anti-inflammatory and metabolic actions of FXR: Insights into molecular mechanisms. *Biochim Biophys Acta BBA - Mol Cell Biol Lipids* (2012) 1821:1443–52. doi: 10.1016/j.bbalip.2012.07.004
166. Nejati Moharrami N, Bjørkøy Tande E, Ryan L, Espevik T, Boyartchuk V. ROR α controls inflammatory state of human macrophages. *PLoS One* (2018) 13:e0207374. doi: 10.1371/journal.pone.0207374
167. Maijenburg MW, Gilissen C, Melief SM, Kleijer M, Weijer K, Ten Brinke A, et al. Nuclear receptors Nur77 and Nurr1 modulate mesenchymal stromal cell migration. *Stem Cells Dev* (2012) 21:228–38. doi: 10.1089/scd.2011.0076
168. Knabl J, Pestka A, Hüttenbrenner R, Plösch T, Ensenaer R, Welbergen L, et al. The liver x receptor in correlation with other nuclear receptors in spontaneous and recurrent abortions. *PPAR Res* (2013) 2013:575604. doi: 10.1155/2013/575604
169. Beltowski J, Semczuk A. Liver X receptor (LXR) and the reproductive system – a potential novel target for therapeutic intervention. *Pharmacol Rep* (2010) 62:15–27. doi: 10.1016/S1734-1140(10)70239-5
170. Banerjee P, Ghosh S, Dutta M, Subramani E, Khaldada J, Roychoudhury S, et al. Identification of key contributory factors responsible for vascular dysfunction in idiopathic recurrent spontaneous miscarriage. *PLoS One* (2013) 8:e80940. doi: 10.1371/journal.pone.0080940
171. Piltonen TT. Polycystic ovary syndrome: Endometrial markers. *Best Pract Res Clin Obstet Gynaecol* (2016) 37:66–79. doi: 10.1016/j.bpobgyn.2016.03.008
172. Achache H, Revel A. Endometrial receptivity markers, the journey to successful embryo implantation. *Hum Reprod Update* (2006) 12:731–46. doi: 10.1093/humupd/dml004
173. Lessey BA, Castelbaum AJ, Sawin SW, Sun J. Integrins as markers of uterine receptivity in women with primary unexplained infertility. *Fertil Steril* (1995) 63:535–42. doi: 10.1016/S0015-0282(16)57422-6
174. Wetendorf M, DeMayo FJ. Progesterone receptor signaling in the initiation of pregnancy and preservation of a healthy uterus. *Int J Dev Biol* (2014) 58:95–106. doi: 10.1387/ijdb.140069mw
175. Stephanou A, Ross R, Handwerger S. Regulation of human placental lactogen expression by 1,25-dihydroxyvitamin D₃. *Endocrinology* (1994) 135:2651–6. doi: 10.1210/endo.135.6.7988455
176. Shin JS, Choi MY, Longtine MS, Nelson DM. Vitamin D effects on pregnancy and the placenta. *Placenta* (2010) 31:1027–34. doi: 10.1016/j.placenta.2010.08.015
177. Murthi P, Yong HEJ, Nguyen TPH, Ellery S, Singh H, Rahman R, et al. Role of the Placental Vitamin D Receptor in Modulating Feto-Placental Growth in Fetal Growth Restriction and Preeclampsia-Affected Pregnancies. *Front Physiol* (2016) 7:43. doi: 10.3389/fphys.2016.00043
178. Barrera D, Avila E, Hernández G, Méndez I, González L, Halhali A, et al. Calcitriol affects hCG gene transcription in cultured human syncytiotrophoblasts. *Reprod Biol Endocrinol RBE* (2008) 6:3. doi: 10.1186/1477-7827-6-3

Conflict of Interest: The authors declare that the research was conducted in the absence of any commercial or financial relationships that could be construed as a potential conflict of interest.

Copyright © 2020 Gupta and Gupta. This is an open-access article distributed under the terms of the Creative Commons Attribution License (CC BY). The use, distribution or reproduction in other forums is permitted, provided the original author(s) and the copyright owner(s) are credited and that the original publication in this journal is cited, in accordance with accepted academic practice. No use, distribution or reproduction is permitted which does not comply with these terms.

Advantages of publishing in Frontiers



OPEN ACCESS

Articles are free to read
for greatest visibility
and readership



FAST PUBLICATION

Around 90 days
from submission
to decision



HIGH QUALITY PEER-REVIEW

Rigorous, collaborative,
and constructive
peer-review



TRANSPARENT PEER-REVIEW

Editors and reviewers
acknowledged by name
on published articles

Frontiers

Avenue du Tribunal-Fédéral 34
1005 Lausanne | Switzerland

Visit us: www.frontiersin.org

Contact us: info@frontiersin.org | +41 21 510 17 00



REPRODUCIBILITY OF RESEARCH

Support open data
and methods to enhance
research reproducibility



DIGITAL PUBLISHING

Articles designed
for optimal readership
across devices



FOLLOW US

@frontiersin



IMPACT METRICS

Advanced article metrics
track visibility across
digital media



EXTENSIVE PROMOTION

Marketing
and promotion
of impactful research



LOOP RESEARCH NETWORK

Our network
increases your
article's readership